Flinders University

UDP-GLYCOSYLTRANSFERASES (UGTs) IN ANTI-CANCER DRUG RESISTANCE

Radwan Ansaar

Bachelor of Science (Biotechnology) (Honours)

Discipline of Clinical Pharmacology
College of Medicine and Public Health
Flinders University, South Australia

November 2024

This thesis has been submitted to Flinders University for the degree of

Doctor of Philosophy

TABLE OF CONTENTS

LIST OF FIGURES

LIST OF TABLES

THESIS ABSTRACT

UDP-glucuronosyltransferases (UGTs) are part of a larger network of drug metabolising enzymes (DMEs) which conjugate sugar donors to lipophilic chemicals to aid in the inactivation and elimination of various molecules, including drugs, toxins and endogenous substances. The liver represents the main detoxifying organ, wherein this process mainly occurs to control systemic circulating levels of drugs, however to a degree a level of local metabolism occurs at the drugs target site, which can at times control therapeutic effect.

Epirubicin (EPI) is a cytotoxic anthracycline that is a mainstay chemotherapy used in the treatment of breast cancer, as can be applicable in various stages of the disease and often relied upon in late-stage cancers. UGT2B7 is thought to be the only DME responsible for EPI metabolism and as such, UGT2B7 levels and activity could be a key determinant of EPI levels systemically and within the tumour target site. Various components of the DME and elimination network can be manipulated by either activation or inhibition to achieve increased inactivation leading to sub-optimal dosage, or inversely, compounding therapeutic effect at the risk of an earlier dose-limiting toxicity. Currently, upregulation of DMEs and drug efflux transporters are thought to be inherent or acquired mechanisms of developing drug resistance, which reflects a key limitation in the application of chemotherapies.

In this thesis, a main objective was to explore the capacity for UGT2B7 to control EPI exposure in breast cancer, gaining insights into the mechanisms surrounding this and whether the modulation of *UGT2B7* could be a viable intervention for overcoming drug resistance to EPI.

Previous literature published by the laboratory (Hu et al., 2015; Hu et al., 2014c) indicated that EPI and nine other cytotoxic drugs (including three anthracyclines) are capable of inducing *UGT2B7*

mRNA in a hepatocellular carcinoma cell line (HepG2). To substantiate these findings, the first part of this thesis project demonstrated the induction of *UGT2B7* mRNA by EPI in breast cancer cell lines of varying subtypes, ranging from luminal to basal, inclusive of a primary triple-negative breast cancer (TNBC) cell line developed in the laboratory. Furthermore, a LC-MS UGT2B7 peptide assay was developed to quantify the induction of UGT2B7 protein in the MDA-MB-231 TNBC cell line. Supportive of the study published by (Hu et al., 2014c), the induction of UGT2B7 by p53 dependent and independent mechanisms was demonstrated using the p53-null cell lines (MDA-MB-231 and MPE-BC-001) and the wildtype-p53 cell line ZR-75-1, showing transcriptional activation by a p53 responsive element on the *UGT2B7* promoter.

A key finding of this thesis project was that increasing UGT2B7 expression conferred resistance to EPI. Specifically, a transgenic UGT2B7 overexpression MDA-MB-231 cell line was shown to be nearly 2-fold (n=4, P=0.01) more resistant to the drug. This led to the formulation of the hypothesis that breast cancer cells could be sensitised to EPI by inhibition of UGT2B7, and therefore a follow-up study was performed to create a model using various approaches including CRISPR, siRNA and UGT-UGT dimerization interactions. This was unsuccessful, due to a range of factors potentially including accessibility of the *UGT2B7* locus, leaving this as a future direction for study. Subsequent *in vivo* studies using the TCGA-BRCA database revealed that UGT2B7 mRNA expression is associated with poor overall survival (OS) in a breast cancer cohort (n=1082, P=0.0247). When the cohort was stratified by subtypes, high UGT2B7 expression was strongly associated with poor OS only in the patient group with basal subtype tumours (n=171, P=8.9 x 10^{-3}), and not in patients with other subtypes of breast cancer. Further stratification of the basal cohort by treatment regimen indicated that high UGT2B7 expression was associated with poorer progression free survival (PFS) only in the subset of patients that received anthracycline containing therapies (i.e. DOX or EPI versus (n=78, P=0.113). These data suggest the UGT2B7, may be a

marker for poor PFS in basal subtyped breast cancer patients receiving anthracyclines. However, further studies using additional datasets are required to confirm these findings. Moreover, the precise mechanistic basis of this association, and in particular, the role of UGT2B7 in controlling intratumoural exposure to anthracyclines, requires further study.

The potential for other anticancer drugs to mediate drug-drug interactions (DDIs) involving UGT2B7 was examined. Firstly, the ability of EGFR-targeting tyrosine kinase inhibitors (TKIs) to either induce UGT2B7 gene expression or inhibit UGT2B7 enzyme activity was explored. In breast cancer cells, TKIs (gefitinib, erlotinib and afatinib) did not affect transcript levels of UGT2B7, nor stimulate the p53 responsive element in the gene promoter. In contrast, gefitinib was able to inhibit the activity of the UGT2B7 enzyme. This was demonstrated using HLMs as a model and epirubicin as the probe substrate. Gefitinib was a moderately-strong inhibitor of epirubicin glucuronidation by UGT2B7 (IC_{50} 68.54 ± 9.56 μM). The selective estrogen receptor modulator (SERM) – tamoxifen also strongly inhibited UGT2B7-mediated epirubicin glucuronidation (IC_{50} 4.082). DDI risks were evaluated using *in vitro-in vivo* extrapolation methods and assuming a reversible inhibition model. For tamoxifen the reversible inhibition (R1) value was well above the threshold for a likely significant DDI (R1=1.4477). However, this was not the case for gefitinib. It is to be noted that, intratumoural levels of both gefitinib and tamoxifen are known to be much higher than plasma levels; for example, tamoxifen can be found in up to 20-fold higher concentrations than plasma (Kisanga et al., 2004; Robinson et al., 1991). Hence, the possibility that both drugs significantly inhibit the glucuronidation of epirubicin within the tumour should be explored in future work. These potential DDIs are of continuing interest because they might be exploited to enhance tumour cell exposure and hence increase the efficacy of epirubicin.

The last chapter of this thesis reports the development of an LC-MS assay to detect epirubicin glucuronide as a selective probe substrate for UGT2B7, which then allowed the estimation of enzyme kinetics with the respective K_m and V_{max} measured as 26.2 ± 5.48 µM and 2896.6 ± 212.8 AU. From these values, along with the physiochemical properties of the drug, a physiologically based pharmacokinetic (PBPK) profile for EPI was developed and validated, which was then utilised to perform a simulation based clinical trial using Simcyp to predict the main determinants of variability in EPI exposure using an oncology cohort. Hereof, 56% of variation in EPI exposure could be accounted for by hepatic UGT2B7 expression, while the remaining 31% was explained by renal UGT2B7 expression, plasma albumin concentration, age, BSA, GFR, haematocrit and sex (R_2 of the model=0.87). With the exception of brain tissue (R2 = 0.56) the PBPK model predicted that EPI plasma and tissue concentrations were poorly correlated (e.g. in muscle, heart, adipose, and liver tissue), supporting the idea that tissue level metabolism of EPI may be an important determinant of local/intratumoural drug levels.

Taken together, the findings from this thesis demonstrated the importance of understanding UGT2B7 regulation both systemically and intratumourally. With the emergence of precision medicine, PBPK based personalised dosing of EPI tailored to UGT2B7 activity might improve the tolerability of the drug and avoid sub-optimal dosing. Moreover, targeted inhibition of UGT2B7 might become an avenue for overcoming EPI resistance and increasing intratumoural EPI exposure. This could increase the effectiveness of EPI by potentially allowing lower systemic dosages and therefore limiting adverse effects.

In the future, trials to assess the effectiveness of combinations of UGT2B7 inhibitors (e.g. tamoxifen) with EPI-containing chemotherapy regimens, might provide the evidence required to translate these findings into novel therapeutic approaches.

DECLARATION

I certify that this thesis does not incorporate without acknowledgment any material previously submitted for a degree or diploma in any university; and the research within will not be submitted for any other future degree or diploma without the permission of Flinders University; and that to the best of my knowledge and belief it does not contain any material previously published or written by another person except where due reference is made in the text.

Signed: Date: 26/11/24

Radwan Ansaar

ACKNOWLEDGEMENTS

This PhD would not be possible without those who have contributed, supported, and uplifted me during this journey. I would like to express my utmost appreciation to those involved.

First and foremost, I would like to express my sincerest gratefulness to Professor Robyn Meech, whose guidance, endless expertise, supportiveness, and mentorship allowed me to take on and complete this PhD. I truly admire your work ethic, passion to learn and caring nature. Your support has instilled me with values that I'll hold true for my personal and professional journey.

To my associate supervisors, Dr Dong Gui Hu and Dr Julie-Ann Hulin, I am incredibly appreciative of your feedback, project guidance and experimental troubleshooting advice. Particularly I would like to thank, Julie-Ann for your timely, in-depth, critical feedback of this thesis, and other written work. Thank you to Professor Ross McKinnon for your insight and broader project perspectives.

To Emeritus Professor Peter Mackenzie, I am thankful for your honest guidance, and advice on this project. Your extensive knowledge in the field is admirable and I have enjoyed learning more of your experiences.

To Professor Andrew Rowland, you have gone above and beyond with your collaborative efforts in support of this project. I would like to express my thanks for enabling me to further develop my research, professional and life skills. You have been an excellent academic role model.

Thank you to my fellow colleagues and PhD students, Dylan Martin, Jai Meyers and Quinn Martin. Your advice, camaraderie, and willingness to partake in friendly exchanges has made working in the lab a positive experience.

I am appreciative of the relationships formed with colleagues and friends at Flinders University, including the other HDR students, those I have worked with, and the members of the teaching team.

I would like to thank Flinders University for providing me with the Flinders University Research Scholarship in support of this work.

Finally, thank you to my parents, family, and loved ones. You have shown belief in me, motivated my work, and moulded the person I am today. Particularly, I'd like to acknowledge my partner, Blessing Sithole, who provided me with a much-needed emotional outlet and the unforgettable times away from the stresses of a PhD. I would never have thought I could achieve this dream, without the infinite love from my support network. This PhD is yours to cherish as much as it mine.

CONFERENCE PROCEEDINGS DERIVED FROM THIS PROJECT

Ansaar, R. (2018) The role of UGT enzymes in cytotoxic drug resistance in breast cancer cells and cancer stem cells, short talk presented to the *ASCEPT 2018 Annual Scientific Meeting*, Adelaide Convention Centre, 27-30 November.

Ansaar, R. (2019) The role of UGT enzymes in cytotoxic drug resistance in breast cancer cells, poster presented to the *ASCEPT 2019 Annual Scientific Meeting*, Rydges Lakeland Resort Queenstown, 26-29 November. Finalist for the Neville Percy Award.

Ansaar, R. (2019) The role of UGT enzymes in cytotoxic drug resistance in breast cancer cells, poster presented at the College of Medicine and Public Health *Emerging Leaders Showcase*, Flinders University, 21-22 November.

Ansaar, R. (2019) The role of UGT enzymes in cytotoxic drug resistance in breast cancer cells, poster presented at the *Cancer Research Day,* Flinders Centre for Innovation in Cancer, 3rd September.

Ansaar, R. (2021) UDP-Glycosyltransferases (UGTs) in Anti-Cancer Drug Resistance, short talk presented at the College of Medicine and Public Health *Emerging Leaders Showcase*, Flinders University, 25-26 November.

SCHOLARSHIPS AND AWARDS IN SUPPORT OF THIS THESIS

Flinders University Research Scholarship (FURS), Flinders University, Australia, awarded from 2019-2022.

ASCEPT Neville Percy Award finalist for the best poster communication at the Annual Scientific Meeting for a Higher Degree student, Queenstown, New Zealand, November 2019.

ASCEPT committee student educational conference travel award to attend and present at the ASCEPT-PAGANZ Joint Scientific Meeting, Queenstown, New Zealand, November 2019.

ABBREVIATIONS USED

Abbreviation	Definition
4-MU	4-Methylumbelliferone
ABC	ATP-binding cassette
ADME	Absorption, distribution, metabolism and excretion
AR	Androgen receptor
AUC	Area under the plasma concentration-time curve
BC	Breast cancer
BCSC	Breast cancer stem cell
BMI	Body mass index
BSA	Body surface area
cDNA	Complementary DNA
CI	Confidence interval
CRISPR	Clustered regularly interspaced short palindromic repeats
CRISPRi	CRISPR interference
CYP	Cytochrome P450
DDI	Drug-drug Interaction
DFS	Disease-free survival
DME	Drug metabolic enzymes
DNA	Deoxyribonucleic acid
DN-inhibition	Dominant-negative inhibition
Dox	Doxorubicin
EC50	Half-maximal effective concentration
EGFR	Epidermal growth factor receptor
EPI	Epirubicin
ER	Estrogen receptor
EV	Extracellular vesicle

gDNA	Genomic DNA
GOF	Gain of function
gRNA	Guide RNA
HER2	Human epidermal growth factor receptor 2
HLMs	Human liver microsomes
HPLC	High-performance liquid chromatography
HR	Hormone receptor
IC50	Half-maximal inhibitory concentration
IHC	Immunohistochemistry
Indel	Insertion-deletion
IV	Intravenous
LC-MS	Liquid chromatography–mass spectrometry
LOF	Loss of function
MBC	Metastatic breast cancer
MDR	Multidrug resistance
MIDS	Model-informed initial dose selection
mRNA	Messenger RNA
NSAID	Non-steroidal anti-inflammatory drug
NSCLC	Non-small cell lung cancer
ORR	Objective response rate
OS	Overall survival
PBPK	Physiologically based pharmacokinetic
pCR	Pathologic complete response
PCR	Polymerase Chain Reaction
PD	Pharmacodynamic
PFS	Progression free survival
PK	Pharmacokinetic
PR	Progesterone receptor
qRT-PCR	Quantitative Real-Time PCR

RISC	RNA-induced silencing complex
RNA	Ribonucleic acid
RTK	Receptor tyrosine kinase
SERD	Selective estrogen receptor degrader
SERM	Selective estrogen receptor modulator
siRNA	Small interfering RNA
SLC	Solute carrier
SNP	Single nucleotide polymorphism
TDM	Therapeutic drug monitoring
TKI	Tyrosine kinase inhibitor
TNBC	Triple-negative breast cancer
TNM	Tumour-Node-Metastasis
UDPGA	Uridine 5’-diphosphoglucuronic acid
UGT	UDP-glucuronosyltransferase
UPLC	Ultra-Performance Liquid Chromatography
WT	Wildtype

CHAPTER 1. REVIEW OF THE LITERATURE

1.1. Breast Cancer

1.1.1. Epidemiology and risk factors

Breast cancer (BC) is the most commonly diagnosed form of cancer in females and is responsible for the most cancer deaths globally, making it a significant health and economic burden worldwide. The Global Cancer Observatory (GLOBOCAN) estimates there were 2.26 million newly diagnosed cases globally, contributing to 11.7% of all cancer diagnoses in 2020 (Sung et al., 2021). From the same dataset, the number of deaths globally in 2020 were estimated to be 684,996 (95% uncertainty interval (UI) 675493.0-694633.0), representing 6.9% of all cancer deaths (Ferlay et al., 2018).

While exceedingly less common, male breast cancer accounts for less than 1% of breast cancer cases and presents as a distinctly different disease (Chen et al., 2020b; Konduri et al., 2020), making it lesser studied in the context of breast cancers. In accordance with this, this literature review highlights the complex heterogeneity of the disease in females, focusing on the origins, classification, prognosis and treatments.

The vast majority of carcinogenesis in breast cancers are sporadic, with the cause of tumour development in the individual unknown. It is considered to be multifaceted in its nature, with a variety of genetic and environmental factors partaking in the role of tumour development (Łukasiewicz et al., 2021). Of the genetic contributors, familial history (of breast or ovarian cancer), ethnicity, and gene mutations, including those considered major risk modifiers, *BRCA1, BRCA2, p53, CDH1, PTEN, STK11*, along with those to a more moderate degree, *ATM, PALB2. BRIP1, CHEK2 and XRCC2*, are also thought to increase the likelihood of breast cancer (Łukasiewicz et al., 2021). This

area is constantly evolving with further detrimental genetic mutations being identified, and their exact level of contribution yet to be determined. Other non-modifiable factors include sex, age, reproductive history, and anatomical predisposition. Environmental and lifestyle causes of the disease include BMI, physical activity, drug and hormone regulators usage, diet and vitamin supplementation, smoking, alcohol, and chemical carcinogen exposure (Łukasiewicz et al., 2021).

1.1.2. Breast anatomy and cancer development

The female breast is composed of glandular tissue (the mammary gland) surrounded by connective tissue stroma (fibrous tissue) which provides support and gives the breast its shape, and adipose (fatty) tissue that fills the spaces between the glandular and fibrous tissue. The mammary gland is the functional unit of the adult breast, wherein they contain lobular units capable of producing milk, and 15-20 ducts that open to carry milk to the nipple (Ellis & Mahadevan, 2013).

Breast cancers can form along the ducts, and also in the terminal end, in the lobule (see Figure 1.1). When originating in the ducts or lobules, it is referred to as a carcinoma, and is the most common site for tumour occurrence. In a rarer instance (<1% of cases), cancer can originate in the supporting connective tissue of the breast and is thereby referred to as a sarcoma (Feng et al., 2018).

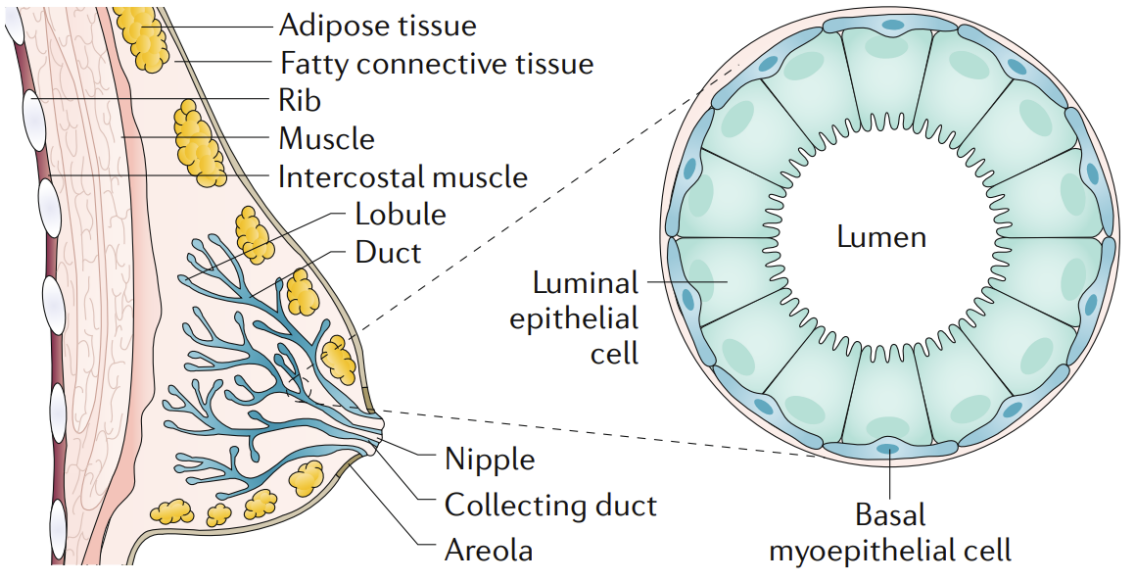

Figure 1.1. Breast cancer anatomy. Breast carcinomas form in the ducts and in the lobules located at the terminal ends of the ducts. They originate in the epithelial cell layer of the lobules, with the proximity of the primary tumour to the lumen being the defining histological marker of progression. Prognosis typically worsens upon tumour migration towards the outer lining (Meng et al., 2016). Figure has been adapted from Harbeck et al. (2019) with permission.

Classification is therefore determined by the presumed cell type of which the tumour originated, along with the invasiveness (how migratory it is). Non-invasive (*in-situ*) breast carcinomas include ductal or lobular carcinoma *in situ* and is the earliest form of breast cancer. Within these *in situ* carcinomas, they can then be further subtyped based on their progression within the epithelial lining of the lobules. Tumours arising in the lumen (centre) of the epithelial lining of the mammary ducts are subtyped as luminal, while further distal tumours arising from the myoepithelial basal layer located beneath the luminal epithelium and adjacent the basement membrane, are called basal. Figure 1.1 shows a cross-sectional diagram of the breast the pathophysiology of cancers arising in different ductal locations. These are also classified by histological markers (to be further explained in 1.1.3).

Invasive breast cancers have begun to migrate from the ducts or lobules and are as such named as invasive ductal or lobular carcinomas. These represent the early stages of breast cancers, with invasive ductal carcinomas being the most common type.

In later stage breast cancers, the cancer has spread (metastasized) to other organs, and thereby is named as metastatic breast cancer (Feng et al., 2018). This initially may affect proximal lymph nodes; however eventually micro-tumour metastases can move through the bloodstream to further major organs in advanced staged cancers (Veronesi et al., 2005). These pathological features determine the prognosis of the disease and dictate treatment options.

1.1.3. Staging and molecular classification

Breast cancer is a highly heterogeneous. Following a diagnosis, the prognosis and most appropriate treatment for an individual is dependent upon the clinical and molecular characteristics of the breast cancer type: this includes the staging and determination of pathologic features such as tumour histological grade and receptor status.

Breast cancer can be staged using the Tumour-Node-Metastasis (TNM) staging classification that is based on the amount of cancerous tissue and its spread within the body (Cserni et al., 2018). In the TNM classification, T refers to tumour size and any spread into nearby tissue; N refers to the spread of cancer into lymph nodes; and M refers to metastasis (spread of cancer to other parts of the body). Metastasized cancers are harder to treat and have poorer prognosis than cancers that remain within the breast (Rice, 2012).

Tumour histological grading can be used to predict the risk of spread and local reoccurrence in carcinomas. The most common system for this is known as the Nottingham Prognostic Index (NPI), which along with factoring in tumour histology, also assesses the lymph node stage, and tumour size (Pereira et al., 1995). By looking at morphological features, including the degree of tubule/gland formation, nuclear pleomorphism, and mitotic frequency, the NPI can provide a more reliable prognostic value than just assessing tumour size (Rakha et al., 2010).

Once a tumour has formed its cell of origin cannot be traced directly, so instead it is inferred from the molecular profile of the tumour ('molecular subtyping'). Current molecular classification divides breast cancers into five clinically relevant intrinsic molecular subtypes based on a 50-gene expression profile (PAM50) (Bertucci et al., 2009; Koboldt et al., 2012). The five subtypes are luminal A, Luminal B, HER2-overexpressing, basal and normal-like. These molecular subtypes are presented in Table 1.1 together with their relative prevalence and prognostic category.

Luminal A cancers are defined by expression of luminal markers and high expression of estrogen receptor alpha (ERα) and its regulatory target progesterone receptor (PR). They also have a relatively low mitotic index as indicated by Ki67 expression. Luminal A cancers are usually dependent on estrogen signalling for growth and have relatively good prognosis. Luminal B cancers also show luminal markers and ERα expression, but they may show low or no expression of PR, a high mitotic index, and a generally higher histological grade than Luminal A tumours (Dai et al., 2015). HER2-enriched tumours show high expression of the human epidermal growth factor receptor 2 (HER2)/erythroblastic oncogene B (*ERRB2*) gene, usually due to gene amplification (Powell, 2012). They are negative for expression of ERα and PR. Basal-like breast cancers are ERα-negative, PR-negative and HER2-negative (Dai et al., 2015) and are hence also called triple-negative breast cancers. However, it is relevant to note that not all TNBC have a basal-like expression profile. In fact, TNBC has been further divided into basal-like immune-activated (BLIA), basal-like immune-suppressed (BLIS), mesenchymal (MES), and luminal androgen receptor (LAR) (Burstein et al., 2015). TNBC/Basal cancers have generally poor prognosis in large part due to limited options for targeted therapy as discussed below.

Table 1.1. Breast cancer subtypes and immunohistochemistry (IHC) classification, along with the association with tumour grade (TNM staging), survival outcomes and prevalence. Table adapted from Dai et al., 2015 under open access permissions.

Intrinsic subtype	IHC status	Tumour grade	Outcome	Prevalence
Luminal A	[ER+|PR+] HER2-KI67-	1/2	Good	23.7%
Luminal B	[ER+|PR+] HER2-KI67+	2/3	Intermediate	38.8%
	[ER+|PR+] HER2+KI67+		Poor	14.0%
HER2 overexpression	[ER-PR-] HER2+	2/3	Poor	11.2%
Basal	[ER-PR-] HER2-, basal marker+	3	Poor	12.3%
Normal-like	[ER+|PR+] HER2-KI67-	1/2/3	Intermediate	7.8%

1.2. Breast Cancer Therapy Guided by Molecular Subtype

Molecular subtyping is a more recent addition to tumour subtyping, and it has significantly improved decisions regarding most appropriate treatment options and therefore improved survival. The cornerstones of treatment for hormone receptor (HR) -positive (ER/PR) or HER2 overexpressing breast cancers are drugs that directly target these growth promoting pathways. However, in the absence of all three receptors (TNBC), treatment options are more limited.

1.2.1. Targeted therapy for ER/PR+ breast cancer

Hormone therapies are used with the overarching aim of limiting estrogenic effects on tumour growth. Due to the reliance on the presence of the ER for effective targeting, these are only used in stage I-III breast cancers upon profiling ER expression.

One approach to blocking estrogenic tumour growth can be achieved by blocking estrogen synthesis via aromatase inhibitors, which inhibit a key enzyme (aromatase) involved in catalysing estrogen synthesis. As estrogen is no longer synthesized in ovarian tissue in postmenopausal women, estrogen synthesis is fully reliant on the conversion via the aromatase enzyme in other tissues – including breast cancer cells (Tremont et al., 2017). Aromatase inhibitors are therefore most effective in postmenopausal women, and the developed treatments include non-steroidal (reversible) drugs such as anastrozole and letrozole, or steroidal (irreversible) aromatase inhibitors such as exemestane (Drăgănescu & Carmocan, 2017; Mustonen et al., 2014; Simpson et al., 2004).

Another approach is focused on limiting the estrogenic effects on tumour cells by using selective estrogen receptor modulators (SERMs) or selective estrogen receptor degraders (SERDs). SERMs act directly on the ER to selectively antagonize/agonize the receptor; dependent on the tissue target, while SERDs directly bind to the ER causing ER degradation (Chen et al., 2022). The most common

SERM used is tamoxifen, which is common for pre and postmenopausal patients, while raloxifene and toremifene are used specifically in postmenopausal patients (Drăgănescu & Carmocan, 2017; Mustonen et al., 2014; Visvanathan et al., 2009). Currently, the only FDA approved SERDs are fulvestrant (Bross et al., 2002) and elacestrant (Bhatia & Thareja, 2023), which are effective against advanced, tamoxifen resistant tumour cells, however it is more active in postmenopausal than premenopausal women, and therefore used as such (Chen et al., 2022; Drăgănescu & Carmocan, 2017).

Cyclin-dependent kinase 4/6 inhibitors (CDKIs) are another targeted therapy that can be used in combination with HR targeting agents in first and second-line therapies. This has a specific use case in HR+/HER2- metastatic breast cancers, with the purpose of disrupting estrogen-regulated cell cycling at the G1 phase (Scott et al., 2017). Currently available drugs have varying affinities for each CDK isoform. These include palbociclib and ribociclib which each have good specificity for CDK4 and CDK6, while abemaciclib is strongly inhibitory towards CDK4 and CDK6, however with higher pan-CDK affinity (Chen et al., 2016). Palbociclib and ribocilib show a high degree of synergism clinically with ER antagonists and as such are a good combinatory approach, while ademaciclib has shown higher effectiveness as a single agent (Chen et al., 2016; Grinshpun et al., 2023).

1.2.2. Targeted therapy for HER2+ breast cancer

HER2 amplification (HER2+) occurs in approximately 25-30% of breast cancers over a variety of different prognostic stages, and typically is associated with poorer outcomes (Spector et al., 2007). A study by Seshadri et al. (1993) observed poorer overall disease-free survival in HER2+ patients, amongst a dataset of 1056 patients, along with a correlation between HER2 amplification and the absence of ER and PR. As such, HER2 can be a useful target for treatment in later staged breast cancers without ER/PR expression, but also combined with chemotherapy in early stages. Current

administrations involve HER2 antibody inhibitors or small molecule tyrosine kinase inhibitors to thwart the tumour proliferative effect associated with HER2 overexpression (Iqbal & Iqbal, 2014).

Currently available HER2 monoclonal antibody therapies include trastuzumab, pertuzumab and margetuximab, of which they mechanistically work by inhibiting HER2 through receptor binding (Wynn & Tang, 2022). Margetuximab is derived from trastuzumab, binding to the same HER2 extracellular domain, however with higher affinity for other receptor variants (Nordstrom et al., 2011). In addition, antibody-drug conjugates have been developed to deliver an additional cytotoxic agent alongside the monoclonal antibody mediated inhibition. These are based off trastuzumab also, and currently available examples of this include ado-trastuzumab emtansine (T-DM1) and trastuzumab deruxtecan (T-DXd) (Wynn & Tang, 2022).

Tyrosine kinase inhibitors (TKIs) are small molecule inhibitors that bind to the to ATP-binding domain of EGFR receptors, thus ablating downstream signalling components of the phosphorylation pathway. These have varying specificity, with some of the newer generations having broader inhibitory effects to the entire HER (EGFR) receptor family. Lapatinib is a first-generation TKI originally developed to target HER1 and HER2 (Untch & Lück, 2010), while neratinib is a second-generation TKI that has broader pan-HER activity (Wynn & Tang, 2022). Tucatinib is a newer third-generation TKI which instead has increased specificity for HER2 with improved efficacy, while also being targeted to reduce undesirable effects (Ulrich & Okines, 2021).

1.2.3. Chemotherapies used in breast cancer

Chemotherapy describes the use of cytotoxic drugs that kill cancer cells by targeting general cellular processes such as cell division (Gustafson & Page, 2013). In general, the use of cytotoxic chemotherapy is not dependant on subtype because the mechanisms of drug action do not rely on specific molecular targets. Cytotoxic drugs also kill normal cells, but the generally higher

proliferative index of the tumour provides a window of opportunity to preferentially kill cancer cells without causing unrecoverable harm to normal tissues. Side effects of these drugs such as alopecia and mucositis are due to the death of fast dividing normal cell populations, such as in hair follicles, and oral and gastrointestinal mucosa (Amjad et al., 2023). These effects are generally reversible once the drug is discontinued. Chemotherapies are quite often used in combination with each other in both adjuvant and neoadjuvant therapy. These can be separated into classes based on their mechanism of action, which will be described herein, along with specific examples used in breast cancer.

Alkylating Agents

DNA alkylating agents attach an alkyl group to DNA to induce cross-linking between DNA strands causing cell-cycle arrest (O'Shaughnessy, 1999; Ogino & Tadi, 2023). Cyclophosphamide is nitrogen mustard that is the main alkylating agent used in breast cancer, as an adjuvant therapy used in several combinations (O'Shaughnessy, 1999). Cisplatin, carboplatin and oxaliplatin are platinum-based alkylating drugs that have varied usage in breast cancer. Cisplatin was the first of the platinum anti-cancer drugs to be used (Wang et al., 2021), while more recently in advanced breast cancers, carboplatin and oxaliplatin have been used (Calderon et al., 2017; Zhang et al., 2022).

Antimetabolites

Antimetabolites are a broader class that inhibit the replication of DNA through a variety of different mechanism of actions based on their sub-classification.

Methotrexate is a folate antagonist that inhibits dihydrofolate reductase, which is essential for catalysing co factors required for pyrimidine and purine nucleotide synthesis pathways, thus impairing cell replication (Koźmiński et al., 2020). While not broadly used as a first line breast cancer

therapy, it has some specific use cases, showing effectiveness in clinical trials (Bazan et al., 2019; Yang et al., 2020a).

Gemcitabine is a synthetic pyrimidine that gets incorporated into DNA, therefore halting DNA polymerase elongation (de Sousa Cavalcante & Monteiro, 2014). It can be used in combination with paclitaxel and acts as a first-line therapy for patients not responsive to anthracyclines (Colomer, 2005).

5-fluorouracil (5-FU) is a fluoropyrimidine which acts as an antimetabolite through impairing key biosynthesis pathways required for DNA replication. This is mainly exerted through the inhibition of thymidylate synthase, which is responsible for synthesising thymidylate – an essential nucleotide in DNA replication. It can also bind to RNA, and disrupt essential RNA processing (Longley et al., 2003). 5-FU has been broadly used in breast cancers from early stage to advanced metastatic cancers (Yoon, 2005). Capecitabine is a precursor of 5-FU, which was designed as a prodrug for 5-FU to mimic its continuous infusion, therefore providing more adequate drug tumour distribution (Venturini, 2002). It is indicated as a treatment for triple negative breast cancer (Varshavsky-Yanovsky & Goldstein, 2020).

Antimicrotubular agents/mitotic inhibitors

Taxanes:

Taxanes form one of the major classes of drugs that target microtubules to disrupt cell proliferation. Paclitaxel and docetaxel share similar mechanisms of action, wherein they bind tubulin, to interfere with mitotic spindles therefore disrupting different mitotic stages of cell division. Due to their differential preference for tubulin binding, docetaxel acts more upon cell cycle stages S, G2, and M, while paclitaxel affects primarily the G2 and M phases (Gligorov, 2004). Paclitaxel exhibits higher

efficacy due to its robust pharmacokinetic properties including longer binding within the cell, which can lead to alternative mechanisms of action, with one being the degradation of the nuclear envelope, causing cell death (Smith et al., 2022). These drugs form important first-line therapies in breast cancer, however recently, cabazitaxel has been synthesized as a docetaxel analog, that could be employed as a second-line therapy for docetaxel resistant cancers, with much higher microtubule suppression at lower concentrations (Azarenko et al., 2014).

Non-taxanes:

Eribulin is a non-taxane based drug that has a unique mechanism of action of inhibiting microtubules by blocking the growth phase of the microtubule, therefore providing cell phase disruption during G2 and M phases (Jordan et al., 2005). Vinorelbine is another non-taxane based microtubule inhibitor which destroys mitotic spindles and stimulates microtubule depolymerization, therefore arresting the cell cycle at the M phase (Capasso, 2012). Ixabepilone has a similar mechanism of action to taxanes, where it binds directly to tubulin subunits, therefore suppressing microtubules and arresting G2 and M cell phases, however due to the differing chemical structure to taxanes, ixabepilone avoids taxane resistant mechanisms, and therefore is a good option for treating taxane-resistance breast cancer (Egerton, 2008; Pivot et al., 2007). Eribulin, vinorelbine and ixabepilone are used in metastatic breast cancer that has failed taxane or anthracycline treatment and can be used as single agents or combined with other chemotherapy (Ibrahim, 2021; O'Shaughnessy et al., 2019; Weber et al., 1995).

Topoisomerase inhibitors (derived from antibiotics)

Doxorubicin is an anthracycline derived from *Streptomyces peucetius*, with primary mechanisms of actions being through DNA intercalation, disruption of topioisomerase DNA repair, and generation of reactive oxygen species (Thorn et al., 2011). Epirubicin is an epimer of doxorubicin that was

synthetically generated because of its favourable toxicity profile and potentially higher antitumour activity (Ganzina, 1983). It therefore has the same mechanism of action as doxorubicin. Both doxorubicin and epirubicin are rarely given in isolation and typically form a myriad of combination therapies, that have become a mainstay in both early and late-stage breast cancers (Khasraw et al., 2012b). Anthracyclines will be further highlighted in section 1.3, as they are an important feature of this study.

1.2.4. Current drug-based treatment approaches based on molecular subtyping

As mentioned previously, treatment options are heavily dependent on the intrinsic tumour subtyping. Thus presents a myriad of available treatment combinations, as summarised in Table 1.2. These will be further elaborated hereon.

Table 1.2. Adjuvant systemic therapies available for specified breast cancer types including phenotypic subtypes. This table has been adapted from Anampa et al. (2015) under open access permissions.

Breast cancer subtype/classification			**Adjuvant systemic therapy**			
Hormone receptors	**HER2 overexpression**	**Intrinsic subtype**	**Endocrine therapy**	**CDK4/6 therapy**	**Anti-HER2 therapy**	**Chemotherapy**
+	–	Luminal A or B	Yes	Yes	No	Yes (if high risk)
+	+	Luminal B or HER2 enriched	Yes	No	Yes	Yes
–	–	Basal	No	No	No	Yes
–	+	HER2 enriched	No	No	Yes	Yes

In hormone receptor positive and HER2 negative cancers, the most common initial approach is reliant on endocrine based therapies combined with a CDK4/6 inhibitor (Hanna & Mayden, 2021; Waks & Winer, 2019). SERMs such as tamoxifen are used as endocrine therapies in pre- or post-menopausal women, while aromatase inhibitors are used in post-menopausal women (including surgically induced menopause) (Waks & Winer, 2019; Yang et al., 2020a). CDK4/6 inhibitors may also be reserved for use in second-line treatment as a monotherapy. Upon the acquisition of hormone resistance, treatment strategies then transition to a single agent chemotherapy.

In HER2+ subtypes, HER2 targeted therapy is used in combination with chemotherapy in ER- cases, otherwise HER2 therapy is combined with endocrine therapy in ER+ instances (Hanna & Mayden, 2021). The usage of anti-HER2 agents such as trastuzumab or pertuzumab (in high-risk cases) may sometimes be used later down the line (von Minckwitz et al., 2017). Several different chemotherapy regimens have been trialled alongside trastuzumab, including topoisomerase inhibitors, alkylating agents or taxanes (Hanna & Mayden, 2021). A standard approach with favourable outcomes and low toxicity is the use of taxanes (paclitaxel) as a single agent combined with trastuzumab or combined with anthracyclines and trastuzumab (Piccart-Gebhart et al., 2005; Tolaney et al., 2017).

In triple negative subtypes the only approved drug-based therapy is chemotherapy, which makes this often relied upon for treatment. No particular chemotherapy regimen is clearly most effective in triple negative breast cancer, and their usage can be before primary treatment options (neoadjuvant), such as surgical intervention or radiotherapy for initial tumour reduction in earlier local cases or afterwards (adjuvant) in metastatic tumours.

In early staged, localized breast cancer, a common neoadjuvant regimen may include taxanes followed by anthracyclines (Rastogi et al., 2008; Rouzier et al., 2005). Other newer advances have trialled antimetabolites with taxanes, the addition of microtubule stabilizing agents to

anthracyclines/alkylating agents or the addition of platinum-based alkylating agents to more traditional anthracycline/taxane based regimens in those with BRCA mutations (Amos et al., 2012; Holanek et al., 2021).

Adjuvant treatment is focused on long-term management and the reduction of reoccurrence. This can either involve taxanes, anthracyclines, or alkylating agents (most likely cyclophosphamide), or several combinations amongst those (Wahba & El-Hadaad, 2015). Recently, antimetabolites have also been trialled following standard adjuvant chemotherapy, which has resulted in improved outcomes (Joensuu et al., 2017).

1.3. Anthracyclines in Chemotherapy

Anthracyclines comprise a class of cytotoxic anticancer drugs derived from *Streptomyces* bacteria, which are commonly used to treat a wide range of cancers (Ormrod et al., 1999). Anthracyclines induce cell death by multiple mechanisms. These include topoisomerase inhibition leading to formation of double strand breaks, DNA intercalation which inhibits DNA/RNA synthesis, deregulation of gene expression through histone eviction from chromatin. In addition, anthracyclines produce unstable free radicals, that damage proteins and cause lipid peroxidation (Stohs., 1995). Cytotoxic potency is greatest in fast replicating cells (Stallard et al., 1990). Anthracyclines freely pass through the cell membrane and bind to nuclear DNA, hence higher concentrations are typically found in cell-dense areas. In general, anthracyclines are extensively distributed to tissue and accumulate in tumour sites (Italia et al., 1983).

Anthracyclines were first used in metastatic breast cancer in the 1970s and were a mainstay of therapy before the advent of taxanes (Friedrichs et al., 2002). The major anthracyclines used clinically are doxorubicin and epirubicin. Anthracyclines are typically used in combination

chemotherapy regimens: commonly fluorouracil, doxorubicin and cyclophosphamide (FAC), or fluorouracil, epirubicin and cyclophosphamide (FEC). When anthracycline containing regimens were initially compared to cyclophosphamide/methotrexate/fluorouracil (CMF) regimens for first line treatment of metastatic breast cancers, the anthracycline-containing regimens showed significantly better responses rates and longer time to progression (Andersson et al., 1999; Colajori et al., 1995). Subsequent studies and meta-analyses supported the superiority of anthracycline containing regimens over CMF (A'Hern et al., 1993).

With the introduction of taxanes (first approved by the FDA in 1996) (Chaurasia et al., 2023; FDA, 1996), anthracycline regimens were no longer the cornerstone of metastatic breast cancer treatment. Aggregate data suggested that first-line FEC had an ORR of 49.4% in metastatic breast cancer (Andersson et al., 1999; Colajori et al., 1995; Conte et al., 2000), whereas first-line, single-agent paclitaxel produced ORRs near 60% (Seidman et al., 1995). Paclitaxel was also effective in patients who had been previously exposed to anthracyclines and showed resistance to these drugs. This prompted studies to determine whether taxane and anthracycline combination regimens would provide further benefit. First-line doxorubicin/paclitaxel combinations produced ORRs from 75% to 95% in advanced breast cancer (Gianni et al., 1995). However, this regimen also led to a high incidence of cardiotoxicity (Gianni et al., 1995) and this was thought to relate to pharmacokinetic interactions as paclitaxel increased plasma concentrations of doxorubicin. The cardiotoxicity associated with doxorubicin is discussed further below.

Overall, anthracyclines have remained an important component of chemotherapy for advanced breast cancer; however, they show dose-limiting toxicities, particularly myelotoxicity and late-onset cardiotoxicity.

1.3.1. Epirubicin in the management of breast cancer

Epirubicin is an epimer of doxorubicin and has a similar efficacy in killing cancer cells, but a more favourable toxicity profile (Khasraw et al., 2012a). Doxorubicin shows marked cardiac toxicity due to generation of free radicals in the cardiomyocyte, which impairs contractility and ultimately results in left ventricular dysfunction (Chatterjee et al., 2010). In severe cases this can lead to congestive heart failure. Epirubicin shows considerably lower cardiotoxicity and lower myelotoxicity. The cumulative dose at which epirubicin causes cardiotoxicity (as measured by change in ejection fraction) is twice as high as that of doxorubicin (Cardinale et al., 2020), which allows for higher dosing (cumulative doses up to 1000mg/m^2) (Conte et al., 2000).

Epirubicin is included in first line therapy regimens for patients with metastatic breast cancers, particularly as part of the FEC regimen discussed above. A phase III study by Conte et al. (1996) found that patients on the FEC regimen had an ORR of 51.3% and a median survival without progression at 9.4 months (n=128).

Currently, standard chemotherapy options for metastatic breast cancer include both an anthracycline and a taxane. A widely used regimen is epirubicin and cyclophosphamide followed by weekly paclitaxel (EC-P regimen) (Yuan et al., 2023). However, recent studies indicate that a regimen of epirubicin plus paclitaxel (EP-P) followed by weekly paclitaxel is equally effective as the cyclophosphamide-containing regimen in hormone-receptor positive, HER2-negative, node-positive metastatic cancer. The cyclophosphamide free regimen also shows less adverse effects such as thrombocytopenia (Yu et al., 2021; Yuan et al., 2023).

In addition to metastatic cancers, anthracycline chemotherapy may also be used in early-stage node-negative, HR-positive, HER2-negative breast cancer patients. While endocrine therapy is the mainstay of systemic treatment for these cancers, many also benefit from adjuvant chemotherapy.

Whether to use chemotherapy typically depends on the risk of recurrence, which is estimated using clinical and/or molecular features. In particular, tumours that are high grade, with high proliferation rates and comparatively lower levels of ER and PR expression, are most likely to benefit from adjuvant anthracycline chemotherapy (Peto et al., 2012). One trial found that epirubicin could be used at higher doses (relative to doxorubicin) in the FEC regimen leading to improved survival outcomes for early stage breast cancers that have poor prognosis (Bonneterre et al., 2005).

1.4. The Principles of Pharmacology

Pharmacology encompasses the study of the effects of drugs in the body, of which there are two core concepts: pharmacodynamics and pharmacokinetics. **Pharmacodynamics** refers to the effects of a drug on biochemical and physiochemical systems in the body, usually though specific molecular target(s). The extent to which the drug can elicit a response at the target(s) determine the magnitude of the therapeutic response. In addition, the drug may elicit on-target or off-target adverse effects. Biochemical responses can include modulation of receptor signalling cascades, enzyme targets, ion channels and transporters, hormones, structural proteins, and more (Randall et al., 2012). Some effects, including adverse effects, may be indirect.

Pharmacokinetics refers to how the body handles the drug. This is commonly described by the ADME principle, which refers to absorption, distribution, metabolism and excretion of the drug. ADME is a systemic process, which begins with the drug entering the bloodstream in a manner that is dependent on the route of administration (Absorption). This is followed by Distribution to various tissues of the body including the relevant target tissue(s). Metabolism describes the biochemical transformation of the drug by drug metabolizing enzymes (DMEs). These reactions may serve to activate or inactivate the compound and can also aid in the excretion of the drug from the body. Typically, most metabolism occurs in the major organs of elimination such as the liver and to a lesser

extent, the kidney and gut. Excretion most commonly occurs via the kidney, although some drugs are predominantly faecally excreted and there are some other minor routes of elimination.

Drug metabolism is of particular interest in molecular pharmacology as variations in expression or function of DMEs have been shown to significantly influence drug disposition. Drug biotransformation in the liver is most studied as it typically has the largest effect on systemic drug clearance and thus overall drug exposure. However, drug metabolism can also occur locally in target tissues, and this may alter local exposure and hence drug efficacy.

1.4.1. Phase I and Phase II Drug Metabolism

Drug metabolism is generally separated in two phases known as Phase I and Phase II. The PharmaADME Consortium (http://www.pharmaadme.org) has identified 298 genes as important for ADME processes with 32 of these defined as 'core ADME genes' (Hovelson et al., 2017; Hu et al., 2020; Hu et al., 2019b). Of these 32 core genes, 23 mediate drug metabolism (12 genes in Phase I and 11 in Phase II), demonstrating how critical the metabolism step is to overall drug disposition.

Phase I drug metabolism typically involves reduction, oxidation or hydrolysis reactions that tend to make lipophilic chemicals more polar by creating or exposing a polar functional group. Of which, the main enzyme family catalysing phase I metabolism is the cytochrome P450 (CYP) family, which typically metabolise compounds by hydroxylation in the presence of an oxygen molecule (Iacopetta et al., 2023; Shakunthala, 2010). Phase II reactions involve attaching a bulky polar group, such as a sugar or sulfonate group, to make the compound even more polar and hence water soluble (Phang-Lyn & Llerena, 2023). The conjugated groups may also provide a negative charge that assists in interaction with anionic transporters thus increasing efflux from the cell. Overall conjugation promotes glomerular filtration and reduces resorption from the kidney tubule, thus facilitating

excretion in urine. An overview of the classical drug clearance process at the level of the cell (e.g. hepatocyte) is shown in Figure 1.2.

1.5. UDP-glycosyltransferases (UGTs)

The largest family of Phase II/conjugation enzymes and most important in terms of fraction of drugs metabolized, are the UDP-glycosyltransferases (UGTs). UGTs conjugate sugars, usually the negatively charged sugar glucuronic acid, to a wide range of lipophilic chemicals of both exogenous and endogenous origin (Meech et al., 2018). This conjugation, called glucuronidation, can reduce the capacity of the chemical to interact with biochemical targets (and thus reduce or block activity) and makes them charged and more hydrophilic, allowing ready excretion from tissues and the body. Conjugation requires a suitable acceptor group, often a carboxyl, hydroxyl, or amino group, which may pre-exist on the substrate or have been generated via a Phase I functionalization reaction. Not all drugs undergo both Phase I and Phase II metabolism and many drugs can undergo conjugation without prior functionalization by Phase I enzymes.

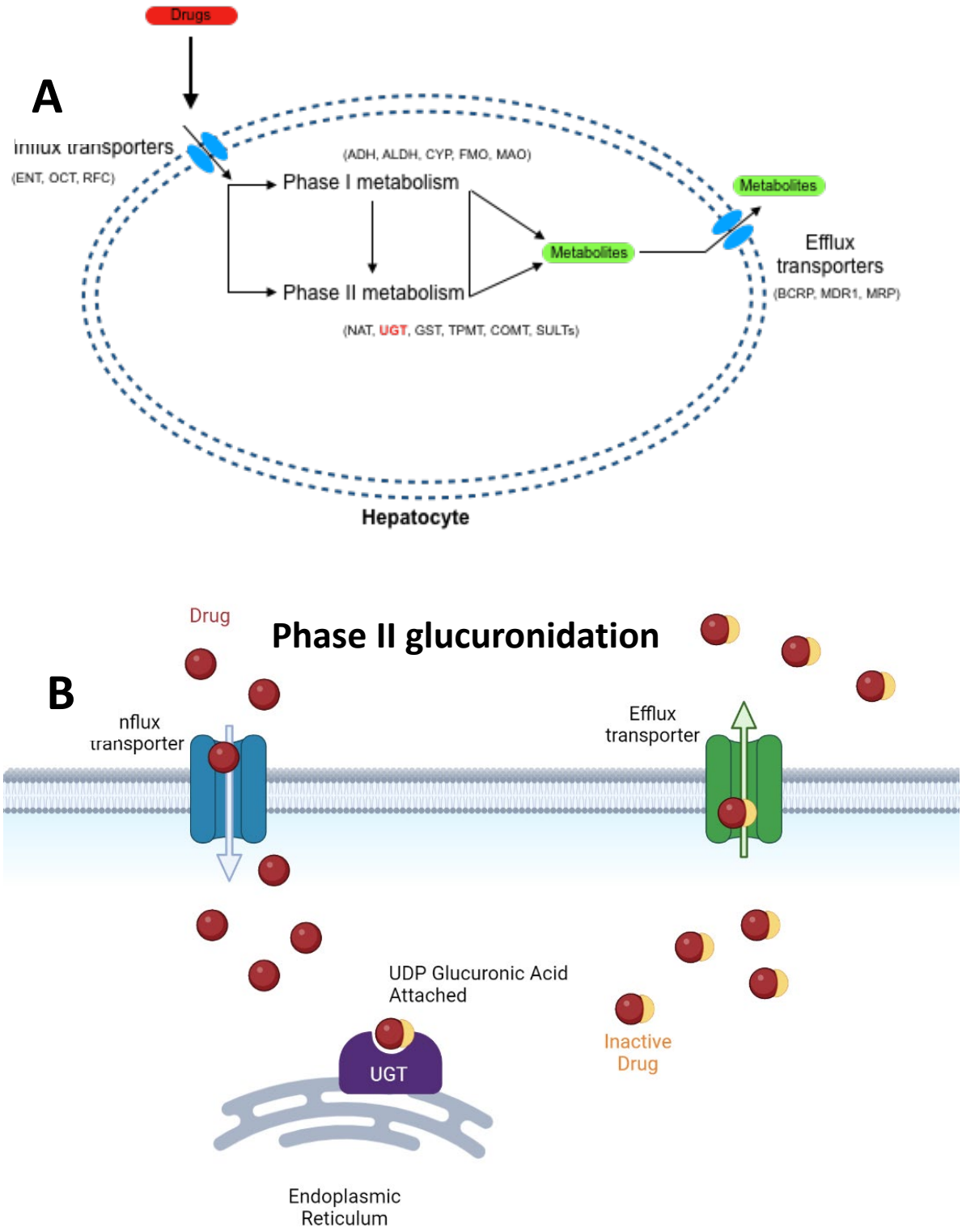

Figure 1.2. A snapshot of drug metabolism in the liver, highlighting phase II drug metabolising enzymes **(A)** UGTs (highlighted in red) are phase II drug metabolising enzymes which perform a detoxifying reaction (glucuronidation) with xenobiotics either independently or depending on a prior phase I reaction. Influx and efflux drug transporters facilitate the uptake and removal of xenobiotics in a hepatocyte (primarily) or other tissue cells. **(B)** Phase II glucuronidation reaction showing the influx of drugs/xenobiotics (shown in red) into the cytosol via drug transporters then the addition of a UDP glucuronic acid (shown in yellow) facilitated by UGT enzymes in the endoplasmic reticulum. This conjugation reaction results in a remaining compound that is inactive and effluxed outside of the hepatocyte via drug transporters. This inactive compound returns to plasma and is readily excretable.

There are 22 functional human UGTs belonging to four UGT families as depicted in the phylogenetic tree of the UGT superfamily in Figure 1.3. The two largest families are UGT1A and UGT2B and all members of these families preferentially conjugate glucuronic acid to their substrates using the UDP-glucuronic acid as an activated nucleotide-sugar donor. UGT3A family contains only 2 members and the UGT8 family contains only 1 member. The UGT3A and UGT8 enzymes do not use UDP-glucuronic acid as a sugar donor and instead conjugate lipophilic substrates with glucose, xylose, N-acetylglucosamine, or galactose depending on the UGT isoform.

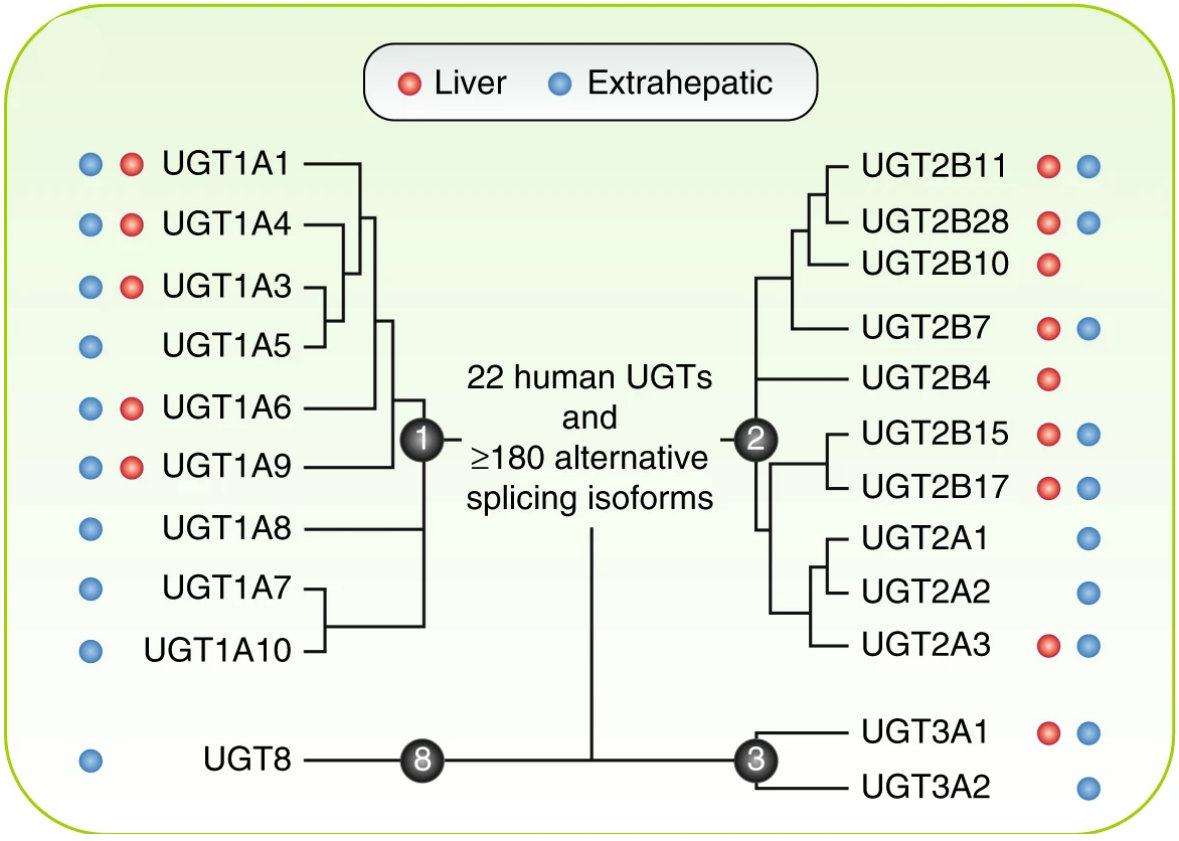

Figure 1.3. Phylogenetic tree showing the relationship between all 22 human UGT isoforms. The UGT superfamily contains four families, UGT1, UGT2, UGT3, UGT8. The UGT2 subfamily is divided into 2 subfamilies UGT2A and UGT2B. Most UGTs are hepatically expressed (indicated by the red dot), Many also have extrahepatic expression (blue dot) and some are exclusively extrahepatic. Figure has been adapted from Allain et al. (2020) under open access permissions.

UGT substrates are extremely structurally diverse, although generally somewhat lipophilic in nature, and include therapeutic drugs, environmental chemicals, toxic by-products of metabolism and various endogenous signalling molecules (Innocenti et al., 2001). In general, the UGT1A and UGT2B isoforms have multiple important drug substrates while the UGT3A and UGT8 enzymes have very few drug substrates and their major function is likely in controlling endogenous metabolism.

Most UGTs are expressed in the liver, and most are also prominently expressed in the other organs of elimination (kidney and intestine). In addition, UGTs typically show gene-specific patterns of expression in other organs and tissues as shown in Table 1.3.

Table 1.3. Tissue specific mRNA expression of UGTs in tissue. Table adapted from (Mubarokah, 2018), wherein detected expression has been denoted by – (not detected) or + (present). Untested tissue expression has been denoted by ND.

		Tissue																					
		Prostate	Breast	Testis	Skin	Oesophagus	Stomach	Small intestine	Colon	Kidney	Lung	Brain	Cerebellum	Thyroid	Thymus	Ovary	Placenta	Cervix	Heart	Trachea	Bladder	Spleen	Uterus	Pancreas
UGT mRNA	1A1	+	+	+	–	–	+	+	+	+	–	+	–	+/–	+/–	–	+/–	–	–	+/–	–	–	+	–
	1A3	ND	–	+/–	ND	–	+	+	+	+	+/–	+	–	+/–	+/–	–	–	–	–	+/–	–	–	+	–
	1A4	ND	–	+/–	ND	–	+	+	+	+	–	+	–	+/–	+/–	–	+/–	–	–	+/–	+	–	+	+
	1A5	ND	–	+	ND	+	+	+	+	+	–	+/–	–	–	+	–	–	+	–	+	+	–	+	–
	1A6	ND	–	+	ND	–	+	+	+	+	+/–	–	–	+/–	+/–	–	+/–	–	–	+	–	+/–	+	–
	1A7	ND	–	+/–	ND	+	+	+	+	+	–	+	–	+/–	+/–	–	+/–	+	–	+	+	–	–	–
	1A8	ND	+/–	+/–	ND	+	–	+	+	+	–	+	–	–	+/–	–	–	–	–	+	+	–	–	–
	1A9	+	+	+	+	+	–	+	+	+	–	+	–	+/–	+/–	–	+/–	–	–	+/–	–	–	–	–
	1A10	ND	–	+/–	ND	+	+	+	+	+	–	+	–	–	+/–	–	+/–	–	–	+	–	–	–	–
	2B4	+	+	+	+	+	–	+	+	+	+	+	–	–	+	–	–	–	+/–	+/–	–	–	–	–
	2B7	–	+	+/–	ND	+	+	+	+	+	+	–	–	–	+/–	–	+/–	–	–	–	–	–	+	+
	2B10	+	+	+	ND	+	–	–	–	+	+	+	–	–	–	–	–	–	–	–	–	–	–	–
	2B11	+	+	+/–	+	–	–	+	–	+	+	+/–	+/–	+/–	–	–	–	–	–	–	–	–	–	+
	2B15	+	+	+	+	+	+	+	+	+	+	+	–	+/–	–	–	–	–	–	+	–	–	–	+
	2B17	+	+	+	+	–	+	+	+	+	+	+/–	+/–	+/–	+	+	+/–	+	–	+	–	+	+	+
	2B28	–	+	–	–	–	–	–	–	–	–	+	–	–	–	–	–	ND	ND	–	+	–	–	–

1.5.1. The role of UGTs in cancer

UGTs have been proposed to play a protective role against cancer (Figure 1.4). In a comprehensive analysis of case-control studies, polymorphisms in *UGT* genes were found to be associated with the risk of developing a variety of different cancers (Bajro et al., 2012; Dura et al., 2012; Hu et al., 2015; Hu et al., 2016; Liu et al., 2009). The mechanisms by which UGTs alter cancer risk and outcomes are not fully defined and may be manifold. The currently identified associations of UGTs with cancer risk have been summarised in Table 1.4.

Table 1.4. *UGT* gene expression has been associated with different cancer types. The data is summarized from Meech et al. (2019) and Hu et al. (2014b). Table adapted from (Wijayakumara, 2021).

Cancer Type	**UGT isoforms indicated to be involved with carcinogenesis and/or progression**
Breast Cancer	UGT1A1, UGT1A6, UGT1A7, UGT2B4, UGT2B15, UGT2B17
Endometrial Cancer	UGT1A1, UGT1A6, UGT2B17
Prostate Cancer	UGT2B15 and UGT2B17, UGT2B28
Liver Cancer	UGT1A7, UGT1A1, UGT1A9, UGT1A6
Lung Cancer	UGT1A1, UGT1A4, UGT1A6, UGT1A7, UGT1A9, UGT2B4, UGT2B7, UGT2B10, UGT2B17
Head and Neck Cancers	UGTA1, UGT1A7, UGT1A10
Colorectal Cancers	UGT1A1, UGT1A3, UGT1A4, UGT1A6, UGT1A7, UGT1A9, UGT2B7, UGT2B15, UGT2B17
Colon Cancer	UGT1A7
Oesophageal Cancer	UGT1A8, UGT2B4
Bladder Cancer	UGT1A7, UGT2B7, UGT1A9, UGT1A6, UGT1A10, UGT1A

UGTs could impact oncogenesis by metabolising and clearing exogenous toxins, including carcinogens and tumour promoters, and by also clearing toxic by-products of endogenous metabolism, including known tobacco related carcinogens (Ren et al., 2000; Wiener et al., 2004a). This protective detoxification activity could reduce the risk of cancer initiation. It may also relate to the metabolism of endogenous lipophilic signalling molecules by UGTs. Many such signalling molecules can promote tumour growth when in excess, such as steroid hormones, fatty acids and bile acids. It is increasingly believed that UGTs can influence cancer progression by altering the levels of these signalling molecules. This function has been most clearly defined in hormone responsive cancers such as prostate cancer, where expression of the androgen conjugating UGT isoform UGT2B17 has been linked to prognostic features such as tumour grade and metastasis (Lévesque et al., 2020; Li et al., 2016; Pâquet et al., 2012). Moreover, in vitro studies have shown that overexpression (Li et al., 2016) or knockdown (Zhu et al., 2018) of UGT2B17 directly affects androgen-regulated cancer cell growth. It is likely that other UGTs have similar roles in controlling cancer growth though metabolism of lipophilic endogenous chemicals that act as ligands for nuclear receptor signalling.

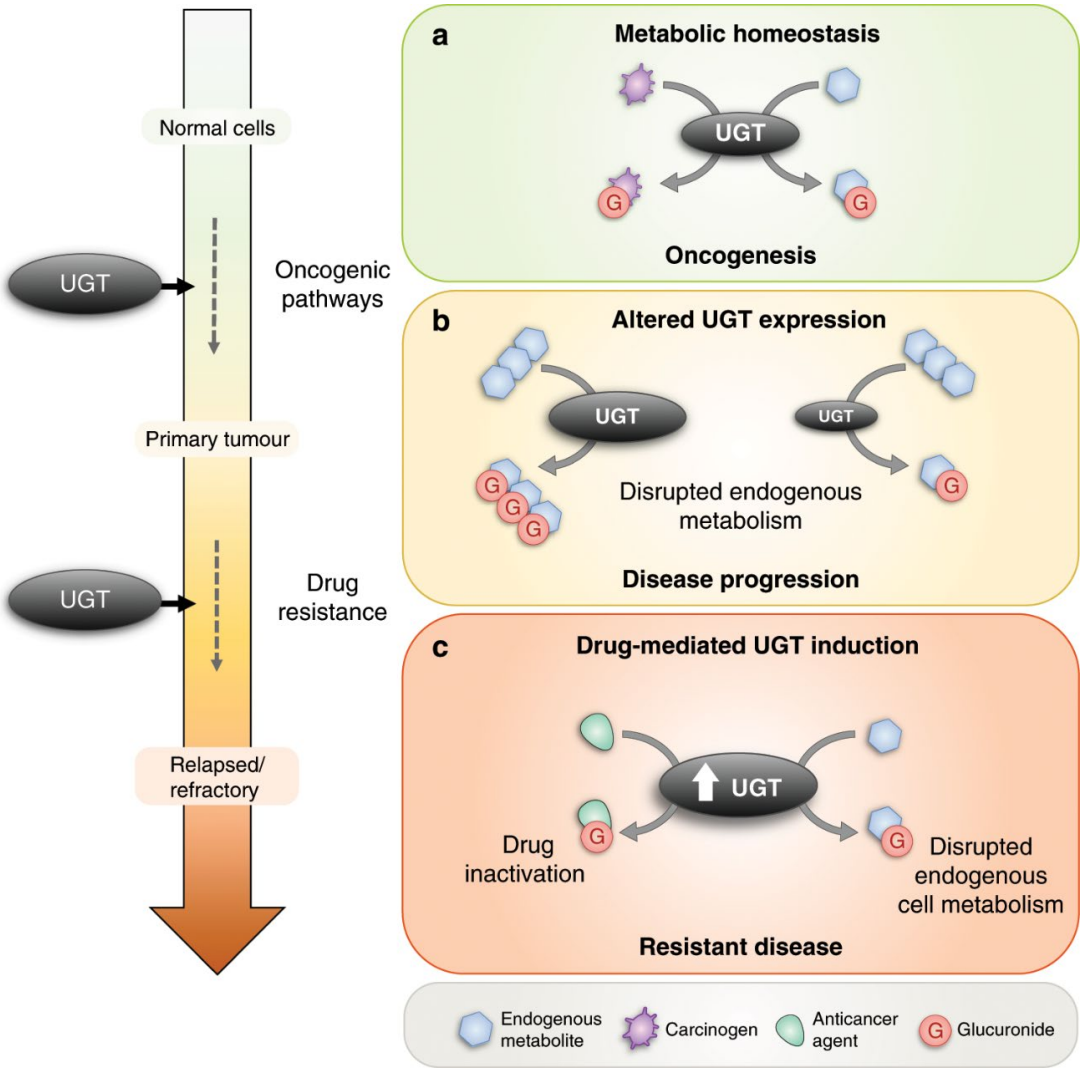

Figure 1.4. UGTs mediate various stages of cancer progression within the cell (Allain et al., 2020) (open access).

The third mechanism by which UGTs may regulate cancer outcomes is the regulation of anti-cancer drug exposure, and thus efficacy, which is the subject of this thesis and will be expanded on in subsequent sections. UGTs are involved in the metabolism of anti-cancer drugs from a wide range of functional and structural classes. These include hormonal drugs, chemotherapy drugs including nucleotide analogues, anthracyclines and alkaloids, and various targeted therapies such as kinase inhibitors. In the case of some drugs, UGT metabolism is a major contributor to exposure and therapeutic outcomes.

Early studies have identified that the active metabolite of the antineoplastic drug, irinotecan (SN-38) developed drug resistance in a lung cancer cell line (PC-7/CPT) through UGT1A amplification, and as a consequence, they were able to re-sensitize the cells to SN-38 by UGT1A inhibition (Gagné et al., 2002; Takahashi et al., 1997). As such, precision dosing centred around *UGT1A1* polymorphisms has been studied, with guided, individualised dosing showing improved responses in avoiding dose-limiting toxicity in cancer treatments (Innocenti et al., 2014).

Sorafenib (antineoplastic tyrosine kinase inhibitor) metabolism has also been shown to be highly decreased by downregulation of UGT1A9 and CYP3A4 in individual tumour hepatic microsomes, implicating these enzymes as major determinants of sorafenib plasma levels, thus providing an avenue for further study of dose-optimization of sorafenib for hepatocellular carcinoma (Ye et al., 2014).

Raloxifene, a SERM used in antiestrogen therapy for breast cancer, has shown associations between *UGT1A8* polymorphisms and a lowered glucuronidation capacity (Kokawa et al., 2013). UGT1A8, which is thought to be solely expressed extrahepatically (Strassburg et al., 1998), is the most active metaboliser of raloxifene, and has been implicated as a major determinant of circulating plasma levels of raloxifene glucuronide, raloxifene-4'-β-glucuronide, based on in-vivo data from human jejunum homogenates (Sun et al., 2013).

Tamoxifen is a well-established SERM, that is a prodrug with its more active metabolites being 4-OH-tamoxifen and endoxifen (Johnson et al., 2004). Lowered glucuronidation was most strongly associated with *UGT1A4* and *UGT2B7* variants, and WT *UGT2B17* and *UGT2B15*, therefore suggesting these genotypes are of prognostic value in mediating the antiestrogenic effects of tamoxifen (Romero-Lorca et al., 2015).

These contributing studies laid an important foundation in highlighting the value of regulating UGT metabolism to alter cancer drug sensitivity intrinsically, and the aforementioned examples are some of the more characterized targets of UGT-mediated drug exposure. In addition to these drugs, a review by Allain et al. (2020) has cited up to 73 anti-cancer drugs which are metabolised by glucuronidation, and therefore may have a degree of various altered target cell sensitivities caused by UGT-mediated metabolism processes. This highlights the importance of understanding the role of individual UGT isoforms in regulating anti-cancer drugs.

1.6. UGT2B7

The aforementioned list of Phase II enzymes considered to be 'core ADME genes', includes 3 *UGT* genes: *UGT1A1, UGT2B15,* and *UGT2B7*. UGT2B7 is of particular interest because it is involved in metabolism of a wide range of drugs and other xenobiotics in the liver and also in other tissues (Meech et al., 2018). Most notably, UGT2B7 substrates include chemotherapeutic drugs, which are further described in the subsequent section.

UGT2B7 is highly expressed in liver and is also significantly expressed in the gut and kidney (see Table 1.3). UGT2B7 has the capacity to glucuronidate a wide range of both endogenous and exogenous compounds. Endogenous substrates include bile acids (e.g. deoxycholic acid, lithocholic acid, hyocholic acid and hyodeoxycholic acid) (Barbier et al., 2009; Gall et al., 1999), retinoic acid (Czernik et al., 2000), and fatty acids (e.g. phytanic acid, docosahexaenoic acid, linoleic acid and metabolites including 13-hydroxyoctadecadienoic acid and 13-oxooctadecadienoic acid (Jude et al., 2001; Little et al., 2002). *UGT2B7* is also involved in estrogen and androgen metabolism, although steroids are considered minor substrates and other UGTs have higher specific activities with sex steroids. The minor steroid substrates of UGT2B7 include oestradiol, estriol, catecholestrogens (e.g.,

4-OH-estrone and 4-OH-estradiol) (Cheng et al., 1998; Gall et al., 1999; Lépine et al., 2004; Turgeon et al., 2001), androgens and their metabolites (e.g., androsterone and androstane-3,17- diol) (Gall et al., 1999; Turgeon et al., 2001), mineralocorticoid and glucocorticoid hormones (Girard et al., 2003; Knights et al., 2009).

UGT2B7 substrates that may be found in the environment include hydroxyestragole (Iyer et al., 2003), deoxynivalenol (mycotoxin) (Maul et al., 2015), trans-3-hydroxycotinine (major metabolite of nicotine) (Yamanaka et al., 2005), and ethanol (Saabi et al., 2013).

UGT2B7 is of pharmacological interest because it has numerous important drug substrates including NSAIDs (Gaganis et al., 2007; Jin et al., 1993b; Mano et al., 2007a), opioids (codeine, morphine, oxycodone) (Coffman et al., 1997; Raungrut et al., 2010; Romand et al., 2017), naloxone (Di Marco et al., 2005), lorazepam (Uchaipichat et al., 2013), and zidovudine (Barbier et al., 2000). A comprehensive list of UGT2B7 drug substrates is provided in Table 1.5. Anticancer drugs that can be metabolized by *UGT2B7* include active tamoxifen metabolites (Sun et al., 2007), the nonsteroidal aromatase inhibitors carbinol (metabolite of letrozole) (Precht et al., 2013) and anastrozole (Kamdem et al., 2010), and the chemotherapy drug epirubicin (Innocenti et al., 2001) which is the subject of this thesis.

Table 1.5. A list of drug substrates metabolised by UGT2B7 (adapted from Meech et al. 2019) (open access).

Drug substrate of UGT2B7	Class	Therapeutic uses	Reference
3'-Azido-3'-deoxythymidine (AZT)	Pyrimidine nucleosides	Antiretroviral	(Barbier et al., 2000)
3-OH-benzodiazepines	Benzodiazepine	Anxiety, seizures and muscle spasms	(Jin et al., 1993b)
Carbinol	Benzene	Metabolite of letrozole (aromatase inhibitor)	(Precht et al., 2013)
Carvedilol	Indole	Hypertension	(Ohno et al., 2004)
Chloramphenicol	Benzene	Antibiotic	(Chen et al., 2010)
Codeine	Morphinans	Analgesic	(Raungrut et al., 2010)
Efavirenz	Benzoxazines	Antiviral	(Bélanger et al., 2009)
Epirubicin	Anthracycline	Chemotherapy	(Innocenti et al., 2001)
Gemfibrozil	Phenol ethers	Lipid regulating agent	(Mano et al., 2007b)
Haloperidol	Organooxygen	Antipsychotic	(Kato et al., 2012)
Lorazepam	Benzodiazepines	Anxiety, seizures and muscle spasms	(Uchaipichat et al., 2013)
Lorcaserin	Benzazepines	Anti-obesity	(Sadeque et al., 2012)
Morphine	Morphinans	Pain-management	(Coffman et al., 1997)
Mycophenolic acid	Isocoumarans	Immunosuppressant	(Picard et al., 2005)
Ornidazole	Azoles	Antibiotic	(Du et al., 2013)
Valproic acid	Fatty Acyls	Anticonvulsant	(Argikar & Remmel, 2009)
Flurbiprofen	Benzene	Non-steroidal anti-inflammatory drug (NSAID) (osteoarthritis)	(Mano et al., 2007a)
Naproxen	Naphthalenes	NSAID (rheumatoid arthritis)	(Jin et al., 1993b)
Ketoprofen	Benzene	NSAID (rheumatoid arthritis)	(Jin et al., 1993b)
Ibuprofen	Phenylpropanoic acids	NSAID (pain/inflammation relief)	(Jin et al., 1993b)
Fenoprofen	Benzene	NSAID (analgesic)	(Jin et al., 1993b)
Tiaprofenic acid	Organooxygen compounds	NSAID (rheumatoid arthritis)	(Jin et al., 1993b)
Benoxaprofen	Azoles	NSAID (analgesic)	(Jin et al., 1993b)
Zomepirac	Organooxygen	NSAID (antipyretic)	(Jin et al., 1993b)
Diflunisal	Benzene	NSAID (analgesic)	(Jin et al., 1993b)
Indomethacin	Indole	NSAID (pain/inflammation relief)	(Jin et al., 1993b)
Mefenamic acid	Benzene	NSAID (analgesic, anti-inflammatory, and antipyretic)	(Gaganis et al., 2007)
Benzo[α]pyrene metabolites			(Jin et al., 1993a)
2-acetylaminofluorene metabolites			(Jin et al., 1993a)

1.7. UGT2B7 Drug-Drug Interactions (DDIs) can Mediate Therapeutic Drug Levels

UGT2B7 is also important in multiple drug-drug interactions (DDIs). DDIs occur when one drug (called the perpetrator drug) affects the metabolism of a second drug (called the victim drug) (Roberts & Gibbs, 2018). This can occur due to either inhibition or induction of ADME factors, particularly DMEs. In most cases, inhibition of DME activity occurs when the perpetrator drug binds to the enzyme and prevents it from carrying out enzymatic biotransformation of the victim drug. In contrast, induction of DME activity generally involves an increase in the amount of the DME expressed, often due to increased gene transcription (Palleria et al., 2013).

UGT2B7 is involved in numerous DDI that are mediated by either enzyme inhibition or induction. One example of the former is the competitive inhibition of UGT2B7 by fluconazole, which leads to reduced metabolism of zidovudine (Uchaipichat et al., 2006). This is predicted to alter the AUC of zidovudine by 41-217% depending on the concentration and frequency of dosing of fluconazole. One example of the latter is the increase in UGT2B7-mediated zidovudine metabolism after treatment with rifampin (Burger et al., 1993). The consequences of this interaction were demonstrated amongst three patients, where administration of 600 mg rifampin increased zidovudine AUC by 2.3 -fold on average, respective to the control participants. Plasma C_{max} was not significantly affected.

Numerous NSAIDs have been implicated as potential victim drugs for DDIs involving UGT2B7. Although glucuronidation has not been well characterized for the majority, S-naproxen inhibition by the UGT2B7 specific inhibitor, fluconazole, is a known example of a NSAID UGT2B7 specific interaction (Bowalgaha et al., 2005; Gaganis et al., 2007). Similarly, Miners et al. (2023) suggest similar mechanisms of inhibition for fenoprofen, carprofen, diflunisal, ketoprofen, and zomepirac

due to their primary clearance pathway being acyl glucuronidation, of which UGT2B7 catalyses for most NSAIDs (Jin et al., 1993b). Although belonging to different drug classes, gemfibrozil and clofibric acid are also majority glucuronidated by UGT2B7 and can be inhibited by fluconazole (Miners et al., 2023; Miners et al., 2021).

Polypharmacy used in opioid analgesics poses a clinical risk and is of high importance in understanding to enable desirable effects, while avoiding unfavourable outcomes. UGT2B7 is a major metabolism pathway of opioids, including morphine, oxycodone, codeine, dihydrocodeine, and buprenorphine (Feng et al., 2017). Morphine is primarily glucuronidated by UGT2B7 to form its major metabolite, morphine-3-glucuronide, and its minor metabolite, morphine-6-glucuronide, both of which are pharmacologically active (Janicki, 1997). Methadone (Gelston et al., 2012), amitriptyline (Wahlström et al., 1994), clomipramine (Wahlström et al., 1994), and mefenamic acid (Uchaipichat et al., 2022) are all examples of inhibitors of UGT2B7 which affect morphine-3-glucuronide and morphine-6-glucuronide formation. Conversely, rifampin ablates the analgesic effect of morphine when co-administered by effectively reducing the AUC of morphine by ~28% (Fromm et al., 1997). Interestingly, while rifampin has been shown to induce UGT2B7, UGT2B7-catalysed metabolites morphine-3-glucuronide and morphine-6-glucuronide were also decreased, making it unclear whether UGT2B7 is induced in this context, as morphine metabolites may also be cleared at an increased rate by induction of p-glycoprotein, therefore increasing efflux of metabolites, as hypothesized by Fudin et al. (2012). A similar relationship between hydromorphone and rifampin has been studied by Lohela et al. (2021), where they both saw reduced hydromorphone AUC and increased hydromorphone-3-glucuronide ratios, with co-administration, thus indicating induction of UGT2B7 by rifampin. A similar phenomenon may be observed with norcodeine (a codeine metabolite formed by CYP3A4) (Thorn et al., 2009), where rifampin results

in increased clearance as evident by increased norcodeine-glucuronide levels in plasma (Caraco et al., 1997), although the UGT isoform involved with metabolising norcodeine is not yet characterized.

While the aforementioned interaction list is not exhaustive, further potential DDIs involving UGTs can be found in a review by Miners et al. (2023). UGT based DDIs remain under-investigated, which therefore represents a gap in the field, where increased studies into the relationships between UGT2B7 substrates and other clinically co-administered inducers/inhibitors are crucial.

Of those UGT2B7 substrates (from Table 1.5) that are likely to be co-administered alongside epirubicin, particularly in the context of cancers, 3'-azido-3'-deoxythymidine (AZT) can be used in the management of various cancers (breast (Melana et al., 1998), colon (Brown et al., 2003), lung (Savaraj et al., 2003), and ovarian (Scanlon et al., 1990) cancer inclusive), as it has antiproliferative and apoptotic activity (Hsieh & Tseng, 2020). Particularly, in HIV-instigated cervical cancer cases, epirubicin may be combined with AZT, although there are limited trials investigating this specific combination. Valproic acid has recently shown therapeutic promise as an anti-cancer agent, where it has been trialled and approved for use in combination with epirubicin (Munster et al., 2009; Münster et al., 2007; Wawruszak et al., 2021). Carvedilol is an antihypertensive used in the instance of anthracycline-related cardiotoxicity (Armenian et al., 2024), although it is primarily indicated for doxorubicin treated patients (Fazio et al., 1998), due to the less than favourable cardiotoxicity caused by doxorubicin, compared to the lowered cardiotoxicity risk with its epimer, epirubicin. In the case of pain management options in cancers, opioids, including morphine and codeine are recommended by the WHO (2018) as first-line treatments in this instance. NSAIDs are commonly used to manage the pain and inflammation in cancers (including breast cancer) and may help lower the risk of secondary breast cancer (Cairat et al., 2020; Lu et al., 2021).

Induction-based DDIs, which are the focus of this thesis, typically require that the perpetrator drug acts to induce a transcriptional regulatory pathway that increases UGT expression. This might be because the drug is a direct ligand for a transcription factor, for example rifampin is a ligand for the transcription factor PXR that induces *UGT2B7* expression. Alternatively, the perpetrator drug may trigger a signalling cascade that leads to activation of a downstream transcription factor. An example of indirect transcription factor activation is the induction of p53 by cytotoxic drugs because of genotoxic stress that leads to pro-apoptotic signalling (Hu et al., 2015). As discussed in later sections, UGT2B7 is a target for regulation by p53 in response to such drugs.

1.8. Role of Genetic Variation in UGT2B7 Drug Exposure and Efficacy

An important aspect of ADME is patient-specific variation in drug exposure that occurs as a result of genetic differences in ADME genes. These differences are typically single nucleotide polymorphisms (SNPs), although they can also involve other types of genetic variation such as insertion-deletion (indel), copy number variation (CNV) and alternative splicing.

1.8.1. Alternative splicing

Transcriptional diversity of UGT2B7 is still an emerging topic of discussion. Currently, there is evidence to suggest the existence of at least four alternative exons (in place of exon 1) upstream of the canonical exon 1, however these are either prematurely terminated due to the presence of stop codons, or likely unable to bind substrates, as they would significantly disrupt the substrate binding domain in the N terminus (Innocenti et al., 2008; Ménard et al., 2011; Sun & Di Rienzo, 2009). There are also two alternative exons upstream of the canonical exon 6, towards the C terminus, however these would not be catalytically active, as they result in C-terminally truncated proteins missing the sugar binding domain, which is essential for glucuronidation (Innocenti et al., 2008; Ménard et al.,

2013). Truncated UGT2B7 proteins are expected to be involved in the modulation of UGT2B7 expression through homodimerization (Lewis et al., 2011), as evidenced by other UGT2Bs (Meech & Mackenzie, 1997), however this has not yet been adequately demonstrated in UGT2B7.

1.8.2. Single nucleotide polymorphisms (SNPs)

Thus, a more studied area has prioritised identifying and characterizing SNPs, as this remains an important direction in understanding factors that may influence enzymatic activity of UGT2B7 (Hu et al., 2014a). Currently several SNPs have been linked to alteration in either *UGT2B7* expression or function as summarized in this section.

The 802C>T (rs7439366) single nucleotide polymorphism (SNP) in exon 2 of *UGT2B7* is a common allelic variant, present in 27% of Asians and 54% of Caucasians (Bernard et al., 2006). It results in a singular histidine to tyrosine substitution at codon 268 often abbreviated as His268Tyr (or H268Y). Moreover, it is in complete linkage disequilibrium with the promoter SNP -161C>T (to be discussed in a following section) (Sawyer et al., 2003) and may be formative of a larger haplotype featuring other UGT2B7 promoter polymorphisms (Hu et al., 2014a). This haplotype appears to result in a net reduction in promoter activity in HepG2 cells, and a reduction in protein expression in human liver microsomes (HLMs) from 12 patients (Hu et al., 2014a). However, individually, based on *in vitro* studies, it is unclear whether H268Y results in increased or decreased activity of UGT2B7 due to conflicting data (Parmar et al., 2011). The H268Y amino acid change did not alter substrate specificity *in vitro* (Jin et al., 1993b) and initial analysis from 28 human liver microsomes donors identified no significant alteration in glucuronidation rates for 3 different substrates (microsomal androsterone, menthol and morphine 3-position) (Bhasker et al., 2000). However, more recently, substrate-dependent altered glucuronidation capacity has been observed *in-vitro and in-vivo*. For

example, in HLMs obtained from 74 subjects, the 24% possessing the homozygous *UGT2B7* H268Y genotype, displayed a reduced level of 4-(methylnitrosamino)-1-(3-pyridyl)-1-butanol glucuronidation, compared to those with the wildtype (WT) *UGT2B7* (Wiener et al., 2004b). Similarly, HLMs carrying the *UGT2B7* H268Y SNP showed reduced activity towards the active metabolites of tamoxifen; 4-OH-TAM and endoxifen by around 2 and 5-fold respectively (Blevins-Primeau et al., 2009).

In contrast, studies of AZT, morphine, and codeine glucuronidation in HLMs identified no apparent differences between *UGT2B7* H268Y and WT HLMs (Court et al., 2003). The *UGT2B7* H268Y variant also showed similar catalytic efficiency to the WT form in the metabolism of mycophenolic acid to mycophenolic acid acyl glucuronide (Bernard et al., 2006). Notably, using a UGT2B7-transfected HEK-293 cell system where UGTs are not endogenously expressed, no significant difference in epirubicin glucuronidation activity was observed between cells that expressed the *UGT2B7* H268Y variant or the WT form (Innocenti et al., 2001). However, this result remains to be confirmed in a more native system such as HLMs.

Interestingly, while the *UGT2B7* H268Y SNP did not alter epirubicin glucuronidation in vitro, it has been linked to outcomes in patients co-treated with epirubicin and tamoxifen. Parmar et al. (2011) genotyped 205 breast cancer patients treated sequentially with epirubicin and tamoxifen and examined whether *UGT2B7*^{His268Tyr} patients have an altered survival outcome when compared to wild type *UGT2B7*^{268His} patients. They found that patients homozygous for the *UGT2B7* ^{268Tyr} allele showed better disease-free survival and reduced incidence of relapse when compared to those possessing at least one *UGT2B7* ^{268His} wildtype allele (i.e. heterozygous or homozygous wildtype). *UGT2B7* $^{268Tyr/Tyr}$ patients on average had a disease-free survival of 8.6 years, while *UGT2B7* $^{268His/His}$ or *UGT2B7* $^{268His/Tyr}$ had a disease-free survival of 7.5 years. Patel et al. (2021) also studied outcomes

for epirubicin-inclusive adjuvant therapy treated gastric cancer patients, however they were unable to find differences in neutropenia or leukopenia in patients who were homozygous for the *UGT2B7* ^{268Tyr} allele. Unlike previous pharmacogenetic studies in breast cancer, they also failed to observe statistically significant differences in overall survival or progression-free survival, relative to the WT genotype. The authors noted that the inconsistencies between these results are likely observed due to the heterogeneity of the different disease types and dosing regimens/treatment types.

Despite differing results between the studied cancers, one interpretation from the Parmar et al. (2011) study in breast cancer, is that the variant form of *UGT2B7* made by the *UGT2B7* ^{268Tyr} allele has a lowered glucuronidation ability of both epirubicin and tamoxifen, and therefore have reduced clearance, and hence greater anti-cancer efficacy. This effect may be substrate-specific, although as noted previously, appears to be applicable to the substrates epirubicin and tamoxifen (and tamoxifen metabolites) *in vitro.*

A newly studied intronic variant of *UGT2B7* designated rs7435335 resulting in the conversion of a G to an A nucleotide has been investigated for clinical prognostic value. It should be noted that this SNP is extremely infrequent on both alleles (homozygous A/A), however a fraction of breast cancer patients are heterozygous for the SNP (G/A). A study by He et al. (2018) showed that from 672 Han Chinese breast cancer patients, 0% are homozygous for the SNP, while 5.3% are heterozygous.

Mou et al. (2019) then compared the rs7435335 G/A genotype to the GG WT genotype (n=190) in ER+ (n=95) and ER- (n=85) breast cancer patients receiving EC-T chemotherapy (75 mg/m^2 of epirubicin, 800 mg of cyclophosphamide, and 75 mg/m^2 docetaxel) to examine associations between this genotype and EC-T efficacy. ER- rs7435335 G/A patients (n=15) had a significantly

higher frequency of achieving pathologic complete response (pCR) (pCR%=66.7% p=0.003). Similarly, ER- rs7435335 G/A patients were associated with significantly higher DFS rates, with the DFS rates being 93.3% and 55.7% (p=0.003) for those possessing the G/A SNP or WT G/G genotype respectively. The rs7435335 SNP also showed a statistically significant correlation between Miller-Payne grade in ER- patients, indicating that the SNP was more prevalent at later tumour stages in this subgroup. These correlations were only present when stratified by ER- subtype, and not as an overall population. While this SNP is associated with positive clinical outcomes and is of interesting prognostic value, it is unclear how it impacts epirubicin pharmacokinetics.

The promoter variant in position -79 relative to the hepatic start site (-125 relative to the translation start site) (RS7668282), is linked to the 268 SNP in the coding region and may form a haplotype. The -79 G>A SNP reportedly decreases transcriptional activity of the promoter by 2-7-fold *in-vitro* in hepatic and colonic cancer cell models (Duguay et al., 2004). In patients the haplotype is associated with lower serum morphine glucuronide concentrations in cancer patients receiving long-term morphine therapy (Duguay et al., 2004). This SNP was also associated with increased haematological toxicity in breast cancer patients receiving FEC (5-fluorouracil, epirubicin, and cyclophosphamide) (Vulsteke et al., 2013). SNPs located in the *UGT2B7* promoter at positions -268 and -102 (relative to the translation start site) in conjunction failed to significantly alter promoter activity in HepG2 (liver cancer) cells, thus has no effect on morphine glucuronidation in patient serum (Holthe et al., 2003).

Another common promoter variant is located at position -161 (rs7668258) relative to the *UGT2B7* translation start site. The -161C>T variant has shown enhanced metabolism of morphine in patient plasma, demonstrated by combined higher rates of morphine-6-glucuronide and morphine-3-glucuronide formation, with exceptionally high levels of glucuronide in the -161 T/T homozygous variant and the -161 C/T heterozygous variant, however most significant differences were observed

in the homozygous variant (Sawyer et al., 2003). Sawyer et al. (2016) examined the effects of this variant on epirubicin clearance in a group of non-metastatic breast cancer patients receiving FEC (5-fluorouracil 500 mg/m^2, epirubicin 100 mg/m^2, cyclophosphamide 500 mg/m^2). Increased epirubicin clearance was observed in patients with the -161 C/T and T/T genotypes relative to the CC genotype. Patients with the -161 C/T and T/T genotypes also had reduced risk of grade 3 and 4 leukopenia, however no differences in overall survival were observed between the groups. Another study by Li et al. (2019) reported reduced cardiotoxicity in the C/T and T/T groups and proposed that reduced toxicity was due to reduced epirubicin exposure. Another follow-up clinical trial was performed by Joy et al. (2021), however they were unable to reproduce the differences in epirubicin clearance rates in patients with these genotypes, although a trend of higher dose-normalized epirubicin plasma concentration in the -161 C/C group did suggest lesser metabolism in C/C patients. Confoundingly, they also reported higher epirubicin AUCs in the C/T and T/T groups respective to the WT C/C group. It is unclear why higher drug exposure would be present with enhanced epirubicin clearance, with the authors suggesting this study had a lesser focus on the pharmacokinetics of the drug and as such, discrepancies in trial conditions explain inconsistencies in PK results. Instead, their study aimed to implement safe epirubicin dose escalation to C/T and T/T genotype patients, as these groups were hypothesized to be receiving sub-optimal dosages. This was successfully accomplished, as they sequentially escalated dosages from first cycle 100 mg/m^2, to second cycle 120 mg/m^2, and third cycle 140 mg/m^2 doses in the T/T group, while the C/T group received an intermediate escalation between the C/C and T/T groups. Increased dosage was well tolerated and no increases in grade 3/4 leukopenia were present. This serves as an important example in tailored dosing based on *UGT2B7* genotyping, warranting further trial of implementing

this with other SNPs. All *UGT2B7* SNPs associated with differential clinical outcomes listed in this section have been summarised in Table 1.6.

The prior discussed data therefore provides *in-vitro* and *in-vivo* evidence suggesting that specific *UGT2B7* SNPs can alter responsiveness and differential treatment outcomes in epirubicin inclusive chemotherapy. This justifies further studies to investigate the prognostic value of *UGT2B7* genotyping in regard to epirubicin pharmacokinetics.

Table 1.6. Clinical parameters associated with differential outcomes linked to *UGT2B7* SNPs in epirubicin included therapies.

***UGT2B7* SNP genotype**	**Treatment/regimen**	**Clinical outcome observed in WT**	**SNP Associated clinical outcome**	**Reference**
UGT2B7 -161 T allele	Adjuvant breast cancer EC-D	7.8% cardiotoxicity in -161 C/C	– Cardiotoxicity reduced to 3.1% (-161 C/T) – Cardiotoxicity reduced to 1.1% (-161 T/T)	Li et al. (2019)
UGT2B7 -161 T allele	Neoadjuvant breast cancer $FE_{100}C$	1.18 ng/mL AUC in -161 C/C	– Increased AUC to 1.35 ng/mL (-161 C/T) – Increased AUC to 1.39 ng/mL (-161 T/T) – No increased leukopenia with tailored dose escalation in -161 C/T (130 mg/m^2) and T/T (140 mg/m^2) patients	Joy et al. (2021)
UGT2B7 -161 T allele	Neoadjuvant breast cancer $FE_{100}C$	103.3 L/hr CL, 76% leukopenia, 10-year RFS 72% in -161 C/C	– Increased CL (134.0L/hr) in -161 C/T and T/T – Reduced leukopenia to 50.0% in -161 C/T 48.7% in -161 T/T – No change in OS – Increased 10-year RFS to 83% in -161 C/T – Decreased 10-year RFS to 61% in -161 T/T	Sawyer et al. (2016)
UGT2B7 His268Tyr	Adjuvant breast cancer epirubicin	Relapse incidence 33.1% and DFS 7.5 years in 268His/His 268His/Tyr	– Relapse incidence reduced to 15.2% and DFS increased to 8.6 years in 268Tyr/Tyr – His268Tyr DFS HR 2.64 (over WT) (better DFS)	Parmar et al. (2011)
UGT2B7 His268Tyr	Adjuvant breast cancer epirubicin/tamoxifen		– His268Tyr DFS HR 5.22 (over WT) (better DFS)	Parmar et al. (2011)

UGT2B7 His268Tyr	Gastric/gastroesophageal cancer postoperative chemoradiation adjuvant 5-FU/leucovorin or epirubicin/cisplatin/5-FU	aOR neutropenia 1.01 and leukopenia aOR 1.14 (his/his)	– aOR neutropenia 0.98 (tyr/tyr) – aOR leukopenia 0.58 (tyr/tyr) (no significant change in aOR for either) – Survival HR p value 1.09 – Progression free HR p value 1.04 (no association with HIS268TYR and survival)	Patel et al. (2021)
UGT2B7 rs7435335	Neoadjuvant breast cancer EC-D	27.1% ER- achieved pCR and 55.7% 3-year DFS rate in GG	– Increased pCR to 66.7% in GA ER- – No significant difference in pCR in ER+ – Increased 44 month DFS rate to 93.3% in GA ER-	Mou et al. (2019)
UGT2B7 rs7668282 (-79)	Neoadjuvant breast cancer FEC	1.01 ratio of febrile neutropenia/without febrile neutropenia	– 0.35 ratio of febrile neutropenia/without febrile neutropenia (lesser ratio of patients with neutropenia compared to WT at primary endpoint p=0.0247)	Vulsteke et al. (2013)

1.9. Targeting Drug Metabolising Enzymes and Efflux Pathways to Overcome Drug Resistance

Multidrug resistance (MDR) remains a significant hurdle in combinatorial cancer therapies, as over 90% of cancer mortality can be attributed to the aforementioned cause (Bukowski et al., 2020). In short, the main factors that cause MDR can be enhanced drug metabolised (by DME), elevated drug efflux (by drug transporters), altered cell cycling to avoid DNA damage and differential cellular growth (by growth signalling), genetic changes (SNPs and gene amplification), and epigenetic effects on gene regulation (Bukowski et al., 2020). The various specific mechanisms will be further explored in this section.

Resistance to cytotoxic drugs such as anthracyclines can occur by many mechanisms, among which are altered uptake or efflux of the drug from cancer cells. ATP-binding cassette (ABC) transporters are known to be involved in multidrug resistance and have been shown to be overexpressed in lung cancer cells, thus increasing drug efflux from the cells and negating the impact of chemotherapy (Cole et al., 1992) (Sun et al., 2012). Kamiyama et al. (2006) found this true in a hepatocellular carcinoma context and observed epirubicin resistance that appeared to be due to ABC transporter upregulation. This has then been suggested to be the case in breast cancer cells (Modi et al., 2022). Such studies suggest that inhibition of efflux transporters may provide a useful avenue for new drug development. Conceptually, such drugs used in combination with cytotoxic drugs that are effluxed by these specific transporters should allow higher levels of the drug to be maintained in the cells and thus be more effective. However, to date there has been little success with this approach in clinical trials (Jaramillo et al., 2018). This could be related to a number of issues, including toxicity

of ABC modulators, which can prevent effective doses being used (Sun et al., 2012), and also overlap and redundancy in ABC transporter activities.

The other superfamily of transporters known as solute carrier (SLC) transporters have also shown evidence of overexpression in cancer cells as they are required for nutrient acquisition in tumours along with absorption, distribution and elimination of drugs (Lin et al., 2015). This makes them another target for overcoming multidrug resistance, but they face similar potential considerations as ABC transporters in terms of whether their inhibition can be achieved without toxicity (Kerhoas et al., 2024).

Aside from altered transport (uptake and efflux), cytotoxic drug efficacy can be affected by biotransformation reactions carried out by drug metabolism enzymes, including Phase I Cytochrome P450 (CYP) enzymes which are involved in oxidative metabolism of drugs, and the Phase II UGT enzymes which were already discussed in detail above. Altered expression levels and functions of CYP enzymes have been shown to affect drug response across a wide range of different classes of drugs (Ahmed et al., 2016). Early work in support of this role involved pharmacogenomic studies showing that single nucleotide polymorphisms (SNPs) of CYP enzymes cause altered pharmacokinetics (drug metabolism and clearance), although it should be noted that the effect sizes associated with SNPs in *CYPs* and *UGTs* are often quite small.

Overexpression of CYP families including 1A, 1B, 2C, 2D, and 3A have been observed in a wide variety of cancers including breast, prostate and liver (Patterson & Murray, 2002). The function of these CYPs in chemotherapy drugs are again for conversion of the active molecules into (generally) inactive metabolites that are no longer cytotoxic (or are less toxic) as shown in Figure 1.2. To date, there have been limited preclinical and clinical studies of CYP inhibition to improve the efficacy of

cytotoxic drugs (Kruijtzer et al., 2002). As examples, CYP3A4 inhibition was shown to increase serum levels of irinotecan and docetaxel due to reduced biotransformation and clearance in the liver in small proof of concept trials (Kehrer et al., 2002) (Bardelmeijer et al., 2002). However, such approaches have not advanced to clinical practice, either because effect sizes are small, and/or because reducing systemic clearance also increases systemic toxicity. In addition, the expression and genetic variation of these targets in liver can be highly variable in patients and patient selection may also have been involved in the poor outcomes of some of these trials (Kruijtzer et al., 2002).

Overall, while these targets appear promising for overcoming multidrug resistance in cancer and studying potential drug-drug interactions (DDIs), they have either not yet been tested extensively in a clinical setting or have not been proven particularly effective in terms of clinical response. Moreover, in contrast to CYPs and drug transporters, there have been no trials testing whether inhibition of UGT or other Phase II metabolic enzymes can increase the bioavailability, or improve the response to, cytotoxic cancer drugs. Indeed, preclinical proof of principle studies are still lacking in this area.

1.10. UGT2B7 is Primarily Expressed in the Liver and Highly Inducible in Hepatocellular Carcinoma and Melanoma Contexts

As previously mentioned, UGTs are expressed in most tissue types, however in accordance with their role in drug metabolism, they are most abundantly expressed in metabolic tissue types including the kidney, gastrointestinal system and most importantly the liver (Allain et al., 2020). Tissue specific expression for each isoform has been depicted in Table 1.3. While it is consistently highly expressed in the liver, UGT2B7 mRNA levels can be highly variable. For example there has been reported instances of 7-fold variability in expression in hepatic liver biopsies from healthy and

diseased (liver fibrosis) patients (Congiu et al., 2002). Furthermore, up to 14-fold variability in UGT2B7 activity (morphine-3-glucuronide formation) has been reported in human liver microsomes (Fisher et al., 2000). While these apparent differences in UGT2B7 expression may be due to inherent physiological variables, it is possible variance may be transiently altered by circulating drug in the system. In specific instances, whereby a substrate is capable of inducing its own metabolising enzyme, repeated dosage of the drug can gradually reduce steady-state drug levels, therefore reducing the effectiveness of the drug. The process of drug induction causing self-metabolism of its own substrate is commonly referred to as autoinduction, and has been reported for chemotherapies used in breast cancer such as cyclophosphamide with CYP enzymes (Hassan et al., 1999). Autoinduction has also been reported in clinically used UGT substrates (Mhaimeed et al., 2022), thus representing a clinical challenge.

Early preliminary unpublished studies from Flinders University Pharmacology laboratories shows UGT2B7 mRNA expression can be induced in HepG2 (liver cancer) cells by various cytotoxic drugs including epirubicin (Figure 1.5A). Further data has built on this and shown that although UGT2B7 expression is lower in breast cancer cell lines than in liver cells (e.g. HepG2), it is still substantially induced (>10-fold) following epirubicin treatment (Figure 1.5B). In both MDA-MB-231 and HepG2 cells, multiple cytotoxic drugs induced UGT2B7 expression, however epirubicin produced the largest fold induction. It is notable that the absolute copy numbers of UGT2B7 mRNA are much higher (at least 500-fold) in HepG2 cells than in MDA-MB-231. In the Caco-2 (colon cancer) cell line, there was no induction of UGT2B7 by any of the drugs (Figure 1.5C). This is potentially, partially due to the fact that Caco-2 cells have a mutated non-functional *p53* gene (which will be described further in the following section), although there are other not-yet characterised pathways capable of inducing UGT2B7 (to be described in Chapter 3), which may be also impaired in Caco-2 cells.

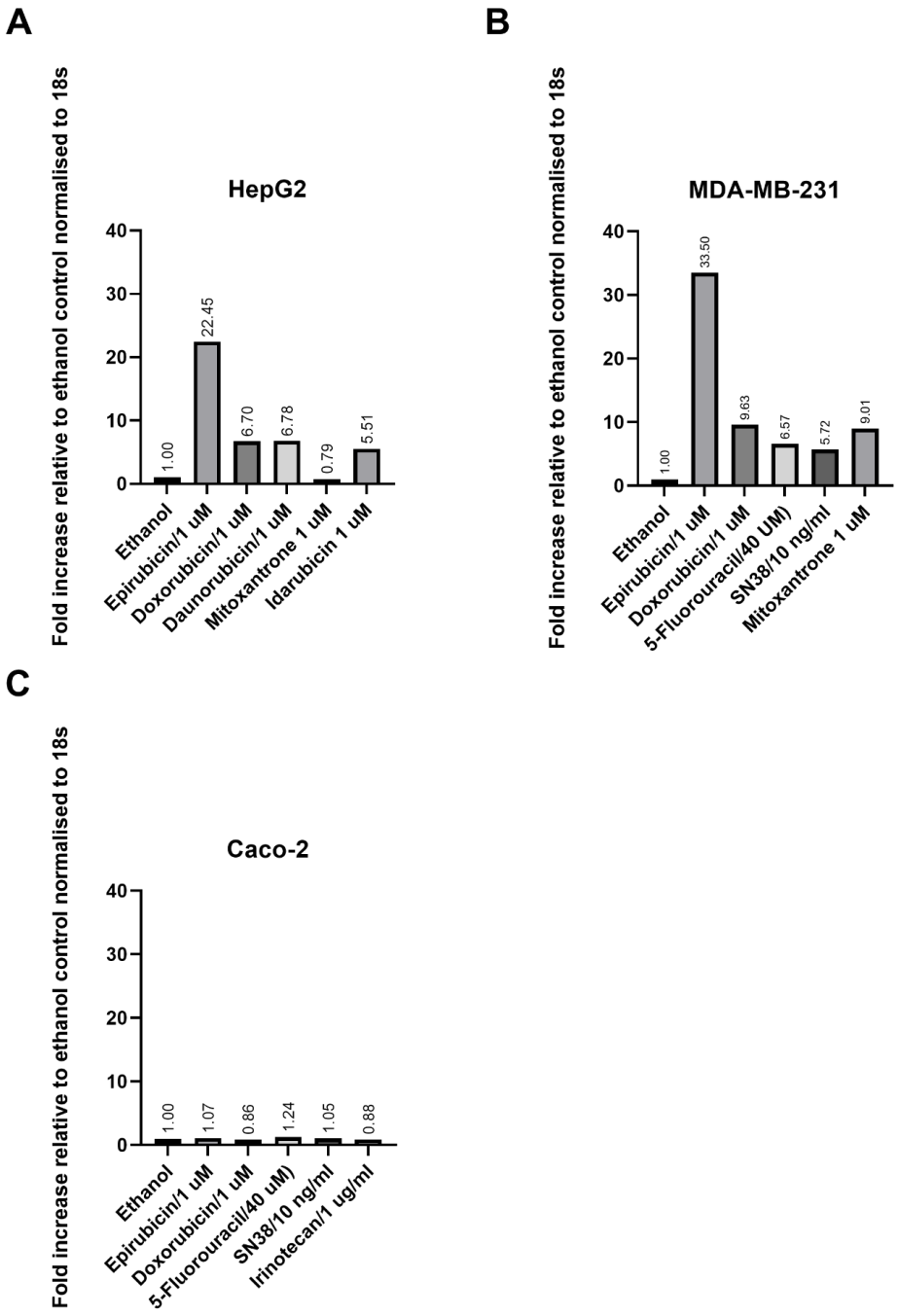

Figure 1.5. Preliminary data of drug induction of UGT2B7 in various cancer cell lines. UGT2B7 mRNA expression was measured by qRT-PCR and normalized to housekeeping gene 18s and shown as fold relative to the vehicle control (ethanol). Experiments were performed by Dong Gui Hu, Clinical Pharmacology, Flinders University. **(A)** In HepG2 liver cancer cells, UGT2B7 is induced by all the drugs (except mitoxantrone) but most potently by epirubicin. **(B)** In MDA-MB-231 breast cancer cells, UGT2B7 is induced by all the drugs but most potently by epirubicin. **(C)** In Caco-2 colon cancer cells, all drugs failed to induce UGT2B7.

In support of these data, a study published by Dellinger et al. (2012) investigated the induction of UGT enzymes by various anti-cancer drugs in SKmel28 (melanoma) cells. From this, they saw epirubicin-mediated induction of UGT2B7, UGT2B10 and UGT2B15 mRNA after 24 hours. To investigate the functional consequences modulating UGT2B7 expression, the authors knocked down UGT2B7 using shRNA in WM115 (primary melanoma) cells. Upon knock-down, the WM115 cells were significantly more sensitive to epirubicin and doxorubicin therapies. When drug sensitivity of WM115 and WM3211 cells were compared (the latter of which naturally do not have detectable expression of UGT2B7), the WM3211 cells showed far greater sensitivity to both doxorubicin and epirubicin. This study combined with previous data therefore prompts interest into investigating similar effects in other forms of tissue, which may be of particular clinical relevance.

The aforementioned data showing induction of UGT2B7 by epirubicin and other anti-cancer drugs, prompted a hypothesis formulated to address the plausibility of autoinduction altering epirubicin circulating plasma level. The proposed hypothesis may be occurring in a one-compartmental model with epirubicin (EPI) inducing UGT2B7 and enhancing epirubicin metabolism. This direct feedback loop in a one-compartmental model can be visualised in Figure 1.6, however it is possible this effect is not only unique to epirubicin and UGT2B7, but also other exogenous drugs. The autoinduction turnover model proposed below describes how the amount of drug input (ln(t)) into the system (EPI) relates to the degradation rate of UGT2B7 ($K_{enz,in}$=$K_{enz,out}$) (i.e. EPI inhibits UGT2B7 degradation, thus increasing UGT2B7 concentration), while the amount of UGT2B7 affects apparent EPI clearance (Cl_{app}), therefore reflecting epirubicin plasma concentration ($C_{p,EPI}$) (i.e. increased UGT2B7 levels promotes EPI clearance, thus lowering the plasma concentration of EPI).

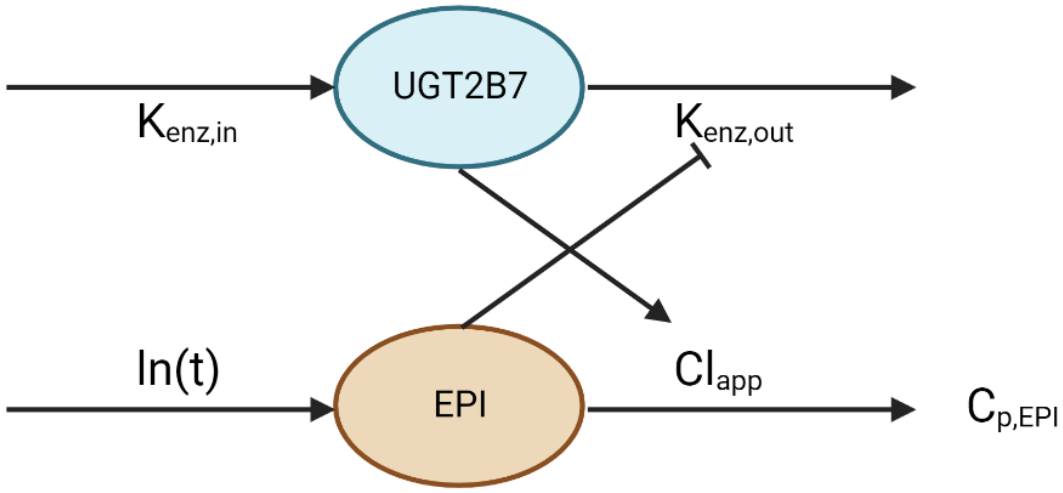

Figure 1.6. Schematic pharmacokinetic diagram of the one-compartmental epirubicin autoinduction model. Enzyme production is stimulated by the substrate thus increasing epirubicin (EPI) inactivation and clearance. The amount of drug (EPI) relates to the rate of enzyme (UGT2B7) degradation ($K_{enz,in}$=$K_{enz,out}$), while the drug input into the system (In(t)) is affected by the enzyme changing the apparent clearance (Cl_{app}) and therefore plasma concentration of drug ($C_{p,EPI}$).

Furthermore, if this induction effect can be substantiated, another key question that needs to be addressed, is the primary mechanism of induction, and whether this underlying mechanism may be a commonality with other anti-cancer drugs.

1.11. Project Outline and Rationale

When taken together with the literature which shows UGT2B7 is a key detoxifier of epirubicin by glucuronidation, it can be hypothesized that the induction of UGT2B7 expression driven by epirubicin, could promote epirubicin clearance and hence cellular survival.

Prior literature and preliminary studies have demonstrated the capacity of epirubicin to induce UGTs, more specifically UGT2B7, in a variety of cancers including, melanoma (Skmel28), liver (HepG2) and preliminarily, in breast cancer (MDA-MB-231). To build upon these findings, this thesis aims to establish a greater understanding of why this occurs in breast cancer and how this suggests

a novel role for UGT2B7 in cytotoxic drug resistance. Cytotoxic drug resistance occurring with epirubicin has larger clinical implications due to it being commonly used in chemotherapeutic regimes for both early and late-stage breast cancer.

As a prior study published from this laboratory (Hu et al., 2014c), identified the p53 pathway as a mechanism of UGT2B7 induction in the liver, validation of this phenomenon occurring within breast tissue will be studied, and whether it is possible to induce UGT2B7 by alternative mechanisms. The tumour suppressor p53 protein, is a hallmark in the prevention of carcinogenesis, as it is typically acts as a checkpoint for cancer, either by aiding in DNA repair or inducing apoptosis (Marei et al., 2021) (to be described in more detail in Chapter 3). Understanding its role in the induction of UGT2B7 could further delineate the multiple roles of UGTs in cancer.

The present study sought to further investigate this in a breast cancer context using cell lines with varying p53 genotype. As such, two model lines were selected to investigate this mechanism of induction; ZR-75-1 cells containing a wildtype fully functional p53, along with MDA-MB-231 cells which possess a R280K missense mutation that affects a core DNA binding domain, thus ablating transcriptional activity resulting in loss of function (Gomes et al., 2018). This could provide further evidence of an alternative mechanism of induction, while validating a similar p53 mechanism of induction in a different tissue context.

As it is anticipated that UGT2B7 may also be highly inducible in breast cancer, the importance of UGT2B7 expression on maintaining a drug-resistant population shall therefore be investigated. To perturb the effect of ectopic UGT2B7 expression stable overexpression cell lines will be created, as well as stable knockout (CRISPR)/knockdown (CRISPRi), transient knockdown of UGT2B7 (siRNA), or interaction-based inhibition of UGT2B7 using chimeric forms of other UGTs. Upon validating and

achieving the desired manipulation of UGT2B7, the functional implications of this will be challenged by exposing a population of breast cancer cells (MDA-MB-231 and ZR-75-1) to clinically relevant drug dosages to evaluate the effects on intratumoural drug resistance/sensitivity.

As chemotherapeutic regimens typically involve combination of different therapy types (i.e. broad targeting cytotoxic therapy together with specific molecular marker targeted therapy), a goal on this study is to determine whether there is any synergistic effect from a UGT2B7 drug induction response on the metabolism of other substrates. To do this, targeted therapies inclusive of tyrosine kinase inhibitors (TKIs) and hormone therapies (tamoxifen) will be tested for interactions with UGT2B7, and if so, whether this enhances/supresses epirubicin metabolism. It is of common clinical practice to include targeted therapies alongside cytotoxics, taking into account the molecular subtyping. By further understanding these interactions, it may aid in guiding beneficial drug combinations.

Since UGTs share very similar sequence homology, it makes it quite difficult to measure specific protein responses attributed to one UGT isoform. Therefore, the development of a UGT2B7-specific peptide assay will enable the accurate quantification of incremental protein level changes in response to UGT2B7 inhibitors/activators, while concurrently this project aims to develop an epirubicin glucuronidation assay, which will specifically measure epirubicin glucuronide formation with the purpose of determining the enzyme kinetics necessary to simulate how epirubicin treatment affects subsequent drug metabolism (i.e. DDIs). The potential applications upon obtaining specific and sensitive UGT2B7 peptide and glucuronidation assays may allow for clinical biomarker detection in predicting optimal patient therapies. Upon utilising these assays to obtain relevant UGT2B7 enzyme kinetics and interactions, a physiochemically based epirubicin pharmacokinetic model will be developed to gain insight into factors relating to drug exposure systemically. Obtaining pharmacokinetic (PK) and pharmacodynamic (PD) information could allow

for model informed prediction of optimised therapeutic windows for epirubicin. The following aims have therefore been proposed, underpinning the plan to investigate the aforementioned experimental goals.

1.11.1. Project aims

Aim 1. To investigate the mechanism of induction of UGT2B7 in several breast cancer contexts.

Aim 2. To evaluate the role of UGT2B7 in drug resistance by examining the functional implications of modulating expression.

Aim 3. To determine whether tyrosine kinase inhibitors (TKIs) or tamoxifen targeted therapies have any effect on UGT2B7 expression and activity and whether the resulting effects are agonistic or antagonistic drug-drug interactions (DDIs).

Aim 4. To develop a physiologically based pharmacokinetic (PK) epirubicin model to identify factors and biomarkers affecting epirubicin variability in exposure and tissue distribution.

CHAPTER 2. MATERIALS AND METHODS

2.1. Experimental Materials

2.1.1. Cell lines

MDA-MB-231 (ATCC® HTB-26™), ZR-75-1 (ATCC® CRL-3438™), MDA-MB-453 (ATCC® HTB-131™), MCF-7 (ATCC® HTB-22™), and HepG2 (ATCC® HB-8065™) cell lines were obtained from The American Type Culture Collection (ATCC) (Manassas, VA). The MFM-223 (ECACC 98050130) cell line was obtained from the European Collection of Authenticated Cell Cultures (ECACC). Metastatic pleural effusion

primary cells (MPE-BC-001) are derived from a malignant pleural effusion from a patient with metastatic triple negative breast cancer. Collected cells were cultured from pleural effusions which were obtained from our collaborators, Professor Sonja Klebe and Dr Ash Hocking (College of Medicine and Public Health, Flinders University) under Southern Adelaide Clinical Human Research Ethics Committee (SAC HREC) (approval number 381.09) and Central Adelaide Local Health Network Human Research Ethics Committee (CALHN HREC) (approval number 14283) approved usage.

Development of breast cancer stable and transient cell line models, mechanistic studies, along with drug toxicity assays, were done primarily using a human epithelial cell line representative of a triple-negative basal B subtype, MDA-MB-231 (ER-/PR-/HER2-) and the human epithelial-like cell line representative of a luminal A subtype, ZR-75-1 (ER+/PR+/-/HER2-), which are both originally derived from breast tissue from the mammary gland of patients with adenocarcinoma and invasive ductal carcinoma respectively. In addition, drug screening experiments were performed in breast cancer cell lines MFM-223 (ER-/PR-/HER2-), MDA-MB-453 (ER-/PR-/HER2-) and MCF-7 (ER+/PR+/HER2-). Any liver representative studies were performed using the hepatocellular carcinoma, epithelial-like HepG2 cell line. Subtyping was classified based on Dai et al. (2017).

2.1.2. Mammalian reporter and expression vectors

The luciferase reporter vectors pGL3-Basic and pRL-null were originally purchased from Promega (Madison, WI). The wildtype and mutated *UGT2B7* promoter regions were previously cloned into pGL3-Basic in the laboratory and were available for use (Hu et al., 2014c). Specific expression vectors used throughout this study are described within the relevant chapters.

2.1.3. Oligonucleotides

DNA oligonucleotides were purchased from Merck Australia (Darmstadt, Germany) or Macrogen (Seoul, South Korea), and were of standard purification quality. Purification typically involved desalting using normal phase chromatography. Sequences of oligonucleotide are listed within the relevant chapters.

2.1.4. Antibodies

The anti- UGT2B7 antibody was developed in our laboratory as previously reported (Hu et al., 2014c). The horseradish peroxidase (HRP)–conjugated goat anti-rabbit secondary antibody (cat no. 31460) and the mouse beta-actin primary monoclonal antibody (BA3R) (MA5-15739) were purchased from Invitrogen. The donkey anti-mouse secondary HRP antibody was purchased from Jackson ImmunoResearch (Cat no. JI-715-035-150).

2.1.5. Chemicals and Reagents

Table 2.1. General chemicals, reagents and kits used in these studies.

Chemical/Reagent (Catalogue number)	Manufacturer
Chemicals	
Ethanol Undenatured 100% AR Packed in HDPE drum (EA043-10L-P)	Chemsupply
Isopropanol (PA013-2.5L-J)	Chemsupply
Methanol (MA004-2.5L-J)	Chemsupply
Thiazolyl Blue Tetrazolium Bromide (MTT) (M2128-500mg)	Merck
Epirubicin Hydrochloride (LKT-E6235-M005)	Sapphire Bioscience
4-Methylumbelliferyl-β-D-glucuronide hydrate (M9130)	Merck
Mammalian Cell Culture	

Dulbecco's Modified Eagle Medium powder (DMEM), high glucose, pyruvate (12800082)	Gibco
RPMI-1640 medium powder (31800089)	Gibco
Foetal bovine serum (FBS) (26140087)	Gibco
Phosphate-buffered saline (PBS) pH 7.4 (10010023)	Gibco
Sodium pyruvate 100mM (11360070)	Gibco
MEM Non-essential amino acid 100x (11140076)	Gibco
Pen Strep 10,000 units/mL (15140122)	Gibco
Trypsin-EDTA (0.5%), no phenol red (15400054)	Gibco
Kanamycin Sulfate (11815024)	Gibco
Ampicillin sodium salt (11593027)	Gibco
Transfection	
Lipofectamine LTX™ Reagent with PLUS (15338100)	ThermoFisher Scientific
Lipofectamine™ 2000 Transfection Reagent (11668030)	ThermoFisher Scientific
Puromycin Dihydrochloride (A1113803)	ThermoFisher Scientific
RNA/DNA Extraction and cDNA Synthesis	
TRIzol™ Reagent (15596026)	Invitrogen
DNAse I enzyme (M0303S)	New England Biolabs
10x DNAse Buffer (B0303S)	New England Biolabs
EDTA 25mM (18068015)	Invitrogen
dNTPs (18427013)	Invitrogen
Random hexamers (N8080127)	Invitrogen
10x Reverse Transcriptase Buffer (30222-2)	Lucigen
NxGen® M-MulV Reverse Transcriptase (30222-2)	Lucigen
RNAse Inhibitor (30281-2)	Lucigen
Glycogen, molecular biology grade (R0561)	Thermofisher Scientific

PCR and Sequencing	
2X GoTaq® Master Mix (A6002)	Promega
Phire Hot Start II DNA Polymerase (F122L)	Thermofisher Scientific
Phire Reaction Buffer (F524L)	Thermofisher Scientific
Phusion™ High-Fidelity DNA Polymerase (F530S)	Thermofisher Scientific
Phusion HF Buffer Pack (F518L)	Thermofisher Scientific
MgCl2 (magnesium chloride) (25 mM) (R0971)	Thermofisher Scientific
QIAquick® PCR Purification Kit (28106)	Qiagen
BigDye™ Terminator v3.1 Cycle Sequencing Kit (4337455)	Applied Biosystems
Agarose Gel Electrophoresis	
100 bp DNA Ladder (with gel loading dye) (N3231S)	New England Biolabs
1 kb DNA Ladder (N3232S)	New England Biolabs
SYBR™ Safe DNA Gel Stain (S33102)	New England Biolabs
Agarose MB (BIOD0012-250G)	Astral Scientific
Luciferase	
Dual-Luciferase® Reporter Assay System (E1960)	Promega
Transformation and Cloning	
LB Medium, Lennox, Powdered (113002132)	MP Biomedicals
Agar, Bacteriological (J637-500G)	Amresco Inc
T4 DNA Ligase Reaction Buffer (B0202S)	New England Biolabs
T4 DNA Ligase (M0202S)	New England Biolabs
Plasmid preparations	
QIAquick Gel Extraction Kit (28706)	Qiagen
QIAprep Spin Miniprep Kit (27106)	Qiagen
QIAGEN Plasmid Midi Kit (12143)	Qiagen
Commercial Antibodies	

Donkey anti-Mouse (H+L) Secondary Antibody, HRP (JI-715-035-150)	Jackson Immuno Research
Goat anti-Rabbit IgG (H+L) Secondary Antibody, HRP (31460)	Invitrogen
Mouse beta-Actin Loading Control Monoclonal Antibody (BA3R) (MA5-15739)	Invitrogen
Western Blotting	
Bio-Rad Protein Assay Dye Reagent Concentrate, 450 ml (#5000006)	Bio-Rad
cOmplete™ Protease Inhibitor Cocktail (11697498001)	Merck
N,N,N',N'-Tetramethyl ethylenediamine (Temed) (MFCD00008335)	Merck
40% Acrylamide/Bis Solution (#1610149)	Bio-Rad
Nitrocellulose membrane 0.45um (1620115)	Bio-Rad
Precision Plus Protein™ WesternC™ Blotting Standards (1610376)	Bio-Rad
SuperSignal™ West Pico Chemiluminescent Substrate (10481755)	ThermoFisher Scientific

2.1.6. General Buffers

1 x Phosphate buffered saline (PBS) (pH 7.4): 137 mM NaCl, 2.7 mM KCl, 10 mM Na_2HPO_4, 2 mM KH_2PO_4

1 x TNES buffer: 50 mM Tris pH 8.8, 400 mM NaCl, 100 mM EDTA, 0.6% SDS

1 x TE buffer (pH 8.0): 1 mM EDTA, 10 mM Tris-Cl

1 x SDS-PAGE transfer buffer: 25 mM Tris (pH 8.3), 192 mM glycine, 20% methanol

1 x Running buffer: 25 mM Tris (pH 8.3), 192 mM Glycine, 0.1% SDS

1 x Tris buffered saline (TBS): 50 mM Tris (pH 7.4), 150 mM NaCl

TBST (+ Tween 20): 0.2% Tween 20 in 1 x TBS

Blotto: 3% or 1% skim milk powder added to TBST

CCMB80 buffer (pH 6.4): 10 mM KOAc, 80 mM $CaCl_2$, 20 mM $MnCl_2$, 10 mM $MgCl_2$, 10% glycerol

RIPA buffer (pH 7.4): 50 mM Tris-HCl (pH 8.0), 1% Igepal CA-630, 150 mM sodium chloride, 0.5% sodium deoxycholate, 0.1% sodium dodecyl sulphate, 1 x protease inhibitor cocktail (Merck)

1 x Tris-acetate EDTA electrophoresis buffer (TAE): 40 mM Tris (pH 8), 20 mM acetic acid, 1 mM EDTA

2.2. Methods

2.2.1. Maintenance of mammalian cell lines

All cell lines were maintained at 37°C in a 5% CO_2 atmosphere. Regular maintenance was undertaken in a sterile environment using a Labconco Biosafety cabinet (Kansas City, Missouri). MDA-MB-231 and HepG2 cells were cultured in Dulbecco's Modified Eagle Medium (DMEM) (high glucose, pyruvate, L-glutamine) (Life Technologies, Carlsbad, California) supplemented with 3.7 g/L sodium bicarbonate, and 10% foetal bovine serum (FBS). MDA-MB-453, ZR-75-1 and MCF-7 cells were cultured in RPMI 1640 medium (with L-glutamine) (Life Technologies, Carlsbad, California) supplemented with 2.0 g/L sodium bicarbonate, and 10% FBS. MPE-BC-001 primary cells grow semi-adherent and cultured in complete RPMI 1640 formulation as above, and 2% pleural effusion supernatant. MFM-223 cells were cultured in Minimal Essential Medium (MEM) (Life Technologies, Carlsbad, California) supplemented with 2 mM glutamine and 10% (FBS). Sub-culturing of cells was routinely performed upon reaching 80-90% confluence. To passage cells, medium was aspirated, and cells were washed with 1 x PBS. Cells were then released from the culture flask by the addition of 0.05% trypsin/0.53 mM EDTA in PBS and incubation at 37°C. Cell density was determined by mixing 10 µL cell suspension with an equal volume of 0.2% trypan blue to count the number of viable

cells. 10 µL was loaded onto a haemocytometer (Hausser Scientific, Horsham, Pennsylvania) and viable cell concentration (cells/mL) was used to calculate the required volume required for carryover of cells. Cells were diluted and resuspended in appropriate fresh medium for continued maintenance. Cell counting and visualization of cells was done using a CKX53 Microscope (Olympus).

2.2.2. Preparation and thawing of cell line frozen stocks

For long term storage, a remaining volume of cell suspension was pelleted by centrifugation at 2,000 rpm for 5 minutes, then the remaining pellet was resuspended in 0.5-1 mL FBS containing 10% DMSO (Merck Australia Darmstadt, Germany). This volume was transferred into Nunc CryoTubes (Merck Australia Darmstadt, Germany) for storage at -80°C. Shortly after, cryopreserved cell lines were transferred on dry ice to liquid nitrogen.

On retrieval of cryopreserved stocks, cells were rapidly thawed in a 37°C water bath then added to the appropriate volume of medium in a flask. The following day, the medium was replaced to remove residual DMSO.

2.2.3. siRNA transfections

For transfections of siRNA, 250 µL of serum-free RPMI was prepared in a microcentrifuge tube with 100 pmol of appropriate siRNA or negative control diluted into the medium. In a second tube, 250 µL of serum-free RPMI was combined with 10 µL of Lipofectamine 2000 (1 µL/10 pmol siRNA). Both tubes were pre-incubated for 5 minutes before combining and incubating at room temperature for 30 minutes to allow formation of oligo-Lipofectamine complexes. Cells were seeded at 6.25×10^5 cells/well in 6-well plates concurrently while lipofectamine complexes were formed. The remaining 500 µL volume was transferred into the 1.5 mL cell suspension in a 6-well plate, to make a total well volume of 2 mL. The culture medium was replenished after 24 hours.

2.2.4. Transfections for stable expression

Lipofectamine LTX (Invitrogen) transfection was used to generate stable cell lines. For 6-well plates, 500 µL of serum free RPMI/DMEM was prepared in a microcentrifuge tube. To this tube, 2.5 µg of plasmid DNA was added, along with 2.5 µL of PLUS reagent. Samples were vortex mixed and incubated at room temperature for 15 minutes. Following that, 7.5 µL of Lipofectamine LTX was added to the tube and incubated at room temperature for a further 30 minutes to allow the formation of DNA-Lipofectamine complexes. Meanwhile, cells were seeded at $6.25x10^5$ cells/well in 1.5 mL medium. Upon completion of the incubation period, the 500 µL mixture was transferred into the respective well to make up a total volume of 2 mL. Twenty-four hours post transfection, the medium was changed to reduce lipofectamine toxicity. Four days after transfection, the cells were given incremental treatments of puromycin (Thermofisher Scientific) (0.2 µg/mL to 0.5 µg/mL), and then maintained at the maximum dose to ensure consistent expression. If fluorescent markers were present, they were visualised using an EVOS M5000 fluorescence microscope (ThermoFisher Scientific)

2.2.5. Extraction of total RNA

Cell lines were harvested for total RNA post treatment or transfections. To extract total RNA, cells grown in monolayer in 6-well plates were washed with PBS and harvested in 1 mL TRIzol reagent (Thermofisher Scientific) to lyse the cells as per the manufacturer's protocol. The TRIzol containing lysed cells was transferred to a microcentrifuge tube and 200 uL chloroform/1mL TRIzol was added and vortexed for 15 seconds (or until cloudy). This was incubated at room temperature for 2-3 minutes to assist in phase separation. The samples were then centrifuged at 11,500 rpm for 15 minutes at 4°C and the top layer containing the aqueous phase was transferred into a fresh tube.

To precipitate the RNA, 500 µL isopropanol/1 mL TRIzol was added to the tube and vortexed vigorously then left at room temperature for 10 minutes. If low amounts of RNA were expected, 5 µg of glycogen (Thermofisher Scientific) was added to act as a carrier to assist in binding to and visualising the RNA. This was then centrifuged at 11,500 rpm for 10 minutes at 4°C. Following centrifugation, the supernatant was removed, the RNA pellet was washed by the addition of 1 mL 75 % ethanol and samples were centrifuged at 7500 g for 5 minutes at 4°C. The RNA pellet was air-dried at room temperature for 5-10 minutes (or until no remaining liquid was observed). The pellet was resuspended in 20-50 µL of nuclease free water (NFW) and heated to 60°C for 10 minutes to redissolve.

2.2.6. Generation of cDNA

cDNA was generated from RNA in a random hexamer-primed M-MuLV reverse transcriptase reaction using the Lucigen NxGen M-MuLV Reverse Transcriptase. Subsequent incubation steps were performed using a DNA Thermal Cycler 480 (Perkin Elmer, Shelton, Connecticut). One or two micrograms of RNA was initially added to a 20 µL reaction containing 2 uL 10 x DNAse buffer (NEB), 1 µL DNAseI (NEB), 0.5 µL RNAse inhibitor (Lucigen) with the remaining volume made up with NFW. This was incubated at 37°C for 10 minutes, and following that, inactivation was achieved by adding 2µL 25mM EDTA and incubating at 75^{o}C for 10 minutes. 10 µL of the DNAseI reaction was transferred to a 20 uL reaction containing 1 µL 10 mM dNTPs, 1 µL 50 µM random hexamers (Invitrogen), 1 µL RNase inhibitor (Lucigen) and nuclease-free water to 17 µL. The reaction mix was incubated at 65°C for 5 mins then stored on ice immediately. Two microlitres 10x M-MuLV Reverse Transcriptase buffer was added and samples incubated at 25°C for 2 mins. Finally, 1 µL NxGen M-MulV reverse transcriptase (Lucigen) was added to bring the final reaction volume up to 20 µL. Samples were incubated at 25°C for 10 mins, then 42°C for 60 mins, then inactivated by incubating

at 85°C for 10 mins. The cDNA product was diluted 5-fold by the addition of 80 µL nuclease-free water, then stored at -80°C or used immediately.

2.2.7. Polymerase Chain Reaction (PCR)

2.2.7.1. Equipment

Qualitative PCR reactions were performed on a Bio-Rad iCycler Thermal Cycler (Hercules, California). qRT-PCR runs were performed using the Rotor-Gene 3000 (Corbett Research, NSW). Subsequent analysis of .rex files were conducted using Rotor-Gene 6000 Series Software 1.7 (Corbett Research).

2.2.7.2. Phusion high-fidelity PCR for cloning DNA fragments

Phusion High-Fidelity DNA Polymerase (Thermofisher Scientific) was used for the cloning from genomic DNA or cDNA, and for sequencing to ensure correct base calling. PCRs with a 20 µL reaction volume were performed as per the manufacturer's specifications (Thermofisher Scientific) using <250 ng of DNA template. Primer Tm's were calculated using the New England BioLabs supplied Ta calculator for specific polymerase used. Thermal cycling conditions for Phusion High-Fidelity PCR consisted of the following steps as recommended by the manufacturer: initial denaturation at 98°C for 30 seconds then 35 cycles of; denaturation at 98°C for 10 seconds, annealing at primer Ta for 30 seconds, extension at 72°C for 30 seconds/Kb. Final extension was at 72°C for 10 minutes, then temperature was held indefinitely at 4°C until they were ready to be analysed.

2.2.7.3. Phire PCR screening of transformed colonies

A 20 µL reaction mix was prepared using Phire Hot Start II DNA Polymerase (ThermoFisher Scientific) as per manufacturers guidelines for each colony to screen for recombinant plasmids. 3 µL of boiled bacterial lysates was generally used as a template. Primer Tm's were calculated using the New

England BioLabs supplied Ta calculator for specific polymerase used. Thermal cycling conditions for Phire PCR consisted of the following steps as recommended by the manufacturer: initial denaturation at 98°C for 30 seconds then 35 cycles of; denaturation at 98°C for 5 seconds, annealing at primer Ta for 5 seconds, extension at 72°C for 15 seconds/Kb. Final extension was at 72°C for 60 seconds, before the reactions were held at 4°C until they were ready to be analysed.

2.2.7.4. Quantitative Real-Time PCR (qRT-PCR)

Real-time PCR was used to quantify levels of mRNA transcripts present in RNA extracted from cells. Primer sets used are detailed in the appropriate chapters. A 20 µL reaction was prepared containing: 1x GoTaq Mastermix (BRYT Green), 0.5 uM each primer, 6 µL nuclease-free water, and 2 µL of diluted cDNA template. The cycling conditions used were a heat activation period of 3 minutes at 95°C; 40 cycles of 95°C for 10 seconds, 60°C annealing for 15 seconds, and 72°C for 20 seconds; and a ramped melt analysis between 55 and 95°C with 4 second, 1°C steps. Data was acquired during the 72°C extension phase. Cycle-Threshold (CT) values were calculated using a 0.08 threshold value, set during the exponential amplification phase. For the interrogated the target genes, the corresponding CT values were normalised to the CT value of the housekeeping 18S ribosomal RNA, using the sequences published by Congiu et al. (2002).

2.2.7.5. PCR clean-up and sequencing

For isolation of specific PCR products from an agarose gel, QIAquick Gel Extraction Kit (Qiagen) was used as per manufacturer's instructions. For general clean-up of PCR products, the QIAquick PCR Purification Kit (Qiagen) was used according to the manufacturer's protocol.

Sequencing services were provided by SouthPath and Flinders Sequencing Facility (SA Pathology, South Australia) using 5 µM forward and/or reverse primers with 100 ng/µL of plasmid template or

10 ng/µL per 100 bp PCR template. Sequencing was performed using the ABI 3130xl Genetic Analyser Sequencer with the BigDye™ Terminator v3.1 Cycle Sequencing Kit (Applied Biosystems). Chromas 2.6.6 (Technelysium, QLD) was used to view chromatogram files of the individual sequences. Sequence trimming, reverse complementation and generation of a consensus sequence was performed using MEGA 11 (Tamura et al., 2021). Reference sequences for comparison were obtained from The National Center for Biotechnology Information (NCBI) and BLAST (Altschul et al., 1990) was used for sequence alignment (NCBI). Visualisation and genomic mapping were done using the UCSC Genome Browser (Kent et al., 2002) and BLAT (Kent, 2002).

2.2.8. Agarose gel electrophoresis

To analyse and visualise PCR products from restriction enzyme digests, plasmids, or PCR screening, agarose gel electrophoresis was used. 1-2% agarose (Astral Scientific) gels were made (depending on the size of the desired product) in TAE buffer containing 1:10,000 SYBR safe gel stain (Thermofisher Scientific) to image under UV light. DNA products were combined with purple gel loading dye (New England Biolabs) to load on the gel. 100 bp or 1 KB (New England Biolabs) DNA ladders (mixed with NEB purple gel loading dye) were ran alongside the samples to approximate the size of the DNA bands. Electrophoresis was performed using the Mini-Sub Cell GT Cell (Bio-Rad) gel electrophoresis tank with an applied current at 80-120 V. DNA gels were imaged using a GelDoc Go Gel Imaging System (Bio-Rad).

2.2.9. Genomic DNA extraction from cells

Cell pellets were collected and used for genomic DNA extraction. Depending on cell volume, 300-600 µL TNES with 350 µg proteinase K (per 600 µL TNES) was used to lyse cells and degrade nucleases and existing protein. Samples were incubated at 55°C for 1 hour. Following incubation, 300-600 µL

(equal volume to TNES) phenol:chloroform (1:1) was added to TNES lysate and vortexed vigorously. This was centrifuged at 11,500 rpm for 15 mins at 4°C. Approximately 500 µL of aqueous phase was transferred to a new tube carefully, avoiding contamination of other phases. Sodium acetate (0.1 vol 3M; 50 ul) was added, along with 1 µL 20 mg/ml glycogen (Thermofisher Scientific) (optional for low concentrations) and 0.6 vol isopropanol (300 µL), then mixed by inversion. Samples were centrifuged at 11,500 rpm for 10 mins at 4°C to pellet the genomic DNA. The supernatant was removed, and the pellet resuspended in 500 µL 80% ethanol and centrifuged at 11,500 rpm for 10 mins at 4°C. The supernatant was removed and the pellet air dried at room temperature for approximately 30 minutes, or at 55°C for approximately 5 minutes. The remaining pellet was resuspended with 20 µL NFW before use in downstream applications.

2.2.10. Quantification of DNA/RNA

A Nanodrop 2000 (Thermofisher Scientific) spectrophotometer was used to determine concentration and purity of DNA and RNA samples. One microlitre of sample was loaded into the spectrophotometer and absorbance was measured at a wavelength of 260 nm (OD_{260}). The DNA/RNA to protein ratio (purity) was measured at OD_{260} versus OD_{280}. An acceptable 260/280 ratio was approximately 1.8 and 2.0 for DNA and RNA respectively. Concentrations were calculated using a modified form of the Beer-Lambert equation to use units of ng-cm/µL. The equation stated by the manufacturer is as follows: $c = (A * \varepsilon)/b$, where c = the nucleic acid concentration in ng/microliter, A is absorbance in AU, ε = the wavelength-dependent extinction coefficient in ng-cm/microliter and b is the pathlength (0.1 cm). For nucleic acids, the extinction coefficients are 50 ng-cm/µL for dsDNA, 33 ng-cm/µL for ssDNA and 40 ng-cm/µL for RNA. Analysis of Nanodrop 2000 files was conducted using the NanoDrop 2000 software 1.6.198 (Thermofisher Scientific).

2.2.11. Quantification of proteins

To calculate total protein concentration in a sample, the Bio-Rad protein assay reagent was used in a microplate format, as per the instructions. Sample protein lysates were diluted 1:10 or as appropriate, and BSA standards were prepared for a range between 0.2 mg/mL to 1 mg/mL. Absorbance was measured at 595 nm using a SpectraMax iD5 Multi-Mode Microplate Reader (Molecular Devices). The BSA standard curve of known concentrations was plotted on an XY-scatter graph in Microsoft Excel, using the rearranged slope to estimate the protein concentration in samples. The result was multiplied to account for the dilution factor.

2.2.12. Luciferase reporter-based assays

Luciferase assays were used to evaluate promoter activity following treatment with epirubicin. These assays were performed using various promoters cloned into the pGL3 Basic Luciferase Reporter Vectors (Promega) using the Dual-Luciferase® Reporter Assay System (Promega). For further details on the promoter constructs, see the relevant chapters. Transfection of the luciferase promoter constructs were performed using Lipofectamine LTX (Invitrogen) as per the protocol specified in section 2.2.4. Transfections were performed in 48 well plates using 5 x 10^5 cells per well. Forty microlitres of serum free RPMI/DMEM (relevant to the growth medium used for the respective cell line) was combined with 0.2 µL PLUS reagent, 8 ng pRL-null (Renilla control) (Promega), 200 ng of reporter construct (empty pGL3 Basic was transfected alongside), and 0.8 µL of Lipofectamine. Twelve hours post transfection, the medium was changed with fresh growth medium. Forty-eight hours after transfection, cells were treated as needed in fresh growth medium. Following 72 hours of drug treatment, the medium was removed, the cells were washed with PBS and 50 µL of passive lysis buffer (Promega) was added to each well. The cell lysates were placed on an orbital shaker for

15 minutes, then stored at -20°C or assayed immediately. To assay for luciferase response, a 20 µL sample of lysate was transferred into a white 96 well plate and an initial luminescence reading was conducted to measure background on the lysates. To minimise carryover luminescence from neighbouring wells, cell lysates were only added to alternate wells of the plate. When ready to assay, 20 µL of Luciferase Assay Reagent II (LAR II) was added to the wells to measure the activity of firefly luciferase expressed from the transfected pGL3-derived vectors. Addition of 20 µL of Stop & Glo Reagent was then added to the same wells to quench the firefly luciferase activity and provide the substrate for the renilla luciferase, and luminescence was measured again. Results were then normalised to Renilla and the empty pGL3 Basic vector, to obtain relative luciferase activities for each sample. Luminescence was measured using the TopCount NXT Microplate Scintillation and Luminescence Counter (Perkin Elmer).

2.2.13. Restriction enzyme digestions

Restriction enzyme digests were performed in 20 µL reactions containing 1 µg DNA template, 1 µL restriction enzyme (New England BioLabs), 2 µL 10X compatible NEBuffer (New England BioLabs) and NFW. Typically, restriction enzyme digests were performed for 60 mins at 37°C, then inactivated by heat at 65°C for 20 minutes. Specific restriction enzymes and cloning sites used are discussed in the relevant chapters.

2.2.14. Ligations and Transformations

Ligations were performed using the NEB Ligation Kit. NEB guidelines were followed, with a recommended total DNA concentration of approximately 100 ng (insert + vector) and a 3-fold molar excess of insert DNA to vector DNA. A 10 µl reaction volume was used, consisting of vector and

insert DNA, 1 x T4 ligation buffer, 1 µl T4 DNA ligase and nuclease-free water. The reaction mix was incubated at room temperature for 2 hours or overnight at 16°C.

Transformations were performed using chemically competent DH5α *Escherichia coli* (*E. coli)* bacteria. Three microlitres of ligation product were incubated with 50 µL of DH5α competent cells on ice for 30 mins, then heat shocked at 42°C for 45 seconds to facilitate uptake of ligated DNA. Cells were then placed back on ice for 2 minutes. Five hundred microlitres of LB medium (antibiotic free) was added to the shocked cells and they were placed in a shaking incubator at 200 rpm for 30-45 minutes (30 minutes for ampicillin expressing vectors, and 45 minutes for kanamycin expressing vectors). Recovered cells (50 µl) were spread on LB agar plates containing ampicillin or kanamycin (100 µg/mL or 40 µg/mL respectively) and incubated overnight at 37°C. Selected colonies were transferred into 50 µL NFW and boiled at 99°C for 10 minutes, and then analysed for appropriate inserts by PCR.

2.2.15. Preparation of competent cells

Competent cells used in transformations were prepared using DH5α *Escherichia coli* (*E. coli)* from a frozen lab stock. An overnight culture of 1 ml DH5α was inoculated into 100 mL LB medium (not containing any antibiotic) and grown at 37°C in a shaking incubator, until reaching an OD_{600} of 0.25-0.3 (without exceeding 0.6). The culture was then centrifuged at 3,000 x g at 4°C for 10 minutes and supernatant removed. The resulting bacterial cell pellet was resuspended in 32 mL cold CCMB80 buffer, then centrifuged at 3,000 x g at 4°C for 10 minutes. Supernatant was again removed, and the cell pellet was resuspended in 4 mL CCMB80 buffer on ice. The 4 mL competent cells were aliquoted into 50 µL and stored at -80°C until use.

2.2.16. Plasmid preparations

Successful clonal colonies were upscaled by inoculating overnight culture in 1-4 mL LB medium (100 µg/mL ampicillin or 40 µg/mL kanamycin) (Gibco) (for small scale plasmid preparation) or in flasks for up to 100 mL LB (for large scale plasmid preparation). These were incubated in the shaking incubator at 37°C overnight. For plasmid DNA isolation and purification, QIAprep Spin Miniprep Kit (Qiagen) or QIAGEN Plasmid Midi Kit (Qiagen) were used as per the manufacturer's instructions.

2.2.17. MTT assays

The Thiazolyl Blue Tetrazolium Bromide (MTT) cell viability assay was used to measure the proliferation of cells in order to quantify cytotoxicity of epirubicin treatments. Details regarding the specific proliferation protocol are outlined in the relevant chapters. The general protocol for MTT was adapted from van de Loosdrecht et al. (1994) and (Scudiero et al., 1988). To measure the viability of cells in medium, 20 µL of 5 mg/mL MTT (in PBS) was added to each well of a 96 well plate. Plates were incubated for 3.5 hours at 37°C, 5% CO_2. Once the cells were fixed, the m was carefully removed to not disturb the stained cells. One hundred and fifty microlitres of MTT solvent (4 mM HCl, 0.1% Nondet P-40 (NP40), made up in isopropanol) was added to each well and the plate was covered in aluminium foil and incubated on the orbital shaker for 15 minutes. The absorbance was measured at 590 nm on the SpectraMax iD5 Multi-Mode Microplate Reader (Molecular Devices).

2.2.18. Western Blotting

2.2.18.1. Preparation of lysates

Cells were collected in PBS using a cell scraper and gentle centrifugation at 1500 rpm for 5 minutes to form a cell pellet. Cells were lysed by the addition of 50-200 µL RIPA buffer (Radioimmunoprecipitation assay buffer; composition as detailed previously) depending on cell

number. To ensure complete homogenisation and lysis, samples were passed through a Becton Dickinson ultra-fine II 30G syringe 10 times and incubated on ice. Cellular debris was removed via centrifugation and lysates were quantified for total protein content as per 2.2.11. SDS loading dye (4x concentrate) was combined with the desired amount of protein in a 20 µL volume and proteins were denatured by heating at 95°C for 5 minutes.

2.2.18.2. Polyacrylamide gel electrophoresis (PAGE)

Proteins were separated by SDS-PAGE gel electrophoresis at room temperature, using a Mini-PROTEAN Tetra electrophoresis chamber (Bio-Rad). Samples were separated at 75 V for 30 minutes through the 4% stacking gel, then 135 V for 1 hour through the 10% separating gel. Once the dye front had reached the end of the gel, the electrophoresis was stopped. Proteins were transferred using a wet-transfer method onto a 0.45 µm nitrocellulose membrane (Bio-Rad) in a cooled Mini Trans-Blot Electrophoretic Transfer Cell (Bio-Rad) filled with transfer buffer. Transfers were run for 1-2 hours at 100V or overnight at 25V at 4°C. Following transfer, membranes were stained using 0.1% Ponceau S to visualise efficiency of transfer and estimate relative protein amounts. To remove the Ponceau S stain, membranes were rinsed with TBST and blocked using 5% Blotto (5% (w/v) skim milk powder in TBST) for 90 minutes at room temperature, or overnight at 4°C on a shaker. Membranes were then rinsed briefly and the primary antibody (refer to 2.1.4 for specific antibodies) was added into 2.5% Blotto and incubated at 4°C on the shaker overnight. The membrane was then rinsed 3X 10 minutes in TBST and the secondary antibody was added in 2.5% Blotto (1:2000) and incubated at 4°C for 3 hours. The membrane was washed by 3X 10 minutes TBST and stored in TBST until imaging. The membranes were imaged using chemiluminescence by the addition of the SuperSignal West Pico PLUS chemiluminescent (ECL) HRP substrate (Thermo Fisher) as per the manufacturer's instructions and imaged using the ImageQuant LAS 4000 (GE Healthcare). Semi-

quantitative comparisons between protein expression were performed using Multi Gauge Software (FUJI Film, Tokyo).

2.2.19. Glucuronidation assays

2.2.19.1. TE buffer lysate and HLM preparation

Cell lysates were prepared in TE buffer and mixed as a homogenate by snap freeze-thawing repeatedly 3 times. These were then passed through a Becton Dickinson ultra-fine II 30G syringe 10 times for further mechanical disruption. These were subject to sonication as mentioned in specific protocols. Protein quantification was performed as per 2.2.11.

2.2.19.2. Epirubicin

i) Human liver microsomes (HLMs) as the enzyme source

Human liver microsomes (HLMs) were diluted to 10 µg/µL and pre-incubated on ice with alamethicin (50 µg/mg protein) for 30 minutes to activate them, as per common practice in UGT activity assays (Boase and Miners (2002)). Introducing pores into the cellular membrane by means of alamethicin removes any latency due to immediate availability of the endoplasmic reticulum-localised UGT enzymes.

Incubations (200 µl total) were prepared sequentially by the addition of sterile distilled water, 4 mM $MgCl_2$, 0.1 M potassium phosphate buffer (pH 7.4), epirubicin hydrochloride (concentration dependent on experiment), and 0.01 mg/mL alamethicin-activated HLMs. Samples were pre-incubated for 5 minutes at 37˚C in a shaking water bath, following initiation of the reaction by the addition of the cofactor UDP-glucuronic acid (5 mM). The reaction was incubated for 2 hours at 37˚C in a shaking water bath, before termination by the addition of 400 µL ice cold methanol with 0.001%

formic acid. The samples were centrifuged for 10 minutes at 10˚C at 4000 g, then 300 µL of supernatant was transferred into an LC-MS vial for a 2 µL fraction to be analysed via LC-MS. During method development (see 6.2.4 for further details) blank reactions were performed which excluded the co-factor in order to confirm the integrity of the peak. Blank reactions excluding the epirubicin substrate or excluding HLMs, were routinely run alongside as appropriate negative controls.

ii) Endogenous UGT expression from cell lysates as the enzyme source

In vitro epirubicin activity assays were performed using *endogenous UGT2B7* expression from cells as the enzyme source. Due to a significantly lower amount of available enzyme in breast cancer cells, when compared to cells of a hepatocellular nature, the protocol was adapted to enable detection of low formation of metabolites. ZR-75-1 cells seeded in a T25 flask were pre-treated for 48 hours with epirubicin at the optimal induction concentration, specific to the cell line (within the nanomolar range). This allowed for adequate available enzyme to be used for in-vitro incubations. TE buffer lysates were prepared from the resulting cell pellet. The lysates were sonicated for 10 cycles using a Sonics Vibracell VCX130 (John Morris Scientific) at 25% amplitude consisting of 20 second pulses, separated by 30 second intervals, to further disrupt the cellular membrane and release the intracellular UGTs. Various concentrations of total protein (mentioned in the specific chapter) were used in the incubation mixture as described above. The glucuronidation reaction was incubated overnight at 37 ˚C in a shaking water bath. The reaction was terminated and prepared for LC-MS analysis as described in the previous section.

2.2.19.3. Liquid chromatography–mass spectrometry (LC-MS) of glucuronides

Epirubicin glucuronide was quantified by liquid chromatography mass spectrometry (LC-MS) performed on an Agilent 1290 infinity liquid chromatography (LC) system linked to an Agilent 6495B

triple quadrupole mass spectrometer (MS; Agilent Technologies, California, US) fitted with a Zorbax Eclipse Plus C18 analytical column (1.8 µM, 2.1 mm x 50 mm; Agilent, California, US). Mobile phase and source conditions were replicated as recently described in (Ansaar et al., 2023). Relative peak areas were recorded, and results were normalised per µg unit of protein. The method development and further details of the small molecule assays are described in the relevant chapters.

2.2.20. LC-MS-based peptide assay for quantification of UGT2B7 protein

Lysates from epirubicin treated cells were subjected to tryptic digestion. Each 200 µL reaction (prepared in Protein LoBind tubes), contained up to 200 µg lysate protein in TE buffer (10 mM Tris-Cl, 1 mM EDTA, pH 8.0), with reagents added to a final concentration of 10 mM dithiothreitol, and 250 mM ammonium bicarbonate and incubated at 60°C for 90 minutes. Iodoacetamide was added to 20 mM and the sample was incubated at 37°C for 60 minutes in the dark. One microgram trypsin gold (Promega) per 50 µg lysate protein was added and the samples were incubated overnight at 37°C in a shaking water bath. Reactions were terminated with 10% v/v formic acid and samples were centrifuged at 11500 RPM at 4°C for 10 minutes. Supernatant (100 µL) was transferred to LC-MS vials and 250 nM/mL UGT2B7 internal stable isotope labelled (SIL) peptide (IEIYPTSLT**K** 587.1562++ m/z c-term labelled) was spiked into the vial. The remaining fraction was used for analysis as described below.

A 10 µL volume of the supernatant was injected into the tandem Triple Quadrupole LC/MS 6495C (Agilent Technologies). Peptides were separated on a reverse phase AdvanceBio Peptide Mapping 2.7 µM, 2.1 mm x 100 mm column (Agilent, California, US). The mobile phase consisted of 90% H_2O, 10% acetonitrile, with 0.1% formic acid. Under a flow rate of 0.3 mL/min the retention time of the diagnostic UGT2B7 peaks was at 3.6 mins. The source parameters were as follows; sheath

gas flow rate of 11 (arbitrary units), gas flow 14 L/min, gas temperature 250°C, nebulizer pressure 20 psi and a capillary voltage varying from 3000-3500V. Multiple reaction monitoring (MRM) mode was used to detect the parental compound (IEIYPTSLTK) of a mass/charge (m/z) of 583.1853++, with the source optimisation for each ion as listed in Table 2.2. The following y ionic transitions were selected as qualifiers or quantifiers: I [y8] - 923.0901+, Y [y7] - 809.9315+, and P [y6] - 646.7569+ (see Table 2.2). A column blank was run alongside to eliminate any contaminant peaks. Human liver microsomes (HLMs) were used as a positive control and for method optimisation.

Table 2.2. Source optimised parameters specific to the respective ionic transitions for LC-MS detection of UGT2B7.

Precursor Ion (m/z)	Product Ion (m/z)	Dwell (seconds)	Fragmentor (V)	Collision Energy (V)	Cell Acceleration (V)	Polarity
587 (ISTD)	931.7	50	380	15	4	Positive
587 (ISTD)	818.4	50	380	17	4	Positive
587 (ISTD)	654.3	50	380	17	4	Positive
583	923.5	50	380	15	4	Positive
583	810.4	50	380	17	4	Positive
583	646.3	50	380	17	4	Positive

Abbreviations used; mass-to-charge ratio (m/z), voltage (V).

2.2.21. Statistical Analysis

Statistical analysis including generating figures, plots and basic statistics was carried out in Microsoft Excel 365. Further statistics were conducted using GraphPad Prism 8.0.2 (GraphPad Software Inc, San Diego, California). Two-tailed independent t-tests were performed to analyse datasets containing a single variable, while multivariate comparisons were analysed using one-way ANOVA tests. Tests were deemed statistically significant with a resulting p value of less than 0.05. The specific statistical analyses used for each dataset are mentioned in the relevant sections.

CHAPTER 3. INDUCTION OF UGT2B7 EXPRESSION BY EPIRUBICIN AS A POTENTIAL MECHANISM FOR CHEMORESISTANCE IN BREAST CANCER

All figures in this chapter have been adapted from a manuscript for intended submission to 'Drug Metabolism and Disposition' entitled "Induction of UGT2B7 Expression by Epirubicin as a Potential Mechanism for Chemoresistance in Breast Cancer" under the following authorship:

Radwan Ansaar[1], Dong Gui Hu[1], Julie-Ann Hulin[1], Lu Lu[1], Sonja Klebe[1], Ash Hocking[1], Andrew Rowland[1], Peter I. Mackenzie[1], Ross I. McKinnon[1] and Robyn Meech[1]

[1] College of Medicine and Public Health, Flinders University, Adelaide, SA

The manuscript is currently in pre-submission. All data included was generated by the primary author and formed as part of the published manuscript, unless clearly stated otherwise. Significant modifications have been made in adapting the manuscript to the structure and formatting of the thesis. More detailed Introduction and Discussion sections have been written specifically for this thesis, and the Results section has been modified for clarity and to provide more detail.

3.1. Introduction

3.1.1. Epirubicin in Breast Cancer Treatment

Anthracyclines are widely used in oncology, usually as a component of combination chemotherapy regimens (Ormrod et al., 1999). In breast cancer, anthracyclines are commonly used in treatment of advanced metastatic forms of disease that do not express hormone receptors (estrogen receptor (ER) and progesterone receptor (PR)) or human epidermal growth factor receptor 2 (HER2) (termed triple negative breast cancer; TNBC). However, they may also be used in combination with both endocrine and anti-HER2 therapies in other breast cancer subtypes. The addition of anthracyclines has been shown to increase disease-free survival when compared to taxane-only containing regimens (Guarneri & de Azambuja, 2022). When used in the neoadjuvant setting in locally advanced breast cancer, they improve breast conservation rate and reduce the probability of postoperative recurrence. Epirubicin (EPI) is the most commonly used anthracycline in the treatment of TNBC, and it is incorporated into many anthracycline containing chemotherapy combinations. Therapeutic responses to epirubicin are dose-dependent both *in vitro* and in clinical studies (Bonneterre et al., 2005; Innocenti et al., 2001; Mandapati & Lukong, 2022; Robert, 1993).

3.1.2. UGT2B7 may mediate both systemic and intratumoral epirubicin metabolism

Glucuronidation is the major pathway for the systemic clearance of epirubicin and its metabolite epirubicinol. The inactive glucuronides exceed the concentration of parent drug within a few hours of intravenous administration and they are rapidly excreted (Robert, 1994). Previous studies

indicate that UGT2B7 is the sole UGT isoform responsible for generating epirubicin- and epirubicinol-glucuronides (Innocenti et al., 2001).

Epirubicin shows rapid and extensive distribution and relatively high hepatic extraction (Cantore et al., 2005; Umekita et al., 1992), suggesting that variation in hepatic metabolism (for example, due to variation in hepatic UGT2B7 activity) may have modest impact on systemic levels and thus efficacy and toxicity (Cottin et al., 1998; Liu et al., 2022; Robert, 1994). However, epirubicin has been reported to accumulate in tumours and other tissues due to its DNA-binding activity (Italia et al., 1983). Thus, it is possible that local, intratumoural epirubicin metabolism plays a significant role in determining the level of epirubicin present within tumour cells. Unfortunately, due to the challenges of measuring intratumoural drug levels *in vivo*, there is a lack of information about inter-individual variation in intratumoural exposure.

We hypothesized that the level of UGT2B7 expression in breast cancer cells could influence intracellular epirubicin levels, which in turn could control the cytotoxic efficacy of the drug. This hypothesis is based in part on previous reports that reducing the level of UGT2B7 expression in melanoma cells increased their sensitivity to epirubicin (Dellinger et al., 2012). Mechanisms that regulate the level of UGT2B7 expression in breast cancer cells have not been studied to date. However, there is an existing literature describing a wide range of transcriptional regulators of the *UGT2B7* gene, as well as mechanisms of induction by chemicals including anti-cancer drugs. This literature is discussed below.

3.1.3. Transcriptional regulation of UGT2B7

Multiple studies over the past two decades have identified mechanisms involved in constitutive and inducible regulation of UGT2B7. These include the identification of numerous transcription

factors which can bind to cis-regulatory elements (e.g. enhancers or silencers) in the promoter region. This literature has been extensively reviewed by Hu et al. (2014b) and will be briefly summarised in this section.

3.1.3.1. Transcription factors primarily involved in constitutive regulation of UGT2B7

Several developmental regulatory factors are proposed to be involved in the tissue-specific patterning of UGT2B7 expression, including hepatocyte nuclear factors 1 and 4 (HNF1, HNF4), constitutive androstane receptor (CAR), and caudal type homeobox 2 (CDX2). Ishii et al. (2000) defined a HNF1 binding site in the *UGT2B7* proximal promoter region. When expressed in liver HepG2 cells, HNF1α bound and activated the promoter, and this could be further enhanced by Oct-1 expression. Gregory et al. (2006) identified two CDX2 transcription factor binding sites in the *UGT2B7* promoter and showed that CDX2 bound and activated the promoter in intestinal-derived Caco2 cells. HNF1α also appeared to cooperate with CDX2 to further enhance the promoter activation. Yueh et al. (2011) used transgene mice expressing a human *UGT2B7* transgene to show a role for HNF4α and CAR in regulation of the *UGT2B7* promoter in liver cells.

3.1.3.2. Transcription factors primarily involved in inducible regulation of UGT2B7

Several transcription factors have been found to mediate inducible regulation of UGT2B7 by different classes of signalling molecules including growth factors and small molecules. These include the activating protein-1 (AP-1) family (Hu et al., 2014a), nuclear factor erythroid 2–related factor 2 (Nrf2) (Duguay et al., 2004; Nakamura et al., 2008) farnesoid X receptor (FXR) (Lu et al., 2005), and p53 (Hu et al., 2015; Hu et al., 2014c). Hu et al. (2014a) identified an AP-1 site in the distal *UGT2B7* promoter. AP-1 complexes are comprised of products of the so-called 'immediate early genes' such as *FOS* and *JUN* that are induced very rapidly after growth factor signalling. An

AP-1 complex comprised of Fra-2 and JunD was found to bind the promoter in HepG2 cells, while c-Fos and c-Jun proteins were found to bind in HuVEC cells (umbilical vein endothelial cells) (Hu et al., 2014b).

Duguay et al. (2004) and Nakamura et al. (2008) reported that Nrf2 binds to an antioxidant response element (ARE) in the distal promoter to induce *UGT2B7* promoter activity (Nakamura et al., 2008). Nrf2 is activated by oxidative stress and certain xenobiotic exposures, thus this induction may be part of a general mechanism to increase cellular detoxification capacity.

Lu et al. (2005) discovered that the bile-acid lithocholic acid can repress UGT2B7 via FXR in Caco-2 cells. Through promoter mutagenesis studies, a repressive FXR responsive element was identified within the proximal promoter region, and therefore has been denoted as the negative FXR response element (NFRE).

A role for p53 in regulation of UGT2B7 by cytotoxic stressors was identified in prior studies published by the Flinders Clinical Pharmacology laboratory (Hu et al., 2015; Hu et al., 2014c). This mode of regulation is central to the studies described in this Chapter. Hence the function of p53 in cancer cells, and the mechanism by which it regulates UGT2B7 are discussed in detail in the next section.

3.1.4. The p53 pathway

Tumour protein P53 (*TP53* or simply p53) is a transcription factor known for regulating critical cellular processes involved in preserving and maintaining genomic integrity (Marei et al., 2021). In accordance with this primary function, it has been well characterized as a cellular stress responsive gene and tumour suppressor. The p53 pathway is largely important in responding to DNA damage, reactive oxygen species (ROS) and hypoxia (Zhu et al., 2020). In order to protect the genome from such oncogenic factors, p53 can induce several protective mechanisms such as controlling

metabolism of glucose and lipids (Gnanapradeepan et al., 2018), activating DNA repair pathways, regulating cell differentiation (Molchadsky et al., 2010) or alternatively promoting cell cycle arrest leading to senescence or apoptosis if the damage is too severe (Zhu et al., 2020). Tight regulation of these processes by p53 are thought to be essential in suppressing tumour formation.

Downstream targets of p53, such as p21 influence core regulatory genes in cell cycling, for example, p21 inhibits Cyclin E/cyclin-dependent kinase (CDK)2 and Cyclin D/CDK4/6 complexes causing G1 cell cycle arrest (Laptenko & Prives, 2006). 14-3-3 sigma is another downstream target of p53 that inhibits Cyclin B/Cdc2 leading to G2 arrest (Harris & Levine, 2005).

Apoptotic targets induced by p53 include p53-upregulated modulator of apoptosis (PUMA) (Yu & Zhang, 2008), Noxa (Shibue et al., 2003), Bax (Chipuk et al., 2004), Bak (Leu et al., 2004), death receptor 5 (DR5) (Wu et al., 1999) and p53-inducible gene 3 (PIG3) (Porté et al., 2009), all of which promote pro-apoptotic functions (Aubrey et al., 2018).

p53 is also implicated as a positive and negative regulator of DNA repair pathways in response to genotoxic stress. It can activate proliferating cell nuclear antigen (PCNA), which acts as an auxiliary protein for DNA polymerases (Morris et al., 1996). Contrastingly, p53 can deregulate DNA polymerase kappa (POLK), although this mechanism of regulation may be unclear (Wang et al., 2004b).

Importantly, oncogenes can also act as inhibitors of p53, for example mouse double minute 2 homolog (MDM2) is a posttranscriptional inhibitor that can degrade p53, leading to uncontrolled cell cycling (Chène, 2003). Therefore, interactions between oncogenes and p53 destabilization have been an important area of study. Post-translational modifications to p53 have also been well researched, with p53 proven to be acetylated, phosphorylated, methylated, ubiquitinated, and

sumoylated at different locations of the protein, with members of these protein families affecting p53 stability in different ways (Marei et al., 2021).

More recently, the functional consequences of p53 mutations have been an area of interest due to it commonly giving rise to cancer progression by altering the DNA binding domain of p53 and affecting subsequent interactions necessary for normal function. In fact, 97% of p53 mutations are located in the core DNA binding domain (Kato et al., 2003). This is then able to disrupt the aforementioned controlled cellular processes, which therefore can induce uncontrollable cellular proliferation by triggering downstream proliferative signaling cascades (Muller & Vousden, 2014). For these reasons, dysregulation of p53 via mutation is a frequent event in cancer and has been referred to as an oncogenic process (Soussi & Wiman, 2015). The occurrence of inactivation of p53 by formed mutations is quite sporadic, and early stage mutations have been thought to be involved with tumourigenesis, while later stage mutations may be perhaps indicative of progression of advanced metastasis (Rivlin et al., 2011). Alternatively, gain of function mutations of p53 have been shown to induce oncogenes c-Myc, epidermal growth factor receptor (EGFR), and telomerase reverse transcriptase (hTERT), as well as inducing downstream cell cycling target, p21 (Rozan & El-Deiry, 2007). While gain of function p53 mutation may have a contradictory role that is not clearly defined in oncogenesis and cancer progression, it may also have a lesser-studied role in contributing to drug resistance, which is of a larger focus of this project.

3.1.5. Regulation of UGT2B7 by p53 in response to cytotoxic stress

p53 mediates responses to cytotoxic stresses induced by cytotoxic chemotherapy drugs. Previous work showed that UGT2B7 expression is regulated by a variety of cytotoxic drugs, including the anthracyclines epirubicin, doxorubicin, daunorubicin and idarubicin (Hu et al., 2015; Hu et al.,

2014c). This work was done in the HepG2 liver cancer cell line, which is derived from a differentiated hepatocellular carcinoma. HepG2 cells can be used as a model for liver cancer; however, due to their moderately differentiated morphology and gene expression pattern, they are also commonly used as a model for the systemic clearance of drugs by normal liver.

Analysis of UGT2B7 and UGT2B10 mRNA expression upon epirubicin treatment showed significant upregulation of both genes, and UGT2B7 protein expression and catalytic activity were also shown to be increased (Hu et al., 2015). A putative p53 responsive element was identified in the *UGT2B7* promoter (Hu et al., 2014c). This element located between nucleotides -251 and -270 (relative to the translation start site), was highly inducible by epirubicin as demonstrated by promoter activity assays. Mutation of the p53 responsive element resulted in loss of promoter activity (Hu et al., 2014c). Involvement of the p53 pathway was further identified using p53-targeting siRNA, which resulted in reduced induction of UGT2B7 by epirubicin as assessed through mRNA quantification. However, it was also found that UGT2B7 (and UGT2B10) can also be induced in a hepatocellular carcinoma cell line (Huh7) that contains a mutated non-functional p53. This suggests that UGT induction by epirubicin can be driven by both p53-dependent and p53-independent pathways.

3.1.6. Induction of UGT2B7 by Epirubicin as a Potential Mechanism for Drug Resistance

As stated previously, we hypothesized that the level of UGT2B7 expression in breast cancer cells could influence intracellular epirubicin levels, which in turn could control the cytotoxic efficacy of the drug. Moreover, the induction of UGT2B7 by epirubicin may be an adaptive process that increases cell survival. To date, induction of UGT2B7 by epirubicin has only been shown in liver cell models (HepG2 and Huh-7) and a melanoma model. Whether induction occurs in breast cancer cells, and by what mechanism, were knowledge gaps addressed in this Chapter.

3.1.7. Aims of Chapter 3

1. Determine the relative expression of UGT2B7 in different breast cancer cell line models, representing both luminal-like hormone receptor positive breast cancer (ER+/PR+/HER2-) and basal-like TNBC (ER-/PR-/HER2-) (Dai et al., 2017).
2. Determine whether epirubicin induces the expression of UGT2B7 at mRNA level and protein and/or activity levels in these cell lines.
3. Define the *UGT2B7* promoter elements that are involved in induction by epirubicin in different breast cancer cell lines.
4. Assess the role of p53 in regulation of the *UGT2B7* promoter by epirubicin in different breast cancer cell lines.

3.2. Materials and Methods

3.2.1. Materials and chemical information

Analytical grade chemicals including epirubicin hydrochloride, nutlin-3a, anduridine 5'-diphosphoglucuronic acid (UDPGA) ammonium salt were purchased from Sigma-Aldrich (St. Louis., Missouri).

3.2.2. Cell culture, drug treatment, RNA extraction, and quantitative reverse-transcription polymerase chain reaction

The breast cancer cell lines MDA-MB-231 (adenocarcinoma), MCF7 (adenocarcinoma), MDA-MB-453 (metastatic carcinoma), and ZR-75-1 (ductal carcinoma) were originally purchased from the ATCC. The breast ductal carcinoma cell line MFM-223 was originally sourced from ECACC. MDA-MB-231 were cultured in Dulbecco's Modified Eagle Medium (DMEM). ZR-75-1, MCF7 and MDA-

MB-453 were cultured in Roswell Park Memorial Institute (RPMI) 1640 Medium. MFM-223 were cultured in Minimal Essential Medium (MEM). All media was supplemented with 10% fetal bovine serum (FBS). All cell lines were maintained under incubation conditions of 37°C in a 5% CO_2 atmosphere. MPE-BC-001 was generated by culture of a malignant pleural effusion from a patient with metastatic TNBC. Collection of pleural effusions and isolation and culture of cells was approved by the Southern Adelaide Clinical Human Research Ethics Committee (SAC HREC) under ethics approval number 381.09 (project entitled 'Molecules associated with growth and vascularisation in the pleura in states of health, disease with a view for treatment of pleural malignancy') and the Central Adelaide Local Health Network Human Research Ethics Committee (CALHN HREC) under ethics approval number 14283. MPE-BC-001 grow semi-adherent and were cultured in RPMI with 10% FBS and 2% pleural effusion supernatant.

For drug treatment, cells were seeded in 6-well plates at $3.2*10^5$ cells/well and cultured for 24 hours until reaching approximately 80% confluency. Cells were treated in triplicate wells with varying doses of epirubicin. Initial screening studies used 1 µM epirubicin, which is within the reported plasma and tissue concentration range (Hunz et al., 2007). Subsequent experiments used a range of epirubicin doses between 200 nM and 1 µM. In some experiments, cells were treated with 10 µM nutlin-3a to induce p53 activity. Cells were harvested 24 or 72 hours later for RNA preparation. Total RNA was extracted using TRIzol (Thermo Fisher Scientific) and cDNA was synthesized from 1 µg RNA using Lucigen NxGen® M-MuLV Reverse Transcriptase. Quantitative reverse-transcriptase PCR (qRT-PCR) was performed using the RotorGene 3000 (Corbett Research, Australia). A 20 µL reaction contained ~100 ng cDNA template, 1X BRYT Green GoTaq Mastermix (Promega), along with a pair of gene-specific primers (500 nM each). qRT-PCR primer sequences for 18s rRNA, p21, UGT2B4, UGT2B7, UGT2B10, UGT2B11, UGT2B15, and UGT2B17 mRNA were as

previously described by Congiu et al. (2002) and Hu et al. (2014c). The GAPDH forward (5' GAGTCCACTGGCGTCTTCAC 3') and reverse (5' GTTCACACCCATGACGAACA 3') primer sequences are provided herein. The qRT-PCR reaction was performed under the following cycling conditions: polymerase activation at 95°C for 3 minutes, 40 cycles of denaturation 95°C for 10 seconds, annealing 60°C for 15 seconds, and extension 72°C for 20 seconds, followed by melt 55-95°C ramping 1°C each step.

3.2.3. Analysis of p53 mutations in MPE-BC-001 cells

To identify mutations within p53 in the MPE-BC-001 cell line, amplicons were generated from cDNA using primers anchored in the 5' UTR (p53E1F 5'- GGACACTTTGCGTTCGGGCT-3') and 3' UTR (p53E1R, 5'-CTTTGAACCCTTGCTTGCAA-3') using Phusion High-Fidelity Polymerase (Thermo Fisher Scientific). PCR products were cloned into the pCR-Blunt vector (Thermo Fisher Scientific) and multiple clones were sequenced using forward and reverse vector primers (M13) (Messing, 1983).

3.2.4. Epirubicin glucuronidation assay

3.2.4.1. Reaction conditions

Lysates were generated from ZR-75-1 and MDA-MB-231 stable cell lines by hypotonic lysis in TE buffer (10 mM Tris-Cl, 1 mM EDTA, pH 8.0). *In vitro* epirubicin glucuronidation assays were performed using 200 µg and 50 µg total protein from ZR-75-1 and MDA-MB-231 lines respectively.

Reactions (200 µL total volume) contained 0.1 M potassium phosphate pH 7.4, 4 mM $MgCl_2$, and 25 µM epirubicin (in DMSO 2% v/v); the epirubicin concentration is equivalent to the Km. After a 5-minute pre- equilibration at 37°C, UDPGA was added to a final concentration of 5 mM to initiate the reaction. Reactions were incubated overnight at 37 °C in a shaking water bath, then

terminated by the addition of 400 µL of ice-cold methanol containing 0.1% formic acid. After centrifuging at 4000 g for 10 min at 10˚C, a 300 µL aliquot of the supernatant was saved.

3.2.4.2. Analysis by liquid chromatography mass spectrometry (LC-MS)

Epirubicin glucuronide was quantified by liquid chromatography mass spectrometry (LC-MS) performed on an Agilent 1290 infinity liquid chromatography (LC) system linked to an Agilent 6495B triple quadrupole mass spectrometer (MS; Agilent Technologies, California, US) fitted with a Zorbax Eclipse Plus C18 analytical column (1.8 µM, 2.1 mm x 50 mm; Agilent, California, US). Mobile phase and source conditions were replicated as recently described in (Ansaar et al., 2023). Relative peak areas were recorded, and results were normalised per µg unit of protein.

3.2.5. LC-MS-based peptide assay for quantification of UGT2B7 protein

Two hundred micrograms of protein lysates from epirubicin treated cells in TE buffer were subjected to tryptic digestion and proteomic analysis as described in 2.2.20.

3.2.6. UGT2B7 promoter luciferase assays

The two *UGT2B7* promoter-luciferase reporter constructs used in this study (2B7 -283/-1 and 2B7 -575/-1) have been previously described (Hu et al., 2014c). The 2B7 -283/-1 construct spans from position -283 nt to the translation start site and the 2B7 -575/-1 construct spans from position -575 nt to the translation start site. Both constructs contain a p53 response element between -251 and -270 nt. The p53 response element has been mutated in the constructs designated -283/-1 MT3 and -575/-1 MT3 via site-directed mutagenesis (Hu et al., 2014a).

MDA-MB-231 and ZR-75-1 cells were seeded in 48 well plates at $5*10^5$ cells/ well and transfected with 200 ng of various pGL3-*UGT2B7* promoter reporter constructs and 8 ng of the pRL-null

internal reference plasmid (Promega), using Lipofectamine LTX (Invitrogen) according to the manufacturer's directions. Twenty-four hours post transfection, the medium was replaced, and cells were treated with 500 nM epirubicin, 10 mM nutlin-3a, or corresponding vehicle controls (ethanol or DMSO). Cells were harvested in passive lysis buffer (Promega) after 72 hours and luciferase activities measured using the Promega dual luciferase assay kit and the Perkin Elmer TopCount NXT. Firefly luciferase readings were normalized over Renilla luciferase readings and the empty pGL3 plasmid.

3.2.7. Statistical Analysis

Statistical analysis was performed using Microsoft Excel (Office 365) and GraphPad Prism. Two tailed t-tests were conducted and a resulting P value of less than 0.05 was considered statistically significant. Cell viability data was used to calculate the half-maximal inhibitory concentration (IC50) in each independent experiment and these values were then compared using an unpaired two-tailed t-test, wherein a P value of less than 0.05 was deemed statistically significant. Unpaired two-tailed t-tests were performed on datasets containing a single variable, while one-way ANOVAs were performed on datasets containing multiple variables. Statistical significance (P value <0.05) has been annotated in the figure or legend.

3.2.8. Analysis of TCGA-BRCA datasets

Clinical and genomic data contained within The Cancer Genome Atlas (TCGA) Breast Invasive Carcinoma (BRCA) project was accessed via the cBioPortal data portal (https://www.cbioportal.org). Detailed methodology of the analysis conducted within this dataset can be found in Chapter 4 (Methods 4.2.14).

3.3. Results

3.3.1. UGT2B7 expression is elevated in aggressive hormone receptor-negative breast cancers

In contrast to several other UGT2B family members, the expression of UGT2B7 has not been extensively characterized in cancers derived from hormone-sensitive tissues such as breast. Using the TCGA-BRCA transcriptome dataset, relationships between breast cancer subtype and UGT2B7 expression were examined. Of the 1084 samples in this dataset, approximately 16% are basal, 7% are Her2-enriched and 64% are luminal A or B subtypes (not shown). When samples were stratified by UGT2B7 mRNA level, the highest UGT2B7 quartile comprised approximately 36% basal, 18% Her2-enriched and 32% luminal A or B subtypes (Figure 3.1A). Moreover, tumours in the top quartile for UGT2B7 expression had significantly higher hypoxia score, mutation count, and aneuploidy score (Appendix Figure 5). Analysis of UGT2B7 in tumours stratified by ERα protein expression showed that UGT2B7 mRNA levels were significantly higher in the cohort of tumours that lack ERα protein (Figure 3.1B). Overall, these data indicate that high UGT2B7 expression is associated with hormone receptor-negative, aggressive breast tumours.

To assess whether UGT2B7 shows a similar pattern of expression in breast cancer cell lines, basal UGT2B7 mRNA levels were measured in a panel of five cell lines representing different breast cancer subtypes (MDA-MB-231, MDA-MB-453, MFM-223, MCF7, ZR-75-1), as well as a primary breast cancer cell line derived in our laboratory from a metastatic TNBC pleural effusion (called MPE-BC-001). UGT2B7 showed the highest level of expression in MDA-MB-231 cells (TNBC), followed by MPE-BC-001 (TNBC), with around 20-50-fold lower mean expression in all other cell lines tested (Figure 3.1C).

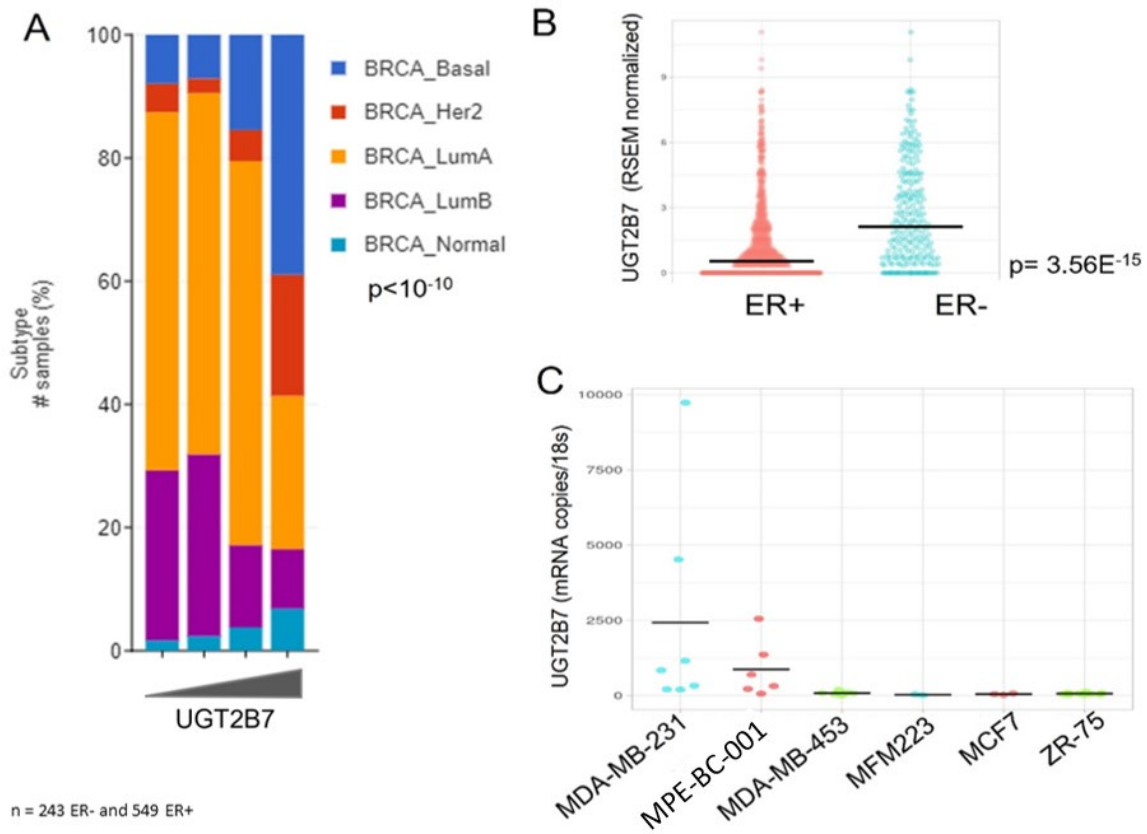

Figure 3.1. UGT2B7 expression in different breast cancer cohorts as defined using the TCGA-BRCA RNA-seq dataset and in breast cancer cell lines. (**A)** Tumours from the TCGA-BRCA dataset were stratified by UGT2B7 expression level and the distribution of subtypes was compared between expression quartiles (quartiles are shown in ascending order (left to right); n = 270 samples per group). Molecular subtyping has been defined by PAM50 classifiers. P values were derived using Chi-squared test. **(B)** Tumours were stratified based on the histopathological marker ER and UGT2B7 expression levels were compared (n = 243 ER- and 549 ER+). P-values were derived using Student's t-test **(C)** UGT2B7 expression levels in cell lines were determined by qRT-PCR and presented as absolute copy numbers relative to 10^9 copies of 18s rRNA. This data is representative of 2-7 technical replicates.

As hormone dysregulation is a feature of carcinogenesis in hormone responsive cancers, UGT2B15 has been implicated as a negatively regulated marker due to its role in inactivating steroids such as androgens (Pâquet et al., 2012). With the prior data suggesting UGT2B7 could be a hallmark of aggressive breast cancers, upregulation of UGT2B7 and downregulation of UGT2B15 was hypothesized to be of prognostic value of tumour subtyping. This was indeed correct, when TCGA-BRCA data were stratified by both UGT2B7 and UGT2B15 expression levels, 86% of

UGT2B7^{high}/UGT2B15^{low} samples were basal subtype, while none of the UGT2B7^{low}/UGT2B15^{high} samples were basal (Figure 3.2).

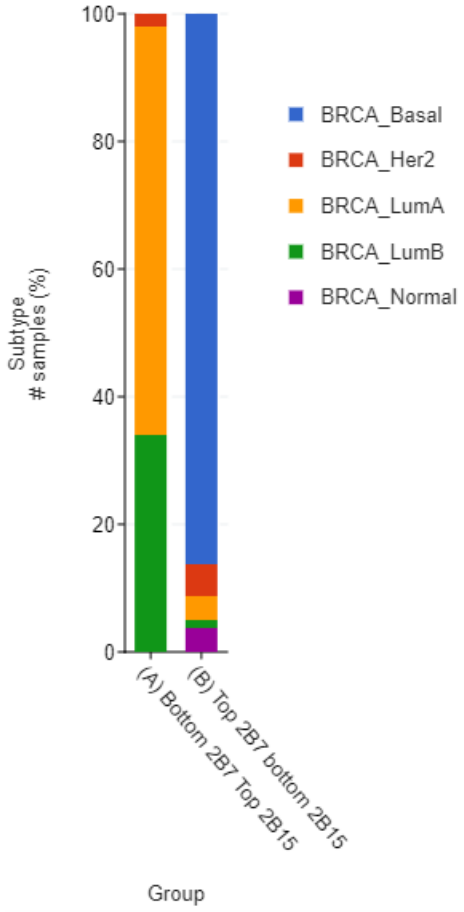

Figure 3.2. UGT2B7 and UGT2B15 expression can be prognostic of Breast Invasive Carcinoma subtyping when stratified by high/low levels. TCGA-BRCA RNA-seq data were stratified by UGT2B7 and by UGT2B15 expression levels using CBioPortal. The group representing the intersection of the top UGT2B7 quartile and bottom *UGT2B15* quartile (n=93) was compared to the group representing the intersection of the top UGT2B15 quartile and bottom UGT2B7 quartile (n=57). Molecular subtyping has been defined by PAM50 classifiers.

3.3.2. Epirubicin induces UGT2B7 expression and activity in breast carcinoma cell lines.

To assess the ability of epirubicin to induce UGT2B7 expression in different breast cancer subtypes, two luminal ER-positive models (ZR-75-1 and MCF-7), one HER2 positive mode (MDA-MB-453) and three TNBC models (MDA-MB-231, MFM-223 and MPE-BC-001) were screened for

changes in UGT2B7 mRNA levels following 72 hours treatment with 1 µM epirubicin. UGT2B7 expression was induced to varying degrees in all six cell lines tested (Figure 3.3). Markedly induction in ZR-75-1 cells was of particular interest in querying due to the low basal levels of UGT2B7, relative to MDA-MB-231 cells (Figure 3.1C).

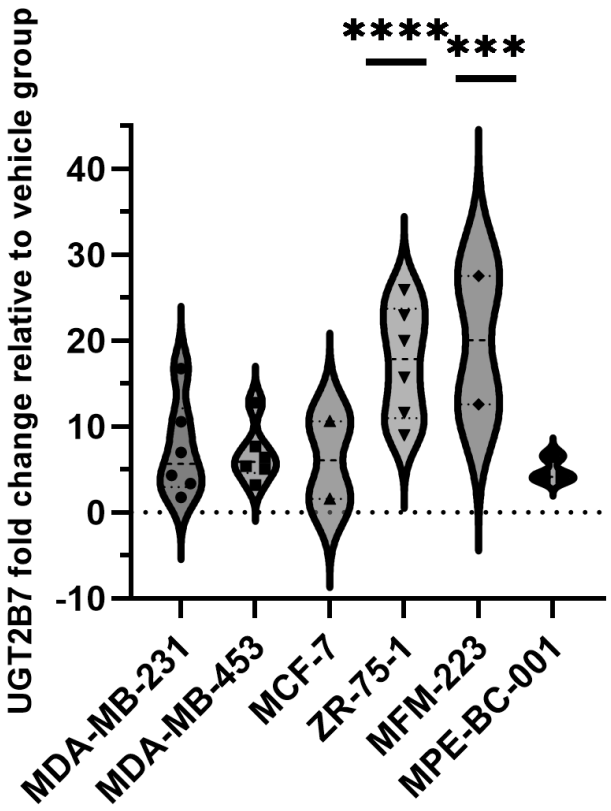

Figure 3.3. qRT-PCR based screen showing UGT2B7 mRNA expression following the treatment of 1 µM epirubicin for 48 hours in breast cancer cell lines. UGT2B7 is induced in all cell lines to a varying degree. ZR-75-1 and MFM-223 cells are significantly induced. Data is presented as fold change relative to vehicle (ethanol) normalised to 18s. The range and distribution is represented by a violin plot of technical replicates n=2-6. A one-way ANOVA was performed with a follow up Dunnett's test (*P <0.05, **P<0.01, ***P<0.001, ****p<0.0001).

Subsequently, from the initial epirubicin induction screen (Figure 3.3), further replication of this was performed using representative models from a luminal-like subtype (ZR-75-1) and a TNBC model (MBA-MB-231), while a primary cancer cell line (MPE-BC-001) was also included, to further substantiate these findings. From this, UGT2B7 mRNA was induced approximately 24-fold in ZR-

75-1 cells at 0.2 µM epirubicin (Figure 3.4A). Induction in ZR-75-1 cells was lower at the higher epirubicin dose of 500 nM, likely due to cytotoxicity. In MDA-MB-231 cells, maximal induction of UGT2B7 mRNA occurred at 1 µM epirubicin and reached approximately 7-fold relative to control (Figure 3.4B). In MPE-BC-001 primary cells, UGT2B7 was induced around 5-fold by 1 µM epirubicin (Figure 3.4C). UGT2B7 induction is partly reliant on an apoptotic response (to be described in the subsequent section), henceforth, induction was assessed at partially cytotoxic concentrations of epirubicin. Similarly, epirubicin induction was characterised in MDA-MB-231 cells, amongst the UGT2B family, of which, seven of the different isoforms saw dose-dependent induction to variable degrees (Figure 3.5).

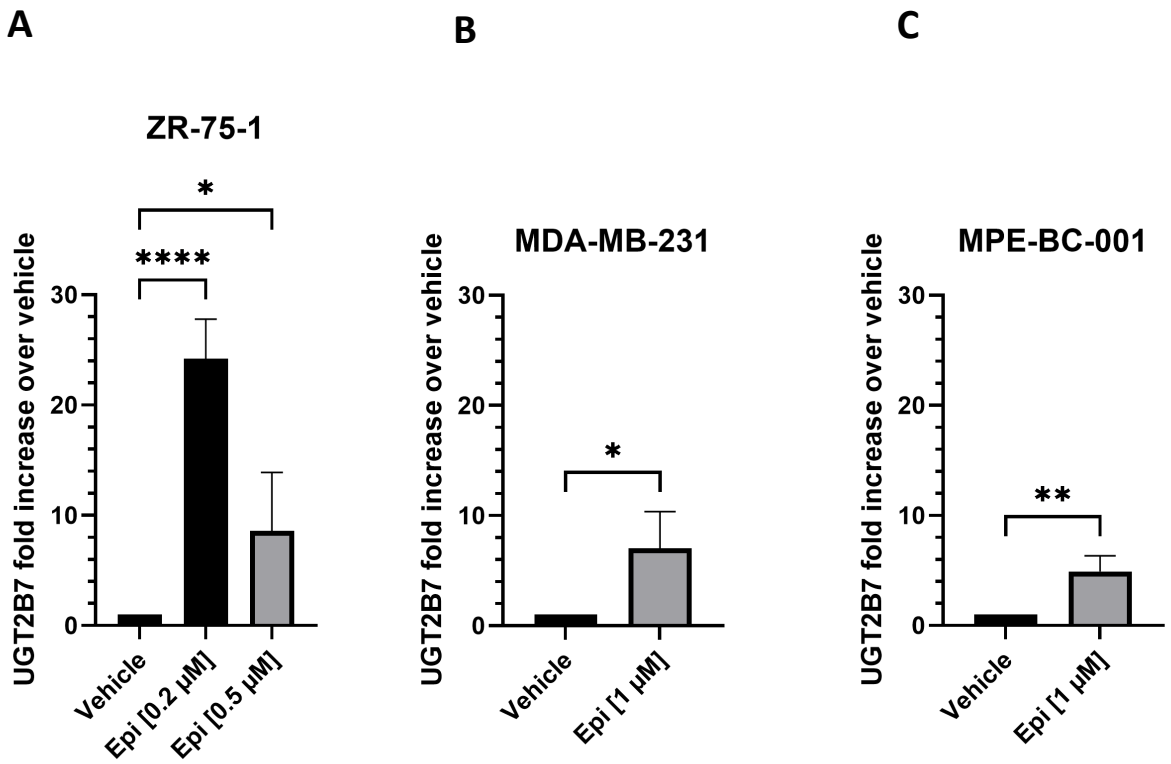

Figure 3.4. **A-C.** Epirubicin upregulates UGT2B7 expression in breast cancer cell lines. Epirubicin (Epi) treatment (72 hrs) increases UGT2B7 mRNA levels in: ZR-75-1 **(A)**, MDA-MB-231 **(B)** and MPE-BC-001 (metastatic primary cell line) **(C)** (n=4). A two-tailed T-test was performed (*P <0.05, **P<0.01).

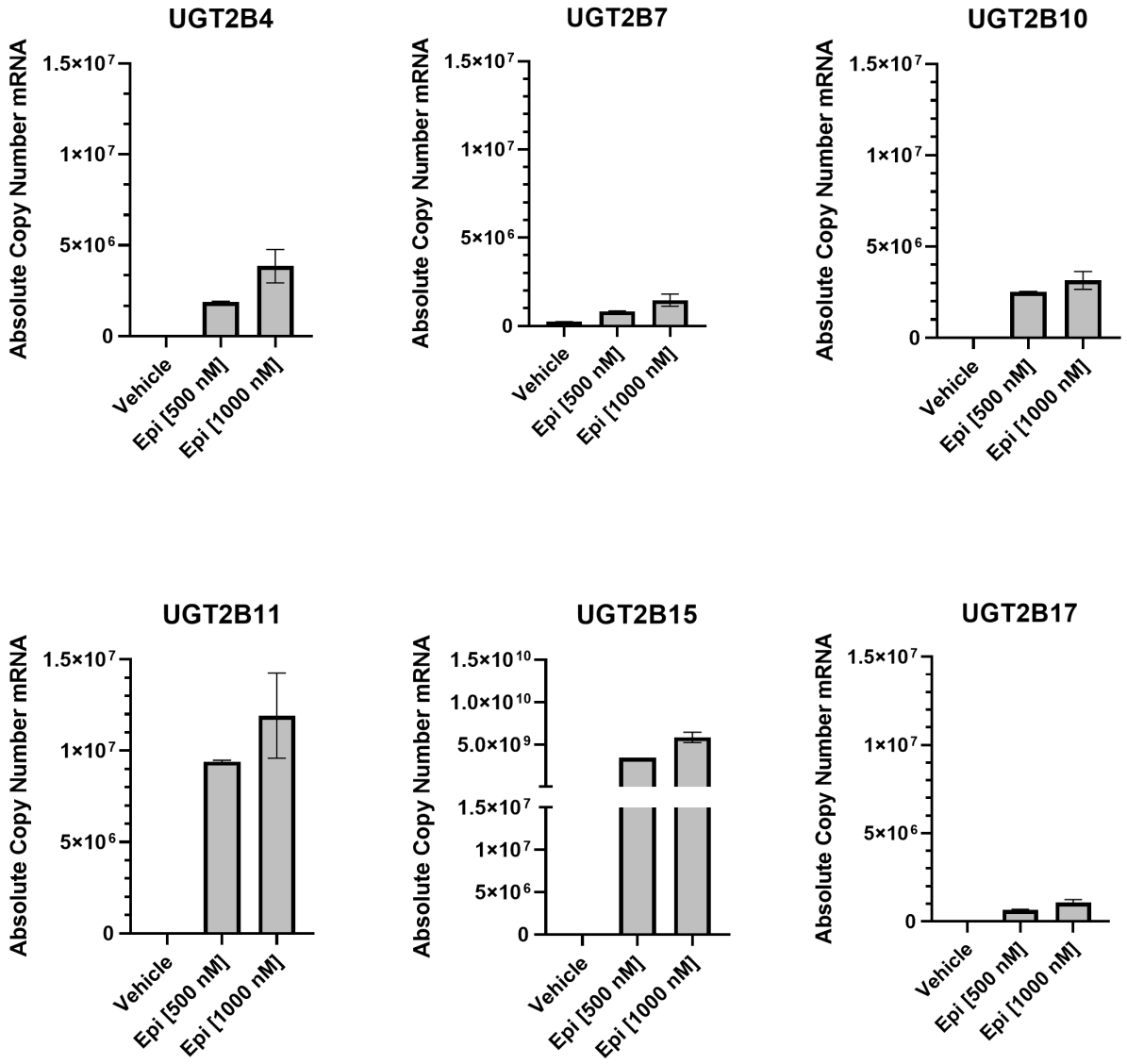

Figure 3.5. mRNA expression of all seven UGT2B family genes is induced by 72h epirubicin treatment (epi) in MDA-MB-231 cells as compared to the vehicle control (ethanol). Data is shown as absolute copy number normalized to copies of the GAPDH housekeeping gene. Data is the average of n=2 biological replicates with 2 technical replicates within each. Error bars represent standard deviation. This data has been obtained from Lu Lu (Clinical Pharmacology, Flinders University, Australia) and plotted with permission.

UGT2B7 induction in the MDA-MB-231 cell line was further characterized at the protein level using a quantitative peptide assay. The specificity of the assay was confirmed using a CRISPR-generated UGT2B7-null HepG2 cell line (Figure 3.6A); furthermore, HepG2 cells were used to demonstrate the capacity of the assay to quantify dose-dependent epirubicin-induction of endogenous UGT2B7 (Figure 3.6B). This can be compared to the epirubicin HepG2 mRNA induction experiments performed by Hu et al. (2014c). Treatment of MDA-MB-231 cells with 1 µM epirubicin induced approximately 2-fold increase in UGT2B7 protein when compared to the control (Figure 3.6C).

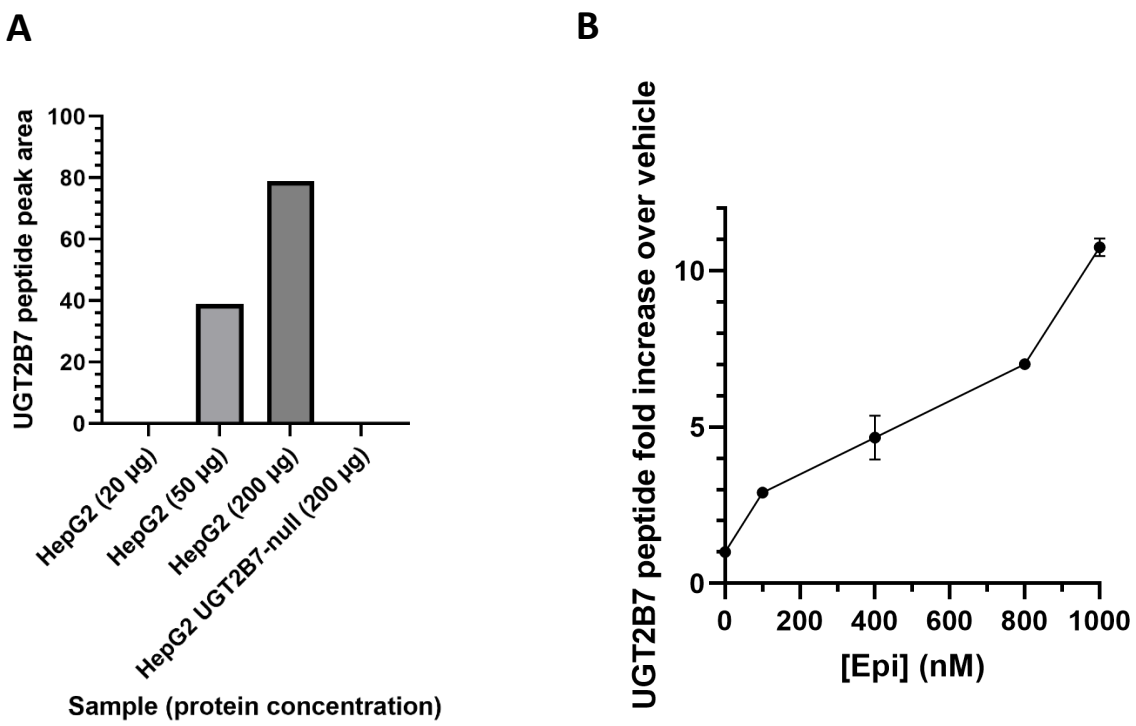

Figure 3.6. Validation of the UGT2B7 specific peptide assay. **(A)** The UGT2B7 peptide assay detects increased levels of UGT2B7 with increased total protein loaded. The UGT2B7-null HepG2 cell line was used as a specificity control demonstrating that it does not detect other UGT isoforms. The null line was generated by CRISPR and previously shown to express no UGT2B7 mRNA (not shown). **(B)** The UGT2B7 peptide assay can detect dose-dependent increases in endogenous UGT2B7 protein in HepG2 cells in response to Epirubicin (Epi) treatment. The experiment was performed in technical duplicate and error bars represent range**. (C)** UGT2B7 protein induction was demonstrated in MDA-MB-231 cells using a specific peptide assay. Protein peak areas were measured following LC-MS detection of a specific UGT2B7 peptide. Data is represented as fold relative to the vehicle (ethanol) control. Three technical replicates were performed, with the error bars representing standard deviation. A two-tailed T-test was performed (*P <0.05; **P<0.01, ***P<0.001).

3.3.3. Epirubicin-mediated induction of UGT2B7 involves both p53-dependent and -independent mechanisms in breast cancer cells.

The next goal was to understand the mechanism of induction of UGT2B7 in breast cancer cells. Previous work published by our laboratory using HepG2 cells found that epirubicin induction of UGT2B7 was p53-mediated (Hu et al., 2014c). However, two of the breast cancer cell lines which demonstrated induction of UGT2B7 by epirubicin in this study (MDA-MB-231 and MPE-BC-001; see Figure 3.4) harbour *p53* mutations. MDA-MB-231 cells carry a well characterized loss of function *p53* mutation, and classical p53 targets such as p21 are not induced in these cells after p53 stabilization by the MDM-inhibitor nutlin-3 (Chipuk & Green, 2006; el-Deiry et al., 1993; Gomes et al., 2018; Shen & Maki, 2011). Interestingly however, previous studies showed that p21 and other pro-apoptotic genes may be induced by cytotoxic stress in a p53-independent manner in this cell line (Lee et al., 2020; Macleod et al., 1995; Tseng et al., 2017). From this study, epirubicin increased p21 mRNA levels 6.4-fold in MDA-MB-231 cells, likely via this p53-independent mechanism (Figure 3.7). The MPE-BC-001 cell line was found to carry R249M, P250del, and V251I mutations, all of which occur in a mutational hotspot and affect the L3 loop (residues M237-P250) that is important for coordination of zinc binding to stabilize the DNA binding domain, thus DNA binding of p53 is likely ablated (Kotler et al., 2018). Only one expressed allele was detected suggesting loss of heterozygosity, which is common in p53-mutant cell lines. Epirubicin was unable to induce p21 mRNA in this model (Figure 3.7). It is possible that MPE-BC-001 cells lack the p53-independent pathway that is deployed by MDA-MB-231 cells to induce p21 in response to cytotoxic stress. As a positive control, it was showed that epirubicin increased expression of p21 robustly (8.2-fold) in p53 wildtype ZR-75-1 cells (Figure 3.7). Overall, these data indicate that

epirubicin can induce UGT2B7 via a p53-independent mechanism in two different p53-mutant breast cancer models; however, the mechanism of induction may differ between these models.

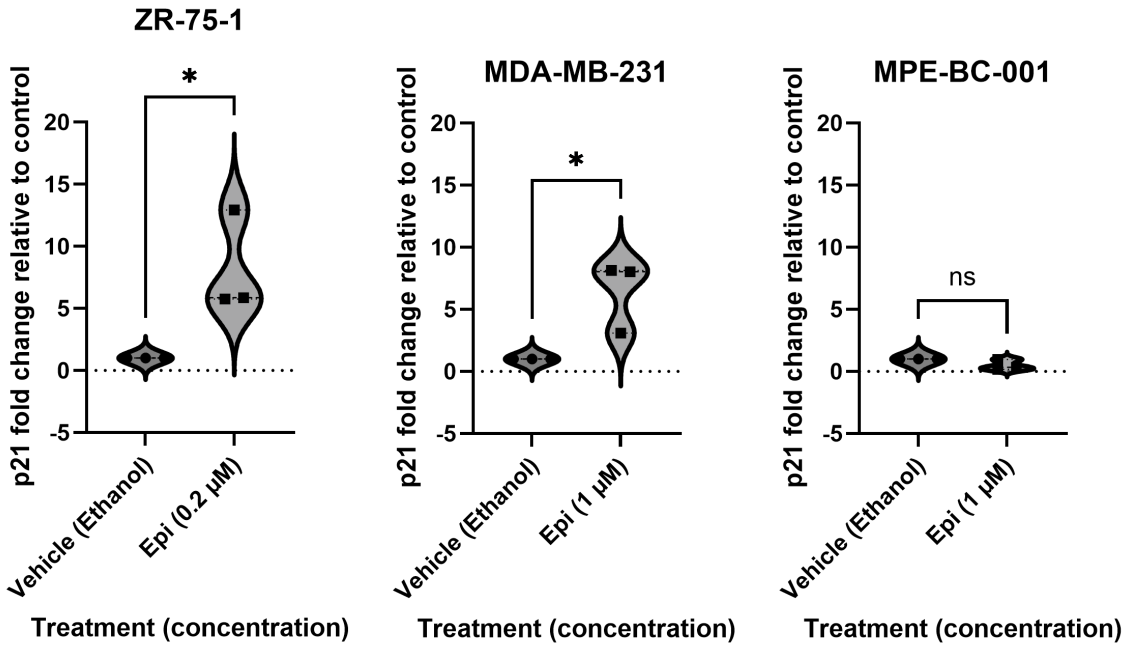

p53 genotype		
Wildtype	R280K missense mutant	R249M, P250del, and V251I mutations

Figure 3.7. Epirubicin (1 µM) treatment (72 hours) induces expression of p21 in ZR-75-1 (p53 wildtype) and MDA-MB-231 cells (p53 R280K missense mutant) but not in the primary MPE-BC-001 cell line (p53 mutations). Relative expression was quantified using qRT-PCR and normalised to expression of 18s rRNA. *P <0.05.

The epirubicin-mediated induction of UGT2B7 was previously investigated in HepG2 liver carcinoma cells, which identified a functional p53 binding site in the proximal region of the *UGT2B7* promoter (Hu et al., 2014c). Herein this work sought to identify whether the same promoter region was involved in induction of UGT2B7 expression in breast cancer cells. For this purpose, luciferase reporter constructs containing segments of the *UGT2B7* promoter were

utilised, spanning from the translation start site to either -283 nt or -575 nt upstream, and encompassing the p53 binding site (Figure 3.8A).

In p53-wildtype ZR-75-1 cells, the *UGT2B7* -283/-1 proximal promoter construct was induced approximately 37-fold by 500 nM EPI, while the -575/-1 construct showed greater induction at approximately 161-fold (Figure 3.8B). Construct -575/-1 MT3 which contains a mutated p53 response element (see Hu et al. (2014c) for further information), showed negligible induction by epirubicin (< 2-fold). Treatment with nutlin-3a induced both the -283/-1 and the -575/-1 promoter constructs in ZR-75-1 cells, although to a lesser extent than epirubicin (Figure 3.8B). The -575/-1 MT3 construct carrying the mutated p53 site was not induced by nutlin-3a. Overall, these data indicate that epirubicin induces the proximal *UGT2B7* promoter via p53 in ZR-75-1 cells, consistent with the mechanism shown previously in HepG2 cells (Hu et al., 2014c).

In p53-mutant MDA-MB-231 cells, the -283/-1 and -575/-1 promoter constructs showed very weak induction by epirubicin (around 2-fold), and this was unaffected by mutation of the p53-response element (Figure 3.8C). Nutlin-3a did not activate any of the constructs, which is consistent with the lack of functional p53 in these cells. These data confirm that p53 is not involved in induction of UGT2B7 mRNA by epirubicin in p53-negative TNBC cells. Moreover, the minimal response of the *UGT2B7* proximal promoter to epirubicin suggests that induction of UGT2B7 mRNA in MDA-MB-231 cells is either controlled by more distal regulatory sequences or is due to post-transcriptional events.

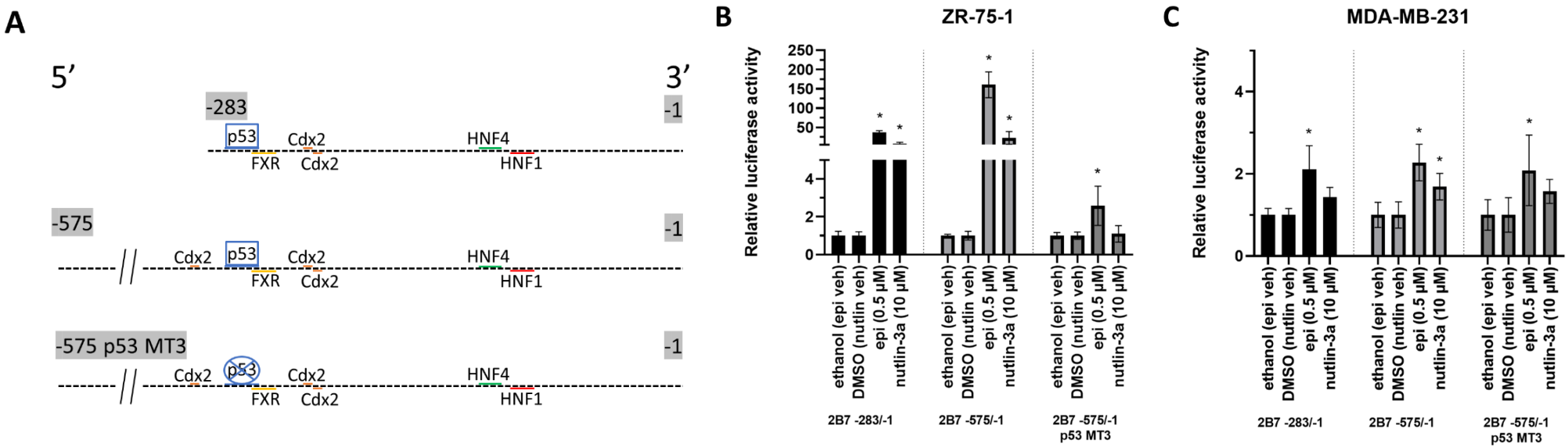

Figure 3.8. Epirubicin-mediated activation of the *UGT2B7* proximal promoter is observed only in breast cancer cell lines with functional p53 **(A)** A schematic of the *UGT2B7* promoter constructs used in the luciferase assays. The common p53 responsive element is shown in blue. The sequence lengths are denoted relative to the translation start codon (ATG). Other previously reported transcription factors have been marked. Caudal-related homeodomain protein 2 (Cdx2) is shown in orange, farnesoid X receptor (FXR) is shown in yellow, and hepatic nuclear factors 4 and 1 (HNF4 and HNF1) are shown in green and red respectively. The sequences have been truncated for formatting and therefore are not to scale. The ZR-75-1 **(B)** or MDA-MB-231 **(C)** cell line was transfected with wildtype or mutated *UGT2B7* proximal promoter constructs and treated with 500 nM epirubicin, 10 mM nutlin-3a or vehicle. The Promega dual luciferase assay kit was used to quantify promoter activity. Wildtype *UGT2B7* promoter activity was robustly induced in ZR-75-1 cells by both epirubicin and nutlin-3a; mutation of the p53 element abolished this response. Wildtype promoter activity was weakly induced in MDA-MB-213 cells by epirubicin; mutation of the p53 element had no effect on the response. *P <0.05; **P<0.01.

3.4. Discussion

Epirubicin is widely used in the treatment of breast cancer. It can be used as neoadjuvant therapy for locally advanced hormone receptor-positive, HER2-positive, or TNBC tumours (Fontaine et al., 2019; Gu et al., 2015; Shan et al., 2020; Untch et al., 2010). It is also used in chemotherapy regimens for metastatic TNBC (Mavroudis et al., 2010). Glucuronidation is a major clearance pathway for epirubicin and UGT2B7 is believed to be solely responsible for this metabolism. A common paradigm in drug metabolism is that the genes encoding drug metabolic enzymes (DME) are often regulated by the chemicals that the enzymes metabolize. This creates a feedback loop that allow dynamic response to changing demands for detoxification as described in the Introduction. With respect to anticancer drugs, this gene induction may occur in organs of elimination, such as liver, and also in the targeted cancer cells. Studies in this Chapter were focused on the potential regulation of UGT2B7 by epirubicin in breast cancer cells.

The extent to which UGT2B7 is expressed in breast cancer has not been well defined previously. Herein it was observed that UGT2B7 mRNA levels were significantly higher in TNBC and basal subtypes than in luminal A/B breast cancers. This contrasts with other UGT2B family members previously studied in breast, such as the steroid conjugating UGT2B15 and UGT2B17 enzymes that are predominantly found in ER+ luminal cancers (Hu et al., 2016). The present study was able to find a strong association between $UGT2B7^{high}$/$UGT2B15^{low}$ and basal subtyping, thus, UGT isoform ratio appears to be a robust marker of cancer subtype. The association of UGT2B7 with basal subtype was recapitulated in cell lines, with markedly higher UGT2B7 expression seen in MDA-MB-231 and MPE-BC-001 cells, relative to other models. Both MDA-MB-231 (Cailleau et al., 1974) and primary MPE-BC-001 are TNBC models that derive from metastatic breast cancer pleural effusions.

The major goal of the studies reported in this Chapter was to determine whether epirubicin induces UGT2B7 expression in breast cancer cells, and to identify the mechanism(s) of induction. Epirubicin did induce UGT2B7 mRNA expression in both ER+ and TNBC cell lines. This finding was consistent with the previous reports of induction of UGT2B7 by epirubicin in hepatocellular carcinoma and melanoma cell lines (Dellinger et al., 2012; Hu et al., 2015). With respect to the mechanism of induction, we investigated the role of the previously identified p53 binding site in the *UGT2B7* proximal promoter (Hu et al., 2014c). We found that the p53 binding site potentially mediated UGT2B7 induction in breast cancer cell lines (ZR-75-1 cells) that carry WT *p53* alleles. It is important to note that it is plausible that in ZR-75-1 cells, UGT2B7 induction may also be occurring through p53-independent mechanisms, as we have not yet confirmed whether epirubicin is able to induce UGT2B7 with a non-functional p53 responsive element. Hu et al. (2014c) were able to demonstrate that knockdown of the p53 RE by siRNA, significantly reduces UGT2B7 induction in HepG2 cells, therefore, this would also need to also be validated in ZR-75-1 cells.

In the context of p53-mutant cells, the proximal promoter appeared to play a minimal, if any, role in UGT2B7 induction, and the mechanism of this induction remains to be fully defined. Induction of pro-apoptotic p53-target genes in cells with loss of function *p53* alleles has been previously reported. For example, pro-apoptotic curcumin increases p21 levels in MDA-MB-231 cells via a mechanism involving SKP2 (Chiu & Su, 2009; Jia et al., 2014; Lee et al., 2020; Macleod et al., 1995; Tseng et al., 2017). Epirubicin also induced p21 in this cell line. In contrast, MPE-BC-001 cells did not show p21 induction, indicating that p53-independent p21 induction is a cell line-specific phenomenon. Given that UGT2B7 was induced by epirubicin in both the MDA-MB-231 and MPE-BC-001 TNBC models, it is probable that the mechanism differs from that previously shown to

induce p21 in MDA-MB-231 cells. Indeed, p53-independent induction mechanisms might be different for detoxification and pro-apoptotic pathways in general.

To begin to identify possible mechanisms of p53-independent induction, other *UGT2B* genes were examined to determine whether they could be induced by epirubicin. All *UGT2B* genes tested (*UGT2B4, 2B10, 2B11, 2B15* and *2B17*) were induced in MDA-MB-231 cells to a similar level as UGT2B7. The *UGT2B* genes are located adjacent to one another in a 0.5Mb region on chromosome 4. Thus, it is possible that the entire gene cluster is induced via epigenetic alterations in chromatin accessibility and long-range regulatory mechanisms such as formation of topologically associated domains. Future studies could test the effects of epirubicin on chromatin accessibility and conformation within the *UGT2B* locus. Further studies should also examine whether post-transcriptional events such as RNA stabilization are involved in increasing UGT2B mRNA levels.

Overall, the presented data supports the idea that UGT2B7 is induced by epirubicin via both p53-dependent and p53-independent mechanisms. The latter could provide a mechanism for drug-induced resistance in TNBCs, over 80% of which carry *p53* mutations (Koboldt et al., 2012). This hypothesis will be addressed directly in the subsequent Chapter 4.

CHAPTER 4. UGT2B7 Expression can Modify the Response of Breast Cancer Cells to Epirubicin

Some of these data (Figures 4.4 & 4.5) in this chapter has been adapted from a manuscript for intended submission to 'Drug Metabolism and Disposition' entitled "Induction of UGT2B7 Expression by Epirubicin as a Potential Mechanism for Chemoresistance in Breast Cancer" under the following authorship:

Radwan Ansaar[1], Dong Gui Hu[1], Julie-Ann Hulin[1], Lu Lu[1], Sonja Klebe[1], Ash Hocking[1], Andrew Rowland[1], Peter I. Mackenzie[1], Ross I. McKinnon[1] and Robyn Meech[1]

[1] College of Medicine and Public Health, Flinders University, Adelaide, SA

The remainder of the Chapter represents original content that has not been submitted for publication.

4.1. Introduction

4.1.1. Glucuronidation as a Possible Mechanism of Anthracycline Resistance

Therapeutic resistance may be intrinsic or acquired during treatment and is a major barrier in cancer treatment. Mechanisms of drug resistance may be pharmacodynamic (alterations in drug targets), pharmacokinetic (alterations in drug exposure), or involve epigenetic shifts in cell state such as stemness and quiescence (Borst, 2012). These mechanisms are not mutually exclusive. The focus of this Chapter is anthracycline resistance, which has the potential to significantly impair the efficacy of anthracycline-containing chemotherapy regimens used in breast cancer. While combination therapy reduces the acquisition of drug resistance (Vasan et al., 2019), anthracycline resistance is an ongoing clinical problem.

To address this problem, initial studies have focused on anthracycline resistance mechanisms circulating around drug efflux transporters, as reviewed by Nielsen et al. (1996). Due to their broad substrate specificity, drug efflux inhibition can be a challenging to implement clinically without leading to toxic effects from disrupting cellular processes (Robey et al., 2018). Thus, the shift has been necessitated to explore other pharmacodynamic targets, and more efficacious pharmacokinetic markers of drug resistance (McGuirk et al., 2021). As of yet, mechanisms other than drug efflux have yet to be well-studied within the context of epirubicin (to be described later). This Chapter aims to address this by focusing on some of the lesser-known pharmacokinetic mechanisms of epirubicin resistance.

As previously discussed in Chapters 1 and 3, epirubicin and epirubicinol are inactivated by glucuronidation (producing 4'-O-β-D-glucuronyl-epirubicin and 4'-O- β-D-glucuronyl-13-S-dihydroepirubicin) (Robert & Bui, 1992). Epirubicin glucuronide is the major metabolite in plasma

accounting for about 50% of the total drug AUC, and represents about one third of the drug found in urine 48 hours after a drug bolus (Cassinelli et al., 1984; FDA, 1999). UGT2B7 is reported to be the sole UGT isoform responsible for this metabolism (Innocenti et al., 2001). Published studies provide evidence that UGT2B7 activity may influence the clinical and cellular response to epirubicin. These publications include several studies that assessed associations between *UGT2B7* polymorphisms and clinical outcomes, and a single *in vitro* study performed on cancer cell lines. These studies are briefly described herein.

4.1.2. *UGT2B7* polymorphisms are associated with epirubicin treatment outcomes.

Several studies have shown that *UGT2B7* genetic polymorphisms are associated with epirubicin response and toxicity in clinical cohorts (Joy et al., 2021; Li et al., 2019; Mou et al., 2019; Parmar et al., 2011; Sawyer et al., 2016). These have been previously described in the Introduction (section 1.8). Most relevantly for this Chapter, a *UGT2B7* promoter SNP (-161 C>T) has been well studied in the context of non-metastatic breast cancer patients receiving FEC (5-fluorouracil 500 mg/m^2, epirubicin 100 mg/m^2, cyclophosphamide 500 mg/m^2). From the aggregated studies; genotypes possessing the T allele have increased epirubicin clearance (Sawyer et al., 2016), reduced risk of leukopenia and cardiotoxicity , and are therefore associated with a higher risk of early disease recurrence (2-year recurrence-free survival; RFS) (RFS by *UGT2B7* -161 genotype: CC=96%, CT=92%, and TT=81%) (Sawyer et al., 2016). This study suggested that UGT2B7 expression level could be a determinant of epirubicin efficacy and toxicity *in vivo*. The effects of the SNP on expression would be expected to occur in a range of tissues in which UGT2B7 is normally expressed. This includes the major organs of elimination (liver, kidney, and intestine), as well as other tissues including the tumour itself. Reduced expression of UGT2B7 in liver may be expected to increase systemic drug exposure and could therefore explain the increased incidence of systemic side effects such as

leukopenia. Delayed disease recurrence may also result from higher levels of systemic exposure and hence higher levels of tumour exposure. However, some studies of polymorphisms that alter UGT2B7 activity report altered epirubicin clearance but minimal change in steady state serum levels. This may be because of the infrequent dosing regimen and rapid distribution into tissues (Robert, 1993, 1994). Epirubicin has a triphasic clearance profile consisting of initial, intermediate and terminal elimination phases of 3 mins, 1 hour and 30 hours, respectively, and its concentration is reported to be high in extrahepatic tissues (Robert, 1993). A distribution study by Italia et al. (1983) found that epirubicin accumulated to varying levels in most tissues including tumours, which may be related to its DNA-binding ability. Overall, these features of epirubicin distribution suggest that intratumoral metabolism may be at least as relevant to its anti-cancer efficacy as hepatic clearance. As discussed below, there are currently limited studies on the importance of UGT2B7 activity within cancer cells.

4.1.3. Intratumoral UGT2B7 levels may control the cellular response to epirubicin.

As previously mentioned in Chapters 1 and 3, there is a single published study examining whether UGT2B7 expression within cancer cells may be a determinant of epirubicin sensitivity. This study by Dellinger et al. (2012), first showed that epirubicin can induce UGT2B7 mRNA expression in cultured metastatic melanoma cells. They then used short-hairpin (sh) RNA, to knockdown UGT2B7 expression by ~60% in the WM115 melanoma cell line. This sensitized the cells to epirubicin, as evident by a change in IC50 from ~218 μM to ~152 μM. Interestingly, the cells were also sensitised to doxorubicin, an epimer of epirubicin (Mordente et al., 2009). Epirubicin is not directly glucuronidated, however, one of its common metabolites (4-O-demethyl-7-deoxydoxorubinolone) has been shown to be glucuronidated. Relative to epirubicin metabolism, glucuronidation is not considered a major pathway for doxorubicin systemic clearance, with the 4-O-demethyl-7-

deoxydoxorubinolone-O-glucuronide accounting for only ~12% of the doxorubicin metabolites excreted in urine (Takanashi & Bachur, 1976). It is currently unknown whether UGT2B7, or a different UGT, is responsible for the production of this doxorubicin metabolite glucuronide. Overall, the Dellinger et al. (2012) study suggested that inhibition of intratumoral drug glucuronidation may be one approach to overcoming anthracycline resistance in the context of melanoma where anthracyclines are poorly effective in due to a high level of intrinsic resistance (Licarete et al., 2020).

UGT2B7 expression within cancer cells might contribute to epirubicin resistance in two ways. First, intrinsically high expression levels may cause reduced intratumoral exposure from the initiation of treatment. Second, because epirubicin treatment induces UGT2B7 expression, it could promote acquisition of resistance in previously sensitive cells during the course of treatment. The model of interest in this project was breast cancer. As shown in Chapter 3, we found that UGT2B7 showed higher intrinsic expression in TNBC subtypes (using both clinical data from the TCGA and breast cancer cell lines) than in hormone-receptor positive subtypes. We also found that UGT2B7 could be induced in both p53 wildtype and mutant breast cancer cell lines.

We hypothesized that intratumoral induction of UGT2B7 expression by epirubicin could contribute to acquisition of epirubicin resistance in breast cancer. In this Chapter, we address this possibility using breast cancer cell line models with UGT2B7 perturbation. In addition, we use RNAseq and clinical data from the TCGA to examine whether there is any association between UGT2B7 mRNA level within tumours, and outcomes for breast cancer patients treated with epirubicin and other drugs. To our knowledge, this is first reported analysis of such associations using these datasets.

4.1.4. Perturbation models to examine the role of UGT2B7 in epirubicin resistance.

In this study we attempted to create both UGT2B7 gain of function (GOF) and loss of function (LOF) models in breast cancer cell lines. GOF models (also called overexpression models) were generated in two different breast cancer cell lines using conventional transgenic overexpression methods. The effects of UGT2B7 on epirubicin clearance and toxicity were then assessed using various *in vitro* assays (Results 4.3.2). The development of UGT2B7 LOF breast cancer models proved to be much more challenging, with **four** different approaches being tested: CRISPR-Cas9 (Results 4.3.4), CRISPRi (Results 4.3.5), siRNA (Results 4.3.6), and dominant-negative inhibition (Results 4.3.7). The basis of these various technologies are described below.

4.1.5. CRISPR-Cas9 and CRISPRi

Clustered regularly interspaced short palindromic repeats (CRISPR) is genomic editing technology originating from the prokaryotic innate immune response (Barrangou, 2015). The CRISPR system uses an endonuclease called CRISPR-associated protein 9 (Cas9) that is directed to the target DNA region of interest by a specific RNA sequence called the guideRNA (gRNA). The guideRNA contains two main regions, the crispr RNA (crRNA) (specific targeting sequence), and a scaffold or tracr RNA which enables binding of the Cas9 complex (Allen et al., 2020). When these regions are fused together and they are referred to as single guide RNA (sgRNA) (Dang et al., 2015). After the sgRNA directs the CRISPR complex to the target DNA sequence, Cas9 generates a double stranded break (DSB) (Ran et al., 2013). CRISPR-Cas9 can be used to generate insertions/deletions (indels) by allowing the DSB to undergo the endogenous DNA repair process known as non-homologous end joining (NHEJ). This process can result in frameshift mutations which can trigger nonsense-mediated decay of the mRNA and hence ablate gene function (Kruminis-Kaszkiel et al., 2018; Tuladhar et al.,

2019). Alternatively CRISPR-Cas9 can be coupled to homology directed repair (HDR) by introducing a repair template allowing more precisely targeted modifications (Ran et al., 2013). These processes have been summarised in Figure 4.1.

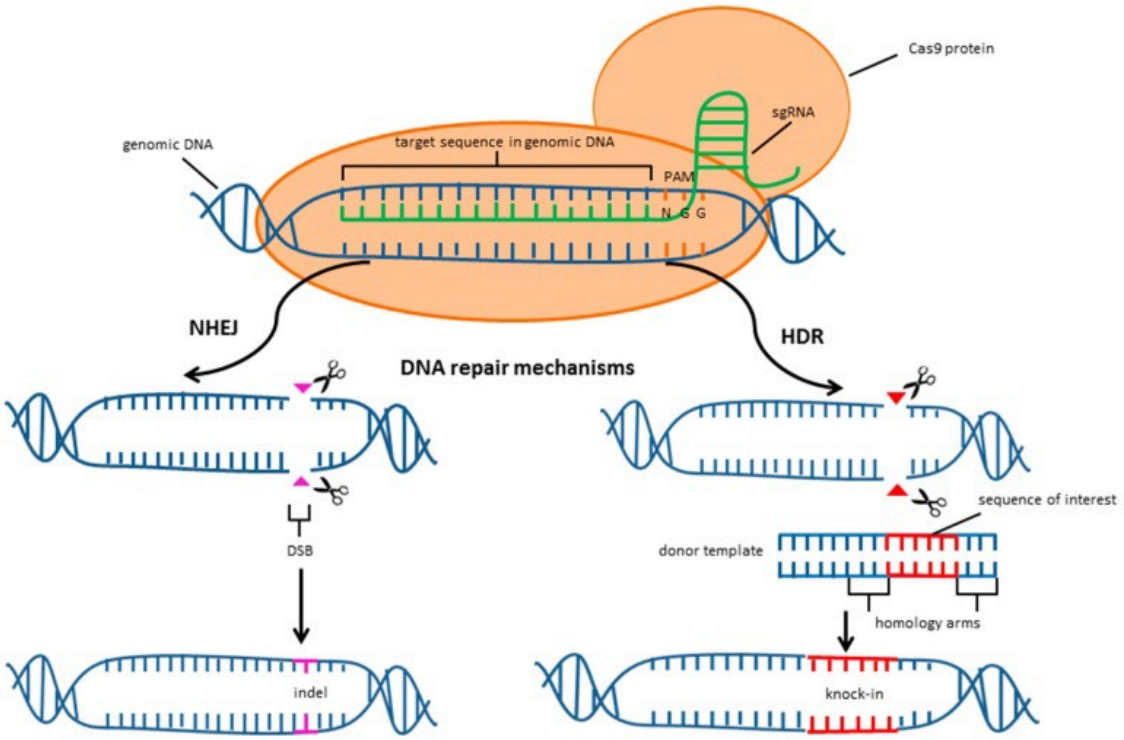

Figure 4.1. The CRISPR-Cas9 system is able to utilise sgRNA to guide and bind the Cas9 complex to the target sequence to effectively introduce endonuclease activity (double-stranded breaks) and direct either non-homologous end joining (NHEJ) to knock-out gene function, or homology directed repair (HDR) to insert a repair template for knock-in. Figure has been reproduced from Kruminis-Kaszkiel et al. (2018) under open access permissions.

The CRISPR system can also be used for gene regulation and epigenetic manipulation. By tandem mutations in both catalytic domains of SpCas9, a variant called dCas9 has been produced that cannot cleave DNA (Adli, 2018). dCas9 binds to the target site and may inhibit the recruitment of transcription factors and RNA polymerases (Adli, 2018). Fusion of transcriptional repressor protein domains such as the Kruppel-associated Box (KRAB) to dCas9 allows site specific recruitment of co-repressors to provide stronger, more reliable repression (Gilbert et al., 2013). Using dCas9 to epigenetically silence gene regulation is known as CRISPR interference (CRISPRi).

A key component of successful CRISPR or CRISPRi experiments is the design of the sgRNA guide sequence. Guide design is usually optimised using tools that predict the cutting efficiency and minimize potential off-target cleavage. Previously in our laboratory, twos gRNAs targeting UGT2B7 had been designed, cloned into a CRISPR-Cas9 expression vector, and tested in HepG2 cells. The first sgRNA targeted exon 1 of *UGT2B7*, the second sgRNA targeted the *UGT2B7* promoter region at the p53 binding site. These CRISPR-Cas9 vectors were transfected into HepG2 cells and stable clonal lines were derived by puromycin selection. Clones were characterized by sequencing to identify indels (insertion/deletion) at the targeted site on each of the two *UGT2B7* alleles. This analysis showed that both constructs could create indels. In the case of the exon 1-targeting construct (hereafter referred to as Cas9-UGT2B7-ex1) some of these indels caused frameshifts within the coding region, leading to loss of functional UGT2B7 expression. An example of a successfully CRISPR-modified HepG2 clone is shown in Figure 4.2. The frame-shifting indel in this clone completely ablated basal UGT2B7 expression and prevented the re-expression of UGT2B7 by epirubicin, as shown via immunoblotting and glucuronidation assays using morphine as a UGT2B7-selective probe-substrate (Figure 4.2B).

Other prior work in this laboratory using CRISPR-Cas9 in breast cancer cell lines identified a limitation of the stable clonal selection process. It was observed that many individual clones that carried the integrated CRISPR-Cas9 vector had altered growth phenotypes that were independent of the presence of any indel at the target site. These phenotypic changes were likely 'integration artefacts' that are due to disruption of unknown genes at the vector integration site, rather than disruption of the targeted gene. There are two potential approaches to overcoming these artefacts: 1) using 'hit-and-run' CRISPR; 2) using CRISPRi methods that do not require clonal selection. In 'hit-and-run' CRISPR, the CRISPR-Cas9 vector is expressed only transiently rather than integrated into

the genome. Cell lines with targeted gene disruption generated by this approach are also called ‘scarless’ knockouts. The challenge of this approach is that the probability of an indel being generated during the short window of transient expression is lower than in stable expression system.

CRISPRi methods do not cause gene mutation but instead cause epigenetic silencing of expression. This method does not require selection and genetic validation of individual clones. Instead, a polyclonal population of integrants with different vector integration sites can be used. The polyclonal approach generally dilutes the effects of individual deleterious integration artefacts. In the present project, pre-validated UGT2B7-taregtting sgRNAs were used to attempt to introduce indels in a breast cancer cell line using the ‘hit-and-run’ CRISPR-Cas9 approach. In addition, we used the polyclonal CRISPRi approach to attempt to epigenetically silence UGT2B7 expression.

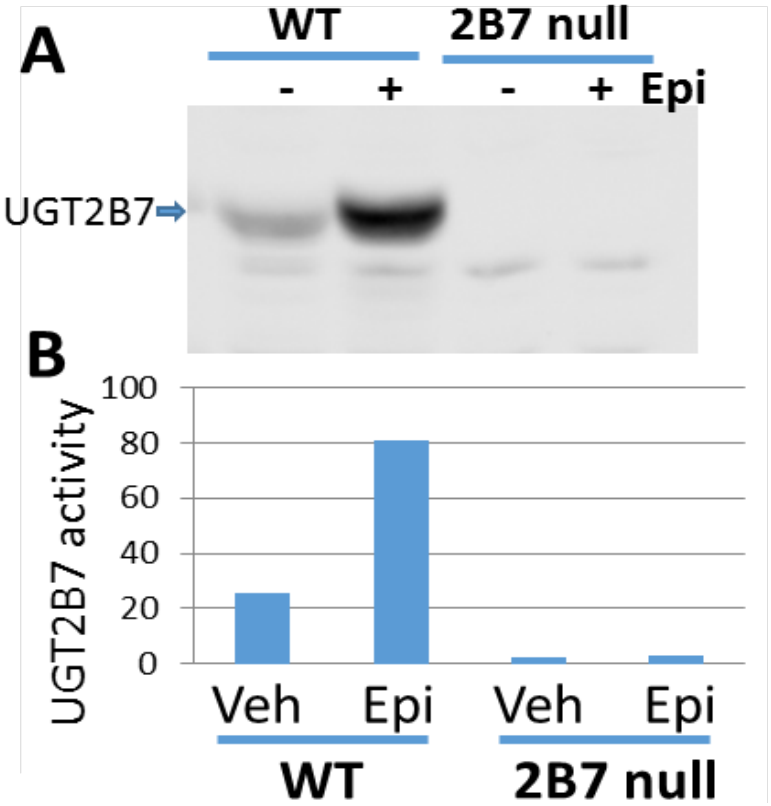

Figure 4.2. (A) *UGT2B7* exon 1 targeting CRISPR sgRNA ablated UGT2B7 protein expression and prevented induction of UGT2B7 by epirubicin in HepG2 cells. **(B)** UGT2B7 morphine-3 glucuronidation activity was essentially abolished by CRISPR knockout . Experiments performed by Dr. Lu Lu (Clinical Pharmacology, Flinders University, Australia).

4.1.6. Short interfering RNAs (siRNAs)

siRNAs are non-coding single-stranded small RNAs between 20-30 nucleotides in length (Dana et al., 2017). siRNAs act as a guide for the RNA-induced silencing complex (RISC), which is able to recognise and bind the complementary sequence in mRNA, leading to inhibition of translation and/or mRNA degradation, and therefore gene silencing (Neumeier & Meister, 2021). Appropriate design of the siRNA sequence is important in achieving efficient gene-knockdown with minimal off target effects. Various tools and software are available for designing specific siRNA, with algorithms typically considering factors such as the affinity for RISC binding to mRNA, siRNA stability, target accessibility, sequence length, and the structural importance of positioning of nucleotides (Pei & Tuschl, 2006).

To obviate the need for this process in the present study, we used a pre-validated UGT2B7-targetting siRNA sequence from literature. This siRNA sequence had been reported to produce 75% inhibition of UGT2B7 mRNA expression and ~44% inhibition of UGT2B7-specific activity in human hepatocytes by Konopnicki et al. (2013).

4.1.7. Dominant-negative enzyme inhibition

An extensive body of literature (reviewed by Hu et al. (2019a)),shows that UGT enzymes form homo- and heterodimers. Moreover, dimerization of active wildtype UGTs with inactive variants has been shown to impair the activity of the former. This process is referred to as dominant-negative inhibition (DN-inhibition) of activity. Many inactive UGT variants are produced naturally by alternative splicing (Tourancheau et al., 2016). Our laboratory previously identified alternative transcripts of the *UGT2B15* and *UGT2B17* genes that produce inactive C-terminally truncated proteins (Hu et al., 2018). Moreover, these truncated proteins could dimerize with full length wildtype UGTs in cells to inhibit their activities. Importantly, they were shown to heterodimerize with UGT2B7 and inhibit its activity by more than 70% (see Figure 4.3 A & B). In this Chapter, we employed the truncated form of UGT2B15 as a tool to induce DN-inhibition of UGT2B7 activity in breast cancer cells.

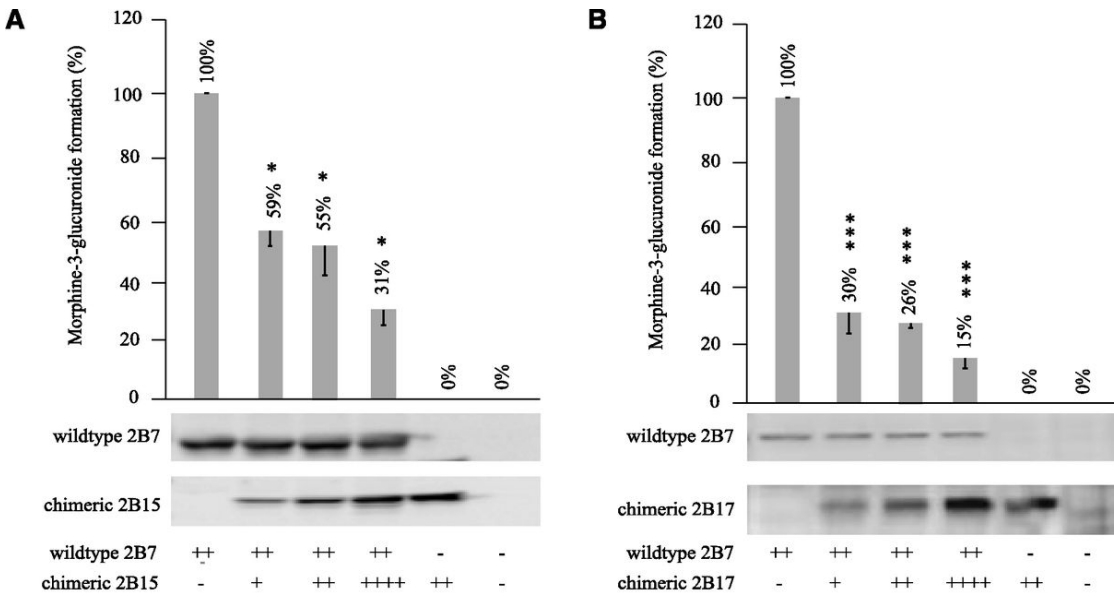

Figure 4.3. Chimeric (truncated) *UGT2B15* and *UGT2B17* variants reduce activity of wildtype (WT) UGT2B7 as assessed using the probe substrate morphine. This inhibitory effect increases in a dose dependant manner. Relative expression from transfection of UGT variant isoforms is indicated by +/-. Figure has been adapted with permission from Hu et al. (2018).

4.1.8. Assays for Measuring Cytotoxic Drug Sensitivity in Cancer Cells

4.1.8.1. Short-term assays

There are many different approaches available to measure the sensitivity of cancer cells to cytotoxic drugs. These assays may be performed *in vitro* using cell lines or primary cells, or *in vivo*, with a common example being the use of xenograft models in mice.

Short term in-vitro cell-line based assays are used to generate dose-response curves that measure the desired pharmacological effect of drugs by either measuring biological response in the form of the half-maximal effective concentration (EC50) (Brooks et al., 2019) or measuring the inhibitory/cytotoxic potential of the drug in the form of the half-maximal inhibitory concentration (IC50) (Larsson et al., 2020). The specified protocols can differ depending on the desired objective of the drug (Sebaugh, 2011). When testing anti-cancer drugs (e.g. cytotoxics), evaluation of potency

typically involves drug-dose response assays in the form of 2D cell culture, wherein the cultured cells are exposed to the drug in incremental doses for up to 72 hours and the cell viability is measured using various cell viability techniques (Larsson et al., 2020). Changes in viable cell numbers can indicate inhibition of cell growth, or cell death. There are several other available rapid screening assays which indirectly measure cell viability by active cellular metabolism (including other colourimetric, fluorometic, luminometric, or dye exclusion assays) (Kamiloglu et al., 2020).

Cells can be counted directly, or by quantifying the incorporation of dyes such as crystal violet (hexamethyl pararosaniline chloride), which binds to cellular proteins and DNA. In the crystal violet assay, dead cells are separated from viable cells by a washing step that exploits their differential adherence to the plate (Feoktistova et al., 2016). Given this method of staining measures the loss of adherence of cells, during cell death this does limit the applicability of this assay to only adherent cell types.

Assays that measure metabolic activity include the colourimetric MTT assay. MTT (3-(4,5-dimethylthiazol-2-yl)-2,5-diphenyltetrazolium bromide) is reduced to formazan only in living cells (Riss et al., 2004). Due to this, it can directly reflect cell mitochondrial health, which is quite versatile as it is applicable to both adherent and non-adherent cell types (Özlem Sultan, 2017). By the addition of DMSO, this method also allows for the solubilisation of formazan crystals in an aqueous solution, which improves the throughput, simplicity, and sensitivity of this assay (Benov, 2021). By combination of these factors, owing to the robust nature of the assay, this has been well established as the gold-standard for drug cytotoxicity studies (van Tonder et al., 2015), which has lead to the selection of this assay in our study to measure short term drug effects.

4.1.8.2. Long-term assays and competition assays

While short-term drug-treatment assays have advantages of speed and scalability, they are may not adequately reflect tumour biology. Clinical chemotherapy regimens typically involve long-term and/or repeated intermittent treatments. Tumours and residual cancer cells that survive the course of treatment may have acquired genetic, epigenetic, and phenotypic changes that can contribute to drug resistance. Long-term assays provide a capacity to assess these changes in the cell population over time. While there is no consensus protocol so far adapted for routine preclinical research, long-term cell viability assays can use 2D (monolayer culture) and 3D (e.g. organoids or spheroids) cell culture methods, the latter better replicating the tumour environment, and may involve repeated cell passaging (Lippert et al., 2011).

To identify the effects of gene perturbation on cell proliferation or survival under drug treatment, it is typical to compare the perturbed and control cell lines in parallel (e.g. in multiwell plates). However, an alternative approach is to combine the modified and control cell types in a co-culture and then measure competition between them. This type of assay can better mimic the natural heterogeneity of tumours and assess whether the gene perturbation provides a selective advantage or disadvantage under various treatment conditions. Co-cultures can also be performed over an extended period by repeatedly passaging the co-cultured cells. Long-term competition assays may be able to detect subtle effects on cell fitness (for example, a small selective advantage of modified cells under drug selection), due to a compounding effect of small shifts in the composition of the population over time. Competition assays require a method to accurately quantify the relative proportions of the different cell types within the co-culture. This may be achieved by tagging the cells with different markers that can be visualized, such as fluorescent proteins, or by using PCR or sequencing methods to quantify genetic markers that differ between the cell types. In this Chapter,

we used both short-term growth/survival assays, and long-term competition assays, to assess the effects of UGT2B7 overexpression on sensitivity to epirubicin.

4.1.9. Aims of Chapter 4

1. Create breast cancer cell lines that stably overexpress UGT2B7 and validate the expression at mRNA, protein, and activity levels.

2. Determine whether UGT2B7 overexpression changes the sensitivity of breast cancer cells to epirubicin in short-term growth assays and long-term competition assays.

3. Develop methods for inhibition of UGT2B7 expression in breast cancer cell lines.

4. Examine whether intratumoural UGT2B7 expression levels correlate with breast cancer outcomes using TCGA-BRCA RNAseq datasets

4.2. Materials and Methods

4.2.1. Materials and chemical information

Analytical grade chemicals including epirubicin hydrochloride, and uridine 5'-diphosphoglucuronic acid (UDPGA) ammonium salt were purchased from Sigma-Aldrich (St. Louis., Missouri).

The pSpCas9(BB)-2A-Puro (PX459) V2.0 plasmid was from Addgene (#62988). This is a newer generation vector containing a mutant Cas9 D10A nickase which is optimized to improve specificity in targeting the intended locus and to generate a higher frequency of double stranded breaks to knockout both target alleles (Ran et al., 2013). The pEF1-IRES-puro (pIRES) backbone containing UGT2B7 cDNA (pIRES-UGT2B7) was originally gifted by Lewis et al. (2011) (Appendix Figure 1). Other vectors were constructed in the laboratory during the project.

4.2.2. Generation of stable UGT2B7 overexpression cell lines

MDA-MB-231 and ZR-75-1 cell lines were cultured as described in Methods 2.2.1. MDA-MB-231 and ZR-75-1 cells were each seeded in 6-well plates at $6.25*10^5$ cells/well and transfected with 2.5 μg of pIRES-UGT2B7 or pIRES control plasmids (previously described; Lewis et al. (2011)), using Lipofectamine LTX. To select for plasmid integration, while undergoing regular passaging, cells were incrementally exposed to increasing concentrations of puromycin dihydrochloride, until cell death was no longer observed. Subsequentially, the cell lines were maintained at highest, stable, concentrations of puromycin dihydrochloride at 0.50 μg/mL and 0.56 μg/mL for MDA-MB-231 and ZR-75-1 lines respectively.

4.2.3. Western Blotting

Western blots were performed from whole cell lysates in RIPA buffer as previously described in 2.2.18. Protein quantity was estimated using the Bio-Rad protein assay dye (see Methods 2.2.11). 100 μg of protein was separated using SDS-PAGE (10%) and blotted onto nitrocellulose membrane. Membranes were probed for UGT2B15 and UGT2B15 chimera proteins using our own rabbit anti-UGT2B15/UGT2B17 antibodies. These antibodies show no cross reactivity with other UGT2B enzymes (Wijayakumara et al., 2015). Membranes were treated with SuperSignal West Pico PLUS Chemiluminescent Substrate (Thermofisher Scientific) and imaged using the ImageQuant LAS 4000 (GE Healthcare).

4.2.4. Epirubicin glucuronidation assays

Epirubicin glucuronidation activity assays were performed using 200 μg of total protein from ZR-75-1 cells lysed in TE buffer. The incubation conditions were consistent with the protocol detailed in 2.2.19.

4.2.5. Liquid Chromatography Mass Spectrometry (LC-MS) Spectral Analysis of Peptide Prescence from Cell lysates

TE lysates were prepared from T25 flasks of ZR-75-1 cells transfected with siRNA (see 4.3.6). Fifty micrograms of total protein was cleaved at tryptic amino acid residues overnight, before analysing UGT2B7 peptide levels using the tandem Triple Quadrupole LC/MS 6495C by Agilent Technologies as detailed in Chapter 2 (Methods 2.2.20).

4.2.6. Cell viability assays.

MDA-MB-231 and ZR-75-1 cell lines overexpressing UGT2B7, and control lines were evaluated for epirubicin sensitivity using cellular viability assays. Six replicate wells for each treatment and cell line were seeded at $8*10^3$ cells per well in a 96 well plate, then treated with epirubicin at doses of 0 (ethanol vehicle control), 20, 50, 100, 200, 400 and 800 nM, for 72 hours. Following drug treatment, 20 µL of 5 mg/mL thiazolyl blue tetrazolium bromide (MTT) (Sigma-Aldrich) reagent was added to each well and incubated at 37°C for 3.5 hours. Culture medium was removed and 150 µL of MTT solvent (4 mM HCl, 0.1% NP40 in isopropanol) was added to the stained cells and incubated for 15 minutes. Absorbance at 590 nm was measured on the DTX 880 Multimode Detector (Beckman Coulter).

4.2.7. Long-term epirubicin selection assays

MDA-MB-231 cells stably expressing UGT2B7 (as used in the cell viability assays) were co-seeded in T25 flasks along with MDA-MB-231 IRES (control line) cells with matching proportions of cells (each at $6.25*10^5$). These were subjected to treatment of 400 nM epirubicin (i.e. approximately IC90) (or vehicle – ethanol) for 48 hours to induce cytotoxic effects on day 0 and day 28 to further assess competitive advantages over a total period of 41 days. Periodic harvesting of cells was done at each

cell passage (including at the initial seeding) (see 2.2.1 for more details), where 1/5th cell volume was carried over to a new flask, while the remaining cell supernatant was centrifuged at 2,000 rpm for 5 minutes and the pellet was retrieved and stored at -20°C for isolation of genomic DNA (gDNA) (see 2.2.9). qRT-PCR (as per 3.2.2) using primers specific to IRES and UGT2B7 plasmids (see 4.2.15 for sequences) were performed on the isolated gDNA. These shared a common reverse primer (IRES plasmid Reverse), with the forward primers differing to selectively amplify either plasmid. Relative plasmid ratios (expressed as UGT2B7% relative to IRES) were used to determine the proportion of the different cell line populations (i.e. IRES or UGT2B7 stable cells) at various time points. Lesser gDNA samples were obtained in the epirubicin treated population due to less frequent passaging (compared to vehicle), from cytotoxicity impaired growth.

4.2.8. CRISPR and CRISPRi constructs

UGT2B7 CRISPR plasmids (targeting *UGT2B7* exon 1 or the proximal promoter p53 site) were previously cloned by Dr Lu Lu (Clinical Pharmacology, Flinders University, Australia). The pSpCas9(BB)-2A-Puro (PX459) vector backbone developed by Feng Zhang (Addgene #62988) was used: Cas9 and puromycin resistance gene (PAC) are expressed as a continuous polypeptide, cleaved into two discrete proteins via the 2A self-cleaving peptide. The guide RNA was inserted at the guide RNA scaffold and its expression is driven by the U6 promoter. The plasmid map is shown in Appendix Figure 3. The sgRNA sequences used in the different constructs are listed in 4.2.15.

The px459 KRABdCas9_2A_PAC 2xU6sgRNA CRISPRi plasmid (see Appendix Figure 4 for map) expresses catalytically inactive dCas9 fused to a KRAB repressor domain and PAC as a continuous polypeptide, cleaved into two discrete proteins via the 2A self-cleaving peptide. This vector was constructed in our laboratory by Prof. Robyn Meech. The px459 KRABdCas9_2A_PAC 2xU6sgRNA

plasmid was used to express two different sgRNA simultaneously. To clone the two sgRNA sequences, the sgRNA oligonucleotides were first cloned into separate px459 KRABdCas9_2A_PAC vector backbones at the BbsI site, creating two vectors with a single sgRNA in each. The U6 promoter and sgRNA cassette was then digested from one vector and ligated into the XbaI site in the vector containing the other U6/sgRNA. This resulted in the px459 KRABdCas9_2A_PAC 2xU6sgRNA vector, with the two sgRNAs driven by separate U6 promoters.

4.2.9. Stable Expression and Selection of Chimeric UGT2B15 and CRISPR/CRISPRi cells

Stable cell lines expressing the chimeric UGT2B15 protein were generated in the lab by Quinn Martin (Clinical Pharmacology, Flinders University, Australia). Briefly, the *UGT2B15* chimeric cDNA was amplified from VCaP cells and cloned into pEF-IRESpuro6 (Hu et al., 2018). ZR-75-1 cells were transfected with 2.5 ug UGT2B15 chimera/IRES plasmids using 7.5 µL Lipofectamine LTX (Thermofisher Scientific) as per the manufacturer's instructions. Similarly, CRISPR cell lines were generated by transfecting px459 CRISPR/CRISPRi constructs (as described in 4.2.8) under the same conditions. In both cases, stable mixed populations were selected for with an initial puromycin concentration of 0.2 µg/mL. This was gradually increased to 0.5 µg/mL, which was maintained for ongoing growth. Expression of the chimeric UGT2B15 was confirmed by qRT-PCR using primers that span the pseudo exon that is spliced into this version of UGT2B15 (*UGT2B29P2* exon 1) replacing the wildtype exon 6. These primers are described below in 4.2.12 and the sequences are presented in 4.2.15.

4.2.10. siRNA Knockdown

ZR-75-1 cells were seeded at $6.25*10^5$ cells/well and reverse transfected in a 6-well plate using Lipofectamine 2000 (Thermofisher Scientific) as per the manufacturer's protocol. Transfections

were performed using 20 or 100 pmol concentrations of UGT2B7 siRNA (as per Konopnicki et al. (2013)) or equal concentrations of FAM-labelled negative control (NC) siRNA. Lipofectamine 2000 was added at a 1:10 siRNA (pmol) to Lipofectamine 2000 (µL) ratio (i.e., 10 µL Lipofectamine 2000 for 100 pmol siRNA). At 24 and 48 hours post transfection, cells were analysed to assess transfection efficiency, using an EVOS Fluorescent Microscope (Life Technologies) with a GFP filter set (470 nm excitation, 525 nm emission) and white light. At 48 hours post transfection, cells were harvested for RNA/proteomic analysis.

4.2.11. mRNA Extraction and Reverse Transcription

Total cell RNA was extracted from cell lines using TRIzol (Invitrogen) as per the manufacturer's protocol. Reverse transcription using Lucigen NxGen M-MuLV reagents was performed as described in 2.2.6, and the resulting cDNA was diluted 5-fold for use in qRT-PCR reactions.

4.2.12. Quantitative Real-Time Polymerase Chain Reaction (qRT-PCR)

Amplification of total UGT2B15 (wildtype and chimeric) and chimeric UGT2B15 from breast cancer cell lines was performed using GoTaq Mastermix (SYBR Green) under the reaction and cycling conditions previously detailed in 2.2.7.4. UGT2B7 expression was measured using specific qRT-PCR primers mentioned in Chapter 3. Standard curve serial dilutions were generated containing known copy numbers of the UGT2B7-IRES plasmid. This allowed for absolute quantification of UGT2B7 cDNA copy numbers in cell lines after UGT2B7 overexpression or knockdown.

UGT2B15 expression was measured using exon 1 spanning primers. Chimeric UGT2B15 was screened using UGT2B15 exon 5 and pseudogene *UGT29P2* exon 1 spanning primers 15E5-qPCR F and 29P2E1-qPCR R as previously referred to by Hu et al. (2018). All primer sequences have been listed in 4.2.15.

4.2.13. Screening of Insertion/Deletion (indel) Events by Sanger Sequence Analysis

Sanger Sequencing was provided by SouthPath and Flinders Sequencing Facility (SA Pathology, South Australia), as detailed in 2.2.7.5. Stable mixed ZR-75-1 CRISPR populations were treated with an inducer - sodium butyrate at a 1 mM concentration for 6 days and sequenced using UGT2B7 CRISPR screening primers (see 4.2.15). The sequence was compared to wildtype UGT2B7 in ZR-75-1 cells using ICE (Inference of CRISPR Edits) by Synthego (https://ice.synthego.com) to rapidly infer the estimated population percentage of insertion/deletion (indel) events from raw traces.

4.2.14. Analysis of TCGA-BRCA datasets

Clinical and genomic data contained within The Cancer Genome Atlas (TCGA) Breast Invasive Carcinoma (BRCA) project was accessed via the cBioPortal data portal (https://www.cbioportal.org) for analysis. The BRCA dataset was stratified by cancer subtype (Basal, Her2, Luminal A, Luminal B) using PAM50 classification. In addition, drug treatment data was obtained from the NCI Genomic Data Commons (https://gdc.cancer.gov/), and the TCGA-BRCA dataset was further stratified by treatment with either an anthracycline-containing regimen (epirubicin or doxorubicin) or a non-anthracycline-containing regimen (neither epirubicin or doxorubicin). For each group of interest, UGT2B7 mRNA expression levels derived from Illumina HiSeq (RSEM, z-scores relative to normal samples) and Overall Survival (OS) and Progression-Free Survival (PFS) data were downloaded via cBioPortal. The survival data include time to death (months) and status (living vs deceased for OS and progression vs censored for PFS). The gene expression and survival data were combined and processed into an appropriate format for analysis using the AutoRPA software (Xie et al. 2020). Default AutoRPA settings were used to construct prognostic staging models based on UGT2B7 expression levels. This process involved two steps, first the RPA algorithm determined whether

there was any partition that was prognostic of survival outcomes. If a partition (referred to as an expression cut-point) was identified, the model performance was assessed and a log rank test statistic determined. For ease of visualization, the Kaplan Meier (KM) plots were generated in cBioPortal using the expression cut-points determined by the RPA algorithm.

4.2.15. Sequences of qRT-PCR primers, Sequencing primers, and sgRNA, siRNA

Table 4.3. Sequences of qRT-PCR primers, Sequencing primers, and sgRNA, siRNA used in this study.

	Sequence (5'-3')
qRT-PCR	
IRES	CTCACTATAGGCTAGCCTCGAGAATT
IRES	CGGAATTGGGCTAGAGCGGC
UGT2B7	CAGAGATTTACCACCCAGTTCATGG
UGT2B7	AGTTGGAGAATTTCATCATGCAACAGA
UGT2B7	TCAGCCAGCAGCTCACCACAGGG
UGT2B15	GTGTTGGGAATATTATGACTACAGTAAC
UGT2B15	TCAGCCAGTAGCTCACCACAGGG
UGT2B15	AATGGCATCTATGAGGCG
UGT2B15	GGACATGTATTTAACATGCC
Sanger	
UGT2B7	TGCAACAGATTAAGAGATGGTCAGA
CRISPR	
UGT2B7	TGCTTTTCAAAAGTGTAGCC
UGT2B7	AATATATTGCATAAGACAGA
siRNA	
UGT2B7	CATTGAAGAGAGTAATTAA

4.3. Results

4.3.1. Development of MDA-MB-231 and ZR-75-1 cell lines stably overexpressing UGT2B7

To assess whether elevated UGT2B7 levels alter epirubicin sensitivity, GOF models were generated using MDA-MB-231 (TNBC) and ZR-75-1 (hormone receptor positive) breast cancer cell lines. The expression vector used carries a UGT2B7 cDNA sequence linked to puromycin acetyltransferase gene via an IRES element. This UGT2B7 expression vector, and the empty vector control (designated IRES in the data shown herein), were integrated into cells using standard transfection methods and selection for puromycin resistance (see 4.2.2). The emerging resistant colonies were allowed to combine in culture and the resulting stable cell lines are therefore polyclonal.

The UGT2B7-MDA-MB-231 and UGT2B7-ZR-75-1 UGT2B7-overexpression lines showed very high levels of exogenous UGT2B7 mRNA (1.2 - 2 x 10^6 copies per 10^9 copies of 18s) relative to the control lines (Figure 4.4A). We next used the UGT2B7 specific peptide assay developed in Chapter 3 to assess whether the amount of UGT2B7 protein was increased in the cell lines. The IRES-MDA-MB-231 control cell line had no detectable basal UGT2B7 protein in this assay, while the UGT2B7-MDA-MB-231 line showed high levels of over-expressed UGT2B7 protein (Figure 4.4B). In contrast to these results, the IRES-ZR-75-1 cell line had a modest basal level of UGT2B7 protein and the UGT2B7-ZR-75-1 stable line only showed a minor increase in in this level (approximately 1.7-fold increase). We also treated both the IRES-ZR-75-1 control and UGT2B7-ZR-75-1 overexpression lines with epirubicin. This showed that the level of UGT2B7 protein exogenously over-expressed in the UGT2B7-ZR-75-1 line was comparable to that induced by epirubicin in the IRES-ZR-75-1 control line (Figure 4.4B).

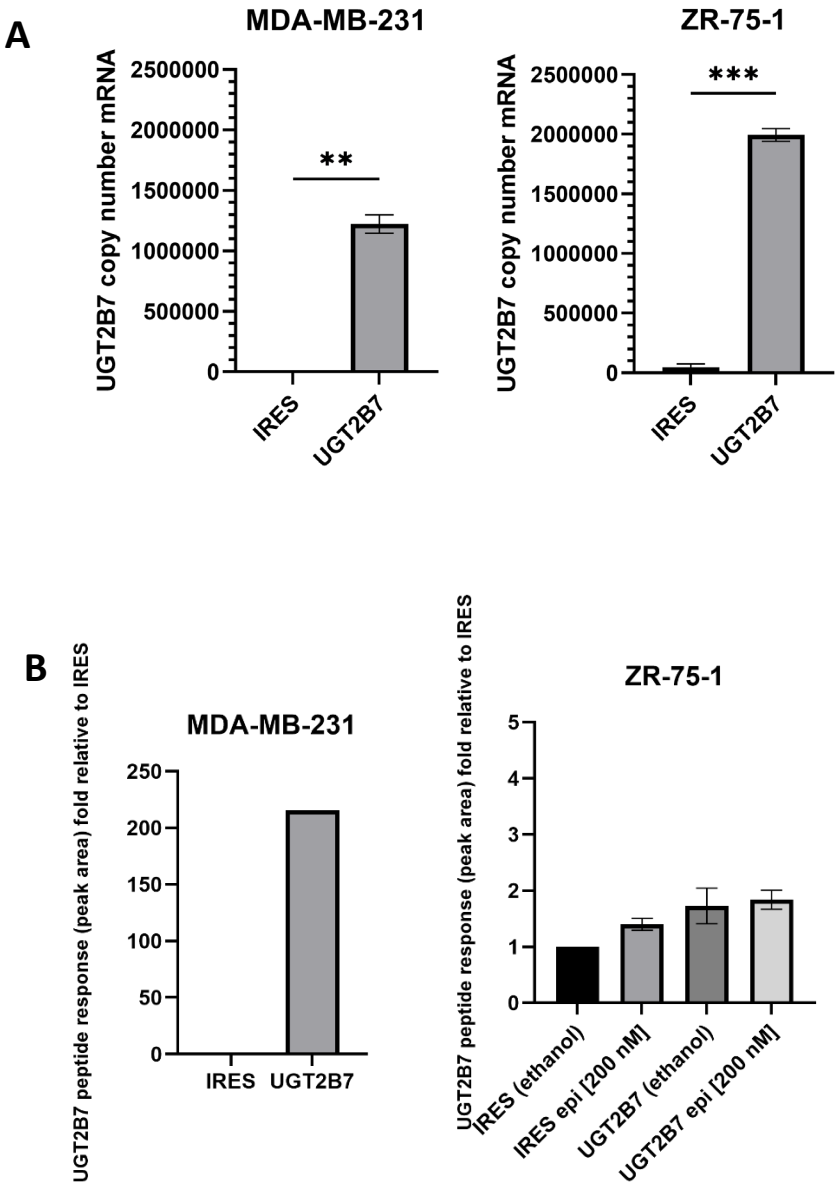

Figure 4.4. Characterization of MDA-MB-231 and ZR-75-1 UGT2B7-overexpression cell lines. (**A)** The level of UGT2B7 mRNA (copy number relative to 18S rRNA) was measured in cells stably transfected with UGT2B7 expression plasmid or the empty vector (IRES) by qRT-PCR. mRNA data consisted of two technical replicates from one biological replicate which then were analysed using a two-tailed unpaired t-test. Asterisks were used to indicate $P<0.05$. Error bars represent standard deviation. (**B)** The level of UGT2B7 protein was measured in the MDA-MB-231 and ZR-75-1 stable lines using a UGT2B7-specific peptide assay. The MDA-MB-231 peptide response is representative data, and therefore is a single biological replicate. ZR-75-1 Control and UGT2B7 lines were additionally treated with 200 nM epirubicin (epi) or vehicle (ethanol) to examine induction of UGT2B7 relative to overexpression. For the treated ZR-75-1 cell lines, a one-way ANOVA followed by a Šídák's multiple comparisons test was performed on a single biological replicate containing two technical replicates. Asterisk were used to denote $P<0.05$. Error bars represent standard deviation.

4.3.2. Elevated UGT2B7 expression promotes epirubicin metabolism and drug resistance in breast cancer cells *in vitro*

The ability of the UGT2B7-MDA-MB-231 overexpression line to metabolize epirubicin was examined using a newly developed highly specific LC-MS assay for epirubicin glucuronide (see Chapter 6 for details of the assay development). The UGT2B7-MDA-MB-231 line showed robust epirubicin glucuronidation activity (Figure 4.5A). The effect of UGT2B7-overexpression on epirubicin sensitivity was then assessed using MTT-based cell viability assays performed over 72 hours. Both the UGT2B7-MDA-MB-231 overexpression line and IRES-MDA-MB-231 control line showed dose-dependent toxicity; however, the UGT2B7-MDA-MB-231 line showed significantly higher cell viability at all epirubicin doses (Figure 4.5B). The half-maximal inhibitory concentration of epirubicin (IC50) was approximately 1.6-fold greater in the UGT2B7-MDA-MB-231 line than the control line (58.85 vs 27.5 nM; n = 4). Similar analyses were performed on the UGT2B7-ZR-75-1 overexpressing cell line compared to the IRES-ZR-75-1 control line. There was no significant difference in viability between the two ZR-75-1 cell lines when treated with a range of epirubicin doses (not shown). This might be due to low levels of exogenous UGT2B7 protein overexpression (see Figure 4.4).

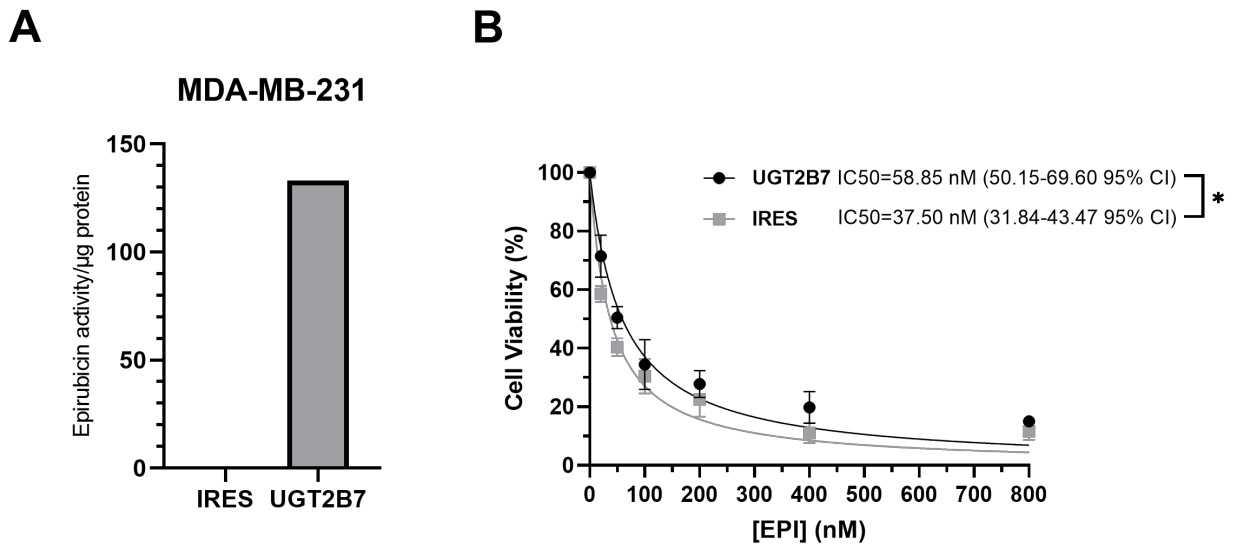

Figure 4.5. Overexpression of UGT2B7 in MDA-MB-231 cells increases epirubicin metabolism and promotes epirubicin resistance. **(A)** Epirubicin glucuronide production (pmol/min/µg protein) was measured in stable MDA-MB-231-UGT2B7 and control vector (IRES) lines. This is representative data and as such was performed in singlicate. **(B)** MDA-MB-231-UGT2B7 and control vector (IRES) lines were treated for 72 hours with epirubicin at a range of doses from 0 to 800 nM. Cell viability was quantified using an MTT asay. Data was plotted using non-linear regression analysis to calculate the half-maximal inhibitory concentration (IC50). The R^2 values for UGT2B7 and IRES were 0.9462 and 0.9593 respectively. The IC50 values calculated from each replicate (n=4) were analysed using a two-tailed unpaired t-test. *P=0.01. 95% confidence interval (95% CI) values are shown.

4.3.3. Assessment of the effect of elevated UGT2B7 expression on epirubicin resistance in long-term competition assays in breast cancer cells

To gain an insight on whether UGT2B7 overexpression gave breast cancer cells a long-term survival advantage, MDA-MB-231 UGT2B7 stable lines (as previously used) were co-cultured with IRES cells and subjected to epirubicin treatment over 4-week intervals, to mimic clinical chemotherapy application. Over a total period of 41 days, relative plasmid proportions were screened using qRT-PCR with cell-line specific markers to estimate population shift. This enables the determination of whether epirubicin treatment enriched the UGT2B7 expressing population, thus conferring elevated drug resistance. Indeed, the frequency of MDA-MB-231 cells

overexpressing UGT2B7 were consistently enriched by epirubicin treatment, as early as two days following the initial treatment (Figure 4.6). This is consistent with the experimental findings from the short-term cell viability assays, as discussed in the previous section. In the vehicle treated group, the UGT2B7 population was also enriched, indicating there is an inherent survival/growth advantage that occurs with overexpression of UGT2B7 without the selective pressure of a drug. This hinders the expected differences in population frequency between the two treatment groups.

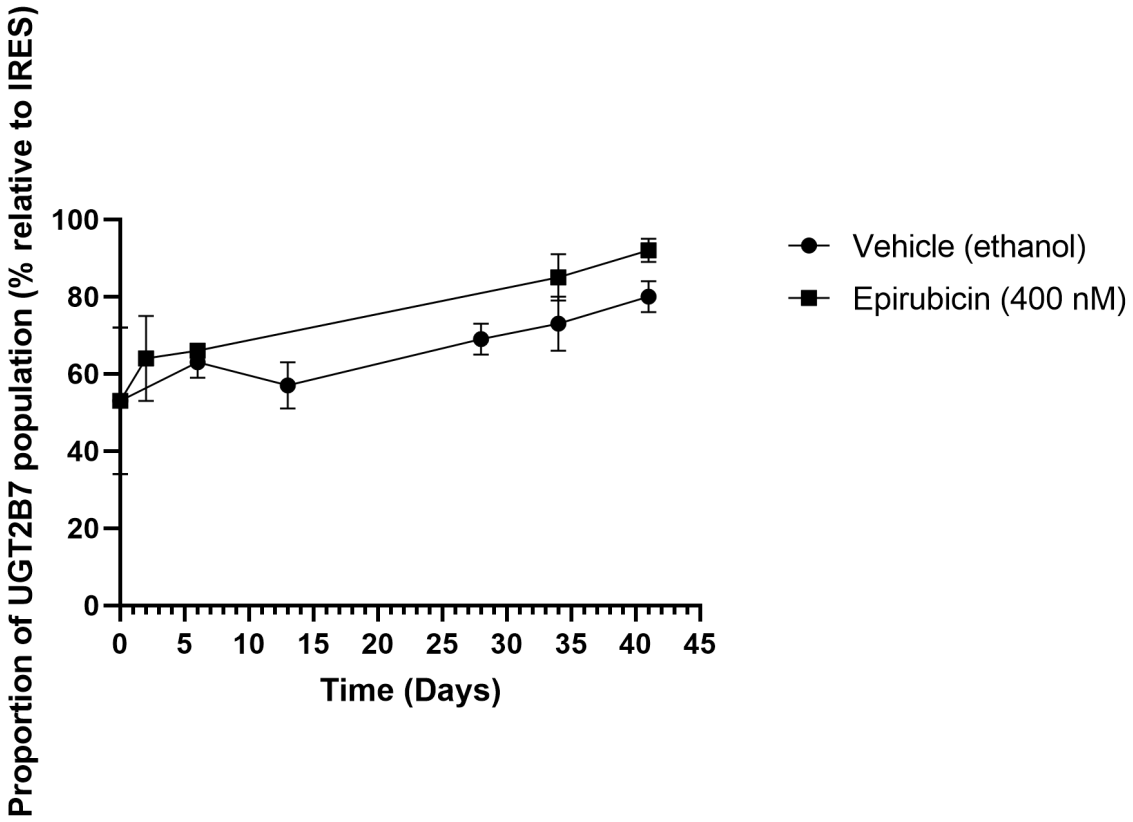

Figure 4.6. Epirubicin competition assay showing a slight long-term selective advantage of MDA-MB-231 cells stably expressing UGT2B7. A stable mixed population was established with a proportion of IRES (empty vector): UGT2B7 seeded at equal ratios. These were treated with 400 nM epirubicin (shown as squares), or the vehicle (ethanol) (shown as circles) on days 0 and 28. Treatment was sustained for a 48-hour period before removing the drug. Genomic DNA was harvested periodically as cells were passaged, and plasmid specific primers were used to differentiate the relative ratio of UGT2B7: IRES expressing cells (expressed as a relative percentage of UGT2B7 stable cells). UGT2B7 cells had an inherent survival advantage in the absence of epirubicin and outcompeted the IRES population, however generally the selective pressure of epirubicin treatment modestly enriched the UGT2B7 population. Two technical replicates of each population (i.e. two flasks for vehicle or epirubicin treated) were maintained for 41 days. Error bars represent standard error of the mean.

4.3.4. Transient and Stable expression of a UGT2B7-targetting CRISPR-Cas9 vector to produce indels in breast cancer cells

To complement the UGT2B7 GOF studies shown in Sections 4.3.1-4.3.2, we sought to develop UGT2B7 LOF models using CRISPR-Cas9 technology. As discussed in the Introduction, previous work in our laboratory had developed UGT2B7-targetting CRISPR-Cas9 vector constructs that successfully produced indels in stably transfected HepG2 cells (e.g. Figure 4.2).

In the present project, the vector targeting *UGT2B7* exon 1 (designated Cas9-UGT2B7-ex1) was used to attempt to introduce indels in UGT2B7 in the ZR-75-1 breast cancer cell line. To avoid integration artefacts that might produce phenotypic alterations (non-specific insertional mutagenesis), we attempted the 'hit-and-run' transient CRISPR-Cas9 approach to produce 'scarless' knockouts.

To test the effectiveness of the Cas9-UGT2B7-ex1 construct in ZR-75-1 cells, we first measured the frequency of indel events in a pool of cells that had been transfected with the vector. The cell population was treated with puromycin after transfection to enrich transfected cells. Genomic DNA was prepared from the cell pool and a region flanking the targeted site in exon 1 was amplified by PCR. The PCR products were subjected to Sanger sequencing. A commercial prediction tool from Synthego called Inference of CRISPR Edits (ICE) was used to estimate the frequency of indels. ICE compares the sequence obtained from unmodified cells to the sequence obtained from the CRISPR-modified cell pool. The comparison is performed within the region adjacent to the protospacer-adjacent motif, which is called the alignment window. Indel events are inferred within a region close to the predicted cut site (called the inference window). Separation between the traces for the control and CRISPR-targeted sequence chromatograms is called discordance. As shown in Figure 4.7A, there was discordance between the sequence of the UGT2B7 PCR product from unmodified

cells (orange trace) and from the CRISPR-pool (green trace). However, the ICE analysis of the UGT2B7 CRISPR pool predicted an indel frequency of only 5% (R^2=0.98) (Figure 4.7B).

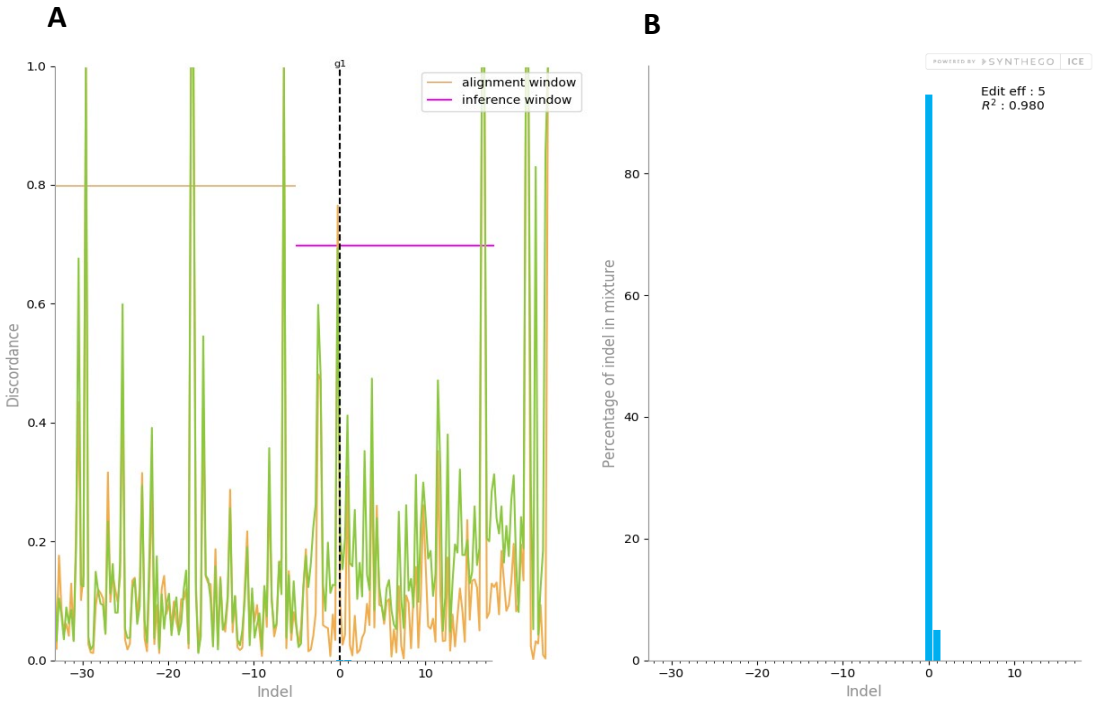

Figure 4.7. ICE analysis conducted on Sanger sequencing from genomic DNA from a ZR-75-1 mixed population expressing a CRISPR-px459 backbone with a sgRNA targeting exon 1 UGT2B7 . **(A)** A discordance plot displaying the level of alignment of the wildtype control (orange) and edited (green) traces relative to the sequence coordinates relative to the cut site. The positioning used for alignment is indicated by the alignment window, while the inference window shows the region around the cut site where deletion events are predicted. The cut site is shown as a black dotted line. **(B)** 5% indel efficiency is estimated in the CRISPR stable population compared to the control, wildtype ZR-75-1 sequence. The R^2 value (Pearson correlation coefficient) indicates goodness of fit of the edited trace relative to the control. A R^2>0.8 is considered sufficient for robust analysis. Figures have been cropped for improved clarity. Raw plots and sequences are available in Appendix Figure 6 and Appendix Figure 7. Analysis was performed using the Synthego ICE Analysis tool (v3) (2019).

The poor CRISPR efficiency was unexpected as UGT2B7 targeting had been previously successful in HepG2 cells. We therefore considered whether the *UGT2B7* locus was less accessible to the targeting complex in ZR-75-1 cells than in HepG2 cells. UGT2B7 expression is higher in HepG2 cells than in breast cancer cell lines (not shown). Low expression is often associated with relatively closed

chromatin, which is controlled by histone modifications. Highly acetylated chromatin is more open and accessible to transcription factors and other nuclear proteins. A known approach to increase histone acetylation is treatment with histone deacetylase inhibitor (HDACi) sodium butyrate. Hence, we treated the transfected cells with 1 mM sodium butyrate for 6 days and genomic PCR and sequencing was performed. Sodium butyrate treatment did appear to increase indel frequency when compared to the untreated population (Appendix Figure 8A, B); however, the increase was minor. Moreover, in this experiment the non-butyrate treated line showed no indels (0% efficiency, R^2=0.98), which was inconsistent with the previous experiment (Figure 4.7B).

Inconsistencies in indel prediction between experiments limits interpretation of the data. However, the overall conclusion was the Cas9-UGT2B7-ex1 vector did not produce a high frequency of indel events in ZR-75-1 cells, nor could it be greatly increased by epigenetic modification of chromatin. This suggested that 'hit-and-run' CRISPR-Cas9 was not likely to be a viable approach to making a LOF model in this cell type as it would be extremely laborious to screen for indels that occurred at 5% or lower frequency, considering that only a fraction of these indels would represent frameshifting events occurring on both alleles on the same cell.

4.3.5. CRISPR interference (CRISPRi) was unable to significantly repress the transcriptional induction of UGT2B7 in ZR-75-1 cells

We next tried to create a UGT2B7 LOF model using CRISPR interference (CRISPRi). This results in knockdown rather than knockout of gene function. Moreover, stable integration methods can be used with selection of a polyclonal population that reduces the impact of individual integration artefacts. A modified version of the CRISPR-Cas9 vector had been previously generated called px459 KRABdCas9_2A_PAC 2xU6sgRNA that uses a dCas9-KRAB repressor fusion protein to induce gene

repression. Two UGT2B7-targeting sgRNA sequences were cloned into the vector backbone: (1) the sgRNA that targets exon1 at a site 528 nt downstream of the translation start site; (2) a sgRNA that targets the proximal promoter p53 site located 290 nt upstream of the translation start site (Figure 4.8A). Using a two-step cloning approach described in the Methods (4.2.8), a double guide construct was generated that contained both sgRNAs, each under the control of their own U6 promoter. The resulting vector is herein referred to as UGT2B7-CRISPRi.

ZR-75-1 cells stably expressing UGT2B7-CRISPRi vector or an empty vector containing no sgRNA (control) were generated using standard transfection followed by transient puromycin selection as described in Methods 4.2.9. To validate that the polyclonal stable lines expressed the sgRNAs and the dCas9-KRAB fusion protein, RNA was prepared, and expression of these sequences was measured by qRT-PCR. Figure 4.8B shows validation of plasmid expression in the cell lines. The use of primers specific to one of a UGT2B7 sgRNAs demonstrated it was only present in the UGT2B7-CRISPRi cell line and not the control line, while dCas9 was present in both cell lines, as expected.

Following confirmation of plasmid expression, the cell lines were evaluated for basal UGT2B7 mRNA expression level, and UGT2B7 induction by epirubicin. Basal UGT2B7 expression was only detected in the control line Figure 4.8C. This suggests that the CRISPRi was functioning as expected and successfully repressed basal expression of UGT2B7. However, more importantly for planned experiments evaluating drug sensitivity, induction of UGT2B7 by epirubicin would need to be inhibited by CRISPRi. Following epirubicin treatment, the control line showed ~46-fold induction. Surprisingly, the UGT2B7-CRISPRi line showed greater induction of UGT2B7 expression following epirubicin treatment (Figure 4.8C). As the CRISPRi knockdown did not appear to inhibit UGT2B7 induction following treatment with epirubicin, this model was deemed not useful for further experiments.

A

B

Plasmid	qRT-PCR primer set	Cycle threshold (Ct)
Plasmid control	UGT2B7 sgRNA	N.D.
	dCas9	18.10
UGT2B7-CRISPRi	UGT2B7 sgRNA	27.12
	dCas9	17.68

C

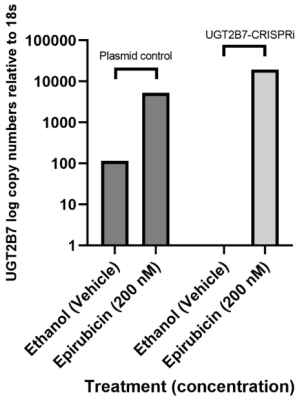

Figure 4.8. Upon confirmation of stable CRISPRi expression, CRISPRi was unable to repress UGT2B7 re-expression by epirubicin **. A.** A schematic map of the UGT2B7 CRISPR sgRNA target regions. The UGT2B7 CRISPR plasmid targets exon 1 (shown in yellow), while the UGT2B7 CRISPRi plasmid features dual sgRNAs targeting exon 1 and the p53 (shown in blue) responsive element (shown in orange). Genomic coordinates are shown in brackets relative to the translation start site (TSS). **B.** qRT-PCR validation of stable expression of the CRISPRi knockdown plasmid, UGT2B7-CRISPRi, and the respective control plasmid with the absence of sgRNAs. The screening primers and corresponding cycle threshold (Ct) mark the broad plasmid detection (dCas9 spanning) and specific detection (UGT2B7 sgRNA spanning) of the transfected plasmids. N.D. denotes no amplification detected within the threshold of quantification. **C**. qRT-PCR of absolute basal and induced UGT2B7 expression in the UGT2B7-CRISPRi cell line, and the control cell line with absent sgRNAs. UGT2B7 was repressed in the UGT2B7-CRISPRi line, however re-expression by 200 nM epirubicin treatment was unable to be inhibited. Cell lines were treated with epirubicin or the ethanol vehicle control for 24 hours. Absolute copy numbers of UGT2B7 were normalised to 18S and displayed on a log scale. Data is representative of 1 biological replicate.

4.3.6. Small interfering RNA (siRNA) did not reduce UGT2B7 mRNA levels in ZR-75-1 cells

As discussed in 4.1.6, previous literature has validated knockdown of UGT2B7 by siRNA (Konopnicki et al., 2013). Although this approach would not provide stable gene knockdown for long-term assays, successful transient knockdown of UGT2B7 would still provide a model suitable for assessing short term changes in drug sensitivity. siRNA corresponding to those reported by Konopnicki et al. (2013) were transfected into ZR-75-1 cells using standard transfection methods. To assess the

efficiency of the protocol, 20 or 100 pmol of a FAM-labelled negative control siRNA was transfected and FAM fluorescence was assessed by fluorescence microscopy at 24 and 48 hours post-transfection (Figure 4.9A-D). The transfection efficiency appeared higher at the higher concentration of siRNA (100 pmol) as expected and was sustained over 48 hours (Figure 4.9B&D).

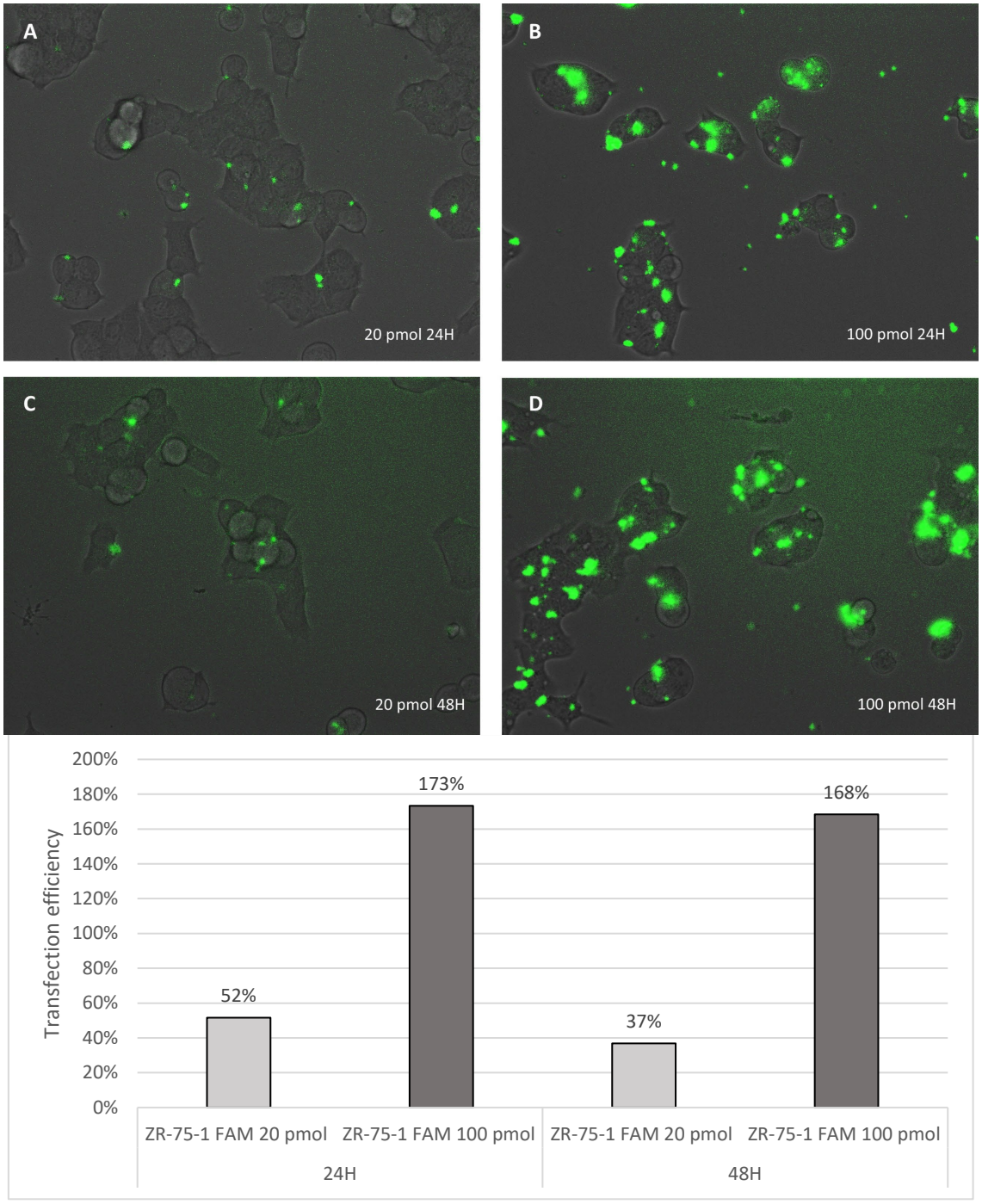

Figure 4.9. FAM overlayed white light images of ZR-75-1 cells transfected with siRNA negative control FAM labelled using Lipofectamine 2000. **A** and **B** show siRNA expression with 20 pmol and 100 pmol siRNA concentrations respectively 24 hours after transfection. **C** and **D** show siRNA expression with 20 pmol and 100 pmol siRNA concentrations respectively 48 hours after transfection. Images obtained using Life Technologies EVOS Fluorescent Microscope measured at excitation 470 nm, 525 nm emission wavelengths under 40X magnification. **(E)** Transfection efficiency estimations respective to the relevant images, 24 (A and B) and 48 (C and D) hours after transfection with either 20 or 100 pmol FAM labelled siRNA.

Based on these pilot experiments, the UGT2B7 and control siRNA were transfected at 100 pmol and UGT2B7 was quantified at 48 hours post transfection. UGT2B7 mRNA was not reduced following transfection of UGT2B7-targeting siRNA (Figure 4.10A), in fact the opposite was observed, which may suggest unintentional non-specific binding, however this result was not replicated. More convincingly, UGT2B7 protein levels were not altered between control and UGT2B7 siRNA transfection conditions (Figure 4.10B).

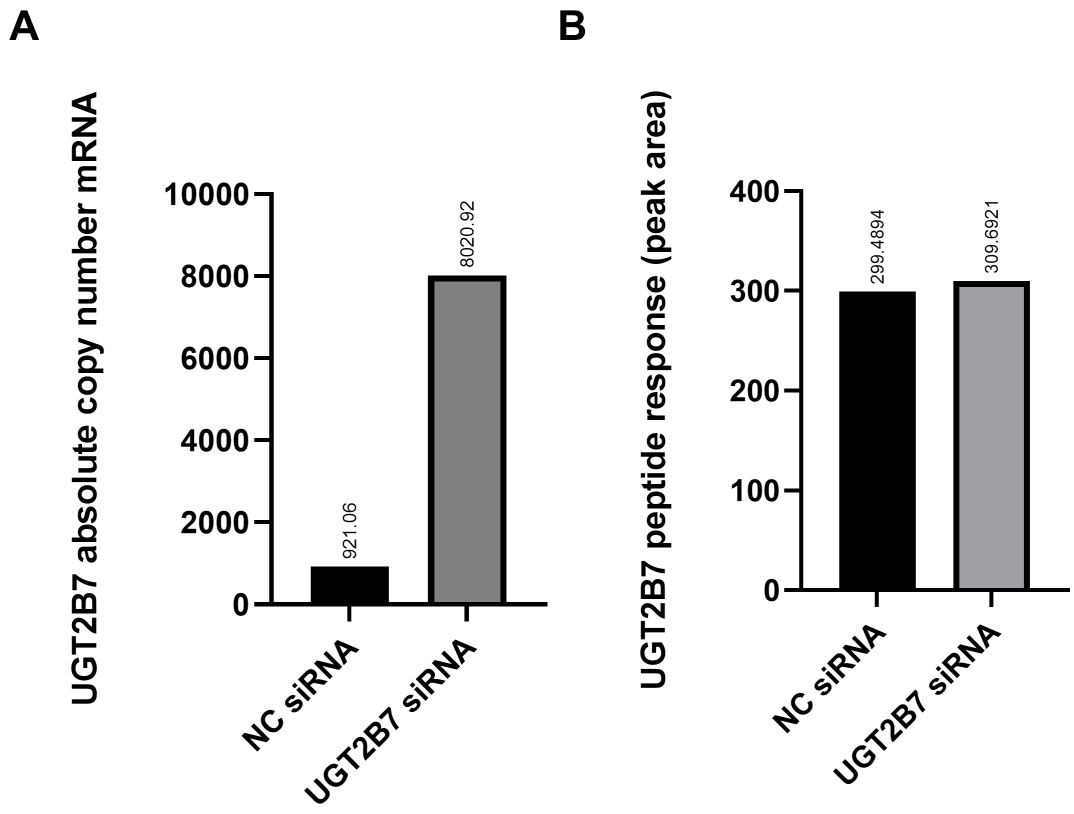

Figure 4.10. (A) UGT2B7 mRNA expression was not consistently inhibited by siRNA. **(B)** LC-MS peptide quantification of UGT2B7 showed no change in response to siRNA. mRNA and peptide levels were quantified 48 hours after transfection of 100 pmol siRNA in ZR-75-1 cells. Statistical analysis was not performed for these experiments (n=1).

Overall, it appeared that the UGT2B7-targeting siRNA was not effective in our ZR-75-1 transfection system. Possible reasons for the discrepancy between our results and the published report on the efficacy of this siRNA are presented in the Discussion.

4.3.7. Dominant negative inhibition as a potential method to suppress UGT2B7 activity in breast cancer cells

Our third approach to developing a UGT2B7 LOF model in breast cancer cells used the DN-inhibition strategy described in the Introduction (section 4.1.7). A C-terminally truncated variant of *UGT2B15* was previously shown to dimerise with UGT2B7 in HEK293T cells and reduce its activity by ~ 70% (Hu et al., 2018). We proposed to exploit this DN-inhibition mechanism to reduce the activity of endogenous UGT2B7 in breast cancer cell lines.

Another student in our laboratory had previously prepared ZR-75-1 cells that stably over-express the C-terminally truncated form of UGT2B15 designated 'chimeric-UGT2B15' because the mRNA contains a pseudoexon derived from a neighbouring pseudogene (PhD candidate Quinn Martin, Clinical Pharmacology, Flinders University). The chimeric-UGT2B15 stable overexpression line was generated by Quinn Martin, as described in Methods 4.2.2. Expression of chimeric-UGT2B15 mRNA was measured in the overexpression line and a control line carrying empty vector via qRT-PCR. The chimeric-UGT2B15 mRNA was expressed at a high level in the overexpression cell line whilst being undetectable in the control line (Figure 4.11A). To examine whether chimeric-UGT2B15 expression caused inhibition of UGT2B7 activity, epirubicin glucuronidation was measured in the chimeric-UGT2B15 overexpression and control cell lines. Epirubicin glucuronidation activity was not altered by expression of the chimeric-UGT2B15 (Figure 4.11B). We suspected that the amount of chimeric-UGT2B15 protein produced in the stable cell line might be insufficient to inhibit UGT2B7, hence we examined chimeric UGT2B15 protein expression by immunoblotting with an antibody that detects the N-terminal region (and hence both wildtype and chimeric forms) of UGT2B15 and UGT2B17. Lysate from a ZR-75-1 cell line expressing wildtype UGT2B17 protein was used as a control for antibody binding. There was no evident expression of chimeric UGT2B15 protein in the

overexpression stable line at the level of the detection of this assay (Figure 4.11C, Appendix Figure 11).

A

Cell line	Cycle threshold (Ct)
UGT2B15 (all variants) (n=2)	
IRES	29.55 +/- 0.44
UGT2B15 chimera	16.73 +/- 0.47
UGT2B15 (chimera specific) (n=1)	
IRES	N.D.
UGT2B15 chimera	14.85

B

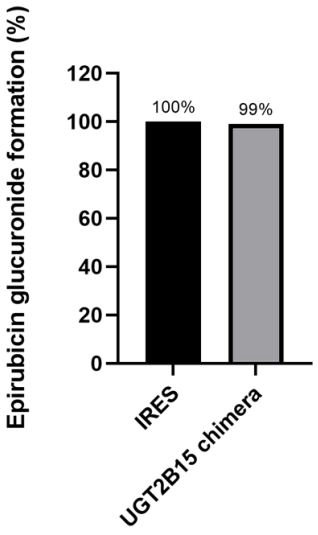

C

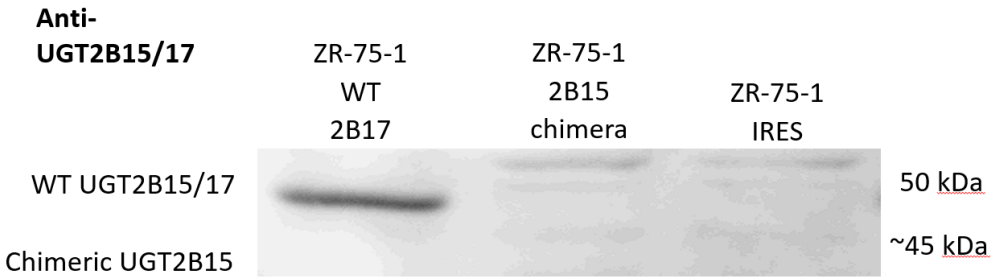

Figure 4.11. Chimeric UGT2B15 protein was not significantly overexpressed in ZR-75-1 cells, and therefore did not inhibit epirubicin glucuronidation. **(A)** *UGT2B15* chimera stably transfected ZR-75-1 cells show increased mRNA expression by qRT-PCR using broadly targeting UGT2B15 (all variants) respective to the IRES control line (as indicated by the raw cycle-threshold (Ct) values). qRT-PCR for *UGT2B15* chimera-specific primers only detects amplicons in the ZR-75-1 UGT2B15 chimera line (shown as raw Ct). **(B)** UGT2B7 activity (epirubicin glucuronidation) is not reduced in the ZR-75-1 UGT2B15 chimera cell line. Epirubicin glucuronide was measured from in-vitro incubations performed overnight after pre-inducing UGT2B7 expression for 48 hours with 200 nM epirubicin. 200 µg of total protein was used for incubations. **(C)** Expression of chimeric UGT2B15 protein was not observed in the immunoblot stained with anti-UGT2B15/UGT2B17 antibody at ~45 kDa. Wildtype (WT) UGT2B15/17 was detected exogenously in ZR-75-1 2B17 stable cells at 50 kDa, however not in the respective control ZR-75-1 IRES stable cells (empty vector). 50 µg of total protein lysates were used. The uncropped Western Blot can be found in Appendix Figure 11.This can be compared to the published Western blot by Hu et al. (2018) (Appendix Figure 12). Figures are presented as

representative data (n=1). Figures A and C has been reproduced with permission from experiments conducted by Quinn Martin (Clinical Pharmacology, Flinders University, Australia).

4.3.8. *In vivo* assessment of the relationship between UGT2B7 levels and breast cancer outcomes using TCGA-BRCA data

In vitro experiments presented herein showed that UGT2B7 GOF promotes resistance of breast cancer cells to epirubicin. Unfortunately, we were unable to generate a complementary LOF model to confirm the role of UGT2B7 at the level of the cancer cell. Endogenous UGT2B7 displays a wide range of expression levels in naturally occurring tumours, thus data from natural tumours provides another potential resource to examine the relationship between intratumoural UGT2B7 expression levels and epirubicin responses. The TCGA-BRCA dataset contains RNA-seq data from 1084 breast tumours (primarily pre-treatment biopsies), as well as clinical and pathological data including patient survival time and cancer subtype. In Chapter 3 TCGA-BRCA data was used to assess the relationship between UGT2B7 expression and cancer subtype. In this Chapter, the same dataset was used to examine associations between UGT2B7 expression level and survival outcomes, with and without drug treatment.

The association of UGT2B7 mRNA expression with overall survival (OS) was assessed in the entire cohort (Figure 4.12A & C) using the recursive partitioning program AutoRPA (Xie et al., 2020). This analysis indicated that higher UGT2B7 expression level was associated with poorer OS (log rank test p-value = 0.0247). However, the survival curves overlapped suggesting a non-proportional hazard (i.e. the effect of UGT2B7 expression is non-proportional over time) and hence the log rank test statistic was not considered reliable. Comparing the high and low UGT2B7 expressing groups (i.e. $UGT2B7^{high}$ and $UGT2B7^{low}$), it was evident that they varied greatly by subtype: the $UGT2B7^{high}$ group contained almost 50% basal tumours while the $UGT2B7^{low}$ group contained only ~ 10% (Figure 4.12B). This is consistent with observations in Chapter 3, where high UGT2B7 expression

was found to associated with the basal subtype. Hence, the cohort was stratified by cancer subtype and the analysis was repeated for each group. In the group of patients with basal subtype tumours (n= 171), high UGT2B7 expression was associated with shorter OS (log rank test statistic p = 8.9×10^{-3}) (Figure 4.12C & D) and shorter PFS (log rank test statistic p = 8.9×10^{-3}) (not shown). In contrast, there was no association of UGT2B7 expression level with OS in patients with Her2 positive, luminal A, or luminal B tumours (Figure 4.12C).

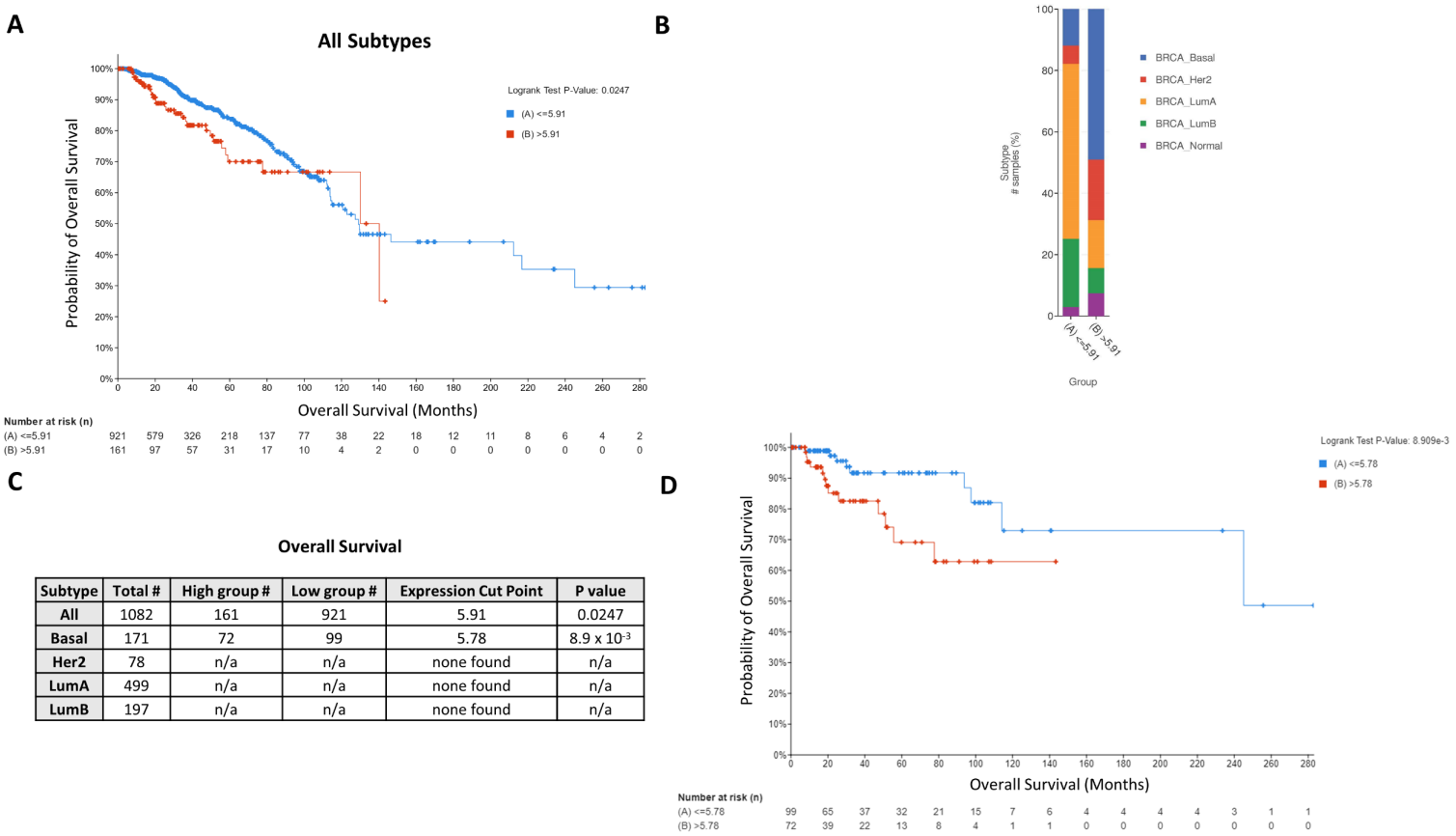

Subtype	Total #	High group #	Low group #	Expression Cut Point	P value
All	1082	161	921	5.91	0.0247
Basal	171	72	99	5.78	8.9×10^{-3}
Her2	78	n/a	n/a	none found	n/a
LumA	499	n/a	n/a	none found	n/a
LumB	197	n/a	n/a	none found	n/a

Figure 4.12. UGT2B7 mRNA expression is associated with poor overall survival (OS), primarily driven by differential survival in the basal subtyped cohort. **(A)** In all breast cancer subtypes, UGT2B7 expression is indicative of poor OS (p=0.0247). Comparisons were performed between $UGT2B7^{low}$ (blue; n = 921) and $UGT2B7^{high}$ (red; n = 161) bins. **(B)** High UGT2B7 mRNA expression (>5.91) grouping enriches the proportion of basal subtyped samples. **(C)** mRNA expression cut points derived from recursive partitioning analysis (RPA) determined UGT2B7 was of prognostic value for OS in unstratified (all) and basal breast cancer subtypes. **(D)** Robust differences in OS between $UGT2B7^{low}$ (blue; n = 99) and $UGT2B7^{high}$ (red; n = 72) are observed in basal subtyped breast cancer. Comparisons were performed using mRNA normalised expression from the TCGA-BRCA dataset recursively partitioned using AutoRPA and visualised using cBioPortal.

We next obtained drug treatment data for the TCGA-BRCA patients from the Genomic Data Commons (GDC). Data was available for 65 drugs or drug combinations. Both the number of patients and the distribution of subtypes varied widely between the drug treatment groups. Hence, the basal subtype cohort was analysed only. Unfortunately, the group treated with epirubicin in this cohort was too small for analysis (n= 7). However, a considerable fraction of this cohort was treated with doxorubicin (n = 71). Previous work in melanoma cells had indicated that UGT2B7 knockdown equally impacted epirubicin and doxorubicin response, suggesting that UGT2B7 may control exposure to both anthracyclines (Dellinger et al., 2012). The basal group was therefore stratified by anthracycline treatment creating two groups: anthracycline treated (DOX or EPI) and non-anthracycline treated (neither DOX nor EPI). Higher UGT2B7 expression was associated with poorer OS in both groups, although the log rank test statistic was not highly significant ($p = 0.049$ and 0.035 respectively) (Figure 4.13A). Progression free survival (PFS) indicates when a patient progressed while on a particular treatment regimen, and hence may be more informative about drug activity (Delgado & Guddati, 2021). Hence PFS was also examined in the anthracycline treated and non-anthracycline treated groups. Higher UGT2B7 expression was associated with poorer PFS only in the anthracycline treated group (log rank test statistic $p = 0.0133$). (Figure 4.13B & C). To further elucidate whether these findings were specific to UGT2B7, UGT2B15 (expressed in ER+ BC tumours) and UGT8 (highly expressed in TNBC) were selected to assess whether any expression levels were associated with differential outcomes of either OS or PFS in the basal tumour cohort. No associations were observed in the basal cohort nor the basal cohort treated with anthracyclines (Appendix Figure 10).

A

Overall Survival					
Drug Regimen (Basal Only)	Total #	High Group #	Low Group #	Expression Cut Point	P Value
Therapy Agnostic	171	72	99	5.78	8.9 x 10(-3)
DOX or EPI	78	32	46	10.81	0.049
No DOX or EPI	93	38	55	5.7	0.035

B

Progression Free Survival					
Drug Regimen (Basal Only)	Total #	High Group #	Low Group #	Expression Cut Point	P Value
Therapy Agnostic	171	n/a	n/a	none found	n/a
DOX or EPI	78	32	46	10.81	0.0113
No DOX or EPI	93	n/a	n/a	none found	n/a

C

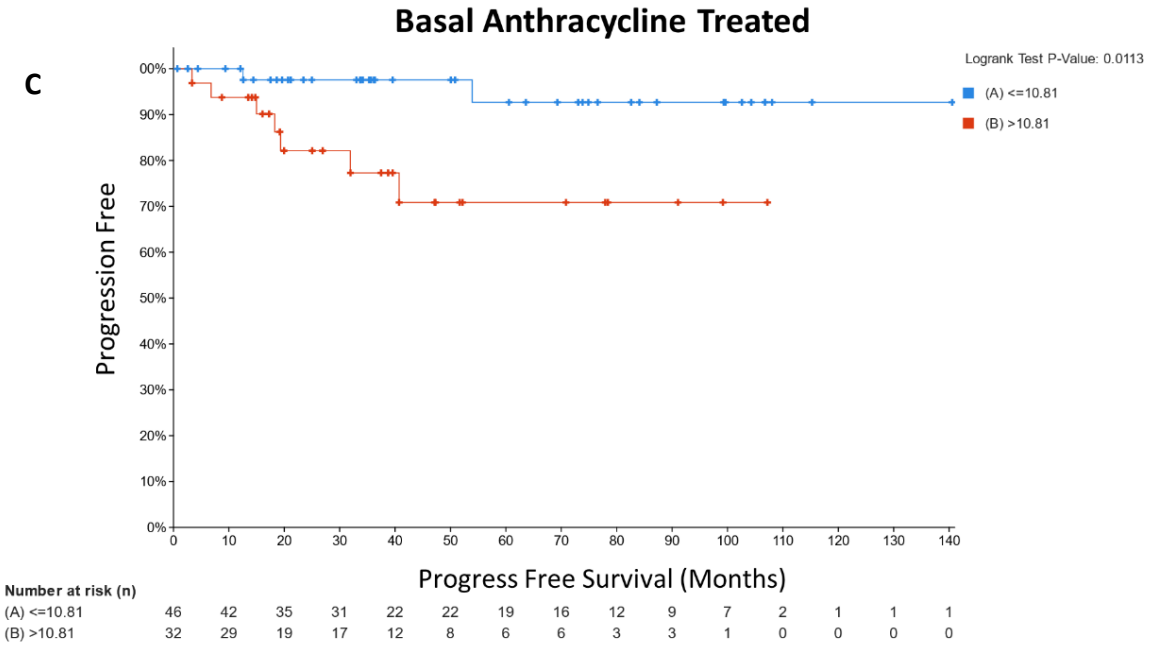

Figure 4.13. Basal subtyped breast cancer patients treated with anthracyclines (doxorubicin (DOX) or epirubicin (EPI)) show decreased progression free survival (PFS) compared to those not stratified by treatments (therapy agnostic) or those receiving alternative drugs. **(A)** UGT2B7 expression was associated with worse overall survival (OS) in basal subtypes irrespective of drug treatments. **(B)** mRNA expression cut points derived from recursive partitioning analysis (RPA) determined UGT2B7 was prognostic of PFS in basal subtypes treated with anthracyclines only. **(C)** UGT2B7 expression was associated with reduced PFS in basal subtypes treated with anthracyclines. Expression was stratified by $UGT2B7^{low}$ (blue; n = 46) and $UGT2B7^{high}$ (red; n = 32) subgroups using a cutoff of 10.81 mRNA normalised expression. Comparisons were performed data obtained from the TCGA-BRCA dataset recursively partitioned using AutoRPA and visualised using cBioPortal.

4.4. Discussion

Intrinsic and acquired anthracycline resistance are barriers to the effectiveness of anthracycline-containing chemotherapy regimens (Holohan et al., 2013). In the case of epirubicin, previously described resistance mechanisms include changes in the primary target topoisomerase II, increased drug efflux, and rewiring of cellular metabolism (Ganapathi & Ganapathi, 2013; McGuirk et al., 2021; Pommier et al., 1994; Szakács et al., 2006; Zheng et al., 2020). Drug efflux has been particularly well studied and epirubicin is known to induce multi-drug resistance through increased expression of *ABCB1* (P-glycoprotein). Several studies have attempted to overcome efflux-mediated resistance using P-glycoprotein inhibitors (Felipe et al., 2018; Yang & Zhang, 2012; Zhu et al., 2013). However, clinical translation is limited by the toxicity of these drugs and collateral harms such as inhibition of cancer-surveilling immune cells (Chen et al., 2020a). Moreover, in one epirubicin-resistant breast cancer model, transporter inhibition restored drug accumulation but did not restore drug-sensitivity, presumably because the cells had evolved redundant resistance mechanisms (Hembruff et al., 2008).

The focus of this project was pharmacokinetic mechanisms of anthracycline resistance mediated by drug glucuronidation within cancer cells. The overall aim of studies in this Chapter was to determine whether UGT2B7 has a specific role in the resistance of breast cancer cells to epirubicin. As mentioned previously, Dellinger et al. (2012) showed that UGT2B7 knockdown in metastatic melanoma cells (WM115) increased their sensitivity to epirubicin and also to its epimer doxorubicin (Mordente et al., 2009). Anthracyclines are not widely used in melanoma; however, they play a significant role in breast cancer treatment. At the beginning of this study, it was unknown whether the level of UGT2B7 expression in breast cancer cells influences their sensitivity to epirubicin. To

address this question, we generated stable UGT2B7 overexpression models, and also attempted to generate knockout/knockdown models for use in phenotypic drug-sensitivity assays. We complemented the studies with analysis of patient data to determine whether there was any relationship between UGT2B7 expression levels in tumours and survival outcomes, with or without anthracycline treatment.

4.4.1. *In vitro* overexpression studies suggest a role of UGT2B7 in epirubicin resistance in breast cancer cells

We generated MDA-MB-231 and ZR-75-1 UGT2B7 overexpression cell lines and characterized them using mRNA, protein and activity assays. It was notable that the amount of exogenous UGT2B7 protein produced in the stable lines (based on peptide detection) did not reflect the amount of mRNA produced. In both MDA-MB-231 and ZR-75-1 overexpression cell lines, UGT2B7 mRNA was increased by many thousands of folds. However, in ZR-75-1 cells, the increase in UGT2B7 protein was less than 2-fold. In MDA-MB-231 cells, UGT2B7 protein overexpression could not be calculated as fold change because basal peptides were not detectable in the control line. UGT2B7 basal levels may be inherently subject to selection bias in the MDA-MB-231 IRES cell line, as basal UGT2B7 protein expression was previously detected in WT MDA-MB-231 cells in Chapter 3 (Figure 3.6).

Overexpression of UGT2B7 increased epirubicin clearance in MDA-MB-231 cells and increased the IC50 for epirubicin. This was consistent with increased metabolic clearance of epirubicin in UGT2B7-MDA-MB-231 cells. This is the first study showing that increased UGT2B7 expression may induce drug resistance in breast cancer. A similar effect on epirubicin sensitivity was not seen in ZR-75-1 cells, which may relate the minor increase in UGT2B7 protein in this cell line.

In addition to short term assays, we performed long-term competition assays by co-culturing the UGT2B7-MDA-MB-231 and control cell lines. We predicted that if UGT2B7 provides a selective advantage to cells under epirubicin treatment, then the UGT2B7 over-expressing line would outcompete the control cells in culture. This type of study could inform studies in more physiologically relevant cancer models, such as patient-derived xenograft models, where gene perturbation can be assessed using animals treated with clinically relevant drug regimens (Charbonneau et al., 2023). Unexpectedly, UGT2B7 over-expressing cells showed enhanced growth independent of drug treatment, as indicated by their over-representation in the mixed population at the end of the study. There was a slight additional survival advantage observed in epirubicin treated conditions. This was partially in accordance with the short-term assays in which UGT2B7-MDA-MB-231 cells showed a growth/survival advantage only with epirubicin treatment and not in vehicle conditions. These findings warrant further investigation using different growth conditions including 3D cultures. Recent work showed that cancer cells have much greater resistance to anthracyclines in 3D organoid culture than in monolayers and can acquire resistance mechanisms that include stemness and diapause (a type of reversible cell stasis) (Dhimolea et al., 2021). A future study could assess whether such 3D growth conditions provide different responses to those observed here in long-term 2D culture assays.

4.4.2. Challenges in generating UGT2B7 knockout/knockdown models

The present study trialled several approaches to generating stable knockout or knockdown of UGT2B7 in breast cancer cells. While this was ultimately without success, some observations from these efforts are worthy of discussion, and may be informative about UGT2B7 biology. We first used the CRISPR-Cas9 approach with a pre-validated CRISPR Cas9 vector targeting *UGT2B7* exon 1. We selected the ZR-75-1 breast cancer cell line for the trial because it showed detectable basal UGT2B7

protein, making it easier to assess knockout. To avoid any artefacts due to vector integration we chose a 'hit-and-run' CRISPR approach that can generate scarless knockouts. This approach typically uses transient transfection of the CRISPR-Cas9 targeting vector followed by limited dilution cloning and screening for indels. The potential disadvantages of the approach are: a) if transfection efficiency is <100% then not all cells will have received the vector; b) in any given cell that did receive vector, an indel event may or may not occur within the period that the vector remains present in the cells (usually several days). These two factors can lead to a low efficiency of indel generation requiring a high number of clones to be screened. Hence before proceeding to any screening, we estimated the indel generation efficiency in a pool of transfected cells using the Inference of CRISPR Edits (ICE) method. We also treated the transfected pool transiently with puromycin to enrich for transfected cells (without clonal selection) before performing ICE. The ICE analysis showed that the indel frequency was only ~ 5%. Of these indels, only around two thirds are expected to change the reading frame; moreover, to create a null model a frameshifting event must occur on both alleles in the same cell. Overall, we considered that the low efficiency made clonal screening unviable.

UGT2B7 expression in ZR-75-1 cells is much lower than in HepG2 cells, which had been previously targeted using CRISPR. Thus, one possible explanation for the low targeting efficiency in ZR-75-1 cells was poor accessibility of the target site due to epigenetic repression of the gene locus. The ability of SpCas9 nuclease to generate dsDNA breaks has been shown to correlate with the absence of repressive histone marks and less condensed chromatin, e.g. euchromatin (Jensen et al., 2017; Uusi-Mäkelä et al., 2018). We therefore attempted to increase chromatin accessibility using sodium butyrate, which causes histone hyperacetylation (by inhibition of histone deacetylase) (Kruh, 1981). The use of sub-millimolar butyrate to enhance the efficiency of CRISPR has previously been reported in literature (Disterer et al., 2012). Rescreening the cell population using ICE after butyrate

treatment suggested a slight increase in indel production. However, it also revealed that ICE was variable in estimating indel efficiencies. A study by Hsiau et al. (2019) that compared ICE with next generation sequencing analysis reported that high quality Sanger traces used for ICE were strongly correlated with Amp-Seq genotyping results with a Pearson r^2 >0.95, but upon using a lower quality trace, there was a lesser correlation (Pearson r^2= 0.88) (Conant et al., 2022). Thus, the variation in ICE results in our experiments probably related to the quality of Sanger sequencing traces used. Overall, we concluded that the editing efficiency using our UGT2B7 CRISPR-Cas9 targeting construct was low in ZR-75-1 cells and could not be meaningfully improved by epigenetic priming with a HDACi. Thus, hit-and-run CRISPR was not a viable option in providing scarless UGT2B7 knock-out.

We proceeded to attempt CRISPRi knockdown of UGT2B7. We used a dual-guide system with CRISPRi vector that induced repression by targeted binding of a dCas9-KRAB fusion protein. One of the sgRNAs used was the same exon 1-targeted sgRNA used in the CRISPR construct. The second sgRNA targeted the p53 responsive element in the *UGT2B7* promoter. We predicted that targeting the repressor complex to locations both upstream and downstream of the TSS could lead to formation of a large repressive complex spanning the TSS and preventing gene transcription. The target sites for the two sgRNA sequences were within the window previously described as suitable for CRISPRi. Specifically, optimal dCas9-KRAB activity has been reported within the window of -50 to +300 bp from the transcription start site (TSS), however strong repression was still observed in the +500 to +600 bp range (Gilbert et al., 2014).

While the data collected from this experiment was only preliminary, it did indicate that basal expression of UGT2B7 was reduced in a polyclonal population of cells carrying the CRISPRi construct. However, when the cells were treated with epirubicin, UGT2B7 mRNA expression was still highly induced. It is possible that p53 was able to displace any KRAB repressor complex assembled at the

promoter. p53 has two transactivation domains (TADs). One of these TADs contains a mixture of highly acidic and hydrophobic residues similar to that seen in the extremely potent viral transactivation protein VP16 (Raj & Attardi, 2017). p53 recruits a number of co-activators including p300/CBP that induces histone acetylation, and also binds directly to the TFIID core transcription machinery (Lee et al., 2010). Thus, the potent gene activating ability of p53 may have overwhelmed dCas9-KRAB repression, suggesting a more potent inhibition strategy is required.

While KRAB repression is thought to be a generally robust method for persistent epigenetic silencing, its effectiveness may be limited at some loci. KRAB's primary repressive mechanism involves interacting with KAP1 (Friedman et al., 1996), which recruits co-repressors such as HP1, SETDB1 (Yeo et al., 2018), and histone deacetylase complexes (Schultz et al., 2001). More potent repression has been achieved in literature (Yeo et al., 2018) by fusing MeCP2 (Methyl-CpG Binding Protein 2) to KRAB, as MeCP2 has a complementary repressive mechanism by binding to methylated DNA (methyl-CpGs) (Schmidt et al., 2020). Other complementary epigenetic silencers include DNA methyltransferases (such as DNMT3A-dCas9) and histone methyltransferases (such as Ezh2-dCas9), and very recent literature recommends combining differently targeting repressors rather than relying on KRAB alone (O'Geen et al., 2019). Unfortunately, within the constraints of this project we were unable to further allocate time and resources to pursuing these newer CRISPRi technologies.

siRNA was also tested as a means of UGT2B7 knockdown in breast cancer cells. A pre-validated sequence was selected from literature that achieved ~75% knockdown of UGT2B7 mRNA in hepatocytes (Konopnicki et al., 2013). While transfection appeared efficient as demonstrated by FAM-labelled control siRNA, we were unable to achieve the desired knockdown of UGT2B7 mRNA, and high siRNA doses may have had off-target effects as suggested by the confounding increase in UGT2B7 mRNA (although we did not attempt to repeat this result). Notably, it has been reported

that the p53 pathway is activated in an off-target manner by a variety of siRNAs, which could in turn increase expression of p53 targets (Scacheri et al., 2004). Most importantly, we saw no change in UGT2B7 protein level at the high dose of siRNA using the peptide assay. The reason for the lack of efficacy of the siRNA in our cells was not clear; however, it is not uncommon for siRNAs to function differently in different cell types. This might relate to differing accessibility of the target site in the mRNA in cells with a different expression of RNA binding proteins. Overall, we chose not to pursue siRNA approaches further.

The last method that we explored to create a UGT2B7 LOF model was stable expression of a truncated UGT protein (called chimeric UGT2B15) that can form inhibitory dimers with UGT2B7. The decision to pursue this approach was partly of convenience, as a ZR-75-1 cell line expressing the truncated form of UGT2B15 (validated by mRNA only) had been previously generated in the laboratory. Thus, we could rapidly assess whether this model had reduced UGT2B7 activity. We confirmed expression of chimeric UGT2B15 at the RNA level and proceeded to test UGT2B7 activity using epirubicin glucuronidation assays. There was no reduction in endogenous epirubicin glucuronidation and subsequent immunoblotting studies suggested that little or no chimeric UGT2B15 protein was made in the stable cell line. Given that the chimeric UGT2B15 protein was previously shown to be robustly expressed in HEK293T cells, this suggested that translation of its mRNA may be specifically suppressed in ZR-75-1 cells. This finding may warrant more study in the future because could indicate a requirement for a defined level of UGT2B enzyme activities in ZR-75-1 cells. This cell line endogenously expresses a several UGTs including UGT2B7, UGT2B15, UGT2B17, UGT2B11 and UGT2B28, and its growth is naturally regulated by steroids (growth is induced by estrogen and suppressed by androgens) (Hickey et al., 2021). This is not the case for HEK293 cells, which lack any *UGT2B* gene expression. Chimeric UGT2B15 is predicted to be able to

heterodimerize with all UGT2B proteins and thus potentially block each of their activities. This could affect essential cell metabolism processes such as lipid homeostasis or steroid signalling.

Aggregate observations from the work discussed in section 4.4.1 and 4.4.2 prompt a tentative hypothesis that UGT2B7 levels may need to be maintained within a narrow range for optimal growth of ZR-75-1 cells, and this might be achieved by translational control e.g. by miRNAs as suggested by Wijayakumara et al. (2017) or by other not-yet defined RNA binding proteins. This may explain why the UGT2B7-ZR-75-1 overexpressing stable line showed very little increase in UGT2B7 protein levels relative to the empty vector containing stable line (see Figure 4.4), despite a very high level of mRNA production from the *UGT2B7* transgene. If UGT2B7 levels outside of the optimal range (higher or lower) produce a growth-disadvantage, it is plausible that protein production may be repressed. This hypothesis could be explored in future studies. If this is indeed the case, an inducible expression system (such as TET-ON) might be used to produce stable lines. Inducible systems are commonly used to stably express genes that alter cell behaviour in a way that compromises the selection process (such as toxic genes).

To summarize this subsection, we were unable to achieve a loss-of-function UGT2B7 model in breast cancer cells to provide a complementary model to the overexpression studies. Since this remains desirable to confirm our hypothesis that intracellular UGT2B7 levels are important determinant of epirubicin response, future work should focus on overcoming the limitations of UGT2B7 knockout/knockdown in breast cancer cells.

Interestingly, during this project, a study was published (Vitale et al., 2020), reporting an increase in epirubicin sensitivity in MDA-MB-231 cells after knockdown of the UGT cofactor precursor, UDP-glucose dehydrogenase. UDP-glucose dehydrogenase synthesizes UDP-glucuronic acid by the

oxidation of UDP-glucose. Knocking down UDP-glucose dehydrogenase reduced the availability of UDP-glucuronic acid, limiting UGT2B7-mediated epirubicin glucuronidation. The authors showed that UDP-glucose dehydrogenase knockdown in epirubicin treated MDA-MB-231 cells significantly increased the expression of pro-angiogenic factors VEGF and FGF-2. Additionally, reduction in UDP-glucose dehydrogenase combined with epirubicin treatment led to a reorganisation in extracellular matrix components, favouring hyaluronan synthesis and contributing to the acquisition of an epirubicin resistant phenotype. This suggests complex processes are involved in the epirubicin resistance in breast cancer cells, potentially involving both glucuronidation and other cellular pathways utilising UDP-sugar donors. As such, multiple cellular mechanisms may need to be targeted to increase the effectiveness of epirubicin, not only drug metabolism.

4.4.3. Clinical data supports an oncogenic role for UGT2B7 in TNBC and a possible role in anthracycline response

Clinical tumour datasets were examined in this Chapter to complement the *in vitro* data. Tumours provide a wide range of UGT2B7 expression levels, and high and low expressors may be considered as natural gain- and loss-of-function models. Higher UGT2B7 expression was associated with poorer overall survival (OS) in the basal subtype independent of drug treatment, but not in other cancer subtypes. This is broadly consistent with our observation that UGT2B7 overexpression in MDA-MB-231 cells provided a growth advantage in long term competition assays that was independent of drug treatment. The mechanism of this potential pro-proliferative effect of UGT2B7 on tumour cells remains to be understood.

The cohort of patients with basal subtype tumours was stratified into anthracycline treated and non-anthracycline treated groups, and both groups showed an apparent association between

UGT2B7 levels and OS; however, the long rank statistics were quite close to the 0.05 threshold for significance. Interestingly, when PFS was examined, only the anthracycline-treated group showed an association between UGT2B7 expression levels and survival. It was not possible to test an association between UGT2B7 expression and epirubicin treatment specifically as the group size was too small. Overall, this analysis suggests that UGT2B7 might be associated with a greater risk of progression in patients with basal tumours undergoing anthracycline treatment, but not those treated with non-anthracycline containing regimens. However, there are several important caveats to this interpretation. First, the analysis is of only one dataset (TCGA-BRCA) and the number of anthracycline treated patients is fairly small. Second, a specific association with anthracycline treatment was only seen with PFS and not with OS.

OS is generally considered the 'gold standard' endpoint in oncology clinical trials as it reflects the outcome most relevant to the patient. However, OS may not always be the best measure when retrospectively assessing the efficacy of a particular drug treatment, because the patient may have received other therapies (e.g. salvage therapies) subsequent to the drug of interest. Thus, OS may reflect the aggregate effect of multiple drugs. PFS indicates the time from randomization to a treatment group until disease progression (or death) (Lebwohl et al., 2009). PFS may or may not be a good surrogate for OS; how well PFS and OS correlate is influenced by the length of the period between progression and death (Chowdhury et al., 2020). PFS can be a good surrogate when this time is short but is less likely to correlate with OS when this time is long, in part because of the variable impact of other salvage therapies that have been used to extend life after progression (Kilickap et al., 2018). However, for this same reason, i.e. it is not influenced by subsequent treatments, PFS can provide advantages when seeking to understand a drug-specific effect on disease control. Overall, while the findings from this analysis are suggestive that intratumoural

UGT2B7 expression may influence the efficacy of anthracycline treatment, these conclusions must be considered tentative until additional datasets can provide a more robust analysis. It is also important to note that the TCGA-BRCA RNA-seq data almost entirely derived from pre-treatment biopsies. Hence if poorer survival was associated with high UGT2B7 levels that occurred *after* anthracycline treatment (due to its transcriptional induction), the dataset would not reveal this. In the future, it would be valuable to seek out RNA-seq data for epirubicin- and/or doxorubicin-treated patients that includes both pre- and post-treatment biopsies.

This project focused primarily on the potential of UGT2B7 to influence the efficacy of epirubicin in breast cancer cells. Dellinger et al. (2012) reported that UGT2B7 knockdown sensitized melanoma cells equally to epirubicin and doxorubicin but did not examine the mechanism of this effect. A valuable future direction would be to determine how UGT2B7 affects doxorubicin response and define its mechanism of action. We presume that UGT2B7 increases resistance to epirubicin through direct glucuronidation, which reduces the amount of active drug in the cells. However, it is not implicit that the same mechanism is responsible for the effect of UGT2B7 on cellular response to doxorubicin. In fact, to date, doxorubicin has not been identified as a UGT2B7 substrate; moreover, epirubicin and doxorubicin have quite different metabolic fates as described below.

All anthracyclines are comprised of a basic structure with two main portions, an amino-sugar moiety (daunosamine) and an anthraquinone ring system referred to as the aglycone (NCBI, 2024) (Figure 4.14A). The planar rings intercalate into DNA while the daunosamine binds in the minor groove. The latter stabilizes the interaction and also blocks the interface where topoisomerase interacts with the DNA, which is central to blockade of DNA replication (Jawad et al., 2019). Hydrogen bonds also form between the anchor region of the anthracycline and guanine residues in DNA, further stabilizing the interaction (Yang et al., 2014) (Figure 4.14A). Epirubicin and doxorubicin are epimers,

meaning that they are chemically identical apart from a single epimeric hydroxyl (OH) group that differs in its spatial orientation between the two molecules (Ganzina, 1983). The epimeric OH group is located in the daunosamine moiety (Figure 4.14B). Glucuronidation of epirubicin by UGT2B7 occurs on this epimeric OH group (Figure 4.14C). This group is not glucuronidated in doxorubicin, possibly because of an unsuitable orientation. Instead, doxorubicin has two main fates: a) reduction by carbonyl reductases (CBR) to form doxorubicinol; b) deglycosidation by CYP450 oxidoreductase (POR) which removes the entire daunosamine group resulting in an aglycone metabolite. When deglycosidation occurs, it is typically coupled to reduction producing the main aglycone metabolite called 7-deoxydoxorubicinolone (Choi et al., 2020; Licata et al., 2000). A study in mice indicated that 7-deoxydoxorubicinolone was the most abundant metabolite found in tissues (heart, liver, and kidney) between 1-4 hrs after doxorubicin administration (van Asperen et al., 1999). It was also the major doxorubicin aglycone metabolite found in plasma in a study of paediatric cancer patients (Siebel et al., 2020). A study using human liver microsomes showed that 7-deoxydoxorubicinolone undergoes o-glucuronidation, with the glucuronic acid group conjugated to the distal aromatic ring in the aglycone (Takanashi & Bachur, 1976) (Figure 4.14D). Similarly, a study using rat liver subcellular fractions showed that 7-deoxydoxorubicinolone was produced in both microsomal and mitochondrial fractions, and that the microsomal fraction rapidly converted this metabolite into more polar forms assumed to be glucuronides or sulphates (Wang et al., 2011). An assessment of doxorubicin metabolites in human urine showed that the glucuronide constituted ~12% of doxorubicin metabolites excreted in urine (with the parent drug and doxorubicinol comprising almost 70%) (Takanashi & Bachur, 1976). It is currently unknown which UGT isoform is responsible for glucuronidation of 7-deoxydoxorubicinolone. It should be noted that epirubicin also undergoes hydrolysis of the daunosamine group to form an aglycone metabolite (which is chemically identical

to the doxorubicin aglycone and presumably has identical metabolite fates), but this is a more minor pathway than for doxorubicin. It has been proposed that the difference in the metabolic fates of epirubicin and doxorubicin may be due to their different intracellular location, with doxorubicin mainly in the cytoplasm and mitochondria where reductases are abundant, and epirubicin mainly in organelles (e.g. endoplasmic reticulum) where UGT2B7 is abundant (Salvatorelli et al., 2006).

To summarize the role of glucuronidation in anthracycline pharmacokinetics more simply: epirubicin is *mainly inactivated by direct glucuronidation* on the daunosamine moiety, while doxorubicin is *mainly inactivated by removal of the daunosamine moiety*, and the major aglycone metabolite then undergoes glucuronidation on an aromatic ring. Because the daunosamine group is important for blockade of topoisomerase-DNA interaction, both daunosamine glucuronidation (by UGT2B7) and hydrolysis (POR) greatly reduce the cytotoxicity of these drugs. However, the aglycone forms still have some toxicity, and in particular can produce ROS and act as mitochondrial poisons (Misiti et al., 2003; Sokolove, 1988).

The results of our survival analyses together with the UGT2B7 knockdown study by Dellinger et al. (2012), suggest that UGT2B7 might be involved in controlling doxorubicin activity. This raises the question of whether this could be mediated by glucuronidation of 7-deoxydoxorubicinolone. Glucuronidation is one of few metabolic pathways that makes drugs more polar and enhances transport, so it is possible that glucuronidation promotes clearance of 7-deoxydoxorubicinolone from the cell. Moreover, clearance of this metabolic end-product could increase the rate of upstream metabolic reactions (i.e. establish a drive effect that increases conversion of doxorubicin to 7-deoxydoxorubicinolone). This might occur in liver, but also in tumour tissues, given that the main enzymes believed be involved in producing 7-deoxydoxorubicinolone, POR and CBR1, are found in breast tumours (Jo et al., 2016; Sneha et al., 2021). Future work could directly test whether

UGT2B7 is responsible for glucuronidation of this metabolite using *in vitro* assays with UGT2B7-expressing cell lysates or microsomes. Finally, it would be valuable to test in cell lines whether UGT2B7 overexpression increases the resistance of cancer cells to doxorubicin and/or its metabolite 7-deoxydoxorubicinolone.

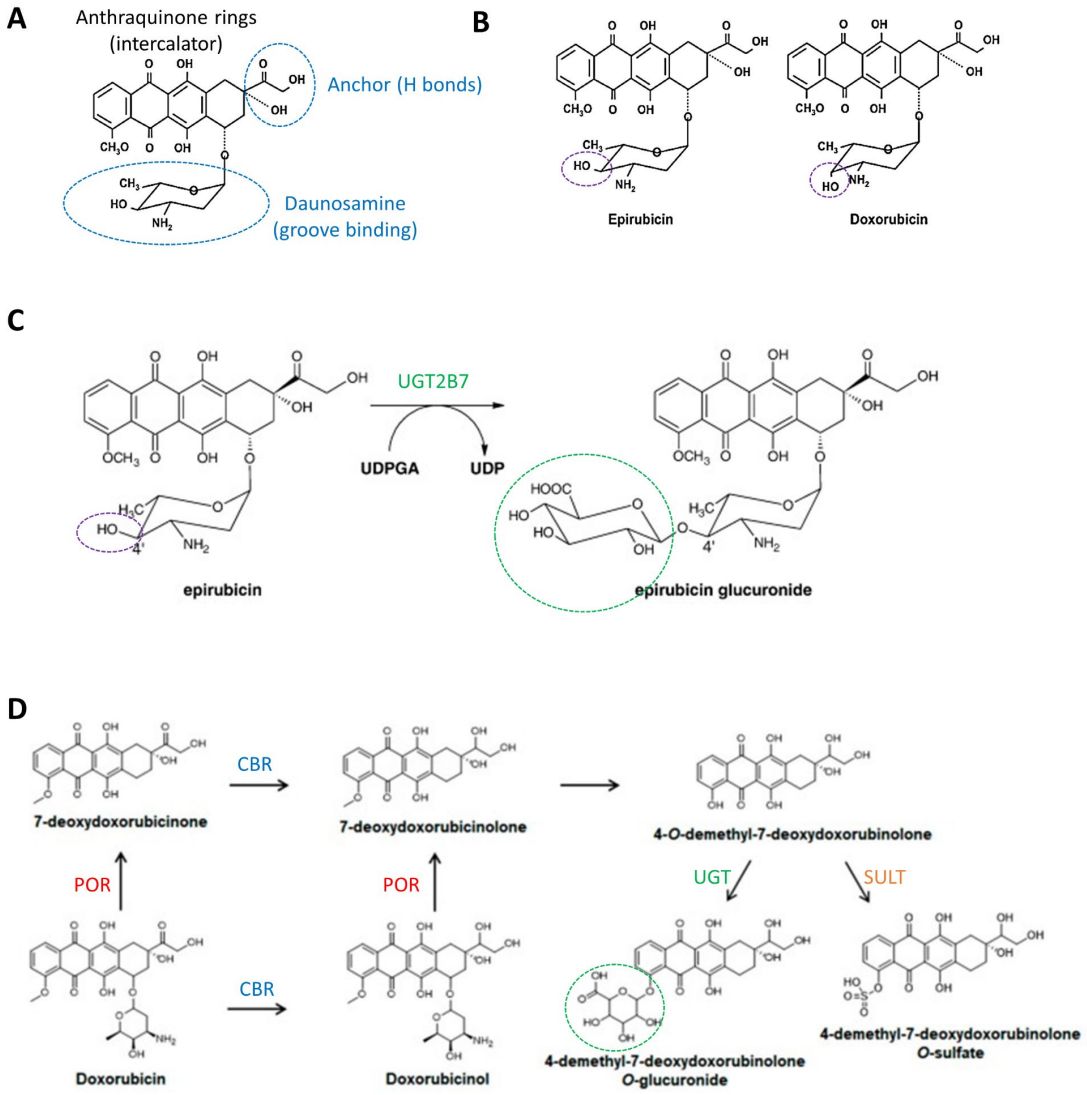

Figure 4.14. Comparison of epirubicin and doxorubicin structures and metabolic fates. **(A)** Structure of epirubicin showing the amino sugar (daunosamine) and aglycone (anthraquinone rings and anchor moieties) components. **(B)** Comparison of epirubicin and doxorubicin structure highlighting the epimeric OH group (purple dashed circle). **(C)** Schematic of epirubicin glucuronidation with the glucuronic acid group highlighted (green dashed circle). **(D)** Metabolic pathways for biotransformation of doxorubicin into doxorubicinol, 7-deoxydoxorubicinone, 7-deoxydoxorubicinolone, and glucuronide and sulphate conjugates of 7-deoxydoxorubicinolone. Note that two rarer metabolites doxorubicinone and doxorubicinolone have been omitted for simplicity. Schematics have been adapted from Choi et al. (2020) (open access), Jawad et al. (2020), and Mazerska et al. (2016) with permissions.

CHAPTER 5. TARGETED BREAST CANCER THERAPIES AS REGULATORS OF UGT2B7 AND THE POTENTIAL FOR SYNERGISTIC EFFECTS IN COMBINATION

5.1. Introduction

5.1.1. Targeted therapies for treatment of breast cancer

Breast cancer targeted therapies, as recently reviewed by Masoud and Pagès (2017), supress cancer cell growth by specifically targeting molecules which aid in cancer cell proliferation and survival. Typically, breast cancer cells overexpress certain receptors, which are involved in crucial cancer cell processes, such as proliferation, migration, cell cycling, angiogenesis and other important pathways (Masoud & Pagès, 2017). Because these processes are often dysregulated specifically in cancers, targeted inhibition is advantageous as there are less adverse effects involved than with untargeted chemotherapies. Use of targeted therapies is typically directed by cancer subtype and analysis of specific molecular markers.

Many luminal-like breast cancers express the estrogen receptor (ER) and progesterone receptor (PR), and these serve as important prognostic markers. As they are overexpressed in approximately 70% of breast cancers (Bae et al., 2015), endocrine therapies have been developed specifically to target these receptors. Tamoxifen is one of the most commonly used endocrine therapies in ER+ breast cancer, as previously described in section 1.2.1.

Another important receptor overexpressed in breast cancer – HER2, belongs to the epidermal growth factor receptor (EGFR/ERBB) family of receptor tyrosine kinases. Cancers with amplification

of the HER2 (*ERBB2*) gene are amenable to targeted therapies including trastuzumab that inhibit HER2 signalling (Bae et al., 2015). When both endocrine and HER2 receptors are present, the outcomes tend to be relatively favourable. Due to the success of targeting HER2 (*ERBB2*) (Han et al., 2022), other receptor tyrosine kinases have also been examined as possible targets for treatment. For hormone receptor positive or HER2 amplified tumours, targeted therapies may also be given in conjunction with or sequential to chemotherapy (Mandapati & Lukong, 2023).

Breast cancer tumours that lack ER and PR expression and do not show HER2 amplification are classified as triple negative breast cancer (TNBC). For this particular subtype, prognosis tends to be the least favourable, partly due to limited treatment options, with endocrine and HER2-targeted therapies unsuitable (de Ruijter et al., 2011; Nofech-Mozes et al., 2009). Chemotherapy forms the mainstay of treatment for TNBC globally, while some countries have also approved PARP inhibitors (e.g. Olaparib) (Mandapati & Lukong, 2023), immunotherapies (e.g. pembrolizumab) (Cortes et al., 2020; Cortes et al., 2022) and the antibody-chemotherapy conjugate sacituzumab govitecan, which delivers SN-38 to cells expressing Trop-2 (Bardia et al., 2021).

5.1.2. Receptor Tyrosine Kinases (RTKs) as targets for cancer treatment

Receptor tyrosine kinases (RTKs), a subclass of protein tyrosine kinases, are a group of transmembrane- cell surface receptors that play an important role in mediating cell-to-cell communication and various cellular processes including cell growth, motility, differentiation and metabolism (Du & Lovly, 2018). All RTK monomers consist of a single hydrophobic transmembrane domain (25-38 aa) and a C-terminal intracellular kinase domain. Structural differences between subclasses emerge due to the differences in the extracellular domain, which confers ligand specificity (Yamaoka et al., 2018) (Figure 5.1).

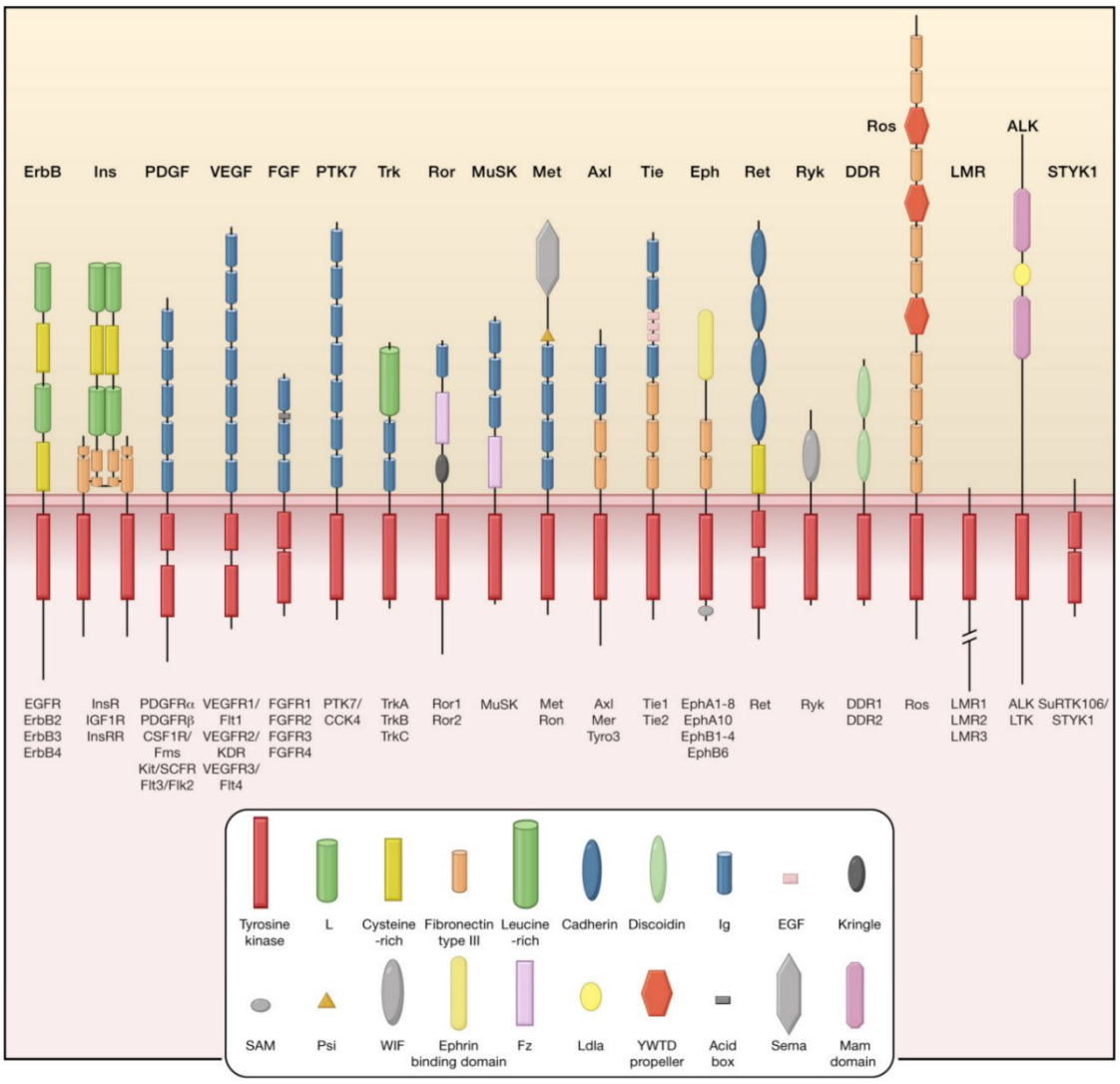

Figure 5.1. Receptor tyrosine kinase (RTK) structure depicted showing the common, catalytically active, intracellular domain as red rectangles, and the extracellular ligand-binding domain variable amongst different RTK subclasses, conferring ligand specificity. Figure has been reproduced from Lemmon and Schlessinger (2010) with permission.

All RTKs can be activated by auto-phosphorylation of the tyrosine residues (Yarden & Sliwkowski, 2001), or by dimerization once the ligand has been bound to the receptor, with the exception being the IGFR subfamily, which does not require the ligand to be bound to dimerize (Yamaoka et al., 2018). Genomic alterations which drive aberrant activation of RTKs are often involved in oncogenesis. The primary mechanisms of dysregulation are gain-of-function mutations, genomic

amplification, chromosomal translocations and autocrine activation (Du & Lovly, 2018; Lemmon & Schlessinger, 2010). There are 58 identified types of RTKs grouped into 20 subclasses (Robinson et al., 2000). Seven of these subclasses are currently targeted in cancer (Ségaliny et al., 2015; Yamaoka et al., 2018), of which the most relevant for this project is Class 1: Epidermal growth factor receptors (EGFR/ERBB).

5.1.3. Class 1 Epidermal growth factor receptors

The present study focused on the epidermal growth factor receptor (EGFR/ERBB) pathway in breast cancer (Jahanzeb, 2008). The ERBB family consists of 4 members, *ERBB1* (EGFR/HER1), *ERBB2* (HER2), *ERBB3* (HER3) and *ERBB4* (HER4) (Murphrey et al., 2023). There are currently 7 known ligands which bind to these receptors: epidermal growth factor (EGF), transforming growth factor-alpha (TGFA), heparin-binding EGF-like growth factor (HBEGF), betacellulin (BTC), amphiregulin (AREG), epiregulin (EREG), and epigen (EPGN) (Singh et al., 2016). Unlike the other receptors, HER2 do not bind any ligand directly, instead initiating signalling through heterodimerization with HER1 and HER3 (Hsu & Hung, 2016). It is also known to form a homodimer in situations wherein it is overexpressed (e.g. cancer) (Gutierrez & Schiff, 2011). HER3 has very minimal tyrosine kinase activity, and instead mainly elicits its function through heterodimerization with the other HER-family members (Black et al., 2019). Downstream signal transduction pathways affected by EGFR family activation include the signal transducer and activator of transcription (STAT), extracellular regulated kinase (ERK) and mammalian target of rapamycin (mTOR) signalling cascades (Wee & Wang, 2017), as indicated in Figure 5.2. This ultimately leads to oncogenic effects such as increased proliferation, survival (Schneider & Wolf, 2009), migration (Ohnishi et al., 2017), adhesion, and angiogenesis (Larsen et al., 2010).

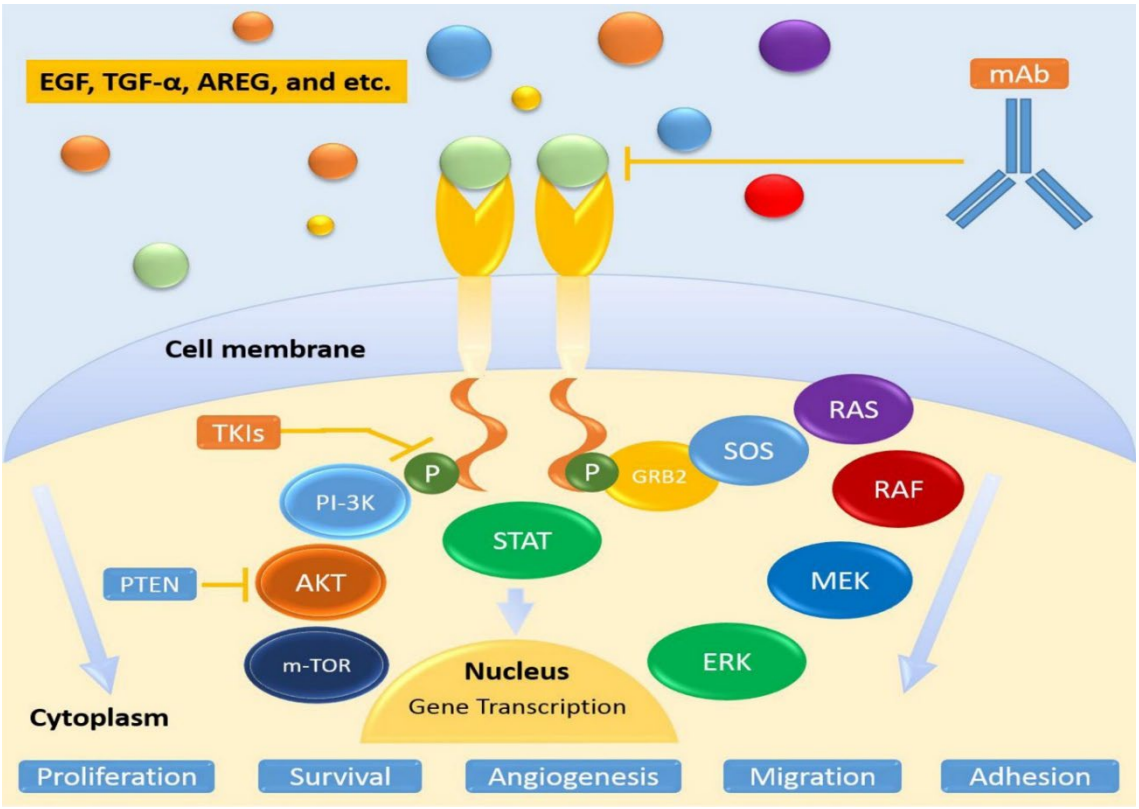

Figure 5.2. A simplified epidermal growth factor (EGF) signalling pathway, depicting the oncogenic effects acted upon by EGF ligands. EGF receptors (EGFR) may activate several downstream pathways including signal transducer and activator of transcription (STAT), extracellular regulated kinase (ERK) and mammalian target of rapamycin (mTOR). Small-molecule inhibitors (tyrosine kinase inhibitors) and monoclonal antibodies (mAb) have been developed to interrupt kinase activity of these EGFRs. This diagram has been reproduced with permission from (Haghgoo et al., 2015)

5.1.4. Tyrosine Kinase Inhibitors

RTKs can be targeted via the extracellular or intracellular domain (Xia et al., 2023) with the intention of disrupting downstream cellular signalling processes that are essential for cancer cell growth. Monoclonal antibody drugs are designed to target the extracellular domain and prevent ligand binding and/or dimerization. Tyrosine kinase inhibitors (TKIs) are small molecule drugs which can either reversibly or irreversibly inhibit the intracellular kinase domain (Thomson et al., 2023;

Yamaoka et al., 2018). As there are structural similarities in the different isoforms of RTKs, broader specificity and stronger inhibition has been developed with each generation of TKIs. Most second and third generation TKIs target more than one HER family member which has advantages in preventing compensatory effects. As the acquisition of drug resistance in targeted therapies has become an increasing problem, the progression to later generation TKIs and combinatorial therapies has helped by inhibiting acquired resistance mechanisms (Wu et al., 2020).

EGFR (*ERBB1*) and HER2 (*ERBB2*) are overexpressed in 40% and 25% of breast cancers respectively, hence they have been thought of as major drivers of tumorigenesis (Masoud & Pagès, 2017). As mentioned previously, HER2 amplification (HER2+) is a recognised molecular subclassification that is prognostic and predictive. Most HER2+ patients are treated as a first line with the monoclonal antibodies trastuzumab and pertuzumab in combination (Iancu et al., 2022). Several trials have shown a role for TKIs including lapatinib, neratinib, and pyrotinib in HER2+ patients (Ji et al., 2024). Lapatinib is a dual EGFR and HER2 inhibitor while neratinib is an EGFR, HER2 and ERBB3 inhibitor. Lapatinib and neratinib are FDA (FDA, 2007; Singh et al., 2018) and TGA (TGA, 2012, 2020) approved for HER2+ metastatic breast cancer, while pyrotinib (pan ERBB inhibitor) is approved for use by the Chinese State Drug Administration (Iancu et al., 2022). These TKIs may be used in combination with trastuzumab (dual inhibition) in HER2+ breast cancer. They may also be used in HER2+ cancer that has become refractory to trastuzumab, generally in combination with chemotherapy (Stanowicka-Grada & Senkus, 2023).

A subset of TNBC show elevation of EGFR signalling suggesting potential for targeting with TKIs that inhibit ERBB1 or other ERBB members (Lyu et al., 2023). However, only a fraction of patients respond to these therapies, and there is considerable interest in identifying ways to potentiate their effects (El Guerrab et al., 2016; McLaughlin et al., 2019) and/or prevent resistance (Iancu et al., 2022).

Overall, there are gaps our understanding that reduce our ability to identify potential responders to TKIs among TNBC patients, and to design rational combination therapies that improve responses.

The last context of interest in which TKIs may be used is hormone receptor positive breast cancer (Jeong et al., 2019). Crosstalk between the ERα and ERBB pathways is now known to be involved in mediating endocrine therapy resistance (Knowlden et al., 2003; Yang et al., 2020b). In particular, a recent study showed that high EGFR expression was associated with poor prognosis in ER+ breast cancers and that EGFR activation could lead to loss of ERα expression and tamoxifen resistance (Jeong et al., 2019). This suggests a potential benefit to dual EGFR and ERα targeting in ER+ breast cancer. There is some evidence to support from clinical trials. For example, gefitinib as an adjunct to anastrozole improved progression-free survival compared to placebo (median progression-free survival, 14.7 vs 8.4 months) (n=93) in previously untreated HR-positive metastatic cancer (Cristofanilli et al., 2010). Gefitinib has been trialled in HR-positive cancer that has developed resistance to endocrine therapy due to upregulation of EGFR. However, while some trials find that gefitinib has efficacy in this context, others do not (Green et al., 2009; Osborne et al., 2011). A summary of the current ERBB family targeting therapies trialled in breast cancer along with their clinical outcomes has been summarized by Iancu et al. (2022) as shown in Table 5.1.

Table 5.1. Overview of the usage of TKIs in breast cancer and their clinical outcomes. Table has been adapted from (Iancu et al., 2022). N, number of total participants; BC, breast cancer; PFS, progression-free survival; TNBC, triple negative breast cancer; EBC, early breast cancer; ABC, advanced breast cancer; MBC, metastatic breast cancer; CBR, clinical benefit rate; BBC, basal-like breast cancer; pCR, pathologic complete response rate; DFS, disease-free survival; OS, overall survival.

Reference	Year	Trial Phase	N	Disease stage, regimen used	Outcome
				Gefitinib	
(Baselga et al., 2005)	2005	II	31	ABC, Gt monotherapy	Reduced clinical antitumor activity
(Green et al., 2009)	2009	II	66	ABC, hormone resistant/negative, Gt monotherapy	Low CBR 11% vs. 7.7%
(Smith et al., 2007)	2007	II	206	EBC, Gt + anastrozole vs. anastrozole	No additional clinical effect
(Polychronis et al., 2005)	2005	II	56	Primary BC, ER, HER2, neoadjuvant, anastrozole + Gt vs. Gt	Significant mean reduction of proliferation related Ki67 index (98% vs. 92.4%)
(Cristofanilli et al., 2010)	2010	II	88	MBC, ER, Gt + anastrozole vs. anastrozole	Increase of PFS by adding Gt
(Carlson et al., 2012)	2012	II	141	MBC, Gt + anastrozole/fulvestrant	Similar CBR, response rates similar with Gt or endocrine therapy alone
(Bernsdorf et al., 2011)	2011	II	181	EBC, neoadjuvant, TNBC vs. nonTNBC	Higher pCR in TNBC, higher toxicity
(Tryfonidis et al., 2016)	2016	II	71	ABC, anastrozole + Gt vs. anastrozole + placebo	No added benefit, higher toxicity; terminated prematurely
				Erlotinib	
(Dickler et al., 2009)	2009	II	69	ABC, unselected BC population, progression under chemo	Minimal efficacy in unselected population
(Lau et al., 2014)	2014	I	N/A	BBC, metformin + Et	Increased apoptosis in a subset of BBC
(Ueno & Zhang, 2011)	2011	I	28	TNBC, xenograft model	Inhibition of metastasis, nonspecific effects
(Guix et al., 2008)	2008	II	52	HR, stage IIIIA	Inhibition of proliferation in ER, not in HER2 or TNBC
				Afatinib	
(Harbeck et al., 2016)	2016	III	508	MBC, HER2, progression on trastuzumab, At + vinorelbine	Reduced efficacy of combination At + vinorelbine
(Cortés et al., 2015)	2015	II	121	Brain MBC progressive or recurrent, HER2	No additional benefit, frequent adverse events

(Hanusch et al., 2015)	2015	II	65	ABC, At + trastuzumab, neoadjuvant	Comparable pCR with other antiHER2, but below expected
				Lapatinib	
(Baselga et al., 2012)	2012	III	455	EBC, HER2, Lt, and Lt + trastuzumab	pCR significantly higher after Lt + trastuzumab vs. trastuzumab alone
	2014	III			
	2014	II			
	2016	III			
	2006	III			
	2010	III			
	2010	III			
	2009	III			
	2010	III			
(de Azambuja et al., 2014)	2014	III	455	EBC, HER2, Lt, Lt + trastuzumab	Event free survival and OS did not differ between groups
(Bonnefoi et al., 2015)	2015	II	122	ABC, HER2, neoadjuvant setting, Lt, Lt + trastuzumab, trastuzumab alone	Modest pCR increase with antiHER2 blockade (60% vs. 52%)
(Piccart-Gebhart et al., 2016)	2016	III	8381	EBC, HER2, adjuvant setting, Lt, Trastuzumab or combination	No improvement in DFS with Lt, but added toxicity
(Geyer et al., 2006)	2006	III	324	ABC, HER2, Lt + capecitabine	Lt + capecitabine was superior to capecitabine alone
(Schwartzberg et al., 2010)	2010	III	1286	MBC, HER2, HR, Lt + letrozole	Significantly higher PFS, ORR and CBR
(Sherrill et al., 2010)	2010	III	1286	MBC, HR, HER2, Lt + letrozole	Lt + letrozole increased PFS interval compared with letrozole alone
(Johnston et al., 2009)	2009	III	1286	MBC, HR, HER2, 1st line therapy	Combined treatment significantly enhanced PFS and CBR
(Blackwell et al., 2010)	2010	III	296	MBC, HeR2, Lt vs. Lt + trastuzumab	Combined treatment improved PFS and CBR
				Neratinib	
(Chow et al., 2013)	2013	I/II	110	MBC, HER2, Nt + paclitaxel	High rate of response, higher toxicity

(Chan et al., 2016)	2016	III	2840	EBC/ABC, HER2, adjuvant setting after chemo and trastuzumab	Improvement of the DFS rate at the 2year follow up
				Canertinib	
(Rixe et al., 2009)	2009	II	198	MBC, progressive or recurrent	No clinically significant activity
				Tucatinib	
(Murthy et al., 2018)	2018	Ib	60	MBC, HER2, progressive BC	Favourable antitumor activity, acceptable toxicity
(Murthy et al., 2020)	2020	II	612	MBC, HER2, progressive BC, Tt combined with trastuzumab and capecitabine	Improved PFS and OS
				Pyrotinib	
(Ma et al., 2017a)	2017	I	38	MBC, HER2	Well tolerated, favourable antitumor activity
(Ma et al., 2019)	2019	II	128	MBC, HER2, Pt combined with capecitabine vs. lapatinib with capecitabine	Improved overall response rate and PFS rate
(Jiang et al., 2019)	2019	III	279	MBC, HER2, Pt combined with capecitabine	Improved PFS; Pt monotherapy antitumor activity

5.1.5. TKI pharmacokinetics and potential roles in resistance.

As mentioned previously, acquired drug resistance is a common hurdle in targeted therapy. This resistance is typically a result of loss of the target (i.e. its expression or functionality) due to mutation or epigenetic changes, or activation of alternative compensatory signalling pathways (Rosenzweig, 2018). However, changes in targeted therapy responses can also involve pharmacokinetic mechanisms. TKIs are subject to several ADME processes that can alter systemic and/or intratumoral exposure (see section 1.9 for more discussion). Relevant pathways for TKIs are transport (uptake and efflux), and metabolism by phase I CYP and Phase II UGT enzymes. The present study focused on EGFR inhibitors (gefitinib, erlotinib, and afatinib); and herein we discuss the pharmacokinetics of these drugs.

Drug efflux transporters have been extensively researched as mediators of drug resistance (Choi & Yu, 2014). ATP-binding cassette (ABC) transporters utilise ATP to facilitate the efflux of drugs from hepatocytes and target cells (Kroll et al., 2021). Upon discovery of their importance in multidrug resistance, three ABC transporters were named – P-glycoprotein/MDR1 (P-gp; multidrug resistance protein 1; *ABCB1*), MRP1 (multidrug resistance associated protein 1; *ABCC1*), and BCRP (Breast Cancer Resistance Protein; *ABCG2*) (Litman et al., 2001). Upregulation of these ABC transporters can limit the effectiveness of anticancer drugs, including TKIs. A strategy for the reversal of multidrug resistance, is concurrently administering ABC inhibitors to reduce drug efflux. This strategy has been used in clinical trials to re-sensitize cancer cells to chemotherapies (as reviewed by He and Wei (2012)). However, these drugs have generally proven too toxic for clinical application (Xiao et al., 2021).

Gefitinib is a high-affinity transport substrate for BCRP, and upregulation of BCRP has been implicated as a potential mechanism for resistance (Ozvegy-Laczka et al., 2004). Gefitinib is also a substrate of P-gp (Kitazaki et al., 2005). Erlotinib is transported by P-gp and BCRP and increased bioavailability of erlotinib has been observed in the absence of these proteins in knockout mice (Marchetti et al., 2008). Afatinib is a substrate of P-gp and BCRP and inhibitors of these transporters can alter its disposition i.e. increasing its exposure, rate of absorption, and therefore bioavailability (FDA, 2013; Wind et al., 2014).

Uptake transporters include the solute carrier (SLC and ELCO) superfamilies, which can control the amount of drug available in plasma and that reaches the target cells (Puris et al., 2023). This area is lesser studied as a mediator of TKI exposure and potential drug resistance, however there is recent evidence suggesting SLC transporters can be inhibited by TKIs (Xiu et al., 2023).

Phase I Cytochrome P450 (CYP) enzymes biotransform many targeted therapy drugs, producing both active and inactive metabolites. Overexpression of CYPs in tumour cells could increase this metabolism altering the pharmacological effect *(Doehmer et al., 1993)*. Gefitinib undergoes extensive biotransformation by CYP3A4, CYP2D6, CYP3A5, and CYP1A1 (Cohen et al., 2003; Li et al., 2007; Zhao et al., 2017). Erlotinib is metabolised by CYP3A4, CYP3A5, and to a lesser extent CYP1A1, CYP1A2, CYP2C8, and CYP2D6 (Johnson et al., 2005; Li et al., 2007). Afatinib however, is mostly excreted as the unchanged drug (minor metabolism by CYP3A4) (FDA, 2013) and therefore unlikely to be affected by changes in CYP enzymes *(Wind et al., 2017)*.

Phase II UGT-mediated glucuronidation is generally an inactivating modification that facilitates efflux from the cells and excretion from the body. Some TKIs have been identified as direct UGT substrates, while for others, their oxidative metabolites are glucuronidated. However, the UGT

isoforms involved are unknown in most cases. In the case of gefitinib, glucuronides have not been reported in human plasma or urine (Ma et al., 2017b; Whirl-Carrillo et al., 2021); however they were identified in mice (Molloy et al., 2021). Erlotinib oxidative metabolites are glucuronidated in humans, with UGT1A1 implicated in this process (Allain et al., 2020). There is emerging evidence suggesting a role for UGT enzymes in resistance to some TKIs. UGT1A expression was linked to altered response to pazopanib (a VEGFR inhibitor) in a broad cell line based sensitivity screen (Allain et al., 2020). Furthermore, clinically in non-small-cell lung cancer, UGT1A levels were overall 3-fold higher in non-responding patients to erlotinib (Allain et al., 2020). Specifically, UGT1A6 mRNA expression was 8-fold higher in patients with an erlotinib-resistant phenotype (López-Ayllón et al., 2015). This could be related to the role of glucuronidation as a route for metabolising erlotinib's oxidative metabolites.

5.1.6. Hormone receptor targeted therapies: Tamoxifen

Estrogen signalling is regulated by estrogen receptors (ERα and ERβ) (Marino et al., 2006), which require the binding of estrogens such as the most potent form, 17β-estradiol (E2) to initiate downstream pathways leading to cellular proliferation as part of breast development. Dysregulation of ERα signalling is a hallmark of breast cancer initiation and progression with around 60% of breast cancers expressing high levels of ERα and showing estrogen-dependent growth (Bocchinfuso & Korach, 1997). Tamoxifen is a well-established and effective drug for hormone receptor (e.g. ERα and progesterone receptor) positive breast cancer (Cuzick et al., 2015). Tamoxifen is a selective estrogen receptor modulator (SERM) with both antagonistic and agonistic properties (Sunderland & Osborne, 1991). In breast tissue, it principally acts as an antagonist of ERα to block the access of 17β-estradiol (E_2) (Yao et al., 2020; Yu & Bender). This ultimately inhibits the transcription of several core estrogen-responsive genes which then impedes estrogen-driven tumour growth (Wang et al.,

2004a). Such genes include *EEIG1* (early estrogen-induced gene 1) and *PDZK1* (PDZ Domain Containing 1) which were identified as being upregulated in breast cancer, and specifically inhibited by tamoxifen (Frasor et al., 2006; Ghosh et al., 2000; Kim et al., 2013). Tamoxifen may be used as neo-adjuvant therapy to shrink tumours before surgery, and post-surgery for at least 5-years to prevent relapse. It is taken as a daily oral dose (Davies et al., 2011).

5.1.7. Tamoxifen pharmacokinetics and potential role in resistance

Tamoxifen is considered a prodrug, as its metabolites (particularly endoxifen and 4-OH-tamoxifen) have more potent anti-estrogenic effects (Hao et al., 2022; Lim et al., 2005). The production of these active metabolites requires the phase I metabolism (oxidation) of tamoxifen by multiple CYP enzymes (CYP2D6, CYP3A4, CYP3A5, CYP2C9, CYP2C19) (Cronin-Fenton et al., 2014). CYP2D6 is considered one of the most important activating enzymes producing 4-OH-tamoxifen which has 100 times the potency of tamoxifen. There is evidence that several *CYP2D6* polymorphisms alter breast cancer outcomes in tamoxifen-treated patients, both increasing and reducing breast cancer recurrence/survival (Cronin-Fenton et al., 2014). Endoxifen and 4-OH-tamoxifen are substrates of the ABCB1 transporter, and knockout of the transporter in mice alters their disposition (Iusuf et al., 2011).

Several UGTs (UGT1A3, UGT1A4, UGT1A8, UGT1A10, UGT2B7 and UGT2B15) are involved in the inactivation of tamoxifen metabolites, with varying specificities for the different metabolite isomers (cis vs trans) (Blevins-Primeau et al., 2009). The putative metabolic cascade is summarized in Figure 5.3. As yet it remains unclear which UGTs are most important for clearance of active tamoxifen metabolites, either through hepatic or intratumoral metabolism. However, as discussed in 5.1.10, there is a compelling argument that UGT2B15 may have a role in clearance of tamoxifen metabolites

in ERα positive cell types, such as breast cancer cells, because the *UGT2B15* gene can be induced by tamoxifen via a ERα mediated pathway.

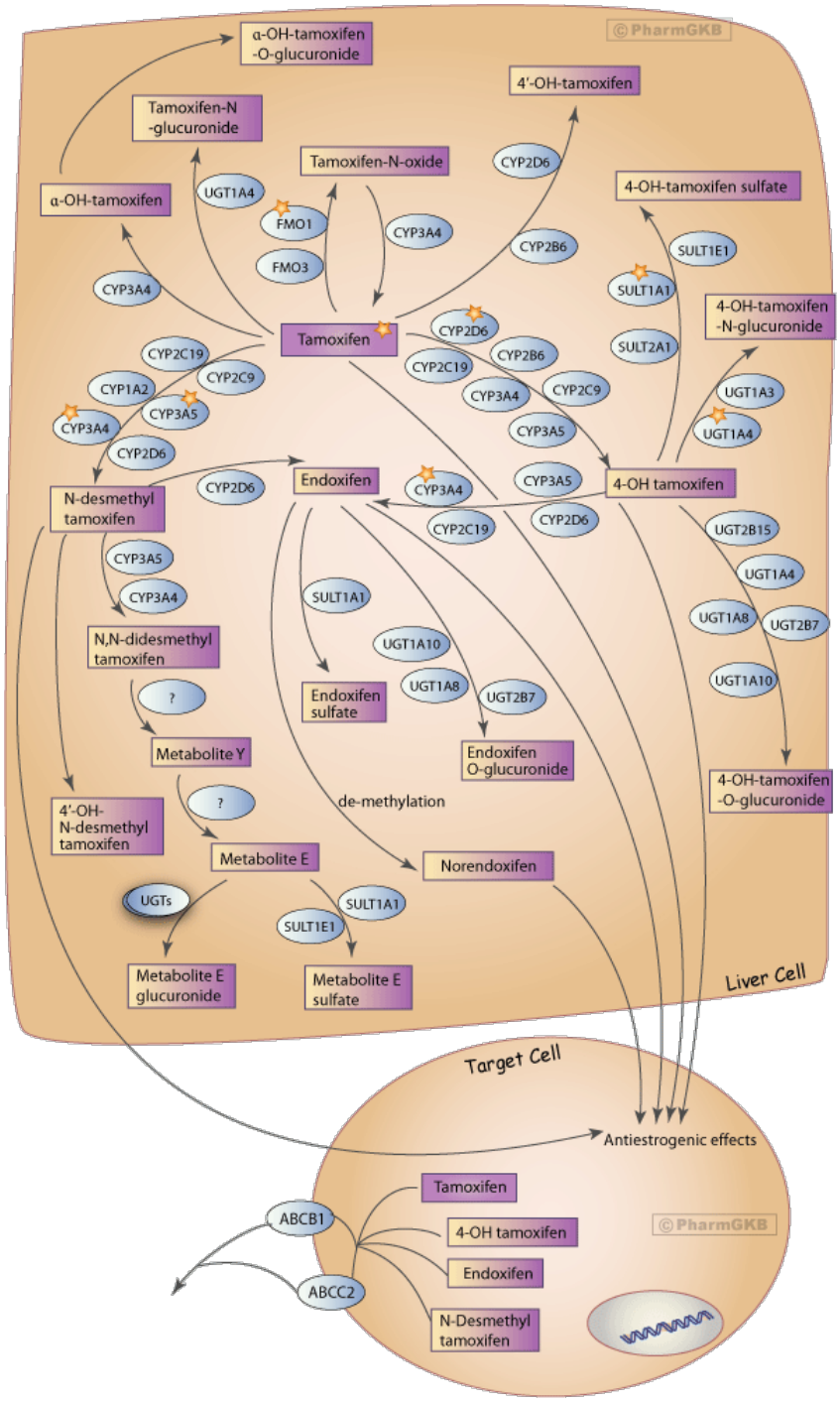

Figure 5.3. The candidate genes involved with the metabolism of Tamoxifen in the liver . Several of the active metabolites (Endoxifen, 4-OH tamoxifen, norendoxifen and N-desmethyl tamoxifen) are responsible for the most potent antiestrogenic effects in the target site as well as the parental compound (tamoxifen). Summarised diagram reproduced with permission by Klein et al. (2013).

5.1.8. Drug Drug Interactions (DDI) and pharmacokinetic enhancement

A discussed in Chapter 1, pharmacokinetic drug-drug interactions (DDIs) occur when one drug (perpetrator) alters the exposure of another drug (victim) as measured by a change in the area under the plasma concentration-time curve (AUC) (Miners et al., 2023). Classically two types of DDIs are defined: inhibition and induction. The mediators of these DDIs are ADME factors, either drug transporters or drug metabolic enzymes (DME); herein we will focus only on the latter.

Inhibition DDIs occur when a drug inhibits the activity of a DME, leading to reduced metabolism of other substrates of that DME (Miners et al., 2023). There are three main types of enzyme inhibition: competitive, non-competitive and uncompetitive. In competitive inhibition, substrate and inhibitor binding are mutually exclusive, this usually occurs when the inhibitor binds at the active site and these inhibitors often structurally resemble substrates (Eun, 1996). However, competitive inhibition can also occur when the inhibitor sterically prevents substrate binding through binding to other sites on the enzyme. A noncompetitive inhibitor does not bind at the substrate binding site and does not prevent substrate binding; however, it does prevent catalysis (Blat, 2010). Uncompetitive inhibition is rarer and occurs when the inhibitor binds only to the enzyme-substrate complex and prevents/decreases enzyme activity, leading to a buildup of trapped substrate (Strelow et al., 2004). While a DDI is a clinical phenomenon, inhibition can be modelled *in vitro* using assays in which the perpetrator drug is added at varying doses to a reaction containing the enzyme and a suitable victim substrate. To determine enzyme specificity, the reaction can use cell lysates or microsomes from a heterologous cell system expressing just one enzyme isoform (Miners et al., 2010). Alternatively liver microsomes may be used with a selective substrate that is metabolized by only one enzyme

isoform (i.e. probe substrate) (Court, 2005). By graphically modelling the enzyme reaction with and without the presence of the inhibitor, using a Lineweaver-Burk plot (double reciprocal) it can delineate the form of inhibition.

Induction DDIs most commonly occur when the perpetrator drug increases the amount of the DME, leading to increased metabolism of other substrates of that DME (Miners et al., 2023). In the majority of reported cases, this is due to transcriptional upregulation of the DME gene (Okey et al., 1986; Sinz et al., 2008). However, it is possible for posttranscriptional events to increase the amount of enzyme in the cell, or even posttranslational changes to increase the activity of the enzyme. The most commonly described example of this involves CYP2E1, wherein ethanol induces protein stabilisation through the ubiquitin-proteasome proteolytic pathway (Novak & Woodcroft, 2000; Roberts et al., 1995). Similarly, pyrazole and isoniazid are also able to induce protein expression of CYP2E1 without a corresponding mRNA increase (Novak & Woodcroft, 2000; Zand et al., 1993). Importantly, induction based DDIs cannot be modelled using purely *in vitro* assays as with inhibition, because they require events that only occur in intact cells. Hence, if induction is suspected, it is generally interrogated in cell-based assays by treating cells with the perpetrator drug and then measuring any change in the expression of the target enzyme at mRNA or protein levels.

Overall, by convention, inhibition based DDIs are presumed to occur at the level of the enzyme/substrate interaction, while induction based DDIs are presumed to occur at the level of gene regulation. However, it should be noted that this is an oversimplification. For example, transcriptional (or other cell-based) events could also reduce the expression of a DME. Similarly, it is possible, but rare, for a drug to directly enhance the activity of an enzyme (Dow et al., 2023).

DDIs are a problem in oncology as cancer patients are often treated with multiple drugs to manage their cancer, pain, treatment related side effects, and comorbidities. Many anti-cancer drugs also have a narrow therapeutic index and high risk of toxicity. The major clinical concerns with DDIs are increased treatment toxicity or reduced efficacy.

While DDIs are typically considered to present a risk of clinical harm, there are some cases where a DDI might be exploited to increase clinical benefit by enhancing drug exposure. The best-known example of this is the use of ritonavir in anti-viral therapy for HIV. Ritonavir is a protease inhibitor that can reduce viral protein production but shows high toxicity (Zhong et al., 2002). It is also a potent CYP3A4 inhibitor that reduces the metabolism of other antivirals, thus allowing them to be more effective with reduced frequency of dosing (Hull & Montaner, 2011). Hence it is now routinely used at a low (subtoxic) dose as a pharmacokinetic enhancer.

There is current interest in applying pharmacokinetic enhancement in oncology, although to date most approaches remain in clinical trials. One clinically approved example is Teysuno that combines the 5-FU prodrug Tegafur with a pharmaco-enhancer. 5-FU has erratic oral bioavailability due to highly variable expression of its catabolizing enzyme dihydropyrimidine dehydrogenase (DPD). Combining Tegafur with a DPD inhibitor (eniluracil) leads to almost 100% oral bioavailability of 5-FU. This allows predictable dosing response and toxicity, and improves the antitumor efficacy and therapeutic index of 5-FU (Schilsky & Kindler, 2000).

The pharmacokinetic enhancement of various TKIs has been demonstrated by the inhibition of CYP3A4, usually involving known CYP3A4 inhibitors; cobicistat, ritonavir, or itraconazole (Westra et al., 2023). This can produce favourable exposure, given a variety of kinase inhibitors are predominantly metabolised by CYP3A4 (Hakkola et al., 2020). Pharmacokinetic boosting by CYP3A4

inhibition has been shown to improve exposure in TKIs such as, axitinib (Lubberman et al., 2017), crizotinib (Hohmann et al., 2021), erlotinib (Boosman et al., 2022), ibrutinib (Tapaninen et al., 2020), and osimertinib (van Veelen et al., 2022). These studies amongst others were recently summarized in a narrative review by Westra et al. (2023), however, whether these approaches will provide a clinical benefit is not yet known, and to date, have mainly been demonstrated on a case-by-case basis.

Interestingly, many TKIs are not only substrates for CYPs, but are also inhibitors of CYP activities. A notable example is erlotinib which is reported to mediate both time-dependent inhibition and induction of CYP3A activity (Calvert et al., 2014; Hakkola et al., 2020; Svedberg et al., 2019). Gefitinib is an inhibitor of CYP2C19 and CYP2D6 (Anwar et al., 2023). Consistent with the minimal metabolism of afatinib by CYP450s, CYP enzymes are not inhibited by afatinib (TGA, 2014). As this project is focused on UGTs, further discussion of the role of TKIs as potential perpetrators of CYP450 mediated DDIs will not be presented here, but the reader is directed to a recent relevant review (Hakkola et al., 2020).

5.1.9. Potential DDIs involving UGTs in which TKIs are perpetrators

Several studies indicate that TKIs can be both victims and perpetrators of DDIs involving UGTs. The ability of TKIs to inhibit various UGTs was investigated by Zhang et al. (2015). They screened the activity of a UGT panel including UGT-1A1, 1A3, 1A4, 1A6, 1A7, 1A8, 1A9, 1A10, 2B4, 2B7, 2B15, and 2B17 in the presence of 4 TKIs- axitinib, imatinib, lapatinib and vandetanib. Imatinib inhibited several UGTs to varying degrees, lapatinib showed strong inhibition of UGT-1A1, 1A4 and 1A7, and vandetinib against UGT1A9. To evaluate whether this inhibition could result in DDIs, Zhang et al. (2015) measured whether lapatinib affected glucuronidation of SN-38 in UGT1A1 recombinant

microsomes. SN-38 is an active metabolite of irinotecan that is a substrate of UGT1A1. The K_i of lapatinib in relation to SN-38 metabolism was 0.6 µM in UGT1A1 supersomes and 1.6 µM in HLMs. The lapatinib inhibition resulted in a predicted increase in SN-38 AUC by 25%. UGT2B17 inhibition by imatinib also predicted an AUC increase of 140% in regard to 4-Methylumbelliferone (4-MU) metabolism. This demonstrates the potential for DDIs caused by TKI-mediated inhibition of UGT activity towards other drugs used in combination in various cancers.

Liu et al. (2010), examined TKI mediated inhibition of a panel of UGTs using a specific enzyme-expressing supersomes and the generic substrate 4-MU. The main focus of their study was the potent inhibition of UGT1A1 activity by erlotinib and gefitinib. They further showed this could inhibit glucuronidation of bilirubin, an endogenous compound solely metabolised by UGT1A1. They modelled this effect, finding that co-administration of erlotinib at 100 mg/day could result in a 30% increase in the AUC of other drugs used in combination if they are primarily metabolised by UGT1A1; moreover, a 150 mg/day erlotinib dose could result in a 10% increase in AUC of bilirubin (Liu et al., 2010). The data from Liu et al. (2010) also showed that gefitinib and erlotinib significantly reduced the activity of UGT2B7 with 4-MU activity (by 71% and 33% respectively), using UGT2B7 supersomes (Figure 5.4). While they did not examine an inhibition profile of UGT2B7 with other substrates, these data suggest that the TKIs might alter exposure to clinically relevant drugs that are UGT2B7 substrates. Afatinib was found to inhibit UGT1A1 and UGT2B7 activities, but at concentrations considerably higher than plasma C_{max} and thus unlikely to occur clinically (TGA, 2014). Overall, the evidence that various TKIs can inhibit UGTs raises the possibility that they could be perpetrators of UGT-mediated DDIs. Depending on the drug combinations, this might lead to adverse effects. Alternatively, it might create synergistic benefits; for example, if the TKI reduces the clearance of another anticancer drug and increases its effective concentration in the tumour.

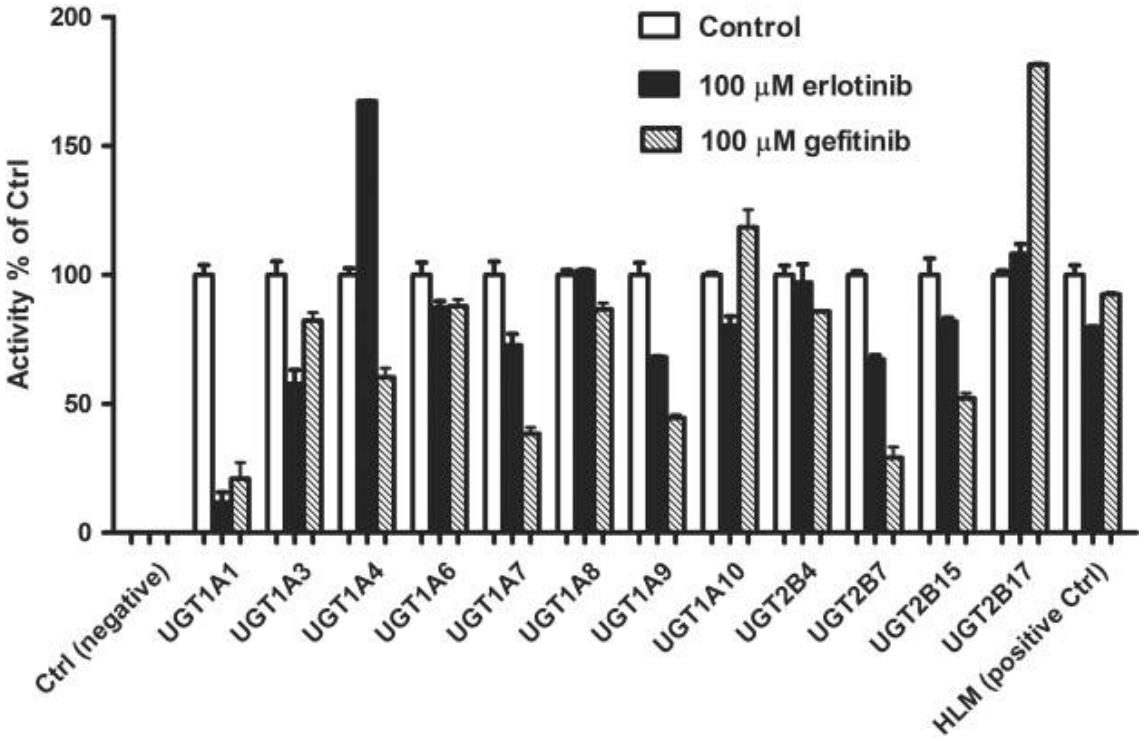

Figure 5.4. Erlotinib and gefitinib show significant alterations in 4-MU activity for various UGT isoforms expressed as recombinant microsomes (supersomes). Primarily less activity is observed in UGT1A1 supersomes treated with erlotinib, while reduction of activity by gefitinib is observed in UGT1A1 and UGT2B7 supersomes. Figure has been reproduced from Liu et al. (2010) with permission.

In addition to inhibition of UGT activities, there is some evidence that TKIs can induce UGT expression. Vemurafenib (PLX4032) is a BRAF targeting TKI which has been shown to induce several UGT2Bs in melanoma cells at the RNA level. As detailed by Dellinger et al. (2012) UGT2B10 and UGT2B15 were strongly induced by vemurafenib in SKmel28 cells, whilst UGT2B7 was modestly induced. It is currently unknown whether any of the EGFR-targeted TKIs can also regulate the expression of *UGT* genes. However, this is an important question, as induction of UGT expression creates the potential for induction based DDIs. Moreover, if the same drug can mediate both UGT induction and inhibition, then these effects may negate each other.

5.1.10. Potential DDIs involving UGTs in which Tamoxifen is the perpetrator

During the course of this study, new literature was published that identified tamoxifen as a novel inhibitor of UGT2B7 activity using the probe substrate naloxone (Hao et al., 2022). Naloxone is near-exclusively metabolised by UGT2B7 (Seo et al., 2014), making it an ideal probe substrate. In their study, they reported the IC_{50} of tamoxifen was 20.1 µM with a K_i of 37.7 µM. As this finding is very new, there is no further literature addressing whether this could result in changes in the metabolism of other drug substrates of UGT2B7. The studies presented in this Chapter sought to investigate this.

Interestingly Hao et al. (2022) also reported that tamoxifen reduced expression of rat Ugt2b1 mRNA in rat livers treated with tamoxifen. This suggests that tamoxifen can both inhibit UGT enzyme activity and *Ugt* gene expression. However, it is unclear how this datum should be extrapolated to humans. The rat Ugt2b1 enzyme shows a broadly similar activity profile for human UGT2B7 substrates (Mackenzie et al., 1997), but there are also major differences in substrate preferences between the rat and human enzymes (King et al., 2000), and it cannot be considered a true homologue.

Previous studies published by our laboratory show that the UGT2B15 and UGT2B17 genes are inducible by active tamoxifen metabolites 4-OH tamoxifen and endoxifen in MCF7 breast cancer cells (Chanawong et al. (2015) and unpublished data from this laboratory). Induction is mediated directly by the liganding of ERα and consequent binding of ERα to estrogen response elements (ERE) in the *UGT2B15* and *UGT2B17* gene promoters (Chanawong et al., 2015). UGT2B15 and UGT2B17 are also induced by oestradiol and its active metabolites by the same mechanism (Hu & Mackenzie, 2009). Given that UGT2B15 can glucuronidate these metabolites, this was proposed as a potential

feedback mechanism for limiting tamoxifen effectiveness in ER-positive cell types, such as breast cancer cells.

In contrast to UGT2B15 and UGT2B17, there is currently no evidence that UGT2B7 is regulated by ERα. Harrington et al. (2006) examined whether several *UGT2B* genes were regulated by oestradiol in MCF7 cells. They detected UGT2B15 induction but could not detect UGT2B7 mRNA in MCF7 cells even after estrogen stimulation. The *UGT2B7* promoter also lacks the conserved EREs found in the *UGT2B15* and *UGT2B17* genes. Thus overall, UGT2B7 is not considered to be an estrogen-responsive gene and is unlikely to be regulated by tamoxifen or its metabolites. However, given the high level of UGT2B7 found in liver, it is likely that it plays a role in systemic clearance of its metabolites.

5.1.11. Aims of Chapter 5

The reviewed literature highlights current gaps in our understanding of interactions between targeted drugs and UGT enzymes. To begin to address some of these gaps, we generated two aims that were focused on possible interactions between targeted therapies and UGT2B7 expression and activity. The knowledge gained from these studies could give insight into new roles for UGT2B7 in drug resistance, DDIs, and possible pharmaco-enhancement in cancer therapy.

Aim 1. Determine whether various EGFR-targeting TKIs induce the expression of UGT2B7 in breast cancer cells.

Aim 2. Determine whether two targeted therapies used in breast cancer can inhibit UGT2B7 mediated glucuronidation of epirubicin.

5.2. Methods

5.2.1. Tyrosine kinase inhibitors

The small molecule tyrosine kinase inhibitors (TKIs) erlotinib HCl (S1023), gefitinib HCl (S5098) and afatinib (S1011) were obtained from Selleckchem (TX, USA), supplied as high purity (>99%) salt forms dissolved in DMSO. The concentrations of the TKIs used in the *in vitro* experiments in this chapter were within the sub-millimolar range comparable to those observed in mean plasma levels and at plasma C_{max}. The reported mean plasma concentrations of each drug included in this study are: 3.11 µM for erlotinib (Lankheet et al., 2015), 0.34 µM for gefitinib (Hegi et al., 2011) and 0.23 µM for afatinib (Tamiya et al., 2017). Due to difficulties in obtaining reliable drug tissue concentrations for these chosen TKIs, the plasma concentrations were used as an initial indicator for the appropriate cell culture treatment concentration to use.

5.2.2. UGT2B7 gene expression analysis

MDA-MB-231, MDA-MB-453 and ZR-75-1 cells were seeded at $6.25*10^5$ cells/well in 6 well plates and treated for 48-hours TKIs at various concentrations, as specified in each figure. UGT2B7 expression (primers specified in 4.2.15) was measured by qRT-PCR as described in 2.2.7.

5.2.3. Luciferase promoter-reporter activity of UGT2B7 in response to TKI stimulation

The pGL3-Basic luciferase reporter constructs containing fragments of the *UGT2B7* promoter (-283/-1, -575/-1, -4926/-1) were already available for use and have been described previously (Hu et al., 2014c).

The various constructs were transfected into ZR-75-1 cells in a 48-well plate using Lipofectamine-LTX (Thermofisher Scientific). A mastermix containing 40 µL serum free RPMI-1640, 0.2 µL PLUS

reagent, 8 ng pRL-null (Renilla control), and 200 ng of the appropriate construct was pre-incubated at room temperature for 15 minutes to equilibrate the mixture. Subsequently, 0.8 µL Lipofectamine-LTX was added and incubated for 30 minutes at room temperature to enable DNA-Lipofectamine complex formation. The mixture was then transferred to the cell containing wells. 24 hours post transfection, various concentrations of erlotinib dissolved in methanol was transferred into the wells in fresh media. Following 72-hour drug treatment, luciferase activity was measured as described in 2.2.12.

5.2.4. Proteomic LC-MS analysis

Two hundred micrograms of protein lysates from TKI treated cells in TE buffer were subjected to tryptic digestion and proteomic analysis as described in 2.2.20.

Further proteomic analysis was conducted in this Chapter using a peptide panel representing multiple drug metabolizing enzymes and drug transporters. This panel was previously developed and validated using internal standard isotope labelled peptides within the laboratory of Professor Andrew Rowland by Ting Wu (unpublished, Flinders University, Clinical Pharmacology).

The panel of peptides screened utilizing this method were as follows:

UGTs: 1A1, 1A3, 1A4, 1A5, 1A6, 1A7, 1A9, 2B4, 2B7, 2B10, 2B15, 2B17

CYP450s: 1A2, 2A6, 2B6, 2C8, 2C9, 2C19, 2D6, 2E1, 3A4, 3A5, 4F2, 4A11, 2C18, 1A1, 4F12, 2J2

Drug Transporters: PMCA4, OATP1B1, OATP1B3, ABCB1 (MDR1/p-gp), OATP2B1, γ-gtp, SLC22A6 (OAT1), Na-k ATPase, OCT1 (SLC22A1), PepT1 (SLC15A1), ABCC2 (MRP2), ABCC4 (MRP4), NTCP (SLC10A1), ASBT (SLC10A2), ABCC3

5.2.5. Epirubicin glucuronidation assay and inhibitor studies

Epirubicin glucuronidation assays were performed as described in Ansaar et al. (2023) (also see Chapter 6 for detailed method development). Epirubicin was used at a concentration of 25 µM (approximately K_m). For inhibition studies, tamoxifen and gefitinib were added to the incubations at a range of 2.5-150 µM. These concentrations were within physiological ranges of drug concentrations and titrated to determine the optimal inhibitory range. 2-hour incubations were performed using alamethicin pre-activated HLMs at 0.01 mg/mL. The substrate incubation time remained short to minimize metabolism-dependent inhibition and inhibitor depletion as per previously published literature (Haupt et al., 2015). Separated supernatant fraction (2 µL) was injected into the tandem Triple Quadrupole LC/MS 6495C (Agilent Technologies, California, US) with the liquid chromatography product separation and mass spectral detection of the epirubicin glucuronide as described (2.2.19) (Ansaar et al., 2023).

5.2.6. Calculation of the inhibitory constant (Ki) of gefitinib and tamoxifen under a competitive inhibition model, and calculation of reversible inhibition (R1)

K_i was inferred from the IC_{50} determined using nonlinear regression analysis, with increasing concentrations of gefitinib/tamoxifen from 10-150 µM and using epirubicin at approximately K_m (25 µM) under the previously described incubation conditions (5.2.5). Calculations were performed using the K_i converter tool (Cer et al., 2009), utilizing the equation for competitive inhibition as described by the authors.

Reversible Inhibition (R1) was calculated using the below formula (FDA, 2019).

$$R1 = 1 + (I_{max,u} / Ki_{,u})$$

Where:

$I_{max,u}$ = the maximal unbound concentration of the inhibitor in plasma

$K_{i,u}$ = unbound inhibition constant estimated using $K_i * F_{u,mic}$

$F_{u,mic}$ = fraction of drug unbound in HLM; equivalent to fraction unbound in the incubation ($F_{u,inc}$)

5.2.7. Statistical analysis

Statistical analysis was performed using Microsoft Excel (Office 365) and GraphPad Prism. Two-tailed *t* tests were conducted on mRNA expression data and a resulting P value of less than 0.05 was considered statistically significant. Two-way ANOVA analysis followed by a post-hoc Dunnett's multiple comparison was performed on luciferase promoter reporter data, with p values less than 0.05 deemed statistically significant. Non-linear regression analysis was conducted in GraphPad Prism to delineate the relationship between UGT2B7 activity and inhibitors using a dose-response curve. The half maximal inhibitory concentration (IC_{50}) has been used to describe the potency of the drug towards enzymatic inhibition. The R^2 value describes the goodness of fit of the data in relation to the non-linear trend.

5.3. Results

5.3.1. UGT2B7 mRNA is not induced by TKIs in breast cancer cells

To assess whether UGT2B7 can be induced by EGFR inhibitors at the mRNA level, breast cancer cell lines (MDA-MB-231 and MDA-MB-453) were treated with gefitinib, erlotinib, or afatinib at 1 µM concentration. No significant change in UGT2B7 mRNA levels were observed following treatment with any of the TKIs (Figure 5.5 A&B). It should be noted that baseline mRNA levels of UGT2B7 were

quite variable between biological replicates, possibly due to stochastic effects that occur when quantifying low mRNA copy numbers. Given the variability of UGT2B7 mRNA levels, we chose to further examine possible regulation of *UGT2B7* transcription using promoter assays. *UGT2B7* promoter constructs of differing lengths were used as previously described in 3.2.6 and shown in schematic form in 3.3.3. Cells were transfected with the *UGT2B7* promoter constructs and then treated with increasing concentrations of erlotinib (0.5 – 5 µM). As shown in Figure 5.5C erlotinib had no significant effect on *UGT2B7* promoter construct activity, at any dose.

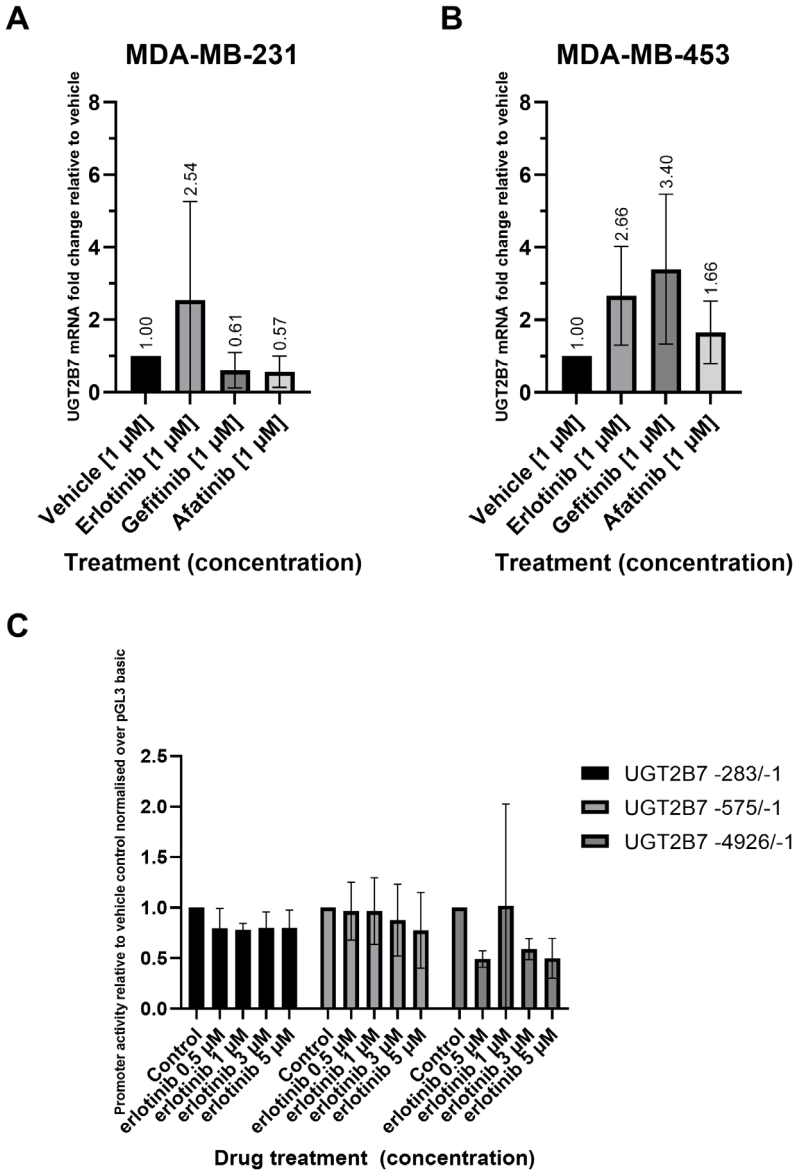

Figure 5.5. No change was observed in UGT2B7 mRNA expression and promoter activity in breast cancer cell lines following treatment with EGFR TKIs . MDA-MB-231 **(A)** or MDA-MB-453 **(B)** cells were treated for 48 hours with the drug treatment. qRT-PCR was performed to show mRNA expression of UGT2B7 in response to EGFR TKIs. Data is represented as fold change relative to the vehicle (methanol) control. Error bars represent standard deviation (+/-). 4 biological replicates were performed for MDA-MB-231 cells, while 1-5 biological replicates were performed for MDA-MB-453 cells. A one-way ANOVA was performed with no treatments reaching statistical significance ($p<0.05$). **(C)** *UGT2B7* luciferase promoter activity in the various sized promoter constructs upon 72-hour treatment with ascending erlotinib doses. The luminescence fold change is expressed as relative to the vehicle control (methanol) and normalised to the internal renilla transfection control and a promoter-less pGL3-Basic. Data represents 3-6 technical replicates combined from 2 biological replicates. A p-value of less than 0.05 is represented with an asterisk. Standard deviation is represented by the error bars.

5.3.2. Proteomic screening for effects of TKIs on ADME gene levels

During this project, our collaborators were developing a LC-MS based proteomic assay to quantify expression of a panel of core ADME proteins (CYPs, UGTs, and drug transporters). We were provided access to the panel to screen for changes in levels of ADME proteins in breast cancer cells after treatment with various TKIs. Unfortunately, in this set of experiments, UGT2B7 was unable to be detected using the proteomic assay. The reason for this discrepancy with previous studies where we detected UGT2B7 peptides in the same cell line (ZR-75-1) was unclear. However, because the peptide panel also detected other ADME factors, it still provided some insight into their potential regulation by TKIs. Figure 5.6 shows the results for those factors for which peptide detection reached the qualifier ion thresholds. For the full list of peptides screened see 5.2.4. UGTs (UGT1A7 and UGT2B17), CYPs (CYP2C19, CYP2E1, CYP2C18, and CYP2J2), ABC efflux transporters (ABCB1 and ABCC2), SLC uptake transporters (SLC22A6 and SLC22A1) and Na-K ATPase were all induced by erlotinib, gefitinib and afatinib to varying degrees. Induction of DMEs was strongest by gefitinib for all enzymes except UGT1A7. Gefitinib also induced uptake transporters SLC22A6 and SLC22A1. Due to the inability to detect UGT2B7 in this assay and other time and resource constraints, we did not proceed further with peptide-based assays in this Chapter.

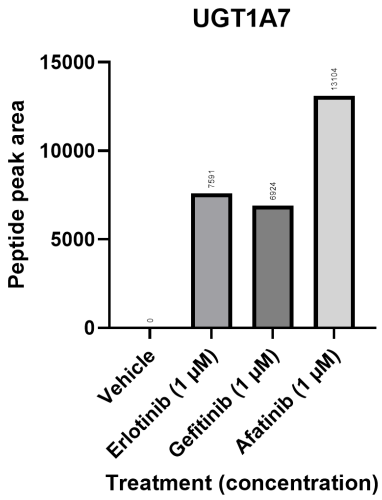
UGT1A7
Peptide peak area
15000
10000
5000
0
0
7591
6924
13104
Vehicle
Erlotinib (1 μM)
Gefitinib (1 μM)
Afatinib (1 μM)
Treatment (concentration)

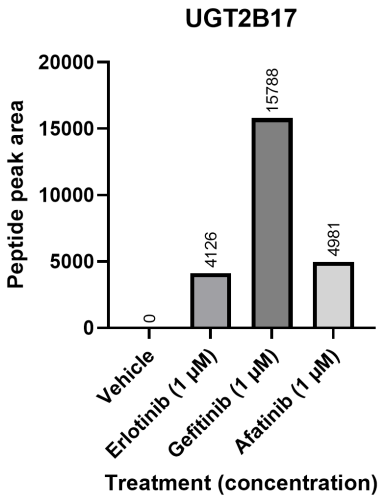
UGT2B17
Peptide peak area
20000
15000
10000
5000
0
0
4126
15788
4981
Vehicle
Erlotinib (1 μM)
Gefitinib (1 μM)
Afatinib (1 μM)
Treatment (concentration)

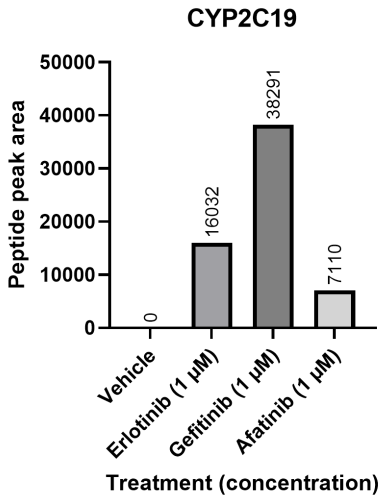
CYP2C19
Peptide peak area
50000
40000
30000
20000
10000
0
0
16032
38291
7110
Vehicle
Erlotinib (1 μM)
Gefitinib (1 μM)
Afatinib (1 μM)
Treatment (concentration)

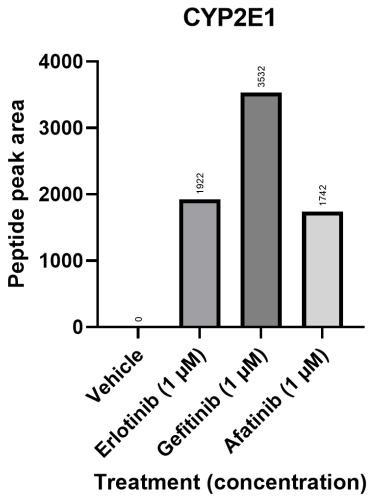
CYP2E1
Peptide peak area
4000
3000
2000
1000
0
0
1922
3532
1742
Vehicle
Erlotinib (1 μM)
Gefitinib (1 μM)
Afatinib (1 μM)
Treatment (concentration)

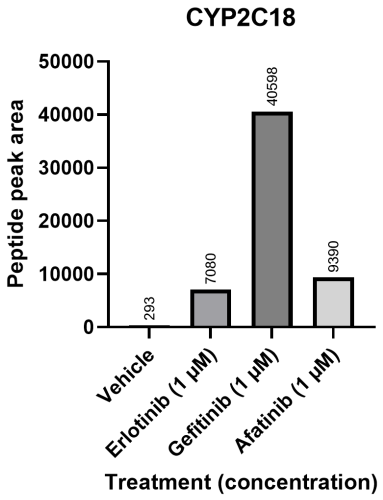
CYP2C18
Peptide peak area
50000
40000
30000
20000
10000
0
293
7080
40598
9390
Vehicle
Erlotinib (1 μM)
Gefitinib (1 μM)
Afatinib (1 μM)
Treatment (concentration)

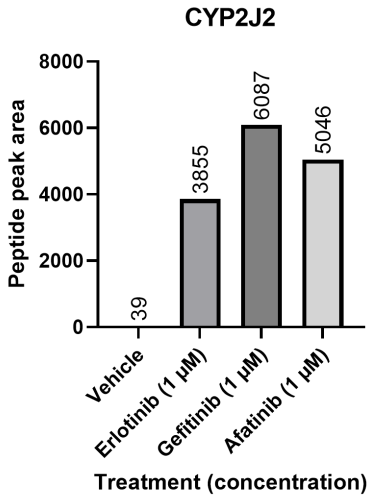
CYP2J2
Peptide peak area
8000
6000
4000
2000
0
39
3855
6087
5046
Vehicle
Erlotinib (1 μM)
Gefitinib (1 μM)
Afatinib (1 μM)
Treatment (concentration)

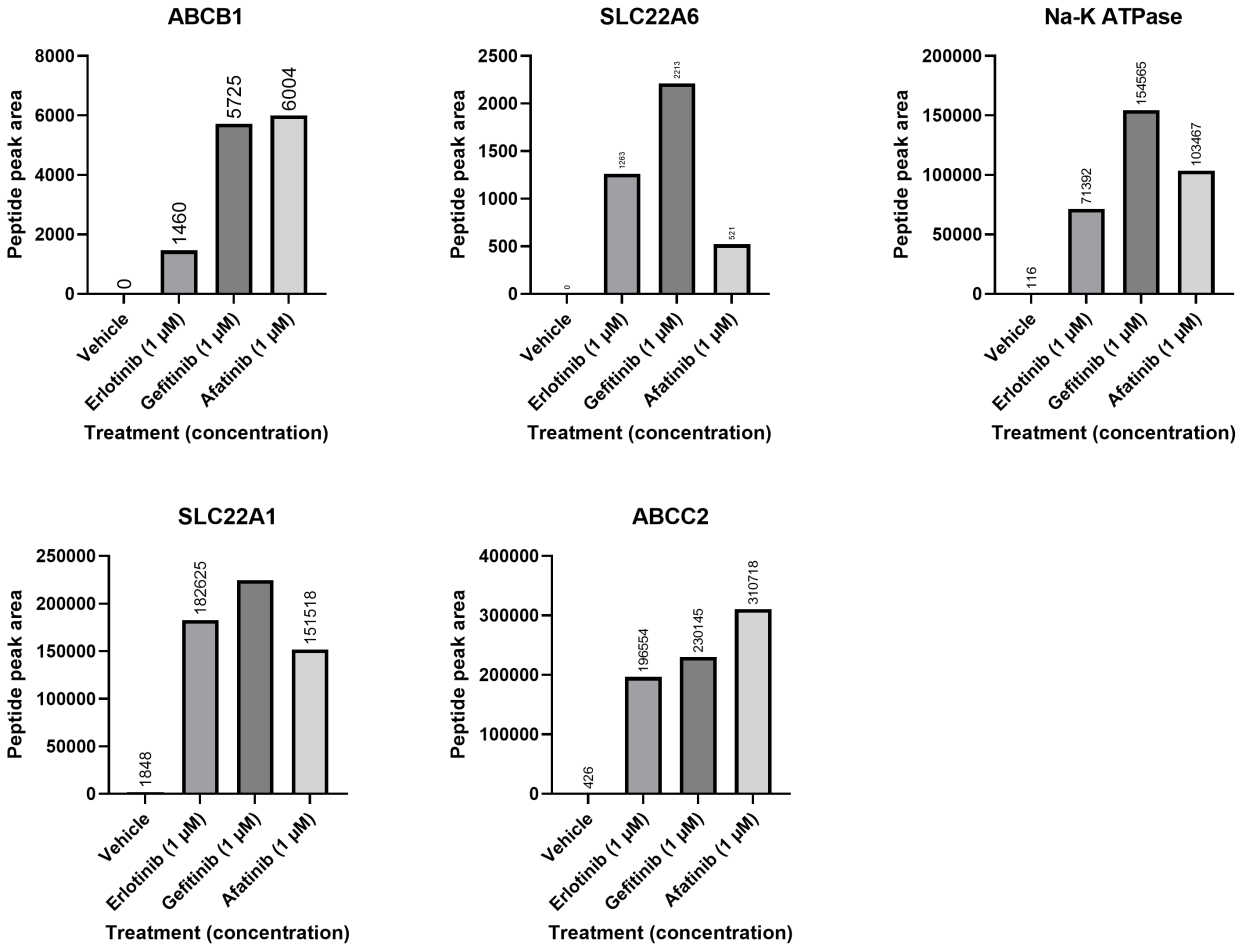

Figure 5.6. UGT and CYP drug metabolising enzyme and drug transporter peptide expression in response to EGFR TKIs at 1 µM treated over 48-hours in ZR-75-1 cells. Results are presented as a screen performed in singlicate. The vehicle for solubilising the drugs was DMSO. Peptides were screened using the LC-MS panel developed by Ting Wu (Flinders University, Clinical Pharmacology), with permission. Only quantifier ions meeting their respective qualifier ions have been depicted.

5.3.3. Gefitinib inhibits UGT2B7 mediated epirubicin metabolism.

Gefitinib was previously shown to be a competitive inhibitor of UGT2B7 in studies using the non-drug substrate 4-MU (Liu et al., 2010). The studies presented in this chapter sought to determine whether gefitinib-also inhibits glucuronidation of the clinically relevant anti-cancer drug epirubicin. Epirubicin was identified as a selective probe substrate for UGT2B7 and a highly specific, quantitative LC-MS-based assay for epirubicin glucuronide was developed as part of this project (detailed in Chapter 6). Here, the in vitro epirubicin glucuronidation assay was used to quantify the inhibitory potential of gefitinib. Glucuronidation assays were performed using HLM as the UGT2B7 enzyme source and gefitinib was added at a range of concentrations. LC-MS analysis revealed a strong inhibitory effect of gefitinib on epirubicin glucuronidation by UGT2B7 (IC_{50} 68.54 ± 9.56 µM) (Figure 5.7).

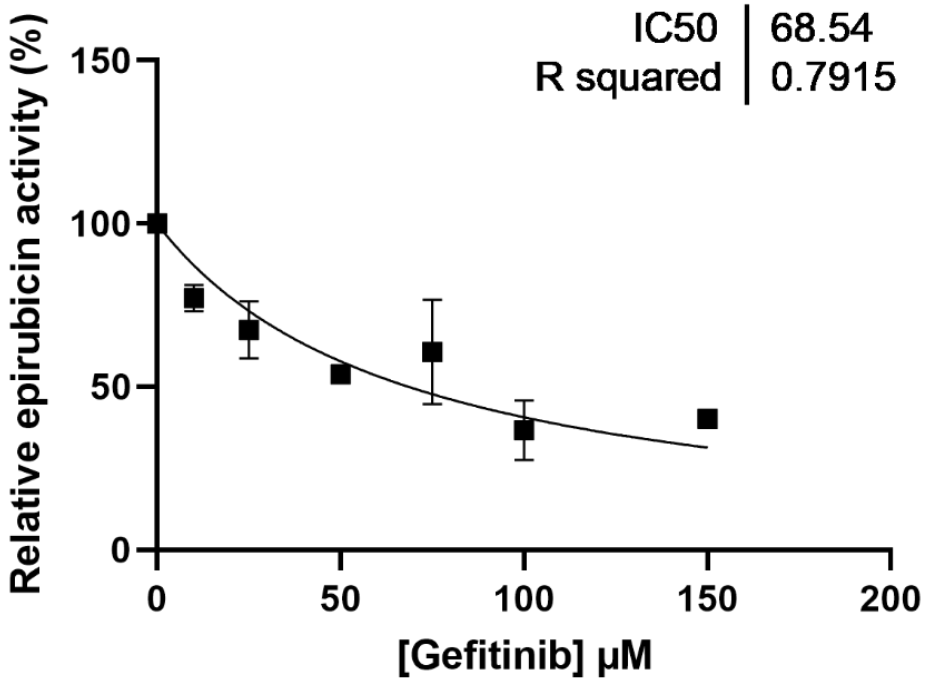

Figure 5.7. Gefitinib is a moderate-strong inhibitor of UGT2B7 activity towards the specific probe substrate epirubicin, shown as epirubicin glucuronide formation (% relative to vehicle control). Incubations were performed using human liver microsomes (HLMs) as the enzyme source. Substrate concentration was at the Km of epirubicin (25 µM). The IC50 was determined as 68.54 ± 9.56 µM using a non-linear regression trend analysis. N=2-4 technical replicates from 2 biological experiments combined.

5.3.4. Tamoxifen inhibits UGT2B7 mediated epirubicin metabolism.

During the course of this project, tamoxifen was identified as a new inhibitor of UGT2B7 via *in vitro* assays with the probe substrate naloxone (Hao et al., 2022). It was of considerable interest to determine whether tamoxifen also inhibited the glucuronidation of the clinically relevant anti-cancer drug epirubicin. The *in vitro* epirubicin glucuronidation assays was therefore applied to quantify the inhibitory potential of tamoxifen. Glucuronidation assays were performed using HLM as the UGT2B7 enzyme source and tamoxifen was added at a range of concentrations. LC-MS analysis revealed an extremely strong inhibitory effect of tamoxifen on epirubicin glucuronidation by UGT2B7 (IC_{50} 4.08 µM).

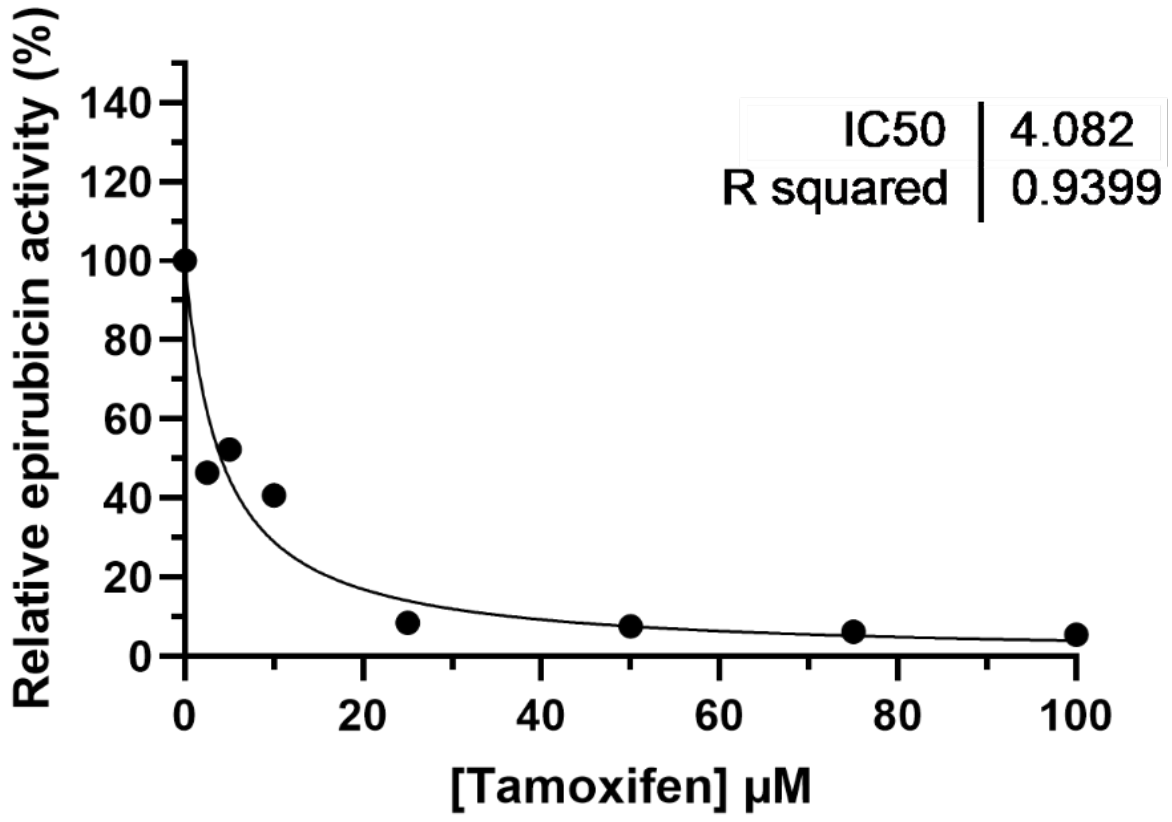

Figure 5.8. Tamoxifen is a strong inhibitor of UGT2B7 activity by the specific probe substrate epirubicin, shown as epirubicin glucuronide formation (% relative to vehicle control). Incubations were performed using human liver microsomes (HLMs) as the enzyme source. Substrate concentration was at the Km of epirubicin (25 µM). The IC50 was determined as 4.082 µM using a non-linear regression trend analysis. N=1 biological replicate.

5.3.5. Basic predictive modelling reveals a potential DDI between epirubicin and tamoxifen

To assess the DDI potential for tamoxifen and gefitinib, both putative inhibitors had inhibitory constant (K_i) values inferred from nonlinear regression analysis. Further DDI risk potential was calculated using the reversible inhibition (R1) estimation equation, provided by the FDA (2019). Table 5.2 shows the values for each of these variables obtained either from our analysis or from literature as appropriate. The value of R1 for gefitinib and tamoxifen was calculated to be 1.000464 and 1.4477 respectively. According to Vieira et al. (2014), if R1 ≥ 1.02 then the drug should be further evaluated for DDI potential. This places tamoxifen significantly above this threshold, indicating a potential DDI risk for use in conjunction with epirubicin. Gefitinib fell below this threshold, suggesting systemic levels of gefitinib are unlikely to reach high enough concentrations to cause a DDI with UGT2B7 substrates.

Table 5.2. The reversible inhibition (R1) calculated values for the proposed inhibitors of this study, tamoxifen and getfitinib. $I_{max,u}$ refers to the maximal unbound concentration of the inhibitor in plasma. K_i was estimated from the IC_{50} values obtained in the study, using the described equations from Cer et al. (2009).F_{umic} is the fraction of drug unbound in HLM; equivalent to fraction unbound in the incubation ($F_{u,inc}$). $K_{i,u}$ is the unbound inhibition constant estimated using K_i * $Fu_{,mic}$. The full calculations of K_i and R1 are detailed in the respective Methods section.

Parameters	**Tamoxifen**	**Reference**	
I_{max} (µM)	0.37	(Binkhorst, 2015)	
F_u	0.00726	(Dickschen et al., 2012)	
$I_{max,u}$ (µM)	0.0026862		
K_i (µM)	2	This thesis	
$F_{u,mic}$	0.003	(Li et al., 2009)	
$K_{i,u}$ (µM)	0.006		
R1			**1.4477**

Parameters	**Gefitinib**	**Reference**	
I_{max} (µM)	0.5	(FDA, 2003)	
F_u	0.034	(Li et al., 2006)	
$I_{max,u}$ (µM)	0.012		
K_i (µM)	34	This thesis	
$F_{u,mic}$	0.76	(Burns et al., 2015)	
$K_{i,u}$ (µM)	25.84		
R1			**1.000464**

5.4. Discussion

The overarching theme of this Chapter was understanding mechanisms of potential DDIs involving targeted anti-cancer drugs and chemotherapies. As discussed in the Introduction (section 5.1), the literature describes complex interactions between UGT enzymes and targeted therapies. Glucuronidation is involved in the metabolism and elimination of many TKIs. Moreover, several studies report that various TKIs can inhibit the activities of several UGTs including UGT2B7 (Liu et al., 2010; TGA, 2014; Zhang et al., 2015). Finally, one study had shown that a TKI could induce the expression of some UGTs including UGT2B7 (Dellinger et al., 2012). Both inhibition and induction of UGT2B7 by TKIs might result in DDIs, wherein the TKI is the perpetrator, and other drug substrates of UGT2B7, such as epirubicin, are potential victims. To better understand the potential for such DDIs, we developed two main aims: first to determine whether TKIs can induce UGT2B7 expression in breast cancer cells; second to determine whether specific targeted drugs inhibit epirubicin glucuronidation by UGT2B7.

5.4.1. ErbB inhibitors do not-induce UGT2B7 expression

A number of approaches were used to assess whether ErbB family targeted TKIs can regulate UGT2B7 expression. Across this set of experiments we tested first generation EGFR-specific TKIs gefitinib and erlotinib, and a second generation dual-specificity TKI afatinib that can inhibit wildtype and mutant EGFR forms as well as HER2 (Yu & Riely, 2013). Moreover, we investigated two cell models with high EGFR expression (MDA-MB-231 TNBC and ZR-75-1), while some experiments also included a line with very low EGFR expression as a control (MDA-MB-453). The mRNA analysis and promoter-reporter assays provided no evidence that any of the tested TKIs can significantly alter UGT2B7 gene expression in breast cancer cell lines. Thus, at this stage the null hypothesis cannot be

rejected. Unfortunately, the proteomic screen did not detect UGT2B7 and hence could not provide further confirmation. Caveats of the gene expression analyses include a low signal to noise ratio caused by high variance in basal UGT2B7 mRNA levels. This is likely due to inherent limitations of the qRT-PCR method when applied to low abundance targets. Future studies might address this using other quantitative methods such as droplet digital PCR, which improves upon qRT-PCR by offering greater precision (reducing variability between replicates), and sensitivity, while eliminating the need for standards (Miotke et al., 2014). In addition, it may be possible to find cell lines with higher basal UGT2B7 expression for analysis (ensuring also that they have sufficiently high EGFR expression to respond to the selected TKIs). The results from the promoter assays also cannot be considered definitive. EGFR signalling is transmitted to the nucleus by a wide variety of transcriptional effectors (Nava et al., 2019; Wee & Wang, 2017). It can also crosstalk with other pathways including ERα signalling. This makes it very challenging to predict binding sites for potential EGFR effectors within the *UGT2B7* promoter. We used the longest available *UGT2B7* promoter segment in our assays to maximize the chance that a relevant regulatory element may be included. However, longer constructs may also have more negative regulatory elements that could dampen any specific effects of EGFR signalling. It is also possible that any elements involved in regulation downstream of EGFR signalling are distal to even the longest promoter segment tested. Recent studies have associated EGFR inhibitors with p53 pathway activation (Huang et al., 2011; Jung et al., 2021); however, given that all promoter constructs tested contained the p53 responsive element, it appears unlikely that this is the case for the UGT2B7.

While no changes in UGT2B7 transcriptional regulation were observed in response to the TKIs, it remains possible that these drugs could modulate post-transcriptional or post-translational processes that control the amount of functional UGT2B7 protein in the cells. Because we did not

successfully measure UGT2B7 protein in these studies, whether TKIs can alter protein production remains to be addressed in the future. It is also possible that TKIs could impact on post-translational modifications that affect UGT activity, such as N-linked glycosylation or phosphorylation. These have been reviewed as mechanisms of UGT2B7 functional modulation by Hu et al. (2019a). In particular, tyrosine kinases have been reported to alter UGT2B7 substrate preference (Mitra et al., 2011). Given that EGFR signalling activates a cascade of protein kinases, it is conceivable that their inhibition might modify UGT phosphorylation. Such assessments could be done using phosphoproteomic methods.

5.4.2. Targeted therapies are potent inhibitors of epirubicin glucuronidation by UGT2B7

5.4.2.1. Gefitinib

Previous work showed that some EGFR-targeted TKIs could inhibit UGT2B7 (Liu et al., 2010). The focus of this part of the study was to determine whether inhibition of UGT2B7 by EGFR-targeted TKIs would affect the metabolism of the chemotherapy drug epirubicin. To assess inhibition, we developed a quantitative and highly specific assay for epirubicin glucuronide (described in detail in Chapter 6). This assay detects the major metabolite found in plasma - epirubicin glucuronide, which accounts for approximately 50% of the drug AUC. In comparison the second most abundant metabolite of epirubicin that is found in plasma – epirubicinol, accounts for 30% of epirubicin AUC, with a portion of that also being glucuronidated, however it is found in quite low concentrations in plasma (FDA, 1999). Whilst the newly developed assay has the sensitivity and specificity necessary to detect epirubicinol glucuronide, this pathway is not relevant in evaluating UGT2B7 activity, as the process requires two-stage metabolism, initially by aldo-keto reductase (ADK) to epirubicinol then conjugation by the UGT to epirubicinol glucuronide (Innocenti et al., 2001), making this not useful for kinetic modelling of UGT2B7.

Gefitinib was a moderate inhibitor of epirubicin glucuronidation in our assay. Previous studies with gefitinib and erlotinib used kinetic analysis to understand the mechanism of inhibition of 4-MU glucuronidation by different UGT isozymes and determined it to be predominantly competitive (as observed by the linear trends of their Lineweaver-Burk analysis) (Liu et al., 2010). However, this mechanism can be substrate specific, and another study found inhibition of UGT1A1-mediated *N*-3-carboxy propyl-4-hydroxy-1,8-naphthalimide (NCHN) glucuronidation by erlotinib to be non-competitive (Cheng et al., 2017). We were unable to calculate the inhibitory constant (K_i) and assess the mode of inhibition because this required absolute quantification of the epirubicin glucuronide using a standard. At the time of writing there is no epirubicin glucuronide standard commercially available. However, we extrapolated using a competitive inhibition model (Cer et al., 2009) to generate a K_i estimate of 34.27 µM for gefitinib. This is commonly accepted, as Haupt et al. (2015) claim predicted K_i values to be within a factor of 2 to experimentally determined K_i values 92% of the time (n=343). However, mode of inhibition is an area that could be further investigated in the future.

Drug-mediated enzyme inhibition observed *in vitro* does not necessarily indicate that a clinically relevant DDI will occur *in vivo*. For example, IC_{50} values greater than 75 µM, are very rarely clinically relevant, as typical drug dosages are unlikely to be high enough to achieve those levels in plasma (Thummel & Wilkinson, 1998). As the IC_{50} for gefitinib fell just below this value (IC_{50} 68.54 µM), we further analysed whether it could result in a DDI using a basic reversible inhibition model to calculate the ratio of intrinsic clearance values of epirubicin (victim) in the absence and in the presence of gefitinib (perpetrator). Reversible inhibition (R1) was calculated using the formula $R1 = 1 + (I_{max,u}/K_{i,u})$ as recommended by the US FDA (FDA, 2019). Definitions for each of the variables are given in the Methods 5.2.6 section.

In this case, the R1 value is much lower, hence it is unlikely that gefitinib would produce DDIs involving UGT2B7 (as measured by increased systemic exposure of the victim drug). One caveat of this analysis is that it considers only the plasma concentration of gefitinib, which is approximately 0.5 µM (Nio et al., 2022). One study has reported that intratumoral levels of gefitinib can be up to 100-fold higher than plasma levels in breast cancer patients (McKillop et al., 2004). Whether these higher gefitinib levels would be sufficient to inhibit UGT2B7 and increase intratumoral epirubicin exposure would need to be tested empirically, e.g. using cell line models.

While preclinical studies have provided support for EGFR inhibition in TNBC models (Abrahams et al., 2024; Brand et al., 2014; Corkery et al., 2009), clinical trials have largely only shown benefit when these drugs are combined with other targeted therapies or chemotherapies (Ou et al., 2024). Relevant to the current study, a phase II trial on ER- invasive breast cancer patients (n=181) found that adding gefitinib (250 mg daily) to neoadjuvant epirubicin/cyclophosphamide (EC) increased pathologic complete response (pCR) from 12% to 17%; however, complete response and overall objective response did not differ and adverse effects were increased (Bernsdorf et al., 2011). Considering both the modest effect of gefitinib on epirubicin glucuronidation and the minimal efficacy of this combination seen clinically, it may be concluded that combining anthracycline and gefitinib is not a particularly promising approach.

5.4.2.2. Tamoxifen

As presented in the introduction, during the course of this project tamoxifen was identified as a novel inhibitor of UGT2B7 activity. In the present study, tamoxifen was found to be a very potent inhibitor of UGT2B7-mediated epirubicin glucuronidation. As discussed in the previous section, in the absence of epirubicin glucuronide standards we could not precisely calculate the inhibitory

constant (K_i) and assess the mode of inhibition. Hence, we extrapolated using a competitive inhibition model to generate a Ki estimate of 2.04 µM for tamoxifen. While UGT2B7 glucuronidates the trans isomers of the active tamoxifen metabolites 4-OH-tamoxifen and endoxifen (Blevins-Primeau et al., 2009), we assume that tamoxifen itself inhibits UGT2B7 activity, largely because in the *in vitro* glucuronidation assay, conversion of tamoxifen to Phase I metabolites is unlikely due to the lack of cofactors for these reactions. This assumption is also supported by the molecular docking experiments performed by Hao et al. (2022), that predicted that tamoxifen itself stably binds to the UDPGA binding domain of UGT2B7.

We further analysed whether tamoxifen could result in a DDI using a basic reversible inhibition model to calculate the ratio of intrinsic clearance values of epirubicin (victim) in the absence and in the presence of tamoxifen (perpetrator) using the formula $R1 = 1 + (I_{max,u} / K_{i,u})$. Upon estimation, the R1 for tamoxifen was considerably above the cut-off of $R1 \geq 1.02$ that is proposed to warrant further evaluation for DDI potential, hence tamoxifen might produce DDIs involving UGT2B7. In addition, intratumoral levels of tamoxifen are reported to be up to 20-fold higher than plasma levels (Kisanga et al., 2004; Robinson et al., 1991), which suggests a possibility of significant intratumoral inhibition of UGT2B7 by tamoxifen. Again, whether this might alter epirubicin exposure could be assessed in cell line models. Interestingly, two studies have reported the combinatorial effects of tamoxifen and epirubicin in cancer cell lines. One study combined tamoxifen and epirubicin in ER-negative Ehrlich's carcinoma ascitic cells (EATC) in mice (Aydiner et al., 1997). The combination decreased proliferation more effectively than either drug alone. They proposed that the mechanism may involve cell-cycle perturbations and did not measure epirubicin exposure (Aydiner et al., 1997). The other study examined the effect of tamoxifen and epirubicin in ER-positive MCF-7 cells and in a cell line called NCI-adr that had been selected for doxorubicin

resistance and showed upregulated P-gp expression (Azab et al., 2005). They found that pre-treating cells with tamoxifen increased epirubicin-induced cytotoxicity by 4-6 fold in both cell lines. The also reported changes in cell cycle dynamics (accumulation of cells in S and G2/M phases) associated with tamoxifen treatment than might enhance the epirubicin response. However, they also found that tamoxifen increased intracellular epirubicin accumulation specifically in the NCI-adr cells. This was not associated with any change in P-gp function. While they did not investigate any changes in epirubicin metabolism in this study, the result does lend some support to the idea that tamoxifen could modulate epirubicin exposure in cancer cells.

Given our interest in whether UGT2B7 inhibitors such as tamoxifen might enhance intratumoral epirubicin exposure, it is important to consider whether these drugs are likely to be co-administered. Use of chemotherapy (concurrent or sequential) during 5-year tamoxifen treatment has been well documented to reduce cancer reoccurrence over a 10-year period (Davies et al., 2011). As described by Davies et al. (2011) in a large-scale meta-analysis, a further reduction of approximately a quarter (in node positive, ER positive women) in 10-year reoccurrence risk was observed by combining tamoxifen with chemotherapy when compared to chemotherapy alone. The TIGER (Austrian tumor of breast tissue: incidence, genetics, and environmental risk factors) breast cancer study (Langsenlehner et al., 2008) described a cohort of 205 patients that received epirubicin (total study n=804), with 59% (120/205) of them also receiving tamoxifen (Parmar et al., 2011). Several European studies such as the French Adjuvant Study Group (FASG) trials have reported use of epirubicin alone or in combination with tamoxifen (Bottini et al., 2005), and have shown suppression of angiogenesis (Mele et al., 2010) and reduced risk of relapse (Wils et al., 1999) when tamoxifen and epirubicin were co-administered. When epirubicin was given as part of a chemotherapy cocktail (FEC) in adjuvant breast cancer regimens, the addition of tamoxifen

showed improved disease-free survival (FASG02 and FASG07 studies) (Namer et al., 2006). These findings and our observations that tamoxifen has significant inhibitory activity on epirubicin metabolism prompt future investigations of tamoxifen as a pharmaco-enhancer of epirubicin response.

5.4.3. Integrating inhibition and induction mechanisms is essential to understand DDIs

A theme of this Chapter was the possibility for inhibition and induction based DDIs to occur concurrently, i.e. for the same (perpetrator) drug to both inhibit enzymatic activity and regulate enzyme expression. In this situation, the net effect on any victim drugs would depend on the relative magnitude of the inhibition and induction effects. Indeed, it is recognized in literature that *in-vitro* to *in-vivo* extrapolation based solely on inhibition of activity is not always a reliable indicator of DDIs, and that possible induction should be factored into the model. Some studies have explored this in animal models. Gabel et al. (2020) demonstrated in mice that repeated injection of tamoxifen increases the formation of 4-OH tamoxifen glucuronides by 1.5-to 2-fold each subsequent injection. This suggests that the mouse Ugt enzyme that mediates 4-OH tamoxifen metabolism is being induced by tamoxifen/4-OH tamoxifen, creating a feedback loop. They then showed that morphine was an *in vitro* inhibitor of 4-OH tamoxifen glucuronidation. However, when morphine and tamoxifen were co-administered *in-vivo*, tamoxifen still increased 4-OH tamoxifen glucuronidation. This suggests that inhibition by morphine was negated by the induction effect of tamoxifen. This example serves to illustrate the importance of considering both inhibition and induction when predicting the overall effect of a potential perpetrator drug on target drug exposure.

Because of the complex interplay of processes that control DME activities, including transcription,

post-translational regulation, and inhibitor binding, all of these factors should be considered when predicting the overall net changes in glucuronidation.

In the present study we investigated the possibility that TKIs might act as both inhibitors of UGT2B7 activity, and also inducers of *UGT2B7* gene expression. We found no evidence for the latter. Hence it is unlikely that any effects of UGT2B7 inhibition by gefitinib would be offset by induction. However, a recent study reported that gefitinib is an inhibitor of the PXR transcription factor in hepatocytes (Abbott et al., 2022). UGT2B7 could potentially be a PXR target, however it remains debated in the literature (Liu et al., 2014; Neumann et al., 2016; Soars et al., 2004; Yueh et al., 2011). Thus future studies could investigate whether gefitinib is able to downregulate (rather than induce) UGT2B7 expression. It should also be noted that we did not investigate induction-based DDIs involving tamoxifen in the present study, because previous studies suggested that UGT2B7 expression is not induced by ERα or by any estrogenic compounds (Hu & Mackenzie, 2009). However, the possibility that tamoxifen or its metabolites can downregulate UGT2B7 expression has not yet been examined.

5.4.4. Potential regulation of ADME factors by TKIs

The last aspect of this Chapter that could direct future experiments is the pilot proteomic screen for regulation of ADME factors by TKIs. Several UGT, CYPs, ATP-binding cassette (ABC) and Solute Carrier (SLC) drug transporters were induced in this screen. However, these effects await confirmation in future studies. A number of these factors are involved in TKI uptake and clearance as previously detailed in 5.1.2, for example, gefitinib, erlotinib, and afatinib are all substrates of P-gp (*ABCB1*). Induction of ABCB1 by these drugs might represent a feedback mechanism to reduce drug exposure (i.e. the TKIs induce their own efflux), protecting the cells from their growth inhibitory

effects. This is consistent with previous reports that elevated ABCB1 levels are involved in resistance to some TKIs (Eadie et al., 2013; He et al., 2021). Gefitinib and afatinib have also been reported as inhibitors of P-gp (FDA, 2013; Kitazaki et al., 2005), if induction of P-gp expression can also, occur, it is unclear what the net effect may be on other P-gp substrates. Mechanisms of induction for these enzymes and transporters will require direct investigation if the induction effects are confirmed in future studies.

5.4.5. Clinical perspectives of DDIs related to targeted therapy inhibition

Epirubicin has multiple adverse effects including cardiotoxicity and neutropenia (Robert, 1993), with the maximum tolerated dose around 150 mg/m^2, (Robert, 1993). Few studies have investigated the potential for epirubicin to be a DDI victim (as indicated by a change in plasma AUC), likely in part because it is infrequently dosed and very rapidly distributed (Tornio et al., 2019). Chan et al (2014) conducted a phase I clinical safety and tolerability study combining vinflunine and epirubicin, due to the potential usage of this combination clinically, but found no meaningful mutual DDIs, however there was still observed synergistic effects (Chan et al., 2014). As discussed above, many anticancer drugs accumulate in tumours. Such drugs might have inhibitory effects that significantly affect intratumoural metabolism of a victim drug, even while systemic exposure (mediated mainly by hepatic metabolism) is unaffected. Assessment of intratumoural drug levels requires post-treatment biopsies which are not routinely performed. Future advances in minimally invasive sampling methods, such as tissue-specific extracellular vesicle (EV) analysis (Rowland et al., 2019; Useckaite et al., 2021), might increase our ability to collect such data. This could facilitate more rationally designed studies to investigate the potential of using inhibitors of drug metabolism as pharmaco-enhancers to increase intratumoral drug exposure.

CHAPTER 6. A PHYSIOLOGICALLY BASED PHARMACOKINETIC MODEL TO PREDICT DETERMINANTS OF VARIABILITY AND EPIRUBICIN EXPOSURE AND TISSUE DISTRIBUTION

This chapter has been peer-reviewed and published in full in MDPI - Pharmaceutics, in the special issue: Role of Pharmacokinetics in Drug Development and Evaluation. It has been reproduced with permissions under the Creative Commons Attribution License.

The final print version was published as:

Ansaar, R., Meech, R. & Rowland, A. 2023. A Physiologically Based Pharmacokinetic Model to Predict Determinants of Variability in Epirubicin Exposure and Tissue Distribution. *Pharmaceutics*, 15(4), 1222. DOI: https://doi.org/10.3390/pharmaceutics15041222

All data included was generated by the primary author and formed as part of the published manuscript, unless clearly stated otherwise. Amendments have been made to conform to the formatting and structure of the thesis.

Author Contributions

Conceptualization, R.M. and A.R.; methodology, A.R.; software, A.R.; validation, R.A. and A.R.; formal analysis, R.A. and A.R.; writing—original draft preparation, R.A.; writing—review and editing, R.A., A.R., and R.M. All authors have read and agreed to the published version of the manuscript.

6.1. Introduction

Epirubicin is member of the anthracycline class of antineoplastic drugs. Anthracyclines are among the most broadly effective classes of antineoplastic drugs, and epirubicin is among the most clinically important drugs in this class. Epirubicin is primarily used in combination therapies for the treatment of breast, gastric, lung and ovarian cancers and lymphomas (Tariq et al., 2016). Epirubicin has emerged as the preferred agent in this class due to the favourable cardiotoxicity profile and similar anti-tumour activity compared to other anthracyclines (Forrest et al., 2013; Tariq et al., 2016).

Epirubicin is administered intravenously (IV) over 3 to 5 min once every 21 days with dosing based on body surface area (BSA; mg/m^2). Despite accounting for BSA, marked inter-subject variability in circulating epirubicin plasma concentration has been reported. Eksborg (1989) reported 10-fold between-subject variability in the area under the plasma concentration time curve (AUC) for epirubicin despite normalising for dose and BSA. As with most antineoplastic drugs, epirubicin has a narrow therapeutic window whereby small differences in exposure can result in marked differences in treatment efficacy and tolerability (Wade et al., 1992). These factors underpin the value of better understanding the physiological and environmental covariates influencing epirubicin exposure, particularly those that can direct a more appropriate initial dose selection. Current initial dose selection for epirubicin based on BSA alone routinely overestimates dose requirement (Gurney et al., 1998) necessitating dose reductions in subsequent cycles due to cardiac and haematologic toxicities (Robert, 1993). Dose reductions and interruptions are most commonly due to reductions in neutrophil and platelet count (Drooger et al., 2015). Grade 3–4 neutropenia occurs in 8.4–54.2% of patients receiving epirubicin and cyclophosphamide (EC)

(90/600 mg/m^2) treatment; thus, haematological toxicity is monitored and dose reductions are implemented between cycles on a case-by-case basis (Liu et al., 2022).

Therapeutic drug monitoring (TDM) is a clinical practice that involves periodic monitoring of drug concentrations in blood serum/plasma at steady state (Kang & Lee, 2009). Doing so, aids in the assessment of optimal dose selection to achieve the desired therapeutic ranges, and therefore, achieving the appropriate therapeutic effects whilst avoiding dose-limiting toxicity. Modern understanding of pharmacokinetic principles have spearheaded the application of TDM, with it being routinely used in a variety of clinical settings, and more recently, being suggested as an emerging viable practice in oncology within the context of cytotoxic drugs (Smita et al., 2022; Stojanova et al., 2022). Of significant advancement, a recent study by Wilhelm et al. (2016) showed the successful implementation of TDM for the use in personalized 5-fluorouracil dosing in metastatic colorectal cancer. They found that on initial treatment, only 33% of patients (n=75) were within the desired 5-FU AUC window, then upon the implementation of TDM, by fourth cycle, they were able to achieve the desired AUC for 54% of patients, with a reduction in commonly associated 5-FU toxicity indicators. TDM may be utilised to guide epirubicin dosing, provided an exposure profile has been developed and a known target therapeutic window is established. Development of PK/PD models can be successfully deployed to inform TDM; however, the infrequent dosing schedule of epirubicin and relatively short terminal half-life (18–45 h) limit practicality in this setting (Kang & Lee, 2009; Ormrod et al., 1999). Additionally, while TDM is appropriate to guide on-treatment dose adjustments for antineoplastic drugs (Fahmy et al., 2021; Mueller-Schoell et al., 2021), it does not support optimal initial (cycle 1) dose selection.

Recently, complementary precision dosing approaches that utilized model-informed initial dose selection (MIDS) have been proposed to support optimal initial dose selection (Rowland et al.,

2018; Sorich et al., 2019; Wills et al., 2021) and supplement on-treatment dose modification strategies such as TDM and toxicity-guided dosing (Kluwe et al., 2021). As implied by the name, MIDS involves the development of quantitative models based upon physiochemical drug properties, preclinical and clinical data to predict physiological levels of drugs which informs drug dosing and safety (Li et al., 2023; Papachristos et al., 2023). Excitingly, MIDS is becoming increasingly accepted and utilised in drug development by pharmaceutical manufacturers and by regulatory bodies (Jones et al., 2015). Quite recently PK/PD modelling has been used to predict thrombocytopenia and other dose limiting toxicity events in the clinical development of PF-06939999, a PRMT5 targeted small molecule inhibitor currently under development for potential use in breast and other cancers (Guo et al., 2022; Kim & Ronai, 2020). This highlights the necessity of developing PK/PD models based upon new and emerging cancer therapies.

Two approaches may be applied to support MIDS: a top-down approach known as population pharmacokinetic (popPK) modelling, and a bottom-up approach known as a physiologically based pharmacokinetic (PBPK) modelling. With popPK modelling, non-linear mixed-effect models are used to describe variability in observed pharmacokinetic (PK) behaviour within a population based on covariates known to influence exposure; this approach may be used to predict future exposure by fitting limited a priori data. In PBPK modelling, physiological data for a population are combined with physiochemical and *in vitro* data for a drug under specific trial conditions to simulate exposure in a virtual population (Shebley et al., 2018; Tsamandouras et al., 2015). Simulated data may be compared to observed data from a matched population to define the performance of the PBPK model. Population PK models for epirubicin have been applied to describe the relation between epirubicin exposure and the incidence of haematologic toxicity (Sandström et al., 2005),

and to associate routinely collected demographic characteristics with epirubicin exposure (Gurney et al., 1998; Ralph et al., 2003).

The development of a PBPK model for epirubicin provides the capacity to (i) define the impact of additional molecular and physiological characteristics that are not routinely collected on epirubicin exposure, (ii) simulate exposure in populations that have not been studied in clinical trials (e.g., different races, age groups, etc.), and (iii) define the likely impact of pharmacogenetic variability on epirubicin exposure. Epirubicin is predominantly cleared by the liver, with renal elimination accounting for 20 to 25% of the dose. The reported primary enzyme involved in the hepatic clearance of epirubicin is UDP-glucuronosyltransferase (UGT) 2B7 (Innocenti et al., 2001). In this regard, reduced UGT2B7 protein expression and/or activity caused by single nucleotide polymorphisms (SNPs) in the *UGT2B7* gene has been associated with increased epirubicin exposure and reduced metabolic clearance (Innocenti et al., 2001). The most notable example of pharmacogenomic-guided epirubicin dosing involved the *UGT2B7* -161C>T SNP. This SNP has been associated with a reduction in epirubicin clearance and increased AUC (Joy et al., 2021; Sawyer et al., 2016); importantly, this SNP has also been demonstrated to predict grade ¾ leucopenia in early breast cancer patients treated with adjuvant or neoadjuvant FEC100 (5-fluorouracil 500 mg/m^2, Epirubicin 100 mg/m^2 and cyclophosphamide 500 mg/m^2).

The primary objective of this study was to identify physiological and molecular characteristics driving variability in epirubicin AUC using PBPK modelling. Identification of these characteristics informs analyses of ‘exposure biomarkers’ for epirubicin that can be evaluated using routinely collected samples from randomised controlled trials and can facilitate non-invasive optimal initial dose selection for this drug (Polasek et al., 2019; Rodrigues & Rowland, 2019). The second objective of this study was to define the association between epirubicin plasma concentration and

tissue concentrations, with a focus on tissues relevant to either the therapeutic efficacy (adipose/breast tissue), or the incidence of toxicity (cardiac, hepatic) for this drug.

6.2. Materials and Methods

6.2.1. Materials and Chemical Information

Epirubicin (hydrochloride) was purchased from Cayman Chemical (Ann Arbor, MI, USA). UDP-glucuronic acid (UDPGA; trisodium salt) was purchased from Sigma-Aldrich (St Louis, MO, USA). Fluconazole was obtained from Pfizer Australia (Sydney, NSW, Australia). Alamethicin (from *Trichoderma viridae*) was purchased from AG Scientific (San Diego, CA, USA). Solvents and other reagents used were of analytical reagent grade or higher.

6.2.2. Human Liver Microsomes

Pooled human liver microsomes (HLMs) were prepared by mixing equal amounts of protein from five human livers (H7, 44-year-old female; H10, 67-year-old female; H12, 66-year-old male; H29, 45-year-old male; and H40, 54-year-old female), obtained from the human liver bank of the Department of Clinical Pharmacology of Flinders University. Approval for the use of human liver tissue in xenobiotic metabolism studies was obtained from the Flinders Clinical Research Ethics Committee. HLMs were prepared by differential centrifugation, as described by Bowalgaha et al. (2005). Microsomes were activated by pre-incubating on ice for 30 min in the presence of alamethicin (50 μg/mg microsomal protein) prior to inclusion in the incubation matrix (Boase & Miners, 2002).

6.2.3. Epirubicin Glucuronidation Assay

Assay conditions for epirubicin glucuronidation by HLMs were optimised for protein concentration, incubation time and epirubicin concentration range (Miners et al., 1988; Rowland et al., 2007). Incubations in a total volume of 200 µL contained $MgCl_2$ (4 mM), potassium phosphate (0.1 M; pH 7.4), epirubicin (in DMSO 2% *v*/*v*), activated HLMs (0.01 mg), and UDPGA (5 mM). A 5 min pre-incubation at 37 °C was performed to thermodynamically equilibrate the mixture; reactions were initiated by the addition of UDPGA. Reactions to form epirubicin glucuronide were performed over 120 min at 37 °C in a shaking water bath and were terminated by the addition of 400 µL of ice-cold methanol containing 0.1% formic acid. The reaction mix was centrifuged at 4000× *g* for 10 min at 10 °C and a 300 µL aliquot of the supernatant fraction was transferred into LC-MS vials. Microsomal incubations were performed in the presence of fluconazole (10–2500 µM) to define the contribution of microsomal UGT2B7 to epirubicin glucuronidation by HLMs.

6.2.4. Quantification of Epirubicin Glucuronide Formation

Epirubicin glucuronide formation was quantified by liquid chromatography mass spectrometry (LC-MS) performed on an Agilent 1290 infinity liquid chromatography (LC) system coupled to an Agilent 6495B triple-quadrupole mass spectrometer (MS; Agilent Technologies, Santa Clara, CA, USA) fitted with a Zorbax Eclipse Plus C18 analytical column (1.8 µM, 2.1 mm × 50 mm; Agilent, Santa Clara, CA, USA). Epirubicin glucuronide was separated from the incubation matrix by using a mobile phase comprising 28% acetonitrile and 0.1% formic acid in water at a flow rate of 0.2 mL/min. Control incubations in the absence of the cofactor (UDPGA), substrate (epirubicin), and

microsomal protein were analysed in parallel to incubation samples to confirm correct product detection.

The MS source parameters were as follows: sheath gas flow rate of 11 L/min, gas flow rate of 14 L/min, gas temperature of 200 °C, nebulizer pressure of 35 psi and capillary voltage of 1500 V. Multiple reaction monitoring (MRM) was used to monitor the precursor transition ion at 720.22 m/z, with the optimised conditions around the product ions listed in Table 6.1. Epirubicin glucuronide was eluted at a retention time of 1.6 min.

Table 6.1: Multiple Reaction Monitoring (MRM) scan parameters for the optimised epirubicin glucuronide ions.

Precursor Ion (m/z)	Product Ion (m/z)	Dwell (seconds)	Fragmentor (V)	Collision Energy (V)	Cell Acceleration (V)	Polarity
720.22	702.2	200	380	15	4	Positive
720.22	361.2	200	380	36	4	Positive
720.22	324.2	200	380	20	4	Positive
720.22	306	200	380	16	4	Positive

6.2.5. Data Analysis (*In Vitro* Kinetics)

The kinetics of microsomal epirubicin glucuronidation (Michaelis constant, Km and maximal reaction velocity, Vmax) were determined by fitting experimental data using the Michaelis–Menten equation in GraphPad Prism 9.3.1 (San Diego, CA, USA). Fluconazole inhibition of microsomal epirubicin glucuronidation was determined by fitting experimental data to the competitive inhibition model using GraphPad Prism 9.3.1 (San Diego, CA, USA). *In vitro* kinetic data

(Km and Vmax) generated in these microsomal incubations were used as input parameters in the PBPK model to describe epirubicin clearance by UGT2B7.

6.2.6. Development and Verification of Epirubicin PBPK Model

6.2.6.1. Structural Model

A full-body PBPK model to simulate the concentration time profile for epirubicin following a single IV dose infused over 3 min was developed using Simcyp® version 19.1 (Certara, Sheffield, UK). The differential equations utilised by Simcyp to construct the PBPK model from physiochemical and *in vitro* data have been described previously by (Rowland Yeo et al., 2010).

6.2.6.2. Development of Epirubicin Compound Profile

The physiochemical, blood binding, distribution and elimination parameters for epirubicin, along with parameters defining induction of UGT2B7 by epirubicin are summarized in Table 6.2. Physiochemical parameters were based on published literature values (Mouridsen et al., 1990), unless specified blood binding and distribution parameters were predicted by the model based on the physiochemical parameters of the drug using in-built functions within the Simcyp simulator. UGT enzymatic expression levels as incorporated by the Simcyp simulator are detailed in Table 6.3.

Microsomal clearance data (assigned to UGT2B7 based on fluconazole inhibition) were based on *in vitro* incubations (see Methods 6.2.3). Renal clearance (CL_R) was calculated based on published clearance values (Robert, 1993). Induction parameters for UGT2B7 were defined based on LC-MS proteomic data using HepG2 cells generated in this laboratory.

Table 6.2: Compound profile for epirubicin based on the physiochemical properties detailed.

Phys Chem	
Molecular Weight (g/mol)	543.52
log Po:w	1.41
Species	Diprotic Base
pKa (Strongest Acidic)	8.010
pKa 2 (Strongest Basic)	10.030
Blood Binding	
B/P	0.729
f_u	0.23
Distribution (full PB-PK model)	
Vss (L/Kg)	25.265
Prediction Method	2
Kp Scalar	25
Elimination	
HLM – UGT2B7 (Km; µM)	26.2
HLM – UGT2B7 (Vmax; pmol/min/mg protein)	2897
HLM – UGT2B7 (fu)	1
Additional clearance - CL_R (L/h)	9.0
Interaction	
UGT2B7 (IndC50; µM)	0.368
UGT2B7 (Indmax)	13.95

Po:w, neutral species octanol: water partition coefficient; B/P, blood-to-plasma partition ratio; fu, fraction unbound; Vss, steady state volume of distribution; CLR, renal clearance; IndC50, inducer concentration to achieve half maximal induction; IndMax, maximal fold induction.

Table 6.3. Mean and range enzymatic expression of UGTs incorporated into the model.

Enzyme	Mean (pmol)	Std Dev	5th centile	95th centile
Liver				
UGT1A1	1685500.93	993902.51	500913.21	3612128.83
UGT1A3	990058.04	566915.04	371500.68	2091593.26
UGT1A4	2202537.56	1079931.96	967923.39	4148718.19
UGT1A5	0.00	0.00	0.00	0.00
UGT1A6	840286.24	422171.05	342314.82	1646158.96
UGT1A7	0.00	0.00	0.00	0.00
UGT1A8	0.00	0.00	0.00	0.00
UGT1A9	1260309.51	713121.23	351967.04	2557354.27
UGT1A10	848.42	424.01	334.97	1651.86
UGT2B4	2263846.38	1110017.02	959048.99	4423238.59
UGT2B7	2965937.20	1512898.54	1143637.73	5894268.63
UGT2B10	276816.45	141780.73	107524.68	536167.74
UGT2B11	0.00	0.00	0.00	0.00
UGT2B15	754277.95	750628.57	62731.22	2139367.98
UGT2B17	153075.36	141330.66	15303.50	417525.92
UGT2B28	0.00	0.00	0.00	0.00
Kidney				
UGT1A1	18873.94	18302.13	3524.75	54716.17
UGT1A3	0.00	0.00	0.00	0.00
UGT1A4	31972.12	27400.22	6617.03	83472.37
UGT1A5	0.00	0.00	0.00	0.00
UGT1A6	13254.10	11197.18	2818.93	34990.87

UGT1A7	48286.99	43588.42	10040.55	129462.17
UGT1A8	18093.15	15089.74	3964.87	46689.78
UGT1A9	273796.48	247215.96	41429.33	742289.63
UGT1A10	62582.66	58719.85	13084.64	166188.26
UGT2B4	1134.54	1038.68	244.67	3012.61
UGT2B7	177510.02	162816.84	41241.74	465485.96
UGT2B10	0.00	0.00	0.00	0.00
UGT2B11	0.00	0.00	0.00	0.00
UGT2B15	346.23	446.85	17.86	1154.06
UGT2B17	0.00	0.00	0.00	0.00
UGT2B28	0.00	0.00	0.00	0.00

6.2.6.3. Population Profile

The epirubicin compound profile was built and verified using the Sim-Cancer population profile. The Sim-Cancer population profile was also used in simulations to characterise the association between epirubicin plasma and tissue concentrations, and to characterise the physiological and molecular parameters associated with variability in epirubicin exposure.

6.2.6.4. Simulated Trial Design

For development of the epirubicin profile, simulations comprised 90 subjects divided across 10 trials with 9 subjects in each trial. During verification of the epirubicin compound profile, simulations were performed in 10 trials comprising age-, sex-, and ethnicity-matched subjects according to the protocol for the observed trial (dosing regimen and number of subjects) described in the following section. Parameters describing epirubicin exposure were assessed over 24 h following a single dose at 9:00 a.m. on day 1.

6.2.6.5. Observed Clinical Data and Compound File Verification

Observed epirubicin pharmacokinetics were obtained from values reported in the literature by Robert et al. (1985). Sixteen metastatic breast carcinoma patients were subjected to a phase III comparative randomised protocol to assess the pharmacokinetics of epirubicin and doxorubicin. The epirubicin group received a combinatorial treatment of epirubicin (50 mg/m^2), 5-FU (500 mg/m^2), and cyclophosphamide (500 mg/m^2). The initial dose of epirubicin was used to study pharmacokinetics. Epirubicin was administered first, followed by administration of the remaining chemotherapies after 1–2 h. Therefore, additional treatment could impact epirubicin pharmacokinetics. Plasma samples were obtained after 5, 10, 20, and 40 min, and after 1, 2, 4, 8, 24, 32, and 48 h for HPLC analysis of the unchanged drug and metabolites. Raw data obtained from this trial were reproduced and plotted for evaluation of the simulated epirubicin compound file.

The epirubicin compound file was further verified by evaluating the impact of UGT2B7 inhibition, which was achieved by simulating the effect of fluconazole coadministration, and by evaluating the impact of renal function (evaluated as glomerular filtration rate; GFR).

6.2.7. Population Characteristics Associated with Variability in Epirubicin Exposure

The verified epirubicin profile was used to evaluate associations between physiological and molecular characteristics of the Sim-Cancer population and the logarithmically transformed epirubicin AUC (LnAUC). Ten trials from the Sim-Cancer population, each comprising 200 subjects, were simulated over 158 h, with a single 120 mg/m^2 epirubicin dosed IV in a fasted state.

Univariate (simple) linear regression was performed using GraphPad Prism 9.3.1 (San Diego, CA, USA). Stepwise multivariate linear regression analysis was performed using IBM® SPSS® Statistics

26 (New York, NY, USA). Linear regression was used to evaluate associations between the physiological and molecular characteristics identified in Table 6.4 and epirubicin LnAUC. Continuous variables were evaluated for normality and non-linearity of association; binary characteristics (sex) were coded as nominal variables. A multivariable linear regression model was developed by stepwise forward inclusion of significant characteristics identified in the univariable regression analysis based on improvement in model R^2. Back transformation of the model-predicted logarithmically transformed AUC was performed to plot correlations between the simulated and model-predicted AUC.

Table 6.4. The mean values and range of all physiological characteristics used in the simple linear regression analysis model. 2000 Sim-Cancer patients were generated in this study.

Physiological Parameter	Mean	Std Dev	5th centile	95th centile	P Value (do values differ from 0)
Age (Years)	66.79	14.04	42.73	88.83	<0.0001
Weight (kg)	70.60	14.09	50.32	95.27	0.004
Height (cm)	165.62	9.73	149.97	181.88	0.0035
BSA (m^2)	1.78	0.20	1.47	2.11	0.0014
BMI (kg/m^2)	25.69	4.41	19.36	33.16	0.2211
Haematocrit (%)	37.64	4.63	30.28	45.70	<0.0001
Albumin (g/L)	38.18	6.90	27.76	49.99	<0.0001
GFR (mL/min/1.73 m^2)	79.80	23.62	47.61	123.08	<0.0001
Albumin (g/L)	38.18	6.905	27.72	50.01	0.0014

LiverUGT2B7 (pmol)	2965937	1512899	1143503	5901583	<0.0001
GutUGT2B7 (pmol)	13751	9171	3974	31676	0.7856
KidneyUGT2B7 (pmol)	177510	162817	41202	466093	<0.0001

6.3. Results

6.3.1. Characterisation of *In Vitro* Epirubicin Glucuronidation

Epirubicin glucuronide formation by HLM was best described by a single-enzyme Michaelis–Menten equation (Figure 6.A). The kinetic parameters derived for epirubicin glucuronidation were a K_m of 26.2 ± 5.48 µM and V_{max} of 2896.6 ± 212.8 AU. The selective UGT2B7 inhibitor fluconazole was included in incubations (final concentration 100 to 2500 µM) to confirm the involvement of UGT2B7 in human liver microsomal epirubicin glucuronidation. The IC_{50} for fluconazole inhibition of epirubicin glucuronidation by HLMs was 770.7 ± 158.1 µM, with a maximal observed inhibition of 75% (Figure 6.B). These data support UGT2B7 as the major enzyme involved in human liver microsomal epirubicin glucuronidation.

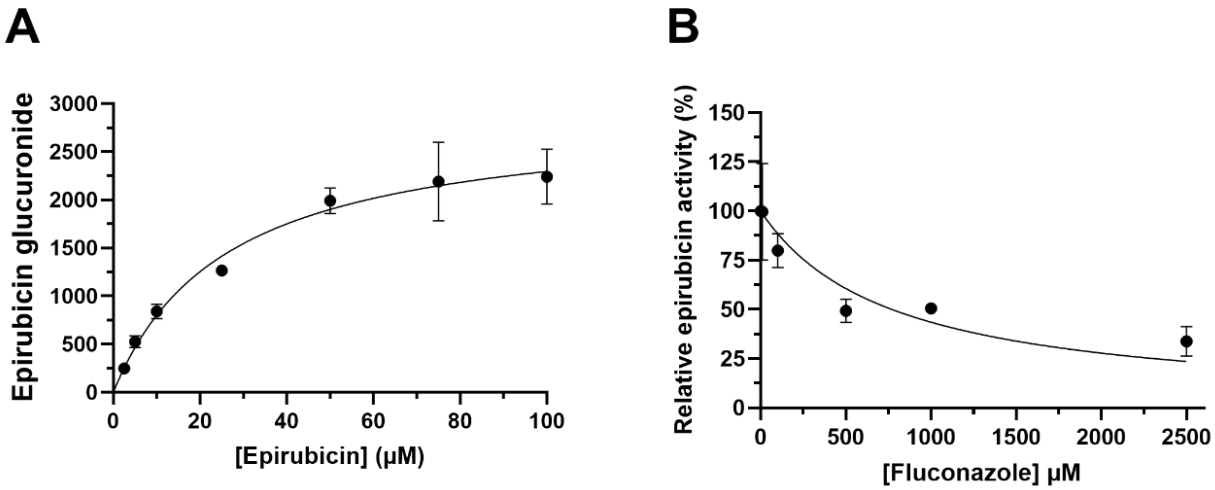

Figure 6.1. The enzyme kinetics of epirubicin metabolism by UGT2B7, in the absence and presence of a canonical UGT2B7 inhibitor (**A**) Michaelis–Menten Kinetics of epirubicin by formation of epirubicin glucuronide in HLMs (R^2 = 0.96). Pooled HLMs (2 mg/mL) were incubated for 2 h with incremental amounts of epirubicin (between 2.5–100 µM) and epirubicin glucuronide was detected in the absence of standards. (**B**) Normalised activity of epirubicin by inhibition of epirubicin glucuronide formation in HLMs. HLMs were incubated for 2 h with 25 µM epirubicin and increasing amounts of fluconazole (between 10–2500 µM). Epirubicin glucuronide was detected, and response was measured relative to the control in the absence of fluconazole. Mean peak area response ± S.D. is measured in arbitrary units. Data were generated in duplicate with standard deviation displayed by error bars.

6.3.2. Verification of the Epirubicin PBPK Model

The accuracy of the epirubicin compound profile was assessed using an age-, sex-, and race-matched single-dose trial (Robert, 1994). Ten simulated trials were performed with epirubicin administered IV at a dose of 50 mg/m^2 in trials comprising 9 female subjects aged between 20 and 50 years. Epirubicin plasma concentration, monitored over 48 h, was used to define the simulated epirubicin maximal concentration C_{max} and AUC. The mean (±SD) simulated AUC and C_{max} in the validation cohort were 1324 ± 20.0 ng/mL·h and 434 ± 42.6 ng/mL, respectively; these values are 1.1- and 1.6-fold higher than the respective measured parameters. The simulated mean (95% confidence interval; CI) and mean observed plasma concentration time profiles are shown

in Figure 6.2. In all cases, the mean simulated epirubicin plasma concentration at each measured time point was within 1.6-fold of the respective observed plasma concentration.

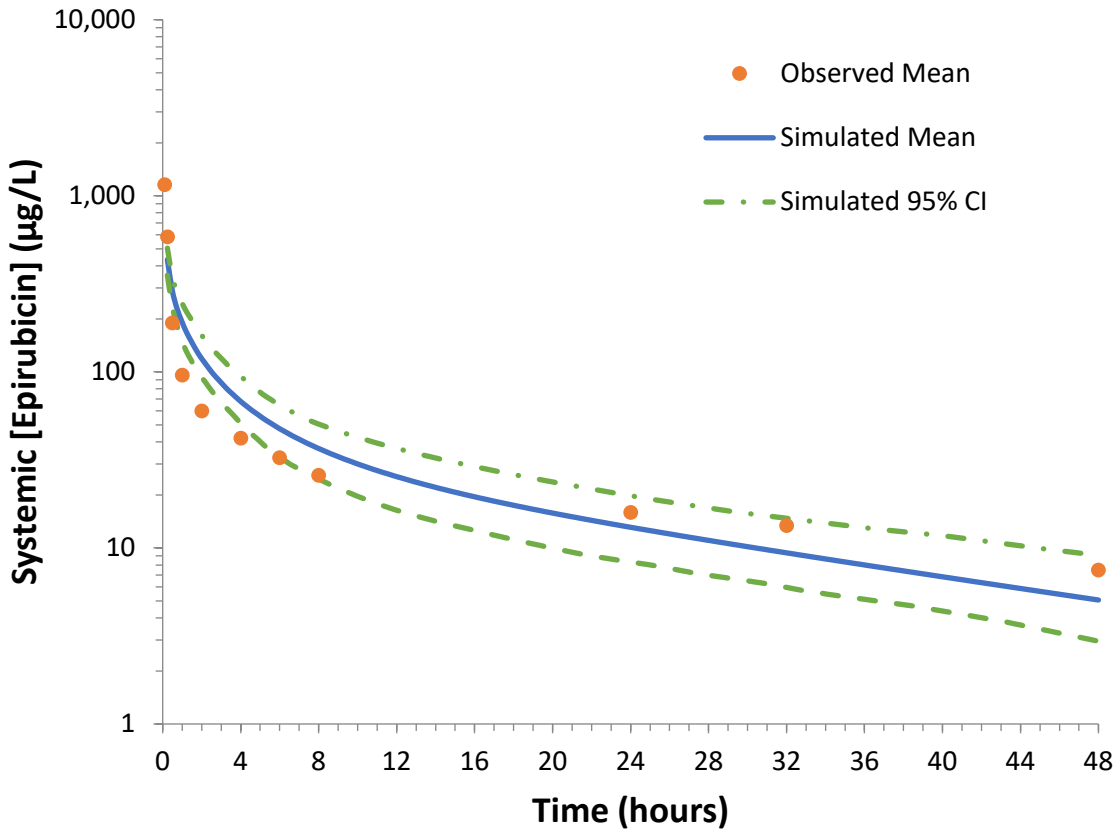

Figure 6.2. Representative overlay showing the simulated and observed epirubicin plasma concentration time curves over 48 h following a single IV dose (50 mg/m^2). The solid blue line represents the mean simulated epirubicin plasma concentration, the dotted green lines represent the 95% confidence interval (CI) for the simulated data and the orange dots represent the mean observed data (Robert, 1994). No data regarding variability in observed data was reported in the original publication.

Consistent with the reported importance of UGT2B7 in epirubicin metabolism *in vivo*, coadministration of steady-state fluconazole (200 mg daily for 7 days) resulted in a 54% increase in the single-dose epirubicin AUC. Notably, as an intravenously administered drug, the C_{max} for epirubicin was only modestly impacted (increased by <5%) (Figure 6.3).

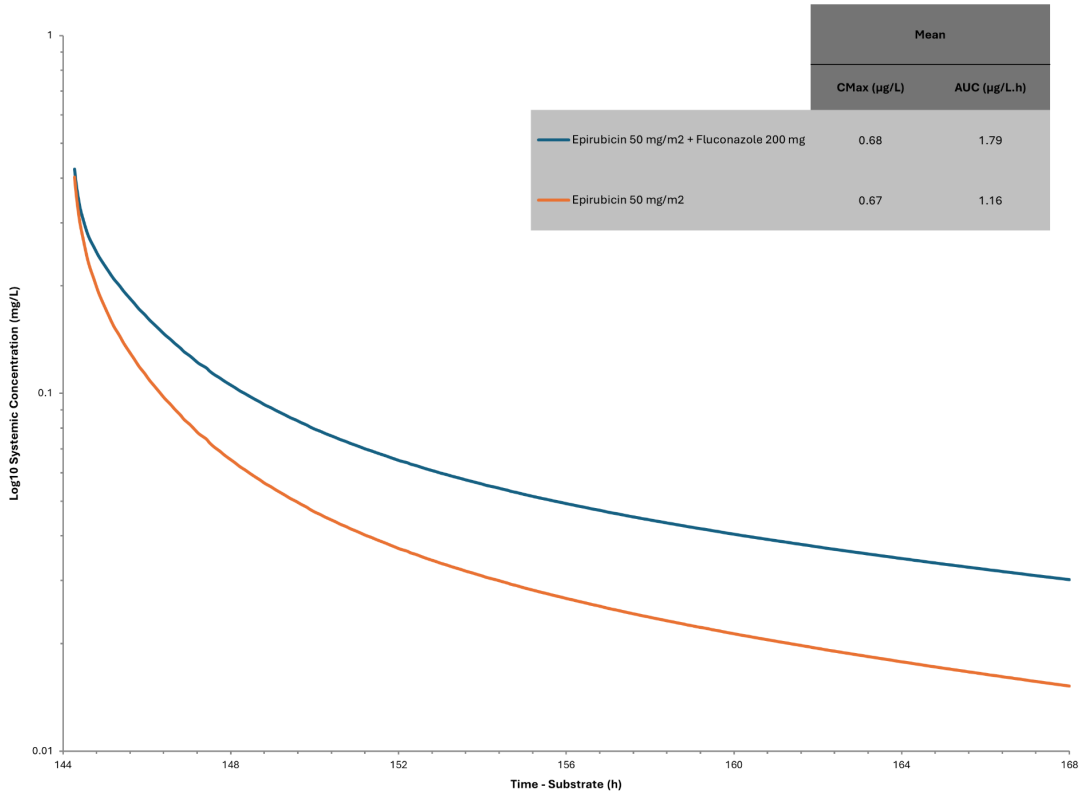

Figure 6.3. Concomitant administration of fluconazole increases epirubicin AUC (relative to epirubicin alone), but not C_{max} . 200 mg/day fluconazole was administered orally over 7 days to achieve steady state. 50 mg/m^2 epirubicin was administered intravenously at the beginning of day 7.

6.3.3. Epirubicin Exposure in Oncology Cohort

The mean, standard deviation (SD) and range of epirubicin AUC and C_{max} values describing exposure to epirubicin in a cohort of 200 oncology patients are reported in Table 6.5. Marked variability in epirubicin AUC and C_{max} was observed; by way of example, AUC values ranged from 2980 to 12,710 ng/mL·h (mean 5374 ng/mL·h). Simulated epirubicin AUC and C_{max} values, and the variability in these parameters, were consistent with observed exposure profiles (Eksborg, 1989).

Table 6.5: Descriptive statistics showing the mean, variance and range of epirubicin exposure in the simulated oncology cohort.

Statistic	AUC (ng/mL.h)	CMax (ng/mL)	Dose (mg)	CL (Dose/AUC) (L/h)
Mean	5374	12683	213.2	41.6
Median	5197	12653	212.1	40.5
Geometric Mean	5252	12654	211.8	40.3
90% confidence interval (lower limit)	5211	12622	211.0	40.0
90% confidence interval (upper limit)	5293	12686	212.7	40.7
5th centile	3776	11296	176.4	26.7
95th centile	7537	14142	253.7	59.8
Skewness	0.99	0.12	0.29	0.50
cv	0.22	0.07	0.11	0.24
Min Val	2980	9678	149.8	14.8
Max Val	12710	15469	302.5	80.9
Fold	4.27	1.60	2.02	5.45
Std Dev	1191	864	24.1	10.2

6.3.4. Epirubicin Clearance Pathways

The mean contribution of renal elimination, defined by the fraction of epirubicin excreted unchanged in the urine (F_e), was 20.95%. The mean contributions of hepatic and renal UGT2B7 to total epirubicin clearance were 75.3% and 4.3%, respectively (Figure 6.4).

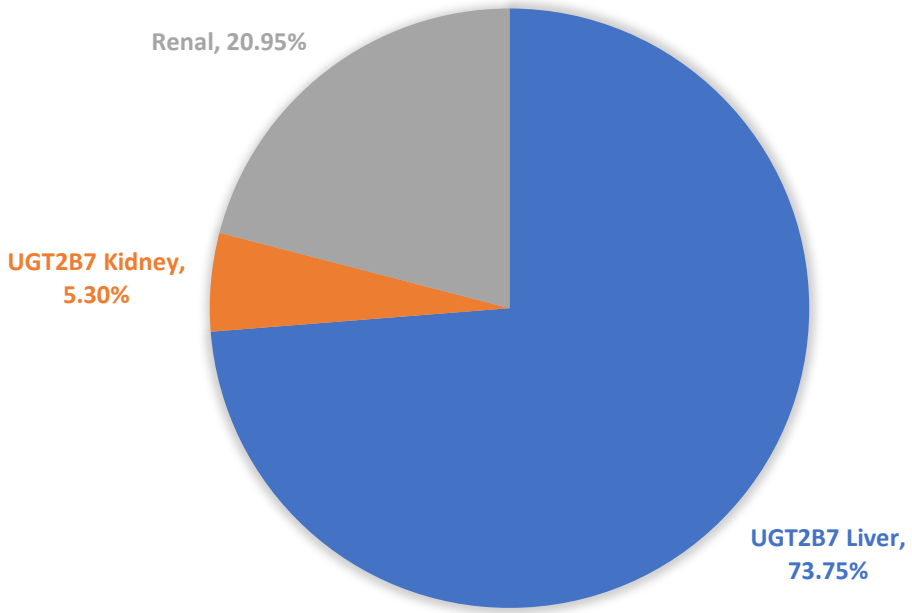

Figure 6.4. A representative pie-chart showing the relative contribution (geometric mean %) of the f_m (hepatic and renal epirubicin) and the f_e unchanged by renal clearance.**Determination of Population Characteristics Affecting Epirubicin Clearance**

The results of univariate linear regression analyses considering the association between molecular and physiological characteristics and epirubicin LnAUC are presented in Table 6.4. Multivariable linear regression modelling by stepwise inclusion of parameters described in Table 6.4 identified hepatic UGT2B7 abundance, albumin concentration, age, renal UGT2B7 abundance, body surface area (BSA), glomerular filtration rate (GFR), haematocrit, and sex as the key covariates associated with variability in epirubicin LnAUC. By accounting for these factors, it was possible to explain 87% of the variability in epirubicin LnAUC within the oncology population (Figure 6.5, Table 6.6 and Table 6.7). The single most important covariate associated with variability in epirubicin LnAUC was hepatic UGT2B7 abundance; accounting for this covariate alone explained 56% of the variability in epirubicin LnAUC. Furthermore, exclusion of body surface area in the model led to a minor decrease in predicted variability to 83% (Table 6.8).

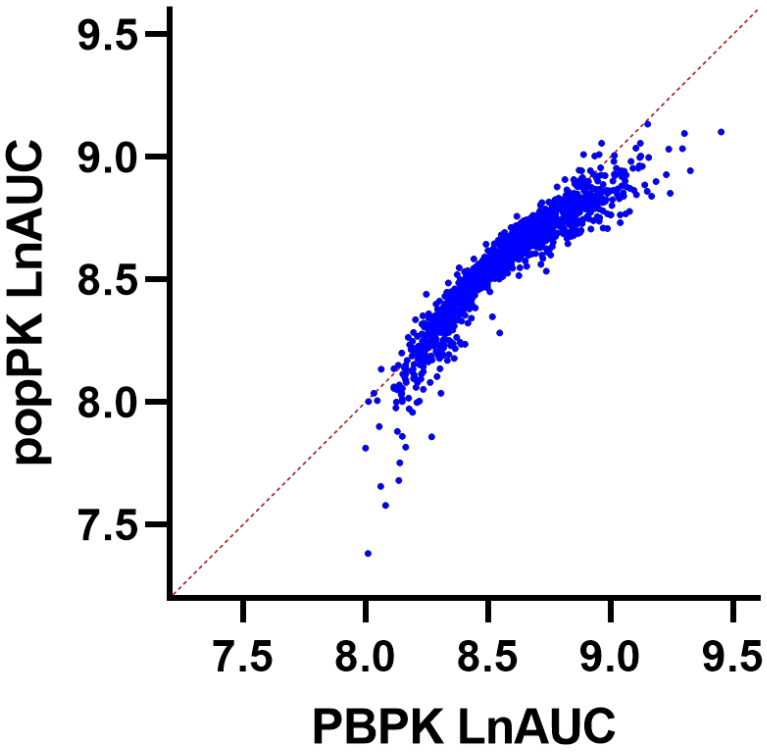

Figure 6.5. Multivariate linear regression analysis showing the correlated relationship between the simulated popPK natural log-transformed AUC (LnAUC) and simulated PBPK LnAUC.

Table 6.6. Multivariate linear regression analysis of the model predicted variables affecting epirubicin LnAUC and their respective linearity regarding LnAUC. R2 of the model is 0.8690.

Variable	Estimated Ln AUC (ng/mL.h)	Standard error	Range (95% CI)	R^2 with other variables	P value
Intercept (constant)	8.211	0.02994	8.152 to 8.269		<0.0001
Sex	-0.03709	0.003901	-0.04474 to -0.02944	0.2216	<0.0001
Age	0.00251	0.000174	0.002169 to 0.002850	0.5024	<0.0001
BSA	0.2669	0.01132	0.2447 to 0.2891	0.4266	<0.0001
Haematocrit	-0.00538	0.000373	-0.006110 to -0.004649	0.005414	<0.0001
Albumin	0.0111	0.000251	0.01060 to 0.01159	0.01572	<0.0001
GFR	-0.00178	0.000106	-0.001983 to -0.001568	0.5261	<0.0001
Liver UGT2B7	-9.77E-08	1.34E-09	-1.004e-007 to -9.510e-008	0.2798	<0.0001
Kidney UGT2B7	-3.24E-07	1.07E-08	-3.454e-007 to -3.033e-007	0.03006	<0.0001

Model variables; sex 0=Female, 1=Male, age (years), body surface area (BSA) (m^2), haematocrit (%), albumin (g/L), glomerular filtration rate (GFR) (mL/min/1.73m^2), liver UGT2B7 (pmol), kidney UGT2B7 (pmol).

Table 6.7. Stepwise multivariate linear regression analysis of predictors of epirubicin LnAUC by sequential addition according to best fit. Cumulative R2 of the final model (h) incorporating all predictors = 0.8690.

Model	R	R^2	Adjusted R^2	Std. Error of the Estimate	R^2 Change
a	.749[a]	0.561	0.561	0.141	0.561
b	.821[b]	0.674	0.674	0.121	0.113
c	.861[c]	0.741	0.740	0.108	0.067
d	.886[d]	0.785	0.784	0.099	0.044
e	.911[e]	0.830	0.830	0.087	0.046
f	.922[f]	0.849	0.849	0.082	0.019
g	.929[g]	0.863	0.863	0.079	0.014
h	.932[h]	0.869	0.868	0.077	0.006

Model predictors; [(a)] LiverUGT2B7 [(b)] LiverUGT2B7, Albumin [(c)] LiverUGT2B7, Albumin, Age [(d)] LiverUGT2B7, Albumin, Age, KidneyUGT2B7 [(e)] LiverUGT2B7, Albumin, Age, KidneyUGT2B7, BSA [(f)] LiverUGT2B7, Albumin, Age, KidneyUGT2B7, BSA, GFR [(g)] LiverUGT2B7, Albumin, Age, KidneyUGT2B7, BSA, GFR, Haematocrit [(h)] LiverUGT2B7, Albumin, Age, KidneyUGT2B7, BSA, GFR, Haematocrit, Sex

Table 6.8. Multivariate linear regression analysis of the model predicted variables affecting epirubicin LnAUC and their respective linearity regarding LnAUC with the exclusion of BSA. R2 of the model is 0.8324.

Variable	Estimated Ln AUC (ng/mL.h)	Standard error	Range (95% CI)	R^2 with other variables	P value
Intercept	8.556	0.02954	8.498 to 8.614		<0.0001
Sex[0]	-0.07619	0.003993	-0.08402 to -0.06836	0.05004	<0.0001
Age	0.003195	0.0001937	0.002816 to 0.003575	0.4880	<0.0001
Haematocrit	-0.005730	0.0004210	-0.006556 to -0.004905	0.003825	<0.0001
Albumin	0.01125	0.0002840	0.01069 to 0.01180	0.01507	<0.0001
GFR	-0.0007297	0.0001087	-0.0009428 to -0.0005166	0.4251	<0.0001
Liver UGT2B7	-9.052e-008	1.476e-009	-9.342e-008 to -8.763e-008	0.2403	<0.0001
Kidney UGT2B7	-2.959e-007	1.206e-008	-3.196e-007 to -2.723e-007	0.01765	<0.0001

Model variables; sex 0=Female, 1=Male, age (years), body surface area (BSA) (m^2), haematocrit (%), albumin (g/L), glomerular filtration rate (GFR) (mL/min/1.73m^2), liver UGT2B7 (pmol), kidney UGT2B7 (pmol).

6.3.6. Associations between Epirubicin Plasma and Tissue Concentration

The concordance between simulated epirubicin plasma and individual tissue concentrations are shown in Figure 6.6. Except for epirubicin concentration in the brain (R^2 = 0.56), there was limited concordance between epirubicin tissue and plasma concentrations (R^2 < 0.22). Notably, while the highest mean tissue AUC was observed in skeletal muscle (169,241 ng/mL·h), the comparatively slow distribution into this tissue resulted in a markedly lower C_{max} compared to other tissues.

Indeed, despite comparable AUCs, the mean epirubicin C_{max} in cardiac tissue (31,952 ng/mL) was >10-fold higher than the epirubicin Cmax in skeletal muscle (2868 ng/mL) (Table 6.9).

Table 6.9: PBPK-predicted epirubicin mean Cmax (ng/mL) and mean AUC (ng/mL·h) in tissue and plasma over 168 h after IV injection in a Sim-Cancer population.

Tissue	Mean Cmax (ng/mL)	Mean AUC (ng/mL.h)
Plasma	979	4,530
Muscle	2,868	169,241
Heart	31,952	144,482
Brain	22,410	147,660
Adipose	1,049	18,680
Liver	13,973	92,446

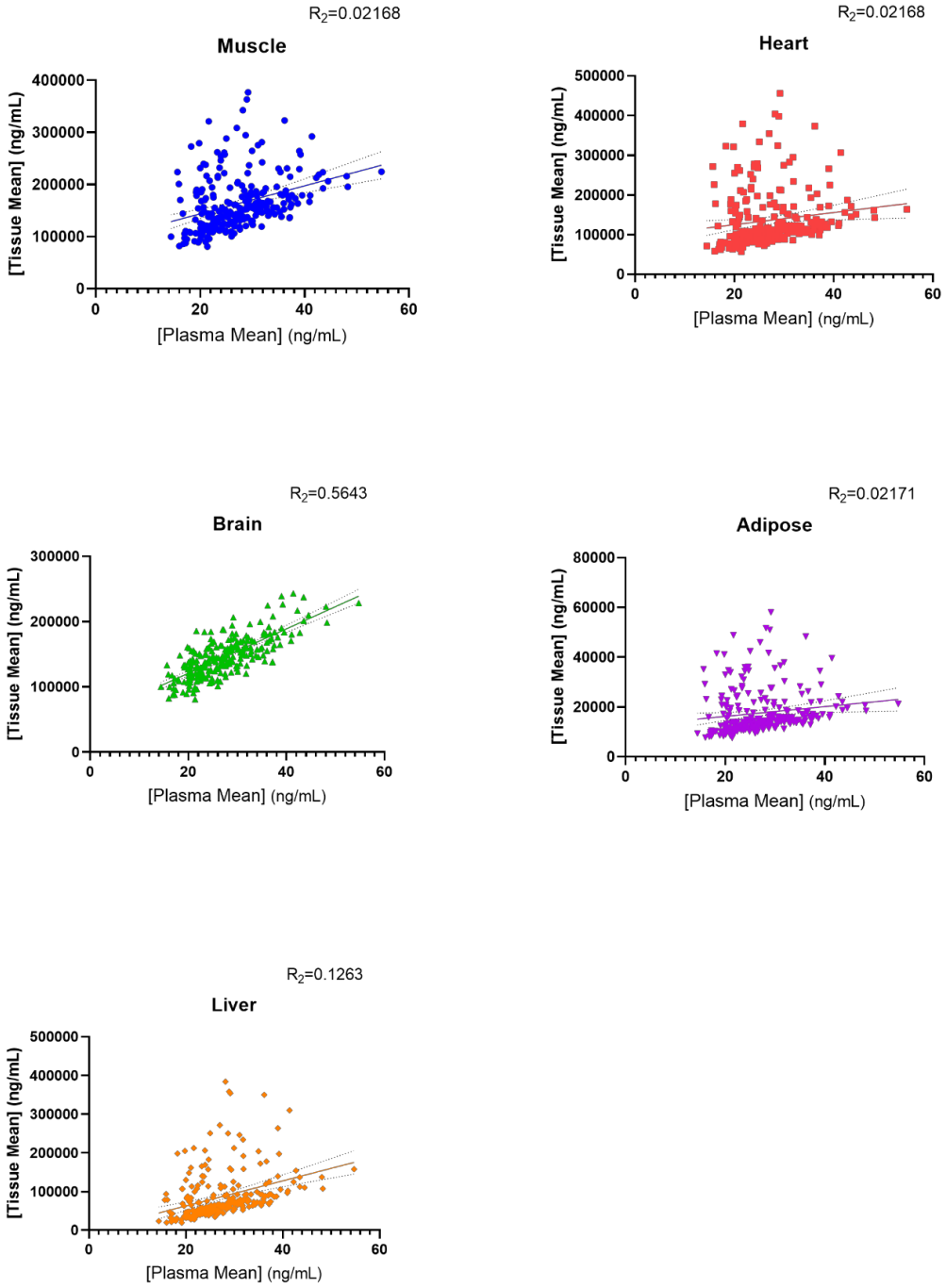

Figure 6.6. Linear regression analysis evaluating the relationship between simulated maximum epirubicin tissue and plasma concentrations in a Sim-Cancer cohort following a single 50 mg/m^2 dose.

6.4. Discussion

The present study describes the development and evaluation of a full-body PBPK model to assess systemic and individual organ exposure to epirubicin. Multi-variable linear regression modelling demonstrated that variability in simulated systemic epirubicin exposure following intravenous injection was primarily driven by differences in hepatic and renal UGT2B7 expression, plasma albumin concentration, age, BSA, GFR, haematocrit and sex. By accounting for these factors, it was possible to explain 87% of the variability in epirubicin in a simulated cohort of 2000 oncology patients aged between 20 and 95 years. The single most important factor in defining simulated systemic epirubicin exposure was hepatic UGT2B7 expression, which alone accounted for 56% of variability in exposure within the simulated cohort.

Current dosing guidelines for epirubicin account for age, BSA, renal function and sex. Typically, epirubicin doses are reduced in patients with a serum creatinine > 5 mg/dL. Epirubicin is quite well tolerated in patients with chronic renal failure undergoing haemodialysis (Gori et al., 2006). Dose reductions in elderly patients are also well tolerated (Nicolella et al., 1996). Data regarding the value of BSA-guided epirubicin dosing are contentious, with multiple studies suggesting that BSA-guided dosing is of limited value (Dobbs & Twelves, 1998; Gurney et al., 1998). In accordance with this, the data presented suggest that incorporating BSA-based dosing into the model only contributes to 4% of exposure variability. This highlights the importance of understanding other contributing variables in epirubicin dosage. Sexual dimorphism around DME expression could perhaps be driven by hormonal differences (Davidson et al., 2019) and may influence epirubicin metabolism; however, further understanding of this is required. Reassuringly, the major factors currently accounted for when guiding epirubicin dosing are consistent with the physiological

parameters identified in the multiple linear regression modelling performed in the current study and with prior non-linear mixed-effects modelling (NONMEM) analyses involving epirubicin. Wade et al. (1992) demonstrated that by accounting for differences in sex and age it was possible to reduce unexplained variability in epirubicin clearance from 50 to 42%. Consistent with the major importance of UGT2B7 expression in defining epirubicin exposure, prior analyses have consistently demonstrated that a large proportion of the variability in epirubicin exposure cannot be accounted for based on routinely collected physiological parameters including age, sex, BSA and renal function. Currently, there is no reliable biomarker to define hepatic UGT2B7 expression in individual patients, and assessment of *UGT2B7* genotype is of limited value (Rodrigues & Rowland, 2019). However, in recent years liver-derived extracellular vesicles (EVs) have emerged as a potential universal ADME biomarker (Achour et al., 2021; Achour et al., 2022; Rodrigues et al., 2021; Rodrigues et al., 2022; Rowland et al., 2019; Useckaite et al., 2021). It is plausible that quantification of UGT2B7 expression in EVs may serve as a robust approach to estimate hepatic UGT2B7 expression in individual patients, thereby supporting dose individualisation for drugs such as epirubicin.

PBPK modelling and simulation is an established tool to support drug discovery and development and is a core element of the regulatory approval process in many jurisdictions (Shebley et al., 2018). Recent studies have further demonstrated the potential role of PBPK in predicting covariates affecting variability in drug exposure resulting from differences in patient characteristics (Rowland et al., 2018; Ruanglertboon et al., 2021; Sorich et al., 2019), giving rise to the intriguing potential for this platform to support model-informed precision dosing (Polasek & Rostami-Hodjegan, 2020; Polasek et al., 2018). This model provides an important foundation for establishing a PK/PD relationship for epirubicin; however, further work on population-based dose

predictive modelling is imperative to inform optimal therapeutic windows for individualized dosage. The major limitation of the current study is the lack of observed clinical data to support the validation of the regression models. Currently, these models are based on a mechanistic systems pharmacology understanding and would require confirmation with *in vivo* clinical data to warrant implementation. A second limitation of the current study is the lack of observed tissue concentration measurements to support the lack of concordance between plasma concentration and tissue concentrations. While the overall simulated volume of distribution (25.265 L/kg) for epirubicin is consistent with reported *in vivo* data (Plosker & Faulds, 1993; Robert, 1993), the specific tissue distribution for this drug *in vivo* has not been reported. Based upon the high distribution volume, it can be reasoned that epirubicin is rapidly and extensively distributed to tissue potentiating tissue accumulation. Simulated epirubicin clearance was consistent with clinical observations of epirubicin plasma clearance as studied by Robert (1994).

Notably, there was limited concordance between systemic epirubicin exposure and the exposure of individual organs to epirubicin. Except for epirubicin concentration in the brain ($R^2 = 0.56$), there was limited concordance between tissue and systemic (plasma) epirubicin concentrations ($R^2 < 0.22$). The highest mean tissue AUC was observed in skeletal muscle (169,241 ng/mL·h); however, the comparatively slow distribution into this tissue resulted in a markedly lower C_{max} compared to other tissues. Indeed, despite comparable AUCs, the mean epirubicin C_{max} in cardiac tissue (31,952 ng/mL) was >10-fold higher than the epirubicin C_{max} in skeletal muscle (2868 ng/mL). The extensive distribution of epirubicin into cardiac tissue is consistent with the well-established cardiac toxicity profile for this drug (Ormrod et al., 1999; Smith et al., 2010). The limited concordance between plasma and cardiac epirubicin concentrations ($R^2 = 0.2188$) indicates

that evaluation of plasma epirubicin concentration is unlikely to be useful in identifying patients at greatest risk of suffering cardiac toxicity when administered epirubicin.

CHAPTER 7. SUMMARY, DISCUSSION AND OVERALL SIGNIFICANCE OF FINDINGS

Breast cancer is a highly heterogeneous disease with a variety of treatment options most often dictated by the molecular subtyping. One of the most common treatments utilised is chemotherapy; a recent study found that around 14% of early-stage node-negative breast cancers and 64% of more advanced node-positive breast cancers are now treated with chemotherapy (Kurian et al., 2018). While there has been an overall decline in the use of chemotherapy over the past few decades, there remains few alternatives for patients indicated with TNBC or those requiring salvage therapy, especially in cases which have progressed beyond the indication of targeted therapies (Wen et al., 2022). A major obstacle in the use of chemotherapies is the acquisition of drug resistance, whereby the tumour develops molecular mechanisms limiting the effectiveness of the drug. While pharmacodynamic mechanisms are most likely to drive resistance to targeted therapies (e.g. loss of the drug target), pharmacokinetic mechanisms are likely to be important in resistance in targeted chemotherapies. Alterations in various ADME processes can lead to reduced exposure of the tumour to the drug, which could reduce efficacy. Moreover, it is logical that changes in ADME processes evolve locally in the tumour as a result of selective pressure (e.g. cytotoxic drug exposure). However, much of our framework for assessing ADME is based on measuring systemic parameters, such as area under the plasma time-concentration curve (AUC) as a measure of drug exposure.

A key player in the drug metabolism process is the UGT superfamily of drug metabolising enzymes, which are relied upon for inactivation of a multitude of clinically used drugs, not only in the liver but also in the target tissue. This project examined the role of UGT2B7 in the potential

development of chemotherapy resistance in breast cancer, and its potential to be involved in DDIs that might provide possibilities for pharmaco-enhancement of chemotherapy.

Chapter 3 focused on understanding the mechanism of induction of UGT2B7 by a commonly used breast cancer chemotherapeutic - epirubicin. The induction of UGT2B7 is of significance because it is the only UGT known to inactivate epirubicin (Innocenti et al., 2001). Previous studies by Hu et al. (2015) had shown that epirubicin could induce UGT2B7 expression in a hepatic carcinoma cell line. Because this cell line is often used as a model for liver, this datum was proposed to be relevant to hepatic induction. In Chapter 3 we explored whether the same induction mechanism occurred in breast cancer cells.

The association of UGT2B7 expression with breast cancer subtype had not been previously established. Using gene expression data from the TCGA-BRCA database, it was deduced that UGT2B7 expression is higher in the basal-like breast cancer subtype and lower in hormone receptor-positive cancers. This result was consistent with analysis of breast cancer cell lines in which TNBC lines (and a primary TNBC cell model) showed higher expression of UGT2B7 than ER+ lines.

The dose-dependent induction of UGT2B7 by epirubicin was demonstrated in cell lines representing different breast cancer subtypes, including luminal-like ER+, basal-like TNBC, and molecular apocrine-like models. Additionally, other members of the UGT2B- family were also induced in a dose-dependent manner, including UGT2B4, UGT2B10, UGT2B11, UGT2B15 and UGT2B17. The *UGT2B7* promoter was activated by epirubicin through the p53 pathway, indicated by the fact that mutation of the p53-responsive element in the proximal promoter prevented activation in breast cancer cell lines with wildtype p53. This was broadly consistent with the

previous study in liver-derived cells by Hu et al. (2014c). Interestingly, there was also induction of UGT2B7 mRNA in cell lines with non-functional p53; however, this did not appear to be mediated via the proximal promoter. This suggests that additional p53-independent mechanism(s) for induction of UGT2B7 exist, which still need to be identified. This may involve other transcription factors that could be identified by analyses focused on more distal regulatory elements. Finally, the induction of multiple *UGT2B* genes by epirubicin suggests that the mechanism might involve chromatin remodelling processes that extend across the whole *UGT2B* locus, and that UGT induction may be part of a generalized adaptive response to cytotoxic stress.

Chapter 4 studies were designed to test the hypothesis that UGT2B7 controls the sensitivity of breast cancer cells to epirubicin. This was achieved by the development of UGT2B7 overexpression models in both TNBC (MDA-MB-231) and luminal ER+ (ZR-75-1) breast cancer cell lines. The MDA-MB-231 UGT2B7-overexpression model showed elevated resistance to epirubicin treatment. This at least partly supported the hypothesis that UGT2B7 can promote epirubicin resistance in breast cancer cells. One of the unexpected findings in this Chapter was the lack of concordance between UGT2B7 mRNA and protein levels in breast cancer cell lines. Although MDA-MB-231 cells had shown higher levels of UGT2B7 mRNA than ZR-75-1 cells (Chapter 3), the UGT2B7 peptide assay only detected baseline (pre-treatment) UGT2B7 protein in ZR-75-1 cells. In contrast, UGT2B7 protein was very robustly induced in MDA-MB-231 cells after epirubicin treatment, whereas the magnitude of induction (relative to baseline) was less in ZR-75-1 cells. This finding could be further investigated in future studies with other follow-up UGT2B7 protein estimation assays, such as immunoblotting, and then potentially via mechanistic studies. Potential mechanisms of post-transcriptional regulation include miRNA-mediated control of mRNA stability and translation. Several miRNAs were previously shown to bind to the *UGT2B7* 3'UTR in liver cells (Hu et al., 2022;

Wijayakumara et al., 2017), and these could be further investigated in the breast cancer context. Finally, to examine the effect of UGT2B7 overexpression in a long-term tumour progression model, we used a competition assay where cells with and without overexpression were combined and passaged over many weeks with or without epirubicin. Unexpectedly, UGT2B7 overexpression provided a growth advantage to breast cancer cells even in the absence of drug selection. There was also a small additional advantage in the context of epirubicin. The reason for the generalized growth advantage could be investigated in the future, one possibility that has been suggested by other unpublished studies from our laboratory is that UGT2B7 is involved in controlling pro-proliferative lipid signalling in cancer cells.

The ability of epirubicin to induce UGT2B7 expression (Chapter 3) combined with the finding that overexpression of UGT2B7 can protect cells from epirubicin toxicity (Chapter 4), suggested a protective feedback loop in which the drug induces its own clearance, thereby reducing exposure and toxicity. This adaptive mechanism by cancer cells could lead to acquired epirubicin resistance. To address this idea, we sought to develop UGT2B7 loss of function (LOF) models.

As previously discussed, *exogenous UGT2B7* overexpression was able to promote epirubicin resistance; however, it remained uncertain whether *endogenous UGT2B7* could be sufficiently induced by epirubicin to also induce resistance. To address this question, we sought to develop a breast cancer model in which *endogenous UGT2B7* was absent (or could not be induced by epirubicin) and test its sensitivity to epirubicin. Several approaches were trialled to achieve UGT2B7 knockout or knockdown, including CRISPR, CRISPRi and siRNA, but none of the methods were effective. As discussed in Chapter 4, the breast cancer cell lines used had generally low basal expression of UGT2B7, which may reflect relatively low chromatin accessibility at the gene locus. Chromatin accessibility has been previously defined as a key limiting factor preventing effective

CRISPR complex binding (Lee et al., 2016), Indeed, Uusi-Mäkelä et al. (2018) noted that successful CRISPR-Cas9 mutagenesis directly correlates with gene expression level. siRNA-directed knockdown was unexpectedly unsuccessful despite use of a previously validated siRNA sequence from literature (Konopnicki et al., 2013). Again, this might relate to different accessibility of the target site for the siRNA in the mRNA between cell types. The last method tested was dominant negative inhibition using a truncated form of UGT2B15 (chimeric UGT2B15) that had been shown previously to inhibit UGT2B7 activity via heterodimerization (Hu et al., 2018). Unexpectedly however, the chimeric UGT2B15 over-expression cell line was found to express only the chimeric UGT2B15 RNA but not the protein. Suppression of translation of chimeric UGT2B15 may occur because the dominant-negative effects of this protein on other UGTs expressed in ZR-75-1 cells interferes with endogenous metabolic processes and impairs cell fitness. This again suggests that cells may maintain tight translational control on UGTs and suggests interesting avenues for further study of UGT regulatory mechanisms (Hu et al., 2022). Finally, this chapter used analysis of clinical data from the TCGA-BRCA database to assess whether high vs low levels of UGT2B7 expression in breast cancer associate with general, or drug-specific, survival outcomes. When the entire breast cancer cohort was examined, we saw association of high UGT2B7 mRNA expression with poorer OS. However, when the cohort was stratified by subtype, association between high UGT2B7 expression and poor OS was only observed in the basal subtype of cancer. This is broadly consistent with the finding in Chapter 4 that overexpression of UGT2B7 provided a growth advantage to a basal-like breast cancer cell line. The basal subgroup was further stratified by drug treatment regimen. Unfortunately, it was not possible to examine association between UGT2B7 expression and epirubicin treatment specifically as there were too few patients receiving epirubicin in the TCGA-BRCA dataset. It was therefore decided to examine the patient group

receiving either of the two anthracycline drugs: epirubicin (EPI) or doxorubicin (DOX). Interestingly, high UGT2B7 expression was associated with poorer PFS, only in the group receiving an anthracycline containing regime (DOX or EPI) and not those receiving non-anthracycline containing regimens (neither DOX nor EPI). However, both groups showed an association between high UGT2B7 expression and poor OS. Further studies using additional cohorts could help to clarify whether there is an association between UGT2B7 expression and anthracycline-specific survival outcomes. Because UGT2B7 is directly responsible for inactivation for epirubicin by glucuronidation, the level of UGT2B7 expression might control the intratumoural exposure to this drug. Doxorubicin undergoes a different metabolic fate to epirubicin and is not directly glucuronidated. Instead, it is converted to a series of metabolites, by differing combinations of reduction or deglycosidation, including an aglycone called 7-deoxydoxorubicinolone (Choi et al., 2020; Licata et al., 2000). Interestingly clearance of 7-deoxydoxorubicinolone does involve glucuronidation (Takanashi & Bachur, 1976), however, no specific UGT isoform has yet been identified as responsible for this pathway. If UGT2B7 is involved in glucuronidation of 7-deoxydoxorubicinolone, this might help enhance overall clearance of doxorubicin, therefore controlling the cytotoxic effect of the drug. These suggestions are in accordance with Dellinger et al. (2012), as they demonstrated that knockdown of UGT2B7 in melanoma cells, re-sensitizes cells to both doxorubicin and epirubicin. Overall, the mechanism(s) underlying the apparent effects of UGT2B7 on doxorubicin activity require further study.

Chapter 5 extended the scope of the project into understanding the possible role of UGT2B7 in targeted therapy and DDIs. Our primary focus was on EGFR inhibitors, which have to date shown limited success in TNBC, despite frequent EGFR overexpression in these cancers. We postulated that EGFR inhibitors could induce UGT2B7 and thus reduce exposure to other drugs that are

UGT2B7 substrates (i.e. an induction based DDI). In the case of epirubicin, this could reduce the efficacy of epirubicin-inclusive chemotherapy. However, neither the first nor second-generation tyrosine kinase inhibitors tested altered the expression of UGT2B7 mRNA. We then directed our attention to inhibition based DDIs involving UGT2B7. Gefitinib had been shown to inhibit UGT2B7 mediated glucuronidation of 4-MU, but the relevance of this for anticancer drugs was unknown. Using a new highly specific assay we were able to show that gefitinib inhibited epirubicin glucuronidation. However *in vitro-in vivo* extrapolation suggested that the inhibition effect would be unlikely to result in a DDI that manifests as a change in the plasma concentration of epirubicin. Our secondary focus in the inhibition studies was on tamoxifen. Tamoxifen had been identified as a new inhibitor of UGT2B7 by a study published during this project. Moreover, literature indicated that tamoxifen combined with epirubicin-inclusive chemotherapy improved outcomes in breast cancer – specifically an increase in disease-free survival (Namer et al., 2006) and reduced risk of relapse (Davies et al., 2011; Wils et al., 1999). We therefore hypothesized that tamoxifen might reduce epirubicin glucuronidation leading to increased tumoural exposure (i.e. a beneficial DDI). Tamoxifen was indeed found to be a strong inhibitor of epirubicin glucuronidation by UGT2B7. Moreover, *in vitro-in vivo* extrapolation (using a reversible inhibition model) suggested that the inhibition effect could result in a significant DDI. In particular, the analysis suggested that tamoxifen has the potential to increase plasma levels of UGT2B7 substrates. To better understand the nature of this interaction, future studies using patient blood samples could assess the pharmacokinetic effects of titrating tamoxifen dose on epirubicin plasma levels. Given in the following chapter, a highly sensitive LC-MS method for measuring epirubicin glucuronidation was developed, this could potentially be applied in the suggested studies in accordance with MIDS. Moreover, given that intratumoural levels of tamoxifen are known to be significantly higher than

plasma levels (Kisanga et al., 2004; Robinson et al., 1991), understanding the occurrence of this interaction within the tumour is of most importance. Previous literature suggests that tamoxifen can increase the cytotoxic effects of epirubicin in ER-negative Ehrlich's carcinoma ascitic cells (EATC, derived from a murine mammary adenocarcinoma) in mice (Aydiner et al., 1997), and in ER-positive MCF-7 and NCI-adr cell lines *in vitro* (Azab et al., 2005), presumably by increased interruption of cell cycling in S and G2/M replication phases. Neither study investigated changes in epirubicin glucuronidation, and as such, investigating whether the observed synergistic effects of the drugs were occurring by pharmacokinetic means, is of significant interest.

Chapter 6 demonstrated the development of a LC-MS based, epirubicin glucuronidation assay, which required method validation using a canonical UGT2B7 inhibitor – fluconazole, to confirm the identification of the correct metabolite of the UGT2B7 specific probe substrate – epirubicin. Upon confirmation of the specificity of this assay, the kinetics of UGT2B7 catalysed epirubicin glucuronidation were analysed using HLMs. Updated methodology eliminating microsomal latency and improving metabolite specificity allowed us to determine a K_m of 26.2 ± 5.48 µM and V_{max} of 2896.6 ± 212.8 AU. The substrate-enzyme affinity for epirubicin was higher than the previously reported K_m value of 568 ± 130 µM that was measured using HPLC (Innocenti et al., 2001). Using the revised kinetic values and the published physiochemical properties of the drug (Mouridsen et al., 1990), a compound profile for epirubicin was constructed using the Simcyp simulator. This enabled the creation of a pharmacokinetic model that would simulate the whole-body metabolism of epirubicin, which in turn could be used to assess the physiological covariates affecting systemic metabolism of epirubicin in an oncology cohort, and the predicted tissue distribution of the drug. Using multi-variate linear regression modelling, it was demonstrated that systemic epirubicin exposure (maintained by mostly liver and partly renal clearance) was primarily driven by

differences in hepatic and renal UGT2B7 expression, plasma albumin concentration, age, BSA, GFR, haematocrit and sex. These factors accounted for 87% of epirubicin variability in exposure. The most significant contributing factor to systemic epirubicin exposure was hepatic UGT2B7 expression, accounting for 56% of the differences in epirubicin variability. This supported the idea that modulation of hepatic UGT2B7 activity could greatly affect the efficacy of epirubicin. Henceforth, the described PBPK model could be further applied to perform PBPK-guided dose-selection forming a bottom-up approach in predicting a priori epirubicin exposure based on demographic factors. This eliminates the invasive nature of precision dosing by TDM and could greatly improve upon current dosing standards. Current epirubicin dosing is typically predicated by body surface area (BSA). From the generated epirubicin PBPK model, upon removing BSA from the model, a minor change in R_2 of 4% was observed therefore indicating that this factor alone is not sufficient to reliably predict epirubicin exposure. This affirms the requirement to improve upon and update current dosing standards to better inform treatment options for clinicians.

Given drug concentrations in plasma are normally indictive of distribution to tissue (Zhang et al., 2019), this was expected to hold true for epirubicin. Confoundingly, aside from in brain tissue (R_2 = 0.56), the remaining simulated tissue concentrations (muscle, heart, adipose, and liver tissue) showed limited correlation with plasma concentrations, indicating there are tissue-specific characteristics or other mechanism regulating the amount of epirubicin accumulation. As reviewed by Zhang et al. (2019), drug uptake, efflux and biotransformation can be factors affecting drug concentration asymmetry between plasma and tissues. These could have a profound impact on the effectiveness of the drug in the target-site.

In the instance of breast cancer, any mechanisms of improving breast-tissue accumulation could improve the intratumoural exposure of epirubicin, resulting in better efficacy. Overall, the work

presented in this thesis has demonstrated that UGT2B7 is an important regulatory component contributing to epirubicin exposure and may play a role in the acquisition of drug resistance. Moreover, the capacity to inhibit UGT activities by exploiting DDI mechanisms may provide new avenues for pharmacokinetic modulation of drug response and resistance in cancer.

APPENDICES

Appendix A. Plasmid Maps

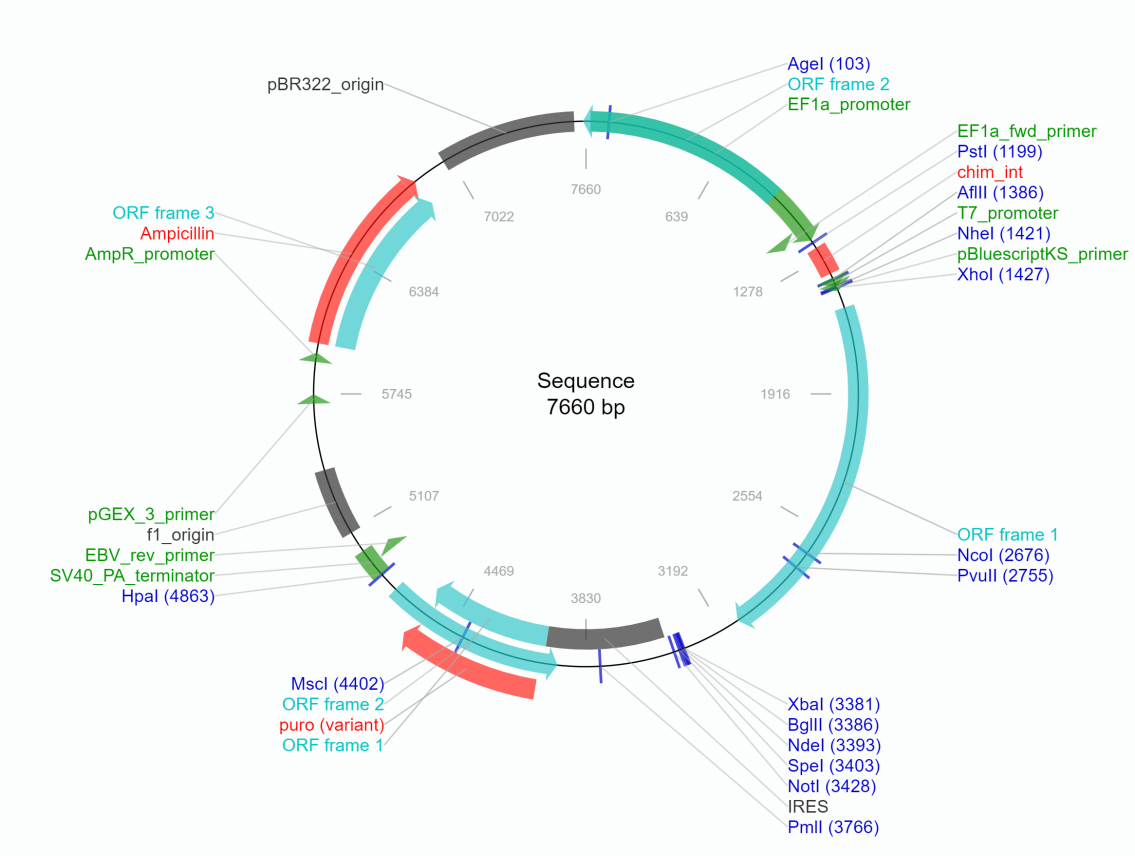

Appendix Figure 1. pEF1-IRES-puro (pIRES) vector carrying a bicistronic cassette including the *UGT2B7* cDNA (ORF 1) linked via an internal ribosome entry site (IRES) to a gene encoding puromycin acetyltransferase (PAC). The ampicillin resistance gene is also depicted. This cassette is constitutively driven by the elongation factor-1 alpha promoter (EF-1 alpha) shown. Restriction enzyme cut sites are shown. Map generated using Addgene. The plasmid was originally cloned by Lewis et al. (2011).

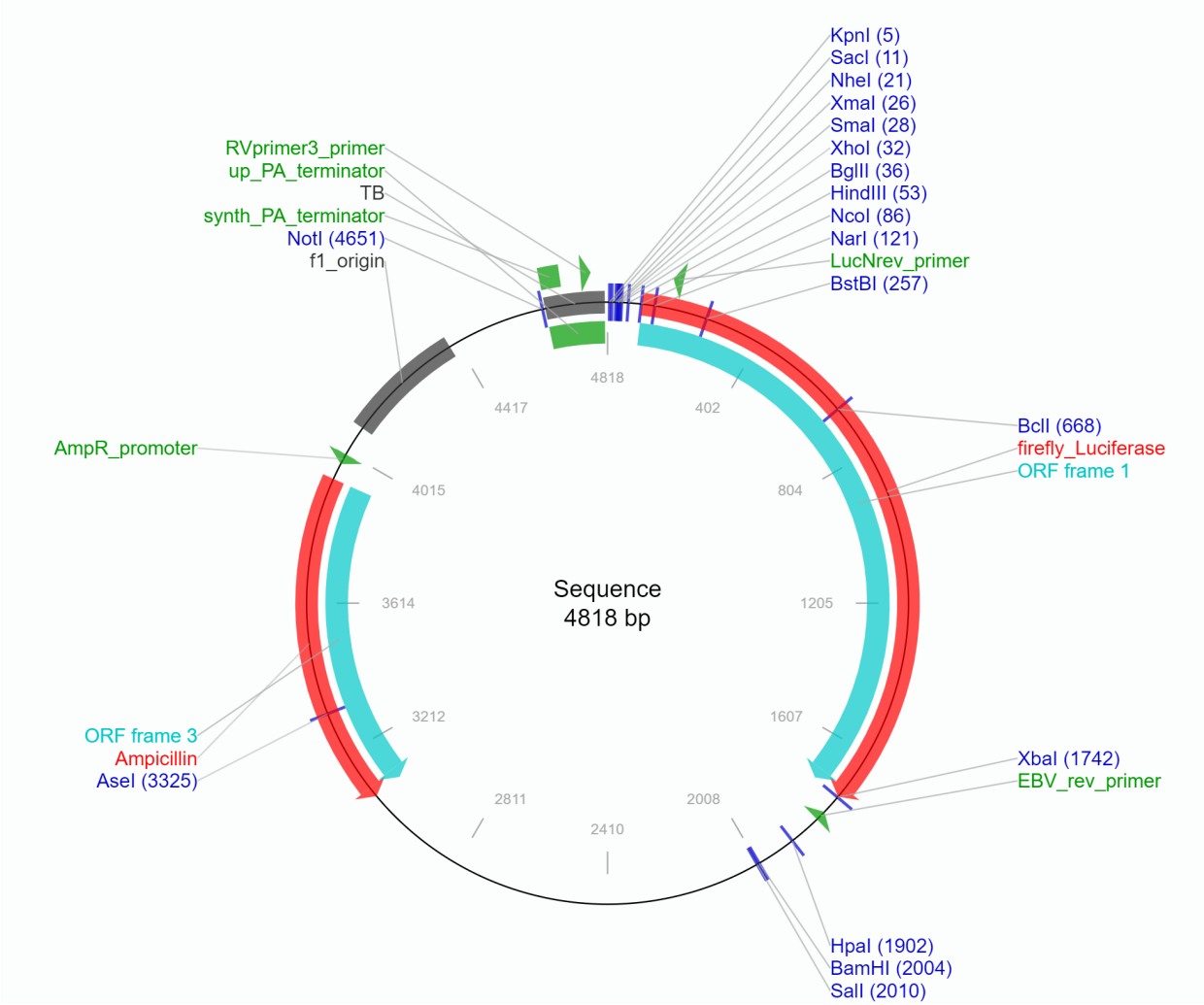

Appendix Figure 2. pGL3-Basic vector containing the firefly luciferase reporter for promoter driven expression studies. Promoters cloned upstream of the luciferase reporter stimulate a quantifiable luminescence-based response. This vector also features ampicillin resistance as depicted. Restriction enzyme cut sites are show. Map generated using Addgene. The plasmid was originally obtained from Promega. Sequence available from Genbank (accession number U47295).

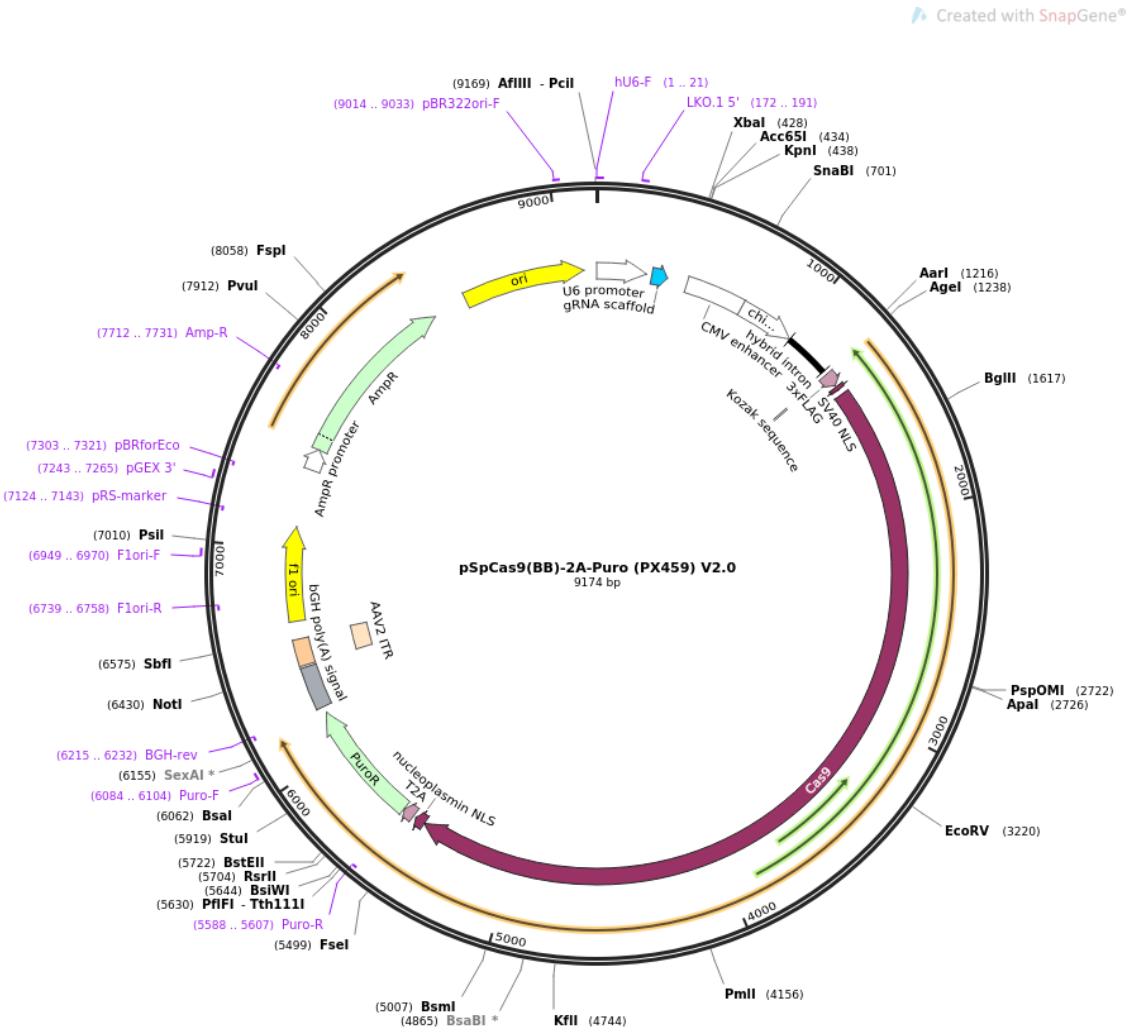

Appendix Figure 3. pSpCas9(BB)-2A-Puro (PX459) plasmid expressing Cas9 and Puromycin resistance gene (PAC) as a continuous polypeptide, cleaved into two discrete proteins via the T2A self-cleaving sequence. Cas9 and PAC expression is driven using the chicken ß-actin promoter. Guide RNA was inserted at the guide RNA scaffold and driven by the U6 promoter. The *UGT2B7* exon 1 targeting guide RNA sequence is 5'-TGCTTTTCAAAAGTGTAGCC-3'. pSpCas9(BB)-2A-Puro (PX459) was originally developed by Feng Zhang (Addgene plasmid # 62988).

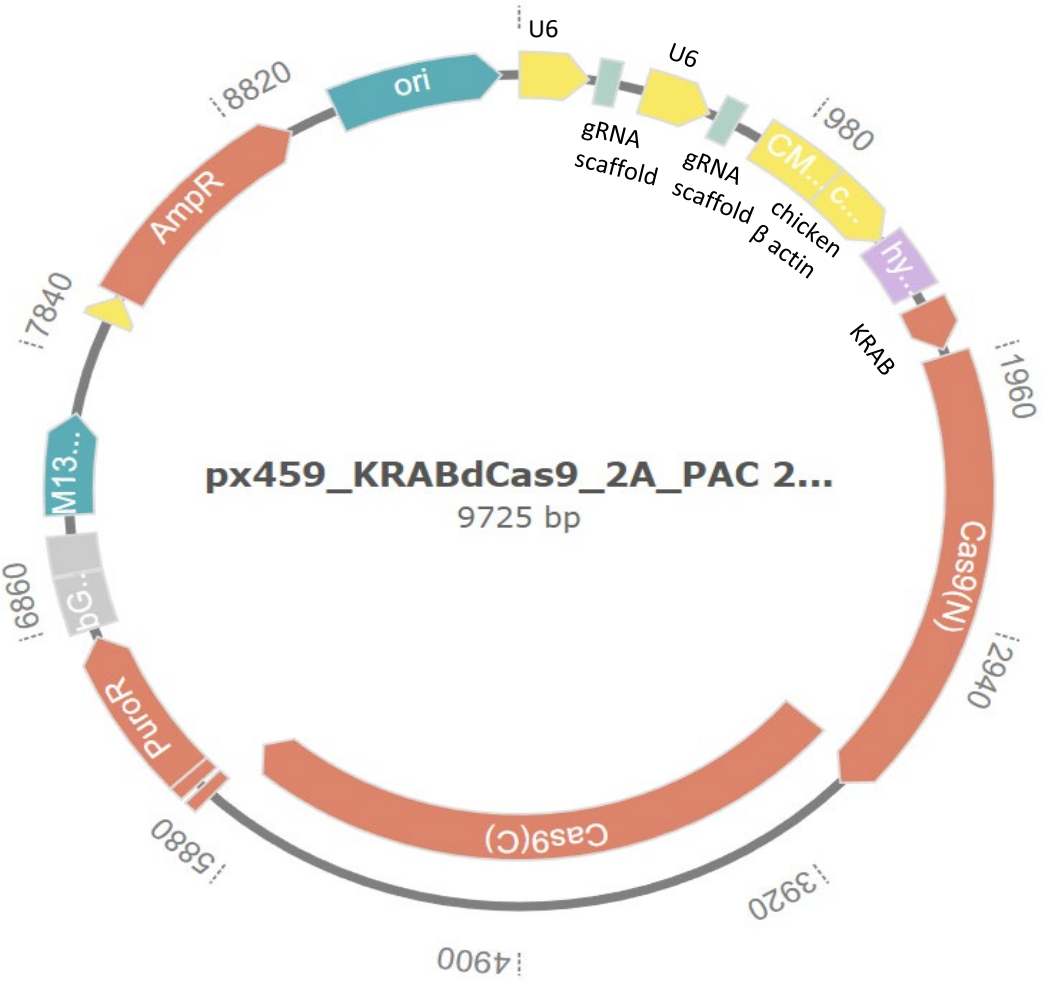

Appendix Figure 4. px459_KRABdCas9_2A_PAC 2xU6sgRNA plasmid expressing dCas9 and Puromycin resistance gene (PAC) as a continuous polypeptide, cleaved into two discrete proteins via the T2A self-cleaving sequence. The KRAB repressor dCas9 (catalytically inactive) and PAC expression is driven using the chicken ß-actin promoter. Two sgRNA scaffolds have been inserted and are driven by separate U6 promoters.

Appendix B. UGT2B7 TCGA expression associations between clinical attributes

A

Clinical Attribute	Attribute Type	Statistical Test	p-Value	q-Value
Subtype	Patient	Chi-squared Test	**$< 10^{-10}$**	**$< 10^{-10}$**
Buffa Hypoxia Score	Patient	Wilcoxon Test	**$< 10^{-10}$**	**$< 10^{-10}$**
Winter Hypoxia Score	Patient	Wilcoxon Test	**$< 10^{-10}$**	**1.56e-10**
Ragnum Hypoxia Score	Patient	Wilcoxon Test	**$< 10^{-10}$**	**8.72e-10**
Mutation Count	Sample	Wilcoxon Test	**$< 10^{-10}$**	**8.72e-10**
Tissue Source Site Code	Sample	Chi-squared Test	**3.77e-10**	**2.64e-9**
Tissue Source Site	Sample	Chi-squared Test	**3.77e-10**	**2.64e-9**
TMB (nonsynonymous)	Sample	Wilcoxon Test	**9.73e-10**	**5.96e-9**
Aneuploidy Score	Sample	Wilcoxon Test	**6.718e-5**	**3.657e-4**
MSI MANTIS Score	Sample	Wilcoxon Test	**1.438e-3**	**7.045e-3**
Fraction Genome Altered	Sample	Wilcoxon Test	0.0158	0.0705
Oncotree Code	Sample	Chi-squared Test	0.0400	0.151
Cancer Type Detailed	Sample	Chi-squared Test	0.0400	0.151
American Joint Committee on Cancer Publication Version Type	Patient	Chi-squared Test	0.0587	0.206
Sex	Patient	Chi-squared Test	0.0717	0.234
Race Category	Patient	Chi-squared Test	0.0912	0.279
Tumor Type	Sample	Chi-squared Test	0.135	0.388
International Classification of Diseases for Oncology, Third Edition ICD-O-3 Histology Code	Patient	Chi-squared Test	0.184	0.501
In PanCan Pathway Analysis	Patient	Chi-squared Test	0.242	0.623
Ethnicity Category	Patient	Chi-squared Test	0.293	0.678

B

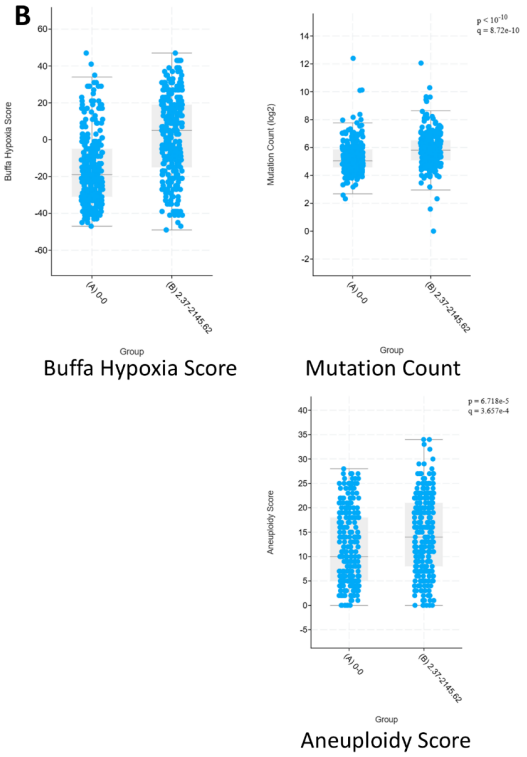

Appendix Figure 5. UGT2B7 expression is associated with genomic instability and tumour hypoxia. **(A)** When TCGA-BRCA samples were stratified into quartiles by UGT2B7 mRNA expression, the top quartile showed significant differences in clinical attributes when compared to the lower quartile (N=1084) **(B)** Three defining clinical attributes (Buffa hypoxia score, mutation count, and aneuploidy score) from this analysis, have been plotted to demonstrate these effects.

Appendix C. Sequencing chromatograms of UGT2B7 directed CRISPR transfectants processed using ICE analysis

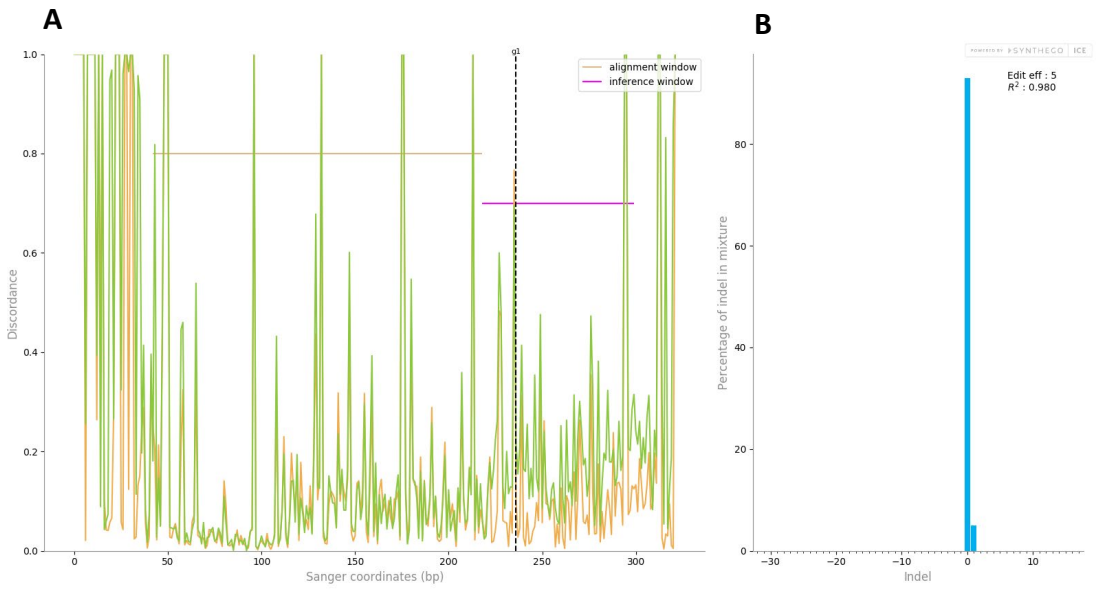

Appendix Figure 6. Raw ICE analysis figures conducted on Sanger sequencing from genomic DNA from a ZR-75-1 polyclonal population expressing a CRISPR-px459 backbone with a sgRNA targeting exon 1 *UGT2B7*. **(A)** A discordance plot displaying the level of alignment of the wildtype control (orange) and edited (green) traces relative to the sequence coordinates. The positioning used for alignment is indicated by the alignment window, while the inference window shows the region around the cut site where deletion events are predicted. The cut site is shown as a black dotted line. **(B)** 5% indel efficiency is estimated in the CRISPR population compared to the control, wildtype ZR-75-1 sequence. The R^2 value (Pearson correlation coefficient) indicates goodness of fit of the edited trace relative to the control. A R^2>0.8 is considered sufficient for robust analysis. Raw sequences are available in Appendix Figure 7. Analysis was performed using the Synthego ICE Analysis tool (v3) (2019).

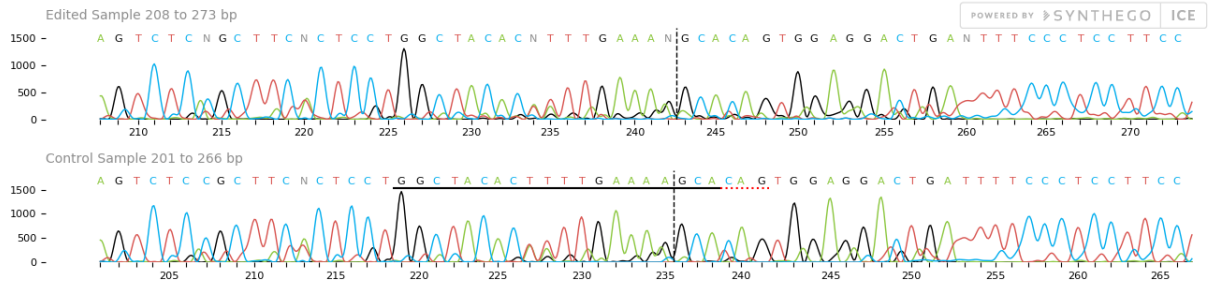

Appendix Figure 7. Raw sequencing chromatogram from genomic DNA of the ZR-75-1 polyclonal population expressing a CRISPR-px459 backbone with a sgRNA targeting exon 1 *UGT2B7*. The edited sample refers to the sequence of the transgenic population, while the control sample refers to the control wildtype ZR-75-1 sequence. Analysis was performed using the Synthego ICE Analysis tool (v3) (2019).

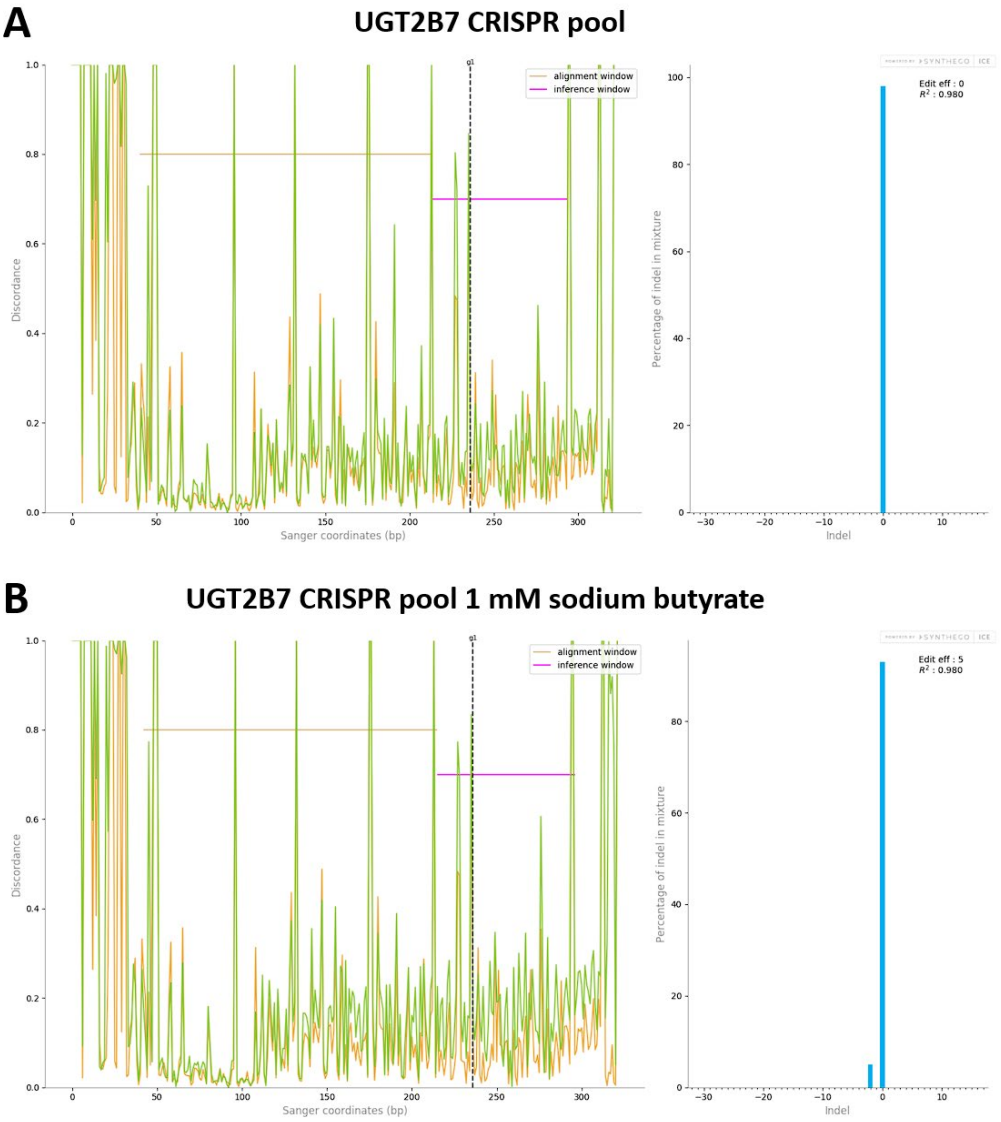

Appendix Figure 8. Raw ICE analysis figures conducted on Sanger sequencing from genomic DNA from a ZR-75-1 polyclonal population expressing a CRISPR-px459 backbone with a sgRNA targeting exon 1 *UGT2B7*. **(A)** The stable CRISPR pool (as in Figure 4.7) was re-sequenced and the resulting ICE analysis estimated a 0% indel efficiency with a R^2 of 0.98. **(B)** The CRISPR polyclonal population (pool) was treated with an epigenetic inducer, sodium butyrate (1 mM) for 6 days and the resulting ICE analysis estimated a 5% indel efficiency with a R^2 of 0.98. Plotted on the left, a discordance plot displaying the level of alignment of the wildtype control (orange) and edited (green) traces relative to the sequence coordinates. The positioning used for alignment is indicated by the alignment window, while the inference window shows the region around the cut site where deletion events are predicted. The cut site is shown as a black dotted line. Plotted on the right, the predicted percentage of indels relative to the position. The R^2 value (Pearson correlation coefficient) indicates goodness of fit of the edited trace relative to the control. A R^2>0.8 is considered sufficient for robust analysis. Raw sequences are available in Appendix Figure 9. Analysis was performed using the Synthego ICE Analysis tool (v3) (2019).

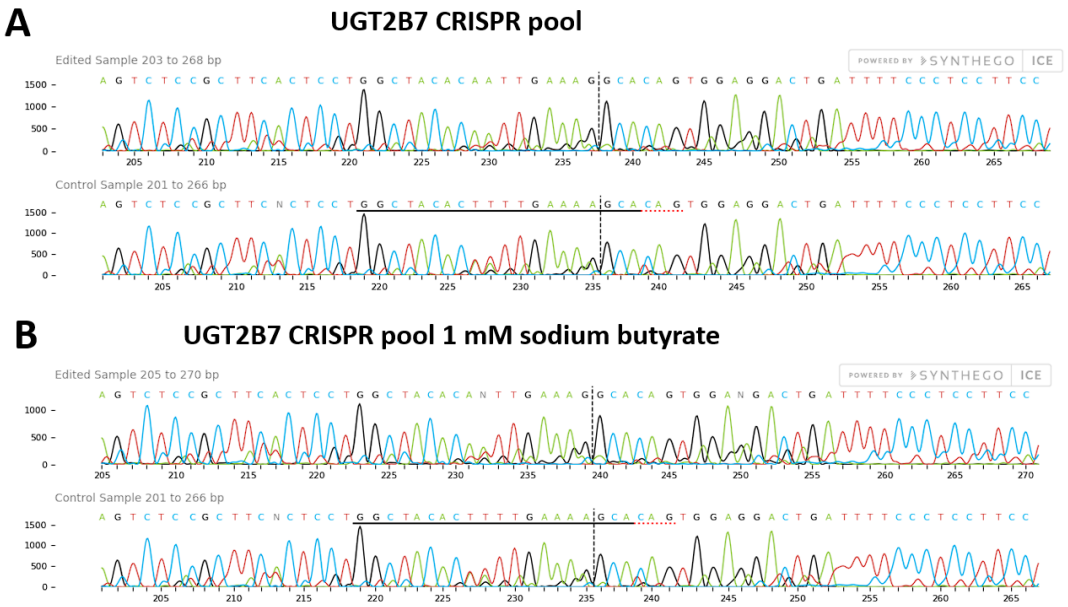

Appendix Figure 9. Raw sequencing chromatogram from genomic DNA of the ZR-75-1 polyclonal population expressing a CRISPR-px459 backbone with a sgRNA targeting exon 1 *UGT2B7* untreated **(A)** or treated with 1 mM sodium butyrate **(B)**. The edited sample refers to the sequence of the transgenic population, while the control sample refers to the control wildtype ZR-75-1 sequence. Analysis was performed using the Synthego ICE Analysis tool (v3) (2019).

Appendix D. UGT8 and UGT2B15 mRNA are not associated with OS and PFS in basal subtyped BC

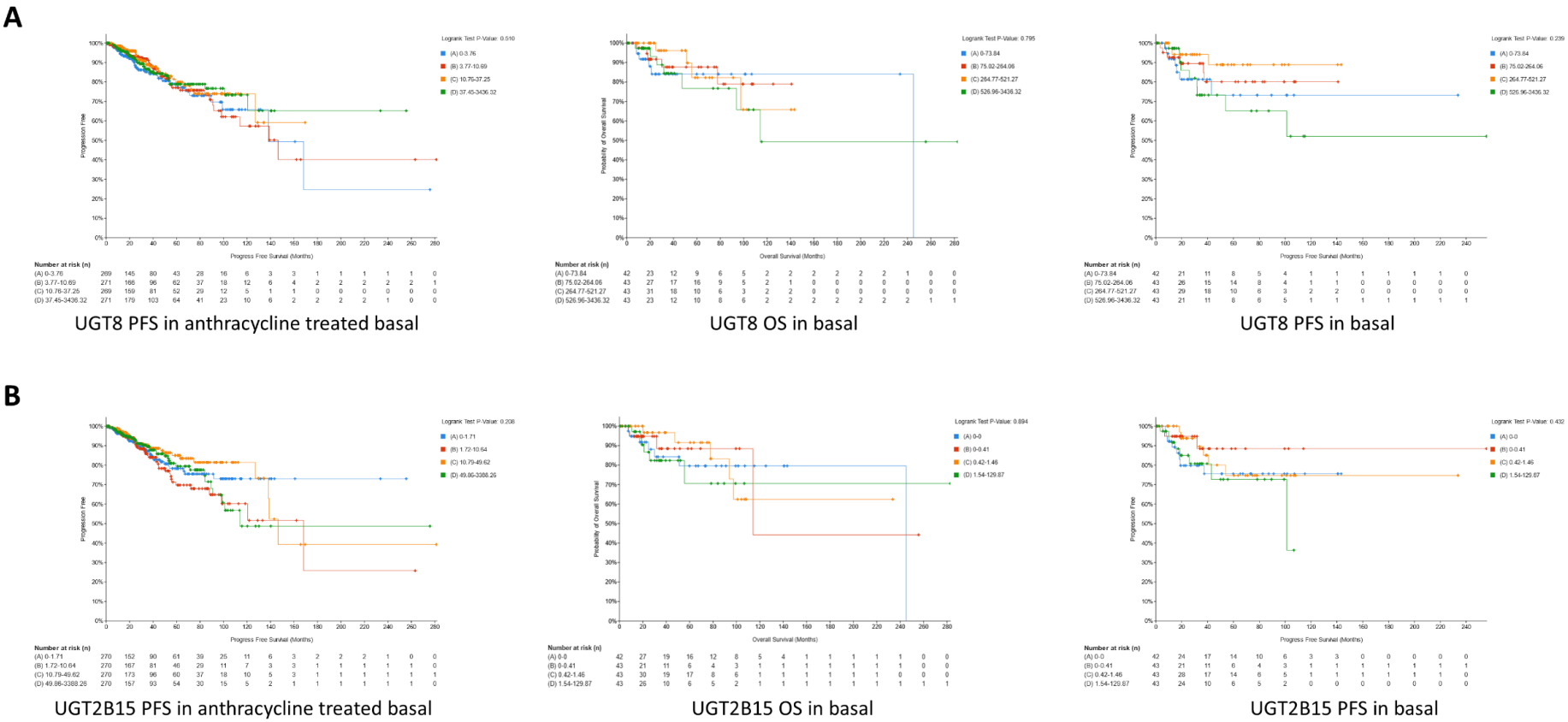

Appendix Figure 10. UGT8 **(A)** and UGT2B15 **(B)** TCGA-BRCA expression levels are not associated with differential overall survival (OS) or progression free survival (PFS) in basal subtyped breast cancer treated with and without anthracycline containing regimines (epirubicin and doxorubicin).

Appendix E. Raw Western blot of chimeric UGT2B15 detection

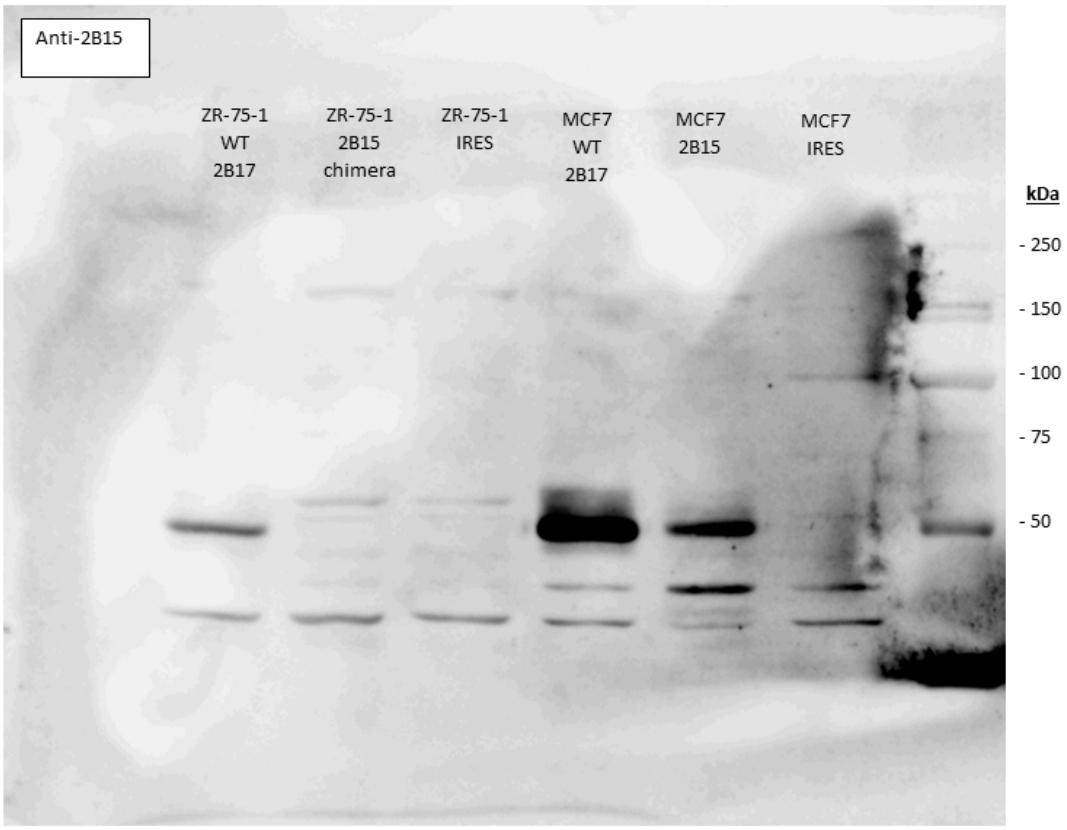

Appendix Figure 11. Raw Western blot showing the detection of wildtype (WT) UGT2B15/17 at 50 kDa in ZR-75-1 cells and MCF7 cells (stably expressing UGT2B15 or UGT2B17) and the absence of chimeric UGT2B15 at 45 kDa . The rabbit anti-UGT2B15/17 antibody was used that recognises wildtype and chimeric variants (Hu et al., 2018). 50 µg of total protein was used from RIPA lysates. Western Blot was performed by Quinn Martin (Clinical Pharmacology, Flinders University, Australia).

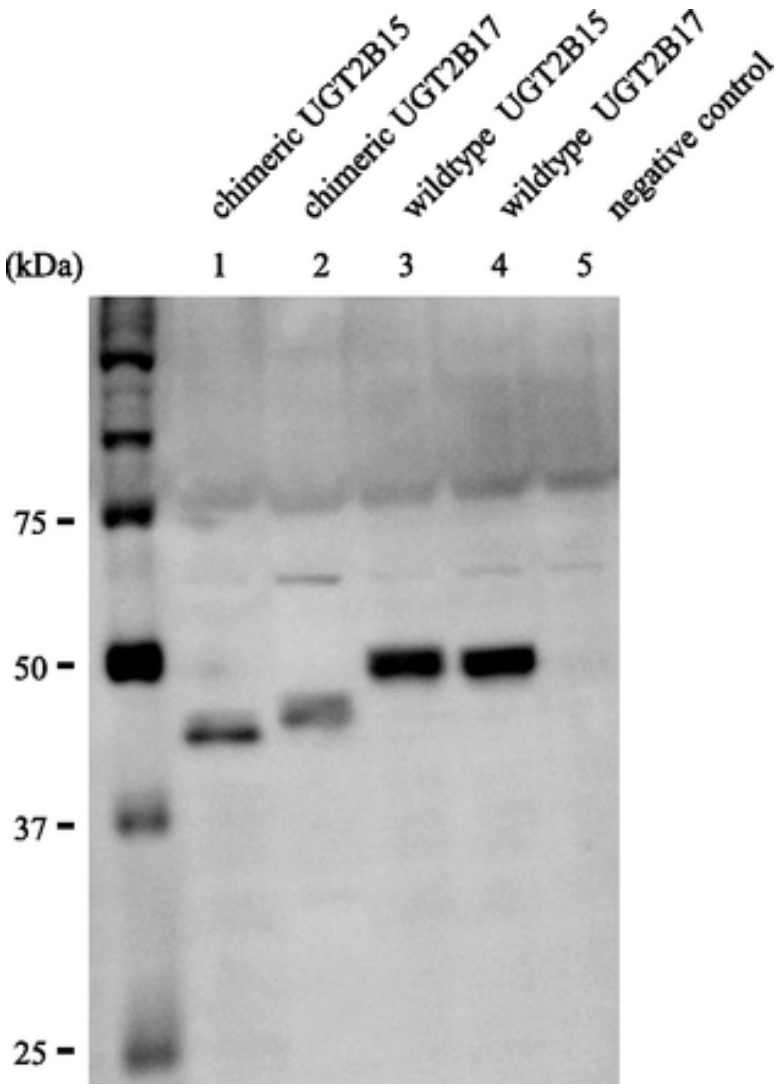

Appendix Figure 12. The published Western Blot by Hu et al. (2018) showing the expression and relative size of chimeric UGT2B15 and UGT2B17 chimeric proteins transiently expressed in HEK-293 cells for 48 hours . The rabbit anti-UGT2B15/17 antibody was used that recognises wildtype and chimeric variants. Figure has been reproduced with permission.

Appendix F. Abstracts Submitted for Conference Proceedings

Ansaar, R. (2018) The role of UGT enzymes in cytotoxic drug resistance in breast cancer cells and cancer stem cells, short talk presented to the *ASCEPT 2018 Annual Scientific Meeting*, Adelaide Convention Centre, 27-30 November.

The role of UGT enzymes in cytotoxic drug resistance in breast cancer cells and cancer stem cells

Radwan Ansaar[1], Lu Lu[1], Tran Nguyen[2], Robyn Meech[1]. Discipline of Clinical Pharmacology, College of Medicine & Public Health, Flinders University[1], Adelaide, SA, Australia; The Centre for Cancer Biology, University of South Australia[2], Adelaide, SA, Australia

Introduction. UDP-glucuronosyltransferases (UGTs) conjugate sugars to lipophilic chemicals as part of a larger network of drug metabolizing enzymes (DMEs) involved in elimination of drugs and toxins. Epirubicin (EPI) is a cytotoxic often used in combination with other drugs to treat breast and other cancers, generally in later stages. UGT2B7 is thought to be the only UGT that metabolizes EPI; our studies show UGT2B7 is induced by EPI in liver cells, which may enhance systemic clearance. However, the role of UGT2B7 in intratumoural clearance, and hence resistance, is unknown.

Aims. To assess whether EPI increases UGT2B7 expression in breast cancer cells and breast cancer stem cells (BCSC), and to determine whether UGT2B7 plays a role in drug resistance in breast cancer cells and/or BCSC.

Methods. MDA-MB-231 breast cancer cells were treated with EPI and UGT2B7 mRNA was quantified by qPCR. UGT2B7-overexpressing cell lines were generated and characterized for response/resistance to EPI. An 'induced BCSC' (iBCSC) model was established by reprogramming MDA-MB-231 cells with pluripotency factors (Oct4/Sox2/Klf4); these were characterized for stem-cell like behaviour, response/resistance to EPI, and gene expression.

Results. Treatment of MDA-MB-231 cells with EPI for 72 hrs induced expression of UGT2B7 by ~4 fold. Increases in the expression of other UGTs and drug efflux ABC transporters were also observed. Ectopic overexpression of UGT2B7 in MDA-MB-231 cells led to increased EPI resistance; the increase in half maximal inhibitory concentration (IC50) averaged ~1.5 fold (n=2). The iBCSC model showed a gene expression profile consistent with epithelial mesenchymal transition

(EMT) and constitutive drug resistance. Although UGTs (including UGT2B7) were not constitutively elevated in iBCSC, treatment with EPI resulted in a much higher UGT2B7 induction (~47 fold) relative to the parental cell line.

Discussion. EPI transcriptionally induces UGT2B7 (and efflux transporters) in breast cancer cells contributing to short-term resistance of these cells to EPI toxicity. BCSC may have both constitutive elevation of genes that contribute to drug resistance (such as efflux transporters) but may also be epigenetically primed to rapidly induce additional mediators of resistance, such as UGT2B7. Understanding the roles of UGTs and transporters in the drug resistant phenotype of BCSC may provide new avenues to enhance the efficacy of cytotoxics in this pathogenic cell population.

Ansaar, R. (2019) The role of UGT enzymes in cytotoxic drug resistance in breast cancer cells, poster presented to the *ASCEPT 2019 Annual Scientific Meeting*, Rydges Lakeland Resort Queenstown, 26-29 November. Finalist for the Neville Percy Award.

The role of UGT enzymes in cytotoxic drug resistance in breast cancer

Radwan Ansaar, Lu Lu, Dong Gui Hu, Ross McKinnon, Peter Mackenzie, Robyn Meech. Discipline of Clinical Pharmacology, College of Medicine & Public Health, Flinders University, Adelaide, SA, Australia

Introduction. UDP-glycosyltransferases (UGTs) are a family of drug metabolising enzymes that facilitate inactivation of xenobiotics, including therapeutic drugs, by conjugating them with sugars (e.g. glucuronic acid). Glucuronidation occurs in the liver to promote systemic detoxification/clearance, and in multiple drug-target tissues resulting in local inactivation. Epirubicin (EPI) is a cytotoxic drug used in combination therapies for breast and other cancers. UGT2B7 is the only UGT known to metabolize EPI. We previously showed that EPI induces UGT2B7 in liver cells, which may enhance systemic clearance. However, the role of UGT2B7 in intratumoural inactivation has not been examined.

Aims. To assess both the regulation and function of UGT2B7 in various breast cancer subtypes in the context of EPI treatment and to understand whether UGT2B7 has a role in drug resistance.

Methods. Realtime-PCR quantification was performed in breast cancer cell lines ZR-75-1 (p53 wildtype) and MDA-MB-231 (p53 R280K missense) to determine whether UGT2B7 expression is increased by EPI treatment. Promoter-reporter assays were used to characterize UGT2B7 induction via p53-dependent and -independent mechanisms. Stable UGT2B7-overexpressing cell lines were generated and characterized for response/resistance to EPI.

Results. 24-hour treatment of ZR-75 cells with 0.5 µM EPI resulted in ~20-fold induction of UGT2B7, whilst treatment of MDA-MB-231 cells with 1 µM EPI induced UGT2B7 ~7-fold (n= 3, $P<0.02$). The proximal UGT2B7 promoter region was induced ~130-fold (n=3, $P<0.09$) by EPI in ZR-75 cells; deletion of the p53 site within this region essentially abolished the activation. In contrast, EPI had negligible effect on UGT2B7 proximal promoter activity in MDA-MB-231 cells. These data suggest that EPI regulates UGT2B7 by p53-dependent and also -independent mechanisms in breast cancer cells. Overexpression of UGT2B7 in MDA-MB-231 increased the IC50 for EPI almost 2-fold (n=3, $P<0.005$).

Discussion. EPI induces UGT2B7 in breast cancer cells. In p53 WT cancers this effect is largely mediated by a proximal promoter p53 site; however, p53-mutant cancers may also induce UGT2B7 by a p53-independent mechanism. Proof of principle that elevation of UGT2B7 can reduce EPI sensitivity suggests that the induction of UGT2B7 by EPI could contribute to resistance to EPI-containing therapies. Further defining these feedback pathways may provide new avenues to enhance the efficacy of cytotoxics by modulating UGT2B7 activity.

Ansaar, R. (2019) The role of UGT enzymes in cytotoxic drug resistance in breast cancer cells, poster presented at the College of Medicine and Public Health *Emerging Leaders Showcase*, Flinders University, 21-22 November.

(Resubmitted from Cancer Research Day, 2019)

The role of UGT enzymes in cytotoxic drug resistance in breast cancer cells

The UDP-glucuronosyltransferase (UGT) family of drug metabolising enzymes are primarily expressed within the liver where they facilitate the addition of sugars to various small molecules, including therapeutic drugs. This process typically inactivates the target molecule and aids in its elimination from the body. Epirubicin (EPI) is a cytotoxic drug often used for the treatment of late stage cancers. UGT2B7 is thought to be the only UGT responsible for EPI metabolism, however, the role of UGT2B7 in intratumoural clearance and drug resistance is unknown. This study aimed to assess regulation of UGT2B7 expression by EPI in breast cancer and to understand the mechanisms underlying drug resistance. Realtime-PCR quantification and promoter studies were performed in breast cancer cell lines to characterise altered UGT2B7 gene expression following EPI treatment. Stable UGT2B7-overexpressing cell lines were generated and characterized for response/resistance to EPI. Treatment with EPI resulted in significant induction of UGT2B7 expression. Increased expression of other UGTs and drug efflux transporters was also observed. UGT2B7 promoter constructs containing the previously identified p53 responsive element were induced by EPI ~128 fold, but only in p53 wildtype cells. Overexpression of UGT2B7 in breast cancer cells led to increased EPI resistance as identified by an increase in half maximal inhibitory concentration. This data suggests that EPI transcriptionally induces UGT2B7 in breast cancer cells and may contribute to short-term resistance of these cells. This is likely induced through both p53 dependent and independent pathways. Understanding the roles of UGTs in drug resistant breast cancer may provide new avenues to enhance the efficacy of cytotoxics in this disease.

Ansaar, R. (2019) The role of UGT enzymes in cytotoxic drug resistance in breast cancer cells, poster presented at the *Cancer Research Day,* Flinders Centre for Innovation in Cancer, 3rd September

The role of UGT enzymes in cytotoxic drug resistance in breast cancer cells

The UDP-glucuronosyltransferase (UGT) family of drug metabolising enzymes are primarily expressed within the liver where they facilitate the addition of sugars to various small molecules, including therapeutic drugs. This process typically inactivates the target molecule and aids in its elimination from the body. Epirubicin (EPI) is a cytotoxic drug often used for the treatment of late stage cancers. UGT2B7 is thought to be the only UGT responsible for EPI metabolism, however, the role of UGT2B7 in intratumoural clearance and drug resistance is unknown. This study aimed to assess regulation of UGT2B7 expression by EPI in breast cancer and to understand the mechanisms underlying drug resistance. Realtime-PCR quantification and promoter studies were performed in breast cancer cell lines to characterise altered UGT2B7 gene expression following EPI treatment. Stable UGT2B7-overexpressing cell lines were generated and characterized for response/resistance to EPI. Treatment with EPI resulted in significant induction of UGT2B7 expression. Increased expression of other UGTs and drug efflux transporters was also observed. UGT2B7 promoter constructs containing the previously identified p53 responsive element were induced by EPI ~128 fold, but only in p53 wildtype cells. Overexpression of UGT2B7 in breast cancer cells led to increased EPI resistance as identified by an increase in half maximal inhibitory concentration. This data suggests that EPI transcriptionally induces UGT2B7 in breast cancer cells and may contribute to short-term resistance of these cells. This is likely induced through both p53 dependent and independent pathways. Understanding the roles of UGTs in drug resistant breast cancer may provide new avenues to enhance the efficacy of cytotoxics in this disease.

Ansaar, R. (2021) UDP-Glycosyltransferases (UGTs) in Anti-Cancer Drug Resistance, short talk presented at the College of Medicine and Public Health *Emerging Leaders Showcase*, Flinders University, 25-26 November.

Mechanisms of acquired chemotherapy resistance in breast cancer cells

The UDP-glycosyltransferase (UGT) drug metabolising enzymes conjugate sugars to small molecules, including therapeutic drugs. This inactivates the target molecule and aids in its elimination. Epirubicin (EPI) is a cytotoxic drug often used in breast cancer (BC) chemotherapeutic regimes, particularly for triple-negative BC which has few therapeutic options. UGT2B7 (2B7) is thought to be the only UGT responsible for EPI inactivation, however, the role of 2B7 in intratumoural clearance and drug resistance is unknown. This study tested the hypothesis that 2B7 expression is induced by EPI in BC cells, and that subsequent metabolism of EPI by the enzyme could lead to drug resistance. qRTPCR quantification and promoter studies were performed in BC cell lines to characterise 2B7 gene expression following EPI treatment. Stable 2B7-overexpressing cell lines were generated and characterized for response/resistance to EPI, while 2B7 CRISPR knockout lines are under development. Treatment with EPI significantly induced expression of 2B7, other UGTs and drug efflux transporters. The p53 responsive element in the 2B7 promoter was induced by EPI specifically in p53 wildtype cells. Overexpression of 2B7 in BC cells led to increased EPI resistance (IC50=1.74-fold increase). These data support the hypothesis of EPI-mediated transcriptional induction of 2B7 in BC lead to the acquisition of EPI resistance. This regulation may involve both p53-dependent and independent pathways. Current work is examining induction of 2B7 and other drug resistance pathways by targeted therapies (e.g. Tyrosine Kinase Inhibitors) to understand whether combination therapies may synergistically promote drug resistance. Understanding mechanisms of acquired drug resistance may enable enhanced BC treatment efficacy.

Appendix G. Manuscripts Published Arising Directly from this Thesis

pharmaceutics

IMPACT FACTOR 5.4 | Indexed in: PubMed | CITESCORE 6.9

Article

A Physiologically Based Pharmacokinetic Model to Predict Determinants of Variability in Epirubicin Exposure and Tissue Distribution

Radwan Ansaar, Robyn Meech and Andrew Rowland

Special Issue
Role of Pharmacokinetics in Drug Development and Evaluation
Edited by
Prof. Dr. David R. Taft

MDPI

https://doi.org/10.3390/pharmaceutics15041222

pharmaceutics

MDPI

Article

A Physiologically Based Pharmacokinetic Model to Predict Determinants of Variability in Epirubicin Exposure and Tissue Distribution

Radwan Ansaar, Robyn Meech and Andrew Rowland *

College of Medicine and Public Health, Flinders University, Adelaide, SA 5042, Australia
* Correspondence: andrew.rowland@flinders.edu.au

Abstract: Background: Epirubicin is an anthracycline antineoplastic drug that is primarily used in combination therapies for the treatment of breast, gastric, lung and ovarian cancers and lymphomas. Epirubicin is administered intravenously (IV) over 3 to 5 min once every 21 days with dosing based on body surface area (BSA; mg/m^2). Despite accounting for BSA, marked inter-subject variability in circulating epirubicin plasma concentration has been reported. Methods: In vitro experiments were conducted to determine the kinetics of epirubicin glucuronidation by human liver microsomes in the presence and absence of validated UGT2B7 inhibitors. A full physiologically based pharmacokinetic model was built and validated using Simcyp® (version 19.1, Certara, Princeton, NJ, USA). The model was used to simulate epirubicin exposure in 2000 Sim-Cancer subjects over 158 h following a single intravenous dose of epirubicin. A multivariable linear regression model was built using simulated demographic and enzyme abundance data to determine the key drivers of variability in systemic epirubicin exposure. Results: Multivariable linear regression modelling demonstrated that variability in simulated systemic epirubicin exposure following intravenous injection was primarily driven by differences in hepatic and renal UGT2B7 expression, plasma albumin concentration, age, BSA, GFR, haematocrit and sex. By accounting for these factors, it was possible to explain 87% of the variability in epirubicin in a simulated cohort of 2000 oncology patients. Conclusions: The present study describes the development and evaluation of a full-body PBPK model to assess systemic and individual organ exposure to epirubicin. Variability in epirubicin exposure was primarily driven by hepatic and renal UGT2B7 expression, plasma albumin concentration, age, BSA, GFR, haematocrit and sex.

Keywords: PBPK; epirubicin; pharmacokinetics; drug exposure

Citation: Ansaar, R.; Meech, R.; Rowland, A. A Physiologically Based Pharmacokinetic Model to Predict Determinants of Variability in Epirubicin Exposure and Tissue Distribution. *Pharmaceutics* **2023**, *15*, 1222. https://doi.org/10.3390/pharmaceutics15041222

Academic Editor: David R. Taft

Received: 23 December 2022
Revised: 21 March 2023
Accepted: 29 March 2023
Published: 12 April 2023

1. Introduction

Epirubicin is member of the anthracycline class of antineoplastic drugs. Anthracyclines are among the most broadly effective classes of antineoplastic drugs, and epirubicin is among the most clinically important drugs in this class. Epirubicin is primarily used in combination therapies for the treatment of breast, gastric, lung and ovarian cancers and lymphomas [1]. Epirubicin has emerged as the preferred agent in this class due to the favourable cardiotoxicity profile and similar anti-tumour activity compared to other anthracyclines [1,2].

Epirubicin is administered intravenously (IV) over 3 to 5 min once every 21 days with dosing based on body surface area (BSA; mg/m^2). Despite accounting for BSA, marked inter-subject variability in circulating epirubicin plasma concentration has been reported. Eksborg [3] reported 10-fold between-subject variability in the area under the plasma concentration time curve (AUC) for epirubicin despite normalising for dose and BSA. As with most antineoplastic drugs, epirubicin has a narrow therapeutic window whereby small differences in exposure can result in marked differences in treatment efficacy and tolerability [4]. These factors underpin the value of better understanding the physiological and

environmental covariates influencing epirubicin exposure, particularly those that can direct a more appropriate initial dose selection. Current initial dose selection for epirubicin based on BSA alone routinely overestimates dose requirement [5] necessitating dose reductions in subsequent cycles due to cardiac and haematologic toxicities [6]. Dose reductions and interruptions are most commonly due to reductions in neutrophil and platelet count [7]. Grade 3–4 neutropenia occurs in 8.4–54.2% of patients receiving epirubicin and cyclophosphamide (EC) (90/600 mg/m^2) treatment; thus, haematological toxicity is monitored and dose reductions are implemented between cycles on a case-by-case basis [8]. Therapeutic drug monitoring (TDM) may be utilised to guide epirubicin dosing, provided an exposure profile has been developed and a known target therapeutic window is established. Development of PK/PD models can be successfully deployed to inform TDM; however, the infrequent dosing schedule of epirubicin and relatively short terminal half-life (18–45 h) limit practicality in this setting [9,10]. Additionally, while TDM is appropriate to guide on-treatment dose adjustments for antineoplastic drugs [11,12], it does not support optimal initial (cycle 1) dose selection.

Recently, complementary precision dosing approaches that utilized model-informed initial dose selection (MIDS) have been proposed to support optimal initial dose selection [13–15] and supplement on-treatment dose modification strategies such as TDM and toxicity-guided dosing [16]. Two approaches may be applied to support MIDS: a top-down approach known as population pharmacokinetic (popPK) modelling, and a bottom-up approach known as a physiologically based pharmacokinetic (PBPK) modelling. With popPK modelling, non-linear mixed-effect models are used to describe variability in observed pharmacokinetic (PK) behaviour within a population based on covariates known to influence exposure; this approach may be used to predict future exposure by fitting limited a priori data. In PBPK modelling, physiological data for a population are combined with physiochemical and in vitro data for a drug under specific trial conditions to simulate exposure in a virtual population [17,18]. Simulated data may be compared to observed data from a matched population to define the performance of the PBPK model. Population PK models for epirubicin have been applied to describe the relation between epirubicin exposure and the incidence of haematologic toxicity [19], and to associate routinely collected demographic characteristics with epirubicin exposure [5,20].

The development of a PBPK model for epirubicin provides the capacity to (i) define the impact of additional molecular and physiological characteristics that are not routinely collected on epirubicin exposure, (ii) simulate exposure in populations that have not been studied in clinical trials (e.g., different races, age groups, etc.), and (iii) define the likely impact of pharmacogenetic variability on epirubicin exposure. Epirubicin is predominantly cleared by the liver, with renal elimination accounting for 20 to 25% of the dose. The reported primary enzyme involved in the hepatic clearance of epirubicin is UDP-glucuronosyltransferase (UGT) 2B7 [21]. In this regard, reduced UGT2B7 protein expression and/or activity caused by single nucleotide polymorphisms (SNPs) in the *UGT2B7* gene has been associated with increased epirubicin exposure and reduced metabolic clearance [21]. The most notable example of pharmacogenomic-guided epirubicin dosing involved the *UGT2B7 -161C>T* SNP. This SNP has been associated with a reduction in epirubicin clearance and increased AUC [22,23]; importantly, this SNP has also been demonstrated to predict grade $\frac{3}{4}$ leucopenia in early breast cancer patients treated with adjuvant or neoadjuvant FEC100 (5-fluorouracil 500 mg/m^2, Epirubicin 100 mg/m^2 and cyclophosphamide 500 mg/m^2).

The primary objective of this study was to identify physiological and molecular characteristics driving variability in epirubicin AUC using PBPK modelling. Identification of these characteristics informs analyses of 'exposure biomarkers' for epirubicin that can be evaluated using routinely collected samples from randomised controlled trials and can facilitate non-invasive optimal initial dose selection for this drug [24,25]. The second objective of this study was to define the association between epirubicin plasma concentration

and tissue concentrations, with a focus on tissues relevant to either the therapeutic efficacy (adipose/breast tissue), or the incidence of toxicity (cardiac, hepatic) for this drug.

2. Materials and Methods

2.1. Materials and Chemical Information

Epirubicin (hydrochloride) was purchased from Cayman Chemical (Ann Arbor, MI, USA). UDP-glucuronic acid (UDPGA; trisodium salt) was purchased from Sigma-Aldrich (St Louis, MO, USA). Fluconazole was obtained from Pfizer Australia (Sydney, NSW, Australia). Alamethicin (from *Trichoderma viridae*) was purchased from AG Scientific (San Diego, CA, USA). Solvents and other reagents used were of analytical reagent grade or higher.

2.2. Human Liver Microsomes

Pooled human liver microsomes (HLMs) were prepared by mixing equal amounts of protein from five human livers (H7, 44-year-old female; H10, 67-year-old female; H12, 66-year-old male; H29, 45-year-old male; and H40, 54-year-old female), obtained from the human liver bank of the Department of Clinical Pharmacology of Flinders University. Approval for the use of human liver tissue in xenobiotic metabolism studies was obtained from the Flinders Clinical Research Ethics Committee. HLMs were prepared by differential centrifugation, as described by Bowalgaha et al. [26]. Microsomes were activated by pre-incubating on ice for 30 min in the presence of alamethicin (50 µg/mg microsomal protein) prior to inclusion in the incubation matrix [27].

2.3. Epirubicin Glucuronidation Assay

Assay conditions for epirubicin glucuronidation by HLMs were optimised for protein concentration, incubation time and epirubicin concentration range [28,29]. Incubations in a total volume of 200 µL contained $MgCl_2$ (4 mM), potassium phosphate (0.1 M; pH 7.4), epirubicin (in DMSO 2% *v*/*v*), activated HLMs (0.01 mg), and UDPGA (5 mM). A 5 min pre-incubation at 37 °C was performed to thermodynamically equilibrate the mixture; reactions were initiated by the addition of UDPGA. Reactions to form epirubicin glucuronide were performed over 120 min at 37 °C in a shaking water bath and were terminated by the addition of 400 µL of ice-cold methanol containing 0.1% formic acid. The reaction mix was centrifuged at 4000× *g* for 10 min at 10 °C and a 300 µL aliquot of the supernatant fraction was transferred into LC-MS vials. Microsomal incubations were performed in the presence of fluconazole (10–2500 µM) to define the contribution of microsomal UGT2B7 to epirubicin glucuronidation by HLMs.

2.4. Quantification of Epirubicin Glucuronide Formation

Epirubicin glucuronide formation was quantified by liquid chromatography mass spectrometry (LC-MS) performed on an Agilent 1290 infinity liquid chromatography (LC) system coupled to an Agilent 6495B triple-quadrupole mass spectrometer (MS; Agilent Technologies, Santa Clara, CA, USA) fitted with a Zorbax Eclipse Plus C18 analytical column (1.8 µM, 2.1 mm × 50 mm; Agilent, Santa Clara, CA, USA). Epirubicin glucuronide was separated from the incubation matrix by using a mobile phase comprising 28% acetonitrile and 0.1% formic acid in water at a flow rate of 0.2 mL/min. Control incubations in the absence of the cofactor (UDPGA), substrate (epirubicin), and microsomal protein were analysed in parallel to incubation samples to confirm correct product detection.

The MS source parameters were as follows: sheath gas flow rate of 11 L/min, gas flow rate of 14 L/min, gas temperature of 200 °C, nebulizer pressure of 35 psi and capillary voltage of 1500 V. Multiple reaction monitoring (MRM) was used to monitor the precursor transition ion at 720.22 m/z, with the optimised conditions around the product ions listed in Table 1. Epirubicin glucuronide was eluted at a retention time of 1.6 min.

Table 1. Multiple Reaction Monitoring (MRM) scan parameters for the optimised epirubicin glucuronide ions.

Precursor Ion (m/z)	Product Ion (m/z)	Dwell (s)	Fragmentor (V)	Collision Energy (V)	Cell Acceleration (V)	Polarity
720.22	702.2	200	380	15	4	Positive
720.22	361.2	200	380	36	4	Positive
720.22	324.2	200	380	20	4	Positive
720.22	306	200	380	16	4	Positive

2.5. *Data Analysis (In Vitro Kinetics)*

The kinetics of microsomal epirubicin glucuronidation (Michaelis constant, Km and maximal reaction velocity, Vmax) were determined by fitting experimental data using the Michaelis–Menten equation in GraphPad Prism 9.3.1 (San Diego, CA, USA). Fluconazole inhibition of microsomal epirubicin glucuronidation was determined by fitting experimental data to the competitive inhibition model using GraphPad Prism 9.3.1 (San Diego, CA, USA). In vitro kinetic data (Km and Vmax) generated in these microsomal incubations were used as input parameters in the PBPK model to describe epirubicin clearance by UGT2B7.

2.6. *Development and Verification of Epirubicin PBPK Model*

2.6.1. Structural Model

A full-body PBPK model to simulate the concentration time profile for epirubicin following a single IV dose infused over 3 min was developed using Simcyp® version 19.1 (Certara, Sheffield, UK). The differential equations utilised by Simcyp to construct the PBPK model from physiochemical and in-vitro data have been described previously by [30].

2.6.2. Development of Epirubicin Compound Profile

The physiochemical, blood binding, distribution and elimination parameters for epirubicin, along with parameters defining induction of UGT2B7 by epirubicin are summarized in Table 2. Physiochemical parameters were based on published literature values [31], unless specified blood binding and distribution parameters were predicted by the model based on the physiochemical parameters of the drug using in-built functions within the Simcyp simulator. Microsomal clearance data (assigned to UGT2B7 based on fluconazole inhibition) were based on in vitro incubations (see Methods section). Renal clearance (CL_R) was calculated based on published clearance values [6]. Induction parameters for UGT2B7 were defined based on LC-MS proteomic data using HepG2 cells generated in this laboratory.

2.6.3. Population Profile

The epirubicin compound profile was built and verified using the Sim-Cancer population profile. The Sim-Cancer population profile was also used in simulations to characterise the association between epirubicin plasma and tissue concentrations, and to characterise the physiological and molecular parameters associated with variability in epirubicin exposure.

2.6.4. Simulated Trial Design

For development of the epirubicin profile, simulations comprised 90 subjects divided across 10 trials with 9 subjects in each trial. During verification of the epirubicin compound profile, simulations were performed in 10 trials comprising age-, sex-, and ethnicity-matched subjects according to the protocol for the observed trial (dosing regimen and number of subjects) described in the following section. Parameters describing epirubicin exposure were assessed over 24 h following a single dose at 9:00 a.m. on day 1.

Table 2. Compound profile for epirubicin based on the physiochemical properties detailed.

Phys Chem	
Molecular Weight (g/mol)	543.52
log Po:w	1.41
Species	Diprotic Base
pKa (Strongest Acidic)	8.010
pKa 2 (Strongest Basic)	10.030
Blood Binding	
B/P	0.729
f_u	0.23
Distribution (full PB-PK model)	
Vss (L/Kg)	25.265
Prediction Method	Rogers and Rowland [32]
Kp Scalar	25
Elimination	
HLM—UGT2B7 (Km; µM)	26.2
HLM—UGT2B7 (Vmax; pmol/min/mg protein)	2897
HLM—UGT2B7 (fu)	1
Additional clearance—CL_R (L/h)	9.0
Interaction	
UGT2B7 (IndC50; µM)	0.368
UGT2B7 (Indmax)	13.95

Po:w, neutral species octanol: water partition coefficient; B/P, blood-to-plasma partition ratio; fu, fraction unbound; Vss, steady state volume of distribution; Kp scalar: scalar applied to all predicted tissue partition values; CLR, renal clearance; IndC50, inducer concentration to achieve half-maximal induction; IndMax, maximal fold induction. Notes: Prediction of tissue distribution based on the model of Rogers and Rowland.

2.6.5. Observed Clinical Data and Compound File Verification

Observed epirubicin pharmacokinetics were obtained from values reported in the literature by Robert, Vrignaud [33]. Sixteen metastatic breast carcinoma patients were subjected to a phase III comparative randomised protocol to assess the pharmacokinetics of epirubicin and doxorubicin. The epirubicin group received a combinatorial treatment of epirubicin (50 mg/m^2), 5-FU (500 mg/m^2), and cyclophosphamide (500 mg/m^2). The initial dose of epirubicin was used to study pharmacokinetics. Epirubicin was administered first, followed by administration of the remaining chemotherapies after 1–2 h. Therefore, additional treatment could impact epirubicin pharmacokinetics. Plasma samples were obtained after 5, 10, 20, and 40 min, and after 1, 2, 4, 8, 24, 32, and 48 h for HPLC analysis of the unchanged drug and metabolites. Raw data obtained from this trial were reproduced and plotted for evaluation of the simulated epirubicin compound file.

The epirubicin compound file was further verified by evaluating the impact of UGT2B7 inhibition, which was achieved by simulating the effect of fluconazole coadministration, and by evaluating the impact of renal function (evaluated as glomerular filtration rate; GFR).

2.7. Population Characteristics Associated with Variability in Epirubicin Exposure

The verified epirubicin profile was used to evaluate associations between physiological and molecular characteristics of the Sim-Cancer population and the logarithmically transformed epirubicin AUC (LnAUC). Ten trials from the Sim-Cancer population, each comprising 200 subjects, were simulated over 158 h, with a single 120 mg/m^2 epirubicin dosed IV in a fasted state.

Univariate (simple) linear regression was performed using GraphPad Prism 9.3.1 (San Diego, CA, USA). Stepwise multivariate linear regression analysis was performed using IBM® SPSS® Statistics 26 (New York, NY, USA). Linear regression was used to evaluate associations between the physiological and molecular characteristics identified in Supplemental Table S1 and epirubicin LnAUC. Continuous variables were evaluated for normality and non-linearity of association; binary characteristics (sex) were coded as nominal variables. A multivariable linear regression model was developed by stepwise forward inclusion of significant characteristics identified in the univariable regression analysis based

on improvement in model R^2. Back transformation of the model-predicted logarithmically transformed AUC was performed to plot correlations between the simulated and model-predicted AUC.

3. Results

3.1. Characterisation of In Vitro Epirubicin Glucuronidation

Epirubicin glucuronide formation by HLM was best described by a single-enzyme Michaelis–Menten equation (Figure 1A). The kinetic parameters derived for epirubicin glucuronidation were a K_m of 26.2 ± 5.48 µM and V_{max} of 2896.6 ± 212.8 AU. The selective UGT2B7 inhibitor fluconazole was included in incubations (final concentration 100 to 2500 µM) to confirm the involvement of UGT2B7 in human liver microsomal epirubicin glucuronidation. The IC_{50} for fluconazole inhibition of epirubicin glucuronidation by HLMs was 770.7 ± 158.1 µM, with a maximal observed inhibition of 75% (Figure 1B). These data support UGT2B7 as the major enzyme involved in human liver microsomal epirubicin glucuronidation.

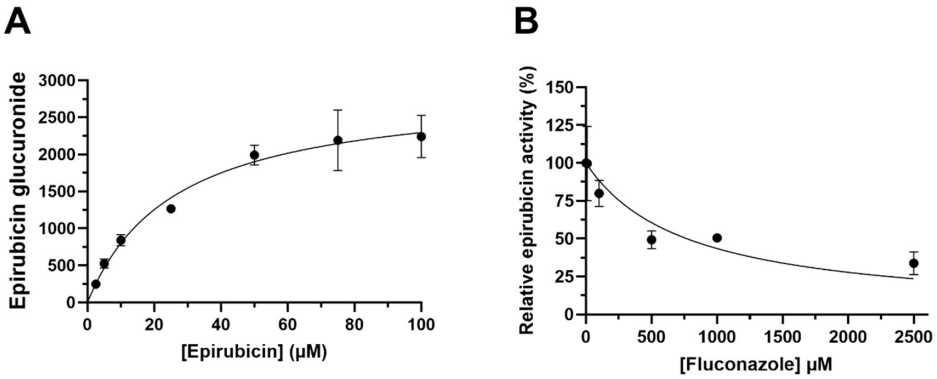

Figure 1. (**A**) Michaelis–Menten Kinetics of epirubicin by formation of epirubicin glucuronide in HLMs (R^2 = 0.96). Pooled HLMs (2 mg/mL) were incubated for 2 h with incremental amounts of epirubicin (between 2.5–100 µM) and epirubicin glucuronide was detected in the absence of standards. (**B**) Normalised activity of epirubicin by inhibition of epirubicin glucuronide formation in HLMs. HLMs were incubated for 2 h with 25 µM epirubicin and increasing amounts of fluconazole (between 10–2500 µM). Epirubicin glucuronide was detected, and response was measured relative to the control in the absence of fluconazole. Mean peak area response ± S.D. is measured in arbitrary units. Data were generated in duplicate with standard deviation displayed by error bars.

3.2. Verification of the Epirubicin PBPK Model

The accuracy of the epirubicin compound profile was assessed using an age-, sex-, and race-matched single-dose trial [34]. Ten simulated trials were performed with epirubicin administered IV at a dose of 50 mg/m^2 in trials comprising 9 female subjects aged between 20 and 50 years. Epirubicin plasma concentration, monitored over 48 h, was used to define the simulated epirubicin maximal concentration C_{max} and AUC. The mean (±SD) simulated AUC and C_{max} in the validation cohort were 1324 ± 20.0 ng/mL·h and 434 ± 42.6 ng/mL, respectively; these values are 1.1- and 1.6-fold higher than the respective measured parameters. The simulated mean (95% confidence interval; CI) and mean observed plasma concentration time profiles are shown in Figure 2. In all cases, the mean simulated epirubicin plasma concentration at each measured time point was within 1.6-fold of the respective observed plasma concentration.

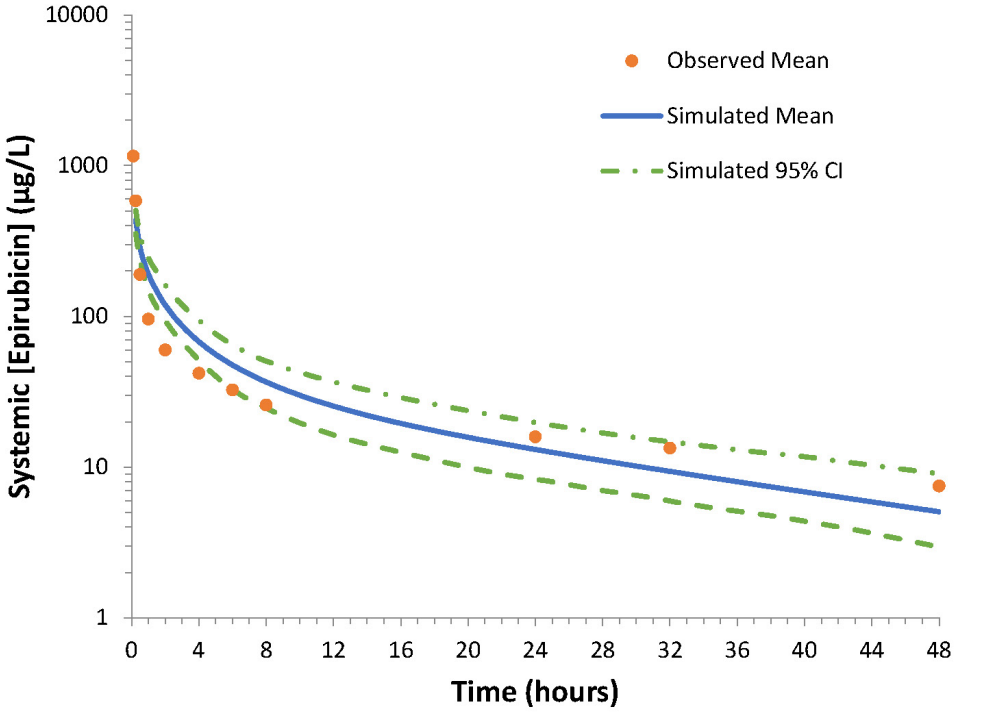

Figure 2. Representative overlay showing the simulated and observed epirubicin plasma concentration time curves over 48 h following a single oral dose (50 mg/m^2). The solid blue line represents the mean simulated epirubicin plasma concentration, the dotted green lines represent the 95% confidence interval (CI) for the simulated data and the orange dots represent the mean observed data [34]. No data regarding variability in observed data was reported in the original publication.

Consistent with the reported importance of UGT2B7 in epirubicin metabolism in vivo, coadministration of steady-state fluconazole (200 mg daily for 7 days) resulted in a 54% increase in the single-dose epirubicin AUC. Notably, as an intravenously administered drug, the C_{max} for epirubicin was only modestly impacted (increased by 5%).

3.3. Epirubicin Exposure in Oncology Cohort

The mean, standard deviation (SD) and range of epirubicin AUC and C_{max} values describing exposure to epirubicin in a cohort of 200 oncology patients are reported in Table 3. Marked variability in epirubicin AUC and C_{max} was observed; by way of example, AUC values ranged from 2980 to 12,710 ng/mL·h (mean 5374 ng/mL·h). Simulated epirubicin AUC and C_{max} values, and the variability in these parameters, were consistent with observed exposure profiles [3].

Table 3. Descriptive statistics showing the mean, variance and range of epirubicin exposure in the simulated oncology cohort.

Statistic	AUC (ng/mL·h)	CMax (ng/mL)	Dose (mg)	CL (Dose/AUC) (L/h)
Mean	5374	12,683	213.2	41.6
Median	5197	12,653	212.1	40.5
Geometric Mean	5252	12,654	211.8	40.3
90% confidence interval (lower limit)	5211	12,622	211.0	40.0
90% confidence interval (upper limit)	5293	12,686	212.7	40.7
5th centile	3776	11,296	176.4	26.7
95th centile	7537	14,142	253.7	59.8
Skewness	0.99	0.12	0.29	0.50
cv	0.22	0.07	0.11	0.24
Min Val	2980	9678	149.8	14.8
Max Val	12,710	15,469	302.5	80.9
Fold	4.27	1.60	2.02	5.45
Std Dev	1191	864	24.1	10.2

3.4. Epirubicin Clearance Pathways

The mean contribution of renal elimination, defined by the fraction of epirubicin excreted unchanged in the urine (F_e), was 20.95%. The mean contributions of hepatic and renal UGT2B7 to total epirubicin clearance were 75.3% and 4.3%, respectively (Figure 3).

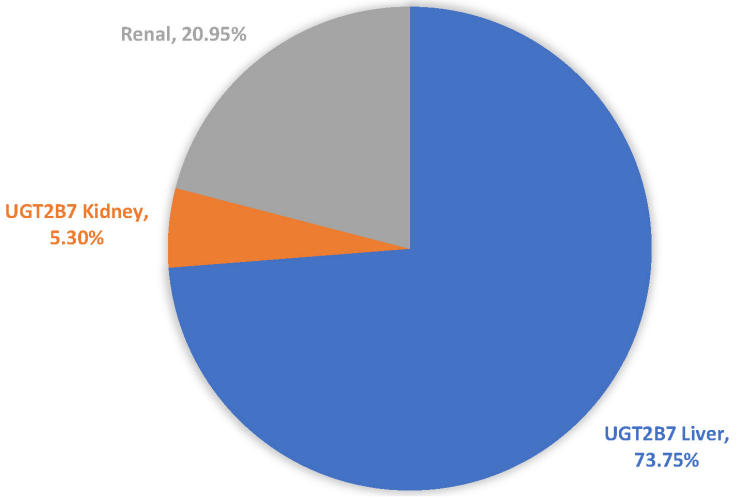

Figure 3. A representative pie-chart showing the relative contribution (geometric mean %) of the f_m (hepatic and renal epirubicin) and the f_e unchanged by renal clearance.

3.5. Determination of Population Characteristics Affecting Epirubicin Clearance

The results of univariate linear regression analyses considering the association between molecular and physiological characteristics and epirubicin LnAUC are presented in Supplemental Table S1. Multivariable linear regression modelling by stepwise inclusion of parameters described in Supplemental Table S1 identified hepatic UGT2B7 abundance, albumin concentration, age, renal UGT2B7 abundance, body surface area (BSA), glomerular filtration rate (GFR), haematocrit, and sex as the key covariates associated with variability in epirubicin LnAUC. By accounting for these factors, it was possible to explain 87% of the

variability in epirubicin LnAUC within the oncology population (Figure 4, Tables 4 and 5). The single most important covariate associated with variability in epirubicin LnAUC was hepatic UGT2B7 abundance; accounting for this covariate alone explained 56% of the variability in epirubicin LnAUC. Furthermore, exclusion of body surface area in the model led to a minor decrease in predicted variability to 83% (Supplemental Table S3).

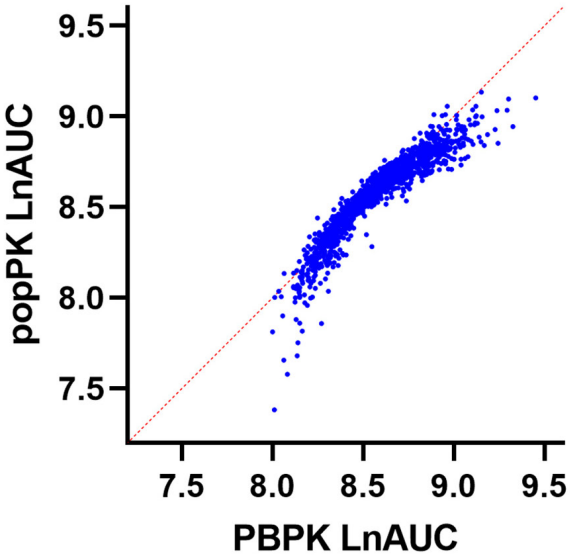

Figure 4. Multivariate linear regression analysis showing the correlated relationship between the simulated popPK natural log-transformed AUC (LnAUC) and simulated PBPK LnAUC.

Table 4. Multivariate linear regression analysis of the model-predicted variables affecting epirubicin LnAUC and their respective linearity regarding LnAUC. R^2 of the model is 0.8690.

Variable	Estimated Ln AUC (ng/mL·h)	Standard Error	Range (95% CI)	R^2 with Other Variables	*p* Value
Intercept (constant)	8.211	0.02994	8.152 to 8.269		<0.0001
Sex	−0.03709	0.003901	−0.04474 to −0.02944	0.2216	<0.0001
Age	0.00251	0.000174	0.002169 to 0.002850	0.5024	<0.0001
BSA	0.2669	0.01132	0.2447 to 0.2891	0.4266	<0.0001
Haematocrit	−0.00538	0.000373	−0.006110 to −0.004649	0.005414	<0.0001
Albumin	0.0111	0.000251	0.01060 to 0.01159	0.01572	<0.0001
GFR	−0.00178	0.000106	−0.001983 to −0.001568	0.5261	<0.0001
Liver UGT2B7	-9.77×10^{-8}	1.34×10^{-9}	-1.00×10^{-7} to -9.51×10^{-8}	0.2798	<0.0001
Kidney UGT2B7	-3.24×10^{-7}	1.07×10^{-8}	-3.45×10^{-7} to -3.03×10^{-7}	0.03006	<0.0001

Model variables; sex 0 = Female, 1 = Male, age (years), body surface area (BSA) (m^2), haematocrit (%), albumin (g/L), glomerular filtration rate (GFR) (mL/min/1.73 m^2), liver UGT2B7 (pmol), kidney UGT2B7 (pmol).

Table 5. Stepwise multivariate linear regression analysis of predictors of epirubicin LnAUC by sequential addition according to best fit. Cumulative R^2 of the final model (h) incorporating all predictors = 0.8690.

Model	R	R^2	Adjusted R^2	Std. Error of the Estimate	R^2 Change
a	0.749 [a]	0.561	0.561	0.141	0.561
b	0.821 [b]	0.674	0.674	0.121	0.113
c	0.861 [c]	0.741	0.740	0.108	0.067
d	0.886 [d]	0.785	0.784	0.099	0.044
e	0.911 [e]	0.830	0.830	0.087	0.046
f	0.922 [f]	0.849	0.849	0.082	0.019
g	0.929 [g]	0.863	0.863	0.079	0.014
h	0.932 [h]	0.869	0.868	0.077	0.006

Model predictors; [(a)] LiverUGT2B7; [(b)] LiverUGT2B7, Albumin; [(c)] LiverUGT2B7, Albumin, Age; [(d)] LiverUGT2B7, Albumin, Age, KidneyUGT2B7; [(e)] LiverUGT2B7, Albumin, Age, KidneyUGT2B7, BSA; [(f)] LiverUGT2B7, Albumin, Age, KidneyUGT2B7, BSA, GFR; [(g)] LiverUGT2B7, Albumin, Age, KidneyUGT2B7, BSA, GFR, Haematocrit; [(h)] LiverUGT2B7, Albumin, Age, KidneyUGT2B7, BSA, GFR, Haematocrit, Sex.

3.6. Associations between Epirubicin Plasma and Tissue Concentration

The concordance between simulated epirubicin plasma and individual tissue concentrations are shown in Figure 5. Except for epirubicin concentration in the brain (R^2 = 0.56), there was limited concordance between epirubicin tissue and plasma concentrations (R^2 < 0.22). Notably, while the highest mean tissue AUC was observed in skeletal muscle (169,241 ng/mL·h), the comparatively slow distribution into this tissue resulted in a markedly lower C_{max} compared to other tissues. Indeed, despite comparable AUCs, the mean epirubicin C_{max} in cardiac tissue (31,952 ng/mL) was >10-fold higher than the epirubicin Cmax in skeletal muscle (2868 ng/mL) (Table 6).

Table 6. PBPK-predicted epirubicin mean Cmax (ng/mL) and mean AUC (ng/mL·h) in tissue and plasma over 168 h after IV injection in a Sim-Cancer population.

Tissue	Mean Cmax (ng/mL)	Mean AUC (ng/mL·h)
Plasma	979	4530
Muscle	2868	169,241
Heart	31,952	144,482
Brain	22,410	147,660
Adipose	1049	18,680
Liver	13,973	92,446

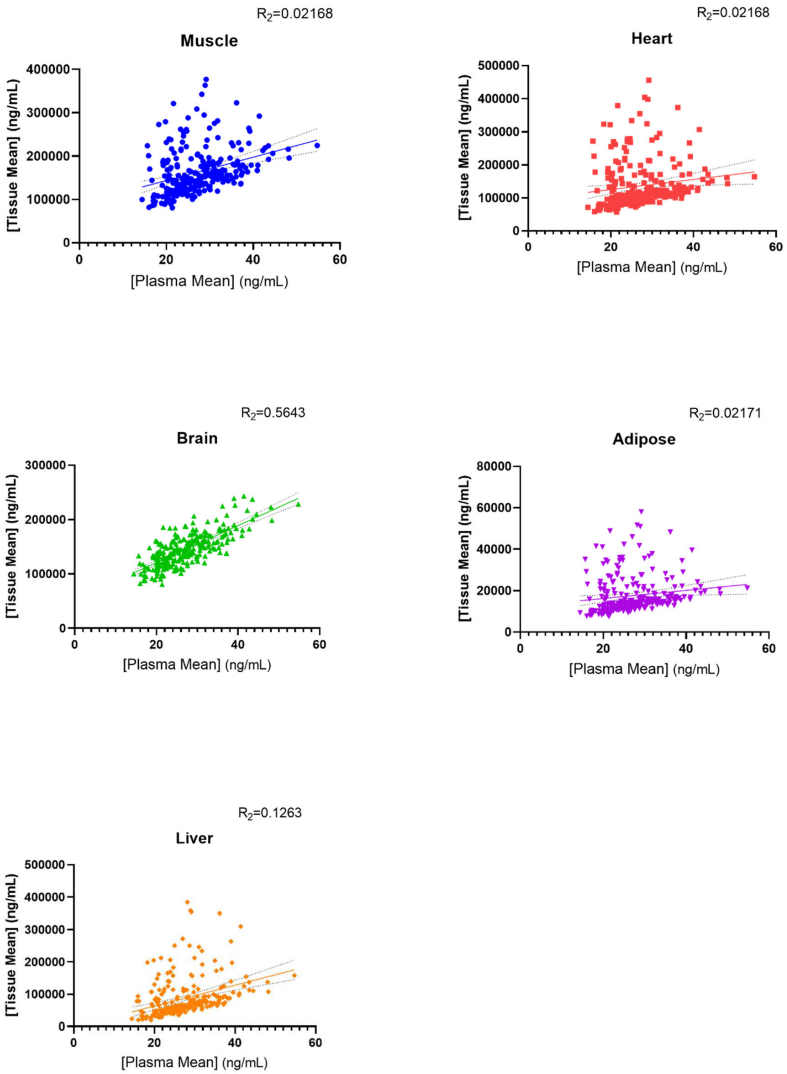

Figure 5. Linear regression analysis evaluating the relationship between simulated maximum epirubicin tissue and plasma concentrations in a Sim-Cancer cohort following a single 50 mg/m^2 dose.

4. Discussion

The present study describes the development and evaluation of a full-body PBPK model to assess systemic and individual organ exposure to epirubicin. Multi-variable linear regression modelling demonstrated that variability in simulated systemic epirubicin exposure following intravenous injection was primarily driven by differences in hepatic and renal UGT2B7 expression, plasma albumin concentration, age, BSA, GFR, haematocrit

and sex. By accounting for these factors, it was possible to explain 87% of the variability in epirubicin in a simulated cohort of 2000 oncology patients aged between 20 and 95 years. The single most important factor in defining simulated systemic epirubicin exposure was hepatic UGT2B7 expression, which alone accounted for 56% of variability in exposure within the simulated cohort.

Current dosing guidelines for epirubicin account for age, BSA, renal function and sex. Typically, epirubicin doses are reduced in patients with a serum creatinine > 5 mg/dL. Epirubicin is quite well tolerated in patients with chronic renal failure undergoing haemodialysis [35]. Dose reductions in elderly patients are also well tolerated [36]. Data regarding the value of BSA-guided epirubicin dosing are contentious, with multiple studies suggesting that BSA-guided dosing is of limited value [5,37]. In accordance with this, the data presented suggest that incorporating BSA-based dosing into the model only contributes to 4% of exposure variability. This highlights the importance of understanding other contributing variables in epirubicin dosage. Sexual dimorphism around DME expression could perhaps be driven by hormonal differences [38] and may influence epirubicin metabolism; however, further understanding of this is required. Reassuringly, the major factors currently accounted for when guiding epirubicin dosing are consistent with the physiological parameters identified in the multiple linear regression modelling performed in the current study and with prior non-linear mixed-effects modelling (NONMEM) analyses involving epirubicin. Wade, Kelman [4] demonstrated that by accounting for differences in sex and age it was possible to reduce unexplained variability in epirubicin clearance from 50 to 42%. Consistent with the major importance of UGT2B7 expression in defining epirubicin exposure, prior analyses have consistently demonstrated that a large proportion of the variability in epirubicin exposure cannot be accounted for based on routinely collected physiological parameters including age, sex, BSA and renal function. Currently, there is no reliable biomarker to define hepatic UGT2B7 expression in individual patients, and assessment of UGT2B7 genotype is of limited value [25]. However, in recent years liver-derived extracellular vesicles (EVs) have emerged as a potential universal ADME biomarker [39–44]. It is plausible that quantification of UGT2B7 expression in EVs may serve as a robust approach to estimate hepatic UGT2B7 expression in individual patients, thereby supporting dose individualisation for drugs such as epirubicin.

PBPK modelling and simulation is an established tool to support drug discovery and development and is a core element of the regulatory approval process in many jurisdictions [18]. Recent studies have further demonstrated the potential role of PBPK in predicting covariates affecting variability in drug exposure resulting from differences in patient characteristics [14,15,45], giving rise to the intriguing potential for this platform to support model-informed precision dosing [46,47]. This model provides an important foundation for establishing a PK/PD relationship for epirubicin; however, further work on population-based dose predictive modelling is imperative to inform optimal therapeutic windows for individualized dosage. The major limitation of the current study is the lack of observed clinical data to support the validation of the regression models. Currently, these models are based on a mechanistic systems pharmacology understanding and would require confirmation with in vivo clinical data to warrant implementation. A second limitation of the current study is the lack of observed tissue concentration measurements to support the lack of concordance between plasma concentration and tissue concentrations. While the overall simulated volume of distribution (25.265 L/kg) for epirubicin is consistent with reported in vivo data [6], the specific tissue distribution for this drug in vivo has not been reported.

Simulated epirubicin clearance was consistent with clinical observations of epirubicin plasma clearance as studied by Robert [34]. Notably, there was limited concordance between systemic epirubicin exposure and the exposure of individual organs to epirubicin. Except for epirubicin concentration in the brain ($R^2 = 0.56$), there was limited concordance between tissue and systemic (plasma) epirubicin concentrations ($R^2 < 0.22$). The highest mean tissue AUC was observed in skeletal muscle (169,241 ng/mL·h); however, the com-

paratively slow distribution into this tissue resulted in a markedly lower C_{max} compared to other tissues. Indeed, despite comparable AUCs, the mean epirubicin C_{max} in cardiac tissue (31,952 ng/mL) was >10-fold higher than the epirubicin C_{max} in skeletal muscle (2868 ng/mL). The extensive distribution of epirubicin into cardiac tissue is consistent with the well-established cardiac toxicity profile for this drug [10,48]. The limited concordance between plasma and cardiac epirubicin concentrations (r^2 = 0.2188) indicates that evaluation of plasma epirubicin concentration is unlikely to be useful in identifying patients at greatest risk of suffering cardiac toxicity when administered epirubicin.

Supplementary Materials: The following supporting information can be downloaded at: https://www.mdpi.com/article/10.3390/pharmaceutics15041222/s1, Table S1: The mean values and range of all physiological characteristics used in the simple linear regression analysis model. Two thousand Sim-Cancer patients were generated in this study. Table S2: Mean and range of enzymatic expression of UGTs incorporated into the model. Table S3: Multivariate linear regression analysis of the model-predicted variables affecting epirubicin LnAUC and their respective linearity regarding LnAUC with the exclusion of BSA. R^2 of the model is 0.8324.

Author Contributions: Conceptualization, R.M. and A.R.; methodology, A.R.; software, A.R.; validation, R.A. and A.R.; formal analysis, R.A. and A.R.; writing—original draft preparation, A.R.; writing—review and editing, R.A. and R.M. All authors have read and agreed to the published version of the manuscript.

Funding: AR is supported by a Research Fellowship from Cancer Council SA (MCRF).

Institutional Review Board Statement: Approval for the use of human liver tissue in xenobiotic metabolism studies was obtained from the Flinders Clinical Research Ethics Committee (059-056).

Informed Consent Statement: Consent was obtained from the donors next of kin.

Data Availability Statement: Data supporting the findings of this study are available from the corresponding author upon reasonable request.

Conflicts of Interest: R.A. and R.M. declare no conflict of interest. A.R. has received unrelated research support from Pfizer Inc., AstraZeneca and Boehringer Ingelheim.

References

1. Tariq, M.; Alam, M.A.; Singh, A.T.; Panda, A.K.; Talegaonkar, S. Improved oral efficacy of epirubicin through polymeric nanoparticles: Pharmacodynamic and toxicological investigations. *Drug Deliv.* **2016**, *23*, 2990–2997. [CrossRef]
2. Forrest, R.A.; Swift, L.P.; Evison, B.J.; Rephaeli, A.; Nudelman, A.; Phillips, D.R.; Cutts, S.M. The hydroxyl epimer of doxorubicin controls the rate of formation of cytotoxic anthracycline-DNA adducts. *Cancer Chemother. Pharmacol.* **2013**, *71*, 809–816. [CrossRef] [PubMed]
3. Eksborg, S. Pharmacokinetics of anthracyclines. *Acta Oncol.* **1989**, *28*, 873–876. [CrossRef] [PubMed]
4. Wade, J.R.; Kelman, A.W.; Kerr, D.J.; Robert, J.; Whiting, B. Variability in the pharmacokinetics of epirubicin: A population analysis. *Cancer Chemother. Pharmacol.* **1992**, *29*, 391–395. [CrossRef]
5. Gurney, H.P.; Ackland, S.; Gebski, V.; Farrell, G. Factors affecting epirubicin pharmacokinetics and toxicity: Evidence against using body-surface area for dose calculation. *J. Clin. Oncol. Off. J. Am. Soc. Clin. Oncol.* **1998**, *16*, 2299–2304. [CrossRef] [PubMed]
6. Robert, J.E. Clinical pharmacology and dose-effect relationship. *Drugs* **1993**, *45* (Suppl. S2), 20–30. [CrossRef] [PubMed]
7. Drooger, J.C.; van Pelt-Sprangers, J.M.; Leunis, C.; Jager, A.; de Jongh, F.E. Neutrophil-guided dosing of anthracycline-cyclophosphamide-containing chemotherapy in patients with breast cancer: A feasibility study. *Med. Oncol.* **2015**, *32*, 113. [CrossRef]
8. Liu, D.; Wu, J.; Lin, C.; Ding, S.; Lu, S.; Fang, Y.; Huang, J.; Hong, J.; Gao, W.; Zhu, S.; et al. The Comparative Safety of Epirubicin and Cyclophosphamide versus Docetaxel and Cyclophosphamide in Lymph Node-Negative, HR-Positive, HER2-Negative Breast Cancer (ELEGANT): A Randomized Trial. *Cancers* **2022**, *14*, 3221. [CrossRef]
9. Kang, J.S.; Lee, M.H. Overview of therapeutic drug monitoring. *Korean J. Intern. Med.* **2009**, *24*, 1–10. [CrossRef]
10. Ormrod, D.; Holm, K.; Goa, K.; Spencer, C. Epirubicin: A review of its efficacy as adjuvant therapy and in the treatment of metastatic disease in breast cancer. *Drugs Aging* **1999**, *15*, 389–416. [CrossRef]
11. Mueller-Schoell, A.; Groenland, S.L.; Scherf-Clavel, O.; van Dyk, M.; Huisinga, W.; Michelet, R.; Jaehde, U.; Steeghs, N.; Huitema, A.D.; Kloft, C. Therapeutic drug monitoring of oral targeted antineoplastic drugs. *Eur. J. Clin. Pharmacol.* **2021**, *77*, 441–464. [CrossRef] [PubMed]

12. Fahmy, A.; Hopkins, A.M.; Sorich, M.J.; Rowland, A. Evaluating the utility of therapeutic drug monitoring in the clinical use of small molecule kinase inhibitors: A review of the literature. *Expert Opin. Drug Metab. Toxicol.* **2021**, *17*, 803–821. [CrossRef] [PubMed]
13. Wills, K.H.; Behan, S.J.; Nance, M.J.; Dawson, J.L.; Polasek, T.M.; Hopkins, A.M.; van Dyk, M.; Rowland, A. Combining therapeutic drug monitoring and pharmacokinetic modelling deconvolutes physiological and environmental sources of variability in clozapine exposure. *Pharmaceutics* **2022**, *14*, 47. [CrossRef] [PubMed]
14. Rowland, A.; Van Dyk, M.; Hopkins, A.M.; Mounzer, R.; Polasek, T.M.; Rostami-Hodjegan, A.; Sorich, M.J. Physiologically Based Pharmacokinetic Modeling to Identify Physiological and Molecular Characteristics Driving Variability in Drug Exposure. *Clin. Pharmacol. Ther.* **2018**, *104*, 1219–1228. [CrossRef]
15. Sorich, M.; Mulflib, F.; van Dyk, M.; Hopkins, A.; Polasek, T.; Marshall, J. Use of predictive analytics to identify physiological and molecular characteristics driving variability in axitinib exposure. *J. Clin. Pharmacol.* **2019**, *59*, 872–879. [CrossRef]
16. Kluwe, F.; Michelet, R.; Mueller-Schoell, A.; Maier, C.; Klopp-Schulze, L.; Van Dyk, M.; Mikus, G.; Huisinga, W.; Kloft, C. Perspectives on Model-Informed Precision Dosing in the Digital Health Era: Challenges, Opportunities, and Recommendations. *Clin. Pharmacol. Ther.* **2020**, *109*, 29–36. [CrossRef]
17. Tsamandouras, N.; Rostami-Hodjegan, A.; Aarons, L. Combining the 'bottom up' and 'top down' approaches in pharmacokinetic modelling: Fitting PBPK models to observed clinical data. *Br. J. Clin. Pharmacol.* **2015**, *79*, 48–55. [CrossRef]
18. Shebley, M.; Sandhu, P.; Riedmaier, A.E.; Jamei, M.; Narayanan, R.; Patel, A.; Peters, S.A.; Reddy, V.P.; Zheng, M.; de Zwart, L.; et al. Physiologically Based Pharmacokinetic Model Qualification and Reporting Procedures for Regulatory Submissions: A Consortium Perspective. *Clin. Pharmacol. Ther.* **2018**, *104*, 88–110. [CrossRef]
19. Sandström, M.; Lindman, H.; Nygren, P.; Lidbrink, E.; Bergh, J.; Karlsson, M.O. Model Describing the Relationship Between Pharmacokinetics and Hematologic Toxicity of the Epirubicin-Docetaxel Regimen in Breast Cancer Patients. *J. Clin. Oncol.* **2005**, *23*, 413–421. [CrossRef]
20. Ralph, L.D.; Thomson, A.H.; Dobbs, N.A.; Twelves, C. A population model of epirubicin pharmacokinetics and application to dosage guidelines. *Cancer Chemother. Pharmacol.* **2003**, *52*, 34–40. [CrossRef]
21. Innocenti, F.; Iyer, L.; Ramírez, J.; Green, M.D.; Ratain, M.J. Epirubicin glucuronidation is catalyzed by human UDP-glucuronosyltransferase 2B7. *Drug Metab. Dispos.* **2001**, *29*, 686–692. [PubMed]
22. Sawyer, M.B.; Pituskin, E.; Damaraju, S.; Bies, R.R.; Vos, L.J.; Prado, C.M.; Kuzma, M.; Scarfe, A.G.; Clemons, M.; Tonkin, K.; et al. A Uridine Glucuronosyltransferase 2B7 Polymorphism Predicts Epirubicin Clearance and Outcomes in Early-Stage Breast Cancer. *Clin. Breast Cancer* **2016**, *16*, 139–144.e3. [CrossRef] [PubMed]
23. Joy, A.A.; Vos, L.J.; Pituskin, E.; Cook, S.F.; Bies, R.R.; Vlahadamis, A.; King, K.; Basi, S.K.; Meza-Junco, J.; Mackey, J.R.; et al. Uridine Glucuronosyltransferase 2B7 Polymorphism-Based Pharmacogenetic Dosing of Epirubicin in FEC Chemotherapy for Early-Stage Breast Cancer. *Clin. Breast Cancer* **2021**, *21*, e584–e593. [CrossRef]
24. Polasek, T.M.; Rayner, C.R.; Peck, R.W.; Rowland, A.; Kimko, H.; Rostami-Hodjegan, A. Toward Dynamic Prescribing Information: Codevelopment of Companion Model-Informed Precision Dosing Tools in Drug Development. *Clin. Pharmacol. Drug Dev.* **2018**, *8*, 418–425. [CrossRef]
25. Rodrigues, A.; Rowland, A. From Endogenous Compounds as Biomarkers to Plasma-Derived Nanovesicles as Liquid Biopsy. *Clin. Pharmacol. Ther.* **2019**, *105*, 1407–1420. [CrossRef]
26. Bowalgaha, K.; Elliot, D.J.; Mackenzie, P.I.; Knights, K.M.; Swedmark, S.; Miners, J.O. S-Naproxen and desmethylnaproxen glucuronidation by human liver microsomes and recombinant human UDP-glucuronosyltransferases (UGT): Role of UGT2B7 in the elimination of naproxen. *Br. J. Clin. Pharmacol.* **2005**, *60*, 423–433. [CrossRef]
27. Boase, S.; Miners, J.O. In vitro-in vivo correlations for drugs eliminated by glucuronidation: Investigations with the model substrate zidovudine. *Br. J. Clin. Pharmacol.* **2002**, *54*, 493–503. [CrossRef] [PubMed]
28. Rowland, A.; Gaganis, P.; Elliot, D.J.; Mackenzie, P.I.; Knights, K.M.; Miners, J.O. Binding of inhibitory fatty acids is responsible for the enhancement of UDP-glucuronosyltransferase 2B7 activity by albumin: Implications for in vitro-in vivo extrapolation. *J. Pharmacol. Exp. Ther.* **2007**, *321*, 137–147. [CrossRef]
29. Miners, J.O.; Lillywhite, K.J.; Matthews, A.P.; Jones, M.E.; Birkett, D.J. Kinetic and inhibitor studies of 4-methylumbelliferone and 1-naphthol glucuronidation in human liver microsomes. *Biochem. Pharmacol.* **1988**, *37*, 665–671. [CrossRef]
30. Rowland Yeo, K.; Jamei, M.; Yang, J.; Tucker, G.T.; Rostami-Hodjegan, A. Physiologically based mechanistic modelling to predict complex drug-drug interactions involving simultaneous competitive and time-dependent enzyme inhibition by parent compound and its metabolite in both liver and gut—The effect of diltiazem on the time-course of exposure to triazolam. *Eur. J. Pharm. Sci.* **2010**, *39*, 298–309.
31. Mouridsen, H.T.; Alfthan, C.; Bastholt, L.; Bergh, J.; Dalmark, M.; Eksborg, S.; Hellsten, S.; Kjaer, M.; Peterson, C.; Skovsgård, T.; et al. Current Status of Epirubicin (Farmorubicin) in the Treatment of Solid Tumours. *Acta Oncol.* **1990**, *29*, 257–285. [CrossRef] [PubMed]
32. Rodgers, T.; Rowland, M. Physiologically based pharmacokinetic modelling 2: Predicting the tissue distribution of acids, very weak bases, neutrals and zwitterions. *J. Pharm. Sci.* **2006**, *95*, 1238–1257. [CrossRef]
33. Robert, J.; Vrignaud, P.; Nguyen-Ngoc, T.; Iliadis, A.; Mauriac, L.; Hurteloup, P. Comparative pharmacokinetics and metabolism of doxorubicin and epirubicin in patients with metastatic breast cancer. *Cancer Treat. Rep.* **1985**, *69*, 633–640.
34. Robert, J. Clinical pharmacokinetics of epirubicin. *Clin. Pharmacokinet.* **1994**, *26*, 428–438. [CrossRef] [PubMed]

35. Gori, S.; Rulli, A.; Mosconi, A.M.; Sidoni, A.; Colozza, M.; Crinò, L. Safety of epirubicin adjuvant chemotherapy in a breast cancer patient with chronic renal failure undergoing hemodialytic treatment. *Tumori J.* **2006**, *92*, 364–365. [CrossRef] [PubMed]
36. Nicolella, D.; Grimaldi, G.; Colantuoni, G.; Belli, M.; Frasci, G.; Perchard, J.; Comella, P. Weekly low dose epirubicin in elderly cancer patients. *Tumori J.* **1996**, *82*, 369–371. [CrossRef]
37. Dobbs, N.A.; Twelves, C.J. What is the effect of adjusting epirubicin doses for body surface area? *Br. J. Cancer* **1998**, *78*, 662–666. [CrossRef] [PubMed]
38. Davidson, M.; Wagner, A.D.; Kouvelakis, K.; Nanji, H.; Starling, N.; Chau, I.; Watkins, D.; Rao, S.; Peckitt, C.; Cunningham, D. Influence of sex on chemotherapy efficacy and toxicity in oesophagogastric cancer: A pooled analysis of four randomised trials. *Eur. J. Cancer* **2019**, *121*, 40–47. [CrossRef]
39. Rodrigues, A.D.; Dyk, M.; Sorich, M.J.; Fahmy, A.; Useckaite, Z.; Newman, L.A.; Kapetas, A.J.; Mounzer, R.; Wood, L.S.; Johnson, J.G.; et al. Exploring the Use of Serum-Derived Small Extracellular Vesicles as Liquid Biopsy to Study the Induction of Hepatic Cytochromes P450 and Organic Anion Transporting Polypeptides. *Clin. Pharmacol. Ther.* **2021**, *110*, 248–258. [CrossRef]
40. Rowland, A.; Ruanglertboon, W.; Van Dyk, M.; Wijayakumara, D.; Wood, L.S.; Meech, R.; Mackenzie, P.I.; Rodrigues, A.D.; Marshall, J.; Sorich, M. Plasma extracellular nanovesicle (exosome)-derived biomarkers for drug metabolism pathways: A novel approach to characterize variability in drug exposure. *Br. J. Clin. Pharmacol.* **2019**, *85*, 216–226. [CrossRef]
41. Rodrigues, A.D.; Wood, L.S.; Vourvahis, M.; Rowland, A. Leveraging Human Plasma-Derived Small Extracellular Vesicles as Liquid Biopsy to Study the Induction of Cytochrome P450 3A4 by Modafinil. *Clin. Pharmacol. Ther.* **2022**, *111*, 425–434. [CrossRef] [PubMed]
42. Useckaite, Z.; Rodrigues, A.D.; Hopkins, A.M.; Newman, L.A.; Johnson, J.G.; Sorich, M.J.; Rowland, A. Role of Extracellular Vesicle-Derived Biomarkers in Drug Metabolism and Disposition. *Drug Metab. Dispos. Biol. Fate Chem.* **2021**, *49*, 961–971. [CrossRef] [PubMed]
43. Achour, B.; Al-Majdoub, Z.M.; Grybos-Gajniak, A.; Lea, K.; Kilford, P.; Zhang, M.; Knight, D.; Barber, J.; Schageman, J.; Rostami-Hodjegan, A. Liquid Biopsy Enables Quantification of the Abundance and Interindividual Variability of Hepatic Enzymes and Transporters. *Clin. Pharmacol. Ther.* **2021**, *109*, 222–231. [CrossRef] [PubMed]
44. Achour, B.; Gosselin, P.; Terrier, J.; Gloor, Y.; Al-Majdoub, Z.M.; Polasek, T.M.; Daali, Y.; Rostami-Hodjegan, A.; Reny, J. Liquid Biopsy for Patient Characterization in Cardiovascular Disease: Verification against Markers of Cytochrome P450 and P-Glycoprotein Activities. *Clin. Pharmacol. Ther.* **2022**, *111*, 1268–1277. [CrossRef] [PubMed]
45. Ruanglertboon, W.; Sorich, M.; Hopkins, A.; Rowland, A. Mechanistic Modelling Identifies and Addresses the Risks of Empiric Concentration-Guided Sorafenib Dosing. *Pharmaceuticals* **2021**, *14*, 389. [CrossRef]
46. Polasek, T.M.; Tucker, G.T.; Sorich, M.J.; Wiese, M.D.; Mohan, T.; Rostami-Hodjegan, A.; Korprasertthaworn, P.; Perera, V.; Rowland, A. Prediction of olanzapine exposure in individual patients using PBPK modelling and simulation. *Br. J. Clin. Pharmacol.* **2018**, *84*, 462–476. [CrossRef]
47. Polasek, T.M.; Rostami-Hodjegan, A. Virtual Twins: Understanding the Data Required for Model-Informed Precision Dosing. *Clin. Pharmacol. Ther.* **2020**, *107*, 742–745. [CrossRef]
48. Smith, L.A.; Cornelius, V.R.; Plummer, C.J.; Levitt, G.; Verrill, M.; Canney, P.; Jones, A. Cardiotoxicity of anthracycline agents for the treatment of cancer: Systematic review and meta-analysis of randomised controlled trials. *BMC Cancer* **2010**, *10*, 337. [CrossRef] [PubMed]

REFERENCES

A'Hern, R. P., Smith, I. E., & Ebbs, S. R. (1993). Chemotherapy and survival in advanced breast cancer: the inclusion of doxorubicin in Cooper type regimens. *Br J Cancer, 67*(4), 801-805. 10.1038/bjc.1993.146

Abbott, K. L., Salamat, J. M., Flannery, P. C., Chaudhury, C. S., Chandran, A., Vishveshwara, S., Mani, S., Huang, J., Tiwari, A. K., & Pondugula, S. R. (2022). Gefitinib Inhibits Rifampicin-Induced CYP3A4 Gene Expression in Human Hepatocytes. *ACS Omega, 7*(38), 34034-34044. 10.1021/acsomega.2c03270

Abrahams, B., Gerber, A., & Hiss, D. C. (2024). Combination Treatment with EGFR Inhibitor and Doxorubicin Synergistically Inhibits Proliferation of MCF-7 Cells and MDA-MB-231 Triple-Negative Breast Cancer Cells In Vitro. *Int J Mol Sci, 25*(5). 10.3390/ijms25053066

Achour, B., Al-Majdoub, Z. M., Grybos-Gajniak, A., Lea, K., Kilford, P., Zhang, M., Knight, D., Barber, J., Schageman, J., & Rostami-Hodjegan, A. (2021). Liquid biopsy enables quantification of the abundance and interindividual variability of hepatic enzymes and transporters. *Clinical Pharmacology & Therapeutics, 109*(1), 222-232.

Achour, B., Gosselin, P., Terrier, J., Gloor, Y., Al-Majdoub, Z. M., Polasek, T. M., Daali, Y., Rostami-Hodjegan, A., & Reny, J. L. (2022). Liquid biopsy for patient characterization in cardiovascular disease: verification against markers of cytochrome P450 and P-glycoprotein activities. *Clinical Pharmacology & Therapeutics, 111*(6), 1268-1277.

Adli, M. (2018). The CRISPR tool kit for genome editing and beyond. *Nature Communications, 9*(1), 1911. 10.1038/s41467-018-04252-2

Ahmed, S., Zhou, Z., Zhou, J., & Chen, S.-Q. (2016). Pharmacogenomics of Drug Metabolizing Enzymes and Transporters: Relevance to Precision Medicine. *Genomics, Proteomics & Bioinformatics, 14*(5), 298-313. 10.1016/j.gpb.2016.03.008

Allain, E. P., Rouleau, M., Lévesque, E., & Guillemette, C. (2020). Emerging roles for UDP-glucuronosyltransferases in drug resistance and cancer progression. *British Journal Of Cancer, 122*(9), 1277-1287. 10.1038/s41416-019-0722-0

Allen, D., Rosenberg, M., & Hendel, A. (2020). Using Synthetically Engineered Guide RNAs to Enhance CRISPR Genome Editing Systems in Mammalian Cells. *Front Genome Ed, 2*, 617910. 10.3389/fgeed.2020.617910

Altschul, S. F., Gish, W., Miller, W., Myers, E. W., & Lipman, D. J. (1990). Basic local alignment search tool. *J Mol Biol, 215*(3), 403-410. 10.1016/s0022-2836(05)80360-2

Amjad, M. T., Chidharla, A., & Kasi, A. (2023). Cancer Chemotherapy. In *StatPearls*. StatPearls Publishing LLC.

Amos, K. D., Adamo, B., & Anders, C. K. (2012). Triple-Negative Breast Cancer: An Update on Neoadjuvant Clinical Trials. *International Journal of Breast Cancer, 2012*(1), 385978. 10.1155/2012/385978

Andersson, M., Madsen, E. L., Overgaard, M., Rose, C., Dombernowsky, P., & Mouridsen, H. T. (1999). Doxorubicin versus methotrexate both combined with cyclophosphamide, 5-fluorouracil and tamoxifen in postmenopausal patients with advanced breast cancer--a randomised study with more than 10 years follow-up from the Danish Breast Cancer Cooperative Group. Danish Breast Cancer Cooperative Group (DBCG). *Eur J Cancer, 35*(1), 39-46. 10.1016/s0959-8049(98)00354-2

Ansaar, R., Meech, R., & Rowland, A. (2023). A Physiologically Based Pharmacokinetic Model to Predict Determinants of Variability in Epirubicin Exposure and Tissue Distribution. *Pharmaceutics, 15*(4), 1222.

Anwar, K., Nguyen, L., Nagasaka, M., Ou, S. I., & Chan, A. (2023). Overview of Drug-Drug Interactions Between Ritonavir-Boosted Nirmatrelvir (Paxlovid) and Targeted Therapy and Supportive Care for Lung Cancer. *JTO Clin Res Rep, 4*(2), 100452. 10.1016/j.jtocrr.2022.100452

Argikar, U. A., & Remmel, R. P. (2009). Effect of Aging on Glucuronidation of Valproic Acid in Human Liver Microsomes and the Role of UDP-Glucuronosyltransferase UGT1A4, UGT1A8, and UGT1A10. *Drug Metabolism and Disposition, 37*(1), 229-236. 10.1124/dmd.108.022426

Armenian, S. H., Hudson, M. M., Lindenfeld, L., Chen, S., Chow, E. J., Colan, S., Collier, W., Su, X., Marcus, E., Echevarria, M., Iukuridze, A., Robison, L. L., Wong, F. L., Chen, M. H., & Bhatia, S. (2024). Effect of carvedilol versus placebo on cardiac function in anthracycline-exposed survivors of childhood cancer (PREVENT-HF): a randomised, controlled, phase 2b trial. *The Lancet Oncology, 25*(2), 235-245. 10.1016/S1470-2045(23)00637-X

Aubrey, B. J., Kelly, G. L., Janic, A., Herold, M. J., & Strasser, A. (2018). How does p53 induce apoptosis and how does this relate to p53-mediated tumour suppression? *Cell Death & Differentiation, 25*(1), 104-113. 10.1038/cdd.2017.169

Aydiner, A., Ridvanogullari, M., Anil, D., Topuz, E., Nurten, R., & Disci, R. (1997). Combined effects of epirubicin and tamoxifen on the cell-cycle phases in estrogen-receptor-negative Ehrlich ascites tumor cells. *Journal of Cancer Research and Clinical Oncology, 123*(2), 113-117. 10.1007/BF01269889

Azab, S. S., El-Demerdash, E., Abdel-Naim, A. B., Youssef, E., El-Sharkawy, N., & Osman, A.-M. M. (2005). Modulation of epirubicin cytotoxicity by tamoxifen in human breast cancer cell lines. *Biochemical Pharmacology, 70*(5), 725-732. 10.1016/j.bcp.2005.03.036

Azarenko, O., Smiyun, G., Mah, J., Wilson, L., & Jordan, M. A. (2014). Antiproliferative Mechanism of Action of the Novel Taxane Cabazitaxel as Compared with the Parent Compound Docetaxel in MCF7 Breast Cancer Cells. *Molecular cancer therapeutics, 13*(8), 2092-2103. 10.1158/1535-7163.MCT-14-0265

Bae, S. Y., Kim, S., Lee, J. H., Lee, H.-c., Lee, S. K., Kil, W. H., Kim, S. W., Lee, J. E., & Nam, S. J. (2015). Poor prognosis of single hormone receptor- positive breast cancer: similar outcome as triple-negative breast cancer. *BMC cancer, 15*(1), 138. 10.1186/s12885-015-1121-4

Bajro, M. H., Josifovski, T., Panovski, M., Jankulovski, N., Nestorovska, A. K., Matevska, N., Petrusevska, N., & Dimovski, A. J. (2012). Promoter length polymorphism in UGT1A1 and the risk of sporadic colorectal cancer. *Cancer Genet, 205*(4), 163-167. 10.1016/j.cancergen.2012.01.015

Barbier, O., Trottier, J., Kaeding, J., Caron, P., & Verreault, M. (2009). Lipid-activated transcription factors control bile acid glucuronidation. *Molecular and Cellular Biochemistry, 326*(1), 3-8. 10.1007/s11010-008-0001-5

Barbier, O., Turgeon, D., Girard, C., Green, M. D., Tephly, T. R., Hum, D. W., & Bélanger, A. (2000). 3'-azido-3'-deoxythimidine (AZT) is glucuronidated by human UDP-glucuronosyltransferase 2B7 (UGT2B7). *Drug Metab Dispos, 28*(5), 497-502.

Bardelmeijer, H. A., Ouwehand, M., Buckle, T., Huisman, M. T., Schellens, J. H., Beijnen, J. H., & van Tellingen, O. (2002). Low systemic exposure of oral docetaxel in mice resulting from extensive first-pass metabolism is boosted by ritonavir. *Cancer Res, 62*(21), 6158-6164.

Bardia, A., Hurvitz, S. A., Tolaney, S. M., Loirat, D., Punie, K., Oliveira, M., Brufsky, A., Sardesai, S. D., Kalinsky, K., Zelnak, A. B., Weaver, R., Traina, T., Dalenc, F., Aftimos, P., Lynce, F., Diab, S., Cortés, J., O'Shaughnessy, J., Diéras, V., Ferrario, C., Schmid, P., Carey, L. A., Gianni, L., Piccart, M. J., Loibl, S., Goldenberg, D. M., Hong, Q., Olivo, M. S., Itri, L. M., & Rugo, H. S. (2021). Sacituzumab Govitecan in Metastatic Triple-Negative Breast Cancer. *New England Journal of Medicine, 384*(16), 1529-1541. 10.1056/NEJMoa2028485

Barrangou, R. (2015). The roles of CRISPR–Cas systems in adaptive immunity and beyond. *Current Opinion in Immunology, 32*, 36-41. 10.1016/j.coi.2014.12.008

Baselga, J., Albanell, J., Ruiz, A., Lluch, A., Gascón, P., Guillém, V., González, S., Sauleda, S., Marimón, I., Tabernero, J. M., Koehler, M. T., & Rojo, F. (2005). Phase II and tumor pharmacodynamic study of gefitinib in patients with advanced breast cancer. *J Clin Oncol, 23*(23), 5323-5333. 10.1200/jco.2005.08.326

Baselga, J., Bradbury, I., Eidtmann, H., Di Cosimo, S., de Azambuja, E., Aura, C., Gómez, H., Dinh, P., Fauria, K., Van Dooren, V., Aktan, G., Goldhirsch, A., Chang, T. W., Horváth, Z., Coccia-Portugal, M., Domont, J., Tseng, L. M., Kunz, G., Sohn, J. H., Semiglazov, V., Lerzo, G., Palacova, M., Probachai, V., Pusztai, L., Untch, M., Gelber, R. D., & Piccart-Gebhart, M. (2012). Lapatinib with trastuzumab for HER2-positive early breast cancer (NeoALTTO): a randomised, open-label, multicentre, phase 3 trial. *Lancet, 379*(9816), 633-640. 10.1016/s0140-6736(11)61847-3

Bazan, F., Dobi, E., Royer, B., Curtit, E., Mansi, L., Menneveau, N., Paillard, M. J., Meynard, G., Villanueva, C., Pivot, X., & Chaigneau, L. (2019). Systemic high-dose intravenous methotrexate in patients with central nervous system metastatic breast cancer. *BMC cancer, 19*(1), 1029. 10.1186/s12885-019-6228-6

Bélanger, A.-S., Caron, P., Harvey, M., Zimmerman, P. A., Mehlotra, R. K., & Guillemette, C. (2009). Glucuronidation of the Antiretroviral Drug Efavirenz by UGT2B7 and an in Vitro Investigation of Drug-Drug Interaction with Zidovudine. *Drug Metabolism and Disposition, 37*(9), 1793-1796. 10.1124/dmd.109.027706

Benov, L. (2021). Improved Formazan Dissolution for Bacterial MTT Assay. *Microbiol Spectr, 9*(3), e0163721. 10.1128/spectrum.01637-21

Bernard, O., Tojcic, J., Journault, K., Perusse, L., & Guillemette, C. (2006). Influence of nonsynonymous polymorphisms of UGT1A8 and UGT2B7 metabolizing enzymes on the formation of phenolic and acyl glucuronides of mycophenolic acid. *Drug Metab Dispos, 34*(9), 1539-1545. 10.1124/dmd.106.010553

Bernsdorf, M., Ingvar, C., Jörgensen, L., Tuxen, M. K., Jakobsen, E. H., Saetersdal, A., Kimper-Karl, M. L., Kroman, N., Balslev, E., & Ejlertsen, B. (2011). Effect of adding gefitinib to neoadjuvant chemotherapy in estrogen receptor negative early breast cancer in a randomized phase II trial. *Breast Cancer Res Treat, 126*(2), 463-470. 10.1007/s10549-011-1352-2

Bertucci, F., Finetti, P., Cervera, N., Charafe-Jauffret, E., Buttarelli, M., Jacquemier, J., Chaffanet, M., Maraninchi, D., Viens, P., & Birnbaum, D. (2009). How different are luminal A and basal breast cancers? *International Journal of Cancer, 124*(6), 1338-1348. 10.1002/ijc.24055

Bhasker, C. R., McKinnon, W., Stone, A., Lo, A. C., Kubota, T., Ishizaki, T., & Miners, J. O. (2000). Genetic polymorphism of UDP-glucuronosyltransferase 2B7 (UGT2B7) at amino acid 268: ethnic diversity of alleles and potential clinical significance. *Pharmacogenetics, 10*(8), 679-685. 10.1097/00008571-200011000-00002

Bhatia, N., & Thareja, S. (2023). Elacestrant: a new FDA-approved SERD for the treatment of breast cancer. *Med Oncol, 40*(6), 180. 10.1007/s12032-023-02045-2

Binkhorst, L. (2015). *Tamoxifen Pharmacokinetics Beyond the Genotyping Era* [Ph.D. thesis]. http://hdl.handle.net/1765/78048

Black, L. E., Longo, J. F., & Carroll, S. L. (2019). Mechanisms of Receptor Tyrosine-Protein Kinase ErbB-3 (ERBB3) Action in Human Neoplasia. *Am J Pathol, 189*(10), 1898-1912. 10.1016/j.ajpath.2019.06.008

Blackwell, K. L., Burstein, H. J., Storniolo, A. M., Rugo, H., Sledge, G., Koehler, M., Ellis, C., Casey, M., Vukelja, S., Bischoff, J., Baselga, J., & O'Shaughnessy, J. (2010). Randomized study of Lapatinib alone or in combination with trastuzumab in women with ErbB2-positive, trastuzumab-refractory metastatic breast cancer. *J Clin Oncol, 28*(7), 1124-1130. 10.1200/jco.2008.21.4437

Blat, Y. (2010). Non-Competitive Inhibition by Active Site Binders. *Chemical Biology & Drug Design, 75*(6), 535-540. 10.1111/j.1747-0285.2010.00972.x

Blevins-Primeau, A. S., Sun, D., Chen, G., Sharma, A. K., Gallagher, C. J., Amin, S., & Lazarus, P. (2009). Functional Significance of UDP-Glucuronosyltransferase Variants in the Metabolism of Active Tamoxifen Metabolites. *Cancer Res, 69*(5), 1892-1900. 10.1158/0008-5472.Can-08-3708

Boase, S., & Miners, J. O. (2002). In vitro-in vivo correlations for drugs eliminated by glucuronidation: investigations with the model substrate zidovudine. *British journal of clinical pharmacology, 54*(5), 493-503. 10.1046/j.1365-2125.2002.01669.x

Bocchinfuso, W. P., & Korach, K. S. (1997). Mammary gland development and tumorigenesis in estrogen receptor knockout mice. *J Mammary Gland Biol Neoplasia, 2*(4), 323-334. 10.1023/a:1026339111278

Bonnefoi, H., Jacot, W., Saghatchian, M., Moldovan, C., Venat-Bouvet, L., Zaman, K., Matos, E., Petit, T., Bodmer, A., Quenel-Tueux, N., Chakiba, C., Vuylsteke, P., Jerusalem, G., Brain, E., Tredan, O., Messina, C. G., Slaets, L., & Cameron, D. (2015). Neoadjuvant treatment with docetaxel plus lapatinib, trastuzumab, or both followed by an anthracycline-based chemotherapy in HER2-positive breast cancer: results of the randomised phase II EORTC 10054 study. *Ann Oncol, 26*(2), 325-332. 10.1093/annonc/mdu551

Bonneterre, J., Roché, H., Kerbrat, P., Brémond, A., Fumoleau, P., Namer, M., Goudier, M.-J., Schraub, S., Fargeot, P., & Chapelle-Marcillac, I. (2005). Epirubicin Increases Long-Term Survival in Adjuvant Chemotherapy of Patients With Poor-Prognosis, Node-Positive, Early Breast Cancer: 10-Year Follow-Up Results of the French Adjuvant Study Group 05 Randomized Trial. *Journal of Clinical Oncology, 23*(12), 2686-2693. 10.1200/JCO.2005.05.059

Boosman, R. J., de Gooijer, C. J., Groenland, S. L., Burgers, J. A., Baas, P., van der Noort, V., Beijnen, J. H., Huitema, A. D. R., & Steeghs, N. (2022). Ritonavir-Boosted Exposure of Kinase Inhibitors: an Open Label, Cross-over Pharmacokinetic Proof-of-Concept Trial with Erlotinib. *Pharm Res, 39*(4), 669-676. 10.1007/s11095-022-03244-8

Borst, P. (2012). Cancer drug pan-resistance: pumps, cancer stem cells, quiescence, epithelial to mesenchymal transition, blocked cell death pathways, persisters or what? *Open Biol, 2*(5), 120066. 10.1098/rsob.120066

Bottini, A., Berruti, A., Brizzi, M. P., Bersiga, A., Generali, D., Allevi, G., Aguggini, S., Bolsi, G., Bonardi, S., Tondelli, B., Vana, F., Tampellini, M., Alquati, P., & Dogliotti, L. (2005). Cytotoxic and antiproliferative activity of the single agent epirubicin versus epirubicin plus tamoxifen as primary chemotherapy in human breast cancer: a single-institution phase III trial. *Endocrine-Related Cancer Endocr Relat Cancer, 12*(2), 383-392. 10.1677/erc.1.00945

Bowalgaha, K., Elliot, D. J., Mackenzie, P. I., Knights, K. M., Swedmark, S., & Miners, J. O. (2005). S-Naproxen and desmethylnaproxen glucuronidation by human liver microsomes and recombinant human UDP-glucuronosyltransferases (UGT): role of UGT2B7 in the elimination of naproxen. *British journal of clinical pharmacology, 60*(4), 423-433. 10.1111/j.1365-2125.2005.02446.x

Brand, T. M., Iida, M., Dunn, E. F., Luthar, N., Kostopoulos, K. T., Corrigan, K. L., Wleklinski, M. J., Yang, D., Wisinski, K. B., Salgia, R., & Wheeler, D. L. (2014). Nuclear Epidermal Growth Factor Receptor Is a Functional Molecular Target in Triple-Negative Breast Cancer. *Molecular cancer therapeutics, 13*(5), 1356-1368. 10.1158/1535-7163.Mct-13-1021

Brooks, E. A., Galarza, S., Gencoglu, M. F., Cornelison, R. C., Munson, J. M., & Peyton, S. R. (2019). Applicability of drug response metrics for cancer studies using biomaterials. *Philos Trans R Soc Lond B Biol Sci, 374*(1779), 20180226. 10.1098/rstb.2018.0226

Bross, P. F., Cohen, M. H., Williams, G. A., & Pazdur, R. (2002). FDA drug approval summaries: fulvestrant. *Oncologist, 7*(6), 477-480. 10.1634/theoncologist.7-6-477

Brown, T., Sigurdson, E., Rogatko, A., & Broccoli, D. (2003). Telomerase inhibition using azidothymidine in the HT-29 colon cancer cell line. *Ann Surg Oncol, 10*(8), 910-915. 10.1245/aso.2003.03.032

Bukowski, K., Kciuk, M., & Kontek, R. (2020). Mechanisms of Multidrug Resistance in Cancer Chemotherapy. *International Journal of Molecular Sciences, 21*(9), 3233. 10.3390/ijms21093233

Burger, D. M., Meenhorst, P. L., Koks, C. H., & Beijnen, J. H. (1993). Pharmacokinetic interaction between rifampin and zidovudine. *Antimicrob Agents Chemother, 37*(7), 1426-1431. 10.1128/aac.37.7.1426

Burns, K., Nair, P. C., Rowland, A., Mackenzie, P. I., Knights, K. M., & Miners, J. O. (2015). The Nonspecific Binding of Tyrosine Kinase Inhibitors to Human Liver Microsomes. *Drug Metabolism and Disposition, 43*(12), 1934-1937. 10.1124/dmd.115.065292

Burstein, M. D., Tsimelzon, A., Poage, G. M., Covington, K. R., Contreras, A., Fuqua, S. A., Savage, M. I., Osborne, C. K., Hilsenbeck, S. G., Chang, J. C., Mills, G. B., Lau, C. C., & Brown, P. H. (2015). Comprehensive genomic analysis identifies novel subtypes and targets of triple-negative breast cancer. *Clin Cancer Res, 21*(7), 1688-1698. 10.1158/1078-0432.Ccr-14-0432

Cailleau, R., Young, R., Olivé, M., & Reeves, W. J., Jr. (1974). Breast tumor cell lines from pleural effusions. *J Natl Cancer Inst, 53*(3), 661-674. 10.1093/jnci/53.3.661

Cairat, M., Al Rahmoun, M., Gunter, M. J., Severi, G., Dossus, L., & Fournier, A. (2020). Use of nonsteroidal anti-inflammatory drugs and breast cancer risk in a prospective cohort of postmenopausal women. *Breast Cancer Research, 22*(1), 118. 10.1186/s13058-020-01343-1

Calderon, L. E., Keeling, J. K., Rollins, J., Black, C. A., Collins, K., Arnold, N., Vance, D. E., & Ndinguri, M. W. (2017). Pt-Mal-LHRH, a Newly Synthesized Compound Attenuating Breast Cancer Tumor Growth and Metastasis by Targeting Overexpression of the LHRH Receptor. *Bioconjug Chem, 28*(2), 461-470. 10.1021/acs.bioconjchem.6b00610

Calvert, H., Twelves, C., Ranson, M., Plummer, R., Fettner, S., Pantze, M., Ling, J., Hamilton, M., Lum, B. L., & Rakhit, A. (2014). Effect of erlotinib on CYP3A activity, evaluated in vitro and by dual probes in patients with cancer. *Anticancer Drugs, 25*(7), 832-840. 10.1097/cad.0000000000000099

Cantore, M., Mambrini, A., Fiorentini, G., Rabbi, C., Zamagni, D., Caudana, R., Pennucci, C., Sanguinetti, F., Lombardi, M., & Nicoli, N. (2005). Phase II study of hepatic intraarterial epirubicin and cisplatin, with systemic 5-fluorouracil in patients with unresectable biliary tract tumors. *Cancer, 103*(7), 1402-1407. 10.1002/cncr.20964

Capasso, A. (2012). Vinorelbine in cancer therapy. *Curr Drug Targets, 13*(8), 1065-1071. 10.2174/138945012802009017

Caraco, Y., Sheller, J., & Wood, A. J. (1997). Pharmacogenetic determinants of codeine induction by rifampin: the impact on codeine's respiratory, psychomotor and miotic effects. *J Pharmacol Exp Ther, 281*(1), 330-336.

Cardinale, D., Iacopo, F., & Cipolla, C. M. (2020). Cardiotoxicity of Anthracyclines. *Front Cardiovasc Med, 7*, 26. 10.3389/fcvm.2020.00026

Carlson, R. W., O'Neill, A., Vidaurre, T., Gomez, H. L., Badve, S. S., & Sledge, G. W. (2012). A randomized trial of combination anastrozole plus gefitinib and of combination fulvestrant plus gefitinib in the treatment of postmenopausal women with hormone receptor positive metastatic breast cancer. *Breast Cancer Res Treat, 133*(3), 1049-1056. 10.1007/s10549-012-1997-5

Cassinelli, G., Configliacchi, E., Penco, S., Rivola, G., Arcamone, F., Pacciarini, A., & Ferrari, L. (1984). Separation, characterization, and analysis of epirubicin (4'-epidoxorubicin) and its metabolites from human urine. *Drug Metabolism and Disposition, 12*(4), 506-510.

Cer, R. Z., Mudunuri, U., Stephens, R., & Lebeda, F. J. (2009). IC50-to-Ki: a web-based tool for converting IC50 to Ki values for inhibitors of enzyme activity and ligand binding. *Nucleic Acids Res, 37*(Web Server issue), W441-445. 10.1093/nar/gkp253

Chan, A., Delaloge, S., Holmes, F. A., Moy, B., Iwata, H., Harvey, V. J., Robert, N. J., Silovski, T., Gokmen, E., von Minckwitz, G., Ejlertsen, B., Chia, S. K. L., Mansi, J., Barrios, C. H., Gnant, M., Buyse, M., Gore, I., Smith, J., 2nd, Harker, G., Masuda, N., Petrakova, K., Zotano, A. G., Iannotti, N., Rodriguez, G., Tassone, P., Wong, A., Bryce, R., Ye, Y., Yao, B., & Martin, M. (2016). Neratinib after trastuzumab-based adjuvant therapy in patients with HER2-positive breast cancer (ExteNET): a multicentre, randomised, double-blind, placebo-controlled, phase 3 trial. *Lancet Oncol, 17*(3), 367-377. 10.1016/s1470-2045(15)00551-3

Chan, S., Campone, M., Santoro, A., Conte, P. F., Bostnavaron, M., & Nguyen, L. (2014). A phase I clinical and pharmacokinetic study evaluating vinflunine in combination with epirubicin as first-line

treatment in metastatic breast cancer. *Cancer Chemother Pharmacol, 73*(5), 903-910. 10.1007/s00280-014-2420-1

Chanawong, A., Hu, D. G., Meech, R., Mackenzie, P. I., & McKinnon, R. A. (2015). Induction of UDP-glucuronosyltransferase 2B15 gene expression by the major active metabolites of tamoxifen, 4-hydroxytamoxifen and endoxifen, in breast cancer cells. *Drug Metab Dispos, 43*(6), 889-897. 10.1124/dmd.114.062935

Charbonneau, M., Harper, K., Brochu-Gaudreau, K., Perreault, A., Roy, L. O., Lucien, F., Tian, S., Fortin, D., & Dubois, C. M. (2023). The development of a rapid patient-derived xenograft model to predict chemotherapeutic drug sensitivity/resistance in malignant glial tumors. *Neuro Oncol, 25*(9), 1605-1616. 10.1093/neuonc/noad047

Chatterjee, K., Zhang, J., Honbo, N., & Karliner, J. S. (2010). Doxorubicin cardiomyopathy. *Cardiology, 115*(2), 155-162. 10.1159/000265166

Chaurasia, M., Singh, R., Sur, S., & Flora, S. J. S. (2023). A review of FDA approved drugs and their formulations for the treatment of breast cancer [Review]. *Frontiers in Pharmacology, 14*. 10.3389/fphar.2023.1184472

Chen, M., LeDuc, B., Kerr, S., Howe, D., & Williams, D. A. (2010). Identification of Human UGT2B7 as the Major Isoform Involved in the O-Glucuronidation of Chloramphenicol. *Drug Metabolism and Disposition, 38*(3), 368-375. 10.1124/dmd.109.029900

Chen, M. L., Sun, A., Cao, W., Eliason, A., Mendez, K. M., Getzler, A. J., Tsuda, S., Diao, H., Mukori, C., Bruno, N. E., Kim, S. Y., Pipkin, M. E., Koralov, S. B., & Sundrud, M. S. (2020a). Physiological expression and function of the MDR1 transporter in cytotoxic T lymphocytes. *J Exp Med, 217*(5). 10.1084/jem.20191388

Chen, P., Lee, N. V., Hu, W., Xu, M., Ferre, R. A., Lam, H., Bergqvist, S., Solowiej, J., Diehl, W., He, Y.-A., Yu, X., Nagata, A., VanArsdale, T., & Murray, B. W. (2016). Spectrum and Degree of CDK Drug Interactions Predicts Clinical Performance. *Molecular cancer therapeutics, 15*(10), 2273-2281. 10.1158/1535-7163.MCT-16-0300

Chen, Y.-C., Yu, J., Metcalfe, C., De Bruyn, T., Gelzleichter, T., Malhi, V., Perez-Moreno, P. D., & Wang, X. (2022). Latest generation estrogen receptor degraders for the treatment of hormone receptor-positive breast cancer. *Expert Opinion on Investigational Drugs, 31*(6), 515-529. 10.1080/13543784.2021.1983542

Chen, Z., Xu, L., Shi, W., Zeng, F., Zhuo, R., Hao, X., & Fan, P. (2020b). Trends of female and male breast cancer incidence at the global, regional, and national levels, 1990–2017. *Breast Cancer Res Treat, 180*(2), 481-490. 10.1007/s10549-020-05561-1

Chène, P. (2003). Inhibiting the p53–MDM2 interaction: an important target for cancer therapy. *Nature Reviews Cancer, 3*(2), 102-109. 10.1038/nrc991

Cheng, X., Lv, X., Qu, H., Li, D., Hu, M., Guo, W., Ge, G., & Dong, R. (2017). Comparison of the inhibition potentials of icotinib and erlotinib against human UDP-glucuronosyltransferase 1A1. *Acta Pharmaceutica Sinica B, 7*(6), 657-664. 10.1016/j.apsb.2017.07.004

Cheng, Z., Rios, G. R., King, C. D., Coffman, B. L., Green, M. D., Mojarrabi, B., Mackenzie, P. I., & Tephly, T. R. (1998). Glucuronidation of catechol estrogens by expressed human UDP-glucuronosyltransferases (UGTs) 1A1, 1A3, and 2B7. *Toxicol Sci, 45*(1), 52-57. 10.1006/toxs.1998.2494

Chipuk, J. E., & Green, D. R. (2006). Dissecting p53-dependent apoptosis. *Cell Death Differ, 13*(6), 994-1002. 10.1038/sj.cdd.4401908

Chipuk, J. E., Kuwana, T., Bouchier-Hayes, L., Droin, N. M., Newmeyer, D. D., Schuler, M., & Green, D. R. (2004). Direct activation of Bax by p53 mediates mitochondrial membrane permeabilization and apoptosis. *Science, 303*(5660), 1010-1014. 10.1126/science.1092734

Chiu, T.-L., & Su, C.-C. (2009). Curcumin inhibits proliferation and migration by increasing the Bax to Bcl-2 ratio and decreasing NF-κBp65 expression in breast cancer MDA-MB-231 cells. *Int J Mol Med, 23*(4), 469-475. 10.3892/ijmm_00000153

Choi, W.-G., Kim, D. K., Shin, Y., Park, R., Cho, Y.-Y., Lee, J. Y., Kang, H. C., & Lee, H. S. (2020). Liquid Chromatography–Tandem Mass Spectrometry for the Simultaneous Determination of Doxorubicin and its Metabolites Doxorubicinol, Doxorubicinone, Doxorubicinolone, and 7-Deoxydoxorubicinone in Mouse Plasma. *Molecules, 25*(5), 1254.

Choi, Y. H., & Yu, A. M. (2014). ABC transporters in multidrug resistance and pharmacokinetics, and strategies for drug development. *Curr Pharm Des, 20*(5), 793-807. 10.2174/13816128005140214165212

Chow, L. W., Xu, B., Gupta, S., Freyman, A., Zhao, Y., Abbas, R., Vo Van, M. L., & Bondarenko, I. (2013). Combination neratinib (HKI-272) and paclitaxel therapy in patients with HER2-positive metastatic breast cancer. *Br J Cancer, 108*(10), 1985-1993. 10.1038/bjc.2013.178

Chowdhury, S., Mainwaring, P., Zhang, L., Mundle, S., Pollozi, E., Gray, A., & Wildgust, M. (2020). Systematic Review and Meta-Analysis of Correlation of Progression-Free Survival-2 and Overall Survival in Solid Tumors. *Front Oncol, 10*, 1349. 10.3389/fonc.2020.01349

Coffman, B. L., Rios, G. R., King, C. D., & Tephly, T. R. (1997). Human UGT2B7 catalyzes morphine glucuronidation. *Drug Metab Dispos, 25*(1), 1-4.

Cohen, M. H., Williams, G. A., Sridhara, R., Chen, G., & Pazdur, R. (2003). FDA Drug Approval Summary: Gefitinib (ZD1839) (Iressa®) Tablets. *Oncologist, 8*(4), 303-306. 10.1634/theoncologist.8-4-303

Colajori, E., Ackland, S., & Anton, A. (1995). IV FEC with epirubicin (E) 50 mg/m2 D1, 8 prolongs time to progression (TTP) with respect to IV CMF D1, 8 given at equimyelosuppressive doses as front line chemotherapy of metastatic breast cancer (MBC): a randomized multinational multicentric phase III trial. Proc ASCO.

Cole, S., Bhardwaj, G., Gerlach, J., Mackie, J., Grant, C., Almquist, K., Stewart, A., Kurz, E., Duncan, A., & Deeley, R. (1992). Overexpression of a transporter gene in a multidrug-resistant human lung cancer cell line. *Science, 258*(5088), 1650-1654. 10.1126/science.1360704

Colomer, R. (2005). Gemcitabine in combination with paclitaxel for the treatment of metastatic breast cancer. *Womens Health (Lond), 1*(3), 323-329. 10.2217/17455057.1.3.323

Conant, D., Hsiau, T., Rossi, N., Oki, J., Maures, T., Waite, K., Yang, J., Joshi, S., Kelso, R., Holden, K., Enzmann, B. L., & Stoner, R. (2022). Inference of CRISPR Edits from Sanger Trace Data. *The CRISPR Journal, 5*(1), 123-130. 10.1089/crispr.2021.0113

Congiu, M., Mashford, M. L., Slavin, J. L., & Desmond, P. V. (2002). UDP glucuronosyltransferase mRNA levels in human liver disease. *Drug Metab Dispos, 30*(2), 129-134. 10.1124/dmd.30.2.129

Conte, P. F., Baldini, E., Gardin, G., Pronzato, P., Amadori, D., Carnino, F., Monzeglio, C., Gentilini, P., Gallotti, P., DeMicheli, R., Venturini, M., Rubagotti, A., & Rosso, R. (1996). Chemotherapy with or without estrogenic recruitment in metastatic breast cancer. A randomized trial of the Gruppo Oncologico Nord Ovest (GONO). *Ann Oncol, 7*(5), 487-490.

Conte, P. F., Gennari, A., Landucci, E., & Orlandini, C. (2000). Role of Epirubicin in Advanced Breast Cancer. *Clinical Breast Cancer, 1*, S46-S51. 10.3816/CBC.2000.s.009

Corkery, B., Crown, J., Clynes, M., & O'Donovan, N. (2009). Epidermal growth factor receptor as a potential therapeutic target in triple-negative breast cancer. *Annals of Oncology, 20*(5), 862-867. 10.1093/annonc/mdn710

Cortes, J., Cescon, D. W., Rugo, H. S., Nowecki, Z., Im, S. A., Yusof, M. M., Gallardo, C., Lipatov, O., Barrios, C. H., Holgado, E., Iwata, H., Masuda, N., Otero, M. T., Gokmen, E., Loi, S., Guo, Z., Zhao, J., Aktan, G., Karantza, V., & Schmid, P. (2020). Pembrolizumab plus chemotherapy versus placebo plus chemotherapy for previously untreated locally recurrent inoperable or metastatic triple-negative breast cancer (KEYNOTE-355): a randomised, placebo-controlled, double-blind, phase 3 clinical trial. *Lancet, 396*(10265), 1817-1828. 10.1016/s0140-6736(20)32531-9

Cortés, J., Dieras, V., Ro, J., Barriere, J., Bachelot, T., Hurvitz, S., Le Rhun, E., Espié, M., Kim, S. B., Schneeweiss, A., Sohn, J. H., Nabholtz, J. M., Kellokumpu-Lehtinen, P. L., Taguchi, J., Piacentini, F., Ciruelos, E., Bono, P., Ould-Kaci, M., Roux, F., & Joensuu, H. (2015). Afatinib alone or afatinib plus vinorelbine versus investigator's choice of treatment for HER2-positive breast cancer with progressive brain metastases after trastuzumab, lapatinib, or both (LUX-Breast 3): a randomised, open-label, multicentre, phase 2 trial. *Lancet Oncol, 16*(16), 1700-1710. 10.1016/s1470-2045(15)00373-3

Cortes, J., Rugo, H. S., Cescon, D. W., Im, S. A., Yusof, M. M., Gallardo, C., Lipatov, O., Barrios, C. H., Perez-Garcia, J., Iwata, H., Masuda, N., Torregroza Otero, M., Gokmen, E., Loi, S., Guo, Z., Zhou, X., Karantza, V., Pan, W., & Schmid, P. (2022). Pembrolizumab plus Chemotherapy in Advanced Triple-Negative Breast Cancer. *N Engl J Med, 387*(3), 217-226. 10.1056/NEJMoa2202809

Cottin, Y., Touzery, C., Dalloz, F., Coudert, B., Toubeau, M., Riedinger, A., Louis, P., Wolf, J. E., & Brunotte, F. (1998). Comparison of epirubicin and doxorubicin cardiotoxicity induced by low doses: evolution of the diastolic and systolic parameters studied by radionuclide angiography. *Clin Cardiol, 21*(9), 665-670. 10.1002/clc.4960210911

Court, M. H. (2005). Isoform-selective probe substrates for in vitro studies of human UDP-glucuronosyltransferases. *Methods Enzymol, 400*, 104-116. 10.1016/s0076-6879(05)00007-8

Court, M. H., Krishnaswamy, S., Hao, Q., Duan, S. X., Patten, C. J., Von Moltke, L. L., & Greenblatt, D. J. (2003). Evaluation of 3'-azido-3'-deoxythymidine, morphine, and codeine as probe substrates for UDP-glucuronosyltransferase 2B7 (UGT2B7) in human liver microsomes: specificity and influence of the UGT2B7*2 polymorphism. *Drug Metab Dispos, 31*(9), 1125-1133. 10.1124/dmd.31.9.1125

Cristofanilli, M., Valero, V., Mangalik, A., Royce, M., Rabinowitz, I., Arena, F. P., Kroener, J. F., Curcio, E., Watkins, C., Bacus, S., Cora, E. M., Anderson, E., & Magill, P. J. (2010). Phase II, randomized trial to compare anastrozole combined with gefitinib or placebo in postmenopausal women with hormone receptor-positive metastatic breast cancer. *Clin Cancer Res, 16*(6), 1904-1914. 10.1158/1078-0432.Ccr-09-2282

Cronin-Fenton, D. P., Damkier, P., & Lash, T. L. (2014). Metabolism and transport of tamoxifen in relation to its effectiveness: new perspectives on an ongoing controversy. *Future Oncol, 10*(1), 107-122. 10.2217/fon.13.168

Cserni, G., Chmielik, E., Cserni, B., & Tot, T. (2018). The new TNM-based staging of breast cancer. *Virchows Archiv, 472*(5), 697-703. 10.1007/s00428-018-2301-9

Cuzick, J., Sestak, I., Cawthorn, S., Hamed, H., Holli, K., Howell, A., & Forbes, J. F. (2015). Tamoxifen for prevention of breast cancer: extended long-term follow-up of the IBIS-I breast cancer prevention trial. *Lancet Oncol, 16*(1), 67-75. 10.1016/s1470-2045(14)71171-4

Czernik, P. J., Little, J. M., Barone, G. W., Raufman, J. P., & Radominska-Pandya, A. (2000). Glucuronidation of estrogens and retinoic acid and expression of UDP-glucuronosyltransferase 2B7 in human intestinal mucosa. *Drug Metab Dispos, 28*(10), 1210-1216.

Dai, X., Cheng, H., Bai, Z., & Li, J. (2017). Breast Cancer Cell Line Classification and Its Relevance with Breast Tumor Subtyping. *Journal of Cancer, 8*(16), 3131-3141. 10.7150/jca.18457

Dai, X., Li, T., Bai, Z., Yang, Y., Liu, X., Zhan, J., & Shi, B. (2015). Breast cancer intrinsic subtype classification, clinical use and future trends. *American journal of cancer research, 5*(10), 2929-2943.

Dana, H., Chalbatani, G. M., Mahmoodzadeh, H., Karimloo, R., Rezaiean, O., Moradzadeh, A., Mehmandoost, N., Moazzen, F., Mazraeh, A., Marmari, V., Ebrahimi, M., Rashno, M. M., Abadi, S. J., & Gharagouzlo, E. (2017). Molecular Mechanisms and Biological Functions of siRNA. *Int J Biomed Sci, 13*(2), 48-57.

Dang, Y., Jia, G., Choi, J., Ma, H., Anaya, E., Ye, C., Shankar, P., & Wu, H. (2015). Optimizing sgRNA structure to improve CRISPR-Cas9 knockout efficiency. *Genome Biology, 16*(1), 280. 10.1186/s13059-015-0846-3

Davidson, M., Wagner, A. D., Kouvelakis, K., Nanji, H., Starling, N., Chau, I., Watkins, D., Rao, S., Peckitt, C., & Cunningham, D. (2019). Influence of sex on chemotherapy efficacy and toxicity in oesophagogastric cancer: A pooled analysis of four randomised trials. *European Journal of Cancer, 121*, 40-47. 10.1016/j.ejca.2019.08.010

Davies, C., Godwin, J., Gray, R., Clarke, M., Cutter, D., Darby, S., McGale, P., Pan, H. C., Taylor, C., Wang, Y. C., Dowsett, M., Ingle, J., & Peto, R. (2011). Relevance of breast cancer hormone receptors and other factors to the efficacy of adjuvant tamoxifen: patient-level meta-analysis of randomised trials. *Lancet, 378*(9793), 771-784. 10.1016/s0140-6736(11)60993-8

de Azambuja, E., Holmes, A. P., Piccart-Gebhart, M., Holmes, E., Di Cosimo, S., Swaby, R. F., Untch, M., Jackisch, C., Lang, I., Smith, I., Boyle, F., Xu, B., Barrios, C. H., Perez, E. A., Azim, H. A., Jr., Kim, S. B., Kuemmel, S., Huang, C. S., Vuylsteke, P., Hsieh, R. K., Gorbunova, V., Eniu, A., Dreosti, L., Tavartkiladze, N., Gelber, R. D., Eidtmann, H., & Baselga, J. (2014). Lapatinib with trastuzumab for HER2-positive early breast cancer (NeoALTTO): survival outcomes of a randomised, open-label,

multicentre, phase 3 trial and their association with pathological complete response. *Lancet Oncol, 15*(10), 1137-1146. 10.1016/s1470-2045(14)70320-1

de Ruijter, T. C., Veeck, J., de Hoon, J. P., van Engeland, M., & Tjan-Heijnen, V. C. (2011). Characteristics of triple-negative breast cancer. *Journal of Cancer Research and Clinical Oncology, 137*, 183-192.

de Sousa Cavalcante, L., & Monteiro, G. (2014). Gemcitabine: Metabolism and molecular mechanisms of action, sensitivity and chemoresistance in pancreatic cancer. *European Journal of Pharmacology, 741*, 8-16. 10.1016/j.ejphar.2014.07.041

Delgado, A., & Guddati, A. K. (2021). Clinical endpoints in oncology - a primer. *Am J Cancer Res, 11*(4), 1121-1131.

Dellinger, R. W., Matundan, H. H., Ahmed, A. S., Duong, P. H., & Meyskens, F. L., Jr. (2012). Anti-cancer drugs elicit re-expression of UDP-glucuronosyltransferases in melanoma cells. *PLoS ONE, 7*(10), e47696-e47696. 10.1371/journal.pone.0047696

Dhimolea, E., de Matos Simoes, R., Kansara, D., Al'Khafaji, A., Bouyssou, J., Weng, X., Sharma, S., Raja, J., Awate, P., Shirasaki, R., Tang, H., Glassner, B. J., Liu, Z., Gao, D., Bryan, J., Bender, S., Roth, J., Scheffer, M., Jeselsohn, R., Gray, N. S., Georgakoudi, I., Vazquez, F., Tsherniak, A., Chen, Y., Welm, A., Duy, C., Melnick, A., Bartholdy, B., Brown, M., Culhane, A. C., & Mitsiades, C. S. (2021). An Embryonic Diapause-like Adaptation with Suppressed Myc Activity Enables Tumor Treatment Persistence. *Cancer cell, 39*(2), 240-256.e211. 10.1016/j.ccell.2020.12.002

Di Marco, A., D'Antoni, M., Attaccalite, S., Carotenuto, P., & Laufer, R. (2005). Determination of drug glucuronidation and UDP-glucuronosyltransferase selectivity using a 96-well radiometric assay. *Drug Metab Dispos, 33*(6), 812-819. 10.1124/dmd.105.004333

Dickler, M. N., Cobleigh, M. A., Miller, K. D., Klein, P. M., & Winer, E. P. (2009). Efficacy and safety of erlotinib in patients with locally advanced or metastatic breast cancer. *Breast Cancer Res Treat, 115*(1), 115-121. 10.1007/s10549-008-0055-9

Dickschen, K., Willmann, S., Thelen, K., Lippert, J., Hempel, G., & Eissing, T. (2012). Physiologically Based Pharmacokinetic Modeling of Tamoxifen and its Metabolites in Women of Different CYP2D6 Phenotypes Provides New Insight into the Tamoxifen Mass Balance. *Front Pharmacol, 3*, 92. 10.3389/fphar.2012.00092

Disterer, P., Papaioannou, I., Evans, V., Simons, J., & Owen, J. (2012). Oligonucleotide-mediated gene editing is underestimated in cells expressing mutated green fluorescent protein and is positively associated with target protein expression. *J Gene Med, 14*, 109-119. 10.1002/jgm.1639

Dobbs, N. A., & Twelves, C. J. (1998). What is the effect of adjusting epirubicin doses for body surface area? *British Journal Of Cancer, 78*(5), 662-666. 10.1038/bjc.1998.556

Doehmer, J., Goeptar, A. R., & Vermeulen, N. P. (1993). Cytochromes P450 and drug resistance. *Cytotechnology, 12*(1-3), 357-366. 10.1007/bf00744673

Dow, L. F., Case, A. M., Paustian, M. P., Pinkerton, B. R., Simeon, P., & Trippier, P. C. (2023). The evolution of small molecule enzyme activators. *RSC Med Chem, 14*(11), 2206-2230. 10.1039/d3md00399j

Drăgănescu, M., & Carmocan, C. (2017). Hormone Therapy in Breast Cancer. *Chirurgia (Bucur), 112*(4), 413-417. 10.21614/chirurgia.112.4.413

Drooger, J. C., van Pelt-Sprangers, J. M., Leunis, C., Jager, A., & de Jongh, F. E. (2015). Neutrophil-guided dosing of anthracycline-cyclophosphamide-containing chemotherapy in patients with breast cancer: a feasibility study. *Med Oncol, 32*(4), 113. 10.1007/s12032-015-0550-x

Du, J., You, T., Chen, X., & Zhong, D. (2013). Stereoselective Glucuronidation of Ornidazole in Humans: Predominant Contribution of UDP-Glucuronosyltransferases 1A9 and 2B7. *Drug Metabolism and Disposition, 41*(7), 1306-1318. 10.1124/dmd.113.051235

Du, Z., & Lovly, C. M. (2018). Mechanisms of receptor tyrosine kinase activation in cancer. *Molecular Cancer, 17*(1), 58. 10.1186/s12943-018-0782-4

Duguay, Y., Báár, C., Skorpen, F., & Guillemette, C. (2004). A novel functional polymorphism in the uridine diphosphate-glucuronosyltransferase 2B7 promoter with significant impact on promoter activity. *Clinical Pharmacology & Therapeutics, 75*(3), 223-233. 10.1016/j.clpt.2003.10.006

Dura, P., Salomon, J., Te Morsche, R. H., Roelofs, H. M., Kristinsson, J. O., Wobbes, T., Witteman, B. J., Tan, A. C., Drenth, J. P., & Peters, W. H. (2012). High enzyme activity UGT1A1 or low activity UGT1A8 and UGT2B4 genotypes increase esophageal cancer risk. *Int J Oncol, 40*(6), 1789-1796. 10.3892/ijo.2012.1385

Eadie, L., Hughes, T. P., & White, D. L. (2013). Increasing Expression Of The Efflux Transporter ABCB1 May Predispose CML Cells To Overt TKI Resistance. *Blood, 122*(21), 5157-5157. 10.1182/blood.V122.21.5157.5157

Egerton, N. (2008). Ixabepilone (ixempra), a therapeutic option for locally advanced or metastatic breast cancer. *P t, 33*(9), 523-531.

Eksborg, S. (1989). Pharmacokinetics of anthracyclines. *Acta Oncol, 28*(6), 873-876. 10.3109/02841868909092323

el-Deiry, W. S., Tokino, T., Velculescu, V. E., Levy, D. B., Parsons, R., Trent, J. M., Lin, D., Mercer, W. E., Kinzler, K. W., & Vogelstein, B. (1993). WAF1, a potential mediator of p53 tumor suppression. *Cell, 75*(4), 817-825. 10.1016/0092-8674(93)90500-p

El Guerrab, A., Bamdad, M., Kwiatkowski, F., Bignon, Y. J., Penault-Llorca, F., & Aubel, C. (2016). Anti-EGFR monoclonal antibodies and EGFR tyrosine kinase inhibitors as combination therapy for triple-negative breast cancer. *Oncotarget, 7*(45), 73618-73637. 10.18632/oncotarget.12037

Ellis, H., & Mahadevan, V. (2013). Anatomy and physiology of the breast. *Surgery (Oxford), 31*(1), 11-14.

Eun, H.-M. (1996). 1 - Enzymes and Nucleic Acids: General Principles. In H.-M. Eun (Ed.), *Enzymology Primer for Recombinant DNA Technology* (pp. 1-108). Academic Press. 10.1016/B978-012243740-3/50004-1

Fahmy, A., Hopkins, A. M., Sorich, M. J., & Rowland, A. (2021). Evaluating the utility of therapeutic drug monitoring in the clinical use of small molecule kinase inhibitors: a review of the literature. *Expert Opinion on Drug Metabolism & Toxicology, 17*(7), 803-821.

Fazio, S., Palmieri, E. A., Ferravante, B., Bonè, F., Biondi, B., & Saccà, L. (1998). Doxorubicin-induced cardiomyopathy treated with carvedilol. *Clin Cardiol, 21*(10), 777-779. 10.1002/clc.4960211017

FDA. (1996). *Docetaxel injection, for intravenous use*. https://www.accessdata.fda.gov/drugsatfda_docs/label/2020/020449s084lbl.pdf

FDA. (1999). *ELLENCE (epirubicin hydrochloride) biopharmaceutics review*. https://www.accessdata.fda.gov/drugsatfda_docs/nda/99/50-778_Ellence_biopharmr.pdf

FDA. (2003). *21-399 IRESSA (gefitinib) clinical review*. https://www.accessdata.fda.gov/drugsatfda_docs/nda/2003/21-399_IRESSA_Pharmr_P1.pdf

FDA. (2007). *Drug Approval Package - Tykerb (Lapatinib) Tablets*. https://www.accessdata.fda.gov/drugsatfda_docs/nda/2007/022059s000TOC.cfm

FDA. (2013). *NDA 201292 Review Addendum – Afatinib*. https://www.accessdata.fda.gov/drugsatfda_docs/nda/2013/201292orig1s000clinpharmr.pdf

FDA. (2019). *In Vitro Drug Interaction Studies - Cytochrome P450 Enzyme- and Transporter-Mediated Drug Interactions Guidance for Industry*. https://www.fda.gov/media/134582/download

Felipe, A. V., Oliveira, J., Moraes, A. A., França, J. P., Silva, T. D., & Forones, N. M. (2018). Reversal of Multidrug Resistance in an Epirubicin-Resistant Gastric Cancer Cell Subline. *Asian Pac J Cancer Prev, 19*(5), 1237-1242. 10.22034/apjcp.2018.19.5.1237

Feng, X. Q., Zhu, L. L., & Zhou, Q. (2017). Opioid analgesics-related pharmacokinetic drug interactions: from the perspectives of evidence based on randomized controlled trials and clinical risk management. *J Pain Res, 10*, 1225-1239. 10.2147/jpr.S138698

Feng, Y., Spezia, M., Huang, S., Yuan, C., Zeng, Z., Zhang, L., Ji, X., Liu, W., Huang, B., Luo, W., Liu, B., Lei, Y., Du, S., Vuppalapati, A., Luu, H. H., Haydon, R. C., He, T. C., & Ren, G. (2018). Breast cancer development and progression: Risk factors, cancer stem cells, signaling pathways, genomics, and molecular pathogenesis. *Genes Dis, 5*(2), 77-106. 10.1016/j.gendis.2018.05.001

Feoktistova, M., Geserick, P., & Leverkus, M. (2016). Crystal Violet Assay for Determining Viability of Cultured Cells. *Cold Spring Harb Protoc, 2016*(4), pdb.prot087379. 10.1101/pdb.prot087379

Ferlay, J., Ervik, M., Lam, F., Colombet, M., Mery, L., Piñeros, M., Znaor, A., Soerjomataram, I., & Bray, F. (2018). Global cancer observatory: cancer today. *Lyon, France: international agency for research on cancer, 3*(20), 2019.

Fisher, M. B., Campanale, K., Ackermann, B. L., VandenBranden, M., & Wrighton, S. A. (2000). In Vitro Glucuronidation Using Human Liver Microsomes and The Pore-Forming Peptide Alamethicin. *Drug Metabolism and Disposition, 28*(5), 560-566.

Fontaine, C., Renard, V., Van den Bulk, H., Vuylsteke, P., Glorieux, P., Dopchie, C., Decoster, L., Vanacker, L., de Azambuja, E., De Greve, J., Awada, A., & Wildiers, H. (2019). Weekly carboplatin plus neoadjuvant anthracycline-taxane-based regimen in early triple-negative breast cancer: a prospective phase II trial by the Breast Cancer Task Force of the Belgian Society of Medical Oncology (BSMO). *Breast Cancer Res Treat, 176*(3), 607-615. 10.1007/s10549-019-05259-z

Forrest, R. A., Swift, L. P., Evison, B. J., Rephaeli, A., Nudelman, A., Phillips, D. R., & Cutts, S. M. (2013). The hydroxyl epimer of doxorubicin controls the rate of formation of cytotoxic anthracycline-DNA adducts. *Cancer Chemother Pharmacol, 71*(3), 809-816. 10.1007/s00280-012-2049-x

Frasor, J., Chang, E. C., Komm, B., Lin, C.-Y., Vega, V. B., Liu, E. T., Miller, L. D., Smeds, J., Bergh, J., & Katzenellenbogen, B. S. (2006). Gene Expression Preferentially Regulated by Tamoxifen in Breast Cancer Cells and Correlations with Clinical Outcome. *Cancer Res, 66*(14), 7334-7340. 10.1158/0008-5472.Can-05-4269

Friedman, J. R., Fredericks, W. J., Jensen, D. E., Speicher, D. W., Huang, X. P., Neilson, E. G., & Rauscher, F. J., 3rd. (1996). KAP-1, a novel corepressor for the highly conserved KRAB repression domain. *Genes Dev, 10*(16), 2067-2078. 10.1101/gad.10.16.2067

Friedrichs, K., Hölzel, F., & Jänicke, F. (2002). Combination of taxanes and anthracyclines in first-line chemotherapy of metastatic breast cancer: an interim report. *European Journal of Cancer, 38*(13), 1730-1738. 10.1016/S0959-8049(02)00144-2

Fromm, M. F., Eckhardt, K., Li, S., Schänzle, G., Hofmann, U., Mikus, G., & Eichelbaum, M. (1997). Loss of analgesic effect of morphine due to coadministration of rifampin. *PAIN, 72*(1), 261-267. 10.1016/s0304-3959(97)00044-4

Fudin, J., Fontenelle, D. V., & Payne, A. (2012). Rifampin reduces oral morphine absorption: a case of transdermal buprenorphine selection based on morphine pharmacokinetics. *J Pain Palliat Care Pharmacother, 26*(4), 362-367. 10.3109/15360288.2012.734903

Gabel, F., Aubry, A. S., Hovhannisyan, V., Chavant, V., Weinsanto, I., Maduna, T., Darbon, P., & Goumon, Y. (2020). Unveiling the Impact of Morphine on Tamoxifen Metabolism in Mice in vivo. *Front Oncol, 10*, 25. 10.3389/fonc.2020.00025

Gaganis, P., Miners, J. O., & Knights, K. M. (2007). Glucuronidation of fenamates: Kinetic studies using human kidney cortical microsomes and recombinant UDP-glucuronosyltransferase (UGT) 1A9 and 2B7. *Biochemical Pharmacology, 73*(10), 1683-1691. 10.1016/j.bcp.2007.01.030

Gagné, J. F., Montminy, V., Belanger, P., Journault, K., Gaucher, G., & Guillemette, C. (2002). Common human UGT1A polymorphisms and the altered metabolism of irinotecan active metabolite 7-ethyl-10-hydroxycamptothecin (SN-38). *Mol Pharmacol, 62*(3), 608-617. 10.1124/mol.62.3.608

Gall, W. E., Zawada, G., Mojarrabi, B., Tephly, T. R., Green, M. D., Coffman, B. L., Mackenzie, P. I., & Radominska-Pandya, A. (1999). Differential glucuronidation of bile acids, androgens and estrogens by human UGT1A3 and 2B7. *The Journal of Steroid Biochemistry and Molecular Biology, 70*(1), 101-108. 10.1016/S0960-0760(99)00088-6

Ganapathi, R. N., & Ganapathi, M. K. (2013). Mechanisms regulating resistance to inhibitors of topoisomerase II. *Front Pharmacol, 4*, 89. 10.3389/fphar.2013.00089

Ganzina, F. (1983). 4'-epi-doxorubicin, a new analogue of doxorubicin: a preliminary overview of preclinical and clinical data. *Cancer Treat Rev, 10*(1), 1-22. 10.1016/s0305-7372(83)80029-2

Gelston, E. A., Coller, J. K., Lopatko, O. V., James, H. M., Schmidt, H., White, J. M., & Somogyi, A. A. (2012). Methadone inhibits CYP2D6 and UGT2B7/2B4 in vivo: a study using codeine in methadone- and buprenorphine-maintained subjects. *British journal of clinical pharmacology, 73*(5), 786-794. 10.1111/j.1365-2125.2011.04145.x

Geyer, C. E., Forster, J., Lindquist, D., Chan, S., Romieu, C. G., Pienkowski, T., Jagiello-Gruszfeld, A., Crown, J., Chan, A., Kaufman, B., Skarlos, D., Campone, M., Davidson, N., Berger, M., Oliva, C., Rubin, S. D.,

Stein, S., & Cameron, D. (2006). Lapatinib plus capecitabine for HER2-positive advanced breast cancer. *N Engl J Med, 355*(26), 2733-2743. 10.1056/NEJMoa064320

Ghosh, M. G., Thompson, D. A., & Weigel, R. J. (2000). PDZK1 and GREB1 are estrogen-regulated genes expressed in hormone-responsive breast cancer. *Cancer Res, 60*(22), 6367-6375.

Gianni, L., Munzone, E., Capri, G., Fulfaro, F., Tarenzi, E., Villani, F., Spreafico, C., Laffranchi, A., Caraceni, A., Martini, C., & et al. (1995). Paclitaxel by 3-hour infusion in combination with bolus doxorubicin in women with untreated metastatic breast cancer: high antitumor efficacy and cardiac effects in a dose-finding and sequence-finding study. *J Clin Oncol, 13*(11), 2688-2699. 10.1200/jco.1995.13.11.2688

Gilbert, L. A., Horlbeck, M. A., Adamson, B., Villalta, J. E., Chen, Y., Whitehead, E. H., Guimaraes, C., Panning, B., Ploegh, H. L., Bassik, M. C., Qi, L. S., Kampmann, M., & Weissman, J. S. (2014). Genome-Scale CRISPR-Mediated Control of Gene Repression and Activation. *Cell, 159*(3), 647-661. 10.1016/j.cell.2014.09.029

Gilbert, L. A., Larson, M. H., Morsut, L., Liu, Z., Brar, G. A., Torres, S. E., Stern-Ginossar, N., Brandman, O., Whitehead, E. H., Doudna, J. A., Lim, W. A., Weissman, J. S., & Qi, L. S. (2013). CRISPR-mediated modular RNA-guided regulation of transcription in eukaryotes. *Cell, 154*(2), 442-451. 10.1016/j.cell.2013.06.044

Girard, C., Barbier, O., Veilleux, G., El-Alfy, M., & Bélanger, A. (2003). Human Uridine Diphosphate-Glucuronosyltransferase UGT2B7 Conjugates Mineralocorticoid and Glucocorticoid Metabolites. *Endocrinology, 144*(6), 2659-2668. 10.1210/en.2002-0052

Gligorov, J. (2004). Preclinical Pharmacology of the Taxanes: Implications of the Differences. *Oncologist, 9*, 3-8. 10.1634/theoncologist.9-suppl_2-3

Gnanapradeepan, K., Basu, S., Barnoud, T., Budina-Kolomets, A., Kung, C.-P., & Murphy, M. E. (2018). The p53 Tumor Suppressor in the Control of Metabolism and Ferroptosis [Review]. *Frontiers in Endocrinology, 9*. 10.3389/fendo.2018.00124

Gomes, A. S., Trovão, F., Andrade Pinheiro, B., Freire, F., Gomes, S., Oliveira, C., Domingues, L., Romão, M. J., Saraiva, L., & Carvalho, A. L. (2018). The Crystal Structure of the R280K Mutant of Human p53 Explains the Loss of DNA Binding. *International Journal of Molecular Sciences, 19*(4), 1184. 10.3390/ijms19041184

Gori, S., Rulli, A., Mosconi, A. M., Sidoni, A., Colozza, M., & Crinò, L. (2006). Safety of epirubicin adjuvant chemotherapy in a breast cancer patient with chronic renal failure undergoing hemodialytic treatment. *Tumori, 92*(4), 364-365. 10.1177/030089160609200421

Green, M. D., Francis, P. A., Gebski, V., Harvey, V., Karapetis, C., Chan, A., Snyder, R., Fong, A., Basser, R., & Forbes, J. F. (2009). Gefitinib treatment in hormone-resistant and hormone receptor-negative advanced breast cancer. *Annals of Oncology, 20*(11), 1813-1817. 10.1093/annonc/mdp202

Gregory, P. A., Gardner-Stephen, D. A., Rogers, A., Michael, M. Z., & Mackenzie, P. I. (2006). The caudal-related homeodomain protein Cdx2 and hepatocyte nuclear factor 1alpha cooperatively regulate the UDP-glucuronosyltransferase 2B7 gene promoter. *Pharmacogenetics and genomics, 16*(7), 527-536. 10.1097/01.fpc.0000215068.06471.35

Grinshpun, A., Tolaney, S. M., Burstein, H. J., Jeselsohn, R., & Mayer, E. L. (2023). The dilemma of selecting a first line CDK4/6 inhibitor for hormone receptor-positive/HER2-negative metastatic breast cancer. *npj Breast Cancer, 9*(1), 15. 10.1038/s41523-023-00520-7

Gu, X., Jia, S., Wei, W., & Zhang, W. H. (2015). Neoadjuvant chemotherapy of breast cancer with pirarubicin versus epirubicin in combination with cyclophosphamide and docetaxel. *Tumour Biol, 36*(7), 5529-5535. 10.1007/s13277-015-3221-9

Guarneri, V., & de Azambuja, E. (2022). Anthracyclines in the treatment of patients with early breast cancer. *ESMO Open, 7*(3), 100461. 10.1016/j.esmoop.2022.100461

Guix, M., Granja Nde, M., Meszoely, I., Adkins, T. B., Wieman, B. M., Frierson, K. E., Sanchez, V., Sanders, M. E., Grau, A. M., Mayer, I. A., Pestano, G., Shyr, Y., Muthuswamy, S., Calvo, B., Krontiras, H., Krop, I. E., Kelley, M. C., & Arteaga, C. L. (2008). Short preoperative treatment with erlotinib inhibits tumor cell proliferation in hormone receptor-positive breast cancers. *J Clin Oncol, 26*(6), 897-906. 10.1200/jco.2007.13.5939

PK/PD model-informed dose selection for oncology phase I expansion: Case study based on PF-06939999, a PRMT5 inhibitor (2022) [2022/11/16] n/a.

Gurney, H. P., Ackland, S., Gebski, V., & Farrell, G. (1998). Factors affecting epirubicin pharmacokinetics and toxicity: evidence against using body-surface area for dose calculation. *J Clin Oncol, 16*(7), 2299-2304. 10.1200/jco.1998.16.7.2299

Gustafson, D. L., & Page, R. L. (2013). Cancer chemotherapy. *Withrow and MacEwen's small animal clinical oncology*, 157-179.

Gutierrez, C., & Schiff, R. (2011). HER2: biology, detection, and clinical implications. *Arch Pathol Lab Med, 135*(1), 55-62. 10.5858/2010-0454-rar.1

Haghgoo, S. M., Allameh, A., Mortaz, E., Garssen, J., Folkerts, G., Barnes, P. J., & Adcock, I. M. (2015). Pharmacogenomics and targeted therapy of cancer: Focusing on non-small cell lung cancer. *European Journal of Pharmacology, 754*, 82-91. 10.1016/j.ejphar.2015.02.029

Hakkola, J., Hukkanen, J., Turpeinen, M., & Pelkonen, O. (2020). Inhibition and induction of CYP enzymes in humans: an update. *Archives of Toxicology, 94*(11), 3671-3722. 10.1007/s00204-020-02936-7

Han, Y., Wu, Y., Xu, H., Wang, J., & Xu, B. (2022). The impact of hormone receptor on the clinical outcomes of HER2-positive breast cancer: a population-based study. *Int J Clin Oncol, 27*(4), 707-716. 10.1007/s10147-022-02115-x

Hanna, K., & Mayden, K. (2021). Chemotherapy Treatment Considerations in Metastatic Breast Cancer. *J Adv Pract Oncol, 12*(Suppl 2), 6-12. 10.6004/jadpro.2021.12.2.11

Hanusch, C., Schneeweiss, A., Loibl, S., Untch, M., Paepke, S., Kümmel, S., Jackisch, C., Huober, J., Hilfrich, J., Gerber, B., Eidtmann, H., Denkert, C., Costa, S., Blohmer, J. U., Engels, K., Burchardi, N., & von Minckwitz, G. (2015). Dual Blockade with AFatinib and Trastuzumab as NEoadjuvant Treatment for Patients with Locally Advanced or Operable Breast Cancer Receiving Taxane-Anthracycline Containing Chemotherapy-DAFNE (GBG-70). *Clin Cancer Res, 21*(13), 2924-2931. 10.1158/1078-0432.Ccr-14-2774

Hao, Z., Xu, J., Zhao, H., Zhou, W., Liu, Z., He, S., Yin, X., Zhang, B., Wang, Z., & Zhou, X. (2022). The inhibition of tamoxifen on UGT2B gene expression and enzyme activity in rat liver contribute to the estrogen homeostasis dysregulation. *BMC Pharmacology and Toxicology, 23*(1), 33. 10.1186/s40360-022-00574-6

Harbeck, N., Huang, C. S., Hurvitz, S., Yeh, D. C., Shao, Z., Im, S. A., Jung, K. H., Shen, K., Ro, J., Jassem, J., Zhang, Q., Im, Y. H., Wojtukiewicz, M., Sun, Q., Chen, S. C., Goeldner, R. G., Uttenreuther-Fischer, M., Xu, B., & Piccart-Gebhart, M. (2016). Afatinib plus vinorelbine versus trastuzumab plus vinorelbine in patients with HER2-overexpressing metastatic breast cancer who had progressed on one previous trastuzumab treatment (LUX-Breast 1): an open-label, randomised, phase 3 trial. *Lancet Oncol, 17*(3), 357-366. 10.1016/s1470-2045(15)00540-9

Harbeck, N., Penault-Llorca, F., Cortes, J., Gnant, M., Houssami, N., Poortmans, P., Ruddy, K., Tsang, J., & Cardoso, F. (2019). Breast cancer. *Nat Rev Dis Primers, 5*(1), 66. 10.1038/s41572-019-0111-2

Harrington, W. R., Sengupta, S., & Katzenellenbogen, B. S. (2006). Estrogen Regulation of the Glucuronidation Enzyme UGT2B15 in Estrogen Receptor-Positive Breast Cancer Cells. *Endocrinology, 147*(8), 3843-3850. 10.1210/en.2006-0358

Harris, S. L., & Levine, A. J. (2005). The p53 pathway: positive and negative feedback loops. *Oncogene, 24*(17), 2899-2908. 10.1038/sj.onc.1208615

Hassan, Svensson, Ljungman, Björkstrand, Olsson, Bielenstein, Abdel, R., Nilsson, Johansson, & Karlsson. (1999). A mechanism-based pharmacokinetic-enzyme model for cyclophosphamide autoinduction in breast cancer patients. *British journal of clinical pharmacology, 48*(5), 669-677. 10.1046/j.1365-2125.1999.00090.x

Haupt, L. J., Kazmi, F., Ogilvie, B. W., Buckley, D. B., Smith, B. D., Leatherman, S., Paris, B., Parkinson, O., & Parkinson, A. (2015). The Reliability of Estimating K_i Values for Direct, Reversible Inhibition of Cytochrome P450 Enzymes from Corresponding IC₅₀ Values: A Retrospective Analysis of 343 Experiments. *Drug Metabolism and Disposition, 43*(11), 1744-1750. 10.1124/dmd.115.066597

He, B.-X., Qiao, B., Lam, A. K.-Y., Zhao, X.-L., Zhang, W.-Z., & Liu, H. (2018). Association between UDP-glucuronosyltransferase 2B7 tagSNPs and breast cancer risk in Chinese females. *Clinical and Experimental Pharmacology and Physiology, 45*(5), 437-443. 10.1111/1440-1681.12908

He, J., Fortunati, E., Liu, D. X., & Li, Y. (2021). Pleiotropic Roles of ABC Transporters in Breast Cancer. *Int J Mol Sci, 22*(6). 10.3390/ijms22063199

He, M., & Wei, M. J. (2012). Reversing multidrug resistance by tyrosine kinase inhibitors. *Chin J Cancer, 31*(3), 126-133. 10.5732/cjc.011.10315

Hegi, M., Diserens, A.-C., Bady, P., Kamoshima, Y., Kouwenhoven, M., Delorenzi, M., Lambiv, W., Hamou, M.-F., Matter, M., Koch, A., Heppner, F., Yonekawa, Y., Merlo, A., Frei, K., Mariani, L., & Hofer, S. (2011). Pathway Analysis of Glioblastoma Tissue after Preoperative Treatment with the EGFR Tyrosine Kinase Inhibitor Gefitinib--A Phase II Trial. *Molecular cancer therapeutics, 10*, 1102-1112. 10.1158/1535-7163.MCT-11-0048

Hembruff, S. L., Laberge, M. L., Villeneuve, D. J., Guo, B., Veitch, Z., Cecchetto, M., & Parissenti, A. M. (2008). Role of drug transporters and drug accumulation in the temporal acquisition of drug resistance. *BMC cancer, 8*(1), 318. 10.1186/1471-2407-8-318

Hickey, T. E., Selth, L. A., Chia, K. M., Laven-Law, G., Milioli, H. H., Roden, D., Jindal, S., Hui, M., Finlay-Schultz, J., Ebrahimie, E., Birrell, S. N., Stelloo, S., Iggo, R., Alexandrou, S., Caldon, C. E., Abdel-Fatah, T. M., Ellis, I. O., Zwart, W., Palmieri, C., Sartorius, C. A., Swarbrick, A., Lim, E., Carroll, J. S., & Tilley, W. D. (2021). The androgen receptor is a tumor suppressor in estrogen receptor–positive breast cancer. *Nature Medicine, 27*(2), 310-320. 10.1038/s41591-020-01168-7

Hohmann, N., Bozorgmehr, F., Christopoulos, P., Mikus, G., Blank, A., Burhenne, J., Thomas, M., & Haefeli, W. E. (2021). Pharmacoenhancement of Low Crizotinib Plasma Concentrations in Patients with Anaplastic Lymphoma Kinase-Positive Non-Small Cell Lung Cancer using the CYP3A Inhibitor Cobicistat. *Clin Transl Sci, 14*(2), 487-491. 10.1111/cts.12921

Holanek, M., Selingerova, I., Bilek, O., Kazda, T., Fabian, P., Foretova, L., Zvarikova, M., Obermannova, R., Kolouskova, I., Coufal, O., Petrakova, K., Svoboda, M., & Poprach, A. (2021). Neoadjuvant Chemotherapy of Triple-Negative Breast Cancer: Evaluation of Early Clinical Response, Pathological Complete Response Rates, and Addition of Platinum Salts Benefit Based on Real-World Evidence. *Cancers (Basel), 13*(7). 10.3390/cancers13071586

Holohan, C., Van Schaeybroeck, S., Longley, D. B., & Johnston, P. G. (2013). Cancer drug resistance: an evolving paradigm. *Nature Reviews Cancer, 13*(10), 714-726. 10.1038/nrc3599

Holthe, M., Rakvåg, T. N., Klepstad, P., Idle, J. R., Kaasa, S., Krokan, H. E., & Skorpen, F. (2003). Sequence variations in the UDP-glucuronosyltransferase 2B7 (UGT2B7) gene: identification of 10 novel single nucleotide polymorphisms (SNPs) and analysis of their relevance to morphine glucuronidation in cancer patients. *The Pharmacogenomics Journal, 3*(1), 17-26. 10.1038/sj.tpj.6500139

Hovelson, D. H., Xue, Z., Zawistowski, M., Ehm, M. G., Harris, E. C., Stocker, S. L., Gross, A. S., Jang, I. J., Ieiri, I., Lee, J. E., Cardon, L. R., Chissoe, S. L., Abecasis, G., & Nelson, M. R. (2017). Characterization of ADME gene variation in 21 populations by exome sequencing. *Pharmacogenetics and genomics, 27*(3), 89-100. 10.1097/fpc.0000000000000260

Hsiau, T., Conant, D., Rossi, N., Maures, T., Waite, K., Yang, J., Joshi, S., Kelso, R., Holden, K., Enzmann, B. L., & Stoner, R. (2019). Inference of CRISPR Edits from Sanger Trace Data. *bioRxiv*, 251082. 10.1101/251082

Hsieh, Y., & Tseng, J.-J. (2020). Azidothymidine (AZT) Inhibits Proliferation of Human Ovarian Cancer Cells by Regulating Cell Cycle Progression. *Anticancer Res, 40*(10), 5517-5527. 10.21873/anticanres.14564

Hsu, J. L., & Hung, M. C. (2016). The role of HER2, EGFR, and other receptor tyrosine kinases in breast cancer. *Cancer Metastasis Rev, 35*(4), 575-588. 10.1007/s10555-016-9649-6

Hu, D. G., Hulin, J.-A., Wijayakumara, D. D., McKinnon, R. A., Mackenzie, P. I., & Meech, R. (2018). Intergenic Splicing between Four Adjacent UGT Genes (2B15, 2B29P2, 2B17, 2B29P1) Gives Rise to Variant UGT Proteins That Inhibit Glucuronidation via Protein-Protein Interactions. *Mol Pharmacol, 94*(3), 938-952. 10.1124/mol.118.111773

Hu, D. G., Hulin, J. u.-A., Nair, P. C., Haines, A. Z., McKinnon, R. A., Mackenzie, P. I., & Meech, R. (2019a). The UGTome: The expanding diversity of UDP glycosyltransferases and its impact on small molecule metabolism. *Pharmacology & Therapeutics, 204*, 107414. 10.1016/j.pharmthera.2019.107414

Hu, D. G., & Mackenzie, P. I. (2009). Estrogen Receptor α, Fos-Related Antigen-2, and c-Jun Coordinately Regulate Human UDP Glucuronosyltransferase 2B15 and 2B17 Expression in Response to 17β-Estradiol in MCF-7 Cells. *Mol Pharmacol, 76*(2), 425-439. 10.1124/mol.109.057380

Hu, D. G., Mackenzie, P. I., Hulin, J.-A., McKinnon, R. A., & Meech, R. (2022). Regulation of human UDP-glycosyltransferase (UGT) genes by miRNAs. *Drug Metabolism Reviews, 54*(2), 120-140. 10.1080/03602532.2022.2048846

Hu, D. G., Mackenzie, P. I., Lu, L., Meech, R., & McKinnon, R. A. (2015). Induction of human UDP-Glucuronosyltransferase 2B7 gene expression by cytotoxic anticancer drugs in liver cancer HepG2 cells. *Drug Metab Dispos, 43*(5), 660-668. 10.1124/dmd.114.062380

Hu, D. G., Mackenzie, P. I., McKinnon, R. A., & Meech, R. (2016). Genetic polymorphisms of human UDP-glucuronosyltransferase (UGT) genes and cancer risk. *Drug Metabolism Reviews, 48*(1), 47-69. 10.3109/03602532.2015.1131292

Hu, D. G., Mackenzie, P. I., Nair, P. C., McKinnon, R. A., & Meech, R. (2020). The Expression Profiles of ADME Genes in Human Cancers and Their Associations with Clinical Outcomes. *Cancers (Basel), 12*(11). 10.3390/cancers12113369

Hu, D. G., Marri, S., McKinnon, R. A., Mackenzie, P. I., & Meech, R. (2019b). Deregulation of the Genes that Are Involved in Drug Absorption, Distribution, Metabolism, and Excretion in Hepatocellular Carcinoma. *J Pharmacol Exp Ther, 368*(3), 363-381. 10.1124/jpet.118.255018

Hu, D. G., Meech, R., Lu, L., McKinnon, R. A., & Mackenzie, P. I. (2014a). Polymorphisms and haplotypes of the UDP-glucuronosyltransferase 2B7 gene promoter. *Drug Metab Dispos, 42*(5), 854-862. 10.1124/dmd.113.056630

Hu, D. G., Meech, R., McKinnon, R. A., & Mackenzie, P. I. (2014b). Transcriptional regulation of human UDP-glucuronosyltransferase genes. *Drug Metabolism Reviews, 46*(4), 421-458. 10.3109/03602532.2014.973037

Hu, D. G., Rogers, A., & Mackenzie, P. I. (2014c). Epirubicin upregulates UDP glucuronosyltransferase 2B7 expression in liver cancer cells via the p53 pathway. *Mol Pharmacol, 85*(6), 887-897. 10.1124/mol.114.091603

Huang, S., Benavente, S., Armstrong, E. A., Li, C., Wheeler, D. L., & Harari, P. M. (2011). p53 modulates acquired resistance to EGFR inhibitors and radiation. *Cancer Res, 71*(22), 7071-7079. 10.1158/0008-5472.Can-11-0128

Hull, M. W., & Montaner, J. S. (2011). Ritonavir-boosted protease inhibitors in HIV therapy. *Ann Med, 43*(5), 375-388. 10.3109/07853890.2011.572905

Hunz, M., Jetter, A., Warm, M., Pantke, E., Tuscher, M., Hempel, G., Jaehde, U., Untch, M., Kurbacher, C., & Fuhr, U. (2007). Plasma and Tissue Pharmacokinetics of Epirubicin and Paclitaxel in Patients Receiving Neoadjuvant Chemotherapy for Locally Advanced Primary Breast Cancer. *Clinical Pharmacology & Therapeutics, 81*(5), 659-668. 10.1038/sj.clpt.6100067

Iacopetta, D., Ceramella, J., Catalano, A., Scali, E., Scumaci, D., Pellegrino, M., Aquaro, S., Saturnino, C., & Sinicropi, M. S. (2023). Impact of Cytochrome P450 Enzymes on the Phase I Metabolism of Drugs. *Applied Sciences, 13*(10), 6045.

Iancu, G., Serban, D., Badiu, C. D., Tanasescu, C., Tudosie, M. S., Tudor, C., Costea, D. O., Zgura, A., Iancu, R., & Vasile, D. (2022). Tyrosine kinase inhibitors in breast cancer (Review). *Experimental and therapeutic medicine, 23*(2), 114-114. 10.3892/etm.2021.11037

Ibrahim, N. K. (2021). Ixabepilone: Overview of Effectiveness, Safety, and Tolerability in Metastatic Breast Cancer [Review]. *Frontiers in oncology, 11*. 10.3389/fonc.2021.617874

Innocenti, F., Iyer, L., Ramírez, J., Green, M. D., & Ratain, M. J. (2001). Epirubicin Glucuronidation Is Catalyzed by Human UDP-Glucuronosyltransferase 2B7. *Drug Metabolism and Disposition, 29*(5), 686-692.

Innocenti, F., Liu, W., Fackenthal, D., Ramírez, J., Chen, P., Ye, X., Wu, X., Zhang, W., Mirkov, S., Das, S., Cook, E., Jr., & Ratain, M. J. (2008). Single nucleotide polymorphism discovery and functional assessment of variation in the UDP-glucuronosyltransferase 2B7 gene. *Pharmacogenetics and genomics, 18*(8), 683-697. 10.1097/FPC.0b013e3283037fe4

Innocenti, F., Schilsky, R. L., Ramírez, J., Janisch, L., Undevia, S., House, L. K., Das, S., Wu, K., Turcich, M., Marsh, R., Karrison, T., Maitland, M. L., Salgia, R., & Ratain, M. J. (2014). Dose-finding and pharmacokinetic study to optimize the dosing of irinotecan according to the UGT1A1 genotype of patients with cancer. *J Clin Oncol, 32*(22), 2328-2334. 10.1200/jco.2014.55.2307

Iqbal, N., & Iqbal, N. (2014). Human Epidermal Growth Factor Receptor 2 (HER2) in Cancers: Overexpression and Therapeutic Implications. *Mol Biol Int, 2014*, 852748. 10.1155/2014/852748

Ishii, Y., Hansen, A. J., & Mackenzie, P. I. (2000). Octamer transcription factor-1 enhances hepatic nuclear factor-1alpha-mediated activation of the human UDP glucuronosyltransferase 2B7 promoter. *Mol Pharmacol, 57*(5), 940-947.

Italia, C., Paglia, L., Trabattoni, A., Luchini, S., Villas, F., Beretta, L., Marelli, G., & Natale, N. (1983). Distribution of 4'epi-doxorubicin in human tissues. *Br J Cancer, 47*(4), 545-547. 10.1038/bjc.1983.86

Iusuf, D., Teunissen, S. F., Wagenaar, E., Rosing, H., Beijnen, J. H., & Schinkel, A. H. (2011). P-Glycoprotein (ABCB1) Transports the Primary Active Tamoxifen Metabolites Endoxifen and 4-Hydroxytamoxifen and Restricts Their Brain Penetration. *Journal of Pharmacology and Experimental Therapeutics, 337*(3), 710-717. 10.1124/jpet.110.178301

Iyer, L. V., Ho, M. N., Shinn, W. M., Bradford, W. W., Tanga, M. J., Nath, S. S., & Green, C. E. (2003). Glucuronidation of 1'-Hydroxyestragole (1'-HE) by Human UDP-Glucuronosyltransferases UGT2B7 and UGT1A9. *Toxicological Sciences, 73*(1), 36-43. 10.1093/toxsci/kfg066

Jahanzeb, M. (2008). Adjuvant trastuzumab therapy for HER2-positive breast cancer. *Clin Breast Cancer, 8*(4), 324-333. 10.3816/CBC.2008.n.037

Janicki, P. K. (1997). Pharmacology of morphine metabolites. *Current Pain and Headache Reports, 1*(4), 264-270. 10.1007/BF02938295

Jaramillo, A. C., Al Saig, F., Cloos, J., Jansen, G., & Peters, G. J. (2018). How to overcome ATP-binding cassette drug efflux transporter-mediated drug resistance? *Cancer Drug Resistance, 1*(1), 6-29.

Jawad, B., Poudel, L., Podgornik, R., & Ching, W.-Y. (2020). Thermodynamic Dissection of the Intercalation Binding Process of Doxorubicin to dsDNA with Implications of Ionic and Solvent Effects. *The Journal of Physical Chemistry B, 124*(36), 7803-7818. 10.1021/acs.jpcb.0c05840

Jawad, B., Poudel, L., Podgornik, R., Steinmetz, N. F., & Ching, W.-Y. (2019). Molecular mechanism and binding free energy of doxorubicin intercalation in DNA. *Physical Chemistry Chemical Physics, 21*(7), 3877-3893. 10.1039/C8CP06776G

Jensen, K. T., Fløe, L., Petersen, T. S., Huang, J., Xu, F., Bolund, L., Luo, Y., & Lin, L. (2017). Chromatin accessibility and guide sequence secondary structure affect CRISPR-Cas9 gene editing efficiency. *FEBS Lett, 591*(13), 1892-1901. 10.1002/1873-3468.12707

Jeong, Y., Bae, S. Y., You, D., Jung, S. P., Choi, H. J., Kim, I., Lee, S. K., Yu, J., Kim, S. W., Lee, J. E., Kim, S., & Nam, S. J. (2019). EGFR is a Therapeutic Target in Hormone Receptor-Positive Breast Cancer. *Cell Physiol Biochem, 53*(5), 805-819. 10.33594/000000174

Ji, W. J., Lu, X., Wang, Y. G., & Chen, L. W. (2024). A comprehensive clinical evaluation of HER2-TKIs in patients with previously treated HER2-positive metastatic breast cancer. *Anticancer Drugs*. 10.1097/cad.0000000000001604

Jia, T., Zhang, L., Duan, Y., Zhang, M., Wang, G., Zhang, J., & Zhao, Z. (2014). The differential susceptibilities of MCF-7 and MDA-MB-231 cells to the cytotoxic effects of curcumin are associated with the PI3K/Akt-SKP2-Cip/Kips pathway. *Cancer Cell Int, 14*(1), 126. 10.1186/s12935-014-0126-4

Jiang, Z., Yan, M., Hu, X., Zhang, Q., Ouyang, Q., Feng, J., Yin, Y., Sun, T., Tong, Z., & Wang, X. (2019). Pyrotinib combined with capecitabine in women with HER2+ metastatic breast cancer previously treated with trastuzumab and taxanes: A randomized phase III study. American Society of Clinical Oncology.

Jin, C.-J., Miners, J. O., Burchell, B., & Mackenzie, P. I. (1993a). The glucuronidation of hydroxylated metabolites of benzo[α]pyrene and 2-acetylaminofluorene by cDNA-expressed human UDP-glucuronosyltransferases. *Carcinogenesis, 14*(12), 2637-2639. 10.1093/carcin/14.12.2637

Jin, C., Miners, J., Lillywhite, K., & Mackenzie, P. (1993b). Complementary deoxyribonucleic acid cloning and expression of a human liver uridine diphosphate-glucuronosyltransferase glucuronidating carboxylic acid-containing drugs. *Journal of Pharmacology and Experimental Therapeutics, 264*(1), 475-479.

Jo, A., Choi, T. G., Jo, Y. H., Jyothi, K. R., Nguyen, M. N., Kim, J.-H., Lim, S., Shahid, M., Akter, S., Lee, S., Lee, K. H., Kim, W., Cho, H., Lee, J., Shokat, K. M., Yoon, K.-S., Kang, I., Ha, J., & Kim, S. S. (2016). Inhibition of Carbonyl Reductase 1 Safely Improves the Efficacy of Doxorubicin in Breast Cancer Treatment. *Antioxidants & Redox Signaling, 26*(2), 70-83. 10.1089/ars.2015.6457

Joensuu, H., Kellokumpu-Lehtinen, P. L., Huovinen, R., Jukkola-Vuorinen, A., Tanner, M., Kokko, R., Ahlgren, J., Auvinen, P., Lahdenperä, O., Kosonen, S., Villman, K., Nyandoto, P., Nilsson, G., Poikonen-Saksela, P., Kataja, V., Junnila, J., Bono, P., & Lindman, H. (2017). Adjuvant Capecitabine in Combination With Docetaxel, Epirubicin, and Cyclophosphamide for Early Breast Cancer: The Randomized Clinical FinXX Trial. *JAMA Oncol, 3*(6), 793-800. 10.1001/jamaoncol.2016.6120

Johnson, J. R., Cohen, M., Sridhara, R., Chen, Y.-F., Williams, G. M., Duan, J., Gobburu, J., Booth, B., Benson, K., Leighton, J., Hsieh, L. S., Chidambaram, N., Zimmerman, P., & Pazdur, R. (2005). Approval Summary for Erlotinib for Treatment of Patients with Locally Advanced or Metastatic Non–Small Cell Lung Cancer after Failure of at Least One Prior Chemotherapy Regimen. *Clinical Cancer Research, 11*(18), 6414-6421. 10.1158/1078-0432.Ccr-05-0790

Johnson, M. D., Zuo, H., Lee, K. H., Trebley, J. P., Rae, J. M., Weatherman, R. V., Desta, Z., Flockhart, D. A., & Skaar, T. C. (2004). Pharmacological characterization of 4-hydroxy-N-desmethyl tamoxifen, a novel active metabolite of tamoxifen. *Breast Cancer Res Treat, 85*(2), 151-159. 10.1023/B:BREA.0000025406.31193.e8

Johnston, S., Pippen, J., Jr., Pivot, X., Lichinitser, M., Sadeghi, S., Dieras, V., Gomez, H. L., Romieu, G., Manikhas, A., Kennedy, M. J., Press, M. F., Maltzman, J., Florance, A., O'Rourke, L., Oliva, C., Stein, S., & Pegram, M. (2009). Lapatinib combined with letrozole versus letrozole and placebo as first-line therapy for postmenopausal hormone receptor-positive metastatic breast cancer. *J Clin Oncol, 27*(33), 5538-5546. 10.1200/jco.2009.23.3734

Jones, H., Chen, Y., Gibson, C., Heimbach, T., Parrott, N., Peters, S., Snoeys, J., Upreti, V., Zheng, M., & Hall, S. (2015). Physiologically based pharmacokinetic modeling in drug discovery and development: A pharmaceutical industry perspective. *Clinical Pharmacology & Therapeutics, 97*(3), 247-262. 10.1002/cpt.37

Jordan, M. A., Kamath, K., Manna, T., Okouneva, T., Miller, H. P., Davis, C., Littlefield, B. A., & Wilson, L. (2005). The primary antimitotic mechanism of action of the synthetic halichondrin E7389 is suppression of microtubule growth. *Molecular cancer therapeutics, 4*(7), 1086-1095. 10.1158/1535-7163.MCT-04-0345

Joy, A. A., Vos, L. J., Pituskin, E., Cook, S. F., Bies, R. R., Vlahadamis, A., King, K., Basi, S. K., Meza-Junco, J., Mackey, J. R., Stanislaus, A., Damaraju, V. L., Damaraju, S., & Sawyer, M. B. (2021). Uridine Glucuronosyltransferase 2B7 Polymorphism-Based Pharmacogenetic Dosing of Epirubicin in FEC Chemotherapy for Early-Stage Breast Cancer. *Clin Breast Cancer, 21*(5), e584-e593. 10.1016/j.clbc.2021.03.001

Jude, A. R., Little, J. M., Bull, A. W., Podgorski, I., & Radominska-Pandya, A. (2001). 13-hydroxy- and 13-oxooctadecadienoic acids: novel substrates for human UDP-glucuronosyltransferases. *Drug Metab Dispos, 29*(5), 652-655.

Jung, S., Kim, D. H., Choi, Y. J., Kim, S. Y., Park, H., Lee, H., Choi, C.-M., Sung, Y. H., Lee, J. C., & Rho, J. K. (2021). Contribution of p53 in sensitivity to EGFR tyrosine kinase inhibitors in non-small cell lung cancer. *Scientific Reports, 11*(1), 19667. 10.1038/s41598-021-99267-z

Kamdem, L. K., Liu, Y., Stearns, V., Kadlubar, S. A., Ramirez, J., Jeter, S., Shahverdi, K., Ward, B. A., Ogburn, E., Ratain, M. J., Flockhart, D. A., & Desta, Z. (2010). In vitro and in vivo oxidative metabolism and glucuronidation of anastrozole. *British journal of clinical pharmacology, 70*(6), 854-869. 10.1111/j.1365-2125.2010.03791.x

Kamiloglu, S., Sari, G., Ozdal, T., & Capanoglu, E. (2020). Guidelines for cell viability assays. *Food Frontiers, 1*(3), 332-349. 10.1002/fft2.44

Kamiyama, N., Takagi, S., Yamamoto, C., Kudo, T., Nakagawa, T., Takahashi, M., Nakanishi, K., Takahashi, H., Todo, S., & Iseki, K. (2006). Expression of ABC transporters in human hepatocyte carcinoma cells with cross-resistance to epirubicin and mitoxantrone. *Anticancer Res, 26*(2a), 885-888.

Kang, J. S., & Lee, M. H. (2009). Overview of therapeutic drug monitoring. *Korean J Intern Med, 24*(1), 1-10. 10.3904/kjim.2009.24.1.1

Kato, S., Han, S. Y., Liu, W., Otsuka, K., Shibata, H., Kanamaru, R., & Ishioka, C. (2003). Understanding the function-structure and function-mutation relationships of p53 tumor suppressor protein by high-resolution missense mutation analysis. *Proc Natl Acad Sci U S A, 100*(14), 8424-8429. 10.1073/pnas.1431692100

Kato, Y., Nakajima, M., Oda, S., Fukami, T., & Yokoi, T. (2012). Human UDP-Glucuronosyltransferase Isoforms Involved in Haloperidol Glucuronidation and Quantitative Estimation of Their Contribution. *Drug Metabolism and Disposition, 40*(2), 240-248. 10.1124/dmd.111.042150

Kehrer, D. F., Mathijssen, R. H., Verweij, J., de Bruijn, P., & Sparreboom, A. (2002). Modulation of irinotecan metabolism by ketoconazole. *J Clin Oncol, 20*(14), 3122-3129. 10.1200/jco.2002.08.177

Kent, W. J. (2002). BLAT—The BLAST-Like Alignment Tool. *Genome Research, 12*(4), 656-664. 10.1101/gr.229202

Kent, W. J., Sugnet, C. W., Furey, T. S., Roskin, K. M., Pringle, T. H., Zahler, A. M., Haussler, & David. (2002). The Human Genome Browser at UCSC. *Genome Research, 12*(6), 996-1006. 10.1101/gr.229102

Kerhoas, M., Le Vée, M., Carteret, J., Jouan, E., Tastet, V., Bruyère, A., Huc, L., & Fardel, O. (2024). Inhibition of human drug transporter activities by succinate dehydrogenase inhibitors. *Chemosphere, 358*, 142122. 10.1016/j.chemosphere.2024.142122

Khasraw, M., Bell, R., & Dang, C. (2012a). Epirubicin: Is it like doxorubicin in breast cancer? A clinical review. *The Breast, 21*(2), 142-149. 10.1016/j.breast.2011.12.012

Khasraw, M., Bell, R., & Dang, C. (2012b). Epirubicin: is it like doxorubicin in breast cancer? A clinical review. *Breast, 21*(2), 142-149. 10.1016/j.breast.2011.12.012

Kilickap, S., Demirci, U., Karadurmus, N., Dogan, M., Akinci, B., & Sendur, M. A. N. (2018). Endpoints in oncology clinical trials. *J buon, 23*(7), 1-6.

Kim, H., Abd Elmageed, Z. Y., Ju, J., Naura, A. S., Abdel-Mageed, A. B., Varughese, S., Paul, D., Alahari, S., Catling, A., Kim, J. G., & Boulares, A. H. (2013). PDZK1 is a novel factor in breast cancer that is indirectly regulated by estrogen through IGF-1R and promotes estrogen-mediated growth. *Mol Med, 19*(1), 253-262. 10.2119/molmed.2011.00001

Kim, H., & Ronai, Z. A. (2020). PRMT5 function and targeting in cancer. *Cell Stress, 4*(8), 199-215. 10.15698/cst2020.08.228

King, C. D., Rios, G. R., Green, M. D., & Tephly, T. R. (2000). UDP-glucuronosyltransferases. *Curr Drug Metab, 1*(2), 143-161. 10.2174/1389200003339171

Kisanga, E. R., Gjerde, J., Guerrieri-Gonzaga, A., Pigatto, F., Pesci-Feltri, A., Robertson, C., Serrano, D., Pelosi, G., Decensi, A., & Lien, E. A. (2004). Tamoxifen and Metabolite Concentrations in Serum and Breast Cancer Tissue during Three Dose Regimens in a Randomized Preoperative Trial. *Clinical Cancer Research, 10*(7), 2336-2343. 10.1158/1078-0432.Ccr-03-0538

Kitazaki, T., Oka, M., Nakamura, Y., Tsurutani, J., Doi, S., Yasunaga, M., Takemura, M., Yabuuchi, H., Soda, H., & Kohno, S. (2005). Gefitinib, an EGFR tyrosine kinase inhibitor, directly inhibits the function of P-glycoprotein in multidrug resistant cancer cells. *Lung Cancer, 49*(3), 337-343. 10.1016/j.lungcan.2005.03.035

Klein, D. J., Thorn, C. F., Desta, Z., Flockhart, D. A., Altman, R. B., & Klein, T. E. (2013). PharmGKB summary: tamoxifen pathway, pharmacokinetics. *Pharmacogenetics and genomics, 23*(11), 643-647. 10.1097/FPC.0b013e3283656bc1

Kluwe, F., Michelet, R., Mueller-Schoell, A., Maier, C., Klopp-Schulze, L., van Dyk, M., Mikus, G., Huisinga, W., & Kloft, C. (2021). Perspectives on model-informed precision dosing in the digital health era: challenges, opportunities, and recommendations. *Clinical Pharmacology & Therapeutics, 109*(1), 29-36.

Knights, K. M., Winner, L. K., Elliot, D. J., Bowalgaha, K., & Miners, J. O. (2009). Aldosterone glucuronidation by human liver and kidney microsomes and recombinant UDP-glucuronosyltransferases: Inhibition by NSAIDs. *British journal of clinical pharmacology, 68*(3), 402-412. 10.1111/j.1365-2125.2009.03469.x

Knowlden, J. M., Hutcheson, I. R., Jones, H. E., Madden, T., Gee, J. M., Harper, M. E., Barrow, D., Wakeling, A. E., & Nicholson, R. I. (2003). Elevated levels of epidermal growth factor receptor/c-erbB2 heterodimers mediate an autocrine growth regulatory pathway in tamoxifen-resistant MCF-7 cells. *Endocrinology, 144*(3), 1032-1044. 10.1210/en.2002-220620

Koboldt, D. C., Fulton, R. S., McLellan, M. D., Schmidt, H., Kalicki-Veizer, J., McMichael, J. F., Fulton, L. L., Dooling, D. J., Ding, L., Mardis, E. R., Wilson, R. K., Ally, A., Balasundaram, M., Butterfield, Y. S. N., Carlsen, R., Carter, C., Chu, A., Chuah, E., Chun, H.-J. E., Coope, R. J. N., Dhalla, N., Guin, R., Hirst, C., Hirst, M., Holt, R. A., Lee, D., Li, H. I., Mayo, M., Moore, R. A., Mungall, A. J., Pleasance, E., Gordon Robertson, A., Schein, J. E., Shafiei, A., Sipahimalani, P., Slobodan, J. R., Stoll, D., Tam, A., Thiessen, N., Varhol, R. J., Wye, N., Zeng, T., Zhao, Y., Birol, I., Jones, S. J. M., Marra, M. A., Cherniack, A. D., Saksena, G., Onofrio, R. C., Pho, N. H., Carter, S. L., Schumacher, S. E., Tabak, B., Hernandez, B., Gentry, J., Nguyen, H., Crenshaw, A., Ardlie, K., Beroukhim, R., Winckler, W., Getz, G., Gabriel, S. B., Meyerson, M., Chin, L., Park, P. J., Kucherlapati, R., Hoadley, K. A., Todd Auman, J., Fan, C., Turman, Y. J., Shi, Y., Li, L., Topal, M. D., He, X., Chao, H.-H., Prat, A., Silva, G. O., Iglesia, M. D., Zhao, W., Usary, J., Berg, J. S., Adams, M., Booker, J., Wu, J., Gulabani, A., Bodenheimer, T., Hoyle, A. P., Simons, J. V., Soloway, M. G., Mose, L. E., Jefferys, S. R., Balu, S., Parker, J. S., Neil Hayes, D., Perou, C. M., Malik, S., Mahurkar, S., Shen, H., Weisenberger, D. J., Triche Jr, T., Lai, P. H., Bootwalla, M. S., Maglinte, D. T., Berman, B. P., Van Den Berg, D. J., Baylin, S. B., Laird, P. W., Creighton, C. J., Donehower, L. A., Getz, G., Noble, M., Voet, D., Saksena, G., Gehlenborg, N., DiCara, D., Zhang, J., Zhang, H., Wu, C.-J., Yingchun Liu, S., Lawrence, M. S., Zou, L., Sivachenko, A., Lin, P., Stojanov, P., Jing, R., Cho, J., Sinha, R., Park, R. W., Nazaire, M.-D., Robinson, J., Thorvaldsdottir, H., Mesirov, J., Park, P. J., Chin, L., Reynolds, S., Kreisberg, R. B., Bernard, B., Bressler, R., Erkkila, T., Lin, J., Thorsson, V., Zhang, W., Shmulevich, I., Ciriello, G., Weinhold, N., Schultz, N., Gao, J., Cerami, E., Gross, B., Jacobsen, A., Sinha, R., Arman Aksoy, B., Antipin, Y., Reva, B., Shen, R., Taylor, B. S., Ladanyi, M., Sander, C., Anur, P., Spellman, P. T., Lu, Y., Liu, W., Verhaak, R. R. G., Mills, G. B., Akbani, R., Zhang, N., Broom, B. M., Casasent, T. D., Wakefield, C., Unruh, A. K., Baggerly, K., Coombes, K., Weinstein, J. N., Haussler, D., Benz, C. C., Stuart, J. M., Benz, S. C., Zhu, J., Szeto, C. C., Scott, G. K., Yau, C., Paull, E. O., Carlin, D., Wong, C., Sokolov, A., Thusberg, J., Mooney, S., Ng, S., Goldstein, T. C., Ellrott, K., Grifford, M., Wilks, C., Ma, S., Craft, B., Yan, C., Hu, Y., Meerzaman, D., Gastier-Foster, J. M., Bowen, J., Ramirez, N. C., Black, A. D., Pyatt, R. E., White, P., Zmuda, E. J., Frick, J., Lichtenberg, T. M., Brookens, R., George, M. M., Gerken, M. A., Harper, H. A., Leraas, K. M., Wise, L. J., Tabler, T. R., McAllister, C., Barr, T., Hart-Kothari, M., Tarvin, K., Saller, C., Sandusky, G., Mitchell, C., Iacocca, M. V., Brown, J., Rabeno, B., Czerwinski, C., Petrelli, N., Dolzhansky, O., Abramov, M., Voronina, O., Potapova, O., Marks, J. R., Suchorska, W. M., Murawa, D., Kycler, W., Ibbs, M., Korski, K., Spychała, A., Murawa, P., Brzeziński, J. J., Perz, H., Łaźniak, R., Teresiak, M., Tatka, H., Leporowska, E., Bogusz-Czerniewicz, M., Malicki, J., Mackiewicz, A., Wiznerowicz, M., Van Le, X., Kohl, B., Viet Tien, N., Thorp, R., Van Bang, N., Sussman, H., Duc Phu, B., Hajek, R., Phi Hung, N., Viet The Phuong, T., Quyet Thang, H., Zaki Khan, K., Penny, R., Mallery, D., Curley, E., Shelton, C., Yena, P., Ingle, J. N., Couch, F. J., Lingle, W. L., King, T. A., Maria Gonzalez-Angulo, A., Mills, G. B., Dyer, M. D., Liu, S., Meng, X., Patangan, M., The Cancer Genome Atlas, N., Genome sequencing

centres: Washington University in St, L., Genome characterization centres, B. C. C. A., Broad, I., Brigham, Women's, H., Harvard Medical, S., University of North Carolina, C. H., University of Southern California/Johns, H., Genome data analysis: Baylor College of, M., Institute for Systems, B., Memorial Sloan-Kettering Cancer, C., Oregon, H., Science, U., The University of Texas, M. D. A. C. C., University of California, S. C. B. I., Nci, Biospecimen core resource: Nationwide Children's Hospital Biospecimen Core, R., Tissue source sites, A.-I., Christiana, Cureline, Duke University Medical, C., The Greater Poland Cancer, C., Ilsbio, International Genomics, C., Mayo, C., Mskcc, & Center, M. D. A. C. (2012). Comprehensive molecular portraits of human breast tumours. *Nature, 490*(7418), 61-70. 10.1038/nature11412

Kokawa, Y., Kishi, N., Jinno, H., Tanaka-Kagawa, T., Narimatsu, S., & Hanioka, N. (2013). Effect of UDP-glucuronosyltransferase 1A8 polymorphism on raloxifene glucuronidation. *European Journal of Pharmaceutical Sciences, 49*(2), 199-205. 10.1016/j.ejps.2013.03.001

Konduri, S., Singh, M., Bobustuc, G., Rovin, R., & Kassam, A. (2020). Epidemiology of male breast cancer. *Breast, 54*, 8-14. 10.1016/j.breast.2020.08.010

Konopnicki, C. M., Dickmann, L. J., Tracy, J. M., Tukey, R. H., Wienkers, L. C., & Foti, R. S. (2013). Evaluation of UGT protein interactions in human hepatocytes: effect of siRNA down regulation of UGT1A9 and UGT2B7 on propofol glucuronidation in human hepatocytes. *Arch Biochem Biophys, 535*(2), 143-149. 10.1016/j.abb.2013.03.012

Kotler, E., Shani, O., Goldfeld, G., Lotan-Pompan, M., Tarcic, O., Gershoni, A., Hopf, T. A., Marks, D. S., Oren, M., & Segal, E. (2018). A Systematic p53 Mutation Library Links Differential Functional Impact to Cancer Mutation Pattern and Evolutionary Conservation. *Molecular Cell, 71*(1), 178-190.e178. 10.1016/j.molcel.2018.06.012

Koźmiński, P., Halik, P. K., Chesori, R., & Gniazdowska, E. (2020). Overview of Dual-Acting Drug Methotrexate in Different Neurological Diseases, Autoimmune Pathologies and Cancers. *Int J Mol Sci, 21*(10). 10.3390/ijms21103483

Kroll, T., Prescher, M., Smits, S. H. J., & Schmitt, L. (2021). Structure and Function of Hepatobiliary ATP Binding Cassette Transporters. *Chemical Reviews, 121*(9), 5240-5288. 10.1021/acs.chemrev.0c00659

Kruh, J. (1981). Effects of sodium butyrate, a new pharmacological agent, on cells in culture. *Molecular and Cellular Biochemistry, 42*(2), 65-82. 10.1007/BF00222695

Kruijtzer, C. M., Beijnen, J. H., & Schellens, J. H. (2002). Improvement of oral drug treatment by temporary inhibition of drug transporters and/or cytochrome P450 in the gastrointestinal tract and liver: an overview. *Oncologist, 7*(6), 516-530.

Kruminis-Kaszkiel, E., Juranek, J., Maksymowicz, W., & Wojtkiewicz, J. (2018). CRISPR/Cas9 Technology as an Emerging Tool for Targeting Amyotrophic Lateral Sclerosis (ALS). *Int J Mol Sci, 19*(3). 10.3390/ijms19030906

Kurian, A. W., Bondarenko, I., Jagsi, R., Friese, C. R., McLeod, M. C., Hawley, S. T., Hamilton, A. S., Ward, K. C., Hofer, T. P., & Katz, S. J. (2018). Recent Trends in Chemotherapy Use and Oncologists' Treatment Recommendations for Early-Stage Breast Cancer. *J Natl Cancer Inst, 110*(5), 493-500. 10.1093/jnci/djx239

Langsenlehner, U., Wolf, G., Langsenlehner, T., Gerger, A., Hofmann, G., Clar, H., Wascher, T. C., Paulweber, B., Samonigg, H., Krippl, P., & Renner, W. (2008). Genetic polymorphisms in the vascular endothelial growth factor gene and breast cancer risk. The Austrian "tumor of breast tissue: incidence, genetics, and environmental risk factors" study. *Breast Cancer Res Treat, 109*(2), 297-304. 10.1007/s10549-007-9655-z

Lankheet, N. A., Schaake, E. E., Burgers, S. A., van Pel, R., Beijnen, J. H., Huitema, A. D., & Klomp, H. (2015). Concentrations of Erlotinib in Tumor Tissue and Plasma in Non-Small-Cell Lung Cancer Patients After Neoadjuvant Therapy. *Clin Lung Cancer, 16*(4), 320-324. 10.1016/j.cllc.2014.12.012

Laptenko, O., & Prives, C. (2006). Transcriptional regulation by p53: one protein, many possibilities. *Cell Death & Differentiation, 13*(6), 951-961. 10.1038/sj.cdd.4401916

Larsen, A. B., Stockhausen, M. T., & Poulsen, H. S. (2010). Cell adhesion and EGFR activation regulate EphA2 expression in cancer. *Cell Signal, 22*(4), 636-644. 10.1016/j.cellsig.2009.11.018

Larsson, P., Engqvist, H., Biermann, J., Werner Rönnerman, E., Forssell-Aronsson, E., Kovács, A., Karlsson, P., Helou, K., & Parris, T. Z. (2020). Optimization of cell viability assays to improve replicability and reproducibility of cancer drug sensitivity screens. *Scientific Reports, 10*(1), 5798. 10.1038/s41598-020-62848-5

Lau, Y. K., Du, X., Rayannavar, V., Hopkins, B., Shaw, J., Bessler, E., Thomas, T., Pires, M. M., Keniry, M., Parsons, R. E., Cremers, S., Szabolcs, M., & Maurer, M. A. (2014). Metformin and erlotinib synergize to inhibit basal breast cancer. *Oncotarget, 5*(21), 10503-10517. 10.18632/oncotarget.2391

Lebwohl, D., Kay, A., Berg, W., Baladi, J. F., & Zheng, J. (2009). Progression-free survival: gaining on overall survival as a gold standard and accelerating drug development. *Cancer J, 15*(5), 386-394. 10.1097/PPO.0b013e3181b9c5ec

Lee, C. M., Davis, T. H., Deshmukh, H., & Bao, G. (2016). 131. Chromatin-Dependent Loci Accessibility Affects CRISPR-Cas9 Targeting Efficiency. *Molecular Therapy, 24*, S54. 10.1016/S1525-0016(16)32940-9

Lee, C. W., Martinez-Yamout, M. A., Dyson, H. J., & Wright, P. E. (2010). Structure of the p53 Transactivation Domain in Complex with the Nuclear Receptor Coactivator Binding Domain of CREB Binding Protein. *Biochemistry, 49*(46), 9964-9971. 10.1021/bi1012996

Lee, K. S., Lee, M. G., Kwon, Y. S., & Nam, K. S. (2020). Arctigenin Enhances the Cytotoxic Effect of Doxorubicin in MDA-MB-231 Breast Cancer Cells. *Int J Mol Sci, 21*(8). 10.3390/ijms21082997

Lemmon, M. A., & Schlessinger, J. (2010). Cell signaling by receptor tyrosine kinases. *Cell, 141*(7), 1117-1134. 10.1016/j.cell.2010.06.011

Lépine, J., Bernard, O., Plante, M., Têtu, B., Pelletier, G., Labrie, F., Bélanger, A., & Guillemette, C. (2004). Specificity and Regioselectivity of the Conjugation of Estradiol, Estrone, and Their Catecholestrogen and Methoxyestrogen Metabolites by Human Uridine Diphospho-glucuronosyltransferases Expressed in Endometrium. *The Journal of Clinical Endocrinology & Metabolism, 89*(10), 5222-5232. 10.1210/jc.2004-0331

Leu, J. I., Dumont, P., Hafey, M., Murphy, M. E., & George, D. L. (2004). Mitochondrial p53 activates Bak and causes disruption of a Bak-Mcl1 complex. *Nat Cell Biol, 6*(5), 443-450. 10.1038/ncb1123

Lévesque, E., Labriet, A., Hovington, H., Allain É, P., Melo-Garcia, L., Rouleau, M., Brisson, H., Turcotte, V., Caron, P., Villeneuve, L., Leclercq, M., Droit, A., Audet-Walsh, E., Simonyan, D., Fradet, Y., Lacombe, L., & Guillemette, C. (2020). Alternative promoters control UGT2B17-dependent androgen catabolism in prostate cancer and its influence on progression. *Br J Cancer, 122*(7), 1068-1076. 10.1038/s41416-020-0749-2

Lewis, B. C., Mackenzie, P. I., & Miners, J. O. (2011). Homodimerization of UDP-glucuronosyltransferase 2B7 (UGT2B7) and identification of a putative dimerization domain by protein homology modeling. *Biochemical Pharmacology, 82*(12), 2016-2023. 10.1016/j.bcp.2011.09.007

Li, H., Hu, B., Guo, Z., Jiang, X., Su, X., & Zhang, X. (2019). Correlation of UGT2B7 Polymorphism with Cardiotoxicity in Breast Cancer Patients Undergoing Epirubicin/Cyclophosphamide-Docetaxel Adjuvant Chemotherapy. *Yonsei Med J, 60*(1), 30-37. 10.3349/ymj.2019.60.1.30

Li, H., Sun, J., Sui, X., Yan, Z., Sun, Y., Liu, X., Wang, Y., & He, Z. (2009). Structure-based prediction of the nonspecific binding of drugs to hepatic microsomes. *Aaps j, 11*(2), 364-370. 10.1208/s12248-009-9113-4

Li, H., Xie, N., Chen, R., Verreault, M., Fazli, L., Gleave, M. E., Barbier, O., & Dong, X. (2016). UGT2B17 Expedites Progression of Castration-Resistant Prostate Cancers by Promoting Ligand-Independent AR Signaling. *Cancer Res, 76*(22), 6701-6711. 10.1158/0008-5472.Can-16-1518

Li, J., Brahmer, J., Messersmith, W., Hidalgo, M., & Baker, S. D. (2006). Binding of gefitinib, an inhibitor of epidermal growth factor receptor-tyrosine kinase, to plasma proteins and blood cells: in vitro and in cancer patients. *Invest New Drugs, 24*(4), 291-297. 10.1007/s10637-006-5269-2

Li, J., Zhao, M., He, P., Hidalgo, M., & Baker, S. D. (2007). Differential Metabolism of Gefitinib and Erlotinib by Human Cytochrome P450 Enzymes. *Clinical Cancer Research, 13*(12), 3731-3737. 10.1158/1078-0432.Ccr-07-0088

Li, L., Qu, J., Song, M., Zhao, Q., Yang, Y., Tan, X., Hu, Y., Li, J., Lin, Y., Feng, H., Yao, S., Keegan, P., & Chen, M. (2023). Flat dose regimen of toripalimab based on model-informed drug development approach [Original Research]. *Frontiers in Pharmacology, 13*. 10.3389/fphar.2022.1069818

Licarete, E., Rauca, V. F., Luput, L., Drotar, D., Stejerean, I., Patras, L., Dume, B., Toma, V. A., Porfire, A., Gherman, C., Sesarman, A., & Banciu, M. (2020). Overcoming Intrinsic Doxorubicin Resistance in Melanoma by Anti-Angiogenic and Anti-Metastatic Effects of Liposomal Prednisolone Phosphate on Tumor Microenvironment. *Int J Mol Sci, 21*(8). 10.3390/ijms21082968

Licata, S., Saponiero, A., Mordente, A., & Minotti, G. (2000). Doxorubicin Metabolism and Toxicity in Human Myocardium: Role of Cytoplasmic Deglycosidation and Carbonyl Reduction. *Chemical Research in Toxicology, 13*(5), 414-420. 10.1021/tx000013q

Lim, Y. C., Desta, Z., Flockhart, D. A., & Skaar, T. C. (2005). Endoxifen (4-hydroxy-N-desmethyl-tamoxifen) has anti-estrogenic effects in breast cancer cells with potency similar to 4-hydroxy-tamoxifen. *Cancer Chemother Pharmacol, 55*(5), 471-478. 10.1007/s00280-004-0926-7

Lin, L., Yee, S. W., Kim, R. B., & Giacomini, K. M. (2015). SLC Transporters as Therapeutic Targets: Emerging Opportunities. *Nature reviews. Drug discovery, 14*(8), 543-560. 10.1038/nrd4626

Lippert, T. H., Ruoff, H. J., & Volm, M. (2011). Current status of methods to assess cancer drug resistance. *Int J Med Sci, 8*(3), 245-253. 10.7150/ijms.8.245

Litman, T., Druley, T. E., Stein, W. D., & Bates, S. E. (2001). From MDR to MXR: new understanding of multidrug resistance systems, their properties and clinical significance. *Cellular and Molecular Life Sciences CMLS, 58*(7), 931-959. 10.1007/PL00000912

Little, J. M., Williams, L., Xu, J., & Radominska-Pandya, A. (2002). Glucuronidation of the Dietary Fatty Acids, Phytanic Acid and Docosahexaenoic Acid, by Human UDP-Glucuronosyltransferases. *Drug Metabolism and Disposition, 30*(5), 531-533. 10.1124/dmd.30.5.531

Liu, D., Wu, J., Lin, C., Ding, S., Lu, S., Fang, Y., Huang, J., Hong, J., Gao, W., & Zhu, S. (2022). The Comparative Safety of Epirubicin and Cyclophosphamide versus Docetaxel and Cyclophosphamide in Lymph Node-Negative, HR-Positive, HER2-Negative Breast Cancer (ELEGANT): A Randomized Trial. *Cancers, 14*(13), 3221.

Liu, J., Yang, X. M., Liu, G., Chang, L. S., Zhang, L. R., & Song, D. K. (2009). [Association between genetic polymorphism of UGT1A7 and susceptibility of bladder cancer]. *Zhonghua Yi Xue Za Zhi, 89*(44), 3122-3125.

Liu, W., Ramírez, J., Gamazon, E. R., Mirkov, S., Chen, P., Wu, K., Sun, C., Cox, N. J., Cook, E., Jr., Das, S., & Ratain, M. J. (2014). Genetic factors affecting gene transcription and catalytic activity of UDP-glucuronosyltransferases in human liver. *Hum Mol Genet, 23*(20), 5558-5569. 10.1093/hmg/ddu268

Liu, Y., Ramírez, J., House, L., & Ratain, M. J. (2010). Comparison of the drug-drug interactions potential of erlotinib and gefitinib via inhibition of UDP-glucuronosyltransferases. *Drug Metab Dispos, 38*(1), 32-39. 10.1124/dmd.109.029660

Lohela, T. J., Poikola, S., Neuvonen, M., Niemi, M., Backman, J. T., Olkkola, K. T., & Lilius, T. O. (2021). Rifampin Reduces the Plasma Concentrations of Oral and Intravenous Hydromorphone in Healthy Volunteers. *Anesth Analg, 133*(2), 423-434. 10.1213/ane.0000000000005229

Longley, D. B., Harkin, D. P., & Johnston, P. G. (2003). 5-Fluorouracil: mechanisms of action and clinical strategies. *Nature Reviews Cancer, 3*(5), 330-338. 10.1038/nrc1074

López-Ayllón, B. D., de Castro-Carpeño, J., Rodriguez, C., Pernía, O., Ibañez de Cáceres, I., Belda-Iniesta, C., Perona, R., & Sastre, L. (2015). Biomarkers of erlotinib response in non-small cell lung cancer tumors that do not harbor the more common epidermal growth factor receptor mutations. *Int J Clin Exp Pathol, 8*(3), 2888-2898.

Lu, Y., Heydel, J. M., Li, X., Bratton, S., Lindblom, T., & Radominska-Pandya, A. (2005). Lithocholic acid decreases expression of UGT2B7 in Caco-2 cells: a potential role for a negative farnesoid X receptor response element. *Drug Metab Dispos, 33*(7), 937-946. 10.1124/dmd.104.003061

Lu, Y. C., Chen, P. T., Lin, M. C., Lin, C. C., Wang, S. H., & Pan, Y. J. (2021). Nonsteroidal Anti-Inflammatory Drugs Reduce Second Cancer Risk in Patients With Breast Cancer: A Nationwide Population-Based Propensity Score-Matched Cohort Study in Taiwan. *Front Oncol, 11*, 756143. 10.3389/fonc.2021.756143

Lubberman, F. J. E., van Erp, N. P., Ter Heine, R., & van Herpen, C. M. L. (2017). Boosting axitinib exposure with a CYP3A4 inhibitor, making axitinib treatment personal. *Acta Oncol, 56*(9), 1238-1240. 10.1080/0284186x.2017.1311024

Łukasiewicz, S., Czeczelewski, M., Forma, A., Baj, J., Sitarz, R., & Stanisławek, A. (2021). Breast Cancer-Epidemiology, Risk Factors, Classification, Prognostic Markers, and Current Treatment Strategies-An Updated Review. *Cancers (Basel), 13*(17). 10.3390/cancers13174287

Lyu, H., Shen, F., Ruan, S., Tan, C., Zhou, J., Thor, A. D., & Liu, B. (2023). HER3 functions as an effective therapeutic target in triple negative breast cancer to potentiate the antitumor activity of gefitinib and paclitaxel. *Cancer Cell Int, 23*(1), 204. 10.1186/s12935-023-03055-w

Ma, F., Li, Q., Chen, S., Zhu, W., Fan, Y., Wang, J., Luo, Y., Xing, P., Lan, B., Li, M., Yi, Z., Cai, R., Yuan, P., Zhang, P., Li, Q., & Xu, B. (2017a). Phase I Study and Biomarker Analysis of Pyrotinib, a Novel Irreversible Pan-ErbB Receptor Tyrosine Kinase Inhibitor, in Patients With Human Epidermal Growth Factor Receptor 2-Positive Metastatic Breast Cancer. *J Clin Oncol, 35*(27), 3105-3112. 10.1200/jco.2016.69.6179

Ma, F., Ouyang, Q., Li, W., Jiang, Z., Tong, Z., Liu, Y., Li, H., Yu, S., Feng, J., Wang, S., Hu, X., Zou, J., Zhu, X., & Xu, B. (2019). Pyrotinib or Lapatinib Combined With Capecitabine in HER2-Positive Metastatic Breast Cancer With Prior Taxanes, Anthracyclines, and/or Trastuzumab: A Randomized, Phase II Study. *J Clin Oncol, 37*(29), 2610-2619. 10.1200/jco.19.00108

Ma, Y., Xin, S., Huang, M., Yang, Y., Zhu, C., Zhao, H., Zhang, Y., Chen, L., Zhao, Y., Li, J., Zhuang, W., Zhu, X., Zhang, L., & Wang, X. (2017b). Determinants of Gefitinib toxicity in advanced non-small cell lung cancer (NSCLC): a pharmacogenomic study of metabolic enzymes and transporters. *The Pharmacogenomics Journal, 17*(4), 325-330. 10.1038/tpj.2016.31

Mackenzie, P. I., Owens, I. S., Burchell, B., Bock, K. W., Bairoch, A., Bélanger, A., Fournel-Gigleux, S., Green, M., Hum, D. W., Iyanagi, T., Lancet, D., Louisot, P., Magdalou, J., Chowdhury, J. R., Ritter, J. K., Schachter, H., Tephly, T. R., Tipton, K. F., & Nebert, D. W. (1997). The UDP glycosyltransferase gene superfamily: recommended nomenclature update based on evolutionary divergence. *Pharmacogenetics, 7*(4), 255-269. 10.1097/00008571-199708000-00001

Macleod, K. F., Sherry, N., Hannon, G., Beach, D., Tokino, T., Kinzler, K., Vogelstein, B., & Jacks, T. (1995). p53-dependent and independent expression of p21 during cell growth, differentiation, and DNA damage. *Genes Dev, 9*(8), 935-944. 10.1101/gad.9.8.935

Mandapati, A., & Lukong, K. E. (2022). Triple negative breast cancer: approved treatment options and their mechanisms of action. *Journal of Cancer Research and Clinical Oncology*. 10.1007/s00432-022-04189-6

Mandapati, A., & Lukong, K. E. (2023). Triple negative breast cancer: approved treatment options and their mechanisms of action. *J Cancer Res Clin Oncol, 149*(7), 3701-3719. 10.1007/s00432-022-04189-6

Mano, Y., Usui, T., & Kamimura, H. (2007a). Predominant Contribution of UDP-Glucuronosyltransferase 2B7 in the Glucuronidation of Racemic Flurbiprofen in the Human Liver. *Drug Metabolism and Disposition, 35*(7), 1182-1187. 10.1124/dmd.107.015347

Mano, Y., Usui, T., & Kamimura, H. (2007b). The UDP-Glucuronosyltransferase 2B7 Isozyme Is Responsible for Gemfibrozil Glucuronidation in the Human Liver. *Drug Metabolism and Disposition, 35*(11), 2040-2044. 10.1124/dmd.107.017269

Marchetti, S., de Vries, N. A., Buckle, T., Bolijn, M. J., van Eijndhoven, M. A., Beijnen, J. H., Mazzanti, R., van Tellingen, O., & Schellens, J. H. (2008). Effect of the ATP-binding cassette drug transporters ABCB1, ABCG2, and ABCC2 on erlotinib hydrochloride (Tarceva) disposition in in vitro and in vivo

pharmacokinetic studies employing Bcrp1-/-/Mdr1a/1b-/- (triple-knockout) and wild-type mice. *Molecular cancer therapeutics, 7*(8), 2280-2287. 10.1158/1535-7163.Mct-07-2250

Marei, H. E., Althani, A., Afifi, N., Hasan, A., Caceci, T., Pozzoli, G., Morrione, A., Giordano, A., & Cenciarelli, C. (2021). p53 signaling in cancer progression and therapy. *Cancer Cell International, 21*(1), 703. 10.1186/s12935-021-02396-8

Marino, M., Galluzzo, P., & Ascenzi, P. (2006). Estrogen signaling multiple pathways to impact gene transcription. *Curr Genomics, 7*(8), 497-508. 10.2174/138920206779315737

Masoud, V., & Pagès, G. (2017). Targeted therapies in breast cancer: New challenges to fight against resistance. *World J Clin Oncol, 8*(2), 120-134. 10.5306/wjco.v8.i2.120

Maul, R., Warth, B., Schebb, N. H., Krska, R., Koch, M., & Sulyok, M. (2015). In vitro glucuronidation kinetics of deoxynivalenol by human and animal microsomes and recombinant human UGT enzymes. *Archives of Toxicology, 89*(6), 949-960. 10.1007/s00204-014-1286-7

Mavroudis, D., Papakotoulas, P., Ardavanis, A., Syrigos, K., Kakolyris, S., Ziras, N., Kouroussis, C., Malamos, N., Polyzos, A., Christophyllakis, C., Kentepozidis, N., & Georgoulias, V. (2010). Randomized phase III trial comparing docetaxel plus epirubicin versus docetaxel plus capecitabine as first-line treatment in women with advanced breast cancer. *Ann Oncol, 21*(1), 48-54. 10.1093/annonc/mdp498

Mazerska, Z., Mróz, A., Pawłowska, M., & Augustin, E. (2016). The role of glucuronidation in drug resistance. *Pharmacology & Therapeutics, 159*, 35-55. 10.1016/j.pharmthera.2016.01.009

McGuirk, S., Audet-Delage, Y., Annis, M. G., Xue, Y., Vernier, M., Zhao, K., St-Louis, C., Minarrieta, L., Patten, D. A., Morin, G., Greenwood, C. M., Giguère, V., Huang, S., Siegel, P. M., & St-Pierre, J. (2021). Resistance to different anthracycline chemotherapeutics elicits distinct and actionable primary metabolic dependencies in breast cancer. *eLife, 10*. 10.7554/eLife.65150

McKillop, D., Raab, G., Eidtmann, H., Furnival, A., Riva, A., Forbes, J., Mackey, J., Spence, M. P., Koehler, M., & Slamon, D. (2004). Intratumoral and plasma concentrations of gefitinib in breast cancer patients: Preliminary results from a presurgical investigatory study (BCIRG 103). *Journal of Clinical Oncology, 22*(14_suppl), 581-581. 10.1200/jco.2004.22.90140.581

McLaughlin, R. P., He, J., van der Noord, V. E., Redel, J., Foekens, J. A., Martens, J. W. M., Smid, M., Zhang, Y., & van de Water, B. (2019). A kinase inhibitor screen identifies a dual cdc7/CDK9 inhibitor to sensitise triple-negative breast cancer to EGFR-targeted therapy. *Breast cancer research : BCR, 21*(1), 77. 10.1186/s13058-019-1161-9

Meech, R., Hu, D. G., McKinnon, R. A., Mubarokah, S. N., Haines, A. Z., Nair, P. C., Rowland, A., & Mackenzie, P. I. (2019). The UDP-Glycosyltransferase (UGT) Superfamily: New Members, New Functions, and Novel Paradigms. *Physiol Rev, 99*(2), 1153-1222. 10.1152/physrev.00058.2017

Meech, R., Hu, D. G., Miners, J. O., & Mackenzie, P. I. (2018). UDP-Glycosyltransferases. In *Comprehensive Toxicology (Third Edition)* (pp. 468-496). Elsevier. 10.1016/B978-0-12-801238-3.65733-1

Meech, R., & Mackenzie, P. I. (1997). UDP-glucuronosyltransferase, the role of the amino terminus in dimerization. *J Biol Chem, 272*(43), 26913-26917. 10.1074/jbc.272.43.26913

Melana, S. M., Holland, J. F., & Pogo, B. (1998). Inhibition of cell growth and telomerase activity of breast cancer cells in vitro by 3'-azido-3'-deoxythymidine. *Clinical cancer research: an official journal of the American Association for Cancer Research, 4*(3), 693-696.

Mele, T., Generali, D., Fox, S., Brizzi, M. P., Bersiga, A., Milani, M., Allevi, G., Bonardi, S., Aguggini, S., Volante, M., Dogliotti, L., Bottini, A., Harris, A., & Berruti, A. (2010). Anti-angiogenic effect of tamoxifen combined with epirubicin in breast cancer patients. *Breast Cancer Res Treat, 123*(3), 795-804. 10.1007/s10549-010-1063-0

Ménard, V., Collin, P., Margaillan, G., & Guillemette, C. (2013). Modulation of the UGT2B7 enzyme activity by C-terminally truncated proteins derived from alternative splicing. *Drug Metab Dispos, 41*(12), 2197-2205. 10.1124/dmd.113.053876

Ménard, V., Eap, O., Roberge, J., Harvey, M., Lévesque, E., & Guillemette, C. (2011). Transcriptional diversity at the UGT2B7 locus is dictated by extensive pre-mRNA splicing mechanisms that give rise to multiple mRNA splice variants. *Pharmacogenetics and genomics, 21*(10), 631-641. 10.1097/FPC.0b013e3283498147

Meng, X., Song, S., Jiang, Z. F., Sun, B., Wang, T., Zhang, S., & Wu, S. (2016). Receptor conversion in metastatic breast cancer: a prognosticator of survival. *Oncotarget, 7*(44), 71887-71903. 10.18632/oncotarget.12114

Messing, J. (1983). New M13 vectors for cloning. *Methods Enzymol, 101*, 20-78. 10.1016/0076-6879(83)01005-8

Mhaimeed, N., Mhaimeed, N., & Shad, M. U. (2022). Pharmacokinetic mechanisms underlying clinical cases of valproic acid autoinduction: A review. *Journal of Affective Disorders Reports, 10*, 100426. 10.1016/j.jadr.2022.100426

Miners, J. O., Lillywhite, K. J., Matthews, A. P., Jones, M. E., & Birkett, D. J. (1988). Kinetic and inhibitor studies of 4-methylumbelliferone and 1-naphthol glucuronidation in human liver microsomes. *Biochem Pharmacol, 37*(4), 665-671. 10.1016/0006-2952(88)90140-2

Miners, J. O., Polasek, T. M., Hulin, J. A., Rowland, A., & Meech, R. (2023). Drug-drug interactions that alter the exposure of glucuronidated drugs: Scope, UDP-glucuronosyltransferase (UGT) enzyme selectivity, mechanisms (inhibition and induction), and clinical significance. *Pharmacol Ther, 248*, 108459. 10.1016/j.pharmthera.2023.108459

Miners, J. O., Polasek, T. M., Mackenzie, P. I., & Knights, K. M. (2010). The In Vitro Characterization of Inhibitory Drug–Drug Interactions Involving UDP-Glucuronosyltransferase. In K. S. Pang, A. D. Rodrigues, & R. M. Peter (Eds.), *Enzyme- and Transporter-Based Drug-Drug Interactions: Progress and Future Challenges* (pp. 217-236). Springer New York. 10.1007/978-1-4419-0840-7_8

Miners, J. O., Rowland, A., Novak, J. J., Lapham, K., & Goosen, T. C. (2021). Evidence-based strategies for the characterisation of human drug and chemical glucuronidation in vitro and UDP-glucuronosyltransferase reaction phenotyping. *Pharmacology & Therapeutics, 218*, 107689.

Miotke, L., Lau, B. T., Rumma, R. T., & Ji, H. P. (2014). High sensitivity detection and quantitation of DNA copy number and single nucleotide variants with single color droplet digital PCR. *Anal Chem, 86*(5), 2618-2624. 10.1021/ac403843j

Misiti, F., Giardina, B., Mordente, A., & Clementi, M. E. (2003). The secondary alcohol and aglycone metabolites of doxorubicin alter metabolism of human erythrocytes. *Brazilian Journal of Medical and Biological Research, 36*.

Mitra, P. S., Basu, N. K., Basu, M., Chakraborty, S., Saha, T., & Owens, I. S. (2011). Regulated phosphorylation of a major UDP-glucuronosyltransferase isozyme by tyrosine kinases dictates endogenous substrate selection for detoxification. *J Biol Chem, 286*(2), 1639-1648. 10.1074/jbc.M110.165126

Modi, A., Roy, D., Sharma, S., Vishnoi, J. R., Pareek, P., Elhence, P., Sharma, P., & Purohit, P. (2022). ABC transporters in breast cancer: their roles in multidrug resistance and beyond. *J Drug Target, 30*(9), 927-947. 10.1080/1061186x.2022.2091578

Molchadsky, A., Rivlin, N., Brosh, R., Rotter, V., & Sarig, R. (2010). p53 is balancing development, differentiation and de-differentiation to assure cancer prevention. *Carcinogenesis, 31*(9), 1501-1508. 10.1093/carcin/bgq101

Molloy, B. J., King, A., Mullin, L. G., Gethings, L. A., Riley, R., Plumb, R. S., & Wilson, I. D. (2021). Rapid determination of the pharmacokinetics and metabolic fate of gefitinib in the mouse using a combination of UPLC/MS/MS, UPLC/QToF/MS, and ion mobility (IM)-enabled UPLC/QToF/MS. *Xenobiotica, 51*(4), 434-446. 10.1080/00498254.2020.1859643

Mordente, A., Meucci, E., Silvestrini, A., Martorana, G. E., & Giardina, B. (2009). New developments in anthracycline-induced cardiotoxicity. *Curr Med Chem, 16*(13), 1656-1672. 10.2174/092986709788186228

Morris, G. F., Bischoff, J. R., & Mathews, M. B. (1996). Transcriptional activation of the human proliferating-cell nuclear antigen promoter by p53. *Proc Natl Acad Sci U S A, 93*(2), 895-899. 10.1073/pnas.93.2.895

Mou, P., Wang, H., An, L., Yin, Q., & Chang, J. (2019). RS7435335 located in the UGT2B7 gene may be a possible genetic marker for the clinical response and prognosis of breast cancer patients receiving neoadjuvant chemotherapy. *Journal of Cellular Biochemistry, 120*(5), 7167-7173. 10.1002/jcb.27990

Mouridsen, H., Alfthan, C., Bastholt, L., Bergh, J., Dalmark, M., Eksborg, S., Hellsten, S., Kjaer, M., Peterson, C., & Skovsgård, T. (1990). Current status of epirubicin (Farmorubicin) in the treatment of solid tumours. *Acta Oncologica, 29*(3), 257-285.

Mubarokah, S. N. (2018). *Regulation of UDP-glucuronosyltransferase 1A genes in the intestine*, Flinders University, College of Medicine and Public Health].

Mueller-Schoell, A., Groenland, S. L., Scherf-Clavel, O., van Dyk, M., Huisinga, W., Michelet, R., Jaehde, U., Steeghs, N., Huitema, A. D., & Kloft, C. (2021). Therapeutic drug monitoring of oral targeted antineoplastic drugs. *European journal of clinical pharmacology, 77*, 441-464.

Muller, P. A. J., & Vousden, K. H. (2014). Mutant p53 in cancer: new functions and therapeutic opportunities. *Cancer cell, 25*(3), 304-317. 10.1016/j.ccr.2014.01.021

Munster, P., Marchion, D., Bicaku, E., Lacevic, M., Kim, J., Centeno, B., Daud, A., Neuger, A., Minton, S., & Sullivan, D. (2009). Clinical and biological effects of valproic acid as a histone deacetylase inhibitor

on tumor and surrogate tissues: phase I/II trial of valproic acid and epirubicin/FEC. *Clin Cancer Res, 15*(7), 2488-2496. 10.1158/1078-0432.Ccr-08-1930

Münster, P., Marchion, D., Bicaku, E., Schmitt, M., Lee, J. H., DeConti, R., Simon, G., Fishman, M., Minton, S., Garrett, C., Chiappori, A., Lush, R., Sullivan, D., & Daud, A. (2007). Phase I trial of histone deacetylase inhibition by valproic acid followed by the topoisomerase II inhibitor epirubicin in advanced solid tumors: a clinical and translational study. *J Clin Oncol, 25*(15), 1979-1985. 10.1200/jco.2006.08.6165

Murphrey, M. B., Quaim, L., Rahimi, N., & Varacallo, M. (2023). Biochemistry, Epidermal Growth Factor Receptor. In *StatPearls*. StatPearls.

Murthy, R., Borges, V. F., Conlin, A., Chaves, J., Chamberlain, M., Gray, T., Vo, A., & Hamilton, E. (2018). Tucatinib with capecitabine and trastuzumab in advanced HER2-positive metastatic breast cancer with and without brain metastases: a non-randomised, open-label, phase 1b study. *Lancet Oncol, 19*(7), 880-888. 10.1016/s1470-2045(18)30256-0

Murthy, R. K., Loi, S., Okines, A., Paplomata, E., Hamilton, E., Hurvitz, S. A., Lin, N. U., Borges, V., Abramson, V., Anders, C., Bedard, P. L., Oliveira, M., Jakobsen, E., Bachelot, T., Shachar, S. S., Müller, V., Braga, S., Duhoux, F. P., Greil, R., Cameron, D., Carey, L. A., Curigliano, G., Gelmon, K., Hortobagyi, G., Krop, I., Loibl, S., Pegram, M., Slamon, D., Palanca-Wessels, M. C., Walker, L., Feng, W., & Winer, E. P. (2020). Tucatinib, Trastuzumab, and Capecitabine for HER2-Positive Metastatic Breast Cancer. *N Engl J Med, 382*(7), 597-609. 10.1056/NEJMoa1914609

Mustonen, M. V., Pyrhönen, S., & Kellokumpu-Lehtinen, P. L. (2014). Toremifene in the treatment of breast cancer. *World J Clin Oncol, 5*(3), 393-405. 10.5306/wjco.v5.i3.393

Nakamura, A., Nakajima, M., Higashi, E., Yamanaka, H., & Yokoi, T. (2008). Genetic polymorphisms in the 5'-flanking region of human UDP-glucuronosyltransferase 2B7 affect the Nrf2-dependent transcriptional regulation. *Pharmacogenetics and genomics, 18*(8), 709-720. 10.1097/FPC.0b013e32830500c9

Namer, M., Fargeot, P., Roché, H., Campone, M., Kerbrat, P., Romestaing, P., Monnier, A., Luporsi, E., Montcuquet, P., & Bonneterre, J. (2006). Improved disease-free survival with epirubicin-based chemoendocrine adjuvant therapy compared with tamoxifen alone in one to three node-positive, estrogen-receptor-positive, postmenopausal breast cancer patients: results of French Adjuvant Study Group 02 and 07 trials. *Annals of Oncology, 17*(1), 65-73. 10.1093/annonc/mdj022

Nava, M., Dutta, P., Zemke, N. R., Farias-Eisner, R., Vadgama, J. V., & Wu, Y. (2019). Transcriptomic and ChIP-sequence interrogation of EGFR signaling in HER2+ breast cancer cells reveals a dynamic chromatin landscape and S100 genes as targets. *BMC Medical Genomics, 12*(1), 32. 10.1186/s12920-019-0477-8

NCBI. (2024). *Compound Summary for CID 443939, Doxorubicin Hydrochloride*. https://pubchem.ncbi.nlm.nih.gov/compound/Doxorubicin-Hydrochloride

Neumann, E., Mehboob, H., Ramírez, J., Mirkov, S., Zhang, M., & Liu, W. (2016). Age-Dependent Hepatic UDP-Glucuronosyltransferase Gene Expression and Activity in Children. *Front Pharmacol, 7*, 437. 10.3389/fphar.2016.00437

Neumeier, J., & Meister, G. (2021). siRNA Specificity: RNAi Mechanisms and Strategies to Reduce Off-Target Effects [Mini Review]. *Frontiers in Plant Science, 11*. 10.3389/fpls.2020.526455

Nicolella, D., Grimaldi, G., Colantuoni, G., Belli, M., Frasci, G., Perchard, J., & Comella, P. (1996). Weekly low dose epirubicin in elderly cancer patients. *Tumori, 82*(4), 369-371.

Nielsen, D., Maare, C., & Skovsgaard, T. (1996). Cellular resistance to anthracyclines. *Gen Pharmacol, 27*(2), 251-255. 10.1016/0306-3623(95)02013-6

Nio, Y., Ishida, H., Matsumoto, N., Kusumoto, S., Kubota, Y., Tsunoda, T., Sasaki, Y., & Fujita, K. I. (2022). Pharmacokinetics of gefitinib in elderly patients with EGFR-mutated advanced non-small cell lung cancer: a prospective study. *BMC Pulm Med, 22*(1), 454. 10.1186/s12890-022-02249-8

Nofech-Mozes, S., Trudeau, M., Kahn, H. K., Dent, R., Rawlinson, E., Sun, P., Narod, S. A., & Hanna, W. M. (2009). Patterns of recurrence in the basal and non-basal subtypes of triple-negative breast cancers. *Breast Cancer Res Treat, 118*(1), 131-137. 10.1007/s10549-008-0295-8

Nordstrom, J. L., Gorlatov, S., Zhang, W., Yang, Y., Huang, L., Burke, S., Li, H., Ciccarone, V., Zhang, T., Stavenhagen, J., Koenig, S., Stewart, S. J., Moore, P. A., Johnson, S., & Bonvini, E. (2011). Anti-tumor activity and toxicokinetics analysis of MGAH22, an anti-HER2 monoclonal antibody with enhanced Fcγ receptor binding properties. *Breast cancer research : BCR, 13*(6), R123. 10.1186/bcr3069

Novak, R. F., & Woodcroft, K. J. (2000). The alcohol-inducible form of cytochrome P450 (CYP 2E1): role in toxicology and regulation of expression. *Arch Pharm Res, 23*(4), 267-282. 10.1007/bf02975435

O'Shaughnessy, J., Kaklamani, V., & Kalinsky, K. (2019). Perspectives on the mechanism of action and clinical application of eribulin for metastatic breast cancer. *Future Oncology, 15*(14), 1641-1653. 10.2217/fon-2018-0936

O'Geen, H., Bates, S. L., Carter, S. S., Nisson, K. A., Halmai, J., Fink, K. D., Rhie, S. K., Farnham, P. J., & Segal, D. J. (2019). Ezh2-dCas9 and KRAB-dCas9 enable engineering of epigenetic memory in a context-dependent manner. *Epigenetics & Chromatin, 12*(1), 26. 10.1186/s13072-019-0275-8

O'Shaughnessy, J. A. (1999). Oral Alkylating Agents for Breast Cancer Therapy. *Drugs, 58*(3), 1-9. 10.2165/00003495-199958003-00001

Ogino, M. H., & Tadi, P. (2023). Cyclophosphamide. In *StatPearls*. StatPearls.

Ohnishi, Y., Yasui, H., Kakudo, K., & Nozaki, M. (2017). Regulation of cell migration via the EGFR signaling pathway in oral squamous cell carcinoma cells. *Oncology letters, 13*(2), 930-936. 10.3892/ol.2016.5500

Ohno, A., Saito, Y., Hanioka, N., Jinno, H., Saeki, M., Ando, M., Ozawa, S., & Sawada, J.-i. (2004). INVOLVEMENT OF HUMAN HEPATIC UGT1A1, UGT2B4, AND UGT2B7 IN THE GLUCURONIDATION OF CARVEDILOL. *Drug Metabolism and Disposition, 32*(2), 235-239. 10.1124/dmd.32.2.235

Okey, A. B., Roberts, E. A., Harper, P. A., & Denison, M. S. (1986). Induction of drug-metabolizing enzymes: Mechanisms and consequences. *Clinical Biochemistry, 19*(2), 132-141. 10.1016/S0009-9120(86)80060-1

Ormrod, D., Holm, K., Goa, K., & Spencer, C. (1999). Epirubicin [journal article]. *Drugs & Aging, 15*(5), 389-416. 10.2165/00002512-199915050-00006

Osborne, C. K., Neven, P., Dirix, L. Y., Mackey, J. R., Robert, J., Underhill, C., Schiff, R., Gutierrez, C., Migliaccio, I., Anagnostou, V. K., Rimm, D. L., Magill, P., & Sellers, M. (2011). Gefitinib or placebo in

combination with tamoxifen in patients with hormone receptor-positive metastatic breast cancer: a randomized phase II study. *Clin Cancer Res, 17*(5), 1147-1159. 10.1158/1078-0432.Ccr-10-1869

Ou, Y., Wang, M., Xu, Q., Sun, B., & Jia, Y. (2024). Small molecule agents for triple negative breast cancer: Current status and future prospects. *Translational Oncology, 41*, 101893. 10.1016/j.tranon.2024.101893

Özlem Sultan, A. (2017). In Vitro Cytotoxicity and Cell Viability Assays: Principles, Advantages, and Disadvantages. In L. L. Marcelo & S. Sonia (Eds.), *Genotoxicity* (pp. Ch. 1). IntechOpen. 10.5772/intechopen.71923

Ozvegy-Laczka, C., Hegedus, T., Várady, G., Ujhelly, O., Schuetz, J. D., Váradi, A., Kéri, G., Orfi, L., Német, K., & Sarkadi, B. (2004). High-affinity interaction of tyrosine kinase inhibitors with the ABCG2 multidrug transporter. *Mol Pharmacol, 65*(6), 1485-1495. 10.1124/mol.65.6.1485

Palleria, C., Di Paolo, A., Giofrè, C., Caglioti, C., Leuzzi, G., Siniscalchi, A., De Sarro, G., & Gallelli, L. (2013). Pharmacokinetic drug-drug interaction and their implication in clinical management. *J Res Med Sci, 18*(7), 601-610.

Papachristos, A., Patel, J., Vasileiou, M., & Patrinos, G. P. (2023). Dose Optimization in Oncology Drug Development: The Emerging Role of Pharmacogenomics, Pharmacokinetics, and Pharmacodynamics. *Cancers, 15*(12), 3233.

Pâquet, S., Fazli, L., Grosse, L., Verreault, M., Têtu, B., Rennie, P. S., Bélanger, A., & Barbier, O. (2012). Differential Expression of the Androgen-Conjugating UGT2B15 and UGT2B17 Enzymes in Prostate Tumor Cells during Cancer Progression. *The Journal of Clinical Endocrinology & Metabolism, 97*(3), E428-E432. 10.1210/jc.2011-2064

Parmar, S., Stingl, J. C., Huber-Wechselberger, A., Kainz, A., Renner, W., Langsenlehner, U., Krippl, P., Brockmöller, J., & Haschke-Becher, E. (2011). Impact of UGT2B7 His268Tyr polymorphism on the outcome of adjuvant epirubicin treatment in breast cancer. *Breast cancer research : BCR, 13*(3), R57-R57. 10.1186/bcr2894

Patel, J. N., Jiang, C., Owzar, K., Mulkey, F., Luzum, J. A., Mamon, H. J., Haller, D. G., Dragovich, T., Alberts, S. R., Bjarnason, G., Willet, C. G., Niedzwiecki, D., Enzinger, P., Ratain, M. J., Fuchs, C., & McLeod, H. L. (2021). Pharmacogenetic study in gastric cancer patients treated with adjuvant fluorouracil/leucovorin or epirubicin/cisplatin/fluorouracil before and after chemoradiation on CALGB 80101 (Alliance). *Pharmacogenetics and genomics, 31*(9), 215-220. 10.1097/fpc.0000000000000442

Patterson, L. H., & Murray, G. I. (2002). Tumour Cytochrome P450 and Drug Activation. *Curr Pharm Des, 8*(15), 1335-1347. 10.2174/1381612023394502

Pei, Y., & Tuschl, T. (2006). On the art of identifying effective and specific siRNAs. *Nat Methods, 3*(9), 670-676. 10.1038/nmeth911

Pereira, H., Pinder, S. E., Sibbering, D. M., Galea, M. H., Elston, C. W., Blamey, R. W., Robertson, J. F., & Ellis, I. O. (1995). Pathological prognostic factors in breast cancer. IV: Should you be a typer or a grader? A comparative study of two histological prognostic features in operable breast carcinoma. *Histopathology, 27*(3), 219-226. 10.1111/j.1365-2559.1995.tb00213.x

Peto, R., Davies, C., Godwin, J., Gray, R., Pan, H. C., Clarke, M., Cutter, D., Darby, S., McGale, P., Taylor, C., Wang, Y. C., Bergh, J., Di Leo, A., Albain, K., Swain, S., Piccart, M., & Pritchard, K. (2012). Comparisons between different polychemotherapy regimens for early breast cancer: meta-analyses of long-term outcome among 100,000 women in 123 randomised trials. *Lancet, 379*(9814), 432-444. 10.1016/s0140-6736(11)61625-5

Phang-Lyn, S., & Llerena, V. A. (2023). Biochemistry, Biotransformation. In *StatPearls*. StatPearls Publishing.

Picard, N., Ratanasavanh, D., Prémaud, A., Le Meur, Y., & Marquet, P. (2005). Identification of the UDP-glucuronosyltransferase isoforms involved in mycophenolic acid phase II metabolism. *Drug Metabolism and Disposition, 33*(1), 139-146. 10.1124/dmd.104.001651

Piccart-Gebhart, M., Holmes, E., Baselga, J., de Azambuja, E., Dueck, A. C., Viale, G., Zujewski, J. A., Goldhirsch, A., Armour, A., Pritchard, K. I., McCullough, A. E., Dolci, S., McFadden, E., Holmes, A. P., Tonghua, L., Eidtmann, H., Dinh, P., Di Cosimo, S., Harbeck, N., Tjulandin, S., Im, Y. H., Huang, C. S., Diéras, V., Hillman, D. W., Wolff, A. C., Jackisch, C., Lang, I., Untch, M., Smith, I., Boyle, F., Xu, B., Gomez, H., Suter, T., Gelber, R. D., & Perez, E. A. (2016). Adjuvant Lapatinib and Trastuzumab for Early Human Epidermal Growth Factor Receptor 2-Positive Breast Cancer: Results From the Randomized Phase III Adjuvant Lapatinib and/or Trastuzumab Treatment Optimization Trial. *J Clin Oncol, 34*(10), 1034-1042. 10.1200/jco.2015.62.1797

Piccart-Gebhart, M. J., Procter, M., Leyland-Jones, B., Goldhirsch, A., Untch, M., Smith, I., Gianni, L., Baselga, J., Bell, R., Jackisch, C., Cameron, D., Dowsett, M., Barrios, C. H., Steger, G., Huang, C. S., Andersson, M., Inbar, M., Lichinitser, M., Láng, I., Nitz, U., Iwata, H., Thomssen, C., Lohrisch, C., Suter, T. M., Rüschoff, J., Suto, T., Greatorex, V., Ward, C., Straehle, C., McFadden, E., Dolci, M. S., & Gelber, R. D. (2005). Trastuzumab after adjuvant chemotherapy in HER2-positive breast cancer. *N Engl J Med, 353*(16), 1659-1672. 10.1056/NEJMoa052306

Pivot, X., Dufresne, A., & Villanueva, C. (2007). Efficacy and safety of ixabepilone, a novel epothilone analogue. *Clin Breast Cancer, 7*(7), 543-549. 10.3816/CBC.2007.n.009

Plosker, G. L., & Faulds, D. (1993). Epirubicin. *Drugs, 45*(5), 788-856. 10.2165/00003495-199345050-00011

Polasek, T. M., Rayner, C. R., Peck, R. W., Rowland, A., Kimko, H., & Rostami-Hodjegan, A. (2019). Toward dynamic prescribing information: codevelopment of companion model-informed precision dosing tools in drug development. *Clinical pharmacology in drug development, 8*(4), 418-425.

Polasek, T. M., & Rostami-Hodjegan, A. (2020). Virtual twins: understanding the data required for model-informed precision dosing. *Clinical Pharmacology and Therapeutics, 107*(4), 742-745.

Polasek, T. M., Tucker, G. T., Sorich, M. J., Wiese, M. D., Mohan, T., Rostami-Hodjegan, A., Korprasertthaworn, P., Perera, V., & Rowland, A. (2018). Prediction of olanzapine exposure in individual patients using physiologically based pharmacokinetic modelling and simulation. *British journal of clinical pharmacology, 84*(3), 462-476.

Polychronis, A., Sinnett, H. D., Hadjiminas, D., Singhal, H., Mansi, J. L., Shivapatham, D., Shousha, S., Jiang, J., Peston, D., Barrett, N., Vigushin, D., Morrison, K., Beresford, E., Ali, S., Slade, M. J., & Coombes, R. C. (2005). Preoperative gefitinib versus gefitinib and anastrozole in postmenopausal patients with oestrogen-receptor positive and epidermal-growth-factor-receptor-positive primary breast cancer: a double-blind placebo-controlled phase II randomised trial. *Lancet Oncol, 6*(6), 383-391. 10.1016/s1470-2045(05)70176-5

Pommier, Y., Leteurtre, F., Fesen, M. R., Fujimori, A., Bertrand, R., Solary, E., Kohlhagen, G., & Kohn, K. W. (1994). Cellular determinants of sensitivity and resistance to DNA topoisomerase inhibitors. *Cancer Invest, 12*(5), 530-542. 10.3109/07357909409021413

Porté, S., Valencia, E., Yakovtseva, E. A., Borràs, E., Shafqat, N., Debreczeny, J. É., Pike, A. C. W., Oppermann, U., Farrés, J., Fita, I., & Parés, X. (2009). Three-dimensional Structure and Enzymatic Function of Proapoptotic Human p53-inducible Quinone Oxidoreductase PIG3*. *Journal of Biological Chemistry, 284*(25), 17194-17205. 10.1074/jbc.M109.001800

Precht, J. C., Schroth, W., Klein, K., Brauch, H., Krynetskiy, E., Schwab, M., & Mürdter, T. E. (2013). The Letrozole Phase 1 Metabolite Carbinol as a Novel Probe Drug for UGT2B7. *Drug Metabolism and Disposition, 41*(11), 1906-1913. 10.1124/dmd.113.053405

Puris, E., Fricker, G., & Gynther, M. (2023). The Role of Solute Carrier Transporters in Efficient Anticancer Drug Delivery and Therapy. *Pharmaceutics, 15*(2). 10.3390/pharmaceutics15020364

Raj, N., & Attardi, L. D. (2017). The Transactivation Domains of the p53 Protein. *Cold Spring Harb Perspect Med, 7*(1). 10.1101/cshperspect.a026047

Rakha, E. A., Reis-Filho, J. S., Baehner, F., Dabbs, D. J., Decker, T., Eusebi, V., Fox, S. B., Ichihara, S., Jacquemier, J., Lakhani, S. R., Palacios, J., Richardson, A. L., Schnitt, S. J., Schmitt, F. C., Tan, P. H., Tse, G. M., Badve, S., & Ellis, I. O. (2010). Breast cancer prognostic classification in the molecular era: the role of histological grade. *Breast cancer research : BCR, 12*(4), 207. 10.1186/bcr2607

Ralph, L. D., Thomson, A. H., Dobbs, N. A., & Twelves, C. (2003). A population model of epirubicin pharmacokinetics and application to dosage guidelines. *Cancer Chemotherapy and Pharmacology, 52*(1), 34-40. 10.1007/s00280-003-0608-x

Ran, F. A., Hsu, P. D., Wright, J., Agarwala, V., Scott, D. A., & Zhang, F. (2013). Genome engineering using the CRISPR-Cas9 system. *Nat Protoc, 8*(11), 2281-2308. 10.1038/nprot.2013.143

Randall, M. D., Kendall, D., & Alexander, S. (2012). *FASTtrack: Pharmacology*. Pharmaceutical Press.

Rastogi, P., Anderson, S. J., Bear, H. D., Geyer, C. E., Kahlenberg, M. S., Robidoux, A., Margolese, R. G., Hoehn, J. L., Vogel, V. G., Dakhil, S. R., Tamkus, D., King, K. M., Pajon, E. R., Wright, M. J., Robert, J., Paik, S., Mamounas, E. P., & Wolmark, N. (2008). Preoperative chemotherapy: updates of National Surgical Adjuvant Breast and Bowel Project Protocols B-18 and B-27. *J Clin Oncol, 26*(5), 778-785. 10.1200/jco.2007.15.0235

Raungrut, P., Uchaipichat, V., Elliot, D. J., Janchawee, B., Somogyi, A. A., & Miners, J. O. (2010). In Vitro–In Vivo Extrapolation Predicts Drug–Drug Interactions Arising from Inhibition of Codeine Glucuronidation by Dextropropoxyphene, Fluconazole, Ketoconazole, and Methadone in Humans. *Journal of Pharmacology and Experimental Therapeutics, 334*(2), 609-618. 10.1124/jpet.110.167916

Ren, Q., Murphy, S. E., Zheng, Z., & Lazarus, P. (2000). O-Glucuronidation of the lung carcinogen 4-(methylnitrosamino)-1- (3-pyridyl)-1-butanol (NNAL) by human UDP-glucuronosyltransferases 2B7 and 1A9. *Drug Metab Dispos, 28*(11), 1352-1360.

Riss, T. L., Moravec, R. A., Niles, A. L., Duellman, S., Benink, H. A., Worzella, T. J., & Minor, L. (2004). Cell Viability Assays. In S. Markossian, A. Grossman, K. Brimacombe, M. Arkin, D. Auld, C. Austin, J. Baell, T. D. Y. Chung, N. P. Coussens, J. L. Dahlin, V. Devanarayan, T. L. Foley, M. Glicksman, K. Gorshkov, J.

V. Haas, M. D. Hall, S. Hoare, J. Inglese, P. W. Iversen, S. C. Kales, M. Lal-Nag, Z. Li, J. McGee, O. McManus, T. Riss, P. Saradjian, G. S. Sittampalam, M. Tarselli, O. J. Trask, Jr., Y. Wang, J. R. Weidner, M. J. Wildey, K. Wilson, M. Xia, & X. Xu (Eds.), *Assay Guidance Manual*. Eli Lilly & Company and the National Center for Advancing Translational Sciences.

Rivlin, N., Brosh, R., Oren, M., & Rotter, V. (2011). Mutations in the p53 Tumor Suppressor Gene: Important Milestones at the Various Steps of Tumorigenesis. *Genes Cancer, 2*(4), 466-474. 10.1177/1947601911408889

Rixe, O., Franco, S. X., Yardley, D. A., Johnston, S. R., Martin, M., Arun, B. K., Letrent, S. P., & Rugo, H. S. (2009). A randomized, phase II, dose-finding study of the pan-ErbB receptor tyrosine-kinase inhibitor CI-1033 in patients with pretreated metastatic breast cancer. *Cancer Chemother Pharmacol, 64*(6), 1139-1148. 10.1007/s00280-009-0975-z

Robert, J. (1993). Epirubicin. Clinical pharmacology and dose-effect relationship. *Drugs, 45 Suppl 2*, 20-30. 10.2165/00003495-199300452-00005

Robert, J. (1994). Clinical pharmacokinetics of epirubicin. *Clin Pharmacokinet, 26*(6), 428-438. 10.2165/00003088-199426060-00002

Robert, J., & Bui, N. B. (1992). Pharmacokinetics and metabolism of epirubicin administered as i.v. bolus and 48-h infusion in patients with advanced soft-tissue sarcoma. *Ann Oncol, 3*(8), 651-656. 10.1093/oxfordjournals.annonc.a058296

Robert, J., Vrignaud, P., Nguyen-Ngoc, T., Iliadis, A., Mauriac, L., & Hurteloup, P. (1985). Comparative pharmacokinetics and metabolism of doxorubicin and epirubicin in patients with metastatic breast cancer. *Cancer Treat Rep, 69*(6), 633-640.

Roberts, A. G., & Gibbs, M. E. (2018). Mechanisms and the clinical relevance of complex drug-drug interactions. *Clin Pharmacol, 10*, 123-134. 10.2147/cpaa.S146115

Roberts, B. J., Song, B.-J., Soh, Y., Park, S. S., & Shoaf, S. E. (1995). Ethanol Induces CYP2E1 by Protein Stabilization: ROLE OF UBIQUITIN CONJUGATION IN THE RAPID DEGRADATION OF CYP2E1. *Journal of Biological Chemistry, 270*(50), 29632-29635. 10.1074/jbc.270.50.29632

Robey, R. W., Pluchino, K. M., Hall, M. D., Fojo, A. T., Bates, S. E., & Gottesman, M. M. (2018). Revisiting the role of ABC transporters in multidrug-resistant cancer. *Nat Rev Cancer, 18*(7), 452-464. 10.1038/s41568-018-0005-8

Robinson, D. R., Wu, Y.-M., & Lin, S.-F. (2000). The protein tyrosine kinase family of the human genome. *Oncogene, 19*(49), 5548-5557. 10.1038/sj.onc.1203957

Robinson, S. P., Langan-Fahey, S. M., Johnson, D. A., & Jordan, V. C. (1991). Metabolites, pharmacodynamics, and pharmacokinetics of tamoxifen in rats and mice compared to the breast cancer patient. *Drug Metabolism and Disposition, 19*(1), 36-43.

Rodrigues, A. D., Van Dyk, M., Sorich, M. J., Fahmy, A., Useckaite, Z., Newman, L. A., Kapetas, A. J., Mounzer, R., Wood, L. S., & Johnson, J. G. (2021). Exploring the use of serum-derived small extracellular vesicles as liquid biopsy to study the induction of hepatic cytochromes P450 and organic anion transporting polypeptides. *Clinical Pharmacology & Therapeutics, 110*(1), 248-258.

Rodrigues, A. D., Wood, L. S., Vourvahis, M., & Rowland, A. (2022). Leveraging human plasma-derived small extracellular vesicles as liquid biopsy to study the induction of cytochrome P450 3A4 by modafinil. *Clinical Pharmacology & Therapeutics, 111*(2), 425-434.

Rodrigues, D., & Rowland, A. (2019). From endogenous compounds as biomarkers to plasma-derived nanovesicles as liquid biopsy; has the golden age of translational pharmacokinetics-absorption, distribution, metabolism, excretion-drug–drug interaction science finally arrived? *Clinical Pharmacology & Therapeutics, 105*(6), 1407-1420.

Romand, S., Spaggiari, D., Marsousi, N., Samer, C., Desmeules, J., Daali, Y., & Rudaz, S. (2017). Characterization of oxycodone in vitro metabolism by human cytochromes P450 and UDP-glucuronosyltransferases. *J Pharm Biomed Anal, 144*, 129-137. 10.1016/j.jpba.2016.09.024

Romero-Lorca, A., Novillo, A., Gaibar, M., Bandrés, F., & Fernández-Santander, A. (2015). Impacts of the Glucuronidase Genotypes UGT1A4, UGT2B7, UGT2B15 and UGT2B17 on Tamoxifen Metabolism in Breast Cancer Patients. *PLoS ONE, 10*(7), e0132269. 10.1371/journal.pone.0132269

Rosenzweig, S. A. (2018). Acquired Resistance to Drugs Targeting Tyrosine Kinases. *Adv Cancer Res, 138*, 71-98. 10.1016/bs.acr.2018.02.003

Rouzier, R., Perou, C. M., Symmans, W. F., Ibrahim, N., Cristofanilli, M., Anderson, K., Hess, K. R., Stec, J., Ayers, M., Wagner, P., Morandi, P., Fan, C., Rabiul, I., Ross, J. S., Hortobagyi, G. N., & Pusztai, L. (2005). Breast cancer molecular subtypes respond differently to preoperative chemotherapy. *Clin Cancer Res, 11*(16), 5678-5685. 10.1158/1078-0432.Ccr-04-2421

Rowland, A., Gaganis, P., Elliot, D. J., Mackenzie, P. I., Knights, K. M., & Miners, J. O. (2007). Binding of Inhibitory Fatty Acids Is Responsible for the Enhancement of UDP-Glucuronosyltransferase 2B7 Activity by Albumin: Implications for in Vitro-in Vivo Extrapolation. *Journal of Pharmacology and Experimental Therapeutics, 321*(1), 137-147. 10.1124/jpet.106.118216

Rowland, A., Ruanglertboon, W., Van Dyk, M., Wijayakumara, D., Wood, L. S., Meech, R., Mackenzie, P. I., Rodrigues, A. D., Marshall, J. C., & Sorich, M. J. (2019). Plasma extracellular nanovesicle (exosome)-derived biomarkers for drug metabolism pathways: a novel approach to characterize variability in drug exposure. *British journal of clinical pharmacology, 85*(1), 216-226.

Rowland, A., Van Dyk, M., Hopkins, A. M., Mounzer, R., Polasek, T. M., Rostami-Hodjegan, A., & Sorich, M. J. (2018). Physiologically based pharmacokinetic modeling to identify physiological and molecular characteristics driving variability in drug exposure. *Clinical Pharmacology & Therapeutics, 104*(6), 1219-1228.

Rowland Yeo, K., Jamei, M., Yang, J., Tucker, G. T., & Rostami-Hodjegan, A. (2010). Physiologically based mechanistic modelling to predict complex drug-drug interactions involving simultaneous competitive and time-dependent enzyme inhibition by parent compound and its metabolite in both liver and gut - the effect of diltiazem on the time-course of exposure to triazolam. *Eur J Pharm Sci, 39*(5), 298-309. 10.1016/j.ejps.2009.12.002

Rozan, L. M., & El-Deiry, W. S. (2007). p53 downstream target genes and tumor suppression: a classical view in evolution. *Cell Death & Differentiation, 14*(1), 3-9. 10.1038/sj.cdd.4402058

Ruanglertboon, W., Sorich, M. J., Hopkins, A. M., & Rowland, A. (2021). Mechanistic modelling identifies and addresses the risks of empiric concentration-guided sorafenib dosing. *Pharmaceuticals, 14*(5), 389.

Saabi, A. A., Allorge, D., Sauvage, F.-L., Tournel, G., Gaulier, J.-m., Marquet, P., & Picard, N. (2013). Involvement of UDP-Glucuronosyltransferases UGT1A9 and UGT2B7 in Ethanol Glucuronidation, and Interactions with Common Drugs of Abuse. *Drug Metabolism and Disposition, 41*(3), 568-574. 10.1124/dmd.112.047878

Sadeque, A. J. M., Usmani, K. A., Palamar, S., Cerny, M. A., & Chen, W. G. (2012). Identification of human UDP-glucuronosyltransferases involved in N-carbamoyl glucuronidation of lorcaserin. *Drug Metabolism and Disposition, 40*(4), 772-778. 10.1124/dmd.111.043448

Salvatorelli, E., Guarnieri, S., Menna, P., Liberi, G., Calafiore, A. M., Mariggiò, M. A., Mordente, A., Gianni, L., & Minotti, G. (2006). Defective One- or Two-electron Reduction of the Anticancer Anthracycline Epirubicin in Human Heart: RELATIVE IMPORTANCE OF VESICULAR SEQUESTRATION AND IMPAIRED EFFICIENCY OF ELECTRON ADDITION *. *Journal of Biological Chemistry, 281*(16), 10990-11001. 10.1074/jbc.M508343200

Sandström, M., Lindman, H., Nygren, P., Lidbrink, E., Bergh, J., & Karlsson, M. O. (2005). Model describing the relations between pharmacokinetics and hematological toxicity of the epirubicin-docetaxel regimen in breast cancer. *Journal of Clinical Oncology, 23*(3), 413-421.

Savaraj, N., Wu, C., Wangpaichitr, M., Kuo, M. T., Lampidis, T., Robles, C., Furst, A. J., & Feun, L. (2003). Overexpression of mutated MRP4 in cisplatin resistant small cell lung cancer cell line: collateral sensitivity to azidothymidine. *Int J Oncol, 23*(1), 173-179.

Sawyer, M. B., Innocenti, F., Das, S., Cheng, C., Ramírez, J., Pantle-Fisher, F. H., Wright, C., Badner, J., Pei, D., Boyett, J. M., Cook Jr, E., & Ratain, M. J. (2003). A pharmacogenetic study of uridine diphosphate–glucuronosyltransferase 2B7 in patients receiving morphine. *Clinical Pharmacology & Therapeutics, 73*(6), 566-574. 10.1016/S0009-9236(03)00053-5

Sawyer, M. B., Pituskin, E., Damaraju, S., Bies, R. R., Vos, L. J., Prado, C. M. M., Kuzma, M., Scarfe, A. G., Clemons, M., Tonkin, K., Au, H.-J., Koski, S., Joy, A. A., Smylie, M., King, K., Carandang, D., Damaraju, V. L., Hanson, J., Cass, C. E., & Mackey, J. R. (2016). A Uridine Glucuronosyltransferase 2B7 Polymorphism Predicts Epirubicin Clearance and Outcomes in Early-Stage Breast Cancer. *Clinical Breast Cancer, 16*(2), 139-144.e133. 10.1016/j.clbc.2015.09.006

Scacheri, P. C., Rozenblatt-Rosen, O., Caplen, N. J., Wolfsberg, T. G., Umayam, L., Lee, J. C., Hughes, C. M., Shanmugam, K. S., Bhattacharjee, A., Meyerson, M., & Collins, F. S. (2004). Short interfering RNAs can induce unexpected and divergent changes in the levels of untargeted proteins in mammalian cells. *Proc Natl Acad Sci U S A, 101*(7), 1892-1897. 10.1073/pnas.0308698100

Scanlon, K. J., Funato, T., Pezeshki, B., Tone, T., & Sowers, L. C. (1990). Potentiation of azidothymidine cytotoxicity in cisplatin-resistant human ovarian carcinoma cells. *Cancer Commun, 2*(10), 339-343. 10.3727/095535490820874128

Schilsky, R. L., & Kindler, H. L. (2000). Eniluracil: an irreversible inhibitor of dihydropyrimidine dehydrogenase. *Expert Opin Investig Drugs, 9*(7), 1635-1649. 10.1517/13543784.9.7.1635

Schmidt, A., Zhang, H., & Cardoso, M. C. (2020). MeCP2 and Chromatin Compartmentalization. *Cells, 9*(4). 10.3390/cells9040878

Schneider, M. R., & Wolf, E. (2009). The epidermal growth factor receptor ligands at a glance. *Journal of Cellular Physiology, 218*(3), 460-466. 10.1002/jcp.21635

Schultz, D. C., Friedman, J. R., & Rauscher, F. J., 3rd. (2001). Targeting histone deacetylase complexes via KRAB-zinc finger proteins: the PHD and bromodomains of KAP-1 form a cooperative unit that recruits a novel isoform of the Mi-2alpha subunit of NuRD. *Genes Dev, 15*(4), 428-443. 10.1101/gad.869501

Schwartzberg, L. S., Franco, S. X., Florance, A., O'Rourke, L., Maltzman, J., & Johnston, S. (2010). Lapatinib plus letrozole as first-line therapy for HER-2+ hormone receptor-positive metastatic breast cancer. *Oncologist, 15*(2), 122-129. 10.1634/theoncologist.2009-0240

Scott, S. C., Lee, S. S., & Abraham, J. (2017). Mechanisms of therapeutic CDK4/6 inhibition in breast cancer. *Semin Oncol, 44*(6), 385-394. 10.1053/j.seminoncol.2018.01.006

Scudiero, D. A., Shoemaker, R. H., Paull, K. D., Monks, A., Tierney, S., Nofziger, T. H., Currens, M. J., Seniff, D., & Boyd, M. R. (1988). Evaluation of a soluble tetrazolium/formazan assay for cell growth and drug sensitivity in culture using human and other tumor cell lines. *Cancer Res, 48*(17), 4827-4833.

Sebaugh, J. L. (2011). Guidelines for accurate EC50/IC50 estimation. *Pharmaceutical Statistics, 10*(2), 128-134. 10.1002/pst.426

Ségaliny, A. I., Tellez-Gabriel, M., Heymann, M.-F., & Heymann, D. (2015). Receptor tyrosine kinases: Characterisation, mechanism of action and therapeutic interests for bone cancers. *Journal of bone oncology, 4*(1), 1-12. 10.1016/j.jbo.2015.01.001

Seidman, A. D., Tiersten, A., Hudis, C., Gollub, M., Barrett, S., Yao, T. J., Lepore, J., Gilewski, T., Currie, V., Crown, J., & et al. (1995). Phase II trial of paclitaxel by 3-hour infusion as initial and salvage chemotherapy for metastatic breast cancer. *J Clin Oncol, 13*(10), 2575-2581. 10.1200/jco.1995.13.10.2575

Seo, K.-A., Kim, H.-J., Jeong, E. S., Abdalla, N., Choi, C.-S., Kim, D.-H., & Shin, J.-G. (2014). In Vitro Assay of Six UDP-Glucuronosyltransferase Isoforms in Human Liver Microsomes, Using Cocktails of Probe Substrates and Liquid Chromatography–Tandem Mass Spectrometry. *Drug Metabolism and Disposition, 42*(11), 1803-1810. 10.1124/dmd.114.058818

Seshadri, R., Firgaira, F. A., Horsfall, D. J., McCaul, K., Setlur, V., & Kitchen, P. (1993). Clinical significance of HER-2/neu oncogene amplification in primary breast cancer. The South Australian Breast Cancer Study Group. *J Clin Oncol, 11*(10), 1936-1942. 10.1200/jco.1993.11.10.1936

Shakunthala, N. (2010). New cytochrome P450 mechanisms: implications for understanding molecular basis for drug toxicity at the level of the cytochrome. *Expert Opin Drug Metab Toxicol, 6*(1), 1-15. 10.1517/17425250903329095

Shan, B.-J., Shen, X.-B., Jin, W., Dong, M.-H., Han, X.-H., Lin, L., Chen, J., Huang, D.-B., Qian, J., Zhang, J.-J., & Pan, Y.-Y. (2020). Standard-dose epirubicin increases the pathological complete response rate in neoadjuvant chemotherapy for breast cancer: a multicenter retrospective study. *Gland Surgery, 9*(4), 1026-1035.

Shebley, M., Sandhu, P., Emami Riedmaier, A., Jamei, M., Narayanan, R., Patel, A., Peters, S. A., Reddy, V. P., Zheng, M., de Zwart, L., Beneton, M., Bouzom, F., Chen, J., Chen, Y., Cleary, Y., Collins, C., Dickinson, G. L., Djebli, N., Einolf, H. J., Gardner, I., Huth, F., Kazmi, F., Khalil, F., Lin, J., Odinecs, A., Patel, C., Rong, H., Schuck, E., Sharma, P., Wu, S. P., Xu, Y., Yamazaki, S., Yoshida, K., & Rowland, M. (2018). Physiologically Based Pharmacokinetic Model Qualification and Reporting Procedures for

Regulatory Submissions: A Consortium Perspective. *Clin Pharmacol Ther, 104*(1), 88-110. 10.1002/cpt.1013

Shen, H., & Maki, C. G. (2011). Pharmacologic activation of p53 by small-molecule MDM2 antagonists. *Curr Pharm Des, 17*(6), 560-568. 10.2174/138161211795222603

Sherrill, B., Amonkar, M. M., Sherif, B., Maltzman, J., O'Rourke, L., & Johnston, S. (2010). Quality of life in hormone receptor-positive HER-2+ metastatic breast cancer patients during treatment with letrozole alone or in combination with lapatinib. *Oncologist, 15*(9), 944-953. 10.1634/theoncologist.2010-0012

Shibue, T., Takeda, K., Oda, E., Tanaka, H., Murasawa, H., Takaoka, A., Morishita, Y., Akira, S., Taniguchi, T., & Tanaka, N. (2003). Integral role of Noxa in p53-mediated apoptotic response. *Genes Dev, 17*(18), 2233-2238. 10.1101/gad.1103603

Siebel, C., Lanvers-Kaminsky, C., Würthwein, G., Hempel, G., & Boos, J. (2020). Bioanalysis of doxorubicin aglycone metabolites in human plasma samples–implications for doxorubicin drug monitoring. *Scientific Reports, 10*(1), 18562. 10.1038/s41598-020-75662-w

Simpson, D., Curran, M. P., & Perry, C. M. (2004). Letrozole: a review of its use in postmenopausal women with breast cancer. *Drugs, 64*(11), 1213-1230. 10.2165/00003495-200464110-00006

Singh, B., Carpenter, G., & Coffey, R. J. (2016). EGF receptor ligands: recent advances. *F1000Res, 5*. 10.12688/f1000research.9025.1

Singh, H., Walker, A. J., Amiri-Kordestani, L., Cheng, J., Tang, S., Balcazar, P., Barnett-Ringgold, K., Palmby, T. R., Cao, X., Zheng, N., Liu, Q., Yu, J., Pierce, W. F., Daniels, S. R., Sridhara, R., Ibrahim, A., Kluetz, P. G., Blumenthal, G. M., Beaver, J. A., & Pazdur, R. (2018). U.S. Food and Drug Administration Approval: Neratinib for the Extended Adjuvant Treatment of Early-Stage HER2-Positive Breast Cancer. *Clin Cancer Res, 24*(15), 3486-3491. 10.1158/1078-0432.Ccr-17-3628

Sinz, M., Wallace, G., & Sahi, J. (2008). Current industrial practices in assessing CYP450 enzyme induction: preclinical and clinical. *Aaps j, 10*(2), 391-400. 10.1208/s12248-008-9037-4

Smita, P., Narayan, P. A., J, K., & Gaurav, P. (2022). Therapeutic drug monitoring for cytotoxic anticancer drugs: Principles and evidence-based practices [Review]. *Frontiers in oncology, 12*. 10.3389/fonc.2022.1015200

Smith, E. R., Chen, Z.-S., & Xu, X.-X. (2022). 11 - Paclitaxel and cancer treatment: Non-mitotic mechanisms of paclitaxel action in cancer therapy. In M. K. Swamy, T. Pullaiah, & Z.-S. Chen (Eds.), *Paclitaxel* (pp. 269-286). Academic Press. 10.1016/B978-0-323-90951-8.00005-9

Smith, I. E., Walsh, G., Skene, A., Llombart, A., Mayordomo, J. I., Detre, S., Salter, J., Clark, E., Magill, P., & Dowsett, M. (2007). A phase II placebo-controlled trial of neoadjuvant anastrozole alone or with gefitinib in early breast cancer. *J Clin Oncol, 25*(25), 3816-3822. 10.1200/jco.2006.09.6578

Smith, L. A., Cornelius, V. R., Plummer, C. J., Levitt, G., Verrill, M., Canney, P., & Jones, A. (2010). Cardiotoxicity of anthracycline agents for the treatment of cancer: Systematic review and meta-analysis of randomised controlled trials. *BMC cancer, 10*(1), 337. 10.1186/1471-2407-10-337

Sneha, S., Baker, S. C., Green, A., Storr, S., Aiyappa, R., Martin, S., & Pors, K. (2021). Intratumoural Cytochrome P450 Expression in Breast Cancer: Impact on Standard of Care Treatment and New Efforts to Develop Tumour-Selective Therapies. *Biomedicines, 9*(3). 10.3390/biomedicines9030290

Soars, M. G., Petullo, D. M., Eckstein, J. A., Kasper, S. C., & Wrighton, S. A. (2004). An assessment of udp-glucuronosyltransferase induction using primary human hepatocytes. *Drug Metab Dispos, 32*(1), 140-148. 10.1124/dmd.32.1.140

Sokolove, P. M. (1988). Mitochondrial sulfhydryl group modification by adriamycin aglycones. *FEBS Lett, 234*(1), 199-202. 10.1016/0014-5793(88)81333-4

Sorich, M. J., Mutlib, F., van Dyk, M., Hopkins, A. M., Polasek, T. M., Marshall, J. C., Rodrigues, A. D., & Rowland, A. (2019). Use of physiologically based pharmacokinetic modeling to identify physiological and molecular characteristics driving variability in axitinib exposure: a fresh approach to precision dosing in oncology. *The Journal of Clinical Pharmacology, 59*(6), 872-879.

Soussi, T., & Wiman, K. G. (2015). TP53: an oncogene in disguise. *Cell Death & Differentiation, 22*(8), 1239-1249. 10.1038/cdd.2015.53

Spector, N., Xia, W., El-Hariry, I., Yarden, Y., & Bacus, S. (2007). HER2 therapy. Small molecule HER-2 tyrosine kinase inhibitors. *Breast Cancer Research, 9*(2), 205. 10.1186/bcr1652

Stallard, S., Morrison, J. G., George, W. D., & Kaye, S. B. (1990). Distribution of doxorubicin to normal breast and tumour tissue in patients undergoing mastectomy. *Cancer Chemother Pharmacol, 25*(4), 286-290. 10.1007/bf00684887

Stanowicka-Grada, M., & Senkus, E. (2023). Anti-HER2 Drugs for the Treatment of Advanced HER2 Positive Breast Cancer. *Curr Treat Options Oncol, 24*(11), 1633-1650. 10.1007/s11864-023-01137-5

Stojanova, J., Carland, J. E., Murnion, B., Seah, V., Siderov, J., & Lemaitre, F. (2022). Therapeutic drug monitoring in oncology - What's out there: A bibliometric evaluation on the topic. *Front Oncol, 12*, 959741. 10.3389/fonc.2022.959741

Strassburg, C. P., Manns, M. P., & Tukey, R. H. (1998). Expression of the UDP-glucuronosyltransferase 1A locus in human colon. Identification and characterization of the novel extrahepatic UGT1A8. *J Biol Chem, 273*(15), 8719-8726. 10.1074/jbc.273.15.8719

Strelow, J., Dewe, W., Iversen, P. W., Brooks, H. B., Radding, J. A., McGee, J., & Weidner, J. (2004). Mechanism of Action Assays for Enzymes. In S. Markossian, A. Grossman, K. Brimacombe, M. Arkin, D. Auld, C. Austin, J. Baell, T. D. Y. Chung, N. P. Coussens, J. L. Dahlin, V. Devanarayan, T. L. Foley, M. Glicksman, K. Gorshkov, J. V. Haas, M. D. Hall, S. Hoare, J. Inglese, P. W. Iversen, S. C. Kales, M. Lal-Nag, Z. Li, J. McGee, O. McManus, T. Riss, P. Saradjian, G. S. Sittampalam, M. Tarselli, O. J. Trask, Jr., Y. Wang, J. R. Weidner, M. J. Wildey, K. Wilson, M. Xia, & X. Xu (Eds.), *Assay Guidance Manual*. Eli Lilly & Company and the National Center for Advancing Translational Sciences.

Sun, C., & Di Rienzo, A. (2009). UGT2B7 is not expressed in normal breast. *Breast Cancer Res Treat, 117*(1), 225-226. 10.1007/s10549-008-0280-2

Sun, D., Jones, N. R., Manni, A., & Lazarus, P. (2013). Characterization of raloxifene glucuronidation: potential role of UGT1A8 genotype on raloxifene metabolism in vivo. *Cancer Prev Res (Phila), 6*(7), 719-730. 10.1158/1940-6207.Capr-12-0448

Sun, D., Sharma, A. K., Dellinger, R. W., Blevins-Primeau, A. S., Balliet, R. M., Chen, G., Boyiri, T., Amin, S., & Lazarus, P. (2007). Glucuronidation of active tamoxifen metabolites by the human UDP glucuronosyltransferases. *Drug Metab Dispos, 35*(11), 2006-2014. 10.1124/dmd.107.017145

Sun, Y.-L., Patel, A., Kumar, P., & Chen, Z.-S. (2012). Role of ABC transporters in cancer chemotherapy. *Chinese Journal of Cancer, 31*(2), 51-57. 10.5732/cjc.011.10466

Sunderland, M. C., & Osborne, C. K. (1991). Tamoxifen in premenopausal patients with metastatic breast cancer: a review. *J Clin Oncol, 9*(7), 1283-1297. 10.1200/jco.1991.9.7.1283

Sung, H., Ferlay, J., Siegel, R. L., Laversanne, M., Soerjomataram, I., Jemal, A., & Bray, F. (2021). Global Cancer Statistics 2020: GLOBOCAN Estimates of Incidence and Mortality Worldwide for 36 Cancers in 185 Countries. *CA: A Cancer Journal for Clinicians, 71*(3), 209-249. 10.3322/caac.21660

Svedberg, A., Vikingsson, S., Vikström, A., Hornstra, N., Kentson, M., Branden, E., Koyi, H., Bergman, B., & Gréen, H. (2019). Erlotinib treatment induces cytochrome P450 3A activity in non-small cell lung cancer patients. *British journal of clinical pharmacology, 85*(8), 1704-1709. 10.1111/bcp.13953

Szakács, G., Paterson, J. K., Ludwig, J. A., Booth-Genthe, C., & Gottesman, M. M. (2006). Targeting multidrug resistance in cancer. *Nat Rev Drug Discov, 5*(3), 219-234. 10.1038/nrd1984

Takahashi, T., Fujiwara, Y., Yamakido, M., Katoh, O., Watanabe, H., & Mackenzie, P. I. (1997). The role of glucuronidation in 7-ethyl-10-hydroxycamptothecin resistance in vitro. *Jpn J Cancer Res, 88*(12), 1211-1217. 10.1111/j.1349-7006.1997.tb00351.x

Takanashi, S., & Bachur, N. R. (1976). Adriamycin metabolism in man. Evidence from urinary metabolites. *Drug Metabolism and Disposition, 4*(1), 79-87.

Tamiya, A., Tamiya, M., Nishihara, T., Shiroyama, T., Nakao, K., Tsuji, T., Takeuchi, N., Isa, S. I., Omachi, N., Okamoto, N., Suzuki, H., Okishio, K., Iwazaki, A., Imai, K., Hirashima, T., & Atagi, S. (2017). Cerebrospinal Fluid Penetration Rate and Efficacy of Afatinib in Patients with EGFR Mutation-positive Non-small Cell Lung Cancer with Leptomeningeal Carcinomatosis: A Multicenter Prospective Study. *Anticancer Res, 37*(8), 4177-4182. 10.21873/anticanres.11806

Tamura, K., Stecher, G., & Kumar, S. (2021). MEGA11: Molecular Evolutionary Genetics Analysis Version 11. *Molecular Biology and Evolution, 38*(7), 3022-3027. 10.1093/molbev/msab120

Tapaninen, T., Olkkola, A. M., Tornio, A., Neuvonen, M., Elonen, E., Neuvonen, P. J., Niemi, M., & Backman, J. T. (2020). Itraconazole Increases Ibrutinib Exposure 10-Fold and Reduces Interindividual Variation-A Potentially Beneficial Drug-Drug Interaction. *Clin Transl Sci, 13*(2), 345-351. 10.1111/cts.12716

Tariq, M., Alam, M. A., Singh, A. T., Panda, A. K., & Talegaonkar, S. (2016). Improved oral efficacy of epirubicin through polymeric nanoparticles: pharmacodynamic and toxicological investigations. *Drug Delivery, 23*(8), 2990-2997. 10.3109/10717544.2015.1136713

TGA. (2012). *Australian Public Assessment Report for lapatinib*. https://www.tga.gov.au/sites/default/files/auspar-lapatinib-121112.pdf

TGA. (2014). *AusPAR Afatinib dimaleate*. https://www.tga.gov.au/sites/default/files/auspar-afatinib-dimaleate-140414.pdf

TGA. (2020). *Australian Public Assessment Report for Neratinib (as maleate)*. https://www.tga.gov.au/sites/default/files/auspar-neratinib-as-maleate-020512.pdf

Thomson, R. J., Moshirfar, M., & Ronquillo, Y. (2023). Tyrosine Kinase Inhibitors. In *StatPearls*. StatPearls Publishing.

Thorn, C. F., Klein, T. E., & Altman, R. B. (2009). Codeine and morphine pathway. *Pharmacogenetics and genomics, 19*(7), 556-558. 10.1097/FPC.0b013e32832e0eac

Thorn, C. F., Oshiro, C., Marsh, S., Hernandez-Boussard, T., McLeod, H., Klein, T. E., & Altman, R. B. (2011). Doxorubicin pathways: pharmacodynamics and adverse effects. *Pharmacogenetics and genomics, 21*(7), 440-446. 10.1097/FPC.0b013e32833ffb56

Thummel, K. E., & Wilkinson, G. R. (1998). IN VITRO AND IN VIVO DRUG INTERACTIONS INVOLVING HUMAN CYP3A. *Annual Review of Pharmacology and Toxicology, 38*(1), 389-430. 10.1146/annurev.pharmtox.38.1.389

Tolaney, S. M., Barry, W. T., Guo, H., Dillon, D., Dang, C. T., Yardley, D. A., Moy, B., Marcom, P. K., Albain, K. S., Rugo, H. S., Ellis, M. J., Shapira, I., Wolff, A. C., Carey, L. A., Overmoyer, B., Partridge, A. H., Hudis, C. A., Krop, I. E., Burstein, H. J., & Winer, E. P. (2017). Seven-year (yr) follow-up of adjuvant paclitaxel (T) and trastuzumab (H) (APT trial) for node-negative, HER2-positive breast cancer (BC). *Journal of Clinical Oncology, 35*(15), 511-511. 10.1200/JCO.2017.35.15_suppl.511

Tornio, A., Filppula, A. M., Niemi, M., & Backman, J. T. (2019). Clinical Studies on Drug-Drug Interactions Involving Metabolism and Transport: Methodology, Pitfalls, and Interpretation. *Clin Pharmacol Ther, 105*(6), 1345-1361. 10.1002/cpt.1435

Tourancheau, A., Margaillan, G., Rouleau, M., Gilbert, I., Villeneuve, L., Lévesque, E., Droit, A., & Guillemette, C. (2016). Unravelling the transcriptomic landscape of the major phase II UDP-glucuronosyltransferase drug metabolizing pathway using targeted RNA sequencing. *Pharmacogenomics J, 16*(1), 60-70. 10.1038/tpj.2015.20

Tremont, A., Lu, J., & Cole, J. T. (2017). Endocrine Therapy for Early Breast Cancer: Updated Review. *Ochsner J, 17*(4), 405-411.

Tryfonidis, K., Basaran, G., Bogaerts, J., Debled, M., Dirix, L., Thery, J. C., Tjan-Heijnen, V. C., Van den Weyngaert, D., Cufer, T., Piccart, M., & Cameron, D. (2016). A European Organisation for Research and Treatment of Cancer randomized, double-blind, placebo-controlled, multicentre phase II trial of anastrozole in combination with gefitinib or placebo in hormone receptor-positive advanced breast cancer (NCT00066378). *Eur J Cancer, 53*, 144-154. 10.1016/j.ejca.2015.10.012

Tsamandouras, N., Rostami-Hodjegan, A., & Aarons, L. (2015). Combining the 'bottom up' and 'top down' approaches in pharmacokinetic modelling: fitting PBPK models to observed clinical data. *British journal of clinical pharmacology, 79*(1), 48-55. 10.1111/bcp.12234

Tseng, T.-H., Chien, M.-H., Lin, W.-L., Wen, Y.-C., Chow, J.-M., Chen, C.-K., Kuo, T.-C., & Lee, W.-J. (2017). Inhibition of MDA-MB-231 breast cancer cell proliferation and tumor growth by apigenin through induction of G2/M arrest and histone H3 acetylation-mediated p21WAF1/CIP1 expression. *Environmental Toxicology, 32*(2), 434-444. 10.1002/tox.22247

Tuladhar, R., Yeu, Y., Tyler Piazza, J., Tan, Z., Rene Clemenceau, J., Wu, X., Barrett, Q., Herbert, J., Mathews, D. H., Kim, J., Hyun Hwang, T., & Lum, L. (2019). CRISPR-Cas9-based mutagenesis frequently

provokes on-target mRNA misregulation. *Nature Communications, 10*(1), 4056. 10.1038/s41467-019-12028-5

Turgeon, D., Carrier, J.-S. b., Lévesque, E. r., Hum, D. W., & Bélanger, A. (2001). Relative Enzymatic Activity, Protein Stability, and Tissue Distribution of Human Steroid-Metabolizing UGT2B Subfamily Members. *Endocrinology, 142*(2), 778-787. 10.1210/endo.142.2.7958

Uchaipichat, V., Rowland, A., & Miners, J. O. (2022). Inhibitory effects of non-steroidal anti-inflammatory drugs on human liver microsomal morphine glucuronidation: Implications for drug-drug interaction liability. *Drug Metabolism and Pharmacokinetics, 42*, 100442. 10.1016/j.dmpk.2021.100442

Uchaipichat, V., Suthisisang, C., & Miners, J. O. (2013). The Glucuronidation of R- and S-Lorazepam: Human Liver Microsomal Kinetics, UDP-Glucuronosyltransferase Enzyme Selectivity, and Inhibition by Drugs. *Drug Metabolism and Disposition, 41*(6), 1273-1284. 10.1124/dmd.113.051656

Uchaipichat, V., Winner, L. K., Mackenzie, P. I., Elliot, D. J., Williams, J. A., & Miners, J. O. (2006). Quantitative prediction of in vivo inhibitory interactions involving glucuronidated drugs from in vitro data: the effect of fluconazole on zidovudine glucuronidation. *British journal of clinical pharmacology, 61*(4), 427-439. 10.1111/j.1365-2125.2006.02588.x

Ueno, N. T., & Zhang, D. (2011). Targeting EGFR in Triple Negative Breast Cancer. *J Cancer, 2*, 324-328. 10.7150/jca.2.324

Ulrich, L., & Okines, A. F. C. (2021). Treating Advanced Unresectable or Metastatic HER2-Positive Breast Cancer: A Spotlight on Tucatinib. *Breast Cancer (Dove Med Press), 13*, 361-381. 10.2147/bctt.S268451

Umekita, N., Awane, Y., Maeshiro, T., Miyamoto, S., Yamada, F., & Matsumine, T. (1992). [A pharmacokinetic study of intra-arterial chemotherapy for prophylactic treatment of liver metastasis after hepatectomy for liver cancer]. *Gan To Kagaku Ryoho, 19*(10 Suppl), 1544-1546.

Untch, M., & Lück, H. J. (2010). Lapatinib - Member of a New Generation of ErbB-Targeting Drugs. *Breast Care (Basel), 5*(s1), 8-12. 10.1159/000285750

Untch, M., Muscholl, M., Tjulandin, S., Jonat, W., Meerpohl, H. G., Lichinitser, M., Manikhas, A. G., Coumbos, A., Kreienberg, R., du Bois, A., Harbeck, N., Jackisch, C., Müller, V., Pauschinger, M., Thomssen, C., Lehle, M., Catalani, O., & Lück, H. J. (2010). First-line trastuzumab plus epirubicin and cyclophosphamide therapy in patients with human epidermal growth factor receptor 2-positive metastatic breast cancer: cardiac safety and efficacy data from the Herceptin, Cyclophosphamide, and Epirubicin (HERCULES) trial. *J Clin Oncol, 28*(9), 1473-1480. 10.1200/jco.2009.21.9709

Useckaite, Z., Rodrigues, A. D., Hopkins, A. M., Newman, L. A., Johnson, J., Sorich, M. J., & Rowland, A. (2021). Role of extracellular vesicle-derived biomarkers in drug metabolism and disposition. *Drug Metabolism and Disposition, 49*(11), 961-971.

Uusi-Mäkelä, M. I. E., Barker, H. R., Bäuerlein, C. A., Häkkinen, T., Nykter, M., & Rämet, M. (2018). Chromatin accessibility is associated with CRISPR-Cas9 efficiency in the zebrafish (Danio rerio). *PLoS ONE, 13*(4), e0196238. 10.1371/journal.pone.0196238

van Asperen, J., van Tellingen, O., Tijssen, F., Schinkel, A. H., & Beijnen, J. H. (1999). Increased accumulation of doxorubicin and doxorubicinol in cardiac tissue of mice lacking mdr1a P-glycoprotein. *Br J Cancer, 79*(1), 108-113. 10.1038/sj.bjc.6690019

van de Loosdrecht, A. A., Beelen, R. H., Ossenkoppele, G. J., Broekhoven, M. G., & Langenhuijsen, M. M. (1994). A tetrazolium-based colorimetric MTT assay to quantitate human monocyte mediated cytotoxicity against leukemic cells from cell lines and patients with acute myeloid leukemia. *J Immunol Methods, 174*(1-2), 311-320. 10.1016/0022-1759(94)90034-5

van Tonder, A., Joubert, A. M., & Cromarty, A. D. (2015). Limitations of the 3-(4,5-dimethylthiazol-2-yl)-2,5-diphenyl-2H-tetrazolium bromide (MTT) assay when compared to three commonly used cell enumeration assays. *BMC Research Notes, 8*(1), 47. 10.1186/s13104-015-1000-8

van Veelen, A., Gulikers, J., Hendriks, L. E. L., Dursun, S., Ippel, J., Smit, E. F., Dingemans, A. C., van Geel, R., & Croes, S. (2022). Pharmacokinetic boosting of osimertinib with cobicistat in patients with non-small cell lung cancer: The OSIBOOST trial. *Lung Cancer, 171*, 97-102. 10.1016/j.lungcan.2022.07.012

Varshavsky-Yanovsky, A. N., & Goldstein, L. J. (2020). Role of Capecitabine in Early Breast Cancer. *J Clin Oncol, 38*(3), 179-182. 10.1200/jco.19.02946

Vasan, N., Baselga, J., & Hyman, D. M. (2019). A view on drug resistance in cancer. *Nature, 575*(7782), 299-309. 10.1038/s41586-019-1730-1

Venturini, M. (2002). Rational development of capecitabine. *Eur J Cancer, 38 Suppl 2*, 3-9. 10.1016/s0959-8049(01)00414-2

Veronesi, U., Boyle, P., Goldhirsch, A., Orecchia, R., & Viale, G. (2005). Breast cancer. *The Lancet, 365*(9472), 1727-1741. 10.1016/S0140-6736(05)66546-4

Vieira, M. L., Kirby, B., Ragueneau-Majlessi, I., Galetin, A., Chien, J. Y., Einolf, H. J., Fahmi, O. A., Fischer, V., Fretland, A., Grime, K., Hall, S. D., Higgs, R., Plowchalk, D., Riley, R., Seibert, E., Skordos, K., Snoeys, J., Venkatakrishnan, K., Waterhouse, T., Obach, R. S., Berglund, E. G., Zhang, L., Zhao, P., Reynolds, K. S., & Huang, S. M. (2014). Evaluation of various static in vitro-in vivo extrapolation models for risk assessment of the CYP3A inhibition potential of an investigational drug. *Clin Pharmacol Ther, 95*(2), 189-198. 10.1038/clpt.2013.187

Visvanathan, K., Chlebowski, R. T., Hurley, P., Col, N. F., Ropka, M., Collyar, D., Morrow, M., Runowicz, C., Pritchard, K. I., Hagerty, K., Arun, B., Garber, J., Vogel, V. G., Wade, J. L., Brown, P., Cuzick, J., Kramer, B. S., & Lippman, S. M. (2009). American society of clinical oncology clinical practice guideline update on the use of pharmacologic interventions including tamoxifen, raloxifene, and aromatase inhibition for breast cancer risk reduction. *J Clin Oncol, 27*(19), 3235-3258. 10.1200/jco.2008.20.5179

Vitale, D., Caon, I., Parnigoni, A., Sevic, I., Spinelli, F., Icardi, A., Passi, A., Vigetti, D., & Alaniz, L. (2020). *Knockdown Of Udp-Glucose Dehydrogenase Facilitates Epirubicin-Resistance In MDA-MB-231 Breast Cancer Cells By Regulation Of Hyaluronan Synthesis*. 10.21203/rs.3.rs-66926/v1

von Minckwitz, G., Procter, M., de Azambuja, E., Zardavas, D., Benyunes, M., Viale, G., Suter, T., Arahmani, A., Rouchet, N., Clark, E., Knott, A., Lang, I., Levy, C., Yardley, D. A., Bines, J., Gelber, R. D., Piccart, M., & Baselga, J. (2017). Adjuvant Pertuzumab and Trastuzumab in Early HER2-Positive Breast Cancer. *N Engl J Med, 377*(2), 122-131. 10.1056/NEJMoa1703643

Vulsteke, C., Lambrechts, D., Dieudonné, A., Hatse, S., Brouwers, B., van Brussel, T., Neven, P., Belmans, A., Schöffski, P., Paridaens, R., & Wildiers, H. (2013). Genetic variability in the multidrug resistance associated protein-1 (ABCC1/MRP1) predicts hematological toxicity in breast cancer patients

receiving (neo-)adjuvant chemotherapy with 5-fluorouracil, epirubicin and cyclophosphamide (FEC). *Annals of Oncology, 24*(6), 1513-1525. 10.1093/annonc/mdt008

Wade, J. R., Kelman, A. W., Kerr, D. J., Robert, J., & Whiting, B. (1992). Variability in the pharmacokinetics of epirubicin: a population analysis. *Cancer Chemother Pharmacol, 29*(5), 391-395. 10.1007/bf00686009

Wahba, H. A., & El-Hadaad, H. A. (2015). Current approaches in treatment of triple-negative breast cancer. *Cancer Biol Med, 12*(2), 106-116. 10.7497/j.issn.2095-3941.2015.0030

Wahlström, A., Lenhammar, L., Ask, B., & Rane, A. (1994). Tricyclic antidepressants inhibit opioid receptor binding in human brain and hepatic morphine glucuronidation. *Pharmacol Toxicol, 75*(1), 23-27. 10.1111/j.1600-0773.1994.tb00319.x

Waks, A. G., & Winer, E. P. (2019). Breast Cancer Treatment: A Review. *JAMA, 321*(3), 288-300. 10.1001/jama.2018.19323

Wang, D.-Y., Fulthorpe, R., Liss, S. N., & Edwards, E. A. (2004a). Identification of Estrogen-Responsive Genes by Complementary Deoxyribonucleic Acid Microarray and Characterization of a Novel Early Estrogen-Induced Gene: EEIG1. *Molecular Endocrinology, 18*(2), 402-411. 10.1210/me.2003-0202

Wang, H., Guo, S., Kim, S. J., Shao, F., Ho, J. W. K., Wong, K. U., Miao, Z., Hao, D., Zhao, M., Xu, J., Zeng, J., Wong, K. H., Di, L., Wong, A. H., Xu, X., & Deng, C. X. (2021). Cisplatin prevents breast cancer metastasis through blocking early EMT and retards cancer growth together with paclitaxel. *Theranostics, 11*(5), 2442-2459. 10.7150/thno.46460

Wang, Y., Katzenmeyer, J. B., & Arriaga, E. A. (2011). Combination of micellar electrokinetic and high-performance liquid chromatographies to assess age-related changes in the in vitro metabolism of Fischer 344 rat liver. *J Gerontol A Biol Sci Med Sci, 66*(9), 935-943. 10.1093/gerona/glr074

Wang, Y., Seimiya, M., Kawamura, K., Yu, L., Ogi, T., Takenaga, K., Shishikura, T., Nakagawara, A., Sakiyama, S., Tagawa, M., & J, O. W. (2004b). Elevated expression of DNA polymerase kappa in human lung cancer is associated with p53 inactivation: Negative regulation of POLK promoter activity by p53. *Int J Oncol, 25*(1), 161-165.

Wawruszak, A., Halasa, M., Okon, E., Kukula-Koch, W., & Stepulak, A. (2021). Valproic Acid and Breast Cancer: State of the Art in 2021. *Cancers (Basel), 13*(14). 10.3390/cancers13143409

Weber, B. L., Vogel, C., Jones, S., Harvey, H., Hutchins, L., Bigley, J., & Hohneker, J. (1995). Intravenous vinorelbine as first-line and second-line therapy in advanced breast cancer. *J Clin Oncol, 13*(11), 2722-2730. 10.1200/jco.1995.13.11.2722

Wee, P., & Wang, Z. (2017). Epidermal Growth Factor Receptor Cell Proliferation Signaling Pathways. *Cancers (Basel), 9*(5). 10.3390/cancers9050052

Wen, J., Ren, L., Li, W., Li, J., Huang, L., Yuan, Z., & Chen, Q. (2022). New classification for advanced breast cancer patients experiencing disease progression during salvage treatment: a single-center retrospective cohort study. *Annals of Translational Medicine, 10*(10), 553.

Westra, N., Touw, D., Lub-de Hooge, M., Kosterink, J., & Oude Munnink, T. (2023). Pharmacokinetic Boosting of Kinase Inhibitors. *Pharmaceutics, 15*(4). 10.3390/pharmaceutics15041149

Whirl-Carrillo, M., Huddart, R., Gong, L., Sangkuhl, K., Thorn, C. F., Whaley, R., & Klein, T. E. (2021). An Evidence-Based Framework for Evaluating Pharmacogenomics Knowledge for Personalized Medicine. *Clin Pharmacol Ther, 110*(3), 563-572. 10.1002/cpt.2350

WHO. (2018). *WHO Guidelines for the Pharmacological and Radiotherapeutic Management of Cancer Pain in Adults and Adolescents*. World Health Organization.

Wiener, D., Doerge, D. R., Fang, J. L., Upadhyaya, P., & Lazarus, P. (2004a). Characterization of N-glucuronidation of the lung carcinogen 4-(methylnitrosamino)-1-(3-pyridyl)-1-butanol (NNAL) in human liver: importance of UDP-glucuronosyltransferase 1A4. *Drug Metab Dispos, 32*(1), 72-79. 10.1124/dmd.32.1.72

Wiener, D., Fang, J. L., Dossett, N., & Lazarus, P. (2004b). Correlation between UDP-glucuronosyltransferase genotypes and 4-(methylnitrosamino)-1-(3-pyridyl)-1-butanone glucuronidation phenotype in human liver microsomes. *Cancer Res, 64*(3), 1190-1196. 10.1158/0008-5472.can-03-3219

Wijayakumara, D. (2021). *Regulation of UDP-glucuronosyltransferases by microRNAs*, Flinders University, College of Medicine and Public Health].

Wijayakumara, D. D., Hu, D. G., Meech, R., McKinnon, R. A., & Mackenzie, P. I. (2015). Regulation of Human UGT2B15 and UGT2B17 by miR-376c in Prostate Cancer Cell Lines. *Journal of Pharmacology and Experimental Therapeutics, 354*(3), 417-425. 10.1124/jpet.115.226118

Wijayakumara, D. D., Mackenzie, P. I., McKinnon, R. A., Hu, D. G., & Meech, R. (2017). Regulation of UDP-Glucuronosyltransferases UGT2B4 and UGT2B7 by MicroRNAs in Liver Cancer Cells. *J Pharmacol Exp Ther, 361*(3), 386-397. 10.1124/jpet.116.239707

Wilhelm, M., Mueller, L., Miller, M. C., Link, K., Holdenrieder, S., Bertsch, T., Kunzmann, V., Stoetzer, O. J., Suttmann, I., Braess, J., Birkmann, J., Roessler, M., Moritz, B., Kraff, S., Salamone, S. J., & Jaehde, U. (2016). Prospective, Multicenter Study of 5-Fluorouracil Therapeutic Drug Monitoring in Metastatic Colorectal Cancer Treated in Routine Clinical Practice. *Clin Colorectal Cancer, 15*(4), 381-388. 10.1016/j.clcc.2016.04.001

Wills, K. H., Behan, S. J., Nance, M. J., Dawson, J. L., Polasek, T. M., Hopkins, A. M., van Dyk, M., & Rowland, A. (2021). Combining therapeutic drug monitoring and pharmacokinetic modelling deconvolutes physiological and environmental sources of variability in clozapine exposure. *Pharmaceutics, 14*(1), 47.

Wils, J. A., Bliss, J. M., Marty, M., Coombes, G., Fontaine, C., Morvan, F., Olmos, T., Pérez-López, F. R., Vassilopoulos, P., Woods, E., & Coombes, R. C. (1999). Epirubicin plus tamoxifen versus tamoxifen alone in node-positive postmenopausal patients with breast cancer: A randomized trial of the International Collaborative Cancer Group. *J Clin Oncol, 17*(7), 1988-1998. 10.1200/jco.1999.17.7.1988

Wind, S., Giessmann, T., Jungnik, A., Brand, T., Marzin, K., Bertulis, J., Hocke, J., Gansser, D., & Stopfer, P. (2014). Pharmacokinetic Drug Interactions of Afatinib with Rifampicin and Ritonavir. *Clinical Drug Investigation, 34*(3), 173-182. 10.1007/s40261-013-0161-2

Wind, S., Schnell, D., Ebner, T., Freiwald, M., & Stopfer, P. (2017). Clinical Pharmacokinetics and Pharmacodynamics of Afatinib. *Clin Pharmacokinet, 56*(3), 235-250. 10.1007/s40262-016-0440-1

Wu, G. S., Burns, T. F., McDonald, E. R., 3rd, Meng, R. D., Kao, G., Muschel, R., Yen, T., & el-Deiry, W. S. (1999). Induction of the TRAIL receptor KILLER/DR5 in p53-dependent apoptosis but not growth arrest. *Oncogene, 18*(47), 6411-6418. 10.1038/sj.onc.1203025

Wu, L., Ke, L., Zhang, Z., Yu, J., & Meng, X. (2020). Development of EGFR TKIs and Options to Manage Resistance of Third-Generation EGFR TKI Osimertinib: Conventional Ways and Immune Checkpoint Inhibitors [Review]. *Frontiers in oncology, 10*. 10.3389/fonc.2020.602762

Wynn, C. S., & Tang, S. C. (2022). Anti-HER2 therapy in metastatic breast cancer: many choices and future directions. *Cancer Metastasis Rev, 41*(1), 193-209. 10.1007/s10555-022-10021-x

Xia, X., Gong, C., Zhang, Y., & Xiong, H. (2023). The History and Development of HER2 Inhibitors. *Pharmaceuticals (Basel), 16*(10). 10.3390/ph16101450

Xiao, H., Zheng, Y., Ma, L., Tian, L., & Sun, Q. (2021). Clinically-Relevant ABC Transporter for Anti-Cancer Drug Resistance. *Front Pharmacol, 12*, 648407. 10.3389/fphar.2021.648407

Xie, Y., Luo, X., Li, H., Xu, Q., He, Z., Zhao, Q., Zuo, Z., & Ren, J. (2020). autoRPA: A web server for constructing cancer staging models by recursive partitioning analysis. *Computational and Structural Biotechnology Journal, 18*, 3361-3367. 10.1016/j.csbj.2020.10.038

Xiu, F., Rausch, M., Gai, Z., Su, S., Wang, S., & Visentin, M. (2023). The Role of Organic Cation Transporters in the Pharmacokinetics, Pharmacodynamics and Drug-Drug Interactions of Tyrosine Kinase Inhibitors. *Int J Mol Sci, 24*(3). 10.3390/ijms24032101

Yamanaka, H., Nakajima, M., Katoh, M., Kanoh, A., Tamura, O., Ishibashi, H., & Yokoi, T. (2005). TRANS-3'-HYDROXYCOTININE O- AND N-GLUCURONIDATIONS IN HUMAN LIVER MICROSOMES. *Drug Metabolism and Disposition, 33*(1), 23-30. 10.1124/dmd.104.001701

Yamaoka, T., Kusumoto, S., Ando, K., Ohba, M., & Ohmori, T. (2018). Receptor Tyrosine Kinase-Targeted Cancer Therapy. *International Journal of Molecular Sciences, 19*(11), 3491. 10.3390/ijms19113491

Yang, F., Teves, S. S., Kemp, C. J., & Henikoff, S. (2014). Doxorubicin, DNA torsion, and chromatin dynamics. *Biochimica et biophysica acta, 1845*(1), 84-89. 10.1016/j.bbcan.2013.12.002

Yang, V., Gouveia, M. J., Santos, J., Koksch, B., Amorim, I., Gärtner, F., & Vale, N. (2020a). Breast cancer: insights in disease and influence of drug methotrexate. *RSC Med Chem, 11*(6), 646-664. 10.1039/d0md00051e

Yang, W. Q., & Zhang, Y. (2012). RNAi-mediated gene silencing in cancer therapy. *Expert Opin Biol Ther, 12*(11), 1495-1504. 10.1517/14712598.2012.712107

Yang, Y., Choppavarapu, L., Fang, K., Naeini, A. S., Nosirov, B., Li, J., Yang, K., He, Z., Zhou, Y., Schiff, R., Li, R., Hu, Y., Wang, J., & Jin, V. X. (2020b). The 3D genomic landscape of differential response to EGFR/HER2 inhibition in endocrine-resistant breast cancer cells. *Biochim Biophys Acta Gene Regul Mech, 1863*(11), 194631. 10.1016/j.bbagrm.2020.194631

Yao, J., Deng, K., Huang, J., Zeng, R., & Zuo, J. (2020). Progress in the Understanding of the Mechanism of Tamoxifen Resistance in Breast Cancer [Review]. *Frontiers in Pharmacology, 11*. 10.3389/fphar.2020.592912

Yarden, Y., & Sliwkowski, M. X. (2001). Untangling the ErbB signalling network. *Nat Rev Mol Cell Biol, 2*(2), 127-137. 10.1038/35052073

Ye, L., Yang, X., Guo, E., Chen, W., Lu, L., Wang, Y., Peng, X., Yan, T., Zhou, F., & Liu, Z. (2014). Sorafenib metabolism is significantly altered in the liver tumor tissue of hepatocellular carcinoma patient. *PLoS ONE, 9*(5), e96664. 10.1371/journal.pone.0096664

Yeo, N. C., Chavez, A., Lance-Byrne, A., Chan, Y., Menn, D., Milanova, D., Kuo, C. C., Guo, X., Sharma, S., Tung, A., Cecchi, R. J., Tuttle, M., Pradhan, S., Lim, E. T., Davidsohn, N., Ebrahimkhani, M. R., Collins, J. J., Lewis, N. E., Kiani, S., & Church, G. M. (2018). An enhanced CRISPR repressor for targeted mammalian gene regulation. *Nat Methods, 15*(8), 611-616. 10.1038/s41592-018-0048-5

Yoon, J. H. (2005). Systemic overview of 5-FU based chemotherapy in breast cancer. *Korean J Clin Oncol, 1*(1), 68-73.

Yu, F., & Bender, W. *The mechanism of tamoxifen in breast cancer prevention*. Breast Cancer Res. 2001;3(Suppl 1):A74. doi: 10.1186/bcr404. Epub 2001 May 29.

Yu, H. A., & Riely, G. J. (2013). Second-generation epidermal growth factor receptor tyrosine kinase inhibitors in lung cancers. *J Natl Compr Canc Netw, 11*(2), 161-169. 10.6004/jnccn.2013.0024

Yu, J., & Zhang, L. (2008). PUMA, a potent killer with or without p53. *Oncogene, 27 Suppl 1*(Suppl 1), S71-83. 10.1038/onc.2009.45

Yu, K. D., Ge, J. Y., Liu, X. Y., Mo, M., He, M., & Shao, Z. M. (2021). Cyclophosphamide-Free Adjuvant Chemotherapy for Ovarian Protection in Young Women With Breast Cancer: A Randomized Phase 3 Trial. *J Natl Cancer Inst, 113*(10), 1352-1359. 10.1093/jnci/djab065

Yuan, P., Kang, Y., Ma, F., Fan, Y., Wang, J., Wang, X., Yue, J., Luo, Y., Zhang, P., Li, Q., & Xu, B. (2023). Effect of Epirubicin Plus Paclitaxel vs Epirubicin and Cyclophosphamide Followed by Paclitaxel on Disease-Free Survival Among Patients With Operable ERBB2-Negative and Lymph Node–Positive Breast Cancer: A Randomized Clinical Trial. *JAMA Network Open, 6*(2), e230122-e230122. 10.1001/jamanetworkopen.2023.0122

Yueh, M. F., Mellon, P. L., & Tukey, R. H. (2011). Inhibition of human UGT2B7 gene expression in transgenic mice by the constitutive androstane receptor. *Mol Pharmacol, 79*(6), 1053-1060. 10.1124/mol.110.070649

Zand, R., Nelson, S. D., Slattery, J. T., Thummel, K. E., Kalhorn, T. F., Adams, S. P., & Wright, J. M. (1993). Inhibition and induction of cytochrome P4502E1-catalyzed oxidation by isoniazid in humans. *Clinical Pharmacology & Therapeutics, 54*(2), 142-149. 10.1038/clpt.1993.125

Zhang, C., Xu, C., Gao, X., & Yao, Q. (2022). Platinum-based drugs for cancer therapy and anti-tumor strategies. *Theranostics, 12*(5), 2115-2132. 10.7150/thno.69424

Zhang, D., Hop, C., Patilea-Vrana, G., Gampa, G., Seneviratne, H. K., Unadkat, J. D., Kenny, J. R., Nagapudi, K., Di, L., Zhou, L., Zak, M., Wright, M. R., Bumpus, N. N., Zang, R., Liu, X., Lai, Y., & Khojasteh, S. C. (2019). Drug Concentration Asymmetry in Tissues and Plasma for Small Molecule-Related Therapeutic Modalities. *Drug Metab Dispos, 47*(10), 1122-1135. 10.1124/dmd.119.086744

Zhang, N., Liu, Y., & Jeong, H. (2015). Drug-Drug Interaction Potentials of Tyrosine Kinase Inhibitors via Inhibition of UDP-Glucuronosyltransferases. *Sci Rep, 5*, 17778. 10.1038/srep17778

Zhao, C., Han, S. Y., & Li, P. P. (2017). Pharmacokinetics of Gefitinib: Roles of Drug Metabolizing Enzymes and Transporters. *Curr Drug Deliv, 14*(2), 282-288. 10.2174/1567201813666160709021605

Zheng, Q., Zhang, M., Zhou, F., Zhang, L., & Meng, X. (2020). The Breast Cancer Stem Cells Traits and Drug Resistance. *Front Pharmacol, 11*, 599965. 10.3389/fphar.2020.599965

Zhong, D.-s., Lu, X.-h., Conklin, B. S., Lin, P. H., Lumsden, A. B., Yao, Q., & Chen, C. (2002). HIV Protease Inhibitor Ritonavir Induces Cytotoxicity of Human Endothelial Cells. *Arteriosclerosis, Thrombosis, and Vascular Biology, 22*(10), 1560-1566. doi:10.1161/01.ATV.0000034707.40046.02

Zhu, C. Y., Lv, Y. P., Yan, D. F., & Gao, F. L. (2013). Knockdown of MDR1 increases the sensitivity to adriamycin in drug resistant gastric cancer cells. *Asian Pac J Cancer Prev, 14*(11), 6757-6760. 10.7314/apjcp.2013.14.11.6757

Zhu, G., Pan, C., Bei, J.-X., Li, B., Liang, C., Xu, Y., & Fu, X. (2020). Mutant p53 in Cancer Progression and Targeted Therapies [Review]. *Frontiers in oncology, 10*. 10.3389/fonc.2020.595187

Zhu, Z., Chung, Y. M., Sergeeva, O., Kepe, V., Berk, M., Li, J., Ko, H. K., Li, Z., Petro, M., DiFilippo, F. P., Lee, Z., & Sharifi, N. (2018). Loss of dihydrotestosterone-inactivation activity promotes prostate cancer castration resistance detectable by functional imaging. *J Biol Chem, 293*(46), 17829-17837. 10.1074/jbc.RA118.004846